SOVIET PHYSICS

JETP

A translation of the Journal of Experimental and Theoretical Physics of the USSR.

SOVIET PHYSICS JETP VOL. 37 (10), NO. 3, pp. 417-636 MARCH, 1960

PRODUCTION OF K⁺ *MESONS BY COSMIC-RAY PROTONS AT 3250 m ABOVE SEA LEVEL*

M. Ya. BALATS, P. I. LEBEDEV, and Yu. V. OBUKHOV

Submitted to JETP editor December 3, 1958

J. Exptl. Theoret. Phys. (U.S.S.R.) **37**, 589-595 (September, 1959)

The spectrum of K^+ mesons in the momentum range up to 0.9 Bev/c produced by cosmic-ray protons was measured at an altitude of 3250 m above sea level (Mt. Alagez). The cross section for the above process is estimated.

EXPERIMENTAL SETUP

A diagram of the experimental setup is given in Fig. 1. Six layers of lead (I — VI), each 50 g/cm² thick, formed the matter in which K mesons were produced in the interaction of cosmic ray particles with lead nuclei. The K^+ mesons leaving the lead were detected by two liquid scintillation counters C_1 and C_2, and fell upon an aluminum absorber A 40 g/cm² in thickness. If the K^+ meson stopped and decayed in the matter of counters C_3 and C_4 or in the lead absorbers D and D′, the array detected the decay of the K^+ meson in those cases when at least one of the shower particles, produced in the same interaction as the K^+ meson, traversed counters C_1 and C_2. It is clear that in such cases, K^+ mesons produced in stars with a small multiplicity were detected by the array with a smaller probability than K^+ mesons produced in stars with a large multiplicity. The estimate of the above effect will be considered later in the discussion of the results.

A triple delayed-coincidence circuit $C_1 + C_2 + C_3(C_4)$ selected the decay events within the time range $(7 - 45) \times 10^{-9}$ sec. The trajectory of the primary particle and the number of the lead layer in which the interaction occurred were determined by means of a 220-channel hodoscope. Thus, the energy of K^+ mesons was determined from their range in lead.

The time of decay of K^+ mesons, i.e., the time between the appearance of a pulse in the counter C_2 and of the pulse in the counter $C_3(C_4)$, was measured with a high-speed oscillograph devel-

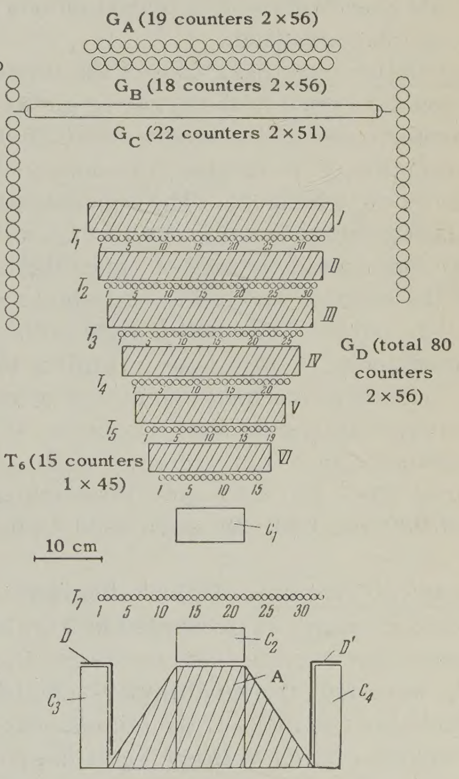

FIG. 1. General diagram of the array.

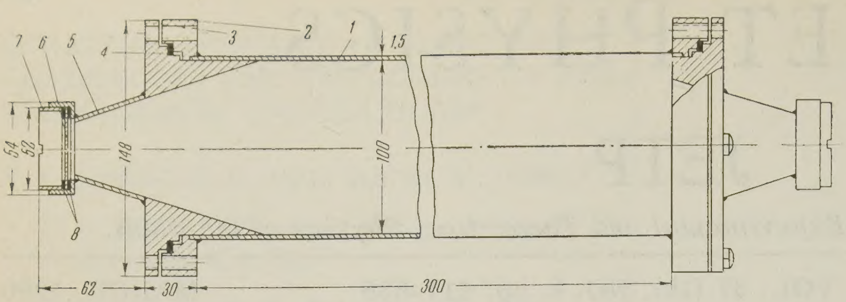

FIG. 2. Construction of the counter. 1 – counter body, 2 – flange, 3 – flange, 4 – fluoroplast washer, 5 – cone, 6 – quartz, 7 – screw, 8 – fluoroplast washer.

oped by us earlier.[1] The signal of triple coincidence $C_1 + C_2 + C_3 (C_4)$ triggered the sweep of the oscillograph and served as the master pulse for the hodoscope. The screen of the cathode-ray tube and the hodoscope panel with neon lamps were photographed on film.

The hodoscope. The position and dimensions of the Geiger-Müller counters are shown in Fig. 1. Trays T_1 and T_7 determine the place of occurrence of the star and the trajectory of the K^+ mesons, and the counters of the groups G_A, G_B, G_C, G_D determine the number of particles falling on the hodoscope from above. The Geiger-Müller counters of group G_C, placed in the front and back of the array, are not shown in Fig. 1.

Each counter of the trays $T_1 - T_7$ and of the groups G_B and G_C was connected to a hodoscope cell with a neon lamp MGKh-90. The counters of the trays G_A and G_D were connected in groups, each of which was connected to a cell with a neon lamp. All neon lamps were placed on one panel, which was photographed.

Scintillation counters. One of the liquid scintillation counters used in the array is shown in Fig. 2. The counter consisted of a brass container filled with a solution of p-terphenyl in doubly-distilled, chemically pure benzene. The concentration of the scintillating substance amounted to 1.4 g/l and was chosen from considerations of small light absorption by the solution and sufficiently large amplitude of the light pulses. For better light collection by the photocathode of the photo-multiplier tube, the inner surfaces of the metal container were lined with polished aluminum foil. Counters C_1 and C_2 measured 300 × 100 × 50 mm, while $C_3(C_4)$ measured 300 × 150 × 40 mm. Photomultiplier tubes of the type FEU-2V were used in the counters.

Electronic circuits. A block diagram of the electronic circuitry is presented in Fig. 3. The photomultiplier signals from counters C_1, C_2, C_3, and C_4 were fed after preliminary amplification and shaping to the input of the coincidence circuit.[2] The resolution curve of this circuit is given in Fig. 4. The method of measuring the time of decay of the K^+ mesons does not differ essentially from the method described earlier.[3]

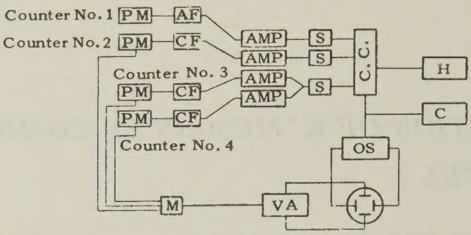

FIG. 3. Block diagram of the array. PM – photomultiplier of type FEU-2V, AF – anode follower, CF – cathode follower, S – shaping circuits, CC – coincidence circuits, H – hodoscope, C – camera control circuits, OS – oscilloscope sweep trigger, VA – vertical amplifier, M – photomultiplier signal mixer.

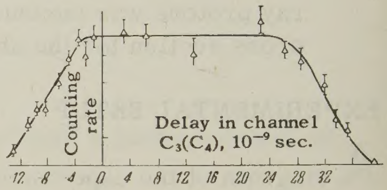

FIG. 4. Resolution curve of the triple coincidence circuit $C_1 + C_2 + C_3 (C_4)$.

To detect K^+ mesons with a mean life of 1.2×10^{-8} sec, the electronic circuit should have a sufficiently high resolving time. In order to measure the time spread of the scintillation-counter system, we determined the time between the pulses of the counters $C_2 - C_3$ and $C_2 - C_4$ corresponding to the simultaneous passage of a particle through the counters.

The data obtained are shown in Fig. 5. The accuracy of the time measurements by means of the counter system $C_2 - C_4$ was 2.2×10^{-9} sec and was determined essentially by the spread of

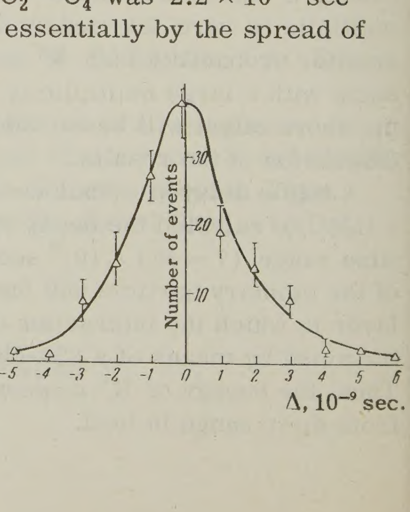

FIG. 5. Time spread of counters C_2, $C_3(C_4)$. The x axis represents the deviation Λ from the mean value of the time interval between the pulses of the counters C_2 and $C_3(C_4)$.

electron trajectories in the photomultiplier and by the counter size.

DECAY SCHEMES

Since the present experiment was not intended to identify the various decay schemes of K^+ mesons, the arrangement of the scintillation counters and the parameters of the electronic circuits were selected to record the most prevalent types of K^+ decay, $K_{\mu 2}$ and $K_{\pi 2}$.

The high energy of the decay μ mesons ($\epsilon_\mu = 152$ Mev, range 104 g/cm^2 Pb) insures good detection by the scintillation counter C_3 (C_4) of a μ meson emerging at any point of the absorber A. The $K_{\pi 2}$ decay scheme was recorded by the array with a somewhat smaller efficiency, in view of the smaller range of the decay π mesons ($E_\pi = 108.5$ Mev, $R = 60$ g/cm^2 Pb), some of which stopped in the absorber and did not reach the counters.

In nuclear interactions in lead, comparatively many π mesons are produced together with the K^+ mesons (the mean life of the π meson is 2.5×10^{-8} sec).

Detection of the $\pi \rightarrow \mu$ decay ($E_\mu = 4$ Mev) was possible only when the π meson stopped and decayed in the scintillating substance of the counter C_3 (C_4) and when at least one particle of the shower passed through counters C_1 and C_2. In such a case, three pulses appeared on the oscillograph screen — one due to the shower particle traversing the counter C_2, one due to the π meson stopping in the scintillator of the counter C_3 (C_4), and one due to the μ meson, which loses not more than 4 Mev in the scintillating liquid. The first two pulses, from counters C_2 and C_3 (C_4), coincide in time.

In the reduction of the data, only the decay events with $A_2/A_3 \leq 5$ were considered, A_2 being the amplitude of the second pulse and A_3 that of the third pulse. This corresponds to a limiting energy π-meson of 20 Mev. It should be noted that such a selection criterion leads to omission of certain similar decays of K^+ mesons, although to a smaller degree, since the energy of secondary products in the K^+ decay is considerably larger.

The contribution of the $\mu \rightarrow e$ decay is small in view of the small value of the chosen time range as compared with the mean life of the μ meson ($\tau_\mu = 2.22 \times 10^{-6}$ sec). In addition, a large fraction of the decay electrons is absorbed in the lead absorbers D and D′.

The mean life of K^+ mesons as measured in the present experiment coincides with the values obtained by other authors.[3-6] This confirms the small admixture of $\pi \rightarrow \mu$ and $\mu \rightarrow e$ decays.

MEASUREMENTS

Four experiments were carried out. In the first experiment, (a), 1200 hours long, the placement of the apparatus was as shown in Fig. 1. Data obtained in this experiment made it possible to obtain the range spectrum of the K^+ mesons in the interval 50 — 350 g/cm^2 Pb, and also the production cross section of K^+ mesons for protons of cosmic radiation. Experiment (b) (200 hours), in which the three lower layers of lead were removed, was devoted to a comparison of the efficiency of the detection of K^+ mesons produced in various layers of lead. Lead layers I — III in experiment (b) differed from layers IV — VI in experiment (a) with respect to the detecting efficiency of the K^+ decay only in their geometry. The third experiment (c) (500 hours) differed from experiment (a) only in that the absorber A was removed in experiment (c). The array detected the decay of K^+ mesons stopping in the matter of the counter C_3 (C_4) and in lead absorbers D and D′. The fourth experiment (d) (196 hours) was carried out to determine the background due to air showers. The placement of the counters was the same as in experiments (a) and (b), but the absorber A and all the six layers of lead were removed. In this experiment, K mesons could be produced and come to rest only in the matter of the counters $C_1 - C_4$.

In reducing the experimental data of all four experiments, decay events satisfying the following conditions were selected:

1) The time between the appearance of pulses in counter C_2 and C_3 (C_4) lies within the range $(7 - 45) \times 10^{-9}$ sec, and the amplitude ratio $A_2/A_3 \leq 5$.

2) The production of K^+ mesons in the lead layers is not connected with an air shower.

3) The trajectory of the particle producing the star does not pass through the side Geiger-Müller counters of the hodoscope (group G_D in Fig. 1).

4) It is possible to determine the layer in which the interaction has occurred from the hodoscope picture.

DISCUSSION OF RESULTS

The number of decays detected in experiments (a), (b), and (c) are given in Table I. In experiment (d), no decay events satisfying the above selection criteria were detected during the 196 hours of operation.

Column 5 of Table I lists the data of the experiment (b), normalized to 1200 hours of operation, with account of the absorption of protons in the three layers of lead, for a nuclear-interaction mean free path equal to 160 g/cm^2. Comparison

TABLE I

No. of layer	Experiment (a) (1200 hrs)		Experiment (b) p stars		Experiment (c) p stars		Momentum range of K particles (Bev/c)	Spectrum of K^+ mesons from experiments (a) and (b)
	p stars	n stars	200 hrs	Normalized to 1200 hrs, taking into account proton absorption	500 hrs	Normalized to 1200 hrs		
I	5	0	5	12	3	7	$0.88 \div 0.95$	12 ± 5
II	7	0	6	14	1	2.4	$0.81 \div 0.88$	18 ± 7
III	5	2	6	14	3	7	$0.72 \div 0.81$	16 ± 7
IV	10	3	—	—	3	7	$0.63 \div 0.72$	37 ± 14
V	15	7	—	—	3	7	$0.54 \div 0.63$	63 ± 11
VI	8	14	—	—	3	7	$0.41 \div 0.54$	43 ± 16
Counters 1 and 2 and the absorber	3	—	2	4.5			$0 \div 0.41$	14 ± 6

of the results of the experiments (a) (column 2) and (b) (column 5) shows that the probability of detection of a K decay is independent (within the limits of statistical errors) of the position of the lead layers relative to the absorber. The data of experiment (c), normalized to 1200 hours of operation, are given in column 7. By comparing these with the data of experiment (a) (column 2), we can determine the ratio of the detected decays in absorber A and in the matter of counters C_3 (C_4).

As already mentioned, the probability of the detection of K mesons stopping in the matter of the counters C_3 (C_4) depends on the multiplicity of the star in which the K meson was produced. This probability decreases with decreasing multiplicity of the star. It is clear that high-energy K mesons are produced with more penetrating particles than K mesons of lower energies. Therefore, the above effect will be especially important for the lower layers of lead.

The experimental data (Table I) for the layers IV — VI give the following ratio of the number of detected decays of K^+ mesons in the matter of counters C_3 (C_4) and in absorber A:

$$N_{\text{counter}}/N_{\text{absorber}} \approx 1.8.$$

The calculated value of this ratio is

$$N_{\text{counter}}/N_{\text{absorber}} = 1.91/0.88 \approx 2.1$$

(see Table II). If we assume that the array detects only 50% of the decay events of K mesons stopping in the matter of counter C_3 (C_4), then the given ratio will be smaller by a factor of two and will equal 1.05. The total detection efficiency of K^+ mesons is then smaller by 35%. Comparing the ratio $N_{\text{counter}}/N_{\text{absorber}}$ found in the experiment with the calculated one, we can conclude that the losses in the detection of decays produced in stars with a small number of prongs are small compared with the statistical error of the experiment. This is most probably due to the fact that most K^+ mesons are produced in stars with a large number of penetrating particles.

In the upper layers of lead, a small number of K particles produced by neutrons was detected (Table I, column 3). This makes it possible to conclude that K mesons are predominantly produced by the charged component of cosmic radiation. The increased number of K^+ mesons produced by neutrons in the lower layers of lead is due to the increase in the solid angle for primary particles. (For protons, the solid angle is limited by the counters of group G_D.)

The observed number of decays of K^+ mesons

TABLE II

	Weight of matter P, kg	$\Omega_\mu/4\pi$	Ω_p, sterad	$P\,\Omega_p(\Omega_\mu/4\pi)$, kg-sterad
Absorber	24.2	0.19	0.19	0,88
Walls of counters and absorbers	7.5	0.5	0.17	0.64
Scintillator	3.5	1	0.17	0.60
Counter shoulders	13.0	0,3	0,17	0.67

---

*$\Omega_\mu/4\pi$ is the solid angle for detection of K^+ meson decay products, Ω_p is the solid angle for protons.

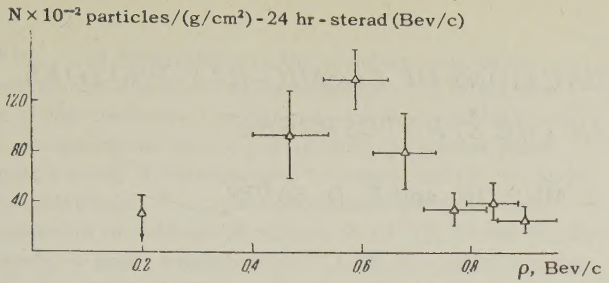

FIG. 6. Momentum spectrum of K^+ mesons.

produced by the charged component in experiments (a) and (b) is given in the last column of Table I. The results are corrected in taking into account the absorption of protons in the lead layers and the nuclear interactions of K^+ mesons with a mean free path[7] $L = 640\ \text{g/cm}^2$. The data are normalized for the same width of the momentum range, 0.1 Bev/c. The momentum range of the K particles corresponding to each layer are shown in the next-to-last column of Table I.

The momentum spectrum of K particles is shown in Fig. 6. The decay curve constructed on the basis of all detected events is shown in Fig. 7. The mean life of the studied particles, as measured in these experiments, is $(10.0 \pm 1.2) \times 10^{-9}$ sec.

The cross section for the production of K^+ mesons by protons can be estimated under the following assumptions:

1) The detection probability of the decay, in the time range given above, is equal to 1, only if a secondary particle falls on one of the side counters C_3 or C_4. The absorption of the decay products in the absorber and in the counter walls is neglected.

2) In the calculation of the solid angles, we shall assume that the K^+-meson trajectory is a continuation of the trajectory of the star-producing particle. (This assumption is confirmed by the fact that the K^+-decay detection efficiency is independent of the position of the lead layer with respect to the absorber.

3) The minimum proton energy necessary for the production of a K meson which can reach the absorber or the counters C_3 and C_4 is ~ 5 Bev. The main inaccuracy of the estimate lies in the uncertainty of this value. However, the small cross section for the production of K mesons for proton energies up to 5 Bev provides the basis for considering such a choice of the limiting energy close to the real one. The proton momentum spectrum at 3200 m above sea level is approximated by the function $N(p)\,dp = A^{-2.7}dp$, where[8] $A = 0.9 \times 10^{-3}$ particle/cm²-sec-sterad (Bev/c), and the angular distribution of protons is of the form[9] $N(\theta)d\theta \sim \cos^6\theta d\theta$. The cross section for the production of K^+ mesons by protons, calculated under the above assumptions, amounts to ¼ of the geometrical cross section and represents the lower limit of the actual value.

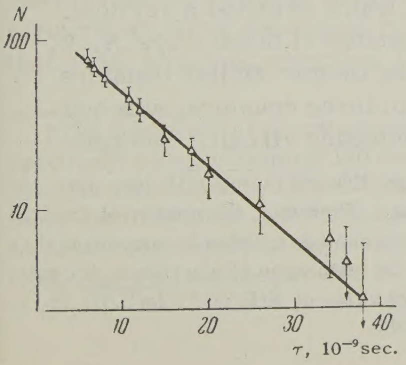

FIG. 7. Integral distribution of mean lives τ.

The results of the experiments show a sharp increase in the cross section for the production of K^+ mesons with increasing energy of the generating protons. From the shape of the given spectrum of K^+ mesons, it can be seen that the spectrum falls in the range of soft K^+ mesons. The observed number of K^+ mesons produced by protons and neutrons indicates the predominant production of K^+ mesons by the charged component of cosmic radiation.

In conclusion, the authors consider it their pleasant duty to express their gratitude to A. I. Alikhanov, G. P. Eliseev, V. A. Lyubimov, and A. G. Meshkovskiĭ for discussion of the results, to A. I. Alikhanian for the facilities for carrying out the experiment at the cosmic station on Mount Alagez, and also to K. A. Zaĭtsev and A. N. Rozanov for help in carrying out the experiment.

---

[1] Balats, Lebedev, and Obukhov, Приборы и техника эксперимента (Instruments and Measurement Engineering) **2**, 63 (1957).

[2] R. L. Garwin, Rev. Sci. Instr. **24**, 618 (1953).

[3] Balats, Lebedev, and Obukhov, JETP **31**, 531 (1956), Soviet Phys. JETP **4**, 436 (1957).

[4] L. Mezzeti and D. W. Keuffel, Phys. Rev. **95**, 858 (1954).

[5] V. Fitch and R. Motley, Phys. Rev. **101**, 496 (1956).

[6] Alvarez, Crawford, Good, and Stevenson, Phys. Rev. **101**, 503 (1956).

[7] Lannutti, Chupp, and Goldhaber, Phys. Rev. **101**, 1617 (1956).

[8] L. I. Potapov and N. V. Shostakovich, Dokl. Akad. Nauk SSSR **106**, 641 (1956), Soviet Phys.-Doklady **1**, 85 (1956).

[9] N. N. Kocharyan, JETP **25**, 364 (1953).

Translated by H. Kasha
119

SOVIET PHYSICS JETP VOLUME 37 (10), NUMBER 3 MARCH, 1960

INVESTIGATION OF PION PRODUCTION IN INTERACTIONS OF COSMIC-RAY PROTONS AND α PARTICLES WITH CARBON NUCLEI IN THE STRATOSPHERE

K. I. ALEKSEEVA, S. I. BRIKKER, N. L. GRIGOROV, V. S. MURZIN, and F. D. SAVIN

Moscow State University

Submitted to JETP editor March 7, 1959

J. Exptl. Theoret. Phys. (U.S.S.R.) **37**, 596-603 (September, 1959)

Pulse ionization chambers and a hodoscope were used to study the interaction of primary protons and α particles with carbon nuclei in the stratosphere at 31° N geomagnetic latitude. The electron cascade initiated in lead by γ quanta from the decay of the neutral π mesons produced in the interaction was investigated. It was found that the primary-particle energy consumed in π^0 production in the interactions between protons or α particles and carbon nuclei in the $\sim 10^{10}$ ev energy range is on the average $(10 \pm 3)\%$ and $(14 \pm 10)\%$ respectively.

INTRODUCTION

UNTIL 1954, no direct measurements had been made of the energy fraction consumed in the production of π mesons in a single act of interaction of cosmic-ray protons with light nuclei. Slight inelasticity of the interaction between nucleons and light nuclei in the energy range of $\sim 10^{10}$ ev was inferred indirectly through a study of the absorption of the nuclear-active particles in cosmic rays[1] and the production of the various secondary components of cosmic radiation in the atmosphere.[2] The validity of this conclusion depended substantially on the assumed value of the cross section for inelastic interactions.

The energy consumed in the production of π^0 mesons can be determined from a measurement of the ionization at the maximum of the cascade shower initiated by the γ quanta produced in π^0-meson decay. By measuring the total ionization produced by all the electrons at the shower maximum, and also the average ionization due to a single electron, we can determine the number of particles N_{max} at the shower maximum. The relation between N_{max} and the energy E of the primary electron or the photon initiating the cascade, given by Belen'kiĭ,[3] makes it possible to determine the average total energy E of the γ quanta produced in the π^0 decay from the number of electrons at the shower maximum, i.e., the average energy $E_{\pi 0} = E$ transferred to π^0 mesons:

$$N_{max} = K(E/\beta)\, E / \sqrt{\ln(E/\beta)}\, \beta, \qquad (1)$$

where $\beta = 6.4 \times 10^6$ ev is the critical energy in lead. Thus, a measurement of the number of electrons at the shower maximum, obtained by measuring the ionization due to these particles, yields directly the energy consumed in the production of π^0 mesons, without the need for any assumption regarding the cross section of the inelastic interaction.*

On September 20, 1954, measurements of the ionization at the maximum of cascade showers produced by γ quanta from the decay of π^0 mesons (average energy of primary protons — $\overline{E}_{0p} = 20$ Bev, that of the primary α particles — $\overline{E}_{0\alpha} = 40$ Bev) were carried out in the stratosphere at an altitude of 25 km and at 31° N geomagnetic latitude. Pulse ionization chambers and a hodoscope were used. The apparatus was lifted into the stratosphere by probe balloons. The results of the measurements were transmitted to the earth by radio.

EXPERIMENTAL SETUP

The arrangement of the counters, ionization chambers, and absorbers, together with a block diagram of the electronic circuits, is shown in Fig. 1. The telescope, which selected a vertical beam of particles, consisted of three trays A, B, and C of self-quenching Geiger-Müller counters. Each tray, consisting of three counters, was connected to a triple-coincidence circuit. The geo-

---

*In the 10^8-10^{10} ev range, $K(E/\beta)/\sqrt{\ln(E/\beta)}$ does not depend strongly on the energy. Therefore, the number of particles at the shower maximum can be regarded as proportional to the energy consumed in the production of π^0 mesons. According to Belen'kiĭ, the average value of $K(E/\beta)/\sqrt{\ln(E/\beta)}$ in the 10^8-10^{10} ev range is 0.080.

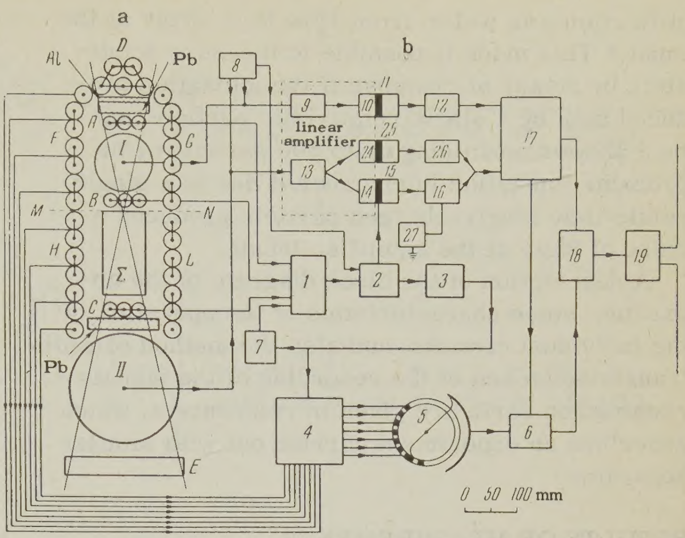

FIG. 1. a) Arrangement of the counters, ionization chambers, and absorbers in the apparatus. b) Block diagram of the electronic circuitry: 1 – triple coincidence circuit, 2 – gating univibrator, 3 – hodoscope master pulse shaping circuit, 4 – hodoscope, 5 – rotary switch, 6 – hodoscope pulse tube, 7 – triple-coincidence gating circuit, 8 – generator of calibration pulses, 9, 10, 13, 14 and 13, 24 – channels of linear amplification, 11, 15, 25 – gating circuits, 12, 16, 26 – pulse-stretching circuits, 27 – blocking of the sensitive channel of the lower chamber, 17 – circuit for simultaneous transmission of pulses from both chambers, 18 – modulator of the transmitter, 19 – transmitter. The elements in the block diagram are marked according to the block diagram of the apparatus in reference 4.

metrical factor of the array was $S\Omega = 9$. The investigated absorber Σ, of 19.5 g/cm^2 graphite, was placed between trays B and C. During the time of flight, the absorber was inserted into the telescope or removed from it every three minutes, so that the measurements with graphite were alternated with background measurements all the time. Two cylindrical pulse ionization chambers were incorporated into the setup, one inside the telescope between the trays A and B (chamber I), and the second below the lower tray C of the hodoscope counters (chamber II).* An absorber consisting of 2 cm of lead and 1 cm of aluminum was placed above the top tray A. The thickness of this absorber was sufficient to insure that practically all particles of the electronic component from the atmosphere underwent an electromagnetic interaction in it and initiated cascade showers, which were efficiently detected by the counters placed above the line MN. The top group D of counters, connected in parallel and actuated by a separate hodoscope cell, covered the total acceptance angle of the apparatus. Therefore, all triple-coincidence events due to single particles inside the acceptance angle of the apparatus were necessarily accompanied by a discharge in counters D (four-fold coincidences). Photons which traversed the instrument underwent conversion in the upper lead absorber, producing electron showers detectable by the instrument. In that case, however, counters D did not discharge. A lead absorber 2 cm thick was placed above chamber II underneath tray C. The γ quanta from the decay of the π^0 mesons produced on carbon were converted in this absorber, and a cascade shower developed which attained its maximum within the absorber. The telescope, the ionization chambers, and the graphite and lead absorbers were surrounded by counters connected to the hodoscope (counters E, F, G, H, L). All the telescope counters were also connected to the hodoscope.*

The setup was triggered (see block diagram, Fig. 1b) by a triple coincidence (block 1) of discharges in the trays A, B, and C of the telescope counters. The resolving power of the triple coincidence circuit was 5×10^{-6} sec and that of the hodoscope cells was 2×10^{-5} sec. The linear amplifiers 9 – 10, 13 – 14, and 13 – 24 (connected to chambers I and II) were gated through junctions 11, 15, and 25, at the moment of passage of a particle through the telescope, by a square pulse of 2×10^{-4} sec duration, the length of the measured pulse being $\sim 1 \times 10^{-4}$ sec. The linearly amplified pulses of chamber I ranged from 10 to $\sim 400\ \mu$v at the amplifier input (the probable pulse due to a single relativistic single-charged particle being 18 μv). For chamber II, which was meant mainly for the detection of showers containing a large number of particles, the range of linear amplification was wider, from 10 μv to ~ 10 mv at the input.* This made it possible to measure accurately by means of chamber II the ionization produced both by a single relativistic particle and by a shower containing up to 500 particles (the probable ionization in chamber II due to a single relativistic singly-charged particle produced a pulse of 25 μv at the amplifier input).

---

*The dimensions of ionization chambers I and II were, respectively: cylinder diameter 100 and 200 mm; length 300 and 300 mm; wall thickness 0.5 and 0.9 mm brass; diameter of internal electrode (steel rod) 3.0 and 6.0 mm. The chambers were filled with spectrally pure argon at 5.0 and 3.0 atmos, respectively, and were operated at 1000 v.

*The counters were filled with a mixture of argon and ethylene. A thin graphite layer spread on the internal surface of the glass walls served as the negative electrode. The wall thickness varied from 1.0 to 1.5 mm. The dimensions of the counters were: A, B, C – diameter 20 mm, length 200 mm; D – diameter 30 mm, length 300 mm (5 pieces); E – diameter 30 mm, length 200 mm (17 pieces); F, G, H, L – diameter 30 mm, length 300 mm (28 pieces).

A description of the block diagram of the apparatus, some characteristics of the operation of the individual circuits, and also the method of radio transmission and of the recording of the signals received on earth are given in reference 4, which describes an experiment carried out with similar apparatus.

RESULTS OF MEASUREMENTS

The hodoscope data were used to determine the nature of the shower and the place of its initiation. In this experiment, we were interested only in events in which charged particles traversed the apparatus. These particles were selected by the discharges they produced in counter group D. Using the hodoscope data, we excluded cascade showers produced by electrons in the upper lead absorber. In that absorber, practically all of the electronic component (~ 98%) underwent cascade multiplication. A shower was considered electron-produced when discharges occurred either a) in more than one counter of trays A or B, or b) in one counter each of trays A and B together with a discharge of at least one counter out of those placed above the graphite absorber (counters F and G located above the line MN). The other detected events represented either singly-charged particles which did not interact with the absorbers (discharge of one counter each in trays A, B, C, and not more than one counter in tray E), or showers in the lower part of the instrument, the particles of which were detected by a counter located below line MN. This category of showers also included electron-nuclear showers emerging from graphite and from the lead located above chamber II. (These showers caused either a) the discharge of one counter each in trays A and B and the discharge of more than one counter in tray C, or b) the discharge of one counter each in A, B, C together with the discharge of at least one counter in the side trays H and L, or together with the discharge of two or more counters in tray E.) Since the showers produced in graphite were recorded against a large background of electron-nuclear showers from the lower lead absorber and of nonlocal showers, the effect due to the carbon was evaluated from the difference of measurements with and without graphite. We disregarded the possible variation in the background of the nonlocal showers upon changing from measurements with the graphite to measurements without it. However, there was no reason to believe this variation to be large.

The particle that produced an electron-nuclear shower in graphite was identified by the ionization produced by this particle in the upper chamber I. Because of the presence of large fluctuations in the ionization in the chamber gas, and also because of fluctuations in pulse size due to the superposition of noise, we assumed that the ionization primary protons in the upper chamber could produce ionization in the range $J/J_0 = 0 - 3.0$, and primary alpha particles could yield $J/J_0 = 3.0 - 7.5$ (where J_0 is the probable ionization due to a relativistic singly-charged particle, and J is the ionization due to the given particle).[4]

Figure 2a shows the ionization spectra of showers in the lower part of the apparatus (below the 2-cm lead layer), obtained at an altitude of 25 km from the data of the lower chamber II, under the condition that the pulse in the upper chamber I was 0 — 3.0 times that due to probable ionization by a relativistic singly-charged particle (this being the range of showers produced by primary protons). A correction is applied to this spectrum for the ionization due to δ showers, based on data obtained on earth, since it could be assumed that all local showers detected at the surface of the earth in the lower part of the apparatus were δ showers. The solid and dotted histograms were obtained for measurements with and without graphite, respectively. The results of the measurement without graphite were multiplied by 1.26 to reduce them to the period of the measurements with graph-

---

*The range of the amplifier connected to chamber II was extended in the following way: after two amplification stages (block 13), the pulse from chamber II was fed simultaneously to the sensitive (14, 15, 16) and "coarse" (24, 25, 26) channels. The pulses were stretched (see description of the block diagram in reference 4) by circuits 16 and 26 and, as long as the pulse from chamber II was small, both stretched pulses were fed to circuit 17. This circuit recorded the longer of the two received stretched pulses, i.e., the pulse from the sensitive channel. If the pulse from chamber II was larger than ~ 400 μv at the amplified input, then the sensitive channel was blocked by circuit 27. As a result of this, only the stretched pulse from the "coarse" channel 24, 25, 26 of chamber II was fed to circuit 17. In order to note the passage of the pulse from the chamber along the "coarse" channel, the voltage pulse from the blocking neon tube in circuit 27 was fed to a marking circuit. As a result, every time the sensitive channel was blocked a voltage pulse appeared on the switch contact connected to the cathode of the neon tube in the marking circuit.

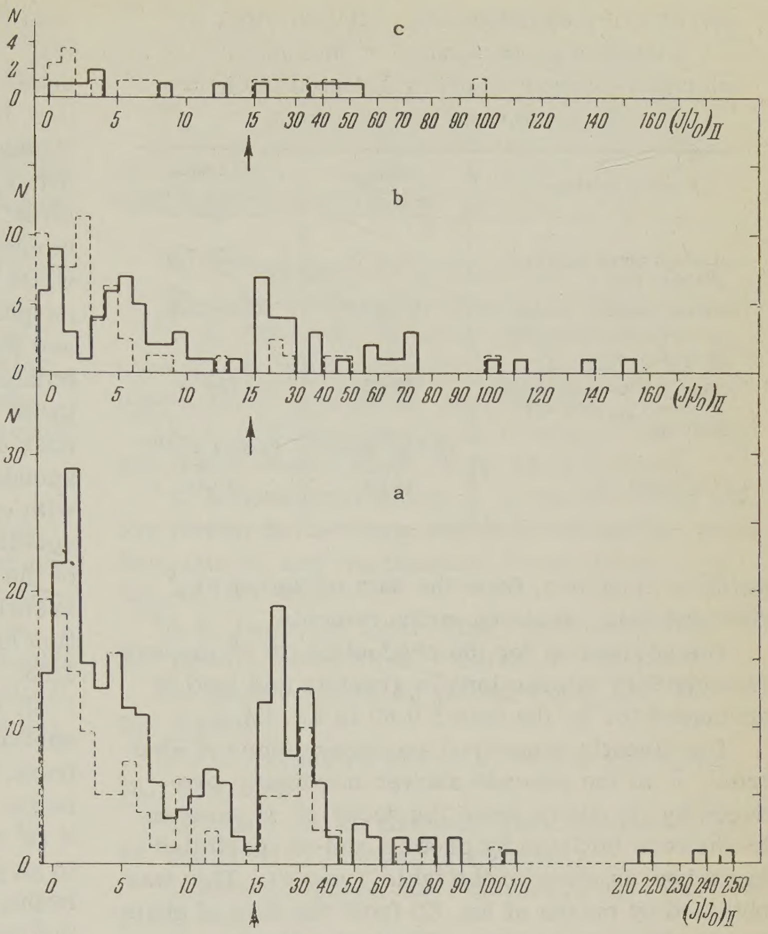

FIG. 2. Ionization spectra in the lower chamber II, obtained in the stratosphere at an altitude of 25 km, in measurements with the graphite absorber (solid line) and without it (dotted line) for pulse in the upper chamber equal a) $0 < (J/J_0)_I < 3.0$; b) $3.0 < (J/J_0)_I < 7.5$; c) $(J/J_0)_I > 7.5$. For ionization values $(J/J_0)_{II} > 15$, the scale of the y axis is compressed by a factor of five. N – number of showers with a given ionization.

ite ($t = 42.3$ min). Equivalent data are shown in Fig. 2b for an ionization range in the upper chamber equal to 3.0 – 7.5 times the probable ionization (range of showers from primary α particles); a correction for δ showers was not introduced here. Figure 2c represents the same for an ionization range in the upper chamber greater than 7.5 times the probable ionization. The excess of the number of showers in measurements with graphite, due to the showers produced on carbon by protons (Fig. 2a)* and by α particles (Fig. 2b), is clearly noticeable. For an ionization in the upper chamber greater than 7.5, the effect of carbon has not been detected, within the limits of the very scant statistical data (Fig. 2c).

Using the data of Fig. 2, we can calculate the average ionization in chamber II under 2 cm of lead per shower initiated in carbon by a proton or an α particle. The average ionization per shower initiated in the carbon, expressed in units of the average ionization due to a relativistic singly-charged particle, gives directly the average number of charged relativistic particles in the shower. To obtain the average number $\bar{\nu}$ of electrons at the shower maximum of a cascade produced by the γ quanta from π^0 decay, we should apply to the measured average number of charged relativistic particles in the shower a correction for the number $\bar{n}$ of penetrating particles in the shower.

A formula for calculating $\bar{\nu}$ on the basis of the obtained ionization spectra was derived from simple considerations, and is of the form

$$\bar{\nu} = 0.80 \left[\frac{\sum (N_i^{C+ph} J_i/1{,}20 J_0) - \sum (N_i^{ph} J_i/1.20 J_0)}{\sum N_i^{C+ph} - \sum N_i^{ph}} - \bar{n} \right]. \quad (2)$$

where J_0 is the probable ionization of a relativistic singly-charged particle, $1.20\ J_0$ is the average ionization of a relativistic singly-charged particle, J_i is the ionization of the given particle, N_i^{C+ph} is the number of showers with a given ionization J_i/J_0 obtained in measurements with graphite in the telescope, N_i^{ph} is the same for measurements without graphite, $\bar{n} = 4.2 \pm 0.5$ is the average number of charged penetrating particles (protons and π mesons) per shower initiated in carbon by a proton (according to our data), and $\bar{n} = 9.1 \pm 0.7$ is the same per shower produced by an α

---

*The absolute number of interactions between protons and carbon nuclei obtained in the present experiment is in agreement with our 1955 data.[5]

Results of measurements of the energy consumed in production of π^0 mesons in electron-nuclear showers initiated in carbon by protons and α particles

Primary particle	Proton $\bar{E}_0 = 20\cdot10^9$ ev	α-particle $\bar{E}_0 = 40\cdot10^9$ ev
Ionization range J/J_0 in chamber I	0—3.0	3.0—7.5
Measured average number of electrons at cascade shower maximum, $\bar{\nu}$	11.4±3.5	32.2±23.0
Number of electrons in the shower N_{max} with corrections	26±8	73±52
$\bar{E}_{\pi^0}$, ev	$(2.1\pm0.6)\cdot10^9$	$(5.8\pm4.2)\cdot10^9$
$(\bar{E}_{\pi^0}/\bar{E}_0)\cdot100$, %	10±3	14±10

particle in carbon, from the data of Rao et al.,[5] obtained from emulsion measurements.

The correction for the production of π^0 mesons in secondary interactions in graphite and lead is accounted for by the factor 0.80 in Eq. (2).

The directly-measured average number of electrons $\bar{\nu}$ at the cascade shower maximum, produced by γ quanta from the decay of π^0 mesons in showers initiated by protons and α particles in carbon, is given in the table (row 2). This was obtained by means of Eq. (2) from the data of chamber II (Figs. 2a and 2b). To obtain N_{max}, we introduced a number of corrections to the measured value of the number of electrons:

1. The ionization pulses from particle showers was expressed in Eq. (2) in units of the average ionization produced in the chamber by relativistic particles. In reality, however, because of a different geometry of the passage of shower particles through the lower chamber, the average path of a single particle in the chamber was somewhat longer than the average path of a shower particle. Therefore, the average ionization due to a single particle was greater than the average ionization due to a shower particle, and the measured number of particles $\bar{\nu}$ was underestimated. Taking into account the difference in the geometry* and also the dependence of the electron momentum on the place of incidence of the particle in the chamber, we found that the measured number of particles, $\bar{\nu}$, had to be multiplied by 1.11.

2. Since no lead scatterer was present in the instrument below chamber II, the energy spectrum of particles as measured by chamber II was harder than the equilibrium spectrum of Tamm and Belen'kiĭ.[3] The spectrum of electrons in the showers under 2 cm of lead, was measured in a cloud chamber, in the absence of backward scattering, by Nassar and Hazen.[7] Since chamber II was made of brass, it was necessary to take into account the effect of transition from lead to copper in the chamber walls. (The effective thickness of chamber walls was ~ 2.3 mm or 1.9 g/cm^2 Cu.) For this purpose, we used experimental data of Hereford and Swann[8] on the range-energy relation (extrapolated) for electrons in copper. According to these data, a range equal to the effective wall thickness of chamber II, $d_{eff} = 1.9$ g/cm^2 Cu, corresponds to 3.8×10^6 ev. The number of electrons with energy $E < 3.8 \times 10^6$ ev, according to the spectrum of Nassar and Hazen,[7] amounts to 25% of the total number; i.e., 25% of the electrons were absorbed in the chamber walls. Hence, the correction factor for the absorption in chamber walls is 1.33.

3. In view of the fact that the measured electron spectrum was harder than the equilibrium spectrum, the scattering in the chamber gas was not large. The scattering in the energy range $E > 4 \times 10^6$ ev, for which $\cos\theta > 0.95$, was assumed to be practically nil. A correction for scattering in the gas chamber was introduced for particles that had an energy less than 4×10^6 ev after passing through the chamber walls. The mean scattering angle in the energy range 0 to 4×10^6 ev was calculated for the electron spectrum of Nassar and Hazen[7] from formula 1.55a of Sec. 22 of the article by Rossi and Greisen.[9] The measured path length and hence the ionization due to the scattering of electrons in the chamber gas, was found to be equal to 10% (correction factor 0.90).

4. To permit comparison of the experimental data with the cascade theory, which deals with an equilibrium spectrum of electrons, we transformed our spectrum to an equilibrium spectrum, taking into account the electrons of the "reverse" current which would flow into the chamber if the chamber were surrounded from all sides by lead and if there were no absorption in the chamber walls. The value of this correction for the "reverse current" was determined by us from the experimental data of Blocker et al.,[10] who used a thin-walled ionization chamber. The correction factor for lead, according to these data, equals 1.70.

The resulting correction factor equals 2.26. It should be noted that a considerable contribution is made to this by the correction for the "reverse current," well-known from experimental data. The contributions of the other corrections are less substantial, and the possible inaccuracy in that determination cannot substantially change the obtained result. The table (row 3) lists the number of electrons at shower maximum, N_{max}, with all corrections. Substituting the result obtained for N_{max} into formula (1) of Tamm and Belen'kiĭ, we find the average energy $\overline{E}_{\pi^0}$, consumed in the production of π^0 mesons, for one shower in carbon, to be $(2.1 \pm 0.6) \times 10^9$ ev for protons and $(5.8 \pm 4.2) \times 10^9$ ev for α particles (row 4 of the table). The average energy of a proton is $\overline{E}_0 = 20 \times 10^9$ ev and that of an α particle is $\overline{E}_0 = 40 \times 10^9$ ev, making the fraction k of the energy consumed in production of π^0 mesons, in interactions involving carbon,

---

*The correction for the difference in the geometry took into account the angular distribution of the electrons emerging from lead, in accordance with the calculations of I. P. Ivanenko.[6]

$$k_p = (10 \pm 3)\ \% \text{ and } k_\alpha = (14 \pm 10)\ \%$$

for protons and α particles respectively. Thus, our result confirms the earlier conclusion[1,2] about the small inelasticity of the interaction of protons with light nuclei in the energy range of $\sim 10^{10}$ ev. The value of k_α obtained for primary α particles under analogous conditions is, within the statistical error of the measurements, not different from the value obtained for protons.

CONCLUSIONS

The average fraction of energy transferred by a $\sim 10^{10}$ ev proton to π^0 mesons in a single act of interaction with a carbon nucleus is equal to 0.10 ± 0.03.

The corresponding value 0.14 ± 0.10 obtained for primary α particles is, within the limits of the statistical error of the measurements, not different from the value obtained for protons.

L. G. Landsberg took part in the experiment.

The authors would like to express their deep gratitude to I. P. Ivanenko for taking part in the discussion of the experimental data.

---

[1] G. T. Zatsepin, JETP **19**, 1104 (1949).

[2] N. L. Grigorov, Usp. Fiz. Nauk **58**, 599 (1956).

[3] S. Z. Belen'kiĭ, Лавинные процессы в космических лучах (Cascade Processes in Cosmic Rays), GTTI 1948, p. 82, 125, and 126.

[4] K. I. Alekseeva and N. L. Grigorov, JETP **37**, 380 (1959), Soviet Phys. JETP **10**, 271 (1960).

[5] K. I. Alekseeva and N. L. Grigorov, JETP **35**, 599 (1958), Soviet Phys. JETP **8**, 416 (1959). Appa, Rao, Daniel, and Neelakantan, Proc. Indian Acad. Sci. **43**, 181 (1956).

[6] I. P. Ivanenko, Dokl. Akad. Nauk SSSR **122**, 367 (1958), Soviet Phys.–Doklady **3**, 962 (1959).

[7] S. Nassar and W. E. Hazen, Phys. Rev. **69**, 298 (1946).

[8] F. L. Herenford and C. P. Swann, Phys. Rev. **78**, 727 (1950).

[9] B. Rossi and K. Greisen, Revs. Modern Phys. **13**, 240 (1941) (Russian Translation).

[10] Blocker, Kenney, and Panofsky, Phys. Rev. **79**, 419 (1950).

Translated by H. Kasha
120

SOVIET PHYSICS JETP VOLUME 37(10), NUMBER 3 MARCH, 1960

NONMESONIC DECAYS OF HYPERFRAGMENTS

I. B. BERKOVICH, A. P. ZHDANOV, F. G. LEPEKHIN, and Z. S. KHOKHLOVA

Radium Institute, Academy of Sciences, U.S.S.R.

Submitted to JETP editor March 12, 1959; resubmitted June 2, 1959

J. Exptl. Theoret. Phys. (U.S.S.R.) **37**, 604-610 (September, 1959)

In a systematic scanning of 47 cm^3 of emulsion irradiated by 4.5-Bev π mesons, 8 double stars were found which were attributed to nonmesonic decays of hyperfragments with $Z = 2$ to 6. In these stars, the connecting track thinned down and one of the secondary tracks had a range $> 5000\,\mu$. The hyperfragments, together with their secondary products, have been identified. Possible decay schemes are proposed for the hyperfragments, assuming one neutron to be emitted.

As is well known, at the present time there is considerable interest in nonmesonic decays of hyperfragments. The number of reliably identified cases is still small, although heavy hyperfragments decay in this way a significant fraction of the time. The difficulty in the analysis lies in the occurrence of neutral particles, and of heavy, short-range fragments among the decay products of the hypernucleus.

In the work reported here, we tried to identify several hyperfragments found in a G-5 emulsion exposed to 4.5 Bev π mesons. That these cases do indeed involve hyperfragments is shown by the facts that the track thinned down toward the end of its range and that the range of one of the secondary particles was more than $5000\,\mu$. The presence of a fast proton is a sufficient but not necessary criterion for the recognition of a hyperfragment. The probability of accidental superpositions in the entire volume scanned is about 10^{-4}, which practically eliminates the possibility of coincidences in the cases we examined. However, in doubtful cases the emulsion was soaked and examined from the opposite side with a long focus objective. Conclusions about the nature of the hyperfragments were based on as exact as possible identifications of the hyperfragment itself and its decay products. The charge of the hypernucleus was determined by measuring the width of the track as a function of the residual range. As a preliminary step, we constructed integral curves for p, α, Li, Be and B to be used for calibration.

In several cases, the charge was found from the thin-down length. The secondary particles were identified by measuring intervals G(R) and scattering $\overline{\alpha}(R)$. In the following we describe the cases considered in detail:

Case No. 264 (Fig. 1). This case was very favorably located in the emulsion. All tracks end in one layer and lie in the same plane. The hypernucleus had charge 3, as found by measurements

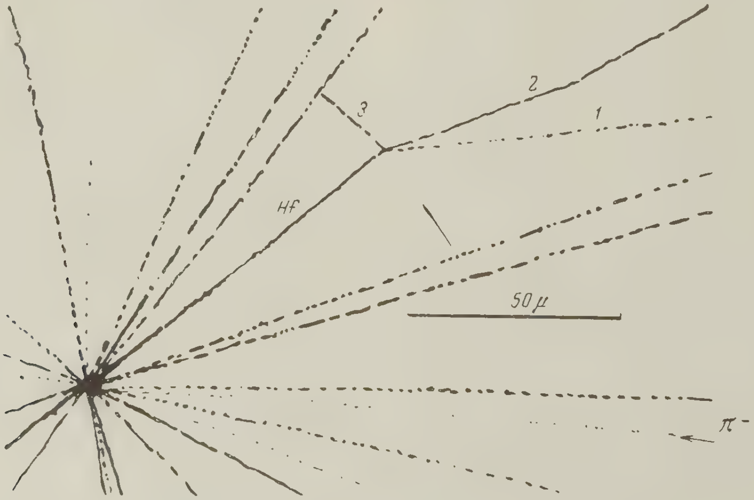

FIG. 1

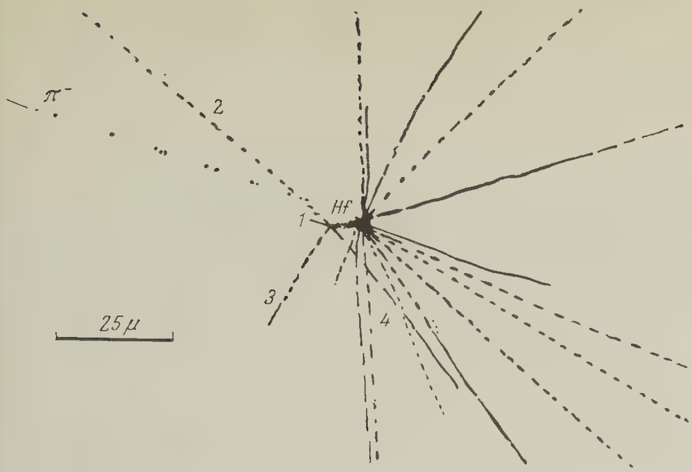

FIG. 2

of the track width and thin-down length. We calculated decay schemes containing one neutron among the products:

1. ${}_\lambda Li^6 \to H^1 + H^1 + H^3 + n$;
2. ${}_\lambda Li^6 \to H^1 + H^2 + H^2 + n$;
3. ${}_\lambda Li^6 \to H^1 + H^3 + H^1 + n$.

The binding energy B_λ corresponding to these possibilities is > 20 Mev.

4. ${}_\lambda Li^7 \to H^1 + H^3 + H^2 + n$;
5. ${}_\lambda Li^7 \to H^1 + H^2 + H^3 + n$.

For these decay schemes, $B_\lambda > 15$ Mev.

6. ${}_\lambda Li^8 \to H^1 + H^3 + H^3 + n, B_\lambda = 5$ Mev.

Comparing this value for B_λ with values obtained by other authors, we concluded that the most probable decay scheme is

$${}_{\lambda_0}Li^8 \to H^1 + H^3 + H^3 + n.$$

Case No. 3013 (Fig. 2). The tracks of all the secondary particles except 2 and 4 are short and inclined, which makes identification difficult. Track 2 is a proton, while tracks 3 and 4 correspond to charge 1. Track 1 was made by a particle having charge not less than 2. Hence, the hypernucleus has a charge of at least 6. Assuming $Z_{Hf} = 6$, calculations on decay schemes give a binding energy $B_\lambda = 70$ Mev. A reasonable value for the binding energy of the λ_0 particle is obtained, together with conservation of energy and momentum, if we assume the decaying nucleus is B^{10} and one neutron is emitted. The most probable decay scheme is the following:

$${}_\lambda B^{10} \to He^4 + H^1 + 2H^2 + n.$$

Case No. 3021 (Fig. 3). The charge of the hypernucleus is 6, as determined by measurements of the track width and the thin-down length. The energy associated with track 4 was found from changes in the ionization under the assumption that the track is that of a proton. Tracks 1 and 2 have charge 2, as found from measurements of the width, while track 3 has charge 1. We calculated all possible decay schemes of ${}_\lambda C^{12}$, ${}_\lambda C^{11}$, and ${}_\lambda C^{10}$, assuming that one neutron was emitted. The most probable decay scheme is

$${}_\lambda C^{12} \to 2He^4 + H^1 + H^2 + n.$$

The binding energy in this case is $B_\lambda \approx 8$ Mev.

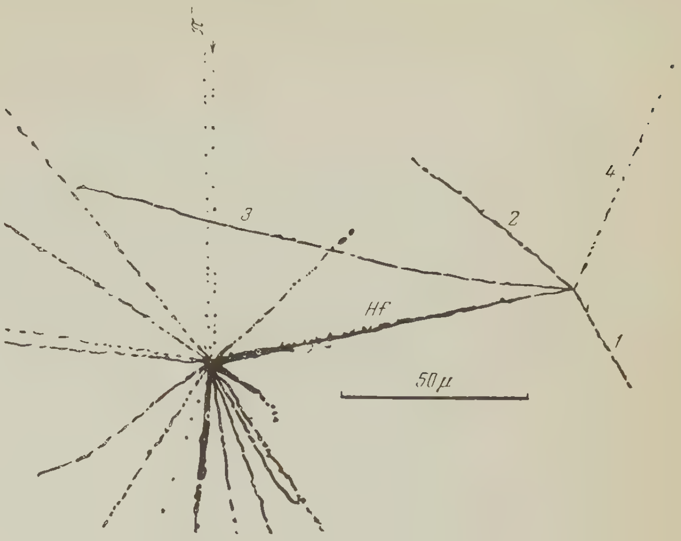

FIG. 3

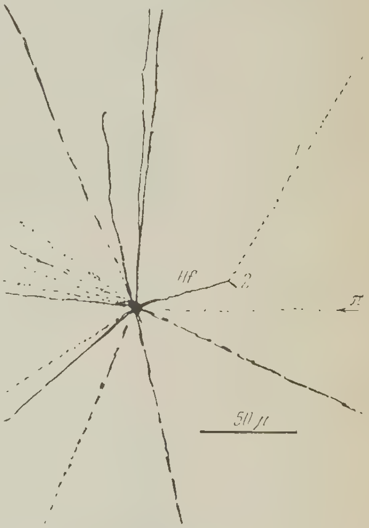

FIG. 4

Case No. 312 (Fig. 4). In this case the hypernucleus has charge 2, as found by measuring the track width. Both the secondary tracks end in the same layer. Track 1 was identified by measuring intervals G(R) and the scattering $\overline{\alpha}(R)$. It turned out that track 1 is a deuteron. Assuming that one neutron was emitted, the following three

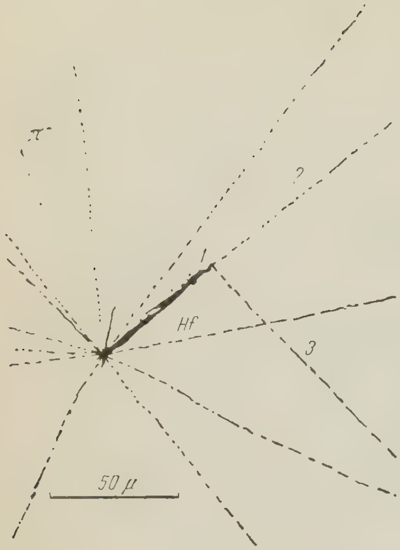

FIG. 5

possibilities were calculated:

1. $_{\lambda_0}\mathrm{He}^6 \to \mathrm{H}^2 + \mathrm{H}^3 + n$, $B_\lambda > 10$ MeV;
2. $_{\lambda_0}\mathrm{He}^4 \to \mathrm{H}^2 + \mathrm{H}^1 + n$, $B_\lambda > 15$ MeV;
3. $_{\lambda_0}\mathrm{He}^5 \to \mathrm{H}^2 + \mathrm{H}^2 + n$, $B_\lambda \approx 1$ MeV.

Comparing these values of B_λ with those given by other authors, we consider that this case corresponds to the decay scheme

$$_{\lambda_0}\mathrm{He}^5 \to \mathrm{H}^2 + \mathrm{H}^2 + n.$$

Case No. 338 (Fig. 5). One of the decay products of the hypernucleus is a heavy fragment. The tracks of the hypernucleus and of the heavy fragment are inclined at the same angle to the plane of the emulsion. The points corresponding to the track widths of the hyperfragment are beyond the range of the calibration curve for boron. The points corresponding to the widths of the heavy fragment correspond to beryllium. The charges of the other tracks were found by ionization measurements and are $Z_1 = 4$, $Z_2 = 1$, and $Z_3 = 1$. The hyperfragment could be either $\lambda_0\mathrm{C}^{12}$ or $\lambda_0\mathrm{C}^{13}$, since analysis of the decay schemes for $\lambda_0\mathrm{C}^{12}$ and $\lambda_0\mathrm{C}^{13}$ both lead to the reasonable value $B_\lambda = 9-10$ Mev. The decay schemes are

$$_{\lambda_0}\mathrm{C}^{12} \to \mathrm{Be}^9 + 2\mathrm{H}^1 + n,$$

$$_{\lambda_0}\mathrm{C}^{13} \to \mathrm{Be}^{10} + 2\mathrm{H}^1 + n.$$

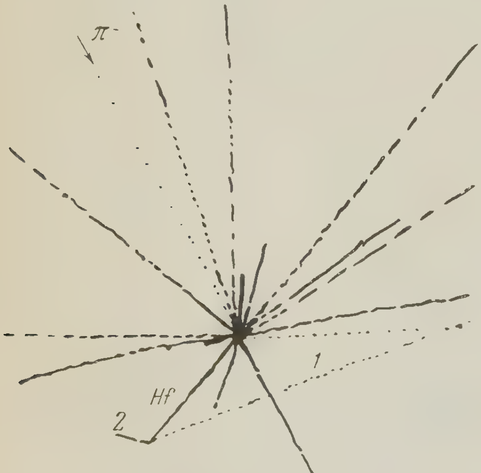

FIG. 7

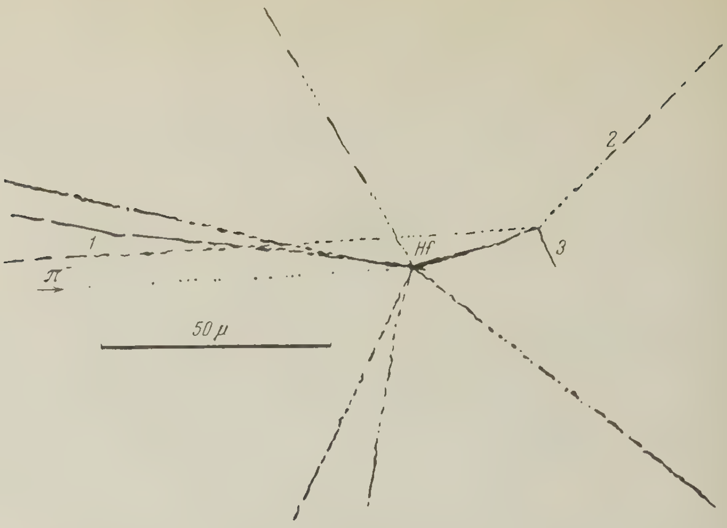

FIG. 6

Case No. 284 (Fig. 6). The track of the hypernucleus is short ($28\,\mu$) but its inclination is also small; comparison of its mean width with the calibrating curves indicate a charge $Z = 4$ for the hypernucleus. This method does not work for track 3. The charge associated with this track was obtained by comparing the charge of the hypernucleus with the charges associated with the other two tracks, the latter charges being obtained from ionization measurements. Analysis of the decay schemes for $\lambda_0\mathrm{Be}$ shows that more than one neu-

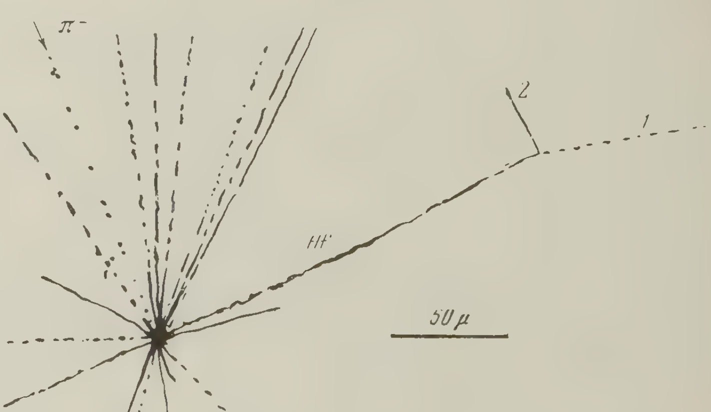

FIG. 8

tron must have been emitted. It is presumed that the decay scheme is either

$$_{\lambda_0}Be^9 \rightarrow H^1 + H^2 + He^4 + 2n,$$

or

$$_{\lambda_0}Be^{10} \rightarrow H^1 + H^2 + He^5 + 2n.$$

Case No. 2711 (Fig. 7). The charge of the hypernucleus is taken to be 2, since along the whole range the track widths lie below the calibrating curve for the α particle. Particle 1 was identified from ionization measurements. The charge of particle 2 cannot be found from width measurements; Z_2 was taken to be 1 on the basis of a comparison between the charges of the hypernucleus and particle 1. Of the three possible decay schemes for λ_0He, we adopt

$$_{\lambda_0}He^5 \rightarrow H^1 + H^3 + n.$$

The value of the binding energy B_{λ_0} found for this decay scheme is the one that lies closest to values quoted in the literature.

Case No. 275 (Fig. 8). The length of the hypernucleus track in this case is 181 μ, and it is but little inclined. Measurements of the track width give the charge with good resolution in Z. The points corresponding to the track widths lie on the calibrating graph near Li. The charge of track 1 is 1, as determined from measurements of the ionization. The charge of the second nucleus is $3 - 1 = 2$. Of all the decay schemes calculated, the most probable one is

$$_{\lambda_0}Li^6 \rightarrow H^1 + He^4 + n$$

This decay scheme gives a binding energy < 8 Mev.

The table below summarizes the cases considered. A characteristic feature of most of these is

Case no.	Primary star	Tracks		Range, μ	Neutron energy, Mev	B_λ Mev
		symbol	particle			
312 (fig. 4)	$11+3\pi$	*Hf*	$_\lambda He^5$	50		~1
		1	H^2	5900		
		2	H^2	3.5*		
		3	n		99	
2711 (fig. 7)	$15+0\pi$	*Hf*	$_\lambda He^5$	77.7		>1
		1	H^1	<15 000		
		2	H^3	16*		
		3	n	—	89	
275 (fig. 8)	$17+0\pi$	*Hf*	$_\lambda Li^6$	181		<8
		1	H^1	>23 000		
		2	He^4	43		
		3	n	—	77	
264 (fig. 1)	$18+3\pi$	*Hf*	$_\lambda Li^8$	87		~5
		1	H^1	9900		
		2	H^3	88		
		3	H^3	22*		
		4	n	—	90	
284 (fig. 6)	$7+0\pi$	*Hf*	$_\lambda Be^9$	28.5		—
		1	H^1	3746		
		2	H^2	2983		
		3	He^4	16*		
		4	$2n$	—	72	
3013 (fig. 2)	$14+0\pi$	*Hf*	$_\lambda B^{10}$	16*		~3
		1	He^4	10*		
		2	H^1	16 500		
		3	H^2	26*		
		4	H^2	47.5		
		5	n	—	72	
3021 (fig. 3)	$12+2\pi$	*Hf*	$_\lambda C^{12}$	94.5		>8
		1	He^1	47		
		2	He^4	48.5		
		3	H^2	135		
		4	H^1	<25 000		
		5	n	—	42	
338 (fig. 5)	$13+0\pi$	*Hf*	$_\lambda C^{12}$	55		~10
		1	Be^9	34		
		2	H^1	821		
		3	H^1	609		
		4	n	—	108	

---

*The indicated mass numbers were assigned on the basis of the adopted decay scheme.

that two nucleons are emitted which carry off most of the energy. This supports the idea that nonmesonic decays of hyperfragments go according to the decay scheme[1]

$$\lambda + N \rightarrow n + N.$$

The fact that in most of the cases one fast proton is emitted gives grounds for supposing that there is a fast neutron among the decay products of the hypernucleus.[2] Hence, most of the nonmesonic decays of hyperfragments which have been described here go according to $\lambda^0 + p \rightarrow n + p$.

H^2, H^3, and He^4 occur among the secondary products of the decay. It is possible that the existence of these particles at the instant of decay is due to an unstable substructure in light nuclei.[3]

The authors would like to thank T. I. Ukolova and S. N. Meleshchenko for their help in making the measurements.

---

[1] Filipkowski, Gierula and Zieliński, Acta Phys. Polon. **16**, 139 (1957).

[2] M. Baldo-Ceolin et al., Nuovo cimento **7**, 328 (1958).

[3] J. Combe, Nuovo cimento Suppl. **3**, 182 (1956).

Translated by R. Krotkov
121

SOVIET PHYSICS JETP VOLUME 37(10), NUMBER 3 MARCH, 1960

SECONDARY STARS CREATED BY THE INTERACTION OF 8.7 Bev PROTONS WITH PHOTOEMULSION NUCLEI

G. B. ZHDANOV, P. K. MARKOV, V. N. STREL' TSOV, M. I. TRET' YAKOVA, CHENG P'U-YING, and M. G. SHAFRANOVA

Joint Institute for Nuclear Research

Submitted to JETP editor March 23, 1959

J. Exptl. Theoret. Phys. (U.S.S.R.) **37**, 611-615 (September, 1959)

The secondary interactions of fast neutrons, protons, and π mesons in a photoemulsion stack bombarded with 8.7-Bev protons were studied. It was found that, on an average, 0.68 ± 0.07 fast neutrons were created in a star. The fast nucleons carried away (55 ± 9)% and the fast π mesons (33 ± 9)% of the energy of the primary particle.

INTRODUCTION

FOR the study of high energy nucleons interacting with nucleons and nuclei, there is a definite interest in the distribution of energy among the secondary nucleons and π mesons. The data in Grigorov's work[1] leads to the result that the average transfer of energy to the fast nucleon after the collision of a 3 — 40 Bev nucleon with a light atom is 70% of the initial value. For the interaction of ~ 9 Bev protons with photoemulsion nuclei, the portion of energy transferred to the fast π's was 20 to 40% of the energy of the primary proton,[2] and the portion transferred to single fast secondary nucleons was equal to (40 ± 20)%.[3]

The goal of our work was to get an estimate of the energy of the fast nucleons and π's formed in the interaction of 8.7 Bev protons with nuclei of the photoemulsion atoms, on the basis of an analysis of the secondary stars.

EXPERIMENTAL ARRANGEMENT

The work was carried out on a stack (composed of 100 emulsion pellicles of the NIKFI-R type) which was bombarded by the inner beam of 8.7 Bev protons in the proton synchrotron of the Joint Institute for Nuclear Research, using an air-driven target introduced into the chamber at the end of each acceleration cycle. The stack was placed in a stainless-steel vacuum container with walls 3 mm thick. The scanning for stars was carried out by areas with a magnification of 300.

The angular half-width of the beam tracks was 0.2°. We counted as secondary stars* those which had no fast-particle track (with ionization $J \leq 1.4 J_0$) forming in the plane of the emulsion an angle from 178° to 180° to the direction of the primary proton tracks.* To determine the stars created by fast secondary neutral and charged particles, we traced the fast particle tracks in 274 secondary stars up to their exit from the stack or until they took part in another star. On the basis of the analysis of these tracings, 677 secondary stars with one or more fast particles were classified in the following way.

1. If at least one of the fast-particle tracks in the star was in the interval 90° — 178° relative to the beam direction, we counted it as formed by a secondary charged particle. The error in estimating such stars was ~ 1%.

2. If the only fast-particle tracks in the star formed angles between 0° and 90°, we counted the star as created by fast neutrons (with energy > 500 Mev). Here the number of stars formed by neutrons, with $n_s = 1$, was overestimated by (18 ± 8)%, in the main on account of the fast secondary charged particles moving in the backward direction.

EXPERIMENTAL RESULTS

The distribution by number of fast particles n_s for stars formed by fast neutrons is given below. The number of stars with $n_s = 1$ was diminished by 18%, corresponding to the results given above. The data for $n_s = 0$ were got by calculation, as shown below.

n_s:	0	1	2	3	4	5	6	Total
Number of stars:	71	83	23	9	2	3	1	192

To estimate the average energy of the fast nucleons, one of the authors (Markov) suggested introducing the relative probability for the appearance of stars with fast-particle numbers $n_s \geq 3$ and $n_s \geq 1$:

---

*The following terminology is used, for brevity: stars formed by protons of the primary beam are called primary; stars formed by particles created in the primary stars are called secondary, and so on.

*By J_0 we always mean the ionization of 8.7-Bev protons.

$$\eta = N\,(n_s \geqslant 3)\,/\,N\,(n_s \geqslant 1).$$

An analysis of the experimental data on the interaction of protons with emulsion nuclei for various energies[3,4] shows that $\eta(E)$ is linearly dependent on the energy in the interval 3 to 9 Bev (Fig. 1),

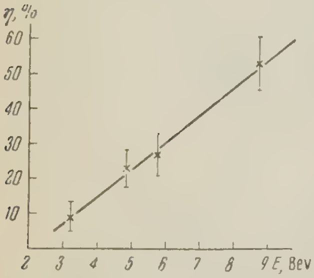

FIG. 1. Dependence of the relative probability η of the appearance of stars with fast-particle numbers $n_s \geqslant 3$ and $n_s \geqslant 1$ on the kinetic energy E of the protons according to references 3 and 4 (the line is drawn by method of least squares).

and this is significant for an estimate of the average energy of secondary particles in a nonmonochromatic spectrum. It is impossible to formulate a similar dependence for the stars formed by neutrons because there are no data corresponding to this in the literature. However, one can suppose that the $\eta(E)$ E dependence for stars formed by protons and neutrons in nuclei is unique, and then one can estimate the average energy by examining the stars formed by neutrons using the E dependence of $\eta(E)$ for stars formed by protons.

From the examined stars formed by neutrons, $\eta = 0.12 \pm 0.03$,* corresponding to (3.7 ± 0.5) Bev. The average energy of the stars formed by neutrons can be determined also by a different method, using the known E dependence of $\overline{n_s(E)}$ for stars formed by protons[5] and analogous to the method used in reference 3 to determine the energy of fast charged particles. It should be noted that this method is not fully independent of the first method. From the n_s distribution of stars created by protons of various energies,[4] one can estimate the portion of stars formed by neutrons with $n_s = 0$ corresponding to an average energy of 3.7 Bev. The answer should be 37%. It is essential here that the percentage of stars with $n_s = 0$ depend linearly on the energy in the 3 – 6 Bev region.[4] Thus the number of stars formed by neutrons should be 192, including stars with $n_s = 0$. The average number of fast particles in a neutron star is $n_s = 0.97 \pm 0.08$, and from this the average energy of neutron stars is obtained as (3.3 ± 0.5) Bev.

It is evident that both estimates agree within the limits of error. We take as the average energy of fast neutrons the average of the energies obtained by the two methods described above, or (3.5 ± 0.5) Bev. The average energy of fast protons will also be taken to be (3.5 ± 0.5) Bev.

By comparing the number of stars created by charged particles with ionization $J \leq 1.4\,J_0$, we can estimate the absolute number of fast neutrons belonging on an average to one star, taking the interaction cross sections of the charged particles and neutrons as equal and independent of the energy. Then for a given geometry the number of secondary stars is proportional to the number of particles created in the primary star. In Fig. 2, the angular distribution of fast charged particles which produced secondary stars is given with and without corrections for ineffective counting of stars in the interval 0° – 5°. The angular distribution of fast charged secondary particles in the range 0° to 90° is also given, from the data in reference 3. To make the two coincide, one must introduce a correction for the geometry for stars formed by fast charged particles coming out at an angle > 20° to the beam direction. After this is done, it turns out that 857 stars from fast charged particles correspond to 192 stars formed by neutrons. Their distribution according to multiplicity is given in the table.

FIG. 2. Angular distribution of fast charged particles: a – originating in primary stars according to reference 3, b – generating observed secondary stars, c – generating secondary stars taking into account corrections for the gap 0°–5°.

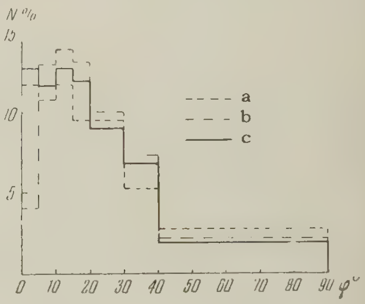

In view of the fact that the average energy of the neutrons producing the observed stars is large, one must suppose that only an insignificant percentage of these neutrons can come out at angles > 20° to the primary proton beam direction. Therefore no geometrical corrections were made for stars formed by neutrons. For angles between 0° and 90° an average of 3.03 fast charged particles[3] were emitted for each primary star. So the average number of fast neutrons per star was equal to

$$192 \cdot 3.03\,/\,857 = 0.68 \pm 0.07.$$

Assuming that the proton-nucleus interaction creates an equal number of fast protons and neu-

---

*Everywhere in this paper, only the statistical error is shown.

Distribution by n_s of stars formed by charged particles with ionization $J \le 1.4 J_0$ at angles of flight $0° - 90°$ to the beam direction

n_s	0	1	2	3	4	5	Total
Number of stars (after introducing corrections)	499*	240	85	24	5	4	857
Experimentally observed number of stars	266	201	64	18	5	2	556

*Stars with $n_s = 0$ were not counted on the entire area. After introducing corrections, their number was 499.

trons* (whose average energy was estimated above) we find that the average energy taken away from a star by the fast particles is (4.8 ± 0.8) Bev, that is, (55 ± 9)% of the energy of the primary proton.

It should be noted that if $\bar{n}_s(E)$ has a smaller value for stars formed by neutrons than for those formed by protons, this circumstance leads to an underestimate of the nucleon energy, as determined by the two methods given above. However, in this same case an additional number of neutron-created stars with $n_s = 0$ involves overestimates, so that the average energy taken away by the nucleons is not essentially changed. Thus, for example, if the energy of the neutrons were underestimated by 1 Bev, the energy carried away by the fast nucleons makes up on the average (63 ± 9)% of the energy of the primary proton.

Knowing the average energy taken away by the fast nucleons and also the average nuclear dissociation energy, equal to (1.0 ± 0.1) Bev per star in agreement with reference 3, it is possible to estimate the average total energy of fast π mesons. It turns out to be (2.9 ± 0.8) Bev per star or (33 ± 9)% of the primary proton energy. Within the limits of statistical error, this value coincides with the results obtained in reference 2.

From reference 3 it is known that the average number of fast charged particles per star is 3.2. If there are 0.68 fast protons to a star, then we get 3.8 ± 0.3 fast π mesons. From this it follows that the average total energy of the pions is (0.8 ± 0.2) Bev.

The methods described so far, of estimating the energy of secondary particles were founded on the determination of the number of particles in the stars they created. Along with this, we measured the angles of flight of the fast particles for stars having $n_s \ge 2$, both relative to the direction of the primary proton beam and to the direction of the generating particle, if the latter was charged. The basic problem in these measurements was in separating the stars created by high energy nucleons and mesons, since in this last case the angular distributions were significantly wider.*

To perform the indicated task it is expedient to assign to each star one angular characteristic, for example, the average flight angle $\bar{\theta}$ of fast particles relative to the primary protons. We could verify here that in the case of the stars from charged particles these average characteristics as a rule changed little in changing over to reading all angles with the direction of the generating particle. In Fig. 3 the distributions by angular characteristics are shown for secondary stars created by neutrons (a) and by fast charged particles making angles ≦ 10° (b) and > 10° (c) to the primary beam.

Even in a cursory comparison of Figs 3a, 3b, and 3c it is evident that stars with average emission angles $\bar{\theta} > 60°$ for fast particles are very rare in group a, somewhat more common in group b, and even more common in group c. Approximate calculations show that the bounding value of the angle $\bar{\theta}$, 60°, roughly corresponds to the transition from stars formed by nucleons to stars formed by π mesons.

A more detailed analysis of Fig. 3 gives the following results:

1. The ratio of the number of fast protons to the number of fast neutrons does not significantly exceed unity.

---

*Thus, for example, there are grounds for supposing that asymmetry between protons and neutrons would show up at the very first in the secondary particles emitted at small angles to the direction of the primary. A subsequent analysis of the angular distributions in the stars we studied showed that the ratio of the numbers of such particles, created by neutral and charged nucleons, could differ from unity by no more than 30%. We got an analogous result on the small deviation from proton-neutron symmetry in the analysis of Fig. 3 below.

*This was due, first, to the lower (average) energies of the mesons in comparison with nucleons and, second, to the velocity being smaller in the center of mass system (of the stationary and incident systems) for equal energies of mesons and nucleons.

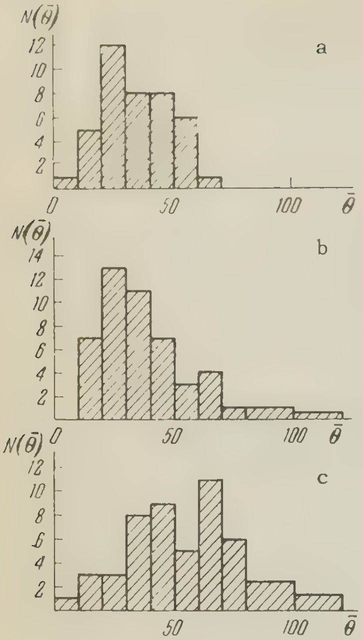

FIG. 3. Distribution of particles by average angle of flight $\bar\theta$ for secondary stars: a – formed by neutrons, b – formed by fast charged particles moving at angles $\phi \lesssim 10°$, and c – at $\phi > 10°$, relative to the primary beam.

2. The ratio of the number of protons and mesons among the particles forming stars with $n_s \geq 2$ is 1.5 to 2, which is evidenced by the significantly higher average energy of protons in comparison with mesons.

3. Among the secondary particles, moving away at angles $\leq 10°$ to the direction of the primary protons, ~ 80% are nucleons.

CONCLUSIONS

The following results were obtained in the work:

1. For the interaction of an 8.7 Bev proton with nuclei of the emulsion atoms, there is an average of (0.68 ± 0.07) fast (with energy > 500 Mev) neutron per star, with average energy (3.5 ± 0.5) Bev.

2. Under the assumption that the number of fast protons and neutrons (calculated for one star) and their average energy are equal, fast nucleons carry away (55 ± 9)% of the energy of the primary particle.

3. The average number of fast (with energy > 80 Mev) π mesons, neutrals included, emitted in one interaction is 3.8 ± 0.3. Their average total energy is (0.8 ± 0.2) Bev.

4. An analysis of the angular distributions of fast tertiary charged particles in secondary stars testifies that ~ 80% of the secondary particles moving at an angle ≤ 10° to the direction of the primary protons are nucleons.

The authors thank M. Ya. Danysh, M. I. Podgoretskiĭ, and I. L. Rozental' for their discussion of a number of questions, and also to the group of workers taking part in the measurements and photoemulsion scanning.

---

[1] N. L. Grigorov, Usp. Fiz. Nauk **58**, 499 (1956).

[2] Bayatyan, Gramenitskiĭ, Nomofilov, Podgoretskiĭ, and Skrzypczak, JETP **36**, 690 (1959), Soviet Phys. JETP **9**, 483 (1959).

[3] Belyakov, Shu-fan, Glagolev, Alkhazhov, Kirillova, Markov, Lebedev, Tolstov, Tzyganov, Shafranova, and Tsyng-se, Proceedings, Annual International Conference on High Energy Physics at CERN, Geneva (1958), pp 309-318.

[4] W. R. Johnson, Phys. Rev. **99**, 1049 (1955).

[5] Bogachev, Shu-fan, Gramenitskiĭ, Kirillova, Lebedev, Lyubimov, Markov, Merekov, Podgoretskiĭ, Sidorov, Tolstov, and Shafranova, Атомная энергия (Atomic Energy) **4**, 281 (1958).

Translated by W. Ramsay
122

SOVIET PHYSICS JETP VOLUME 37(10), NUMBER 3 MARCH, 1960

ON THE MAGNETIZATION PROCESS IN FERROMAGNETS

L. V. KIRENSKIĬ, M. K. SAVCHENKO, and I. F. DEGTYAREV

Physics Institute of the Siberian Division, Academy of Sciences, U.S.S.R.

Submitted to JETP editor March 31, 1959

J. Exptl. Theoret. Phys. (U.S.S.R.) **37**, 616-619 (September, 1959)

The dynamics of the domain structure during magnetization were studied in crystals of silicon iron containing 3% silicon, using the powder figure method and the magneto-optical Kerr effect. It is shown that magnetization is achieved in the general case by the following processes: displacement of the domain walls, rearrangement of the domain structure, rotation of the magnetization vector in the direction of the field, and the paraprocess. The rotation process terminates technical magnetization; the process of boundary displacement precedes the rearrangement of the domain structure and completes it.

INTRODUCTION

IN the absence of a magnetic field, according to contemporary ideas, a ferromagnetic crystal is divided into separate regions of spontaneous magnetization — domains. The domains are separated from one another by a bounding layer of thickness $0.6 - 0.9\,\mu$.[1] The domain configuration in a given crystal is determined from the minimization of its free energy.[2] The domain structure is adequately revealed by the method of powder figures,[3] and the domain configurations obtained in experiments are very close to those required by the theory.

The magnetization of a ferromagnet, according to contemporary views,[4] is composed of the process of boundary displacement, the rotation process and the paraprocess. The process of boundary displacement can be both reversible and irreversible. During irreversible boundary displacement uneven changes of the magnetization occur — the Barkhausen jumps.

On the completion of the displacement process the crystal is magnetized to saturation as a whole along one of the axes of easy magnetization closest to the direction of the field; the rotation process is considered complete when the magnetization vector is parallel to the field vector.

The processes of boundary displacement and rotation partially overlap in some comparatively small portion of the technical part of the magnetization curve.

The processes of boundary displacement and rotation undoubtedly occur and can be easily revealed by motion pictures of powder figures.[5] The paraprocess is observed in strong fields and is completely irreversible.

If the process of magnetization does, in fact, take place as described above, then when studying the Barkhausen effect in a single crystal disc with positive anisotropy constant — the disc being cut in a plane of the type (110) — the following picture should apply.

Since the domain structure of such a crystal consists of plane-parallel domains magnetized along and in the opposite direction to the [001] axis lying in the plane of the disc, then a Barkhausen jump will correspond only to a portion of the ferromagnet, the magnetic moment of which undergoes an irreversible rotation through 180°.

Therefore, a measuring coil detecting the Barkhausen jumps detects such a jump completely if the axis of the coil coincides with the [001] direction and only partially for any other direction. Since an apparatus for studying Barkhausen jumps detects only those above a certain size, then the maximum number of jumps should be detected in the direction of the easy axis, while in a direction normal to this axis no jumps should in general be detected by the coil.

It is essential to dispose the detecting coil accurately, but not the direction of the magnetizing field. For the latter it is important that the component along the axis of easy magnetization be different from zero.

However, detailed studies of the Barkhausen effect lead to directly contrary results.[6] The maximum number of jumps appears in the [110] direction, perpendicular to the axis of easy magnetization. In the direction of easy magnetization the number of jumps is a minimum.

The experimental fact given above cannot be explained by assuming that the mechanism of the jumps is an irreversible displacement of part of the boundary held up somewhere at magnetic inhomogeneities in the crystal. Also, the maximum number of jumps corresponds approximately to the maximum value of the magnetic permeability, which for a uniformly increasing magnetic field should depend only on the speed of displacement of the boundaries between domains, because only in these places in a ferromagnetic single crystal is the magnetic permeability essentially greater than unity — being close to it anywhere inside the domains.

However, direct measurement of the speed of boundary motion in a uniformly increasing field shows that the maximum speed of boundary motion corresponds to the initial portion of the magnetization curve,[5] which does not as a rule correspond with the maximum magnetic permeability.

The said divergences of some of the experimental data from the theoretical scheme of magnetization show that experiments should be made aimed at finding more precisely the mechanism of the magnetization process in ferromagnets.

EXPERIMENTAL ARRANGEMENT

The investigation was carried out on crystals of silicon iron with 3% silicon content. The specimens were cut in the form of plates 30 x 6 mm or discs of diameter 20 mm. The specimen thicknesses were 0.3 mm or less. The specimen surfaces coincided with the (110) planes or were close to them. In the plates the long side coincided with the [001] direction. The specimens were annealed in vacuum for two to three hours at a temperature of 1000°C, were subsequently cooled slowly in the furnace, and then polished electrolytically.

The change of the domain structure of the specimens in a magnetic field of increasing strength was studied by the powder-figure method and the method of meridional magneto-optical Kerr effect.[7] For visual observations and photography of the domain structure by the magneto-optical method, the specimens were coated with a uniform layer of iron oxide.[7] The domain structure was studied by the powder method simultaneously on opposite surfaces of

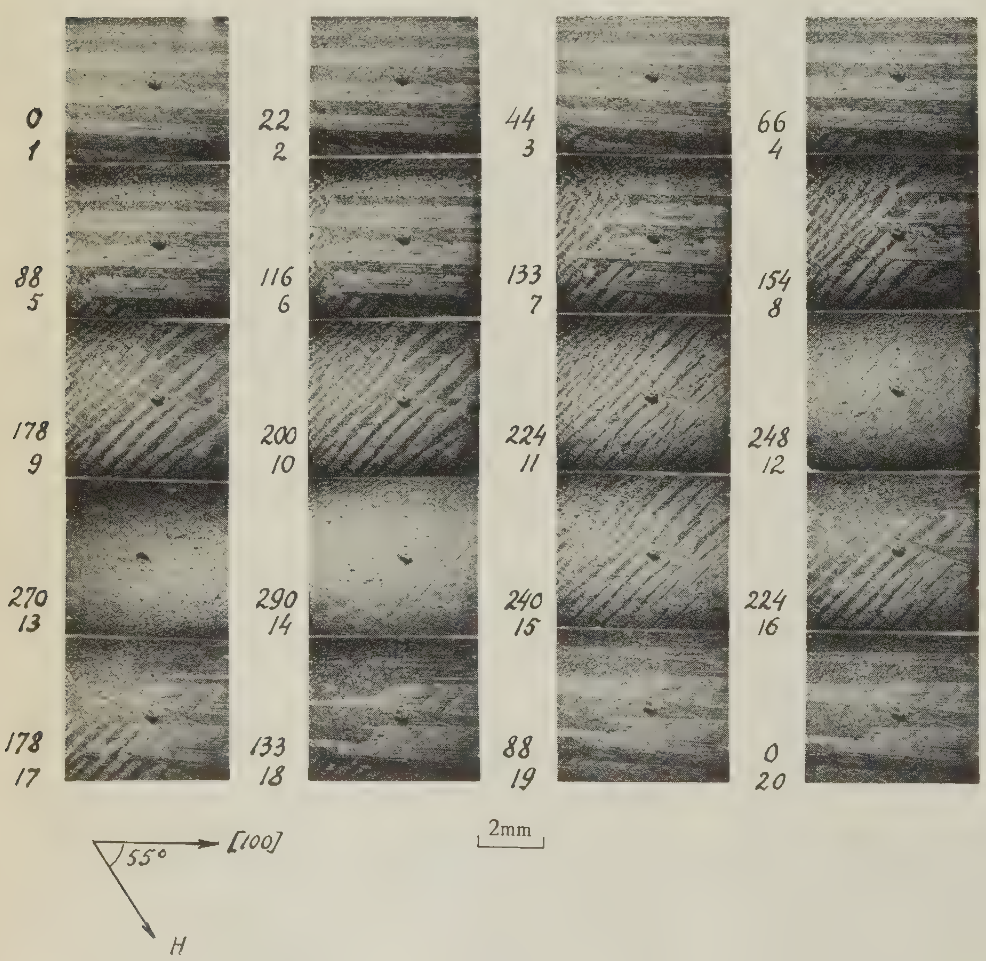

FIG. 1. Dynamics of the domain structure in a changing magnetic field inclined at an angle of 55° to the axis of easy magnetization. Numbers on the left: values of the external field in oe; below them, serial numbers of the frames.

a specimen. The observations were made using two MIM-6 microscopes, arranged vertically with objectives pointing towards each other, so that the optical axes of the microscopes coincided accurately.

OBSERVATIONAL RESULTS AND THEIR ANALYSIS

Magneto-optical observations: Using a specimen in the form of a disc of diameter 20 mm and thickness 0.3 mm, observations were made on the dynamics of the domain structure during magnetization along different directions in the plane of the specimen. For magnetization in the easy direction only displacements of the 180° boundaries were observed. In Fig. 1 the change of domain structure is shown during magnetization of the same specimen at an angle of 55° to the easy axis. With no field the original appearance is of parallel dark and light strips, which correspond to domains magnetized along and opposite to the [001] axis (Fig. 1, Frame 1). Apart from the main features, small wedges are seen, showing that the surface of the specimen has a small inclination to a crystallographic plane of the type (110). In fields less than 100 oe, widening of the light strips is mainly observed (Fig. 1, Frames 2 — 5). In fields of 100 — 200 oe, rearrangement of the domain structure occurs (Fig. 1, Frames 6 — 10). By visual observation of this rearrangement, its clearly pronounced erratic nature was apparent.

With further growth of the field up to 300 oe the displacement of the domain walls of the newly

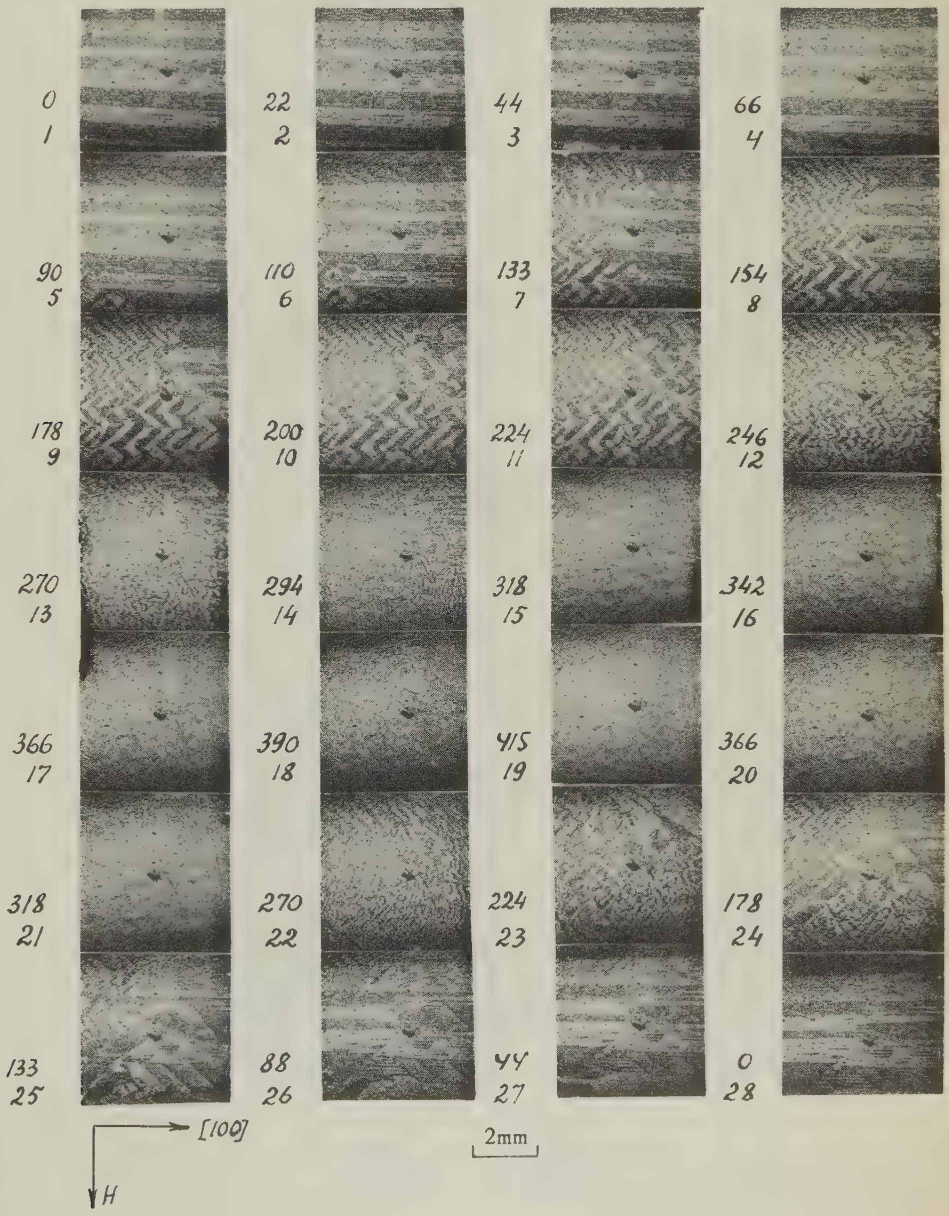

FIG. 2. Dynamics of the domain structure in a changing magnetic field directed along an axis of the type [110] perpendicular to the axis of easy magnetization. Numbers on the left: values of the external field in oe, and below them serial numbers of the frames.

formed structure is observed (Fig. 1, Frames 11 – 14).

In fields above 300 oe no structure is observed, since technical saturation has been reached. On diminishing the value of the field the process takes place in the reverse order (Fig. 1, Frames 15 – 20). The domain walls observed at the end are considerably distorted (Fig. 1, Frame 20). After demagnetization by an alternating field, the domain structure returns again to the original.

Similar changes of the domain structure are also observed during magnetization along other different angles – greater than 30° – to the easy axis. A typical feature of the structures arising due to rearrangement is that the direction of the dark and light strips in them is perpendicular to the difficult axis closest to the magnetic field vector. Thus, on changing the angle between the vector **H** and the [001] direction from 0 to 360°, new structures can be observed with only two directions of the strips, perpendicular to the two axes of difficult magnetization lying in the plane of the specimen.

A considerably more complicated rearrangement of the domain structure is observed during magnetization at an angle of 90° to the easy axis, i.e. along the [110] direction. The results of these observations are given in Fig. 2. On applying the magnetic field the process of boundary displacement is hardly noticeable (Fig. 2, Frames 1 – 4). In fields from 90 to 200 oe, rearrangement of the domain

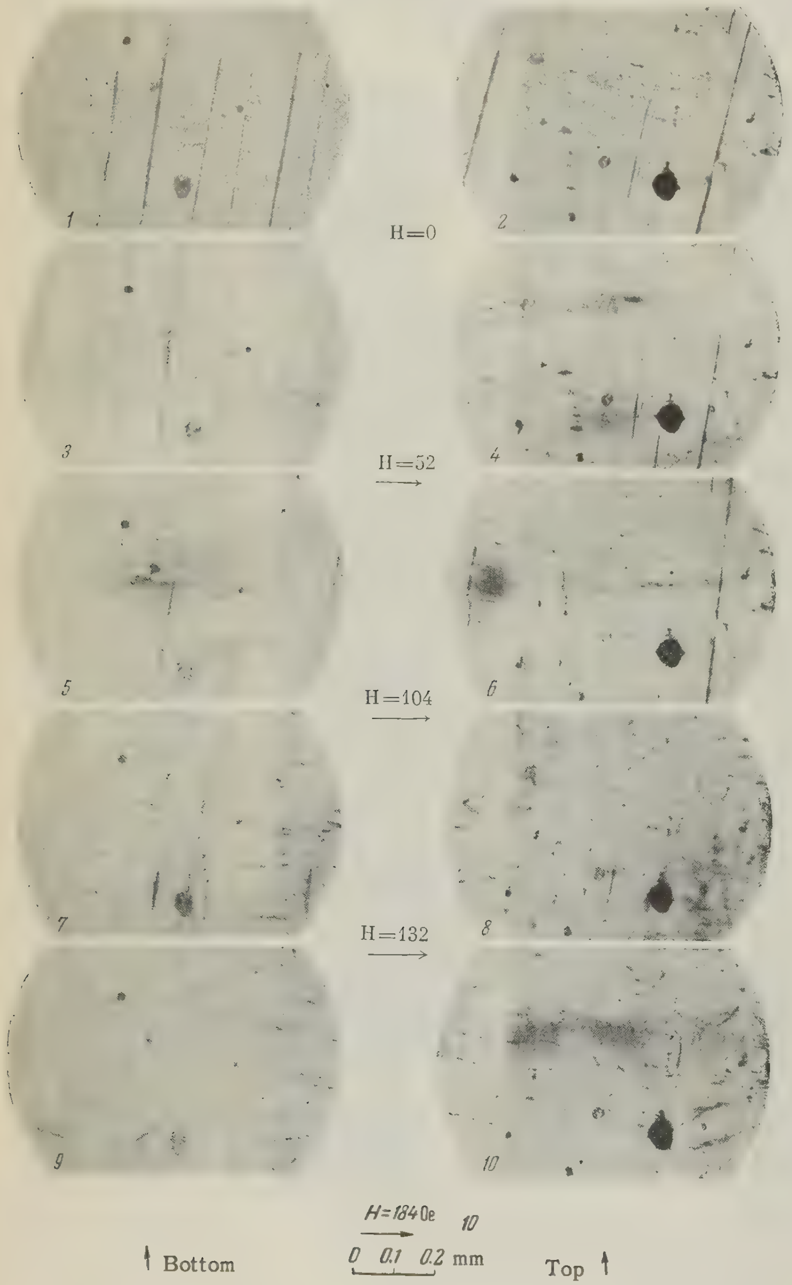

FIG. 3. Dynamics of the domain structure on opposite sides of a crystal in an increasing magnetic field. The domain structure does not penetrate the crystal.

structure takes place. Structures arise consisting of broken strips (Fig. 2, Frames 5 — 10). In this case both directions, characterising structures of this kind, appear simultaneously. With further increase of the field, sub-division into smaller domains takes place and the figures take the form of fine winding strips with preferential direction along the [110] axis, i.e., along the field (Fig. 2, Frames 11 — 19). On reducing the field the process takes place in the reverse order, but the characteristic directions are less clearly displayed (Fig. 2, Frames 20 — 28). As is seen from this figure and also from visual observations, throughout the entire process of magnetization in fields up to 400 oe boundary displacement is not observed, and the rearrangement of the structure which occurs takes place in the form of jumps during which separate volumes of the specimens reverse their magnetization.

It is apparent that such sharp structure changes are caused by major changes of the domain structure inside the crystal.

Similar changes of domain structure were observed by the magneto-optical method on several specimens. On specimens of thickness 200 — 400 μ the rearrangement of domain structure already described was, as a rule, observed. On specimens of thickness 100 μ and less, such complicated changes of structure were not often observed, and displacement of the boundaries of the original figures predominated; only during magnetization in a direction close to an axis of the type [110] did new structures arise in the form of fine winding lines oriented along the [110] axis.*

Powder-figure observations: In Fig. 3 are shown powder-figures taken on opposite sides of the same crystal. As is seen from this figure, the domain structure does not go right through and undergoes a significant change inside the crystal. On the upper surface the entire width of one domain and parts of two others are seen, whereas on the lower surface are seen a large number of parallel domains of approximately equal thickness. On increasing the field (directed horizontally) the structures also change in different fashions. The structure on the upper surface is almost unchanged up to a field of 100 oe; then destruction of the domains commences, and finally in very strong fields a new structure appears. On the lower surface boundary displacement is more clearly observed, which is broken up in the end by rearrangement of the domain structure.

It is interesting to remark that the domains that were getting smaller as the field increased directly before the rearrangement of the entire domain structure, increased somewhat in volume and were then destroyed.

Thus, the magnetization process in a ferromagnetic crystal is not restricted to the processes of boundary displacement, rotation and the paraprocess. The process of domain structure rearrangement plays an important role in the magnetization process; it is accompanied by a large number of Barkhausen jumps and corresponds to the maximum magnetic permeability.

---

*The changes of domain structure described are observed most clearly on looking through the motion-picture films taken during the work on the magneto-optical effect.

[1] L. V. Kirenskiĭ and V. V. Veter, JETP **35**, 819 (1958), Soviet Phys. JETP **8**, 568 (1959).

[2] L. D. Landau and E. M. Lifshitz, Sow. Phys. **8**, 153 (1935).

[3] F. Bitter, Phys. Rev. **38**, 1903 (1931); N. S. Akulov and M. V. Dehtjar, Ann. physik, 750 (1932).

[4] S. V. Vonsovskiĭ and Ya. S. Shur, Ферромагнетизм (Ferromagnetism) Gostekhnizdat (1948); R. Bozorth, Ferromagnetism, Van Nostrand, N. Y., 1951.

[5] L. V. Kirenskiĭ and V. D. Dylgerov, Физика металлов и металловедение (Physics of Metals and Metal Research) **3**, 216 (1956); Kirenskiĭ, Dylgerov, and Savchenko, Izv. Akad. Nauk SSSR, Ser. Fiz. **21**, 1168 (1957), Columbia Tech. Transl. p. 1157.

[6] Ivlev, Il'yushenko, and Aseeva, Izv. Akad. Nauk SSSR, Ser. Fiz. **21**, 1250 (1957), Columbia Tech. Transl. p. 1239.

[7] L. V. Kirenskiĭ and I. F. Degtyarev, JETP **35**, 584 (1958), Soviet Phys. JETP **8**, 403 (1959).

Translated by K. F. Hulme
123

NUCLEAR INTERACTIONS OF 8.7-Bev PROTONS IN PHOTOGRAPHIC EMULSIONS

G. B. ZHDANOV, V. M. MAKSIMENKO, M. I. TRET' YAKOVA, and M. N. SHCHERBAKOVA

P. N. Lebedev Physics Institute, Academy of Sciences, U.S.S.R.

Submitted to JETP editor April 4, 1959

J. Exptl. Theoret. Phys. (U.S.S.R.) 37, 620-633 (September, 1959)

Inelastic interactions of 8.7-Bev protons with photoemulsion nuclei were studied and, in particular, the interaction cross section, multiple production of particles and their angular distribution. From comparison with calculations based on the statistical theory, some conclusions are drawn concerning the existence of interactions of peripheral (nucleon-nucleon) type, as well as the role of secondary interactions inside the complex nucleus.

THIS work was carried out with a small part of one of the photo-emulsion stacks irradiated with the primary 8.7-Bev proton beam inside the accelerating chamber of the proton synchrotron of the Joint Institute for Nuclear Research.*

Photoemulsion layers of type NIKFI-R and thickness ~ 450 μ were exposed without backing, and had a track-density of 27 – 30 grains per 100 μ for relativistic particles. Scanning along the track of the primary particles was carried out with 630-fold magnification. In all, about 25,000 tracks with total length ~ 300 m were scanned.

1. INELASTIC INTERACTION CROSS SECTION

The method of scanning along the tracks of the proton beam was almost 100% efficient in finding interactions, even in the case where the interaction resulted in the proton being deflected through an angle of 2° and greater without emission of any other charged particles.

The desired mean free path λ for interaction with photoemulsion nuclei was determined in the way usually done when this method is used.

In Table I we give the corresponding λ's for two types of interactions, star production and "pure" scattering (for angles greater than 5° and between 1° and 5°).† In the latter case, corrections were introduced for the efficiency of measuring similar scatterings and were determined by comparing the angular distributions in the plane of the photo-emulsion and in the perpendicular direction.

TABLE I

Type of Interaction	λ cm
Star production	35.0±1.3
Scattering through angles $\theta_l > 5°$	1750±500
Scattering through angles $1° \leqslant \theta_l \leqslant 5°$, without correction	750±150
The same, with correction for counting efficiency	500±100

The value of λ for the totality of interactions indicated in lines 1 and 2 of Table I do not differ, within the limits of experimental error, from results in the literature,[1,2] nor does the mean free path for star formation differ from results obtained for protons of energy 1 to 6 Bev.[3-5] However, to obtain the mean free path characterizing the inelastic interactions of protons with nuclei as usually defined, one must include all interactions other than elastic.

For protons of a given energy, this task reduces basically to taking account of processes of diffraction scattering by the various nuclei of the photoemulsion, in which a few (not more than three) particles are "boiled off." This can be seen, in particular, from Table II, where we show our distributions with angle θ_l of a single fast particle undergoing two types of interaction:* "pure" scattering without production of visible stars and stars of the type $n_s = 1$, $n_g = 0$, $n_b = 1 - 3$. Table II shows that, within the limits of statistical error,

---

*The error in energy determination was less than 5%.

†In Table I and the following, θ_l denotes the angle of deflection of a fast particle relative to the direction of the primary beam, the half-width of which constituted ± 0.2°. The analogous angle in the center-of-mass (c.m.) system is denoted by θ_0.

*We employ the following nomenclature for the number of particles with different ionizing powers: n_s corresponds to ionization $J \leqslant 1.5J_{min}$, n_g to $J = (1.5-5)J_{min}$, n_b to $J > 5J_{min}$. The boundary between "grey" and "black" tracks was less definite (tracks were separated visually) and corresponded, on the average, to an energy somewhat larger than the 30 Mev usually employed for protons.

TABLE II. Angular distributions for interactions of type $n_b = n_g = 0$, $n_s = 1$ (scattering) and type $n_s = 1$, $n_g = 0$, $n_b = 1 - 3$ (stars)*

θ_l, degrees	<1	1–2	2–3	3–4	4–5	5–10	10–30	>30	Total number of cases
$n_g = n_b = 0$	—	13	9	8	1	5	8	2	46
$n_g = 0$, $n_b = 1-3$	2	7	12	13	1	8	10	7	60

*Scatterings with angles <1° were not counted. Cases with angles 2, 3° etc. were included in columns 2–3°, 3–4°, respectively, etc.

the angular distributions for both types of interaction were the same.

Cronin, Cool, and Abashian[6] give theoretical angular distributions for light (C) and heavy (Pb) nuclei for an incident of momentum of 0.95 Bev/c and for various assumptions about the form factors of these nuclei. By extrapolating the data of these authors to momenta ~ 10 Bev, it is easy to see that the great majority (not less than 95%) of the cases of diffraction scattering by photoemulsion nuclei go through angles θ_l less than 1 – 1.5°. From these considerations, we believe it possible to include as diffraction scattering all interactions satisfying the following two conditions

a) $n_s = 1, \quad n_g = 0, \quad n_b \leqslant n_{b_0} = 3;$
b) $\theta_l < \theta_0 = 2°$.

The resulting value for the mean free path λ for inelastic interactions with photoemulsion nuclei, taking into account errors connected both with statistical fluctuations and with the uncertainty of how to take the diffraction scattering into account, is $\lambda_{\text{inel}} = 34 \pm 2$ cm.

In so far as the total geometrical cross section for all photoemulsion nuclei, determined from the relation $\sigma_{\text{geom}} = \pi\,(1.38 \times 10^{-13}\,\text{cm})^2 A^{2/3}$, corresponds to a mean free path $\lambda_{\text{geom}} \cong 27$ cm, the value for λ_{inel} obtained above means that the so-called transparency of the photoemulsion nuclei is, on the average, 20%.

2. DISTRIBUTION ACCORDING TO THE NUMBERS OF FAST AND SLOW PARTICLES

The number of interactions which can be interpreted as pure charge exchange, the incident proton going into a neutron without appreciable loss of energy, is very small; of 520 stars, there were only 17 cases of type $n_s = 0$, corresponding to a cross section of only 3% of the cross section for inelastic interaction with photoemulsion nuclei. In these 17 cases, the charge exchange was, apparently, sometimes accompanied by production of neutral mesons.

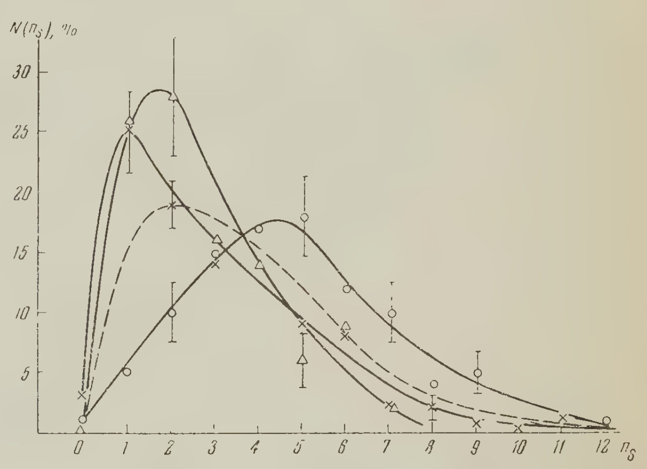

FIG. 1. Distribution of interactions of various types with respect to the number of fast particles n_s: Δ – $n_b = 0$ to 2, $n_g = 0$, $\bar{n}_s = 3.0 \pm 0.15$; × – $n_b = 3$ to 8, $n_g = 0$ or $1 \leqslant n_b + n_g \leqslant 8$, $n_g > 0$, $\bar{n}_s = 3.1 \pm 0.1$; ○ – $n_b + n_g \geqslant 9$, $\bar{n}_s = 4.8 + 0.15$. The dashed curve is the distribution summed over all stars, $\bar{n}_s = 3.7 \pm 0.05$.

In Figs. 1 – 3 we give the distribution of stars with number of fast particles n_s, and with number of slow particles n_b and n_g for interactions of different types. From these distributions, the presence of a rather noticeable correlation between the values of any two quantities of the three quantities (n_b, n_g, n_s) is evident. Calculation of the corresponding coefficients of pairwise correlation* k leads to the following values

$$k\,(n_b,\ n_g) = 0.60; \quad k\,(n_b,\ n_s) = 0.42;$$
$$k\,(n_g,\ n_s) = 0.35.$$

From consideration of Figs. 1 – 3 it also follows that the character of the distribution with number of particles, selected for a large number of fast ($n_s \geq 7$) or slow ($n_g > 1$ and $n_b > 8$) particles differs essentially from the mean distributions. An analogous conclusion, as will be shown below, follows from consideration of the angular

---

*The correlation coefficients were determined by the usual formula $k(x, y) = (\overline{xy} - \bar{x}\bar{y})[D(x)D(y)]^{-1/2}$, where D is the dispersion of the quantities x and y.

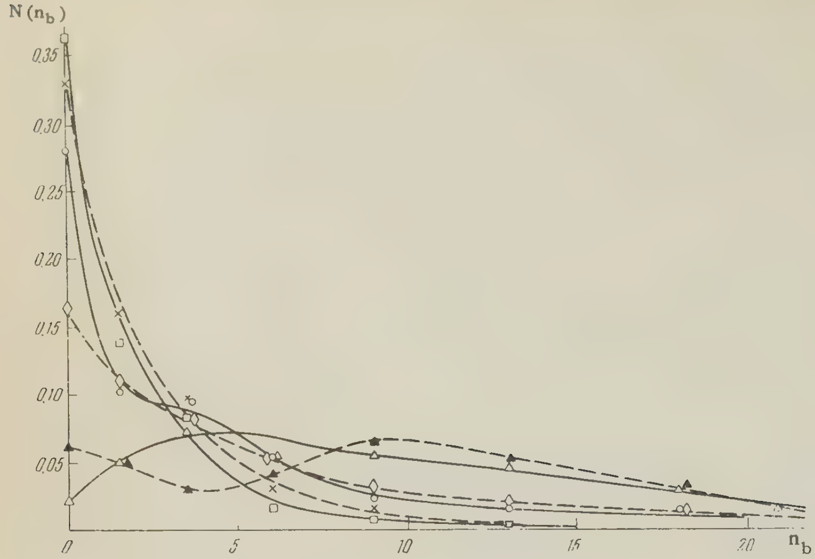

FIG. 2. Distribution of interactions of various types with number of black tracks n_b: □ – $n_g = 0$, ○ – $n_g = 1$, Δ – $n_g > 1$, × – $n_s = 1(0)$, ◇ – $n_s = 2-6$, ▲ – $n_s \geqslant 7$.

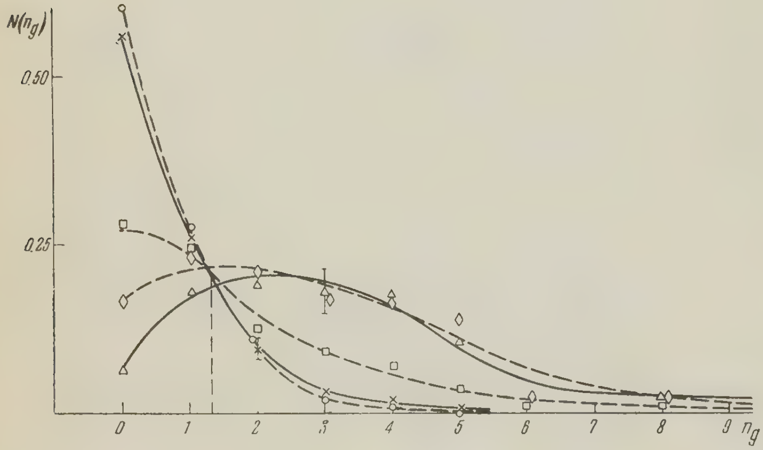

FIG. 3. Distribution of interactions of various types with number of grey tracks n_g: × – $n_b + n_g \leqslant 8$, Δ – $n_b + n_g > 8$, ○ – $n_s = 1(0)$, □ – $n_s = 2-6$, ◇ – $n_s \geqslant 7$.

distributions of fast particles. On the other hand, a large part of the interactions selected by their small number of fast and slow particles, differs in angular distribution but little from nucleon-nucleon ones.

3. ANGULAR DISTRIBUTION OF FAST AND SLOW PARTICLES

Determination of the spatial angles θ_l for relativistic particles and grey tracks was carried out, as a rule, from two angles θ_1 and θ_2, projections of the angle θ_l on the plane of the photoemulsion and on the plane perpendicular to it, going through the track of the primary proton. The angles were determined accurate to 1 – 2°.

In Figs. 4 – 6 the integrated angular distributions of relativistic particles are given for stars, divided into groups in dependence on the numbers n_s (Fig. 4), n_b (Fig. 5) or n_g (Fig. 6). To construct the curve for the case $n_s = 1$ in Fig. 4, corrections for the case of diffraction scattering of primary protons on nuclei were introduced.

We calculated the theoretically expected angular distribution of relativistic particles (given in Figs. 4 – 6) in nucleon-nucleon interactions for isotropic emission of charged particles in the c.m. system of the two colliding nucleons and for the momentum distribution predicted by the statistical theory (see Figs. 7a and 7b). In addition to this, analogous angular distributions were obtained under the assumption of collisions in a "tube" of nuclear matter consisting of two and four nucleons.*

As can be seen from Fig. 4, and especially from Figs. 5 and 6, there is a rather large group of interactions for which the angular distribution of fast particles is, apparently, somewhat broader than in the case of "pure" interaction with the maximum (with respect to length) possible "tube" of nuclear matter in the photoemulsion. In these same interactions, a very large number of slow particles are emitted on the average. This number is signifi-

---

*Angular distributions for the case of a tube of two nucleons are not given on Figs. 4-6 because of lack of space.

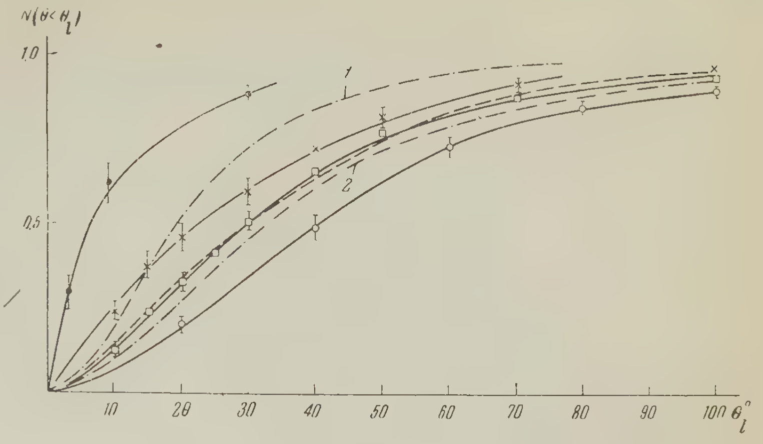

FIG. 4. Integral angular distributions of relativistic particles in stars with various numbers n_s (W is the proportion of stars of given n_s among the total number of stars): ● – $n_s = 1$ (W ≈ 20%), × – $n_s = 2,3$ (W = 32%), □ – $n_s = 4$–6 (W = 34%), ○ – $n_s \geqslant 7$ (W = 11%). The dashed curve shows the summed distribution. The dashed-dotted curves give the angular distributions calculated from the statistical theory for the interaction of the primary proton with one (1) and four (2) nucleons of the nucleus, simultaneously.

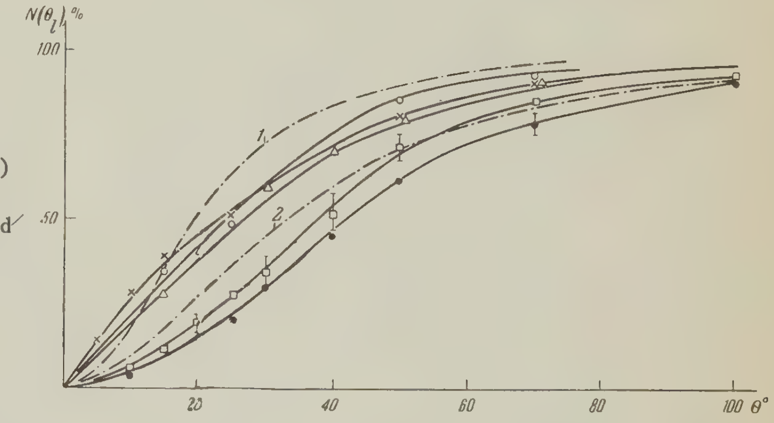

FIG. 5. Integral angular distributions of relativistic particles in stars with various numbers n_b (W is the proportion of stars with given n_b): ○ – $n_b = 0$ (W = 11%) × – $n_b = 1$–3 (W = 35%), Δ – $n_b = 4$–8 (W = 30%), □ – $n_b = 9$–12 (W = 12%), ● – $n_b \geqslant 13$ (W = 12%). The dashed dotted curves are calculated for cases of interaction with one (1) or four (2) nucleons.

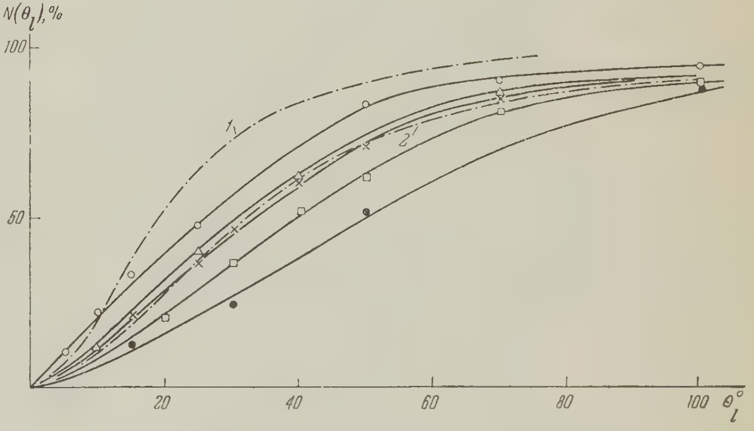

FIG. 6. Integral angular distribution of relativistic particles in stars with various numbers n_g (W is the proportion of stars with given n_g): ○ – $n_g = 0$ (W=46%), Δ – $n_g = 1$ (W = 24%), × – $n_g = 2, 3$ (W = 20%), □ – $n_g = 4$–6 (W = 8%), ● – $n_g \geqslant 7$ (W = 2%). Curves 1 and 2 are calculated for the cases of one and four nucleons, respectively.

cantly larger than in stars of higher energy ($\geq 10^{12}$ ev).

The angular distribution of grey tracks is given on Fig. 8. It can be seen from this figure that the distribution is almost the same in stars of different types and is practically independent of the energy of the particle. In addition, it practically coincides with the angular distributions of strongly ionizing particles from interactions of 1.5-Bev π mesons[7] with photoemulsion nuclei.

Calculations show that if the first interaction of the incident nucleon is with "tubes" of nuclear matter of various dimensions, the total number of grey tracks should be, on the average, significantly less (at most, two), and their angular distribution essentially narrower, than observed in the experiment. This discrepancy, in our view, can be explained only by taking into account the secondary interactions inside the nucleus of the π mesons produced. In addition, a special kinematical analysis demonstrated that even in the cases where there was only one grey track, the corresponding slow proton could not, as a rule, be considered as a recoil from a primary nucleon-

TABLE III. Dependence of the width of the angular distributions on the number of particles n_s produced

	n_s	1	2,3	4—6	7—9	≥10
Experiment	$\theta_{1/2}$	~7°*	23°	30°	39°	47°
	$\cot\theta_{1/2}$	~8*	2.35	1.73	1.23	0.93
Calculation	$\cot\theta_{1/2}$	3.0	2.15	1.67	1.4	1.15
	l	1	2	3	4	6

*The values of $\theta_{1/2}$ and cot $\theta_{1/2}$ are those obtained after introducing corrections for diffraction scattering.

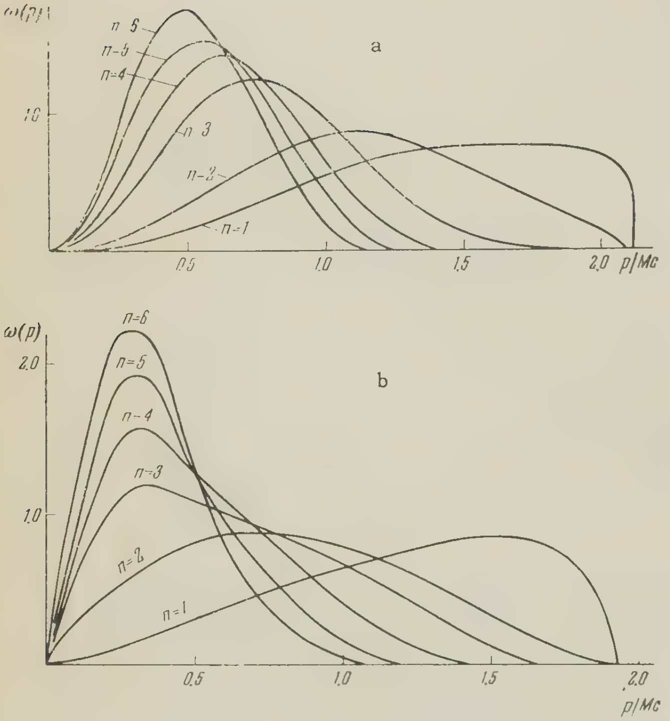

FIG. 7. Momentum spectra of particles in 8.5-Bev nucleon-nucleon interactions according to the statistical theory: a – nucleons, b – π mesons; n is the multiplicity of meson production; M is the nucleon mass; ω(p) dp gives the number of particles with momentum in the interval p, p + dp (normalized to unity).

nucleon interaction.*

The coincidence of the angular distribution of grey tracks with the analogous distribution for meson stars, which we noted above, appears to indicate that the observed particles are mainly recoil protons from π mesons having energies not exceeding 1.5 Bev. The assumption about the presence of secondary interactions of π mesons inside the nucleus allows us to give a qualitative explanation for the breadth of the angular distribution of fast particles in the group of interactions with a large number of fast and slow particles, and also the broader distribution of grey particles and simultaneous increase in the number of grey and black tracks.

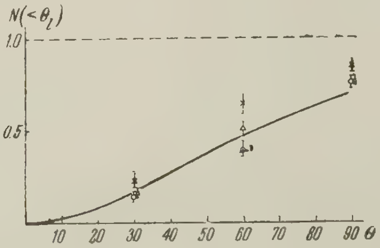

FIG. 8. Integral angular distributions of grey particles: × – J = 1.4 – 2.0 J_{min}; ○ – J > 2 J_{min}; $\overline{\cot\theta_l} \geqslant 3$; Δ – J > 2 J_{min}, $\overline{\cot\theta_l} < 3$; The continuous curve gives the distribution of strongly ionizing particles in stars from 1.5-Bev π mesons according to the data of reference 7.

4. ANALYSIS OF THE ANGULAR DISTRIBUTIONS

1. From the analysis of the distributions shown in Fig. 4, it follows first that there is a close relation between the width of the angular distribution and the number of particles produced. If we characterize the width of the distribution by the median angle $\theta_{1/2}$ and the corresponding value $\gamma_c' = \cot\theta_{1/2}$, then we obtain the pattern displayed in Table III.

In the same table we give the calculated values of $\cot\theta_{1/2} = \gamma_c\beta_c/\overline{\beta}_0$ (γ_c is the Lorentz factor of the c.m. system) for the cases of interaction of the incident nucleon with several nucleons of the nucleus (l is the number of nucleons participating in the interaction) under the assumption that the secondary particles are emitted symmetrically (in the c.m. system) with mean* velocity $\overline{\beta}_0 = 0.7\,c$; β_c is the velocity of the c.m. system.

In comparing Table III and Fig. 4, it should be kept in mind that the small difference between experimental and calculated values of cot $\theta_{1/2}$ in Table III is somewhat accidental. It can be seen by comparing the calculated curve (1 on Fig. 4) with the experimental curve for n_s = 2 and 3,

---

*The corresponding quantitative criteria were kindly communicated to us by N. G. Birger and Yu. A. Smorodin. They were employed in their paper.[8]

*As established in the calculations referred to above, roughly these velocities were obtained from the statistical theory for the cases $l = 1$ and $l = 4$ after averaging over the velocities of all nucleons and mesons.

TABLE IV. Connection between the angular characteristic of stars and their distribution with number of black tracks

n_s	$\bar{\theta}_l$ deg	Relative number of cases, in per cent				Total number of cases
		$n_b = 0,1$	$n_b = 2-5$	$n_b = 6-10$	$n_b \geqslant 11$	
$n_s = 2,3$	<14	72%	15%	13%	—	39
	14–24	41%	39%	16%	5%	44
	>24	20%	40%	22%	19%	86
$n_s = 4-6$	<14	~50%	50%	—	—	4
	14–24	37%	47%	13%	3	30
	>24	14%	26%	26%	34%	139

taking into account the non-monochromatic nature of the spectra of particles produced, that the agreement between calculations and experiment is not satisfactory. In addition, because of the inevitable fluctuations in the number of particles n_s produced in a given type of nuclear interaction, the cases, chosen only by the quantity n_s, should certainly represent a mixture of interactions of the incident nucleon with various numbers of nucleons in the nucleus. This directs attention to the correspondence between the angle $\theta_{1/2}$ for stars with small n_s ($n_s = 2$ and 3) and the calculated value of the angle $\theta_{1/2}$ for nucleon-nucleon interactions, as well as the large (by comparison with the predictions of the statistical theory of a given nucleon-nucleon collision) number of collisions with production of only a few particles.* Both of these facts indicate that, together with collisions with several nucleons of the nucleus and with the lowering of the value of γ_c, collisions can also take place with little inelasticity and larger value of γ_c (i.e., γ_c larger than that γ_{cn} which should obtain for the nucleon-nucleon interaction). The latter can, apparently, be ascribed either to peripheral interaction[9] of the incident nucleon with one of the nucleons of the stationary nucleus, or to peripheral interaction with the nucleus as a whole as a consequence of diffraction phenomena.[10] In the former case, values of γ_c either less than, equal to, or greater than γ_{cn} are possible; in the second case, $\gamma_c > \gamma_{cn}$ only. The presence of interactions with increased values of γ_c follows also from the analysis of stars with $n_s = 1$ (see Fig. 4).

2. It is clear that the number of slow particles in the star, $n_h = n_b + n_g$, is not a very suitable quantity to use in separating different types of nuclear interaction in the photoemulsion. In fact, we calculated the correlation coefficients $k(n_h, \xi)$ and $k(n_s, \xi)$ between the quantities n_h (or n_s) and the angular characteristics of individual interactions ξ. As angular characteristic, we employed in one calculation the mean cotangent of emission of fast particles ($\xi_2 = \overline{\cot\,\theta_l}$) and, in another calculation, the quantity l obtained by selecting stars by three angular characteristics — the mean cotangent of emission of fast particles, the mean and half value of the same angle. It turned out that in all cases the correlation coefficient lay between 0.30 and 0.45, i.e., the degree of correlation between the number of slow particles n_h and the angular characteristics of the star ξ did not exceed that for the number of fast particles n_s, and this was not greater than the degree of correlation between the quantities n_h and n_s.

3. It seems to us that in the case of the given primary energy, the angular characteristics of the stars (ξ) are a more definite indicator of the type of interaction than the number of slow particles n_h emitted from the nucleus, i.e., the degree of excitation of the nucleus, in so far as n_h mainly characterizes the secondary processes, and ξ more the primary ones.

Table IV illustrates the differing character of the interaction for stars with differing angular characteristics $\xi_1 = \bar{\theta}_l$. It can be seen that for low values of n_s, the distribution of the stars with angular characteristics is far from being invalidated by fluctuations, and has a definite physical meaning in the clarification of the mechanism of nuclear interaction.*

In the following analysis, the quantity ξ_2 is, in our view, a more convenient angular characteristic for the stars than ξ_1, especially for interactions with large values of γ_c. In fact, with an isotropic distribution of particles in the c.m.s., after transforming in the well-known way to angles in the laboratory system (l.s.),

$$\cot\theta_l = \frac{\gamma_c}{\sin\theta_0}\left(\frac{\beta_c}{\beta_0} + \cos\theta_0\right), \tag{1}$$

---

*This will be discussed in detail below.

*In essence, Table IV gives only a more detailed confirmation of the fact that the correlation coefficient between the quantities n_h and ξ differs from zero. An analogous picture is found in the analysis of stars according to the number of grey tracks n_g and with the choice of the quantity $\xi_2 = \overline{\cot\,\theta_l}$ as angular characteristic.

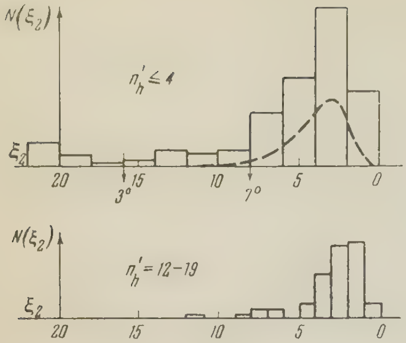

FIG. 9. Distribution of stars with angular characteristic $\xi_2 = \overline{\cot\theta_l}$ for various values of the sum $n_h' = n_b + 3n_g$.

we obtain rather simple features for the function describing the distribution of particles with the quantity $\cot\theta_l$. In particular a) the "half value" $(\cot\theta_l)$, i.e., the value for which the integral distribution S $(< \cot\theta_l)$ is 50%, is equal to $\gamma_c\beta_c\,(\overline{1/\beta_0})$, and, is determined, thus, not solely by the quantity γ_c, but by some effective value of the particle velocity in the c.m. system; b) the mean value $\xi_2 = \overline{\cot\theta_l}$ differs from $(\cot\theta_l)_{1/2}$ by the factor $\overline{1/\sin\theta_0} = \pi/2$; c) the spread in angular characteristic relative to $(\overline{\cot\theta_l})_{1/2}$ is approximately proportional to γ_c.

In Fig. 9 we show the distributions with angular characteristic $\xi_2 = \overline{\cot\theta_l}$ for stars with $n_s \geq 2$, plotted in groups depending on the number of slow particles emitted — more precisely, on the quantity $n_h' = n_b + 3n_g$. There the calculated (dashed) curve for fluctuations in the quantity ξ_2 is also plotted, giving somewhat of an overestimate of the role of these fluctuations. As can be seen from Fig. 9, for stars with a small number of slow particles ($n_h' \leq 4$) there is a rather noticeable group of cases for which the angular distribution is essentially different from that proposed by the statistical theory. As n_h' is increased, such anomalous cases disappear, and the center of mass of the distribution of stars is displaced towards smaller values of ξ_2.

4. Starting from the model in which the initial proton interacts with a "tube" of nuclear matter of mass l (in units of the nucleon mass) we tried to carry out a qualitative breakdown of all observed stars with 4 groups. These groups are characterized by values of l of 1, 2, 4, and also $l < 1$; the final value denotes the part of the interactions giving an angular distribution narrower than the nucleon-nucleon one.* As clarified by the following analysis, the quantity γ_c, which can formally be taken to describe the angular distribution of particles in this group, is equal to about 5, which corresponds roughly to the center of mass of the incident nucleon together with one of the virtual π mesons of the stationary nucleon.

The task of breaking down the observed distributions into groups, each of which possesses a given angular distribution and, consequently, a given (aside from fluctuations) value of the quantity ξ_2, was carried out in the following way. First of all, mean values of ξ_2 for each of the groups ($l = 1$, $l = 2$ and $l = 4$) and fluctuations of the quantity ξ_2 about its mean values were calculated, using in this results of the statistical theory. After this, several intervals of values of ξ_2 were chosen, namely,

$$\Delta_1(\xi_2) = 6 \text{ to } 3; \quad \Delta_2(\xi_2) = 3 \text{ to } 1.5: \quad \Delta_3(\xi_2) < 1.5.$$

and the probability of each of the group falling into one or the other of intervals was determined, taking the corresponding fluctuations into account.* Assuming that none of these intervals contained interactions of the type $l < 1$, we have the following three equations for three unknowns:

$$\begin{aligned} W_{11}N_1 + W_{12}N_2 + W_{11}N_4 &= A, \\ W_{21}N_1 + W_{22}N_2 + W_{24}N_4 &= B, \\ W_{31}N_1 + W_{32}N_2 + W_{31}N_4 &= C. \end{aligned} \qquad (2)$$

The quantities on the right-hand side are the number of stars known from experiments for which the value of ξ_2 falls in the interval Δ_1, Δ_2, or Δ_3. On the left-hand side are the calculated values W_{ik} of the probability of stars of the k-th group ($l = k$) falling into the i-th interval of values of ξ_2. Solution of the system (2) leads to the following values of the number of interactions in each of the groups:†

$$N_1 \approx N_2 \approx N_4 \approx 25\%\, N_0,$$

where N_0 is the total number of stars. Here the accuracy of the evaluations of each of the quantities (N_1, N_2, N_4) was 20 — 25%.

The same calculations showed that of the fluctuations from the remaining 25% of the stars falling into the "zeroth" interval of values of ξ_2 ($\xi_2 > 6$), no more than $1/5$ could belong to interactions of the type $l = 1$, and, consequently, $4/5 \cdot 0.25 = 20\%$ belonged to the interactions of the type $l < 1$.

In order to check the degree of agreement between our breakdown of interactions into groups

---

*Here and in the following, in all cases with $l \geqslant 1$, it will be assumed that all particles are distributed isotropically in the c.m. system.

*These fluctuations were calculated assuming isotropic and independent distributions of particles: protons (p) and mesons (π), where for $l = 1, 2, 4$, stars containing, respectively, $1p + 2\pi$, $1p + 3\pi$ and $1p + 4\pi$ were chosen as typical.

†Estimates carried out by us showed that these relative probabilities agree satisfactorily with the existing data on the spatial distribution of the density of nucleons in the nucleus.

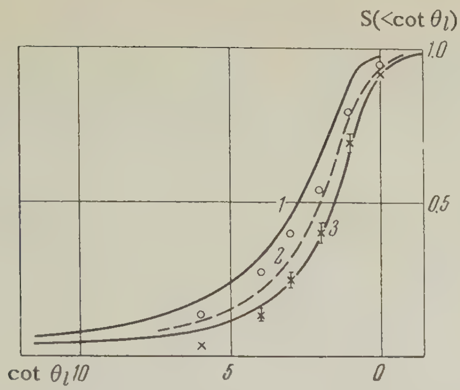

FIG. 10. Angular distributions of fast particles in interactions of various types. Experimental values: × – stars with $\overline{\cot\theta_l} = 1.5$ to 3.0; ○ – stars with $\overline{\cot\theta_l} = 2.5$ to 4.5. Theoretical curves: 1 – for interactions with $l = 1$, 2 – for $l = 2$, and 3 – for $l = 4$.

and predictions of the statistical theory, we carried out a supplementary analysis of the angular distributions of fast particles $S\ (<\cot\theta_l)$ and the multiplicity of production n_s. In Fig. 10 we show the experimental data on the angular distributions of particles in stars for two intervals of $\xi_2 : \xi_2 = 4.5$ to 2.5 and $\xi_2 = 3.0$ to 1.5. Also shown are the calculated distributions for interactions of type $l = 1$, $l = 2$ and $l = 4$. Comparison of calculation and experiment shows that in the first interval of ξ_2, as one would expect, there is mainly a mixture of interactions of type $l = 1$ and $l = 2$. However, in the second interval, one finds a distribution which is somewhat broader (in angle) than one would expect for an interaction of type $l = 4$.

5. In a somewhat different aspect, the same question can be elucidated by analyzing the mean values of the quantity $\xi_3 = \Sigma\ (\sin\theta_l)^{-1}$ for various groups of stars, separated by a simpler criterion — according to the number of slow particles. Here the quantity ξ_3 is convenient in that it is connected in a simple way with some effective value of the transverse momentum of the particle $(p_\perp)_{\text{eff}}$, namely

$$K\sum_{i=1}^{n_s} p_\perp / \sin\theta_l = K(p_\perp)_{\text{eff}}\,\zeta_3 = E_0 - \Delta E, \tag{3}$$

where K is the mean ratio of the total number of fast particles in the star to the number of charged particles, E is the energy of the primary proton and ΔE is the excitation energy of the nucleus, or, more precisely, the energy taken up by the nonrelativistic particles.

In Table V are given the experimental and calculated values of $\overline{\xi}_3$ and the corresponding values of $(p_\perp)_{\text{eff}}$ for stars of various types, where we have taken $K = 3/2$ and $\Delta E = 1$ Bev.[1] From consideration of the lower-left half of Table V, it can be seen how regularly the values of $(p_\perp)_{\text{eff}}$ decrease with increasing n_s; this is connected, apparently, with the fact that, for given l, an increase in the number of particles n_s produced leads to a decrease in the mean momentum of each of them. However, the value of $(p_\perp)_{\text{eff}}$ averaged over all n_s turns out to be higher than the theoretical one; and this difference cannot be explained only by an admixture of interactions with small l. It is considerably more likely that the transverse momenta of the highest energy particles increase because of the secondary interactions inside the nucleus.

In so far as the upper left-hand part of the table is concerned, we see there that, on the contrary, the value of $(p_\perp)_{\text{eff}}$ is low (compared with the theoretical one) and does not even depend on the multiplicity n_s. It would appear that this fact can be only partially explained by an admixture of interactions with $l > 1$, but mainly by an admixture of interactions having the anomalously narrow angular distribution $(l < 1)$.

We tried to check the assumption that the high value of $(p_\perp)_{\text{eff}}$ in the former case could be explained by cascade processes inside the nucleus in "pure" form. With this in mind, we carried out a

TABLE V: Comparison of experimental and calculated values of the quantity $\overline{\xi}_3$ and corresponding values $(p_\perp)_{\text{eff}}$

Experiment*				Theory			
	n_s	$\overline{\xi}_3$	$(p_\perp)$ eff/μc		Type of particle	$\overline{\xi}_3$	$(p_\perp)$ eff/μc
$n_g \leqslant 1,\ n_h \leqslant 4$	2—3	24.5	1.5	$l = 1$	p	5	2.4
	4—6	22	1.6		π	10	
	$\geqslant 7$	24	1.5		$p + \pi$	15	
	$(n_g + n_h) < 11$						
$n_g + n_h > 8$	2—3	7.1	5.1	$l = 4$	p	7	1.5
	4—6	13	2.8		π	16	
	$\geqslant 7$	19.5	1.8		$p + \pi$	23	
	$\overline{n}_s = 5$	13.5	2.7				

*The accuracy in the experimental data is 15% in the upper half of the table and 5% in the lower.

TABLE VI. Proportion of stars (percent) with different l for given n_s

n_s	$l < 1$	$l = 1$	$l = 2$	$l \geqslant 3$ ($l = 4$)
1	$\geqslant 50$	~ 25	~ 15	~ 5
2–3	$\geqslant 25$	~ 30	~ 20	~ 20
4–6	$\leqslant 10$	~ 25	~ 30	~ 40
$\geqslant 7$	—	$\leqslant 10$	~ 20	~ 80

TABLE VII. Distribution of the number of stars with n_s for given l

	l	$n_s = 1$	$n_s = 2–3$	$n_s = 4–6$	$n_s \geqslant 7$	$\bar{n}_s$
Experiment	<1	55(±15)%	35(±12)%	≤10%	—	1.5—2.0
Experiment	1	20(±10)%	40(±10)%	40(±10)%	<10%	3.3±0.3
Theory		≈7%	≈46%	≈46%	0.6%	≈3.3
Experiment	2	10(±4)%	30(±7)%	50(±15)%	10(±5)%	4.0±0.4
Theory		~0.5%	≈14%	≈65%	≈20%	≈4.8
Experiment	$\geqslant 3$	4(±2)%	25(±7)%	40(±15)%	30(±10)%	5.0±0.5
Theory		—	≈5%	≈40%	≈55%	≈6.75

TABLE VIII. Proportion of stars with various l for given n_b and n_g

	$l < 1$	$l = 1$	$l = 2$	$l > 3$		$l < 1$	$l = 1$	$l = 2$	$l \geqslant 3$
$n_b \leqslant 3$	35%	35%	20%	10%	$n_g = 0$	≥30%	~30%	~20%	~15%
$n_b = 4–8$	≥15%	~25%	~30%	~30%	$n_g = 1$	≥15%	~25%	~30%	~30%
$n_b = 9–15$	—	~15%	~25%	~60%	$n_g = 2,3$	~10%	~20%	~30%	~40%
$n_b \geqslant 16$	—	≤10%	~15%	~80%	$n_g \geqslant 4$	—	~10%	~20%	~70%
$\bar{n}_b(l)$	2—3	4—5	6—8	10—12	$\bar{n}_g(l)$	≤0.5	≈0.8	≈1.25	≈2

very approximate calculation of this process according to the following scheme. We assumed that in the subsequent interactions of the primary proton with each of the l nucleons in the nucleus, only one fast nucleon remained, carrying off 70% of the initial energy, and that the remaining 30% of the energy was distributed among the mesons, the number of which was determined by the value of γ_c, according to the statistical theory.[11] We assumed also that in the process of interaction with other nucleons in the nucleus, all mesons of energy up to 550 Mev (total energy $5\mu c^2$) are absorbed and that only mesons of energy greater than 550 Mev are scattered. It is easy to show that this way of considering the process can lead to a value for the multiplicity* for given l which is significantly higher. None the less, in the case of $l = 4$, for example, calculation with this scheme gives $n_s = 5.5$, i.e., a value larger than observed in experiment. For a conclusive decision on the applicability of the model of cascades inside the nucleus in "pure" form, it would be necessary to carry out more rigorous calculations using accurate experimental data on the characteristics of nucleon and π-meson interactions at the various energies.

6. We turn now to a determination of the number of fast and slow particles (n_s, n_b and n_g) in interactions with different values of the quantity l. Grouping all observed stars of given n_s, n_b or n_g first according to the angular characteristics of the fast particles (ξ_2), and then carrying out a regrouping according to l by solving the system of equations (2), we obtained the results given in Tables VI — VIII. From Table VI it follows that interactions with a large number of fast particles correspond mainly to interaction of the incident nucleon with several nucleons of the nucleus. If we assume that the excitation energy ΔE of the nucleus is proportional to either the quantity n_b or n_g, which, in turn, turn out to be proportional to each other (for given l), then it follows from Table VIII that the excitation energy increases with increasing l, but somewhat more slowly than l. The data in Table VII shows that the model of interaction of the incident nucleon with a "tube" of nuclear matter leads to a high value for the multiplicity n_s. Starting from an analysis of the distribution of stars with n_s it thus follows that the interaction of nucleons in a complex nucleus has a character intermediate between that of the pure "tube" and pure cascade models.

In order to answer the question about the simultaneous or successive character of the interaction of the incident nucleon with the nucleons in the nucleus, it would be necessary to study the corresponding energy characteristics for mesons and nucleons.

---

*This is connected, first of all, with the fact that, according to the statistical theory, appreciably less than 70% of the initial energy should be kept, on the average, by one fast nucleon.

CONCLUSIONS

1. The mean free path for inelastic interaction of 8.7-Bev protons with photoemulsion nuclei is equal to 34 ± 2 cm.

2. In the interactions discussed, in a significant part of the cases ($\geq 15\%$) stars are formed which can apparently be related to processes of peripheral nucleon-nucleon interactions. These stars are characterized by a small number of fast particles ($n_s = 1-2$) which emerge at small angles (of the order of 5° on the average) relative to the direction of the incident proton.

3. Processes of "pure" charge exchange, i.e., processes in which fast charge particles are not formed, account for about 3% of all interactions in photoemulsions.

4. A significant part (about 25%) of the interactions with photoemulsion nuclei hardly differ, in angular distribution and mean multiplicity of fast particle production, from interactions of the nucleon-nucleon type, calculated with the usual statistical theory.

5. The angular distribution of grey tracks depends only very weakly on the angular distribution of fast particles and differs little from the distributions found in interactions of 1.5-Bev π mesons with photoemulsion nuclei. It can be assumed that the origin of grey particles in this case is connected to a significant degree with secondary interactions of π mesons of energy ~ 1 Bev.

6. The monotonic broadening of the angular distributions with increasing multiplicity of fast particle production corresponds to the picture of interactions intermediate between the representations of successive and simultaneous interactions of the primary nucleon with nucleons of the complex nucleus.

In conclusion, the authors would like to express their deep gratitude to Academician V. I. Veksler for the possibility of being able to work with part of the photoemulsion stack, irradiated in the proton synchrotron of the Joint Institute for Nuclear Research, to M. I. Podgoretskiĭ, I. M. Gramenitskiĭ, K. D. Tolstov, and R. M. Lebedev of the Joint Institute for discussion of the data obtained, scientific worker of the Acad. Sci. Physics Institute, E. A. Zamchalova, for helping in the preparation of the photoemulsion stack for irradiation, and also to Prof. N. A. Dobrotin, I. L. Rozental', D. S. Czernawski and N. G. Birger for valuable advice in the discussion of results.

---

[1] Bogachev, Shu-fen', Gramenitskiĭ et al., Атомная энергия (Atomic Energy) **4**, 281 (1958).

[2] Bogachev, Bunyatov, Merekov, and Sidorov, Dokl. Akad. Nauk SSSR **121**, 617 (1958), Soviet Phys–Doklady **3**, 785 (1959).

[3] Lock, March, Muirhead, and Rosser, Proc. Roy. Soc. **A230**, 215 (1955).

[4] Smith, Leavitt, Shapiro, et al., Phys. Rev. **92**, 851 (1953).

[5] Cavanaugh, Haskin, and Schein, Phys. Rev. **100**, 1263 (1955).

[6] Cronin, Cool, and Abashian, Phys. Rev. **107**, 1121 (1957).

[7] J. E. Crew and R. D. Hill, Phys. Rev. **110**, 177 (1958).

[8] N. G. Birger and Yu. A. Smorodin, J. Exptl. Theoret. Phys. (U.S.S.R.) **36**, 1159 (1959), Soviet Phys. JETP **9**, 823 (1959).

[9] D. Czernawski, Postepy Fizyki **9**, 653 (1958) [Poland].

[10] I. I. Ivanchik, J. Exptl. Theoret. Phys. (U.S.S.R.) **36**, 617 (1959), Soviet Phys. JETP **9**, 427 (1959); I. Ya. Pomeranchuk and E. L. Feĭnberg, Dokl. Akad. Nauk SSSR **93**, 439 (1953).

[11] Belen'kiĭ, Maksimenko, Nikishov, and Rozental', Usp. Fiz. Nauk **62**, 1 (1957).

Translated by G. E. Brown
124

SOVIET PHYSICS JETP VOLUME 37 (10), NUMBER 3 MARCH, 1960

ON THE ABSORPTION OF π^+ MESONS WITH ENERGIES OF ABOUT 50 Mev BY CARBON NUCLEI

J. V. LABERRIGUE-FROLOVA, M. P. BALANDIN, and S. Z. OTVINOVSKIĬ

Joint Institute for Nuclear Research

Submitted to JETP editor April 4, 1959

J. Exptl. Theoret. Phys. (U.S.S.R.) **37**, 634-638 (September, 1959)

Stars arising from the absorption of π^+ mesons with an energy of 50 ± 20 Mev in carbon nuclei were investigated with the aid of a propane bubble chamber. The formation cross section of such stars was equal to 145 ± 36 mb. The distribution of stars according to the number of prongs was obtained, the average number of prongs being 2.6 ± 0.3. A significant anisotropy in the angular distribution of prongs relative to the direction of motion of the π^+ meson was observed. The basic source of this anisotropy was evidently a pre-absorption scattering of π^+ mesons from the individual nucleons inside the nucleus. The distribution of two-pronged stars by angles between the prongs is given.

A significant number of stars from the interaction of low-energy π^+ mesons with carbon nuclei were found while looking through photographs obtained earlier[1] in a study of π^+-μ^+-e^+ decay using a propane bubble chamber[2] of diameter 9 cm and depth 7 cm.

The inelastic interactions of π^+ mesons with complex nuclei has been studied with scintillation counters, photoemulsions, and Wilson cloud chambers. The investigations carried out with scintillation counters[3-5] consisted of measuring the attenuation of the π^+ beam intensity and did not allow separation of the absorption of π^+ mesons from other inelastic processes. In the work with photographic plates,[6-8] it was impossible to identify the nuclei involved in the interaction. Finally, the work with cloud chambers[9-10] was restricted to an investigation of only the energetic prongs of the stars (for example, Byfield et al.[10] considered prongs belonging to protons with energies ≥40 Mev), since the carbon target, unavoidably relatively thick, absorbed the low-energy charged particles. Under these conditions the photograph of the event was far from complete.

In spite of this large amount of work, it is interesting to investigate the inelastic interactions of π^+ mesons with complex nuclei using a bubble chamber, since this enables us to get additional information on the subject through some peculiarities of the method. For example, using the bubble chamber for the solution of similar problems, it is possible simultaneously to identify the nucleus involved in the interaction, to separate the absorption of π^+ mesons from other inelastic processes, and to get a fuller photograph of the event than in cloud chambers, since protons with energies ≥ 3 Mev, corresponding to prong lengths ≥ 0.5 mm, can be observed.

In connection with the above it seemed interesting to us to investigate with the propane bubble chamber the character of the stars coming from the absorption of low energy π^+ mesons by carbon nuclei. This question was investigated with a propane bubble chamber earlier,[11] but only for 250 — 270 Mev pions. Since in our case the pion energies were quite a bit lower than 250 Mev, it is interesting to compare the results we obtained with the results of reference 11.

The conditions of the experiment, a diagram of which is given in reference 1, were the following. The formation of π^+ mesons took place in a polyethylene target placed in the 670-Mev proton beam from the synchrotron chamber. The mesons coming from the target were deflected by an electromagnet to pass through a collimator in a four-meter concrete shield into the measurement area, where the bubble chamber was located. A filter to slow down the pions was placed immediately in front of the chamber. All the photographs were taken for two values of the energy of the pions as they came out of the collimator. In this work only those photographs were examined which were taken for an incident pion-beam energy of 273 Mev, that is, when the mesons incident on the collimator came from a target 30 cm thick at an angle 0° to the direction of the incident proton beam, and when a 15.5 cm thick copper filter was placed in front of the chamber. The average pion energy in the middle of the chamber was 50 ± 20 Mev for this filter. The estimate of the error in the value of the energy of the pions was made by an analysis of their absorption curve in copper, obtained with scintillation counters. The pion energy losses in going through the propane chamber were also taken into consideration.

The scanning and analysis of the photographs taken was done on a reprojector;[12] the scanning, as already described, was done while the work was being carried out.[1] To eliminate distortions dependent on the regions of the chamber a region with a diameter of 6 cm was separated and only those stopping and interaction events which occurred in this region were noted. The pion interaction events with both hydrogen and carbon were determined.

To separate out the elastic scattering of pions from hydrogen, measurements were made of the angles between the pion track and each of the secondary tracks in all cases where the given interaction could have taken place. It was reckoned that elastic pion scattering on hydrogen took place wherever the measured angles satisfied the kinematic relations.

Among the stars showing up in the scanning were stars occurring both with and without the absorption of a pion. Those stars were counted as occurring without pion absorption one of whose prongs had the form characteristic of π^+-μ^+-e^+ decay. To decide which of the remaining stars occurred with pion absorption, the length of each prong was determined; and the longest prong, according to probability, was ascribed to a π^+ meson and the others to protons. If the bubble density of the track assigned to the pion did not markedly increase towards the end, then 1 — 1.5 cm was added to its length, corresponding to the known path of a pion to its full stop. Then the energy of all the particles in a star was found under the assumption that each of them stopped inside the chamber. It was taken that the star formation occurred with pion absorption if the energy of all the particles added to the binding energy of the original carbon nucleus was greater than the binding energy of the residual nucleus plus 70 Mev. From all the possible residual nuclei, that one was chosen whose binding energy was the closest to the binding energy of the original carbon nucleus. Whenever this condition was not fulfilled, but either all the particles of the star stopped in the chamber or all the particles which did not terminate inside had strong blackening for a sufficiently great length, so that none of them could be a π^+-meson track, we considered that we had here too a π^+ absorption process, although some of these might have been actually charge exchanges of a π^+-meson with a carbon nucleus. This method of choice was justified by the fact that, for pion energies of the order of 50 Mev, the upper limit of the charge exchange cross section is only a few percent of the absorption cross section,[13] so that this process could not essentially influence the character of the results. All the rest of the stars, satisfying none of the conditions enumerated above, were placed by us in the "doubtful" group. Typical photographs of stars occurring with π^+-meson absorption, are given in Figs. 1 and 2.

In all, 2360 stereo photographs were scanned, and 180 stars satisfying the conditions for π^+-meson absorption were discovered. Eight of these 180 stars had an indeterminate number of prongs. In addition, 65 stars were found which by our conditions of selection were accounted "doubtful." Considering that half of the "doubtful" stars occurred with π^+ absorption by carbon nuclei, and taking into account an admixture of μ^+ mesons in the pion beam, determined from the absorption curve of pions in copper, the absorption cross section for π's with energies 50 ± 20 Mev by carbon atoms was found to be 145 ± 36 mb.

The distribution of stars formed by π^+ mesons in their absorption by carbon nuclei is given by the solid line in Fig. 3 in terms of the number of prongs. In constructing this distribution, only those prongs were considered whose length was not less than 0.5 mm, and it was supposed that half the "doubtful"

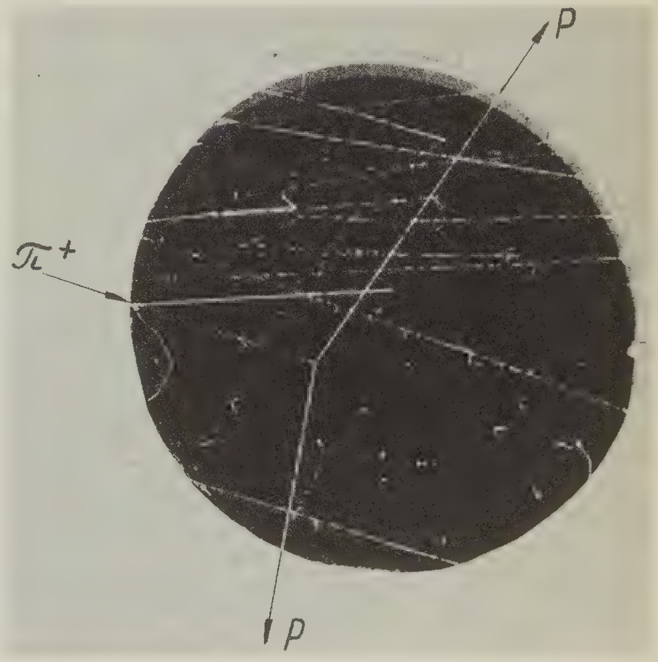

FIG. 1. Two-pronged star resulting from the absorption of a π^+ meson by a carbon nucleus.

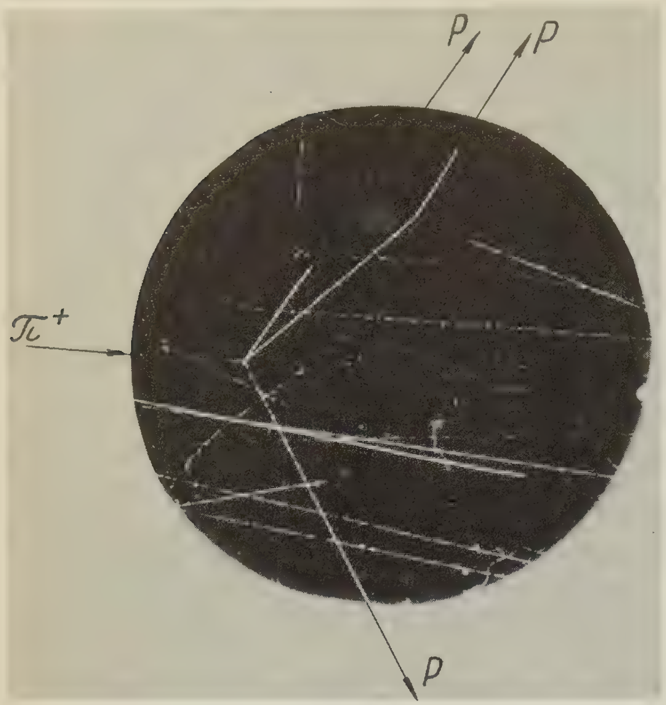

FIG. 2. Three-pronged star resulting from the absorption of a π^+ meson by a carbon nucleus.

stars occurred with π^+-meson absorption by carbon nuclei. The experimental points in Fig. 3 are shown together with their errors, calculated using statistical considerations and the fact of the presence of "doubtful" stars, which were the basic source of errors for one- and two-pronged stars. In the same figure, the dotted line shows an analogous distribution obtained in reference 11 for 115 stars formed by π^+ mesons of energy 250 — 270 Mev upon being absorbed by carbon nuclei. It is evident from Fig. 3 that the distributions shown of stars according to number of prongs agree well with each other, within the limits of experimental error. This obviously indicates the absence of a strong dependence in these similar distributions on the energy of the incident π^+ mesons. We further note that the star distributions obtained are characterized in their dependence on the number of prongs by an average of 2.6 ± 0.3 prongs. To calculate the error in the average number, statistics and the presence of "doubtful" stars were taken into account.

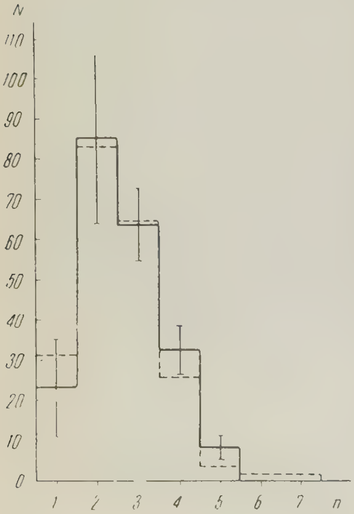

FIG. 3. Distribution of stars by number of prongs. N — number of stars, n — number of prongs in the stars. The solid line is the results of the present work, the dotted line is the data obtained in reference 11 for 115 stars produced in the absorption of 250-270 Mev energy π^+ mesons by carbon nuclei.

For 172 stars formed by π^+ mesons during their absorption by carbon nuclei, a distribution of prongs was constructed as a function of the magnitude of the angle ϑ, the projection of the angle between the direction of motion of the π^+ meson and the prong onto the plane perpendicular to the optical axes of the stereo camera. It is evident from this distribution, shown in Fig. 4, that there was observed a strong anisotropy of prongs relative to the direction of motion of the π^+ meson. In fact, the number of prongs N_f in the forward hemisphere relative to the π^+ meson direction of motion was 1.81 times greater than the number of prongs N_b in the back hemisphere. If the degree of observed anisotropy is characterized by the ratio $(N_f - N_b)/(N_f + N_b)$, this quantity is equal to 0.29 ± 0.05. Again, the error calculation for the magnitude of the anisotropy took into account statistics and the presence of "doubtful" stars. To trace the variation of the anisotropy as a function of the number of prongs in the stars, the ratio $(N_f - N_b)/(N_f + N_b)$ was calculated for stars with various numbers of prongs. The following data were obtained:

Number of prongs in star:	1	2	3	4	5
$\frac{N_f - N_b}{N_f + N_b}$:	$1.00^{+0.29}_{-0.56}$	$0.36^{+0.09}_{-0.1}$	0.36 ± 0.08	0.18 ± 0.09	0.20 ± 0.16

It is evident from these data that some tendency is observed for the anisotropy to increase as the number of prongs in a star decreases. The observed anisotropy cannot be connected with the

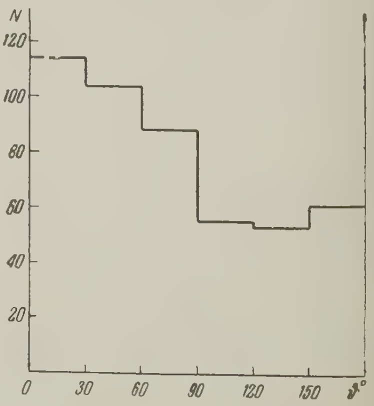

FIG. 4. Angular distribution of prongs relative to the direction of motion of the π^+. θ is the projection of the angle between the π^+ meson direction of motion and the prong on the plane perpendicular to the optical axes of the stereo camera. N is the number of prongs in each 30° interval of the angle θ.

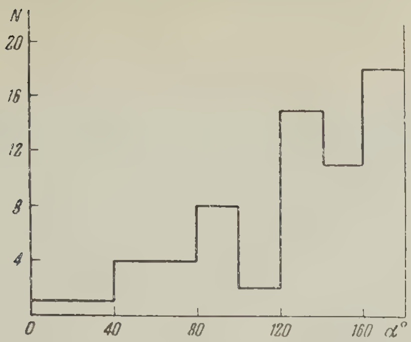

FIG. 5. Distribution of two-pronged stars as a function of the angle between the two prongs. α is the angle between the two prongs, N is the number of two-pronged stars, and the interval of the angle α is 20°.

process of absorption of a π^+ meson by a nucleon pair. This result is not hard to understand if one considers the kinematical relations or makes use of the experimental data on the distribution of two-pronged stars in terms of the angle α between the two prongs. One can see from this distribution, shown in Fig. 5, that there exists a significant group of stars in the α interval 120° to 180° which evidently correspond to the known process of π^+-meson absorption by a nucleon pair. The proton distribution in this group as a function of the magnitude of the angle ϑ is isotropic, as should be expected from the kinematic relations. This fact strengthens the result obtained before about the impossibility of explaining the observed anisotropy by absorption of the π^+ meson by a nucleon pair.

It is reasonable to suppose that the chief sources of anisotropy are quasi-elastic scattering of π^+ mesons by protons and their exchange scattering by neutrons inside the nucleus, since in these processes the protons can only be ejected in the forward hemisphere relative to the π^+-meson direction of motion. Under this supposition, there ought to exist (as an analysis of the data shows), besides the stars resulting from π^+-meson absorption without previous scattering by inside nucleons, a significant group of stars in which the π^+ meson experiences a quasi-elastic or exchange scattering from individual nucleons inside the nucleus and is then absorbed. Of course, the picture of star formation proceeding with π^+-meson absorption in two states is highly schematic, since the time separation of these two processes inside the nucleus is rather arbitrary.

If the values of the cross sections of the processes $\pi^+ + p \rightarrow \pi^+ + p$, $\pi^+ + n \rightarrow \pi^0 + p$, $\pi^+ + n \rightarrow \pi^+ + n$ and the processes $\pi^- + n \rightarrow \pi^- + n$, $\pi^- + p \rightarrow \pi^0 + n$, $\pi^- + p \rightarrow \pi^- + p$ are taken into account, one can conclude, on the basis of the hypotheses given above, that the degree of anisotropy $(N_f - N_b)/(N_f + N_b)$ for the stars occurring with π^--meson absorption must be significantly less than that observed in the present work.

In closing, we are glad to thank B. M. Pontecorvo for his advice and his interest in the work. We also thank V. A. Moiseenko, V. Trifonov and E. Yurova for performing many measurements. One of the authors of the article, J. V. Laberrigue-Frolova, wishes to express her great appreciation to Prof. D. I. Blokhintsev and Prof. V. P. Dzhelepov for their hospitality at the Joint Institute for Nuclear Research. She cherishes the memory of Joliot-Curie, through whose initiative she came to work at Dubna.

---

[1] Balandin, Moiseenko, Mukhin, and Otvinovskiĭ, JETP **36**, 424 (1959), Soviet Phys. JETP **9**, 296 (1959).

[2] M. P. Balandin and V. A. Moiseenko, Тезисы докладов на Всесоюзной конференции по физике частиц высоких энергий (Theses of the reports of the All-Union Conference on the Physics of High Energy Particles), Moscow (1956).

[3] D. H. Stork, Phys. Rev. **93**, 868 (1954).

[4] Isaacs, Sachs, and Steinberger, Phys. Rev. **85**, 803 (1952).

[5] Ignatenko, Mukhin, Ozerov, and Pontecorvo, JETP **31**, 545 (1956), Soviet Phys. JETP **4**, 351 (1957).

[6] G. Bernardini and F. Levy, Phys. Rev. **84**, 610 (1951).

[7] B. Rankin and H. Bradner, Phys. Rev. **87**, 553 (1952).

[8] Blau, Oliver, and Smith, Phys. Rev. **91**, 949 (1953).

[9] A. Shapiro, Phys. Rev. **84**, 1063 (1951).

[10] Byfield, Kessler, and Lederman, Phys. Rev. **86**, 17 (1952).

[11] Kan-Chang, Tso-Tsiang, Da-Tsao, Dubrovskiĭ, Kladnitskaya, and Solov'ev, JETP **35**, 899 (1958), Soviet Phys. JETP **8**, 625 (1959).

[12] Vasilenko, Kozodaev, Sulyaev, Filippov, and Shcherbakov, Приборы и техника эксперимента (Instruments and Measurement Engineering) **6**, 34 (1957).

[13] R. Wilson and J. P. Perry, Phys. Rev. **84**, 163 (1951).

Translated by W. Ramsay
125

SOVIET PHYSICS JETP VOLUME 37(10), NUMBER 3 MARCH, 1960

MULTIPOLARITIES OF GAMMA TRANSITIONS IN Tm^{169}

V. M. KEL' MAN, R. Ya. METSKHVARISHVILI, B. K. PREOBRAZHENSKIĬ, V. A. ROMANOV, and V. V. TUCHKEVICH

Leningrad Physico-technical Institute, Academy of Sciences, U.S.S.R.

Submitted to JETP editor April 9, 1959

J. Exptl. Theoret. Phys. (U.S.S.R.) **37**, 639-642 (September, 1959)

The ratios of the internal conversion coefficients of 63, 94, 110, 130.5, 177 and 198 kev γ quanta in the L-subshells of Tm^{169} have been found. From these data, we determine the multipolarities of the transitions and, in the case of mixed radiations, the percentages of components in the mixture.

THE gamma spectrum and conversion electron spectrum of excited Tm^{169}, formed by electron capture from radioactive Yb^{169} (half-life 32 days), have been studied by many authors.[1-9] The Tm^{169} nucleus is highly deformed, and one sees very clearly in its level scheme* (Fig. 1) the rotational band with $K = \frac{1}{2}$ (the levels at 0, 8.4, 118, and 139 kev). The lowest level of this band, with spin $\frac{1}{2}$ and positive parity, is the ground state of Tm^{169}. The levels at 316 and 379 kev are associated with single-particle excitation of the nucleus, while the level at 379 together with the one at 473 kev form the rotational band with $K = {}^7\!/_2$. Most of the γ transitions are mixtures of dipole and quadrupole. Up to now the composition of the mixtures has not been determined sufficiently accurately, and the data from different papers differ markedly from one another. The most accurate determination of the mixture percentages was made in reference 5. These authors used, in addition to other methods for determining the multipolarities, the measurement of the ratio of the conversion coefficients in the L-subshells. They made these measurements quite accurately for the conversion of the 130.5 kev line. For the harder γ rays at 177 and 198 kev, they made only an approximate determination of the ratio $L_I : L_{III}$.

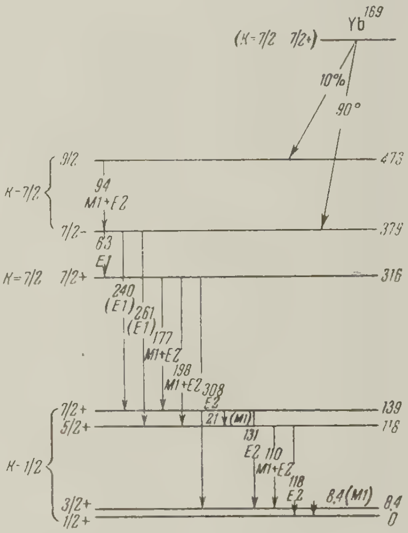

FIG. 1. Level scheme of Tm^{169}.

In the present paper we give results of measurements of the ratios of conversion coefficients of γ quanta with energies 63, 94, 110, 130.5, 177, and 198 kev in the L-subshells of Tm^{169}. We have determined the multipolarities of the transitions, and the percentages of the mixture in cases of mixed radiation. The measurement of the ratio of intensities of conversion lines from the first γ ray listed was done on a double-focusing β-ray spectrometer in which the relative half-width of the line was 0.4% (in momentum). The remaining measurements were done on a β-spectrometer constructed in analogy to an optical spectrometer.[10,11] It consists of a magnetic deflection system (prism) and two magnetic lenses. The source was a thin layer of Yb^{169} placed on a strip of aluminum foil. Its dimensions were $5 \times 1\ \mathrm{mm}^2$. The preparation of the source was accomplished as follows. A tantalum target was irradiated with 680-Mev protons at the synchrocyclotron of the Joint Institute for Nuclear Studies. The rare earths produced by spallation reactions were separated by the ion exchange method on a sulfostirol cation KU-2, using ammonium lactate[12,13] as a complexing agent. The principal activity of a particular element was concentrated in 1 or 2 drops of the ammonium lactate solution (concentration 0.2 to 0.4 M in the lactate) emerging from the column.

---

*This level scheme is taken from reference 4, but the multipolarity assignments have been corrected in accordance with the results of the present work.

Even careful evaporation of these drops directly onto the source results in some tarring of the lactate and formation of some residue. If the source is prepared on a thin aluminum foil or organic film, heating to burn off the residue is not possible. Therefore the lactate drops carrying the activity were first evaporated onto another backing, and then the activity was taken up in a drop of ~ 1% solution of acetic acid, which was placed on the source backing and evaporated. In this way the activity was almost completely transferred.

Using this method, we separated and deposited on an aluminum foil the Lu fraction, which contains Lu^{169}. The latter decays with a period of ~ 2 days to Yb^{169}.[14] The measurements of the conversion spectrum of Tm^{169} were begun about a month after the separation of the Lu fraction, so that the radioactive lutecium isotopes had had time to decay sufficiently and the main activity was that of Yb^{169}. The measurements of the internal conversion lines of the 130.5-kev line in the L-subshells of Tm^{169} were done three months after the separation, because the L_I conversion line is superimposed on a strong line from K-conversion of the 181.4 kev γ ray accompanying the Lu^{172} — Yb^{172} decay (Lu^{172} half-life is 6.7 days).

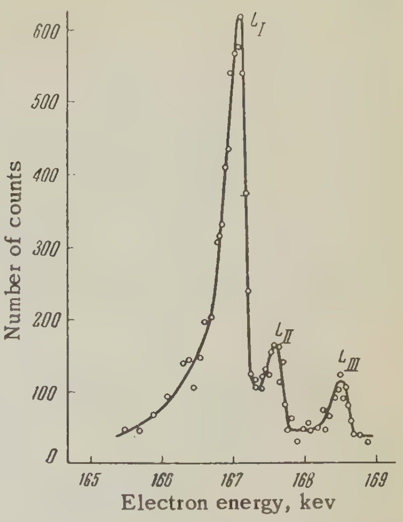

FIG. 2. Conversion lines of 177 kev radiation in the L-subshells of Tm^{169}.

Because the source was quite thick, the resolving power of the spectrometer cited in reference 11 (instrumental relative half-width of line = 0.04%) could not be reached. It therefore seemed reasonable to reduce the resolution of the instrument and thus raise its luminosity. For this purpose we reduced the focal separation of the lenses from 120 to 50 cm and brought the source and detector correspondingly closer to the lenses. This reconstruction of the instrument increased the instrumental half-width by a factor of about 2.4, but the solid angle increased by a factor of 5 or 6, reaching a value of ~ 0.1% of 4π. The relative half-width found in the experiment, resulting from slowing down of electrons in the source, was 0.12 — 0.20% (in momentum). In all cases the lines were resolved sufficiently well for the later graphical separation. To illustrate this, we show in Figs. 2 and 3 the conversion lines of the 177 and 198 kev radiations in the L-subshells of Tm^{169}.

The ratios of the internal conversion coefficients and the multipolarities determined from them are given in the table. The percentage composition of the mixed radiations was determined

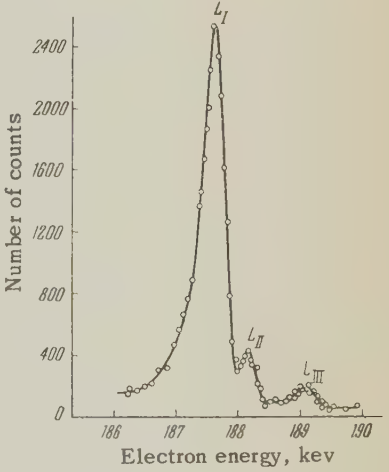

FIG. 3. Conversion lines of 198 kev radiation in the L-subshells of Tm^{169}.

Multipolarities of γ-transitions and ratios of conversion coefficients in L-subshells for Tm^{169}

Energy of transition in kev	$L_I : L_{II} : L_{III}$	Multipolarity of transition found from ratio:		Average value
		L_{II}/L_I	L_{III}/L_I	
63	1 : (0.44±0.01) : (0.50±0,02)	$E1$	$E1$	$E1$
94	1 : (0.179±0.006) : (0,085±0,005)	96.2% $M1+$ +3.8% $E2$	96.9% $M1+$ +3.1% $E2$	96.5% $M1+$ +3.5% $E2$
110	1 : (0.133±0.003) : (0.053±0.002)	97.5% $M1+$ +2.5% $E2$	97.5% $M1+$ +2.5% $E2$	97.5% $M1+$ +2.5% $E2$
130.5	(0.23±0.01) : (1.09±0.03) : 1	$E2$	$E2$	$E2$
177	1 : (0.24±0.01) :(0.137±0,006)	82% $M1+$ +18% $E2$	82% $M1+$ +18% $E2$	82% $M1+$ +18% $E2$
198	1 : (0.135±0.002) : (0.063±0.001)	93% $M1+$ +7% $E2$	90% $M1+$ +10% $E2$	91.5% $M1+$ +8.5% $E2$

independently from the ratios L_{II}/L_I and L_{III}/L_I, which were compared with the corresponding theoretical ratios.[15] The average of these two values was taken for the final result.

Our results confirm the level scheme shown in Fig. 1. An interesting point is the large admixture of E2 to the M1 radiation in the 177 and 198 kev transitions. This is apparently caused by K-forbiddenness of the transition from the 316-kev level to the lower levels.

---

[1] S. A. E. Johansson, Phys. Rev. **100**, 835 (1955).

[2] B. R. Mottelson and S. G. Nilsson, Z. Physik **141**, 217 (1955).

[3] Cork, Brice, Martin, Schmid, and Helmer, Phys. Rev. **101**, 1042 (1956).

[4] Hatch, Boehm, Marmier, and DuMond, Phys. Rev. **104**, 745 (1956).

[5] Mihelich, Ward, and Jacob, Phys. Rev. **103**, 1285 (1956).

[6] Baranov, Polevoĭ, Rodionov, and Shishkin, Атомная энергия (Atomic Energy) **3**, 256 (1957).

[7] Gromov, Dzhelepov, and Preobrazhenskiĭ, Izv. Akad. Nauk SSSR, Ser. Fiz. **22**, 775 (1958), Columbia Tech. Transl. p. 770.

[8] E. N. Hatch and D. E. Alburger, Phys. Rev. **110**, 1116 (1958).

[9] U. Capeller and R. Klingelhoefer, Z. Physik **150**, 375 (1958).

[10] Kel'man, Kaminskiĭ, and Romanov, Izv. Akad. Nauk SSSR, Ser. Fiz. **18**, 148, 209 (1954).

[11] Kel'man, Romanov, Metskhvarishvili, and Kolyunov, JETP **32**, 39 (1957), Soviet Phys. JETP **5**, 24 (1957).

[12] Preobrazhenskiĭ, Lilova, Dobronravova, and Teterin, Ж. неорг. химии (Journal of Inorganic Chemistry) **1**, 2294 (1956).

[13] B. K. Preobrazhenskiĭ, ibid. **3**, 119 (1958).

[14] Gorodinskiĭ, Murin, Pokrovskiĭ, and Preobrazhenskiĭ, Izv. Akad. Nauk SSSR, Ser. Fiz. **21**, 1004 (1957), Columbia Tech. Transl. p. 1005.

[15] L. A. Sliv and I. M. Band, Таблицы коэффициентов внутренней конверсии гамма-излучения (Tables of Internal Conversion Coefficients of Gamma-Radiation), vol. 2, Moscow-Leningrad, 1958.

Translated by M. Hamermesh
126

SOVIET PHYSICS JETP VOLUME 37(10), NUMBER 3 MARCH, 1960

KNOCK-ON ALPHA PARTICLES PRODUCED BY FAST NUCLEONS

V. I. OSTROUMOV and R. A. FILOV

Leningrad Polytechnic Institute

Submitted to JETP editor April 11, 1959

J. Exptl. Theoret. Phys. (U.S.S.R.) 37, 643-650 (September, 1959)

We investigate the cross section for knock-out of α particles with energies > 30 Mev from photographic emulsion nuclei bombarded by 100, 140, 200, 360, and 660 Mev protons. The knock-out of the particles by cascade nucleons is computed under the assumption that the intranuclear nucleons have definite momenta. It is found that there is an appreciable probability of formation of α substructures in light nuclei such as C^{12} or O^{16}, as well as in the diffuse region of heavy nuclei.

INTRODUCTION

THE prevalent opinions concerning the mechanism of splitting of nuclei by high-energy particles is based on the Serber-Goldberger idea of individual collisions between the incident particle and the intranuclear nucleons. The nucleus is considered as a Fermi gas whose particles — the neutrons and protons — interact weakly with each other. The presence of other nucleons during the instant of collision of two particles does not influence directly the results of the collision. The experimental disintegration data obtained during the past ten years, principally with photoemulsions, have demonstrated the correctness of these ideas. However, there are also certain facts that disagree with this simplified picture of the interaction. In particular, it has been established in many investigations that the cascade process which develops inside the nucleus upon incidence of a high energy particle involves not only the nucleons but also the more complex formations such as α particles. Thus, one must admit that there exist inside the nucleus more or less stable complexes, capable of leaving the nucleus when the latter collides with a fast nucleon. This point of view finds confirmation in the Brueckner model.[1,2] The strong correlation between nucleons, which according to this model does take place in a real nucleus, should lead to the formation of a quasi-stable complex, consisting of two, three, etc. nucleons. Paired and quadruple configurations, i.e., quasi-deuterons and alpha groups, have apparently the highest probabilities.[3,4]

An investigation, by Meshcheryakov and his associates,[5] of fast deuterons emitted from light nuclei under the influence of 660-Mev protons has shown these deuterons to be connected with the elastic collisions between the protons and the intranuclear deuteron groups. Barton and Smith,[6] in an analysis of the disintegration of He and Li by high energy photons, have also concluded that these nuclei contain correlated neutron-proton pairs, although their estimate of the quasi-deuteron momentum is somewhat lower than the value obtained in reference 5.

Rotenberg and Wilets[4] note that the probability of production of nucleon complexes is considerable in the peripheral region of the nucleus, where the density of nuclear matter is lower. On the other hand, the mean free paths of the deuterons and α particles are found to be less than the dimension of the heavy nucleus[7-9] and one can therefore expect the collision processes, which cause the complex particles to be emitted from the nucleus in the cascade stage to occur in the surface layer.

Interesting results, which also confirm the suggested knock-on origin of the α particles, have been obtained by Cüer et al.[10,11] in photoemulsion investigations of stars produced by 180- and 340-Mev protons on C^{12}. A kinematic analysis of the reaction $C^{12}(p, 3\alpha p')$ made it possible for Cüer et al. to conclude that in 30% of the cases this reaction proceeds via scattering of the incident proton by the α group contained in the C^{12} nucleus. The kinetic energy of the intranuclear α particles was found to be approximately 5 — 10 Mev. To reconcile these conclusions with the results of other researches, it was proposed that the α substructures were short-lived and dissociated rapidly into nucleons. Serebrennikov[12] estimated their lifetimes and obtained a value of $\sim 4 \times 10^{-23}$ sec. Naturally, this figure says nothing of the contribution of the α-particle states to the total wave function of the nucleus, since the probability of α-group production can also be large. Hodgson[13] has found that the probability of finding each nucleon in bound state in the α particle is approximately 0.4 for light nuclei (C, N, O) and for the peripheral region of heavy nuclei (Ag and Br). Hodgson's calculations, however, did not take into account the momentum of the α particle proper, with which the proton collides. Nor did he take into consideration the fact that the scattering process occurs in the potential well of the nucleus and that the α particle is in a state with negative total energy. An allowance for these factors may change considerably the results obtained in reference 13.

Finally, mention should be made of the paper by Schiff,[14] in which are calculated the probabilities of the electric monopole transitions in C^{12} and O^{16} on the basis of the independent-particle model and the α-particle model. The experimental value of the transition matrix element was found to lie between the two calculated ones.

Our own investigation is devoted to a further study of the existence inside the nucleus of the α particles capable of participating in the cascade process as a whole. To exclude the influence of impurity particles produced by evaporation, we investigated only the disintegration of emulsion nuclei accompanied by an emission of α particles with energies greater than 30 Mev. The experimental values of the cross sections for their emission were compared with calculated cross sections of elastic collisions between nucleons and He_2^4, obtained with allowance for the motion of the α particle proper.

EXPERIMENT

We used in the experiment photographic plates with fine-grain nuclear emulsion type P-9, in which it is possible to distinguish, with good accuracy, the tracks of doubly-charged particles from singly-charged particle tracks. The plates were irradiated in the synchrocyclotron of the Joint Institute for Nuclear Research in an external collimated beam of 660, 360, 200, 140, and 100 Mev protons. The proton energy was reduced by a copper block of suitable thickness. Magnetic lenses were used to clear the extraneous particles from the beam after passage through this block.

The procedure used to pick the stars for analysis, and the criteria used for classifying these stars according to the nature of the nucleus on which the star was produced, were described elsewhere.[15] The intensity of the beam was determined from the number of stars per unit volume of the investigated emulsion. The mean free path of protons of respective energies for star production was taken from various sources.[16]

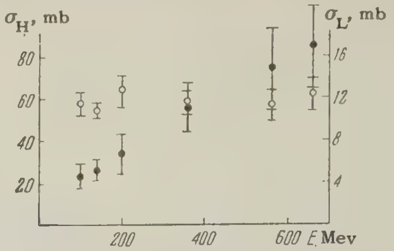

FIG. 1. Cross section for the emission of α particles with energies greater than 30 Mev from light nuclei (open circles – right-hand scale) and heavy nuclei (full circles – left-hand scale) of the emulsion at different energies of bombarding protons. The point for the 560-Mev energy was taken from reference 17.

The experimentally-obtained cross sections for the emission of α particles with energies greater than 30 Mev, at various bombarding proton energies, are shown in Fig. 1 separately for the light and heavy nuclei of the emulsion.* The errors in the experimental values, indicated on the diagram, include the statistical errors in the α-particle count and in the density of stars in the emulsion, and also the error due to the geometric corrections for the exit of the α-particle tracks from the selected emulsion layer. The same diagram shows the cross sections as determined indirectly from the α-energy spectra given by Vaganov et al.[17]

CALCULATION OF THE CROSS SECTIONS

To determine the probability of elastic collision between a nucleon and an α particle, in which the latter acquires a large momentum (corresponding to more than 30 Mev energy outside the nucleus), it is necessary to have experimental data on the differential cross sections over a wide range of angles and energies. We used the results summarized in the review of Hodgson[18] on the cross sections of elastic scattering of neutrons and protons, with energies up to 70 Mev, by He_2^4. The experimental curves were extrapolated to higher energies (up to ~ 300 Mev). We note that the experimental data available on the differential cross sections for the elastic scattering of nucleons by helium fit satisfactorily the following formula

$$d\sigma(\theta, E)/d\omega = C(\theta)\exp\{-k(\theta)\sqrt{E}\}, \qquad (1)$$

---

*The cross sections obtained previously[15] for the production of fast α particles at 360 and 660 Mev were found to be overestimated, owing to an error that crept into the determination of the particle current.

where $d\sigma(\theta, E)/d\omega$ is the differential cross section for scattering of a nucleon of energy E by the helium nucleus through an angle θ (in the center-of-mass system, calculated per unit solid angle), and C and k are functions that depend only on the scattering angle. These coefficients are listed in Table I. For E = 90 Mev, Eq. (1) is in satisfactory agreement with the Heidman formula,[19] up to ~75°. We assume that (1) remains in force up to 300 Mev nucleon energy. It should be noted, incidentally, that extrapolation to such energies was carried out only for angles less than 60°, since the contribution of larger angles was found to be negligible.

TABLE I

θ, deg	C, mb	k, Mev$^{-1/2}$
30	4.1	0.12
45	3.3	0.28
60	2.1	0.35
75	1.4	0.40
90	0.4	0.37
105	0.3	0.32
120	0.2	0.28
135	0.4	0.31
150	0.7	0.33
165	1.5	0.37

The cross sections for the knock-out of fast α particles by nucleons was carried out for He_2^4 nuclei with kinetic energies W = 0, 5, 10, and 20 Mev. The binding energy of the α particle in the nucleus (B = 4 Mev) was also taken into account. According to Igo and Thaler[8] the depth of the potential well of the Ag nucleus for α particles is approximately 35 Mev and one can therefore assume that in the heavy nuclei the α particles will have energies up to 30 Mev. This figure should probably be reduced for the lighter nuclei.

We are interested in those cases of elastic collisions between a nucleon of energy E and an α group of kinetic energy W, which cause the latter to leave the nucleus with energy T > 30 Mev. Obviously T depends not only on E, W, and the scattering angle θ, but also on the relative directions of the initial momenta of the nucleon and of the target particle. We denote the angle between these two vectors by $\varphi (0 \leq \varphi \leq \pi)$.

The resultant velocity of the recoil particle depends, in the laboratory system, also on the angle of rotation of the scattering plane relative to the plane that is determined by the initial momenta of the colliding particles (we shall denote this angle by β). Figure 2 illustrates the geometry of the collision. Using the laws of elastic collision between two moving particles in the nonrelativistic form, and using the geometric relations derived from Fig. 2, we obtain the condition that must be satisfied by the quantities, E, W, θ, φ, and β if the α particle is to leave the nucleus with energy greater than 30 Mev:

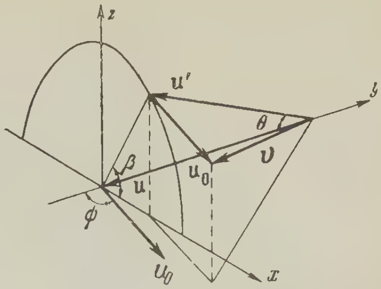

FIG. 2. Velocity vector diagram: xy – plane defined by the vectors of the momenta of the incident nucleon and of the α particle, **u** – velocity of the α particle in the c.m.s. prior to colliding with the nucleon, **u'** – the same after colliding with the nucleon, $\mathbf{u}_0$ – velocity of the center of mass, **v** – velocity of the recoil α particle in the laboratory system; θ – scattering angle in the c.m.s.

$$\begin{aligned} &1.5\sqrt{EW}\cos\varphi + (\cos\theta\cos\psi + \sin\theta\sin\psi\cos\beta) \\ &\quad\times\Big\{E^2 + W^2 + \frac{17}{4}EW - 4EW\cos^2\varphi \\ &\quad+ 3(E - W)\sqrt{EW}\cos\varphi\Big\}^{1/2} \geqslant 3.1B + 94 + W - E. \end{aligned} \tag{2}$$

The angle ψ is determined from the relation

$$\cot\psi = \frac{-4\sqrt{EW}\cos\varphi + \sqrt{EW} - 2(E - W)}{5\sqrt{EW}\sin\varphi}. \tag{3}$$

Inequality (2) defines the region of permissible values of φ and β for specified E, W, and θ. The cross section of interest to us, that for differential scattering with production of a fast α particle, is

$$\frac{d\sigma(E, W, \theta)}{d\omega} = \iint \frac{d\sigma_0(E, W, \theta, \varphi)}{d\omega} P(E, W, \theta, \varphi, \beta)\, d\varphi d\beta, \tag{4}$$

where $d\sigma_0/d\omega$ is the cross section for scattering the free α particles, taken from Eq. (1) with allowance for the dependence of the particle energy on the angle φ; P is the statistical weight of the states in which φ and β satisfy condition (2).

It is natural to assume that the distribution of the intranuclear α particles is isotropic with respect to the directions of their momenta, and also that the scattering is actually symmetrical (i.e., the cross section is independent of β). Then

$$\frac{d\sigma}{d\omega} = \frac{1}{2\pi}\int_0^{\pi} \frac{d\sigma_0}{d\omega}\beta_{max}(\varphi)\sin\varphi d\varphi. \tag{5}$$

The value of β_{max} is determined as a function of φ, θ, E and W from Eq. (2).

The cross section curve represented by Eq. (5)

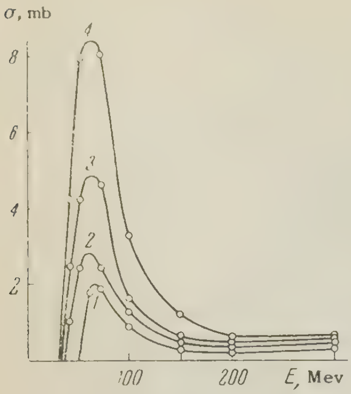

FIG. 3. Cross section for the knock-out of an α particle with energy greater than 30 Mev by a nucleon of energy E, at various energies of motion of the α particle in the nucleus. 1) for W = 0; 2) W = 5; 3) W = 10; 4) W = 20 Mev.

can be integrated over all possible angles θ, starting with a certain $\theta_{\min}$, to find the total cross section for the knock-out of a fast alpha particle by a nucleon of energy E. We note that in our case the nucleon energy must be reckoned from the bottom of the potential well, since it will exceed the energy of the nucleon outside the well by approximately 30 Mev.

Figure 3 shows points corresponding to the calculated cross sections for various choices of the initial α-particle kinetic energy.

PROBABILITY OF EXISTENCE OF ALPHA PARTICLES IN THE NUCLEUS

The curves shown in Fig. 3 indicate that the most effective region for the knock-out of alpha particles with T > 30 Mev is the nucleon-energy region from 50 – 70 Mev (corresponding to nucleon energies from 30 – 50 Mev outside the nucleus), and that the cross section decreases with further increase in energy. The dependence $\sigma_\alpha(E)$ shown in Fig. 4 is evidence, however, of the opposite: as the energy of the bombarding protons increases, the probability of emission of fast α particles increases monotonically. This contradiction can be eliminated by assuming that the emission of the α particle is due to secondary nucleons produced in the nuclear cascade process, the number of which increases continuously with increasing beam energy. One can then assume approximately that the yield of α particles per single nuclear disintegration induced by a proton of energy E_0 will be

$$\sigma_\alpha(E_0)=\int_0^{E_0}\sigma(E)\,n(E)\,N_{\text{eff}}\,dE. \tag{6}$$

Here $\sigma(E)$ is the cross section shown in Fig. 3, n the number (per disintegration) of cascade nucleons of energy E passing through a nuclear surface layer that contains N_{eff} alpha particles.

We introduce a quantity w, defined by the relation

$$N_{\text{eff}}=Nw, \tag{7}$$

where N is the maximum possible number of α groups in the surface layer. The size of this layer is determined, as already indicated, by the free path of the α particle in the nuclear matter. In accordance with experiment[7-9], we assume that the latter is 2.5×10^{-13} cm. If we take the density distribution functions of the nucleons in the nucleus in the following form[20]

$$\rho(r)=\rho_0\,\frac{1+\exp(-c/a)}{1+\exp[(r-c)/a]},$$

we obtain N = 12 for Ag and Br. For the light nuclei, we can assume N = 3.

The unknown quantity in (6), which can be written in the following form

$$\sigma_\alpha(E_0)=Nw\bar{n}(E_0)\int_0^{E_0}f(E)\,\sigma(E)\,dE, \tag{6a}$$

is w, since σ_α is measured experimentally, and the average number of cascade nucleons n and their energy distribution f(E) can be calculated by the Monte Carlo method.[21] The probabilities w for the existence of α groups, calculated from (6a), are listed in Table II.

Figure 4 shows the mean value of w vs. the energy W. If it is assumed that the kinetic energy of the α particles in the nucleus amounts to 10 Mev, it follows from our calculations that in light nuclei such as C^{12} and O^{16}, and also in the diffusion region of the heavy nuclei, the nucleons spend half their lifetimes in the form of alpha complexes.

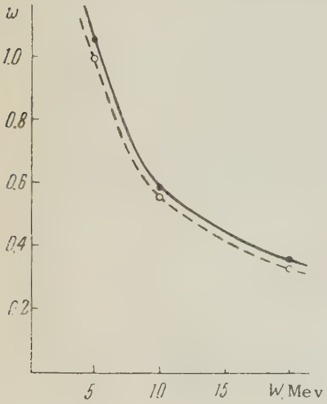

FIG. 4. Dependence of the calculated value of w on the assumed value of the energy of internal motion of the α particles, W, in light (open circles) and heavy (full circles) emulsion nuclei.

DISCUSSION OF THE RESULTS

The values of w, found in our experiments, remain approximately constant as the energy of the incident protons changes. This circumstance serves as an indication of the correctness of the chosen model for the production of fast α particles. There is no assurance, however, that these calculations are not subject to systematic errors

TABLE II

E_0, Mev	Nuclei Ag and Br				Nuclei C, O, N			
	W, Mev							
	0	5	10	20	0	5	10	20
100	2,19	1.00	0,56	0.34	2.40	1.05	0.62	0.37
140	1,99	0,91	0,51	0.32	2.01	0.93	0,52	0,31
200	2.04	0,93	0,54	0.32	2.19	0,99	0.57	0,34
360	2.60	1,07	0.58	0.36	2.15	1.02	0,54	0.32
560	2.61	1.21	0,66	0,41	2.01	0,95	0,55	0,33
660	2.58	1.17	0,65	0.40	2.14	1.00	0.58	0.34
average	2.33	1.05	0.58	0.36	2.15	0,99	0,56	0,33

which may either overestimate or underestimate w by the same amount for all beam energies. This pertains primarily to the cross sections used for the elastic scattering of the nucleons by the free α particles, and also to the extrapolation of Eq. (1). In addition to this source of error, there exist others, for example, corrections for the probability of emission of a recoil α particle from the surface layer of the nucleus, for the effect of the Pauli principle (which forbids certain collisions between nucleons and α particles) etc., none of which are accounted for here. These factors result in an increase of w. Factors that contribute to a decrease of w include: the presence among the observed fast α particles of a certain fraction of particles due to some other mechanism (for example, according to Ostroumov et al.,[15] the admixture of evaporated α particles with energies > 30 Mev amounts to $5-10\%$), the presence in the nucleus of α particles with greater velocities than assumed by us, the knock-out of alpha particles by cascade nucleons, which for some reason or another do not leave the nucleus, and consequently are not taken into account in the calculations by the Monte Carlo method, etc.

As can be seen from Fig. 2, the principal contribution to the process of impact production of fast α particles is from nucleons with energies $60-70$ Mev, scattered at angles of approximately $120-150°$. In the laboratory system, the α particle moves after the collision in a direction close to the initial direction of the nucleon. But since we take $\bar{n}$ in Eq. (6a) to mean the number of observed nucleons, i.e., the cascade nucleons that leave the nucleus, the direction of motion of the α particle will also be such that the latter is capable of leaving the nucleus. Nor is allowance for the Pauli principle likely to cause great changes in the calculations. In fact, a 70-Mev nucleon colliding with an α particle loses approximately 35 Mev and remains with an energy greater than the Fermi level. Furthermore, one can assume that the formation of nucleon complexes will contribute to a weakening of the effect of the Pauli principle.

As regards the correctness of the choice of the W, nothing more specific can be added to what has already been said in the introduction. In all probability there is a certain distribution of α particles by momenta in the nucleus, and perhaps, as shown by the results of Cüer,[11] this distribution is quite broad; without knowing its form, it is difficult to calculate the contribution of the high-energy α particles to the computed cross section. As to the correctness of the extrapolation of Eq. (1), it is seen from Fig. 1 that nucleons with energies $200-300$ Mev contribute little to the total cross section and possible errors in the extrapolation will not affect greatly the calculated values of w. Summarizing, we can assume that the foregoing factors, not accounted for in our calculation, act in opposite directions and cancel each other out to a considerable extent. It should be added that the value of w is quite sensitive to the form of the energy spectrum of the cascade nucleons, particularly in the region of small energies, and that a modification of the form of the function $f(E)$, which changes with changing energy of the bombarding proton, may lead to a certain modification of w.

The value of w can also be estimated for the Ag and Br nuclei by using the data of Ostroumov,[22] in which the relative contribution of cascade α particles of all energies is determined. This estimate leads to $w \sim 0.5-0.6$, which does not disagree greatly with our results and the data of Hodgson.[13] It should be noted that Hodgson assumed $N = 15$ for heavy nuclei and a $N = 3.3$ for light nuclei, while in our calculations these values are respectively 12 and 3.

It can be assumed that a certain fraction of the tracks of doubly-charged particles in the stars belongs to the He_2^3 nuclei. The emission of nuclei of the light helium isotope is connected, apparently, with the same processes as the emission of α particles. An additional source may be the reaction produced when an α particle is struck by a fast nucleon [for example, of the type $He_2^4(p, d)He_2^3$]. It would be interesting to determine experimentally the relations between the yields of the isotopes of He and H, due to the impact mechanism, and to compare them with the cross sections of the corresponding processes. This would throw light on the probability of realization of various groupings of nucleons in the nuclei.

A considerable similarity was established in reference 15 between the emission of fast α particles and that of fragments. This similarity, in light of the results of the present paper, can serve as a certain basis for stating that multiply-charged particles are emitted from a nucleus, to a considerable extent, via elastic or quasi-elastic collisions between nucleons or their complexes and corresponding instantaneous nuclear substructures. It appears to us therefore that further research in this direction is of importance, not only to clarify the nature of fragmentation but also from the point of view of understanding the internal structure of the nucleus.

In conclusion, the authors express their gratitude to O. V. Lozhkin for help in the performance of the experiment, to E. I. Prokof'eva, N. R. Novikova, and E. V. Fadina for preparation of the plates. The authors are also indebted to N. A. Perfilov for continuous attention to the investigation and for participation in the discussion of the results.

---

[1] Brueckner, Eden, and Francis, Phys. Rev. **98**, 1445 (1955).

[2] H. A. Bethe, Phys. Rev. **103**, 1353 (1956).

[3] A. I. Baz', JETP **31**, 831 (1956), Soviet Phys. JETP **4**, 704 (1957).

[4] M. Rotenberg and L. Wilets, Phys. Rev. **110**, 1126 (1958).

[5] Azhgireĭ, Vzorov, Zrelov, Meshcheryakov, Neganov, and Shabudin, JETP **33**, 1185 (1957), Soviet Phys. JETP **6**, 911 (1958).

[6] M. Q. Barton and J. H. Smith, Phys. Rev. **110**, 1143 (1958).

[7] C. E. Porter, Phys. Rev. **100**, 1400 (1955).

[8] G. Igo and R. M. Thaler, Phys. Rev. **106**, 126 (1957).

[9] H. J. Watters, Phys. Rev. **103**, 1763 (1956).

[10] Cüer, Combe, and Samman, Compt. rend. **240**, 1527 (1955); P. Cüer and J. Combe, J. phys. radium **16**, 29 (1955); J. Combe, J. phys. radium **16**, 445, 1955; J. Combe, Suppl. Nuovo cimento **3**, 182 (1956).

[11] P. Cüer and A. Samman, J. phys. radium **19**, 13 (1958).

[12] Yu. I. Serebrennikov, Dissertation, Leningrad Polytech. Inst., 1959.

[13] P. E. Hodgson, Nucl. Phys. **8**, 1 (1958).

[14] L. J. Schiff, Phys. Rev. **98**, 1281 (1955).

[15] Ostroumov, Perfilov, and Filov, JETP **36**, 367 (1959), Soviet Phys. JETP **9**, 254 (1959).

[16] E. L. Grigor'ev and L. P. Solov'eva, JETP **31**, 932 (1956), Soviet Phys. JETP **4**, 801 (1957); Bernardini, Booth, and Lindenbaum, Phys. Rev. **85**, 826 (1952); Lees, Morrison, Muirhead, and Rosser, Phil. Mag. **44**, 304 (1953); S. Jannelli and F. Mezzanares, Nuovo cimento **4**, Suppl. No. 2, 939 (1956). L. S. Vermain, Phys. Rev. **82**, 596 (1951).

[17] P. A. Vaganov and V. I. Ostroumov, JETP **33**, 1131 (1957), Soviet Phys. JETP **6**, 871 (1958).

[18] P. E. Hodgson, Adv. Phys. **7**, 25 (1958).

[19] J. Heidmann, Phil. Mag. **41**, 444 (1950).

[20] L. R. B. Elton, Nucl. Phys. **5**, 173 (1958).

[21] Morrison, Muirhead, and Rosser, Phil Mag. **44**, 1326 (1953); Bernardini, Booth, and Lindenbaum, Phys. Rev. **88**, 1017 (1952); Metropolis, Bivins, Storm, Miller, Friedlander, and Turkevich, Phys. Rev. **110**, 204 (1958).

[22] V. I. Ostroumov, JETP **32**, 3 (1957), Soviet Phys. JETP **5**, 12 (1957).

Translated by J. G. Adashko
127

FORMATION OF NEGATIVE HYDROGEN IONS ON AN INCANDESCENT TUNGSTEN SURFACE

V. I. KHVOSTENKO and V. M. DUKEL'SKIĬ

Leningrad Physico-Technical Institute, Academy of Sciences, U.S.S.R.

Submitted to JETP editor April 13, 1959

J. Exptl. Theoret. Phys. (U.S.S.R.) 37, 651-653 (September, 1959)

Formation of H^- ions on an incandescent tungsten surface has been observed. The temperature dependence of the ratio of the negative-ion current to the electron current in the 2600 — 2900° K range yields a value of 0.8 ± 0.1 ev for the electron affinity of the hydrogen atom.

ACCORDING to quantum-mechanical calculations, the electron-affinity energy of the hydrogen atom is 0.754 ev.[1] Using this value, it is easy to calculate from the Saha-Langmuir formula that the probability of alpha capture of an electron by a hydrogen atom, evaporated from the surface of tungsten at 2400° K, is 6×10^{-9} (assuming the work function of the tungsten to be 4.5 ev).

In the case of such small α, one must take into account, in a study of the negative surface ionization, the possibility of formation of negative ions not only on the surface of the cathode, but also under the surface, via interaction between the thermionic electrons emitted from the cathode and the gas molecules. In the case of hydrogen, the processes in the volume may be: 1) formation by impact of H^- ions from molecules H_2, and also from the H_2O molecules that are always present in the residual gas in the equipment; 2) radiative capture of slow electrons by the hydrogen atoms, produced upon dissociation of the hydrogen molecules on the surface of the incandescent tungsten.

We have shown earlier[2] that H^- ions are not produced from H_2 and H_2O molecules by collision with electrons of energy less than 5 ev. To eliminate such H^--ion production it was enough to create in the surface-ionization experiments conditions under which the electrons emitted by the cathode could not acquire an energy greater than 5 ev. Under the conditions of our experiment, the effect of radiative capture was small compared with surface ionization, and could therefore be neglected.*

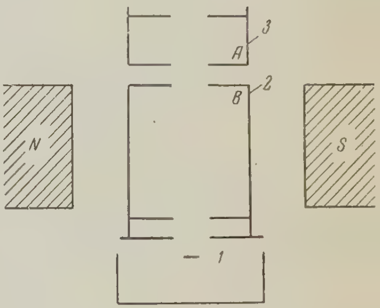

FIG. 1. Diagram of the ion source. 1 – tungsten ribbon 1.5 × 10 mm (cathode), 2 – cylinder (anode), 3 – mass-analyzer tube.

Figure 1 shows schematically the apparatus used. The cathode was an electrically-heated incandescent tungsten ribbon 1. The temperature of the central portion of the ribbon was measured with an optical pyrometer. The potential difference V used to draw out the electrons and negative ions was applied between the cathode 1 and cylinder 2. This potential difference was not more than 4 volts, to prevent the electrons that enter cylinder 2 together with the ions from producing H^- ions in this volume. The electrons were deflected by a transverse magnetic field of ~ 60 oe to the wall of cylinder 2 and were kept out of the space AB, where the negative ions (which were hardly moved by the magnetic field) were accelerated to 1000 ev before entering the mass analyzer 3. The ion current was measured with an electron multiplier connected to an electrometer amplifier.[2]

We first ascertained what occured in the apparatus with the cathode incandescent, but in the absence of hydrogen. For this purpose, after establishing maximum vacuum (1×10^{-6} mm Hg) in the equipment and adjusting the mass analyzer for H^--ion registration, we measured the ion current for various values of the drawing potential V. At a cathode temperature of 2300° K, no H^- ions could be observed for V ranging from 0.1 to 3.5 v. The H^--ion current became measurable at $V = 3.7$ volts and increased rapidly with increasing V. These ions were apparently due to the interaction between the electrons and the traces of water vapor in the apparatus.

---

*The ratio of the H^--ion current due to radiative capture to the current due to surface ionization is approximately $4n_e\overline{Q}d/\overline{v}\alpha$, where n_e is the number of electrons emitted from 1 cm² of cathode surface per second, $\overline{Q}$ the mean value of the effective cross section for radiative capture (at an electron energy of 1 ev, $Q = 2 \times 10^{-22}$ cm² at the maximum[3]), d the length of the path on which the capture can take place, $\overline{v}$ the mean velocity of the H atoms evaporated from the cathode, and α is the degree of surface ionization. At a cathode temperature of 2700°K and d = 0.1 cm, this ratio was less than 0.02.

When hydrogen was admitted to the instrument (pressure $\sim 10^{-4}$ mm Hg) we observed H^- ions even at drawing potentials from 0.5 to 3.5 volts. Under these conditions we observed clearly the effect of surface ionization, undistorted by the interaction of the electrons with the H_2O and H_2 molecules. We measured in this interval of V the dependence of the H^--ion current I_i at the output of the mass spectrometer on the temperature T of the cathode, within the range from 2200 to 2900° K. Simultaneously we measured the electron current I_e in cylinder 2. Figure 2 shows one of the curves obtained for the dependence of the ratio I_i/I_e on the cathode temperature. The current I_i was on the order of 10^{-16} amp; the noise level was smaller by a factor 10 − 20.

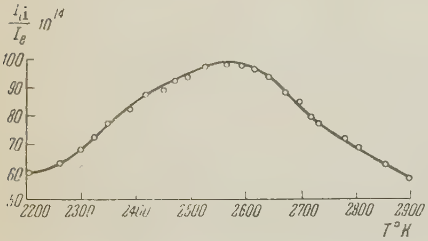

FIG. 2. Dependence of the ratio of the H^--ion current to the electron current on the cathode temperature (hydrogen pressure 2×10^{-4} mm Hg, V = 3.0 v).

It is known that observation of surface ionization with production of negative ions can be used to determine the electron affinity ϵS of an atom. At $\alpha \ll 1$, the negative-ion current density is given by

$$i_i = \varepsilon n_0 A \exp\{\varepsilon(S - \varphi^*)/kT\}, \tag{1}$$

where n_0 is the number of atoms evaporated from 1 cm^2 of cathode surface per second, and $\epsilon\varphi^*$ is the effective work function of the Saha-Langmuir formula for a polycrystalline surface. The saturation electron current density is determined from the Richardson-Dushman formula

$$i_e = BT^2 \exp(-\varepsilon\varphi_R / kT). \tag{2}$$

In the case of an inhomogeneous surface the electron emission, like the emission of negative ions, is predominantly from sections that have the low work function. This may justify setting φ^* in Eq. (1) equal to φ_R in Eq. (2). After having done this and after taking the ratio i_i/i_e, we can eliminate φ

$$\frac{i_i}{i_e} = \frac{\varepsilon n_0 A}{BT^2} \exp(\varepsilon S/kT), \tag{3}$$

hence

$$\log_{10} \frac{i_i T^2}{i_e} = \log_{10} \frac{\varepsilon n_0 A}{B} + \frac{5.04 \cdot 10^3}{T} S. \tag{4}$$

Ionov[4] confirmed experimentally the correctness of Eq. (4) in the case of formation of negative iodine ions on the surface of tungsten. Under the conditions of our experiments, the electron current was far from its saturation value (2 or 3 orders of magnitude less). It must be assumed, however, that (3) and (4) should be valid also in the absence of saturation, since the energy distributions of the ions and electrons emitted from the surface of the incandescent metal are the same.[5]

It is seen from Fig. 2 that in the interval from 2200 to 2550° K the ratio I_i/I_e increases with temperature. At these temperatures, apparently, the coefficient of dissociation of hydrogen molecules on the surface of tungsten is still less than unity and therefore n_0 depends on the temperature. To determine the energy of the electron affinity from (4), we used the temperature interval from 2600 to 2900° K, in which n_0 can be assumed constant. In this temperature interval, the points corresponding to the value of $\log_{10}(I_i T^2/I_e)$ as functions of $5.04 \times 10^3/T$ fit well a straight line. The value of the energy of electron affinity ϵS of the hydrogen atom, determined from the slope of this line, was found to be 0.8 ± 0.1 ev.

The correctness of the value obtained (in spite of its low accuracy) can be considered as a successful test of our method. In this connection, prospects are uncovered of using surface ionization to determine the electron affinities of other atoms, for which this quantity is of the same order of magnitude as for the hydrogen atom.

---

[1] E. A. Hylleraas and J. Midtal, Phys. Rev. **103**, 829 (1956); **109**, 1013 (1958).

[2] V. I. Khvostenko and V. M. Dukel'skiĭ, JETP 33, 851 (1957), Soviet Phys. JETP 6, 657 (1958).

[3] S. Chandrasekhar, Astrophys. J. **102**, 223 (1945).

[4] N. I. Ionov, JETP 17, 272 (1947).

[5] N. I. Ionov, JETP 18, 96 (1948).

Translated by J. G. Adashko
128

PRODUCTION OF COMPOUND NUCLEI BY BOMBARDMENT OF V *AND* Nb *WITH* O^{16}, C^{12}, *AND* C^{13} *IONS*

A. S. KARAMYAN and A. A. PLEVE

Submitted to JETP editor April 17, 1959

J. Exptl. Theoret. Phys. (U.S.S.R.) **37**, 654-662 (September, 1959)

The production of compound nuclei in the reactions $V^{51}_{23} + O^{16}_{8} \to Ga^{67}_{31}$ and $Nb^{93}_{41} + C^{12,13}_{6} \to Ag^{105,106}_{47}$ was investigated. The results are given in the form of excitation functions for the evaporation of different numbers of nucleons. Comparison of these reactions with reactions induced by light particles and involving compound nuclei close to Ga^{67} and Ag^{105} shows that in the case of heavy ions evaporation of a specified number of nucleons occurs at a somewhat higher excitation energy. A possible explanation is that the large angular momentum which the heavy ion contributes to the compound nucleus significantly affects the deexcitation process.

Along with the production of a compound nucleus and subsequent evaporation of nucleons, reactions were observed in which very energetic particles were emitted (60 Mev with two particles). This is not consistent with the statistical theory.

INTRODUCTION

THE production of compound nuclei by bombarding medium-weight nuclei with multiply-charged heavy ions was studied in reference 1, where the cross sections for the reactions

$$V^{51}(C^{12},\ 2n)Cu^{61} \text{ and } V^{51}(N^{14},\ xn)Zn^{65-x},\ x = 1,2,\ldots,\ 5$$

were reported as functions of ion energy. In agreement with the statistical theory the excitation functions that were obtained were characteristic of neutron evaporation from uniformly heated compound nuclei. At high excitation energies, however, instead of the expected sharp falling-off of the cross section for the emission of two or three neutrons the curves were relatively flat over an interval of a few dozen Mev.

This shape of the excitation function for reactions induced by protons is accounted for by a direct interaction between the incident particle and individual nucleons of the target nucleus. Neutrons emitted as a result of such interactions possess energies considerably exceeding the energies of neutrons evaporated from compound nuclei in thermodynamic equilibrium. For reactions involving multiply-charged ions this effect was accounted for in reference 1 by the idea of "local heating," the possibility of which was pointed out by Bethe[2] in 1938. According to Bethe, because of the extremely short mean free path of the incident particle in nuclear matter the entire excitation energy is distributed among a few nucleons and evaporation from a heated "spot" can take place before thermal equilibrium of the entire system is established. As a result of this mechanism, evaporating nucleons will obviously carry away energy much higher than that corresponding to the temperature of a uniformly heated nucleus. At high excitation energies 2 or 3 neutrons can therefore be emitted instead of 4 or 5, with correspondingly higher energies. This can account for the flat portions of the excitation functions at high energies for reactions with the emission of 2 or 3 neutrons. The detection of a similar effect when 4 or 5 neutrons are emitted would require considerably higher ion energies than those used in our experiments.

For the purpose of elucidating the reactions induced by multiply-charged ions we compared the excitation functions for these reactions with the corresponding functions for the reactions $Cu^{63,65}(p, xn)Zn$, where $x = 1, 2, \ldots, 5$.[3] When copper is irradiated by protons the compound nuclei Zn^{64} and Zn^{66} are formed, which are close to the compound nuclei Cu^{63} and Zn^{65} that result when vanadium is bombarded by carbon and nitrogen. It was found that the excitation functions for the evaporation of a specified number of neutrons in reactions induced by multiply-charged ions are shifted by 10 to 15 Mev toward higher excitation energies. This shift may result from the fact that compound nuclei may have different momenta depending upon whether they were formed by the fusion of target nuclei with ions or with protons. For example, the compound nucleus Zn^{64} with 80

Mev excitation energy, resulting from the $Cu^{63} + p$ reaction, has maximum angular momentum $L_{max} \approx 10\ \hbar$; the Zn^{65} nucleus with the same excitation energy, resulting from the $V^{51} + N^{14}$ reaction, has $L_{max} \approx 50\ \hbar$.

The present work has continued the study of interactions between multiply-charged ions and medium-weight nuclei, with special attention to the departures from the evaporation model. At the Atomic Energy Institute of the USSR Academy of Sciences 102-Mev oxygen ion beams were produced, making it possible to extend the investigation of interactions between multiply-charged ions and vanadium. The interactions of accelerated C^{12} and C^{13} ions with niobium were also studied.

EXPERIMENTAL PROCEDURE

The excitation functions for the reactions $V^{51}(O^{16}, xn)Ga$ and $Nb^{93}(C^{12,13}, xn)Ag$ were derived by measuring the activity induced in stacked foils. In earlier experiments vanadium had been deposited on an aluminum backing, but in the present experiment the foils were made of pure vanadium and niobium.* An activation analysis showed a lead content in the niobium of not more than 0.006%. The absence of a backing made chemical separation unnecessary and increased the likelihood of detecting products with half-lives of the order of a few minutes. This procedure also eliminates errors involved in the determination of the chemical yield and from the residual background of the backing material, and considerably reduces the error in determining the thickness of the target material.

Foils 2 to 3 μ thick were used for convenience of measurement and were irradiated in the internal beam of the 150-cm cyclotron. The energies of the O^{16}, C^{13}, and C^{12} ions were 102, 83, and 77 Mev, respectively. In reference 4 the beam was determined to be monoenergetic to within 2%, from the line width at half maximum. The entire energy spectrum of accelerated C^{12} ions was specially studied at the cyclotron terminal radius, and it was found that low-energy ions constituted only a few per cent of the total beam intensity.

Reactions were identified mainly by means of the half-lives of β-active products. In some instances additional information for the identification was obtained by determining the end-point energies of β spectra associated with specified half-lives; for this purpose aluminum absorbers were used. β particles were recorded by means of standard apparatus employing end-window counters and special holders which insured identical counting conditions for all foils and which permitted variation of the solid angle.

The apparatus used in absolute activity measurements was calibrated by means of a counter with known efficiency, which was available through the kindness of S. A. Baranov.

INTERPRETATION OF MEASUREMENTS

Lifetimes and decay schemes in the isotope tables of reference 5 were used in calculating cross sections. This information for the reactions of interest is shown more compactly in Figs. 1 and 2, using the conventional notation. For nuclei with unknown relative β-decay probability in the positron-capture branch it was assumed that all decay takes place through the emission of positrons. Therefore in such cases only the lower limits of the cross sections were determined; the corresponding excitation functions are represented by dashed lines in the figures. Excitation energies were calculated using tabulated nuclear masses,[6] as follows:

$$E^* = (m_1 + m_2 - M)\,c^2 + \frac{m_2}{m_1 + m_2} E,$$

where m_1, m_2, and M are respectively the masses of the incident ion, the target nucleus and the compound nucleus in its ground state, and E is the kinetic energy of the ion at the foil. E was determined from stopping powers given in reference 7 and the experimental range-energy curves for accelerated carbon and oxygen ions in Al, Cu, and Ni given in reference 4.

Since compound nuclei resulting from reactions with heavy ions possess considerable recoil energy, in determining the energy dependence of cross sections it was necessary to introduce a suitable correction to account for the passage of recoil nuclei from one foil to another. To this end we determined separately the mean range in vanadium of Ga^{67} nuclei produced in the $V^{51} + O^{16}$ reaction. When 102-Mev oxygen ions are used, the energy of the Ga^{67} recoil nuclei is 24 Mev; reference 8 gives for fission fragments in this energy region the following approximate expression for the range-energy relation:

$$R = R_0 (E/E_0)^{1/2}.$$

When R_0 is determined experimentally at E_0

---

*Pure vanadium which could be rolled was provided by M. S. Makunin, a graduate student at the Metallurgical Institute, U.S.S.R. Academy of Sciences. In rolling the vanadium and niobium we were greatly assisted by B. V. Blinov of the All-Union Institute of Measurements, and by V. M. Plotko of the Joint Institute for Nuclear Research.

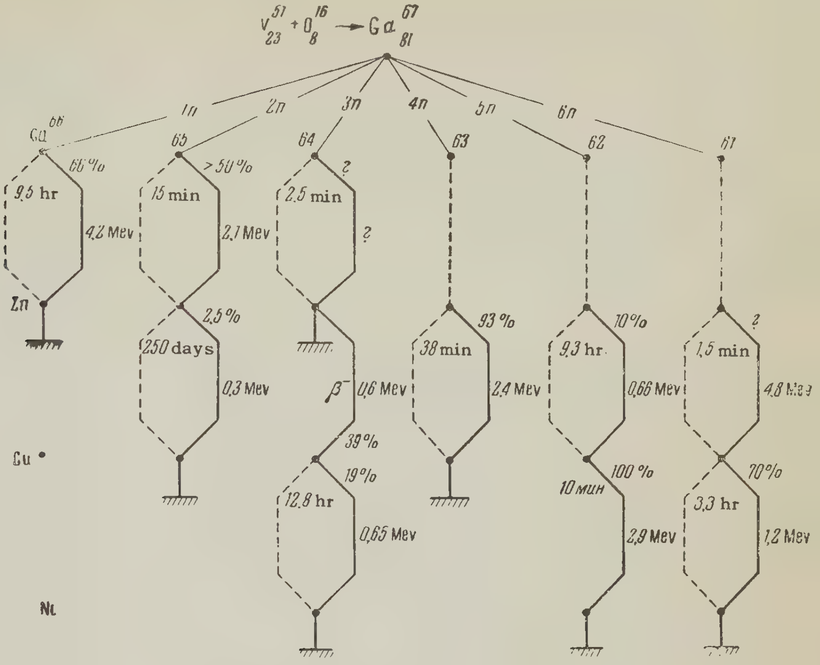

FIG. 1. Scheme of nucleon-emission and radioactive-product decay for the reaction $V^{51} + O^{16}$.

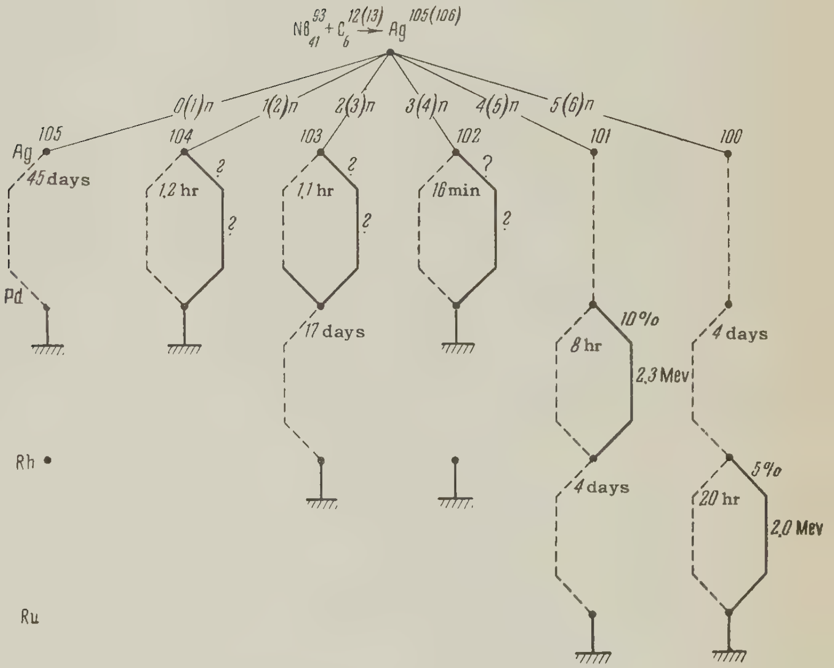

FIG. 2. Scheme of nucleon-emission and radioactive-product decay for the reaction $Nb^{93} + C^{12,13}$.

= 24 Mev, this formula enables us to calculate R for other energies. The calculation showed that the correction to the excitation functions to account for compound-nucleus recoil is almost independent of energy; a common shift is found for all excitation functions toward higher energies, amounting to 4 and 1 Mev for vanadium and niobium, respectively.

ESTIMATE OF ERROR

The sources of systematic errors in our experiments may have been errors associated with the measurements of ion currents, inaccurate branching ratios in the tables, calibration of the measuring equipment by means of a 4π counter and additional unaccounted-for systematic errors. When we exclude the last possibility the total systematic error of our cross section values should not exceed 17%.

Accidental errors which can distort excitation functions are much more important; these may arise through inaccurate analysis of the decay curves (5%), inaccurate weighing of the foils (1%) and inexact correspondence of foil positions with respect to the counters (2%). Our estimates thus show that the relative cross sections were determined to within 8%.

The initial ion energies given in reference 4 were determined to within 2%; this degree of error thus applies to the energy at the first foil. As the ions are slowed down the error increases and amounts to 10% at the last foil.

RESULTS

Figures 3 — 5 show the excitation functions of various reactions resulting from the irradiation of vanadium by oxygen and of niobium by carbon. The numbers of protons and of neutrons emitted by the compound nuclei are indicated without representing the order of their emission. The dashed lines pertain to reactions for which only the lower limits of the cross sections were determined. We shall now consider the curves for vanadium and niobium in greater detail.

Vanadium. The complete fusion of O^{16} and V^{51} results in compound nuclei of Ga^{67} with excitation energies from 39 to 90 Mev. The lower limit of the excitation energy represents kinetic energy of the oxygen ions which equals the Coulomb threshold of the reaction; the upper limit is the maximum ion energy, which was 102 Mev in our experiments.

Figure 3 shows that in the given range of excitation energies the compound nucleus decays through the emission of both neutrons and protons, with the number of evaporated particles varying from 2 to 5. The probability for the evaporation of a single neutron is evidently very small for excitation energies exceeding 40 Mev. We were unable to detect a reaction product accompanied by the emission of only a single neutron, and the cross section for such a reaction must therefore be considerably smaller than 1 mb.

The β^+ activity of Ga^{65} was used to record the reaction (O^{16}, 2n); in this case we know only that the positrons represent more than half of the total number of decays. In the calculation of the cross section it was assumed that Ga^{65} emits only positrons; therefore the true cross section lies somewhere below twice the given value. The variation of this cross section was studied up to excitation energies of 60 Mev; at higher energies uncertainty results from the decay of Cu^{62}, which is produced in the reaction (O^{16}, 2p3n) and has a half-life close to that of Ga^{65}.

The (O^{16}, 3n) reaction was identified in a somewhat unusual manner. Reaction products in almost all foils of the pile exhibited β activity with a half-life of 2.8 hours and an end-point energy of 0.6 Mev. The shape of the excitation function and the position of its peak indicate that this activity can only result from the emission of 3 or 4 particles. The reactions (O^{16}, 3p) and (O^{16}, p2n) result in stable nuclei, and the (O^{16}, 2pn) reaction is easily identified from the 12.8-hour half-life of Cu^{64}. All possible reactions involving the emission of four particles are excluded similarly; this activity was therefore assigned to Ga^{64}, which is the reaction product that accompanies three neutrons.

This identification is possible if we assume either that a) the tabular value of the Ga^{64} half-life is incorrect or b) Ga^{64} had an isomeric state

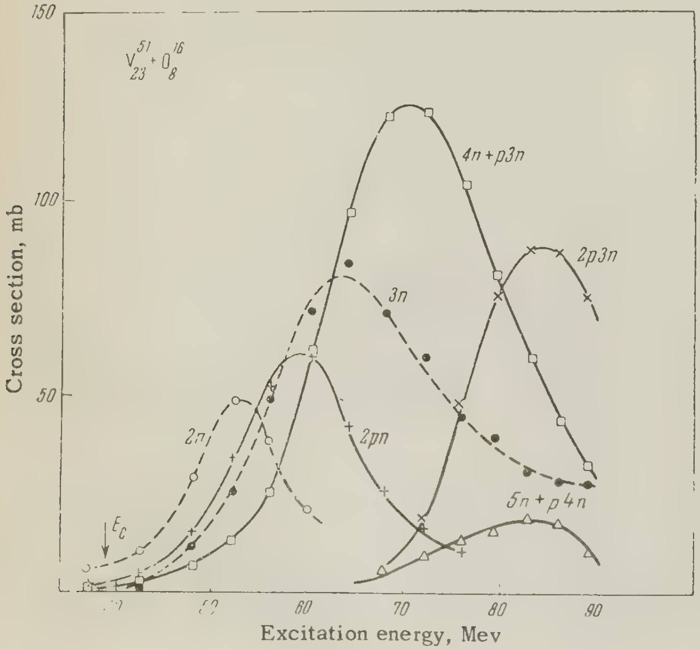

FIG. 3. Excitation functions for the reaction $V^{51} + O^{16}$.

with a half-life of 2.8 hours. The slow falling-off of the excitation function above 75 Mev may possibly result from the fact that at such energies the reactions (O^{16}, 6n) and (O^{16}, p5n) can occur, resulting in the formation of Cu^{61}, which has a similar half-life of 3.3 hours and 1.2-Mev end-point energy. Such activity corresponding to an excitation energy of 75 Mev was actually detected among the foils. Cu^{64} as the product of (O^{16}, 2pn) is easily detected from its 13-hour β activity with the spectral limit $E_\beta \sim 0.5$ Mev. The excitation functions of (O^{16}, 4n) and (O^{16}, p3n) are combined since both reactions are identified by the same product Zn^{63}, with a half-life of 38 minutes and 2.4-Mev β end-point energy. Ga^{63}, the product of a "4n" reaction, is unknown but apparently has a short half-life.

The situation is similar with respect to the reactions (O^{16}, 5n) and (O^{16}, p4n), which are recorded by means of the 9.3-hour emission from Zn^{62}. In this case a complication results from the small difference between the half-lives of Zn^{62} and of Cu^{64}, which is formed in a 2pn reaction. The separation of the products according to β-particle energies is not especially accurate.

In the 75 — 90 Mev range of excitation energies 10-minute β activity was observed, with a peak which indicates that it must be associated with the emission of 5 or 6 particles. Figure 1 shows that this activity can only result from (O^{16}, 2p3n), which produces Cu^{62}.

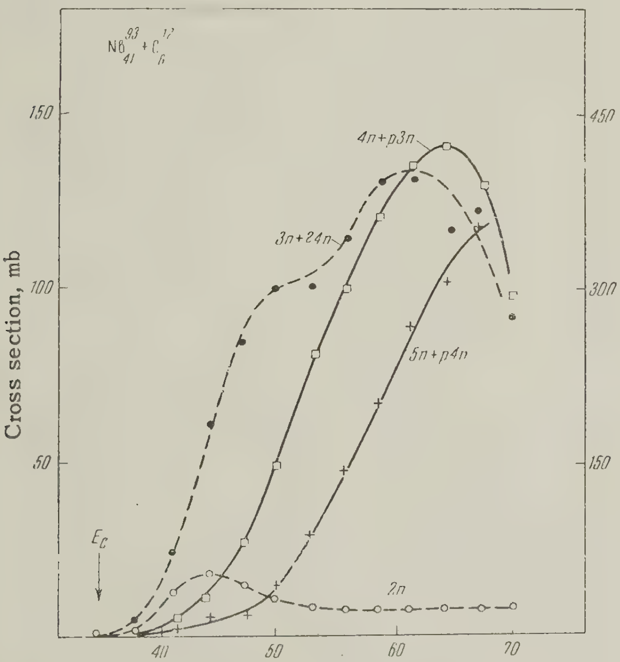

FIG. 4. Excitation functions for the $Nb^{93}+C^{12}$ reaction. On the left — the scale for "2n" and "3n + ?4n" reactions; on the right — the scale for "4n + p3n" and "5n + p4n" reactions.

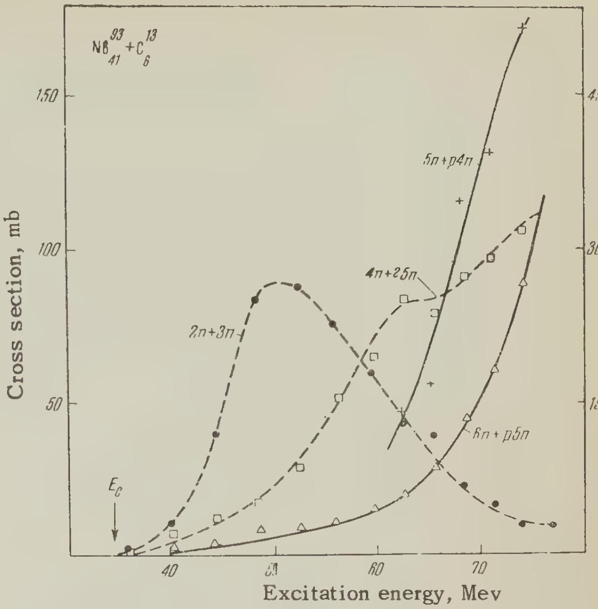

FIG. 5. Excitation functions for the $Nb^{93}+C^{13}$ reaction. On the left — the scale for "2n + 3n" and "4n + ?5n" reactions; on the right — the scale for "5n + p4n" and "6n + p5n" reactions.

Niobium. Excitation functions for the interaction between carbon and niobium were obtained in the excitation energy range 35 — 70 Mev. The conditions which determine the limits of this range have been considered above. The excitation functions of $Nb^{93}(C^{12}, xn)Ag^{105-x}$ and of $Nb^{93}(C^{13}, xn)Ag^{106-x}$ are given in Figs. 4 and 5, respectively. The method of calculating the respective cross sections in these figures will be considered together, but all quantities pertaining to the irradiation of niobium by C^{13} (Fig. 5) will be enclosed in parentheses. Ag^{104} and Ag^{103}, which are produced by the evaporation of 1 (2) and 2 (3) neutrons from the compound nucleus, have almost indistinguishable half-lives of 1.2 and 1.1 hours, respectively. We have no data on the β-ray end-point energies and branching of the decay schemes. Therefore the excitation function in Figs. 4 and 5 is designated by 1n + 2n (2n + 3n) and is actually the lower limit of the sum of the cross sections for the emission of 1 and 2 (2 and 3) neutrons. The evaporation of 3 (4) neutrons yields Ag^{102}, for which we also know only its 16-minute half-life. The cross section has an inflection point at 50 (65) -Mev excitation energy, very great width and a peak which is distant from the peak of the excitation function for the emission of 2 (3) neutrons. The curve appears from its shape to be the sum of two curves with a relative displacement along the horizontal axis. Some nucleus with a half-life of ~ 16 minutes is evidently formed in addition to Ag^{102}; this may be Ag^{101}, resulting from the evaporation of 4 (5) neutrons, or Tc^{101}, which results from the emission of 4 protons (4 protons + 1 neutron). The tables contain no data on Ag^{101}; we know that Tc^{101} exhibits β^- decay with a 15-minute half-life and 1.2-Mev end-point energy. We were unable to determine which of these reactions actually occurs; the lower limit of the excitation function in the figures is therefore designated arbitrarily by 3n + 4n (4n + 5n). Ag^{101}, which is formed following the evaporation of 4 (5) neutrons, decays with an unknown but apparently short half-life and is transformed into Pd^{101}, which has a half-life of 8 hours, a 2.3-Mev β-energy limit and 10% relative probability for positron emission. Aside from the reaction with the evaporation of 4 (5) neutrons, Pd^{101} may result from the emission of 3 neutrons and 1 proton (4 neutrons and 1 proton); the corresponding curves in the figure are designated by 4n + p3n (5n + p4n).

The evaporation of 5 (6) neutrons results in the production of Ag^{100}, which apparently has a very short lifetime. Pd^{100} decays purely by electron capture with a half-life of 4 days, and its daughter element, 20-hour Rh^{100}, emits positrons with energies up to 2 Mev in 5% of its decays. The identification of the reaction accompanied by the emission of 5 (6) neutrons was made by means of the 4-day activity and end-point energy of the Pd^{100} β spectrum. However Rh^{101}, which is the product of a reaction involving the emission of 4 (5) particles, also exhibits a 4-day half-life and conversion electrons; therefore in calculating the cross section for the 5 (6)-particle case we introduced a correction determined by means of the absorption curves. The approximate character of this correction considerably reduces the accuracy of the 5 (6)-particle excitation function.

We note that when Nb was irradiated by C^{13} nuclei almost the same amount of 16-hour activity was detected in all foils. This activity, which had a cross section ≥ 10 mb, was not identified.

CONCLUSIONS

From Figs. 3, 4, and 5 and from a comparison of our results with those in references 3 and 9, which present data for reactions induced by protons and α particles, we may draw the following conclusions:

1. Differences in the excitation functions distinguish the competing processes in which different numbers of nucleons are evaporated from heated compound nuclei. The absolute cross sections which take into account reactions resulting in stable nuclei are so large that we may consider the formation of a stable nucleus to be the principal process for medium-weight nuclei in our range of excitation energies.

2. A comparison of the excitation function peaks observed for reactions induced by multiply-charged ions, protons and α particles shows that in the case of the multiply-charged ions all excitation functions are shifted toward higher energies (by 10 — 15 Mev for V + O and by 7 — 8 Mev for Nb + C). The probable explanation of this shift is that in all instances compound nuclei are formed with identical charges, masses and excitation energies but quite different angular momenta. The large angular momentum contributed by a multiply-charged ion creates an extra centrifugal barrier and thus results in the emission of particles with kinetic energy greater than 2T, T being the temperature of the nucleus. Moreover, the angular momentum carried away by evaporating nucleons is small, so that after the emission of a certain number of particles the residual nucleus, with an excitation energy above the nucleon binding energy, possesses such large angular momentum that particle evaporation is impossible. This residual nucleus will be deexcited through the emission of a γ-ray cascade. Therefore in reactions involving multiply-charged ions the energy carried away by photons is greater than the 8 Mev which is ordinarily assumed for other types of reactions.

3. To verify the departure from predictions based on the evaporation model which was observed in reference 1 (see the Introduction) the following experiments were performed: a) The $V^{51}(C^{12}, 2n)Cu^{61}$ cross section was measured again very carefully, using pure vanadium foils and high-energy carbon ions; b) the dependence of $Nb^{93}(C^{12}, 2n)Ag^{103}$ on ion energy was measured several times. All of these experiments showed that reactions involving the emission of two neutrons have a cross section ~ 10 mb at excitation energies up to 70 — 80 Mev. The emission of two neutrons at such high excitation energies apparently indicates a direct interaction between the incident nucleus and nucleons of the target nucleus.

We note in conclusion that the determination of the relative probabilities of direct interactions and the production of compound nuclei will require further more detailed investigations of both the excitation functions and the angular and energy distributions of the emitted particles.

The authors are deeply indebted to Professor G. N. Flerov for valuable suggestions during the experimental work and for a discussion of the results.

---

[1] Karamyan, Gerlit, and Myasoedov, JETP **36**, 621 (1959), Soviet Phys. JETP **9**, 431 (1959).

[2] H. A. Bethe, Phys. Rev. **53**, 675 (1938).

[3] J. W. Meadows, Phys. Rev. **91**, 885 (1953).

[4] Yu. Ts. Oganesyan, JETP **36**, 936 (1959), Soviet Phys. JETP **9**, 661 (1959).

[5] Strominger, Hollander, and Seaborg, Revs. Modern Phys. **30**, 585 (1958).

[6] V. A. Kravtsov, Usp. Fiz. Nauk **54**, No. 1 (1954).

[7] G. W. C. Kaye and T. H. Laby, Tables of Physical and Chemical Constants and Some Mathematical Functions, Longmans, New York, 1948 (Russ. Transl. IIL, 1949, p. 242).

[8] B. Rossi and H. Staub, Ionization Chambers and Counters, McGraw-Hill, New York, 1949 (Russ. Transl. IIL, 1951, p. 233).

[9] K. G. Porges, Phys. Rev. **101**, 225 (1956).

Translated by I. Emin
129

SOVIET PHYSICS JETP VOLUME 37(10), NUMBER 3 MARCH, 1960

SCATTERING OF 5–10 Mev PROTONS ON He^3

K. P. ARTEMOV, S. P. KALININ, and L. N. SAMOĬLOV

Submitted to JETP editor April 17, 1959

J. Exptl. Theoret. Phys. (U.S.S.R.) **37**, 663-666 (September, 1959)

The angular distribution of protons, elastically scattered on He^3, has been measured for five values of the incident energy. The protons were recorded by their tracks in photographic plates. The differential cross sections so obtained are compared with theoretical values calculated under two different assumptions regarding the character of the exchange force. The nucleon-nucleon interaction with Serber exchange forces is in better agreement with experiment. The energy dependence of the cross section does not reveal the discreet levels in the Li^4 nucleus.

THE elastic scattering of protons, at different energies, by He^3 is of interest for determining the states of Li^4 and similarly the excited states of the α particle.

The well-known 22-Mev excited state of He^4 is ascribed isotopic spin $T = 0$;[1] consequently, the ground state of Li^4 cannot be similar to this state of He^4. On the basis of the experimental data mentioned in reference 1, it is necessary to assume that the excited state in He^4 with isotopic spin $T = 1$ is at an excitation energy of 24 or 25 Mev. The similar ground state of Li^4 must be unstable with respect to the decay to $He^3 + p$. The existence of this state would be revealed in resonance effects in p-He^3 scattering (or n-T scattering), although the width of the level is large. In this connection, it is desirable to have systematic data on p-He^3 scattering over a wide energy interval.

On the other hand, from a comparison of the experimental data on the scattering of nucleons on light nuclei (in particular, of protons on He^3) with the corresponding theoretical calculations it is possible to try to extract information concerning the forces acting between two nucleons in a many nucleon system.

Experiments on the scattering of protons on He^3 described in the literature are at $E_p^{Lab} = 1.01$, 1.60, 2.25, and 3.52;[2] 4.97,[3] 8.6,[4] and 9.75[5] Mev. In the present work we obtain curves for the angular distribution of protons scattered on He^3 nuclei at $E_p^{Lab} = 9.6$; 8.6; 7.9; 6.8 and 5.5 Mev.

9.6-Mev protons were obtained from the cyclotron directly, while lower-energy protons were obtained by slowing them down ahead of the collimator of the scattering chamber. The gas-filled target had windows closed with iron foil of thickness 6 mg/cm^2 and filled with He^3 to a pressure of about 800 mm mercury. Another target, but empty, was exposed to measure the background, which turned out to be very small for all scattering angles, with the exception of the smallest angle (20°). At 20°, the background increased with decreasing proton energy from 20% at 9.6 Mev to 70% at 5.5 Mev. The proton current in the target was measured using a Faraday cylinder, placed after the target and joined to the integrator.[6] The scattered protons were recorded on photographic plates, situated 125 mm from the center of the gas-filled target at angles from 20 up to 155° at 15° intervals. Each plate was placed at an angle of 4° to the scattered protons. All the plates were exposed together, but the magnitude of the exposure at different angles was regulated by a remotely controlled shutter, placed between the target and each of the plates. In counting the number of proton tracks in the plates, those tracks were chosen which had a given direction and originated in the surface of the emulsion.

The measured results for the differential cross sections for the scattering of protons on He^3 are presented in Figs. 1 to 5 (the energy of the proton is given in the laboratory system). The data of Sweetman (black points) are also included in Fig. 2 and taken from reference 4.

Theoretical calculations of the p-He^3 scattering cross section have been carried out recently by Bransden and Robertson[7] and also by Innas et al.[4] The calculations in reference 7 were carried out using Wheeler's[8] resonating-group structure method. The spatial dependence of the interaction potential between each pair of nucleons was chosen to be a Gaussian:

$$V(r) = V_0 e^{-\mu r^2}$$

with $V_0 = -45$ Mev and $\mu = 0.2669 \times 10^{26}$ cm^{-2}, while two forms were taken for the exchange op-

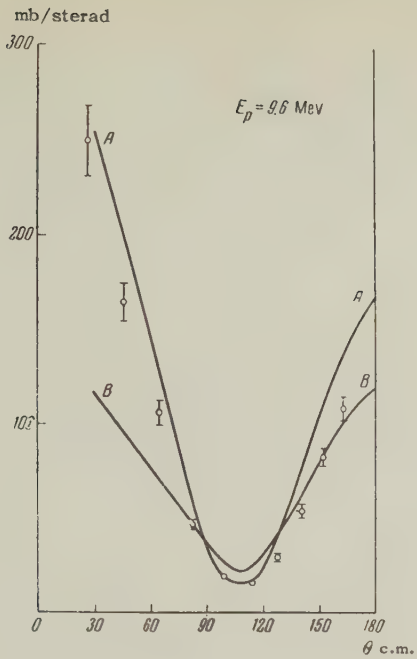

FIG. 1

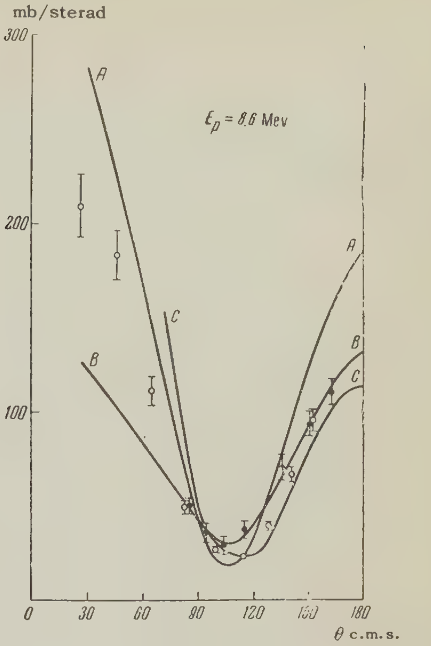

FIG. 2

erator, Serber's and symmetric. The theoretical curves for both variants are drawn in the figures: (A) $\sigma(\theta)$ for Serber exchange forces[7] and (B) for symmetric exchange force.[7] The curves were obtained by interpolation of the angular distributions p-He^3 scattering given in reference 7. It is seen that the symmetric variant consistently disagrees with the experimental data. The Serber variant overestimates the absolute magnitude of the cross section at all angles of the interval, but reproduces the angular distribution better. With increasing energy the agreement of the Serber variant with the experimental data improves. It is possible, that with a slight change in the parameters of the potential (for example the spatial dependence) the Serber variant might be in better agreement with the experimental data over the entire energy interval.

In reference 4, the scattering of protons on He^3 is calculated using the optical model and taking into account spin-orbit coupling. The calculations were carried out with the p-He^3 interaction potential in the form of a square well of depth V_0 and for a "shaped" well:

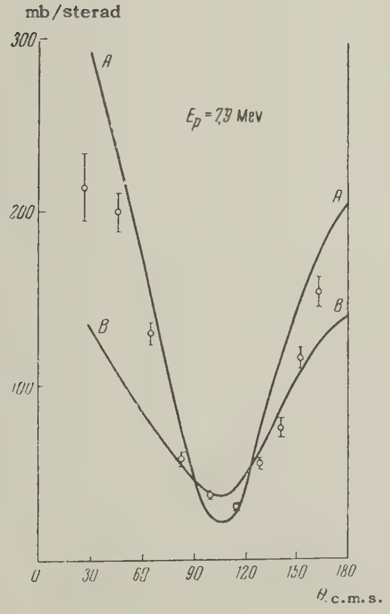

FIG. 3

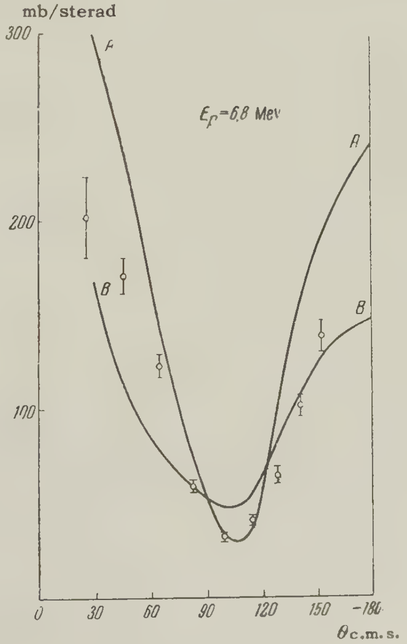

FIG. 4

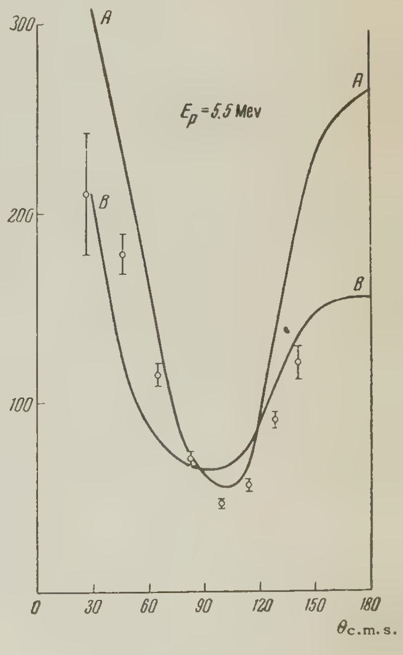

FIG. 5

$$V = -V_0/[1 - \exp\{(r - R)/d\}]$$

with $V_0 = 30$, 36, and 42 Mev, $d = 0.5 \pm 0.1 \times 10^{-13}$ cm, and $R = (1.26\,A^{1/3} + 0.7) \times 10^{-13}$ cm. The energy of the spin-orbit coupling was taken as a rectangular well in the form: $1.2\,(\beta V_0/R^2)\,\boldsymbol{\sigma}\cdot\mathbf{L}$, while for a "shaped" well:

$$\beta\left(\frac{1}{r}\,\frac{\partial V}{\partial r}\right)(\sigma\mathbf{L}), \qquad \beta = \hbar^2/\mu Mc^2,$$

where μ is the meson mass and M is the nucleon mass.

In Fig. 2 is drawn the differential cross section $\sigma(\theta)$, calculated in reference 4 using the optical model and taking into account spin-orbit coupling with $V_0 = 36$ Mev (curve C). It is seen that it is in qualitative agreement with the experimental results. Theoretical curves for $\sigma(\theta)$ at 9.6, 7.9, 6.8, and 5.5 Mev are not given and therefore comparison with experimental data cannot be made. However, curves for $E_p^{\mathrm{Lab}} = 4.97$ and 9.75 Mev with V_0 equal to 30 and 36 Mev are presented in reference 4 and they are in qualitative agreement with the experimental data of Sweetman[3] and Lovberg,[5] respectively.

The satisfactory agreement between theory and experiment in p-He^3 scattering in the non-resonance domain, up to proton energies of ~ 10 Mev, apparently indicates the absence of resonance effects in the scattering in this energy domain. This indicates that the Li^4 nucleus does not have a well defined state with a life-time noticeably greater than the time of the nuclear collision. Therefore the assumption made in reference 1 on the ground state of Li^4 and similarly on the second excited state of He^4 with an energy of 24 or 25 Mev and isotopic spin $T = 1$ is not confirmed by p-He^3 scattering experiments.

---

[1] Bogdanov, Vlasov, Kalinin, Rybakov, Samoĭlov, and Sidorov, Тр. Всесоюзн. конф. по ядерн. реакциям при малых и средних энергиях (Trans. All Union Conf. on Nuclear Reactions at Small and Intermediate Energies), U.S.S.R. Acad. Sci. Press, p. 7 (1957).

[2] Famularo, Brown, Holmgren, and Stratton, Bull. Amer. Phys. Soc. **28**, 24 (1953); Phys. Rev. **93**, 928 (1954).

[3] D. Sweetman, Phil. Mag. **46**, 358 (1955).

[4] Innas, Hossain, and Islam, Rept. on 2nd. United Nations International Conf. on the Peaceful Uses of Atomic Energy, **14**, 140 (1958).

[5] R. Lovberg, Phys. Rev. **103**, 1393 (1956).

[6] A. A. Kurashov and A. F. Linev, Приборы и техника эксперимента (Instrum. and Meas. Engg.) No. 2, 70 (1957).

[7] B. H. Bransden and H. H. Robertson, Proc. Phys. Soc. **72**, 770 (1958).

[8] J. A. Wheeler, Phys. Rev. **52**, 1107 (1937).

Translated by K. Smith
130

SOVIET PHYSICS JETP VOLUME 37(10), NUMBER 3 MARCH, 1960

POSITRON SPECTRUM OF Eu^{152} *AND* Eu^{152m}

S. F. ANTONOVA, S. S. VASILENKO, M. G. KAGANSKIĬ, and D. L. KAMINSKIĬ

Submitted to JETP editor April 18, 1959

J. Exptl. Theoret. Phys. (U.S.S.R.) **37**, 667-671 (September, 1959)

A low background β spectrometer was employed to study the spectrum of positrons produced in the decay of Eu^{152} and Eu^{152m}. It was found that β^+ decay of Eu^{152} takes place to the first (2^+) and second (4^+) excited states of Sm^{152}. The end-point energies of the partial spectra are 713 kev and 470 kev and their intensities are respectively 1.4×10^{-4} and 5×10^{-5} β^+ per decay. Formation of Sm^{152} in the ground and first excited states occurs in the positron decay of the Eu^{152m} isomer. The endpoint energies of the partial spectra are 890 kev and ~ 770 kev and the intensities are respectively 6×10^{-5} and 2×10^{-5} β^+ per decay. The excitation energy of the Eu^{152} isomer is deduced from the difference of the endpoint energies of the β^+ spectra and is found to be (55 ± 6) kev. Pair conversion coefficients and the multipolarities of a number of γ transitions are derived from the positron internal pair conversion spectra.

1. INTRODUCTION

It is known that a change in the number of neutrons in a nucleus from $N = 88$ to $N = 90$ also involves an abrupt change in the form of the nucleus. Therefore it is of considerable interest to study radioactive Eu^{152} and its isomer Eu^{152m}, which decay to ${}_{62}\mathrm{Sm}^{152}_{90}$ and ${}_{64}\mathrm{Gd}^{152}_{88}$. Electron capture, β^- decay, and γ radiation have been comparatively well investigated for these nuclei. Less has been done to study the positron decay of Eu^{152} and Eu^{152m}. Grodzins and Kendall[1] detected β^+ decay of the isomer Eu^{152m}. Earlier Kaminskiĭ and Kaganskiĭ[2] showed the existence of β^+ decay of Eu^{152}. A more detailed study of the positron decay of Eu^{152} and Eu^{152m} shows that the data of references 1 and 2 must be substantially supplemented. When the present experiment was almost completed we became aware of some of the results of the work of Alburger, Ofer, and Goldhaber,[3] which had not yet been published. In general, their results agree with ours.

2. EXPERIMENTAL METHOD

A magnetic spectrometer of the sector type with double focusing as shown schematically in Fig. 1 was used to study the positron spectrum. The spectrometer used in our experiment is different from the detector described in reference 2. As can be seen in Fig. 1 the detector consists of two Geiger counters situated one meter from each other and connected to a coincidence circuit. The first counter was placed at the focus of the spectrometer. β particles passing through the first counter were then focused with a magnetic lens on the second counter. The real advantage of such a counting system is the combination of a very small background and efficient detection of charged particles. The dependence of the detector efficiency on the energy of the particles is shown in Fig. 2 (by efficiency we mean the ratio of the number of coinci-

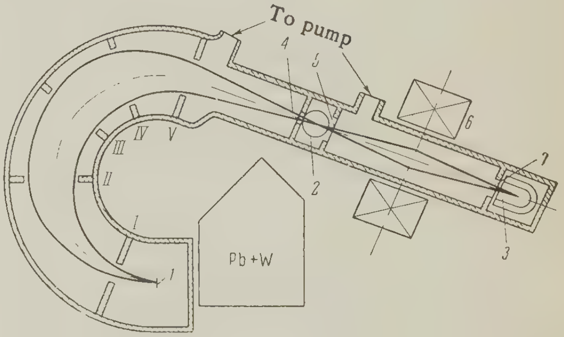

FIG. 1. Design of the β spectrometer. 1 – source; 2 and 3 – Geiger counters; 4, 5 and 7 – collodion films 0.2 mg/cm²; 6 – magnetic lens; I to V – baffles.

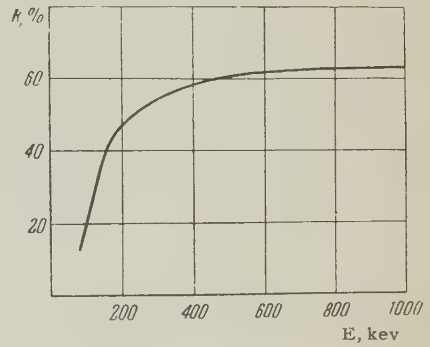

FIG. 2. Dependence of efficiency on β-particle energy.

dences to the number of pulses registered by the first counter). This dependence on energy resulted from the scattering of β particles in the first counter and in the films that separate the Geiger counters from the vacuum chamber.

In measuring the positron spectrum of Eu^{152} and Eu^{152m} the spectrometer background was 2 to 3 orders lower than the intensity of the spectra being studied. The solid angle of the spectrometer was 0.5% of 4π and the resolution was 1%.

The sources used were obtained from europium oxide of a natural isotope compound irradiated by slow neutrons. The sources were prepared by percipitation from an emulsion and were 1 to 2 mg/cm^2. In control experiments we used thinner sources, 0.2 mg/cm^2 which were prepared by electrolysis of europium chloride.[4]

3. RESULTS

Results of the measurements of the positron spectra of $Eu^{152,154}$ are shown in Fig. 3, which includes the correction for the dependence of the detector efficiency on positron energy. As can be seen from Fig. 3 the positron spectra are very complex. Sharp breaks in the spectrum at $H\rho = 1920$ gauss cm and $H\rho = 2460$ gauss cm are evidently caused by internal pair conversion of γ quanta with the energies $E_\gamma = 1280$ kev and $E_\gamma = 1409$ kev.

Insofar as the energy distribution of pair conversion positrons is known,* the corresponding spectra (a and b in Fig. 3) can be separated by the size of the break. After subtracting the pair conversion spectra the remaining spectrum was analyzed with a Fermi plot. Analysis shows that this spectrum consists of two β^+-groups having the allowed shape with end-point energies of (713 ± 3) kev and (470 ± 10) kev. These partial β^+ spectra are shown in Fig. 3 (c and d).

Our measurements were taken several years after the irradiation of the sources. An attempt to evaluate the half-life of the positron spectrum gave the value ~ 10 years. In accordance with data in reference 2, this means that the positron spectrum shown in Fig. 3 is determined by the decay of the long-lived isotopes of Eu^{152} and Eu^{154}. In accordance with available data in reference 6, γ quanta with the energy $E_\gamma = 1280$ kev and consequently one of the pair conversion spectra arise from the decay of Eu^{154}. The other spectrum of pair conversion positrons is connected with the 1409-kev transition and results from the decay of Eu^{152}. Both β^+ spectra must be ascribed to the positron decay Eu^{152} to Sm^{152} since the difference between end point energies of these groups agrees perfectly with the energy separation between the first and second excited states of Sm^{152}.

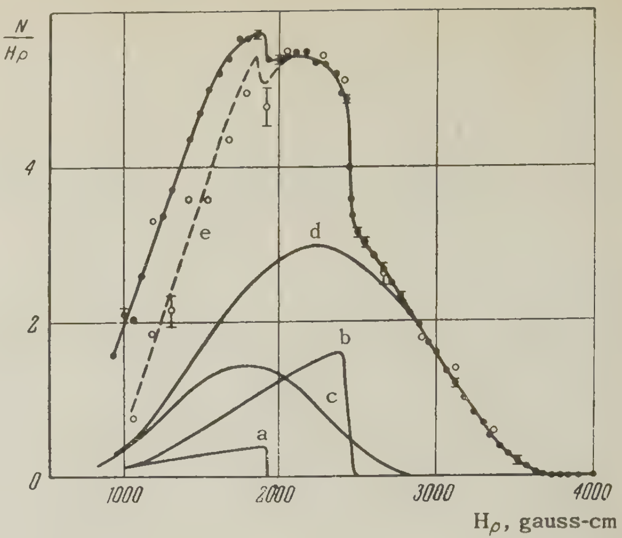

FIG. 3. Positron spectrum of $Eu^{152,154}$ measured with source thickness of 2 mg/cm^2. Curve e is a sum spectrum of the four components. Points on curve e are the result of measurements with a source 0.2 mg/cm^2 thick.

Figure 4 shows the decay scheme of Eu^{152} which includes the data on positron decay obtained in our experiments. The intensities of partial β^+ groups were determined by comparing the corresponding spectra with the pair conversion spectrum associated with the 1409-kev transition. The probability of the 1409-kev transition in accordance with available data is taken equal to 25% (see Fig. 4), while the pair conversion coefficient was determined by the method described in reference 2, from the ration of the areas of the spectra of K-electron conversion and positron pair conversion. The value of the pair conversion coefficient is Γ

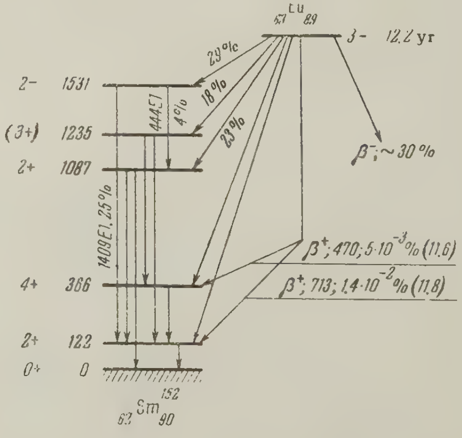

FIG. 4. Decay of Eu^{152} to Sm^{152}.

---

*The pair conversion spectrum of positrons in our case, Z = 62 to 64, was assumed the same as for Z = 84 for which Jaeger and Hulme did the calculation.[5]

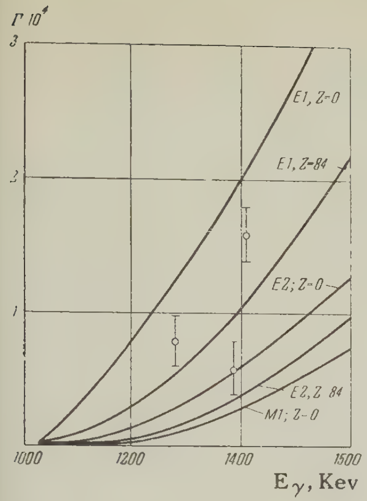

FIG. 5. Dependence of the pair-conversion coefficient on the energy and multipolarity of transition. Points are the result of our measurements.

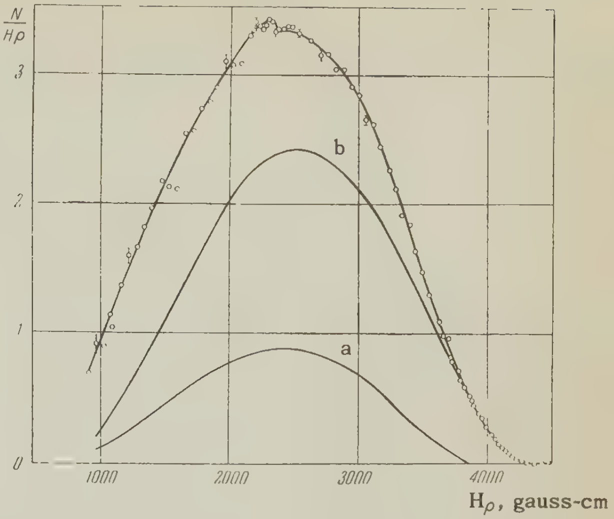

FIG. 6. Positron spectrum of Eu^{152m}. Source thickness 1.5 mg/cm².

= $(1.6 \pm 0.2) \times 10^{-4}$ as can be seen in Fig. 5, and agrees with the multipolarity E1 established for this transition by other methods. The pair conversion coefficient $\Gamma = (0.8 \pm 0.2) \times 10^{-4}$ for the 1280-kev transition also corresponds to a multipolarity E1. Thus for the calculation of Γ the relative intensity of this γ transition was taken equal to $I_{1280} = 0.35\ I_{1409}$ in agreement with data given by Dzhelepov and others.[7]

After separating from the spectrum the four components shown in Fig. 3 there remains a surplus of positrons in the energy region below 250 kev. Control measurements carried out with a considerably thinner source (0.2 mg/cm²) showed that this surplus was caused by scattering in the comparatively thick sources used in the basic measurements. Results of these measurements are shown in the same figure.

In our experiments the positron decay of Eu^{154} was not detected. However, on the basis of available data on the mass difference of Eu^{154} and Sm^{154} we can assume the presence of β^+ decay of Eu^{154} with an end-point energy of ~1 Mev. According to our experiments the probability of such a decay is less than 10^{-6} positron per decay of $Eu^{152,154}$.

Figure 6 shows the results of measurements of the positron spectrum of the Eu^{152m} isomer. Measurement of the half-life of this spectrum gave the value $T_{1/2} = 9.2$ hours. In contrast to the positron spectrum of Eu^{152} (in Fig. 3), there are few positrons here which result from pair conversion. The fact that in the decay of the 9.2-hour isomer, the γ transitions with an energy of more than $2mc^2$ are comparatively weak confirms this. We made a more detailed study of spectra in the 380-kev energy region. The measurements showed (see Fig. 6) the presence of a small break at 364 kev which corresponds to the γ-transition energy $E\gamma = 1386$ kev. Calculation of the pair conversion coefficient for this transition gave the value $\Gamma = (0.6 \pm 0.3) \times 10^{-4}$, which gives a multipolarity E2 (see Fig. 5); for the calculation the intensity of the γ quanta was taken as equal to 0.7% to correspond with Marklund's data.[8]

An analysis of the β^+-spectrum, using the Fermi plot method, showed the presence of two components of β^+ decay with the energies (890 ± 5) kev and ~770 kev. These components were identified as the positron decays of Eu^{152m} to the ground and first excited states of Sm^{152}. Figure 7 shows the decay scheme of the 9.2-hour isomer (according to Marklund's data[8]) which includes the results obtained in our work. The intensity of the β^+ spectrum was determined from the ratio of the areas of the positron and electron spectra. Inasmuch as the value for the spin of the isomeric state still remained undetermined (0^- or 1^-) it was of considerable interest to determine the form

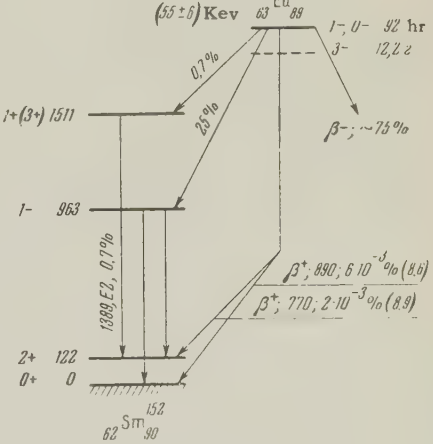

FIG. 7. Decay of Eu^{152m} to Sm^{152}.

	Alburger et al.[3]		Our data	
	End-point energy, kev	Intensity, β^+ per decay	End-point energy, kev	Intensity, β^+ per decay
Eu^{152}	715±10	$1.6 \cdot 10^{-4}$	713±3	$(1.4 \pm 0.2) \cdot 10^{-4}$
	470±30	$0.8 \cdot 10^{-4}$	470±10	$(0.5 \pm 0.1) \cdot 10^{-4}$
Eu^{152m}	895±5	$7 \cdot 10^{-5}$	890±5	$(6 \pm 1) \cdot 10^{-5}$
	~770	$4 \cdot 10^{-5}$	770±30	$(2 \pm 0.5) \cdot 10^{-5}$

of the β^+ spectrum corresponding to the decay of Eu^{152m} to the first excited state of Sm^{152}. The unique form for the spectrum would give for the spin of Eu^{152m} the value 0^-. However, the attempt to establish the form of the spectrum in our work was unsuccessful because of the comparatively small difference between the end-point energies of the components (120 kev) and consequently a certain arbitrariness in separating them.

The table shows the data for positron decay of Eu^{152} and Eu^{152m} obtained by us and also by Alburger et al.[3] As can be seen from the table, the results in reference 3 generally agree with our work. The only real difference is in the intensity of the low energy components. The reason for this is not yet clear since the experimental part of reference 3 has not yet been published. We determined the energy of the metastable state for the end point energies of β^+ decay of Eu^{152} and Eu^{152m}. Our data gives this energy as (55 ± 6) kev.

The authors wish to thank Professor L. A. Sliv for his constant attention and interest in our work.

[1] H. Kendall and L. Grodzins, Bull. Am. Phys. Soc. Ser. II, **1**, 164 (1956).

[2] D. L. Kaminskiĭ and M. G. Kaganskiĭ, JETP **35**, 926 (1958), Soviet Phys. JETP **8**, 646 (1959).

[3] Alburger, Ofer, and Goldhaber, Phys. Rev. (in press); Phys. Rev. Lett. **1**, 479 (1958).

[4] B. V. Bobykin and K. M. Novik, Izv. Akad. Nauk SSSR, Ser. Fiz. **21**, 1556 (1957), Columbia Tech. Transl. p. 1546.

[5] J. C. Jaeger and H. R. Hulme, Proc. Roy. Soc. (London) **A148**, 703 (1935).

[6] B. S. Dzhelepov and L. K. Peker, Схемы распада (Decay Schemes), M. 1958.

[7] Dzhelepov, Zhukovskiĭ, and Nedovesov, Izv. Akad. Nauk SSSR, Ser. Fiz. **19**, 296 (1955), Columbia Tech. Transl. p. 269.

[8] I. Marklund, Nucl. Phys. **9**, 83 (1958/1959).

Translated by Genevra Gerhart
131

SOVIET PHYSICS JETP VOLUME 37(10), NUMBER 3 MARCH, 1960

THE ANISOTROPY OF MAGNETORESISTANCE AND THE TOPOLOGY OF FERMI SURFACES OF METALS

N. E. ALEKSEEVSKIĬ and Yu. P. GAĬDUKOV

Institute for Physical Problems, Academy of Sciences, U.S.S.R.

Submitted to JETP editor April 24, 1959

J. Exptl. Theoret. Phys. (U.S.S.R.) 37, 672-677 (September, 1959)

The anisotropy of magnetoresistance has been studied for single crystals of Ag, Au, Cu, Sn, Pb, Tl, and Ga. Stereographic projections of the singular field directions have been constructed, and some considerations about the topology of the Fermi surface of metals are discussed on the basis of these.

IN this paper we describe some* results of a further study of the anisotropy of magnetoresistance in single crystals of Au, Cu, Sn, Pb, Tl and Ga, which we examined earlier,[1] and also of Ag single crystals investigated for the first time.

For most of the metals the measurements were made on 10 — 15 specimens with different orientations of the crystallographic axes relative to the specimen axis. The orientation was determined by back-scattering Laue photography or by an optical method.†

The purity of the specimens used can be expressed as the ratio $\rho(300°)/\rho(4.2°)$ (the ratio of the resistance at room temperature to that at 4.2°K), which was about 10,000 for Sn, Pb and Ga, 3000 for Tl, and 1000 for Au, Cu and Ag. The specimen diameters were large enough for size effects not to affect the results.

All measurements were made at $T = 4.2°K$, since lowering the temperature further would not have produced any significant reduction in conductivity. The residual resistances in zero field, ρ_0, were very low and necessitated the determinations of emf's of the order of 10^{-8} v. For this a potentiometric system was used with a photo-multiplier connected to the output with negative feedback. The sensitivity of this arrangement was a few times 10^{-10} v.

The rotation diagrams for Cu and Ag are shown in Figs. 1 and 2; these give the dependence of relative change of resistance, $\Delta\rho_H/\rho_0 = \rho_H/\rho_0 - 1$, for constant field, $H = 23{,}500$ oe, on the angle ϑ through which H is turned in the plane perpendicular to the specimen axis. The angular dependence of the resistance of Pb and Ga is shown in polar coordinates in Figs. 3 and 4.

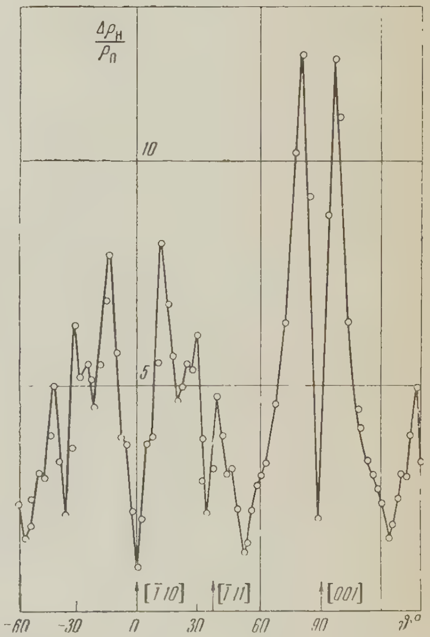

FIG. 1. Copper single crystal. [110] axis along the specimen axis. T = 4.2°K, $\rho(300°)/\rho(4.2°) = 728$; H = 23,500 oe.

From a study of the anisotropy in the resistance of silver it was found that as for other metals,[1] the resistance reaches complete saturation for directions of the minima in the resistance rotation diagram, and in the directions of the maxima increases indefinitely almost as the square of the field (Fig. 5). From this observation we may conclude[2] that silver has an open Fermi surface.

As for gold, the resistance of some specimens of Cu and Ag were averaged over ϑ (from 0 to 180°) at several values of the field (from 8000 to 24,000 oe). These average values are plotted in Fig. 6 and $\overline{\Delta\rho_H/\rho_0}$ is seen to vary linearly with field. We may then assume that Kapitza's law (linear increase of resistance with field[3]) for

---

*The authors hope soon to describe in full all the experiments and the results.

†The authors are grateful to G. É. Karstens for help with the determinations of orientation.

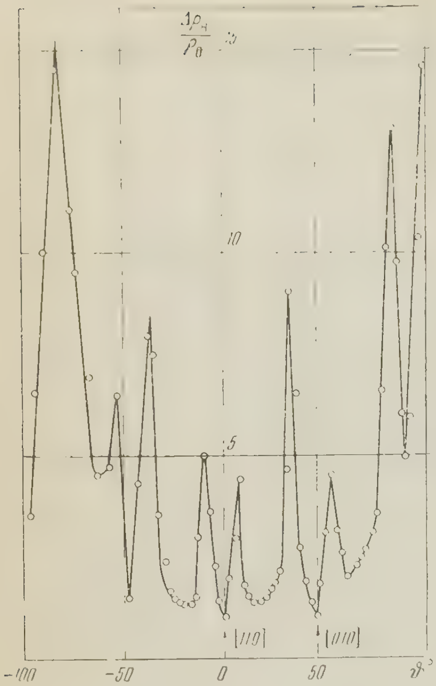

FIG. 2. Silver single crystal. [001] axis approximately (± 5°) along the specimen axis. T = 4.2°K, $\rho(300°)/\rho(4.2°) = 741$; H = 23,500 oe.

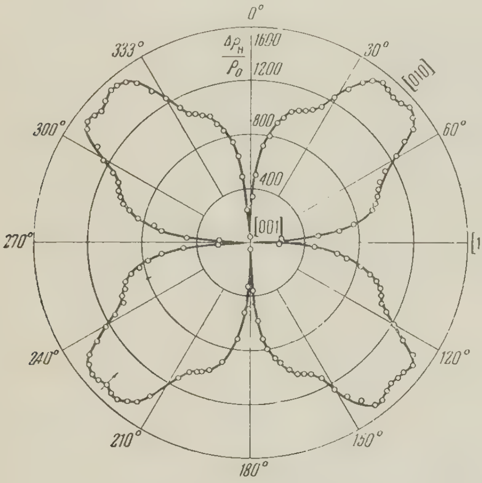

FIG. 3. Lead single crystal. [001] axis coincident with specimen axis. T = 4.2°K, $\rho(300°)/\rho(4.2°) = 8{,}750$; H = 23,500 oe.

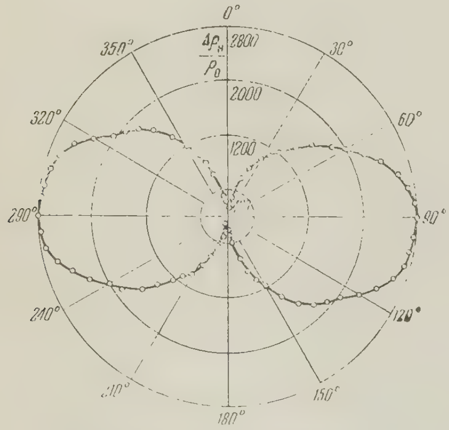

FIG. 4. Gallium single crystal. T = 4.2°K, $\rho(300°)/\rho(4.2°) = 28{,}000$; H = 23,500 oe.

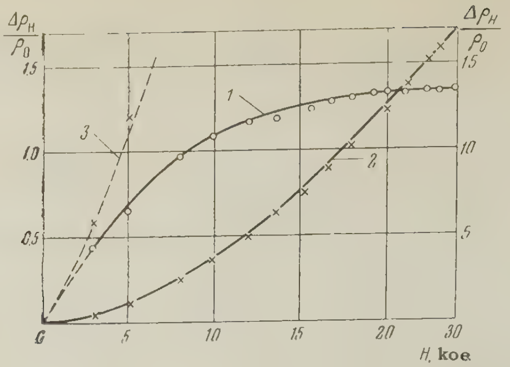

FIG. 5. Silver single crystal (see Fig. 2). Magnetoresistance for fixed angle ϑ: curve 1 for $\vartheta = 0$ (min), curves 2 and 3 for $\vartheta = 80°$(max); T = 4.2°K. The left hand ordinate scale refers to curves 1 and 3, the right hand to curve 2.

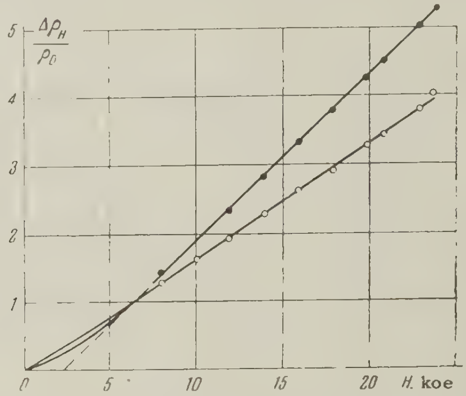

FIG. 6. The resistance averaged over ϑ for several values of magnetic field. ● – Cu [110] single crystal (see Fig. 1), ○ – Ag [001] single crystal (see Fig. 2).

polycrystalline Cu and Ag is a consequence of the averaging of various laws of resistance increase, as for Au.[1]

The variation of half-widths of the narrow maxima and minima in the rotation diagrams of Au, Cu, Pb and Sn were investigated. It was found that the half widths of the maxima decrease with increasing magnetic field (as 1/H), while those of the minima stay the same (Fig. 7). The results are in good agreement with the theory of Lifshitz and Peschanskiĭ.[4]

An interesting transition of a minimum into a maximum can be seen in the rotation diagram for lead and tin: for one and the same direction (for example, the [010] direction in Sn, shown in Fig. 8) the depth of the minimum progressively decreases as the current direction relative to the crystallographic axes varies. This change in the minimum can be regarded as confirming the relation

$$\rho = B(H/H_0)^2 \cos^2 \alpha + A, \qquad (1)$$

where α is the angle between the direction of open trajectories and the current direction.[4]

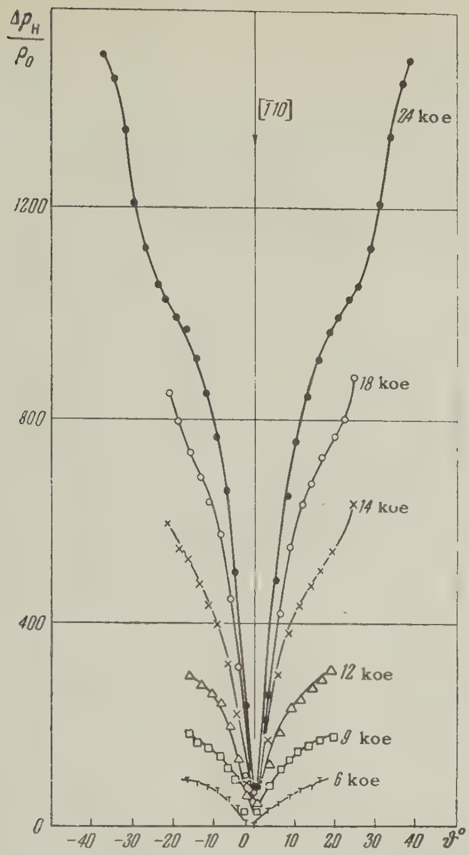

FIG. 7. The change in shape of the narrow minima in the rotation diagram for lead (Pb [001], see Fig. 3); T = 4.2°K.

The appearance of the rotation diagrams of Tl and Ga depends little on the specimen orientation and the dependence of $\Delta\rho/\rho_0$ on ϑ agrees well with (1). We may deduce from this that Tl and Ga have Fermi surfaces in the form of corrugated planes.[5]

From the data for Au, Cu and Ag specimens of various orientations, stereographic projections can be constructed of the singular magnetic field directions (directions of the maxima and of narrow minima etc.). Such a projection (for Ag) is shown in Fig. 9. The shaded regions and the thick lines joining them correspond to the field directions for which the resistance increases quadratically with field. The stereographic projections for Au and Cu are sufficiently close to that for Ag.

By comparison with the theory of Lifshitz and Peschanskiĭ,[4,5] an analysis of the stereographic projections points to the Fermi surfaces of these metals — "the space net" — being formed from "corrugated cylinders" with axes along the body and face diagonals of the reciprocal lattice. The data available[4,6] indicate that the Fermi surface of copper also has open directions along the edges of the reciprocal lattice.

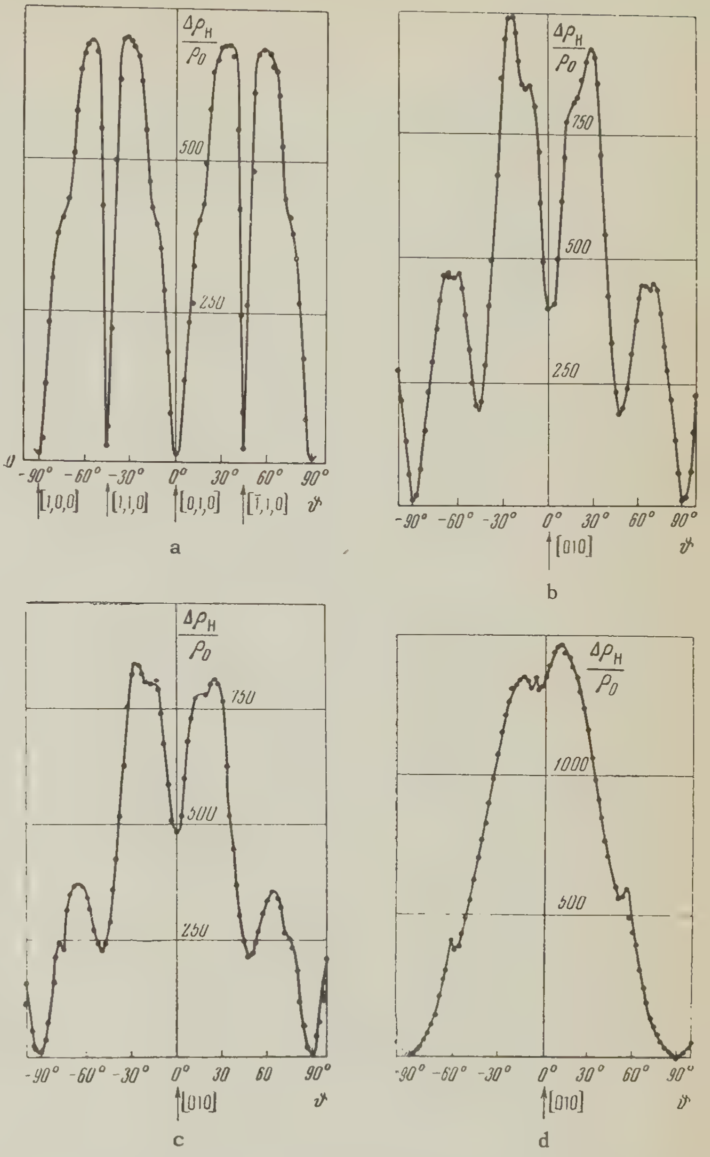

FIG. 8. Tin single crystals. The change in the depth of the minimum for fixed direction of the field H = 23,500 oe and varying current direction (specimen orientation); a – Sn I, $\varphi = 0°$; b – Sn II, $\varphi = 26°$; c – Sn III, $\varphi = 36°$; d – Sn IV, $\varphi = 51°$. (φ is the angle between the specimen axis, in the (100) plane, and the [001] axis.)

The stereographic projections of lead and tin cannot be interpreted so unambiguously. Nevertheless, we can say that a Fermi surface of lead formed by broad cylinders in the [111] direction, and in tin by broad cylinders in the [010] and [110] directions of the reciprocal lattice do not contradict the experimental data.* It is possible that these surfaces would appear more complicated if studied in more detail. It would seem likely that metals with the same crystal lattice will have nearly the

---

*In our previous paper[1] the direction [001] for Sn should read [100].

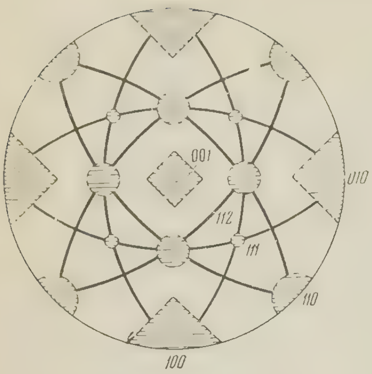

FIG. 9. Stereographic projection of the singular field directions for silver.

same form of Fermi surface. This is apparently true for Au, Cu, and Ag, which have body centered cubic lattices. However, if we compare the galvanomagnetic characteristics of these metals with the results for lead, which is also body centered cubic, it is easily seen that there is a considerable difference (Figs. 1, 2, and 3). While the resistance of Au, Cu, and Ag only varies quadratically over a narrow range of angles, the quadratic region in Pb occupies almost the whole rotation diagram, and saturation is found only in a narrow interval. An analogy can be found between the rotation diagrams of Pb and Sn, which have different lattices and belong to the same column of the periodic table. The diagrams for Tl and Ga are also similar and they are in the same column of the table and have different lattices.

These facts suggest a possible connection between the form of the angular dependence of resistance (for metals with open Fermi surfaces) and the position in the periodic table. It is probable that further study will clarify the reasons for metals having similar galvanomagnetic properties. All the available data show that, contrary to previous ideas, a large number of metals have open Fermi surfaces.

The results presented here, together with data from earlier work,[7,8] indicate that Au, Cu, Ag, Pb, Sn, Tl, Ga, Zn, and Cd have open Fermi surfaces. Bi and In[9,10] probably have closed surfaces, as do possibly Al, Be and Na,[8,11] for which a small anisotropy in resistance is characteristic. It may be that Al has a Fermi surface with very narrow regions of open directions.[1,12] The old division into metals with $n_1 = n_2$ and metals with $n_1 \neq n_2$ (n_1 and n_2 are the numbers of electrons and holes) still holds for metals with closed surfaces. There is no strong resistance anisotropy, dependent on magnetic field, for these metals; for the first case the resistance increases quadratically and in the second the resistance is independent of field for large fields. This classification is meaningless for metals with open Fermi surfaces.

It is a pleasure to express our thanks to Academician P. L. Kapitza for his constant interest in the work. We also thank Professor I. M. Lifshitz and V. G. Peschanskiĭ for discussion of the results.

---

[1] N. E. Alekseevskiĭ and Yu. P. Gaĭdukov, JETP **35**, 554 (1958), Soviet Phys. JETP **8**, 383 (1959); JETP **36**, 447 (1959), Soviet Phys. JETP **9**, 311 (1959).

[2] Lifshitz, Azbel', and Kaganov, JETP **31**, 63 (1956), Soviet Phys. JETP **4**, 41 (1957).

[3] P. L. Kapitza, Proc. Roy. Soc. **A123**, 292 (1929).

[4] I. M. Lifshitz and V. G. Peschanskiĭ, JETP **35**, 1251 (1958), Soviet Phys. JETP **8**, 875 (1959).

[5] V. G. Peschanskiĭ, Thesis, Khar'kov State University (1959).

[6] A. B. Pippard, Phil. Trans. Roy. Soc. **A250**, 325 (1957).

[7] Lazarev, Nakhimovich, and Parfenova, JETP **9**, 1169 (1939).

[8] E. S. Borovik, Thesis, Physico-technical Institute, Academy of Sciences, Ukrainian S.S.R., Khar'kov (1954).

[9] L. Schubnikow and W. J. de Haas, Leiden Comm. 210a (1930).

[10] E. S. Borovik, Dokl. Akad. Nauk SSSR **69**, 767 (1949).

[11] E. Justi and H. Scheffers, Z. Physik **39**, 105 (1938).

[12] B. Lüthi and J. L. Olsen, Nuovo cimento **3**, 840 (1956).

Translated by R. Berman
132

SOVIET PHYSICS JETP VOLUME 37(10), NUMBER 3 MARCH, 1960

DIFFRACTION OF X-RAYS BY POLYCRYSTALLINE SAMPLES OF HYDROGEN ISOTOPES

V. S. KOGAN, B. G. LAZAREV, and R. F. BULATOVA

Submitted to JETP editor April 29, 1959

J. Exptl. Theoret. Phys. (U.S.S.R.) 37, 678-683 (September, 1959)

Comparison of the interference patterns obtained in the scattering of x-rays by polycrystalline samples of hydrogen isotopes indicates the existence of isotopic polymorphism. The structural difference between hydrogen and deuterium and the structural proximity of the latter to tritium give evidence that the polymorphism is connected not with dissimilarity of energy spectra but with difference of atomic weights. The observed structural differences of the hydrogen isotopes are in accord with the hydrogen-deuterium state diagram.[1] The parametric data cited in this work as characterizing the structures of the hydrogen isotopes (tritium and deuterium have a tetragonal lattice with $c/a = 1.73$ and $a = 3.3$ and 3.35 A, respectively; hydrogen has either a hexagonal lattice with $c/a = 1.73$ and $a = 3.7$ A or a tetragonal lattice with $c/a = 0.82$ and $a = 4.5$ A), although in accord with density data and with the results of x-ray investigations of isotope mixtures, still need improvement of precision by methods permitting the production of more complete interference patterns.

As previously[1] reported, the scattering of x-rays by polycrystalline samples of hydrogen, deuterium, and their mixtures yields diffraction patterns differing from each other, depending upon the isotopic composition of the samples. The dissimilarity of the diffraction patterns secured with hydrogen and deuterium permitted the supposition that they had different crystalline structures. This difference in crystalline structure may be due both to inequality of the atomic weights and the disparity of the energy spectra of their molecules. To elucidate the relative influence of these factors, it appeared interesting to obtain the diffraction pattern of the scattering of x-rays by samples of the third hydrogen isotope — tritium, which is closer to deuterium in atomic weight, but closer to hydrogen in energy spectrum because, like hydrogen, it has a half-integral spin.

Tritium samples were obtained and x-rayed in the apparatus schematically shown in Fig. 1. The construction of the apparatus takes into account not only the fact that the radioactive tritium irradiates the x-ray film even during brief contact with it, but also that the decay product of tritium is helium, the entrance of which, together with the investigated gas, into the apparatus and consequently into the evacuated space of the helium Dewar flask occasions deterioration of the vacuum and rapid boil-off of the helium. In order to preclude its contact with gaseous helium, the x-ray film was placed outside the Plexiglas chamber 4, used to seal the apparatus. In this chamber a narrow groove is machined out, leaving a wall with a thickness of 0.3 mm. Such a wall freely transmits x-rays but completely absorbs the slow electrons emitted in the decay of tritium.

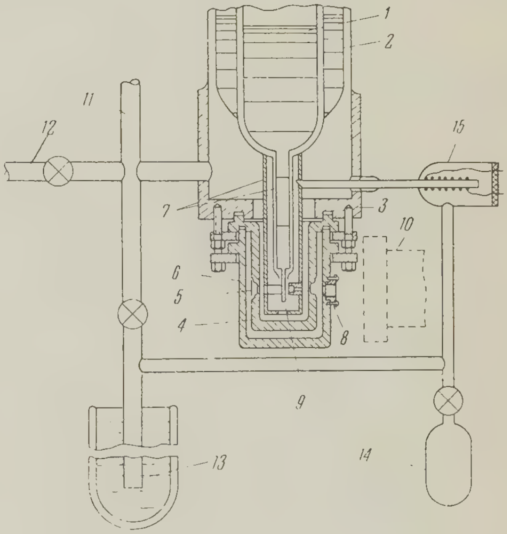

FIG. 1. Cryostat for x-ray photographs of samples of solid hydrogen isotopes: 1) metallic Dewar helium flask, 2) metallic Dewar nitrogen flask, 3) flange with fastening to seal the apparatus, 4) plexiglas chamber sealed to the apparatus, 5) x-ray film, 6) thick-walled safety chamber of plexiglas, 7) shields at nitrogen temperature, 8) beryllium window for admitting x-rays into the chamber, 9) copper capillary cooled from within by liquid helium (serves as the base for condensing samples of solid hydrogen isotopes from the gaseous phase), 10) sharp-focussing x-ray tube, 11) pipe branch to manometer tubes, 12) pipe branch to pump, 13) pipe cooled by liquid helium (serves for removing tritium present in the apparatus after it has warmed up), 14) flask containing tritium, 15) palladium filter.

To prevent the possible escape of tritium into the atmosphere in the event of rupture of the thin plexiglass, a second thick-walled enclosure 6 is provided, with a beryllium window 8 for the passage of the x-rays.

The helium was separated from the gas entering into the apparatus by a palladium filter, 15. The gas fed into the apparatus was condensed on a copper capillary, 9, cooled by liquid helium from within.

The apparatus for x-ray photography of hydrogen and deuterium differs from that described above by having a valve with a fine adjustment in place of the palladium filter; the x-ray film is not situated outside the plexiglass chamber, but located within it, thus eliminating the need for an internal chamber with a thin wall.

It should be noted that we did not succeed in eliminating all the fog from the tritium x-ray pictures. Apparently, it is due to the x-rays produced when β-electrons are slowed down in the sample substance. The intensity of this radiation amounts to $\sim 10^{-5}$ of the original beam intensity from the x-ray tube and is, of course, sufficient to produce considerable fogging of the x-ray film in a 2 or 3 hour exposure. The tritium vaporized after the helium Dewar flask has warmed up is collected in a tube, 13, which is cooled by liquid helium.

An x-ray pattern of a polycrystalline tritium sample is shown in Fig. 2. From a comparison with patterns of hydrogen and deuterium (Fig. 3) it is evident that in interference pattern character tritium is closer to deuterium than to hydrogen.

The character of the diffraction patterns obtained for hydrogen isotopes requires some supplementary remarks. As already pointed out in a previous communication,[1] the peculiarities of the method employed to obtain the samples (a transparent layer of condensed gas on a copper rod which is not transparent to x-rays) occasion the appearance of extraneous lines on the pattern, the causes of which are clear from Fig. 4. The use of lead screen 7 eliminates both of the extraneous lines 6 and 6′, while lead screen 8 removes one of the extraneous lines 6 and one of the principal lines 5′. The patterns shown in Figs. 2, 3a, and 3b were taken in Fe K_α radiation with a manganese filter. Patterns a and b in Fig. 3 were taken with screen 7 and do not have the extraneous lines; Fig. 2 was taken with screen 8 and shows one principal line and one extraneous one (marked by dashes). Pattern c in Fig. 3 was taken without screens and it displays all the principal and supplementary lines.*

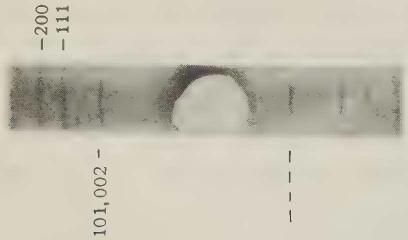

FIG. 2. X-ray pattern of tritium. Lines 200 and 111 are the standard copper lines from the capillary; 101 and 002 are the tritium lines. The extraneous line of type 6′ (see Fig. 4) is indicated by the dashes.

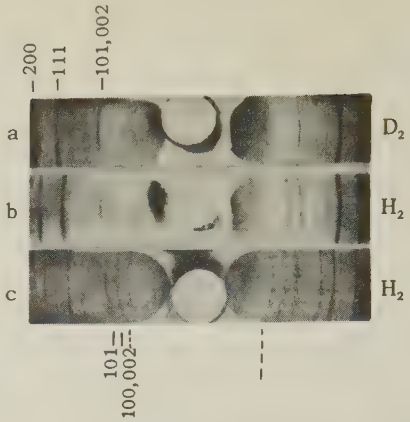

FIG. 3. X-ray pattern of deuterium and hydrogen. 200 and 111 are the copper lines; 101 and 002 are the deuterium lines; 101, 100 and 002 are the hydrogen lines (the indicated indices are for hexagonal lattice). The dashes point to the extraneous lines in the hydrogen x-ray pattern, taken without lead screens.

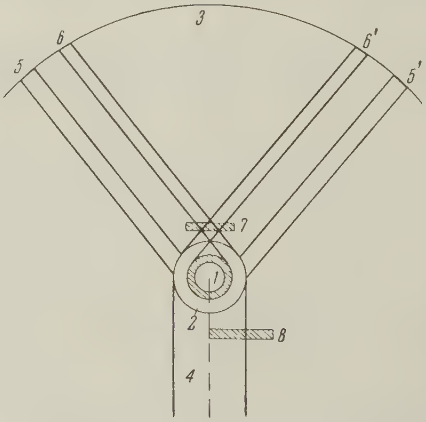

FIG. 4. Diagram of the arrangement for getting diffraction pictures from a layer of gas condensed on the copper capillary and transparent to x-rays. 1) copper capillary, 2) layer of condensed gas, 3) x-ray film, 4) primary beam, 5 and 5′) principal refracted rays, 6 and 6′) supplementary (extraneous) refracted rays, 7) lead screen to eliminate both extraneous rays, 8) lead screen to eliminate one extraneous ray (6) and one principal ray (5′).

In previous work on the structure of hydrogen[2,3] and deuterium,[3] the extraneous lines were not sifted

---

*The distance between the principal and supplementary lines is somewhat greater than would result from the diagram in Fig. 4, since the latter does not take into account the dispersion of the primary beam.

Isotope:	Hydrogen		Deuterium	Tritium
Possible syngony and space group	Tetragonal C_4^5	Hexagonal D_{6n}^4	Tetragonal C_4^5	Tetragonal C_4^5
Number of molecules per unit cell	2	6	2	2
Absence of lines at small angles	001, 100	001	001, 100	001, 100
Lines present in the pattern	110 and 101	100, 002 and 101	101, 002	101, 002
sin ϑ*	0.298 and 0.335	0.298 and 0.335	0.330	0.335
c/a	0.82	1.73	1.73	1.73
c, A	3.75	6,49	5.86	5.78
c^{**}_{extrap}, A	3,68	6,42	5,79	5.71
a_{extrap}, A	4,5	3.7	3.35	3.3
Density at 4.2° K, g/cm^3	0,09	0.089	0,205	0.324
Data in literature on density at 4.2° K	0.089 [4]		0.205 [4	0.27[5]***

*Corrected for the diameter of the copper capillary and the thickness of the layer of condensed gas. The effective diameter of the cassette was determined for each pattern on the basis of the copper lines.

**The value of c_{extrap} for deuterium was obtained by extrapolating the graph in Fig. 5. Hydrogen and tritium were photographed only in Fe radiation. The same extrapolation law was adopted for them as for deuterium.

***Density value cited for 20.6°K. If the variation of this density with temperature is taken to be the same as for deuterium,[4] extrapolation to 4.2°K gives a value of 0.32 g/cm^3, which is in good agreement with the value secured from the x-ray data.

out, so that, naturally, the conclusions contained in these reports with regard to the structure of hydrogen and deuterium must be reconsidered.

After removal of the extraneous lines, there remain two lines on each of the hydrogen patterns and one line on each of the deuterium patterns. These lines are seen at small angles, since with increasing angle the intensity of the diffraction is sharply diminished on account of the angular dependence of the atomic and thermal factors. The small number of interference lines on the patterns of the hydrogen isotopes does not permit reliable indexing and the determination of the law of interference extinction, and thus an unambiguous selection of the space groups. However, this might still be attempted with a certain degree of reliability.

Knowing the densities of hydrogen, deuterium,[4] and tritium[5] it can be shown (if consideration is restricted to the simplest cubic, tetragonal, and hexagonal syngonies) that the lines present in the patterns do not represent reflections from the planes with the smallest indices. This immediately permits the establishment of a series of extinctions at the smallest angles and thereby reduces the range of possible space groups. Thus it proves possible to propose one most probable space group for deuterium and tritium, and two for hydrogen between which a final choice could not be made on the basis of the available patterns. The results of the calculations are presented in the table.

In calculating the lattice parameters on the basis of lines not only few in number, but also arrayed at small angles, the following method was employed to render possible extrapolation up to 90°.* Using the same object under identical conditions, x-ray photographs were taken with different radiation sources. The lattice parameters calculated according to the lines in these photographs, located in dependence upon the wavelength at the different respective angles, furnished the set of values needed for executing the extrapolation. Figure 5 shows the extrapolation line for the parameter c of the deuterium lattice, calculated on the basis of the single line 002, taken with four radiation sources.

The accuracy of the calculated lattice parameters shown for hydrogen and deuterium in the table, as well as the choice of the space group for deuterium, is corroborated by the results of x-ray structural analysis for samples of hydrogen-deuterium mixtures: in the range of solid solutions an increase in the concentration of deuterium occasions

---

*To reduce the relative error in determining the lattice parameters.

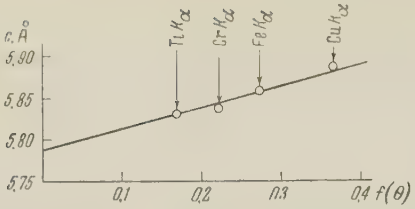

FIG. 5. Extrapolation graph for the parameter c of deuterium (the value of c is determined in accordance with line 002, in patterns taken with each of four radiation sources: Cu K_α, Fe K_α, Cr K_α, Ti K_α). The abscissas represent

$$f(\theta)=\frac{1}{2}\left[\frac{\cos^2\theta}{\sin^2\theta}+\frac{\cos^2\theta}{\theta}\right]$$

a decrease of the average volume per molecule, while an increase in the concentration of hydrogen causes a decrease of this volume. This agrees with the tabulated data, from which it is seen that the volume per molecule in the deuterium lattice (~ 33 A^3) is smaller than the value in the hydrogen lattice (~ 38 A^3). At both of the solid-solution limits (15% and 80% deuterium by volume) the mean volume per molecule is ≈ 35 A^3.

Patterns of deuterium samples with large hydrogen admixtures (20% hydrogen by volume) have not one line, like those of pure deuterium, but two closely spaced lines. This corresponds to a change in the ratio of the tetragonal lattice axes up to values at which coincidence of the lines 101 and 002 no longer occurs. A magnified pattern of such a mixture is presented in Fig. 6; it was taken without a filter and without lead screens, so that the lines of Fe K_β and the extraneous lines of type 6 (Fig. 4) are visible in it.

The foregoing data on the structures of the hydrogen isotopes should not be considered definitive until they have been confirmed by some other method permitting the display of a larger number of interferences. The most effective would probably be the neutron diffraction method, which possesses the advantage that its application is not subject to so sharp a decrease of interference intensity with increasing scattering angle. Thus the use of neutron diffraction would in considerable measure remove the difficulty encountered in the observation of interferences in the scattering of x-rays in such light objects as the hydrogen isotopes, and which yields only one or two interference lines at small angles.

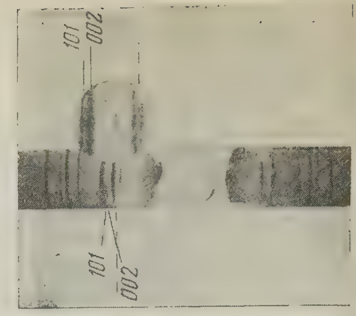

FIG. 6. Enlarged pattern of a hydrogen-deuterium mixture (80% deuterium by volume). 101 and 002 are the lines of a solid solution of hydrogen in deuterium. The dashes point to the extraneous lines of type 6 and 6′ (see Fig. 4).

However, independently of the results of the experiments which will be undertaken for the more accurate determination of the structures of the hydrogen isotopes, it is already possible, from the character of the interference patterns, to affirm a difference in the structures of hydrogen and deuterium and a close similarity of the structures of deuterium and tritium. The solid-liquid phase diagram for the hydrogen-deuterium system,[1] in which there is no region occupied by a continuous series of solid solutions right up to the melting point, is also in accord with the fact that these isotopes crystallize in lattices of different structure.

The existence of the phenomenon of isotopic polymorphism, observed in the hydrogen isotopes,[3] was recently corroborated by studies of the structure of helium isotopes, in which it was shown that He^3 has a second modification, different in structure from He^4.[6]

The authors express their thanks to M. N. Massalitin for the construction of the cryostats used in this work.

---

[1] Kogan, Lazarev, and Bulatova, JETP **34**, 238 (1958), Soviet Phys. JETP **7**, 165 (1958).

[2] Keesom, De Smedt, and Mooy, Comm. Phys. Univ. Leiden, 209d (1930).

[3] Kogan, Lazarev, and Bulatova, JETP **31**, 541 (1956), Soviet Phys. JETP **4**, 593 (1957).

[4] Wooley, Scott, and Brickwedde, J. Res. N. B. S. **41**, 379 (1948).

[5] E. R. Grilly, J. Amer. Chem. Soc. **73**, 5307 (1951).

[6] Schuch, Grilly, and Mills, Phys. Rev. **110**, 775 (1958).

Translated by J. E. Viscardi
133

SOVIET PHYSICS JETP VOLUME 37(10), NUMBER 3 MARCH, 1960

INVESTIGATION OF A SHOWER CONSISTING OF 200,000 PARTICLES AND RECORDED IN A NUCLEAR PHOTOGRAPHIC PLATE

N. L. GRIGOROV and M. A. KONDRAT'EVA

Institute of Nuclear Physics, Moscow State University

Submitted to JETP editor April 30, 1959

J. Exptl. Theoret. Phys. (U.S.S.R.) **37**, 684-689 (September, 1959)

Electron-sensitive photographic plates were used to investigate the lateral and angular distributions of particles of a large shower that developed in lead. It is shown that at a shower energy on the order of 4×10^{13} ev the lateral distribution of all particles and the angular characteristics of the particles in the central portion of the shower are in agreement with the cascade theory.

1. LATERAL DISTRIBUTION OF PARTICLES; NUMBER OF PARTICLES, AND SHOWER ENERGY

A very large electron-photon shower, with an axis inclined 15° to the normal to the plane of the plate, was found on a NIKFI type R plate (200 μ), exposed in 1956 on Mt. Aragats in apparatus with ionization-chambers.[1] Figure 1 shows a microphotograph of the central portion of this shower.

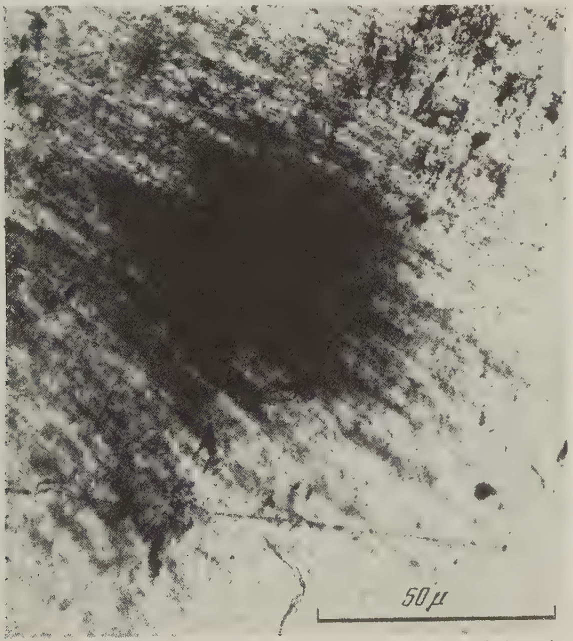

FIG. 1. Microphotograph of the central portion of the shower.

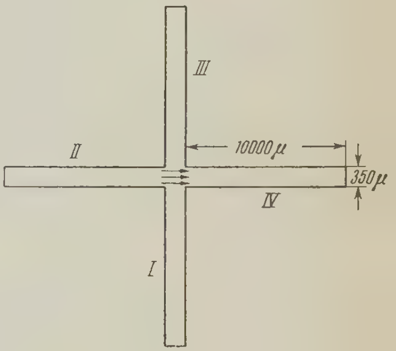

FIG. 2. Relative positions of the traced sections of the shower. The arrows indicate the direction of the projection of the shower axis.

Using the RA-1 drawing apparatus, mounted on one of the eyepieces of the MBI-2 microscope set at magnification 1350, all the particles of the shower and of the background were transferred to paper. These particles were located in four-mutually perpendicular sections at distances $500\,\mu \leq r \leq 10{,}000\,\mu$ from the axis of the shower (Sections I and III are perpendicular to the direction of the shower-axis projection, while II and IV are parallel to the projection, see Fig. 2). To determine the background on a given plate, all the tracks of relativistic particles were traced on several sections 2 — 5 cm outward from the center of the shower. The background was found to be $(1.02 \pm 0.03) \times 10^{-3}$ particle/μ^2. After subtracting the background, we obtained the lateral distribution of the shower particles in the distance interval $500 \leq r \leq 10{,}000\,\mu$.

At distances $r < 500\,\mu$ from the axis, the particle density is too great to be determined directly. Therefore the data on the lateral distribution at small distances from the shower axis were obtained by photometry with a MF-4 microphotometer. For this purpose, a negative of the shower, magnified 30 times, was obtained on a photographic film and the photometric evaluation was made at a magnification 30, with a slit 1.1×5.0 mm. If these slit dimensions are referred to the true size of the shower, we find that the photometry covered a shower section measuring $1.2\,\mu \times 5.6\,\mu$, i.e., an area of $6.8\,\mu^2$. The photometric results were compared with the calibration of the nuclear emulsion, made with electrons of energy $E \gtrsim 1$ Mev. The density $\rho(r)$ thus obtained, together with the density at $r > 500\mu$, is shown in Fig. 3.

Figure 3 shows also the function of the lateral distribution for $E_0 = 4 \times 10^{13}$ ev for a shower at the maximum of its development ($S = 1.0$), obtained by interpolation from the data of Kamata and Nishimura.[2] The lateral distribution of Kamata and Nishimura agrees well with the experimental lateral distribution. The discrepancy in the region $r < 100\mu$ may indicate that this shower is an electron-nuclear shower, generated in lead.

The number of the particles in the shower was counted separately in the following regions. 1) $0 \leq r \leq 250\mu$, where $\rho(r)$ was determined by photometry, $N_1 = 10{,}000$ particles. 2) Summation by rings (for $250\mu \leq r \leq 10{,}000\mu$) yields $N_2 = 150{,}000$ particles, i.e., $N_1 + N_2 = 160{,}000$ particles. 3) At $r > 10^4\mu$, a power law $\rho(r) = B/r^3$ or $\rho(r) = B/r^4$ is assumed; if $\rho(r) \sim r^{-3}$, then $N_3 = 88{,}000$ particles, and if $\rho(r) \sim r^{-4}$, then $N_3 = 42{,}000$ particles.

Since scattering is stronger in lead than in air, $\rho(r)$ is expected to drop off at large distances no faster than in air. Then, assuming $\rho(r) \sim r^{-3}$ at $r > 10{,}000\mu$, we obtain $N_0 = 160{,}000 + 88{,}000 = 248{,}000$ particles. The error in the total number of particles, due to errors in the determination of $\rho(r)$, is approximately 20%. Thus, $N_0 = (248 \pm 50) \times 10^3$ particles.

If it is assumed that the shower is observed at the maximum of its development, i.e., $N_0 = N_{max}$, we can determine the energy of the soft component of this shower from the following formula

$$N_{max} = 0.17\,(E/\beta)/\sqrt{\ln (E/\beta)} = N_0. \qquad (1)$$

From (1) we obtain $E_0 \geq E = (3.6 \pm 0.7) \times 10^{13}$ ev.

Were this shower to be created by a primary electron (photon), ordinary cascade theory would give $t_{max} = \ln (E_0/\beta) = 15.5$ t-units. But we observe the shower at a depth $t = 21.7$ t-units, i.e., six t-units deeper than the maximum of the number of particles. This difference is either due to the Pomeranchuk-Migdal effect, or else we deal with an electron-nuclear shower of high energy.

2. ANGULAR DISTRIBUTION OF PARTICLES

A. Distribution of particles about the shower axis. Figure 4 gives an idea of the character of

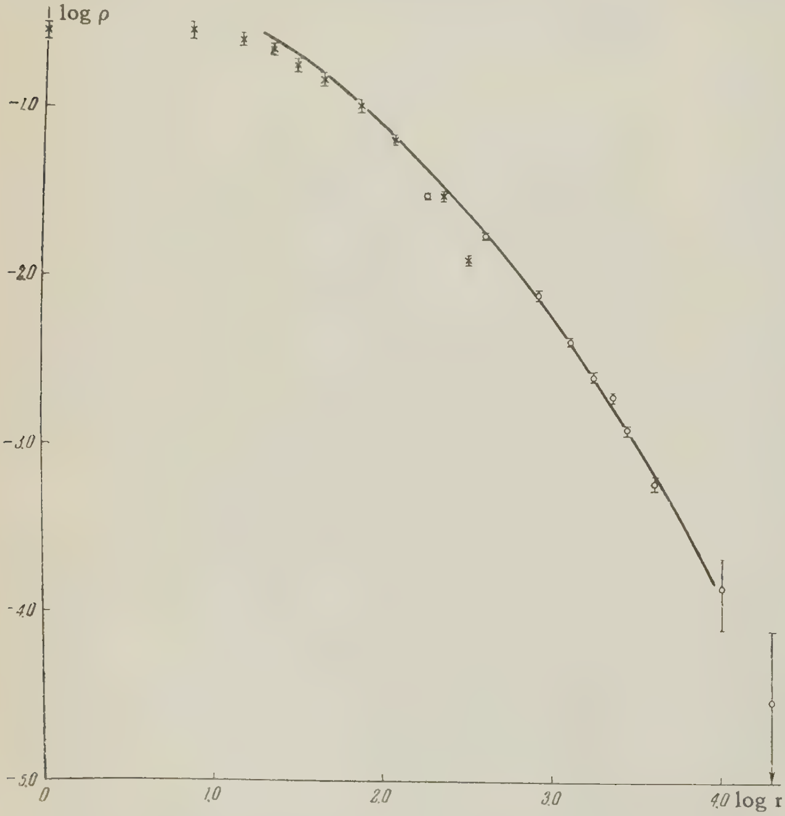

FIG. 3. Lateral distribution of shower particles. Abscissa – logarithm (to the base 10) of the distance from the center of the shower in microns; ordinate – logarithm (to the base 10) of the density of the shower particles ρ (particles/μ^2), × – photometry data, mean-squared error; o – data obtained by counting the number of particles directly, statistical error; solid line – theoretical curve obtained from the Kamata and Nishimura data.[2]

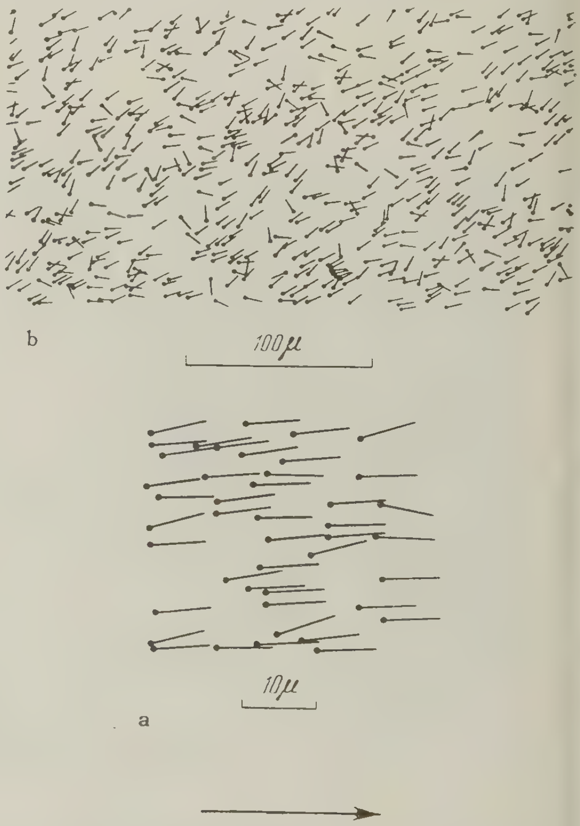

FIG. 4. Angular distribution of particles at a distance 100μ (a) and 600μ (b) from the center of the shower. The dashes represent the projections of the particle tracks on the emulsion plane, the dots represent the points where the particles enter the emulsion, and the arrow represents the direction of the projection of the core of the shower.

the angular distribution of particles in the shower. The figure shows the projections of the particle tracks in two sections, $100\,\mu$ and $600\,\mu$ away from the center of the shower.

It is seen from Fig. 4, that at a given distance r from the shower axis the projections of the particle tracks follow on the average a certain common direction, determined by an angle $\bar{\lambda}$. A detailed measurement of the angles λ_i between the projections of the track and of the shower core on the plane of the emulsion shows that as the distance r from the center of the shower increases, the average angle $\bar{\lambda}$ of a particle group increases first in proportion to r, and then at a slower rate.

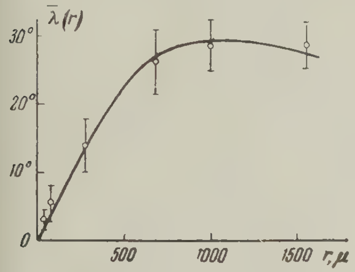

FIG. 5. Dependence of $\bar{\lambda}$ on the distance r from the center of the shower. Mean-squared errors.

Figure 5 shows the results of the measurements of $\bar{\lambda}$ at various distances r from the center of the shower in sections I and III. Since sections I and III in the emulsion plane are perpendicular to the projection of the shower core, the quantity $x = r/\tan\bar{\lambda}$ gives the coordinate of the point to which the continuations of the projections of the shower-particle tracks converge. This point is located from 0.84 mm (for tracks with $r = 43\,\mu$) to 1.84 mm (for tracks with $r = 1000\,\mu$) from the center of the shower (in the emulsion plane). Thus, over a wide range of distances from the center of the shower, the particles have at each point of the shower a common direction, inclined to the shower axis at an angle $\bar{\theta}$ given by $\tan\bar{\theta} = r/y$, where y is the height of the cone, measured along the axis of the shower from the plane of observation, and r is the distance from the center of the shower in a plane perpendicular to the shower axis. We can readily obtain the value of y from the known values of x and of the angle β_0 between the shower axis and the normal to the emulsion plane.

$$x = y\sin\beta_0.$$

From these relations we obtain the connection between the angles $\bar{\lambda}$ and $\bar{\theta}$

$$\bar{\theta} = \tan^{-1}(\sin\beta_0\tan\bar{\lambda}). \qquad (2)$$

The shower considered has $\beta_0 = 15°$, and thus $y = 3.9\,x$ and $\bar{y} = 3.9\,\bar{x}$. The average over the range $43\,\mu \le r \le 1000\,\mu$ is (1.2 ± 0.23) mm. Thus, $\bar{y} = (4.7 \pm 0.9)$ mm. The shower unit in lead is 5.2 g/cm^2 or 4.6 mm. Consequently, $\bar{y} = (1.0 \pm 0.2)$ t-units and $\bar{\theta}(r) = \tan^{-1} \times [r/(1.0 \pm 0.2)]$ for $r \le 0.2$ t-units.

B. Distribution of the particles about the mean direction. If one takes an area, with dimensions considerably smaller than the distance r from the area to the center of the shower, then the particles that strike this area, which have a common mean direction determined by the angle $\bar{\lambda}$, are distributed in some manner relative to this mean direction (see Fig. 4). The average spread, $\overline{\Delta\lambda} = \sum^{n}\Delta\lambda_i/n$ (where $\Delta\lambda_i = |\lambda_i - \bar{\lambda}|$), was determined for all sections (I, II, III, and IV) and at various distances r from the center of the shower. The dependence $\overline{\Delta\lambda}(r)$ is shown in Fig. 6.

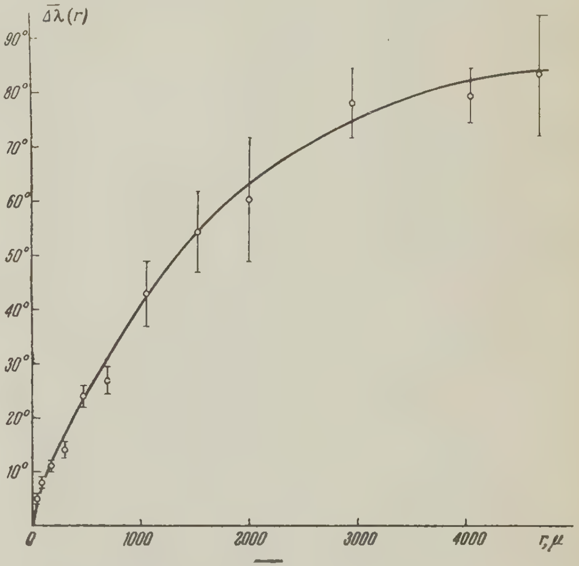

FIG. 6. Dependence of $\overline{\Delta\lambda}$ on the distance r from the center of the shower. Mean-squared errors.

The fact that the projections of the particle tracks are distributed about the angle $\bar{\lambda}(r)$ in the emulsion plane denotes that the particles have a certain distribution in space about the angle $\bar{\theta}(r)$ between the particle group and the shower axis. To evaluate the distribution of the particles about a mean direction, specified by an angle $\bar{\theta}(r)$, we measured the angles λ_i and $\Delta\theta_i$, where $\Delta\theta_i = |\theta_i - \bar{\theta}|$ is the angle between the track of the i-th particle and the mean direction corresponding to $\bar{\theta}(r)$. The measurements were made $850\,\mu$ from the center of the shower, in sections I and III. The distribution of the particles about the angles $\Delta\theta_i$ is shown in Fig. 7, which also shows the Gaussian distribution. As can be seen from the diagram, the distribution of the particles about $\bar{\theta}(r)$ is Gaussian, i.e., $n(\theta) = C\exp\{-\theta^2/2\Delta\theta^2\}$. From

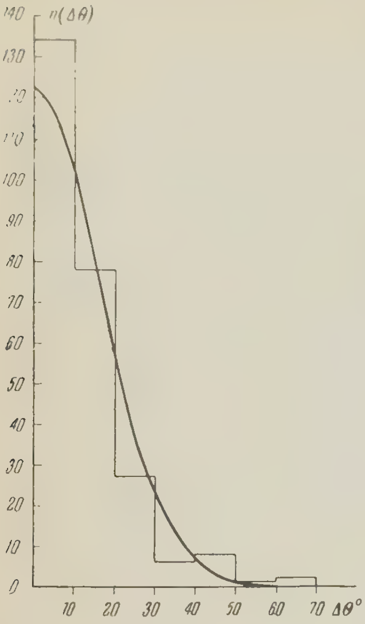

FIG. 7. Distribution about the angles $\Delta\theta_i$, obtained for particles at a distance 850μ from the center of the shower. Curve – Gaussian distribution.

these measurements, performed for $r = 850\,\mu$, we obtained $\overline{\Delta\lambda} = 33°$ and $\overline{\Delta\theta} = 13°$.

It is impossible to measure $\overline{\Delta\theta}$ at smaller distances directly, since the particle density is too high. We therefore proceeded as follows. Calculation has shown that $\overline{\Delta\lambda}$ and $\overline{\Delta\theta}$ are linearly related up to $\Delta\theta \sim 10°$. Using the coefficient of proportionality between $\overline{\Delta\lambda}$ and $\overline{\Delta\theta}$, determined experimentally for $r = 850\,\mu$ $(\overline{\Delta\theta}/\overline{\Delta\lambda} = 0.4)$, we were able to evaluate $\overline{\Delta\theta}$ from the known $\overline{\Delta\lambda}$. Thus, we obtained $\overline{\Delta\theta}$ for various r and from the known $\overline{\Delta\theta}$, assuming the $\overline{\Delta\theta}$ to be due essentially to Coulomb scattering of the particles, we determined the effective energies of the shower particles at various distances from the center of the shower, namely $E = E_s/\overline{\Delta\theta}$, where $E_s = 21$ Mev.

The data obtained in this manner were compared with the data of Guzhavin and Ivanenko,[3] who calculated $\theta_x E/E_s$ for electrons (θ_x is the mean of the projections of the angles between the particles and the shower axis on the plane in which the shower axis is located) as a function of $\tilde{x}_0 = x_0 E/E_s$ (x_0 is the distance from the shower axis, in t-units). The values for θ_{exp} were determined from (2). (see table).

x_0	$\overline{\Delta\theta} = 0.4\overline{\Delta\lambda}$, deg	E, ev	$\tilde{x}_0$	θ_x	θ_{exp}
0.01	1.6	$7.5 \cdot 10^8$	0.357	0.6	0.7
0.04	4.8	$2.5 \cdot 10^8$	0.476	2.1	2.7
0.10	9.2	$1.3 \cdot 10^8$	0.620	4.6	6.1
0.20	15.2	$0.8 \cdot 10^8$	0.760	8.1	8.5

The agreement obtained cannot be deemed absolute, since θ_x and θ_{exp} differ somewhat, but it can be stated that our data (within the limits of the assumptions made) do not contradict the cascade theory.

The authors express deep gratitude to A. V. Podgurskaya, who participated in the 1956 expedition on Mt. Aragats, to P. M. Smirnov, who observed this interesting event, and to A. I. Plekhova for help in the reducing of the shower data.

---

[1] Brikker, Grigorov, Kondrateva, Podgurskaja, Savel'eva, Sobinjakov, and Sestoperov, Nuovo cimento **8**, Suppl. No. 2, 733 (1958).

[2] K. Kamata and J. Nishimura, Progr. Theoret. Phys. Suppl. No. 6, 93 (1958).

[3] V. V. Guzhavin and I. P. Ivanenko, JETP **36**, 1509 (1959), Soviet Phys. JETP **9**, 1070 (1959).

Translated by J. G. Adashko
134

SOVIET PHYSICS JETP VOLUME 37 (10), NUMBER 3 MARCH, 1960

ON THE THEORY OF MAGNETIC-MOMENT RELAXATION IN FERRODIELECTRIC SUBSTANCES

V. G. BAR'YAKHTAR

Physico-Technical Institute, Academy of Sciences, Ukrainian S.S.R.

Submitted to JETP editor February 9, 1959

J. Exptl. Theoret. Phys. (U.S.S.R.) **37**, 690-694 (September, 1959)

The relaxation of magnetic moment and the equalization of temperatures between spin waves and lattice in a ferrodielectric substance are investigated at low temperatures $T \ll \Theta_c$. For $T \gg \Theta_1$, $\Theta_1 = \Theta_c(\mu M_0/\Theta_c)^{4/7}$ a Bose distribution corresponding to the nonequilibrium magnetic moment is first set up, then the equilibrium value of the magnitude of the magnetic moment is established and, finally, a rotation of the magnetic moment to its equilibrium direction occurs. For $T \ll \Theta_1$ the magnetic moment assumes its equilibrium value simultaneously with the establishment of the Bose distribution of the spin waves, and then the magnetic moment rotates to its equilibrium direction.

Simple formulas are obtained which describe the temperature equalization of the spin waves and the lattice, and the relaxation of the magnetic moment.

1. In the paper by Akhiezer, Peletminskiĭ and the present author[1] the relaxation of magnetic moment in a ferrodielectric substance was investigated in the temperature range $\Theta_c \gg T \gg \Theta_c(\mu M_0/\Theta_c)^{4/7}$ (μ is the Bohr magneton, M_0 is the equilibrium magnetic moment per unit volume, Θ_c is the Curie temperature) and the relaxation constants were calculated. In doing this it was established that the slowest process is the rotation of the magnetic moment towards the axis of easiest magnetization.

In this paper we investigate in greater detail the establishing of the magnitude of the magnetic moment and the equalization of the lattice and the spin-wave temperature in the case when there is no deviation of the magnetic moment from the equilibrium direction. We also consider the relaxation of the magnetic moment and the leveling out of temperatures in the ferrodielectric at temperatures $T \ll \Theta_1$ [for the sake of brevity we shall use the notation $\Theta_1 = \Theta_c(\mu M_0/\Theta_c)^{4/7}$].

We start the investigation of relaxation processes in a ferrodielectric with the kinetic equation for the distribution function of the spin waves

$$\dot{n}_k = \dot{n}_k^{st} \equiv L_k\{n, N\},$$

$$L_k\{n, N\} = L_k^e\{n\} + L_k^w\{n\} + L_k^p\{n, N\} + L_k^a\{n\} \qquad (1)$$

(the expressions for L_k^e, L_k^w, L_k^p, and L_k^a are given in reference 1).

In the temperature range $\Theta_c \gg T \gg \Theta_1$ the principal role in the setting up of the Bose distribution in the spin wave system is played by the exchange interaction ($L_k^e \gg L_k^w$, L_k^p, L_k^a) as a result of which during a time $\sim (\hbar/\Theta_c)(\Theta_c/T)^4$ the following distribution is established

$$n_k = \left[\exp\left(\frac{\varepsilon_k - \gamma}{T_s}\right) - 1\right]^{-1}. \qquad (2)$$

This distribution is a solution of the equation $L_k^e\{n\} = 0$.

The chemical potential γ and the temperature of the spin waves T_s are determined in such a case by the absolute value of the magnetic moment of the sample

$$\mathfrak{M}^2 = \left(\int M dv\right)^2 = (M_0 V)^2 - 4\mu M_0 V \sum_{k \neq 0} n_k \qquad (3)$$

and by the energy of the spin system.

The presence of the weak interactions taken into account by means of the operators L_k^w, L_k^a, L_k^p brings about the situation that γ and T_s vary slowly with time [compared to the time required for the establishment of the distribution (2)]. Variation with time of γ and T_s leads to the variation with time of the phonon temperature T_p.

On substituting into the collision integral $L_k\{n, N\}$ the distribution function for the spin waves (2) and the phonon distribution function

$$N_{fs} = [\exp(\hbar\omega_{fs}/T_p) - 1]^{-1}$$

and on expanding in terms of the quantities γ and $\Delta T = \Delta T_s - \Delta T_p$, which characterize small deviations of the system from complete thermodynamic equilibrium, we obtain

$$L_{\mathbf{k}}\{n,\ N\} = \gamma\,(\partial L_{\mathbf{k}}/\partial\gamma)_0 + \Delta T\,(\partial L_{\mathbf{k}}/\partial\Delta T)_0, \qquad (4)$$

where the subscript 0 means that the values of the derivatives of the collision integral are taken at $\gamma = 0$, $\Delta T = 0$.

The time variation of the quantities γ, $\Delta T_s = T_s - T$, $\Delta T_p = T_p - T$ (T is the equilibrium temperature) can be determined from the following equations

$$\sum_{fs} \hbar\omega_{fs}\dot{N}_{fs} = -\sum_{\mathbf{k}} \varepsilon_{\mathbf{k}} L_{\mathbf{k}}\{n,\ N\},$$

$$\sum_{\mathbf{k}} \dot{n}_{\mathbf{k}} = \sum_{\mathbf{k}} L_{\mathbf{k}}\{n,\ N\}, \qquad \sum_{\mathbf{k}} \varepsilon_{\mathbf{k}}\dot{n}_{\mathbf{k}} + \sum_{fs} \hbar\omega_{fs}\dot{N}_{fs} = 0. \qquad (5)$$

The first equation determines the amount of heat transmitted from the lattice to the spin wave, the second equation determines the change in the total number of spin waves which determines γ, while the third relation between ΔT_s, ΔT_p, and γ represents the law of conservation of energy. By using (4) and (5) these equations can easily be put into the following form

$$c_s\Delta\dot{T}_s + c_p\Delta\dot{T}_p - \dot{\gamma}\sum_{\mathbf{k}} \varepsilon_{\mathbf{k}}\,\partial n_{\mathbf{k}}/\partial\varepsilon_{\mathbf{k}} = 0,$$

$$c_p\Delta\dot{T}_p = A_{T\gamma}\gamma + A_{TT}\,\Delta T,$$

$$-\dot{\gamma}\sum_{\mathbf{k}} \partial n_{\mathbf{k}}/\partial\varepsilon_{\mathbf{k}} + \Delta\dot{T}_s\sum_{\mathbf{k}} \partial n_{\mathbf{k}}/\partial T = A_{\gamma\gamma}\gamma + A_{\gamma T}\,\Delta T, \qquad (6)$$

where

$$A_{T\gamma} = -\sum_{\mathbf{k}} \varepsilon_{\mathbf{k}}(\partial L_{\mathbf{k}}/\partial\gamma)_0, \qquad A_{\gamma\gamma} = \sum_{\mathbf{k}} (\partial L_{\mathbf{k}}/\partial\gamma)_0,$$

$$A_{TT} = -\sum_{\mathbf{k}} \varepsilon_{\mathbf{k}}(\partial L_{\mathbf{k}}/\partial\Delta T)_0, \qquad A_{\gamma T} = \sum_{\mathbf{k}} (\partial L_{\mathbf{k}}/\partial\Delta T)_0,$$

$$c_s = \frac{15\,\zeta(^3/_2)}{32\,\pi^{3/2}}\frac{V}{a^3}\left(\frac{T}{\Theta_c}\right)^{3/2}, \qquad c_p = \frac{2\pi^2}{5}\frac{V}{a^3}\left(\frac{T}{\Theta_D}\right)^3,$$

c_s and c_p are the spin and the phonon heat capacities, a is the lattice constant, Θ_D is the Debye temperature, V is the volume of the sample. It may be shown that the quantities $A_{T\gamma}$ and $A_{\gamma T}$ are related by the equation $A_{T\gamma} = -TA_{\gamma T}$.

The values of the quantities A as functions of the temperature may be obtained by considering the specific form of the collision integrals. We shall give here only the final formulas obtained for a uniaxial ferrodielectric. If $T \gg \Theta_D^2/\Theta_c,\ \Theta_1$, then

$$A_{\gamma\gamma} = -\frac{1}{5\pi}\frac{V}{a^3}\frac{\mu M_0}{\hbar}\frac{\mu M_0}{\varepsilon_0\Theta_c}\left(\frac{T}{\Theta_c}\right)^2.$$

$$A_{T\gamma} = \frac{1}{6\pi^2}\frac{V}{a^3}\frac{\hbar}{\rho a^5}\,\delta^2\left(\frac{\mu M_0}{\Theta_c}\right)^2\left(\frac{T}{\Theta_c}\right)^2,$$

$$A_{TT} = \frac{4\pi}{15}\frac{\hbar}{\rho a^5}\,[2\beta_1^2 + (2\beta_1 + \beta_2)^2]\left(\frac{T}{\Theta_c}\right)^4 \equiv \frac{4\pi}{15}\frac{\hbar}{\rho a^5}\beta_e^2\left(\frac{T}{\Theta_c}\right)^4, \qquad (7)$$

where ρ is the density of the substance, $\epsilon_0 = \mu H_0 + \mu\beta M_0$ is the energy of the spin wave with $\mathbf{k} = 0$, β is the anisotropy constant, δ is the magnetostriction constant, and β_1 and β_2 are numerical constants of the order of magnitude of unity, which appear as coefficients in the Hamiltonian of the exchange interaction between the spin waves and the phonons [the Hamiltonians of the interactions of the spin waves with each other and of the spin waves with the phonons are given in reference 1, formulas (2) – (5)].

By assuming that γ, ΔT_s, and ΔT_p vary with time as $e^{-\lambda t}$, we obtain the following values for the relaxation constants when $T \gg \Theta_D^2/\Theta_c,\ \Theta_1$:

$$\lambda_1 \approx \frac{\mu M_0}{\hbar}\frac{\mu M_0}{\sqrt{\varepsilon_0\Theta_c}}\frac{T}{\Theta_c}, \qquad \lambda_2 \approx \frac{\hbar}{\rho a^5}\beta_e^2\left(\frac{T}{\Theta_c}\right)^{5/2}. \qquad (8)$$

The relaxation constant λ_1 is determined primarily by the relativistic magnetic interaction which describes the fusion of two spin waves into one and the splitting of one spin wave into two. The relaxation constant λ_2 is associated with the exchange interaction between the spin waves and the phonons describing creation and absorption of a phonon by a spin wave. Thus, if $M_0 \sim 10^3$ G, $\epsilon_0 = \mu(H + \beta M_0) \sim 10^{-16}$ erg, $\Theta_c \sim 10^3$ °K, $T \sim 10^2$ °K, then $\lambda_1 \sim 3 \times 10^6\ \text{sec}^{-1}$, $\lambda_2 \sim 10^9\ \text{sec}^{-1}$. It may be seen from (8) that the inequality $\lambda_2 \gg \lambda_1$ holds in the temperature range $T \gg \Theta_c\mu M_0/\beta_e^2\sqrt{\epsilon_0\Theta_c} \sim 10$°K.

The time variation of the difference ΔT between the temperatures of the spin waves and of the phonons, and of the difference in the magnitudes of the magnetic moment $\mathfrak{M}$ is determined, according to (3), (2), and (6), by the following formulas

$$\frac{\mathfrak{M} - \overline{\mathfrak{M}}}{M_0V} = \frac{\mathfrak{M}_0 - \overline{\mathfrak{M}}}{M_0V}\frac{e^{-\lambda_1 t} + \alpha e^{-\lambda_2 t}}{1 + \alpha}$$

$$+ \frac{\varepsilon_0}{\Theta_c}\left(\frac{\lambda_1}{\lambda_2}\right)^2\left(\frac{T}{\Theta_c}\right)^{1/2}\frac{\Delta T_0}{T}\,(e^{-\lambda_2 t} - e^{-\lambda_1 t}),$$

$$\frac{\Delta T}{T} = \frac{\Delta T_0}{T}\frac{e^{-\lambda_2 t} + \alpha e^{-\lambda_1 t}}{1 + \alpha}$$

$$+ 9\left(\frac{\varepsilon_0\Theta_c}{T^2}\right)^{1/2}\frac{\Theta_c}{T}\frac{\mathfrak{M}_0 - \overline{\mathfrak{M}}}{M_0V}\,(e^{-\lambda_1 t} - e^{-\lambda_2 t}), \qquad (9)$$

where $\alpha \approx 2(\lambda_1/\lambda_2)^2(\epsilon_0/T)^{1/2} \ll 1$, $\overline{\mathfrak{M}}$ is the equilibrium value of the magnetic moment at a given temperature, $\mathfrak{M}_0$ is the initial value of the magnetic moment, ΔT_0 is the initial temperature difference.

If these initial data are such that $\Delta T_0 = 0$, then

$$\mathfrak{M} - \overline{\mathfrak{M}} \approx (\mathfrak{M}_0 - \overline{\mathfrak{M}})\,(e^{-\lambda_1 t} + \alpha e^{-\lambda_2 t})/(1 + \alpha).$$

Since $\alpha \ll 1$ and $\lambda_2 \gg \lambda_1$, then

$$\mathfrak{M} - \overline{\mathfrak{M}} \approx (\mathfrak{M}_0 - \mathfrak{M})\,e^{-\lambda_1 t}. \qquad (10)$$

From this it can be seen that the magnetic moment relaxes during a time of the order of $\tau_{\mathfrak{M}} = 1/\lambda_1$.

If at zero time $\mathfrak{M}_0 = \overline{\mathfrak{M}}$, then the leveling out of the temperatures is described by the formula

$$\Delta T = \Delta T_0 (e^{-\lambda_2 t} + \alpha e^{-\lambda_1 t}) / (1 + \alpha). \tag{11}$$

We note that the leveling out of the temperatures proceeds at different rates during the initial and final stages of the process. Since the quantity λ_2 is sufficiently great ($\sim 10^9\ \mathrm{sec}^{-1}$ at $T \sim 100°\mathrm{K}$) then, apparently, experimentally it is very difficult to observe the initial stage of the leveling out of the temperatures between the spin waves and the lattice. The complex nature of the relaxation, as has been shown by Kaganov and Tsukernik,[2] leads to a complicated frequency dependence of the magnetic permeability of the ferrodielectric, by studying which one can make conclusions with respect to the interaction processes between spin waves and phonons in the ferrodielectric.

2. Let us now consider the question of the relaxation of the magnetic moment in the temperature region $\epsilon_0 < T \ll \Theta_1$. At such temperatures the average probability of the splitting of a spin wave into two and of the fusion of two spin waves into one which is given[3] by:

$$W_w = \frac{\mu M_0}{\hbar} \frac{\mu M_0}{\Theta_c} \left(\frac{T}{\Theta_c}\right)^{1/2} \ln^2 \frac{T}{\mu M_0}, \tag{12}$$

will be considerably larger than the average probability of the scattering of a spin wave by a spin wave due to the exchange interaction[1,4]

$$W_e \approx (\Theta_c / \hbar)(T / \Theta_c)^4. \tag{13}$$

This means that in the temperature region under consideration the principal role in the kinetic equation for the distribution function of spin waves (1) is played by the operator $L_{\mathbf{k}}^{w}$, while the other collision integrals $L_{\mathbf{k}}^{e}$, $L_{\mathbf{k}}^{a}$, $L_{\mathbf{k}}^{p}$ may be regarded as small perturbations.

It may be easily seen that the solution of the equation $L_{\mathbf{k}}^{w}\{n\} = 0$ is of the form

$$n_{\mathbf{k}} = \begin{cases} n_0, & \mathbf{k} = 0, \\ [\exp(\varepsilon_{\mathbf{k}} / T_s) - 1]^{-1}, & \mathbf{k} \neq 0. \end{cases} \tag{14}$$

In order of magnitude the time for setting up this distribution is equal to $\tau_W = 1/W_W$. We note that the distribution (14) also makes the collision integral $L_{\mathbf{k}}^{e}$ equal to zero.

The parameters of the distribution T_s and n_0 are determined by the energy of the spin system and by the component of the magnetic moment of the sample perpendicular to the axis of easiest magnetization

$$\mathfrak{M}_\perp^2 = 4\mu M_0 V n_0 \tag{15}$$

(in the state of complete thermodynamic equilibrium $\mathfrak{M}_\perp = 0$). The absolute value of the magnetic moment of the sample attains its equilibrium value at a given temperature simultaneously with the establishment of the distribution (14).

The establishment in a ferrodielectric of complete thermodynamic equilibrium is due to weak interactions described in the kinetic equation by the collision integrals $L_{\mathbf{k}}^{a}$ and $L_{\mathbf{k}}^{p}$. Due to these interactions the temperature of the spin waves and the lattice temperature approach their equilibrium values slowly (in comparison with τ_W), while the magnetic moment slowly rotates towards its equilibrium direction.

By utilizing the expressions for the distribution functions of the spin waves (14) and of the phonons, and also the kinetic equation (1), we can obtain the system of equations for determining the variation with time of n_0 and $\Delta T = T_s - T_p$:

$$\Delta \dot{T} + \frac{\varepsilon_0}{c_s} \dot{n}_0 = B_{T0} n_0 + B_{TT} \Delta T, \qquad \dot{n}_0 = B_{00} n_0, \tag{16}$$

where

$$B_{TT} = (1/c_s + 1/c_p) \sum_{\mathbf{k}} \varepsilon_{\mathbf{k}} (\partial L_{\mathbf{k}} / \partial \Delta T)_0, \quad B_{00} = (\partial L_0 / \partial n_0)_0,$$

$$B_{T0} = (1/c_s + 1/c_p) \sum_{\mathbf{k}} \varepsilon_{\mathbf{k}} (\partial L_{\mathbf{k}} / \partial n_0)_0 \equiv a^3 B'_{T0} / V.$$

In the case that $\epsilon_0 < T \ll \Theta_1$, Θ_D^2 / Θ_c we have

$$B_{TT} \approx -\frac{\beta_1^2 \hbar}{\rho a^5} \left(\frac{T}{\Theta_c}\right)^2 \exp\left(-\frac{\Theta_t^2}{4\Theta_c T}\right), \qquad B_{00} \approx -\frac{\mu M_0}{\hbar} \frac{\mu M_0}{\Theta_c} \left(\frac{T}{\Theta_c}\right)^2,$$

$$B'_{T0} \approx -\frac{\hbar \varepsilon_0}{\pi^3 \rho a^5} \left(\frac{\gamma \mu M_0}{\Theta_c}\right)^2 \left(\frac{\varepsilon_0}{T}\right)^2 \left(\frac{\Theta_D}{T}\right)^2 \exp\left(-4 \frac{\varepsilon_0 \Theta_c}{\Theta_t^2} \frac{\varepsilon_0}{T}\right),$$

where $\Theta_t = \hbar s_t / a$, and s_t is the speed of transverse sound.

By assuming that the time variation of the quantities n_0 and ΔT is given by $e^{-\lambda t}$ we shall obtain the following values for the relaxation constants:

$$\lambda' = -B_{00}, \quad \lambda'' = -B_{TT}. \tag{17}$$

In the case that $\epsilon_0 < T \ll \Theta_D^2 / \Theta_c$, Θ_1 we have

$$\lambda' \approx \frac{\mu M_0}{\hbar} \frac{\mu M_0}{\Theta_c} \left(\frac{T}{\Theta_c}\right)^2, \qquad \lambda'' \approx \frac{\beta_1^2 \hbar}{\rho a^5} \left(\frac{T}{\Theta_c}\right)^2 \exp\left(-\frac{\Theta_t^2}{4\Theta_c T}\right). \tag{18}$$

From (15) and (16) we obtain

$$\Delta T = \Delta T_0 e^{-\lambda'' t} + (B'_{T0} / \lambda'')(\mathfrak{M}_{\perp 0} / 2M_0 V)^2 (e^{-\lambda' t} - e^{-\lambda'' t}),$$
$$\mathfrak{M}_\perp^2 = \mathfrak{M}_{\perp 0}^2 e^{-\lambda' t}, \tag{19}$$

where ΔT_0 and $\mathfrak{M}_{\perp 0}$ are the initial temperature difference and the initial value of the transverse component of the magnetic moment of the ferrodielectric.

These formulas show that λ' has a simple physical meaning: $2/\lambda'$ is the relaxation time for the perpendicular component of the magnetic moment.

If the deviation from the equilibrium state of the ferrodielectric is associated only with a difference in the temperatures of the spin waves and of the lattice, then the time for the leveling out of the temperatures is determined by the quantity $\tau = 1/\lambda''$. If $\Delta T_0 = 0$, then in the course of relaxation of the magnetic moment the temperatures of the spin waves and of the lattice will increase at the expense of conversion into heat of the energy associated with the deviation of the magnetic moment of the sample from its equilibrium direction. The time for the establishment of a common temperature under these conditions is equal to half the relaxation time of the transverse component of the magnetic moment.

The author expresses his gratitude to S. V. Peletminskiĭ for aid in this work and to A. I. Akhiezer and M. I. Kaganov for valuable discussions.

---

[1] Akhiezer, Bar'yakhtar, and Peletminskiĭ, JETP **36**, 216 (1959), Soviet Phys. JETP **9**, 146 (1959).

[2] M. I. Kaganov and V. M. Tsukernik, JETP (in press).

[3] A. I. Akhiezer, J. Phys. (U.S.S.R.) **10**, 217 (1946).

[4] M. I. Kaganov and V. M. Tsukernik, JETP **35**, 474 (1958), Soviet Phys. JETP **8**, 327 (1959).

Translated by G. Volkoff
135

SOVIET PHYSICS JETP VOLUME 37 (10), NUMBER 3 MARCH, 1960

NONRESONANCE ABSORPTION OF ELECTROMAGNETIC WAVES IN A MAGNETOACTIVE PLASMA

B. N. GERSHMAN

Radiophysics Institute, Gorkiĭ State University

Submitted to JETP editor February 16, 1959

J. Exptl. Theoret. Phys. (U.S.S.R.) **37**, 695-704 (September, 1959)

The absorption (attenuation) outside the gyromagnetic resonance regions is analyzed from the general equation for three types of high-frequency waves. Both collisions and the specific plasma-absorption mechanisms are taken into account.

IN an earlier paper by the present author[1] the propagation of electromagnetic waves in a plasma in a fixed magnetic field was subjected to a kinetic analysis, in which the thermal motion of the electrons was taken into account. A dispersion equation was obtained for the propagation of the three kinds of characteristic waves: ordinary, extraordinary, and plasma. However, absorption was not considered in reference 1. This gap has been filled to some extent in papers by Sitenko, Stepanov, and Tkalich.[2-4] These authors, however, considered only particular cases. Hence it seems desirable to make a more general analysis, taking account of both collisions and the specific plasma attenuation mechanisms which were first treated by Landau.[5] This approach leads to a number of new results (attenuation of the ordinary wave at low frequencies, a more detailed description of collisions, etc.). Furthermore, a number of points in the calculations given in references 1—4 are supplemented or refined.

In the present work chief attention is given to absorption outside the gyromagnetic resonance regions. Absorption in these regions will be considered in another paper (together with the evaluation of the absorption coefficients given in the formulas that follow).

1. We start from a linearized system consisting of the kinetic equation and the electrodynamic equations*

$$\frac{\partial f}{\partial t} + \mathbf{v}\nabla_r f - \frac{e}{m}\mathbf{E}\nabla_{\mathbf{v}} f_0 - \frac{e}{mc}[\mathbf{v}\times\mathbf{H}_0]\nabla_{\mathbf{v}} f + \nu f = 0,$$

$$\operatorname{curl}\mathbf{H} = -\frac{4\pi e}{c}\int \mathbf{v} f d\tau_{\mathbf{v}} + \frac{1}{c}\frac{\partial \mathbf{E}}{\partial t}, \quad \operatorname{curl}\mathbf{E} = -\frac{1}{c}\frac{\partial \mathbf{H}}{\partial t},$$

$$\operatorname{div}\mathbf{E} = -4\pi e\int f d\tau_{\mathbf{v}}, \quad \operatorname{div}\mathbf{H} = 0, \tag{1.1}$$

where f_0 is the equilibrium distribution function, f is a small deviation from f_0, e and m are the mass and charge of the electron, and $\mathbf{E}$ and $\mathbf{H}$ are the self-consistent electric and magnetic fields. Collisions of electrons with other particles are taken into account directly by introducing the term νf in the first equation in (1.1), where ν is the effective number of collisions of electrons with other particles. We assume that f_0 is Maxwellian and characterized by a temperature T

$$f_0 = N(m/2\pi\varkappa T)^{3/2}\exp(-mv^2/2\varkappa T), \tag{1.2}$$

where N is the equilibrium electron density (N is independent of the coordinates because the plasma is uniform) and κ is the Boltzmann constant.

The system above can be solved by the method given by Landau.[5] In considering propagation in a uniform infinite medium we expand the variables $\mathbf{E}$, $\mathbf{H}$, and f in Fourier integrals in the coordinates (for example, $\mathbf{E} = \int \mathbf{E}_{\mathbf{k}} e^{i\mathbf{k}\cdot\mathbf{r}} d\tau_{\mathbf{k}}$) and consider the equations for the Fourier components characterized by given values of the wave vector $\mathbf{k}$. Then we apply the operational technique, assuming that the values of the nonequilibrium distribution at the initial time $f_{\mathbf{k}}(t=0)$ are given. The solution shows that the asymptotic nature of the behavior of the field is determined by the quantity e^{pt}, where $p = -i\omega - \gamma$ (ω is the frequency and γ the damping factor). Carrying out the appropriate calculations it is possible to obtain the dispersion equation which relates p and the wave vector $\mathbf{k}$.

It is also of interest to consider another formulation of the problem: in this case, at an arbitrary time t the values of the nonequilibrium function $f_\omega(z=0)$ are given in the plane $z=0$ (here and below it is assumed that propagation is along the z axis; f_ω is a spectral component of f).

In this formulation the problem can also be solved by the Landau technique.* In this case the asymptotic behavior of the fields as a function of the coordinate z (for $z > 0$) is determined by $\exp(-qz + ikz)$, where k is the wave number and q is the amplitude of the absorption factor. In the analysis below we use the solution of the problem in the second formulation, although the corresponding formulas for the first formulation are also given.

---

*It is assumed that ion motion can be neglected. In the presence of a fixed magnetic field H_0 this assumption is justified only when $\omega \gg \Omega_H$, where ω is the frequency of the propagating wave and Ω_H is the gyromagnetic frequency of the ions.

We obtain the dispersion equation in the same way as in reference 1. The original system of equations differs from that considered earlier in that collisions are taken into account. Furthermore the boundary conditions are somewhat different from those in reference 1, in which the analysis has been carried out for the first formulation of the problem. This new approach provides results which are much more general. For this reason we do not repeat the entire derivation here. We summarize the important steps and indicate the assumptions which are made.

The dispersion equation can be written in the form

$$\begin{vmatrix} E_1[A_1]-1 & E_1[A_2] & E_1[A_3] \\ E_2[A_1] & E_2[A_2]-1 & E_2[A_3] \\ E_3[A_1] & E_3[A_2] & E_3[A_3]-1 \end{vmatrix} = 0, \qquad (1.3)$$

where the elements of the determinant are given by the relations ($j = 1, 2, 3$)

$$E_1[A_j] = \frac{4\pi ei}{\omega(c^2\tilde{k}^2-\omega^2)}\{(c^2\tilde{k}^2\sin^2\alpha-\omega^2)\,I_1[A_j]$$
$$+\,c^2\tilde{k}^2\sin\alpha\cos\alpha I_3[A_j]\},$$
$$E_2[A_j] = -\frac{4\pi ei\omega}{c^2\tilde{k}^2-\omega^2}\,I_2[A_j],$$
$$E_3[A_j] = \frac{4\pi ei}{\omega(c^2\tilde{k}^2-\omega^2)}\{c^2\tilde{k}^2\sin\alpha\cos\alpha I_1[A_j]$$
$$+\,(c^2\tilde{k}^2\cos^2\alpha-\omega^2)\,I_3[A_j]\}. \qquad (1.4)$$

Here α is the angle between the wave vector **k** and the magnetic field H; $\tilde{k} = k + iq$. Furthermore we assume that the condition

$$|\delta| = |(\varkappa T/m)(\tilde{k}/\omega_H)^2\sin^2\alpha| \ll 1, \qquad (1.5)$$

is satisfied. For weakly damped waves this condition is violated only when there is a weak anisotropy and $\omega_H \ll \omega$ ($\omega_H = eH_0/mc$ is the electron gyromagnetic frequency). If (1.5) is satisfied the quantities $I_i[A_j]$ can be written in the form

$$I_1[A_1] = -(eN/2m)\,[J_0^+ + J_0^-$$
$$+\,\delta(J_0^{++} + J_0^{--} - J_0^- - J_0^+)],$$
$$I_1[A_2] = -I_2[A_1] = -(icN/2m)\,[J_0^- - J_0^+$$
$$+\,\delta\langle 2(J_0^+ - J_0^-) + J_0^{--} - J_0^{++}\rangle],$$
$$I_2[A_2] = -(eN/2m)\,[J_0^+ + J_0^-$$
$$+\,\delta\,\langle 4J_0 - 3(J_0^+ + J_0^-) + J_0^{++} + J_0^{--}\rangle],$$
$$I_3[A_1] = I_1[A_3] = (\tilde{k}\sin\alpha\, eN/2m\omega_H)(J_1^- - J_1^+),$$
$$I_3[A_2] = -I_2[A_3]$$
$$= -(i\tilde{k}\sin\alpha\, eN/m\omega_H)\,[J_1 - \tfrac{1}{2}(J_1^+ + J_1^-)],$$
$$I_3[A_3] = -(2\pi eN/m)\;[J_2 + \delta\,\langle -J_2 + \tfrac{1}{2}(J_2^+ + J_2^-)\rangle]. \qquad (1.6)$$

Here

$$J_0 = \sqrt{\frac{m}{2\pi\varkappa T}}\int\limits_C \frac{1}{-i\omega+\nu+i\tilde{k}v_z\cos\alpha}\exp\left(-\frac{mv_z^2}{2\varkappa T}\right)dv_z. \qquad (1.7)$$

The integrals J_1 and J_2 are obtained from J_0 by adding the factors v_z and $mv_z^2/2\pi\kappa T$ respectively; the integrals denoted by ± are obtained by replacing the frequency ω by $\omega \mp \omega_H$ respectively in the denominator of the integrand while in the integrals denoted by ++ and −− the frequency ω is replaced by $\omega \mp 2\omega_H$.

The integration is carried out along a contour C which bypasses the singularities of the integrands from below (in the plane of v_z). We see that collisions can be taken formally into account by replacing $-i\omega$ with $-i\omega + \nu$. However this substitution cannot be made everywhere, but only in integrals such as that given in (1.7). The relations in (1.6) are obtained by expanding in terms of the small parameter δ. In this case account is taken of the thermal corrections in the first approximation (only terms proportional to the temperature T are retained).

Substituting (1.4) in (1.3) and making use of (1.6) we arrive at the dispersion equation

$$i\omega\omega_0^6\{2\pi J_2 J_0^+ J_0^- - (\tilde{k}^2\sin^2\alpha/2\omega_H^2)\,J_0^- J_1^{+2}$$
$$+\,\delta\,[2\pi J_2\langle J_0(J_0^+ + J_0^-) - 4J_0^+J_0^- + J_0^+J_0^{--} + J_0^-J_0^{++}\rangle$$
$$+\,2\pi J_0^+J_0^-\langle -J_2 + \tfrac{1}{2}(J_2^+ + J_2^-)\rangle]\}$$
$$+\,\omega_0^4\{-J_0^+J_0^-(c^2\tilde{k}^2\sin^2\alpha - \omega^2)$$
$$-\,\pi J_2(J_0^+ + J_0^-)\langle c^2\tilde{k}^2(1+\cos^2\alpha) - 2\omega^2\rangle$$

---

*In solving the problem it is necessary to expand all variables in Fourier time integrals and to use the operational method with respect to the variable z. In the remaining calculations the method is the same as that used for solving the problem in the first formulation.

$$+ (c^2\widetilde{k}^3/\omega_H)\sin^2\alpha\cos\alpha\,\langle J_1(J_0^- - J_0^+) + J_0^+J_1^- - J_1^+J_0^-\rangle$$

$$+\widetilde{k}^2\sin^2\alpha/\omega_N^2 + \langle c^2\widetilde{k}^2(1+\cos^2\alpha) - 2\omega^2\rangle J_1^{+2}/4$$

$$+\delta[(c^2\widetilde{k}^2\sin^2\alpha - \omega^2)\langle 4J_0^+J_0^-$$

$$- J_0(J_0^+ + J_0^-) - J_0^+J_0^{--} - J_0^-J_0^{++}\rangle - \pi(c^2\widetilde{k}^2\cos^2\alpha - \omega^2)$$

$$\times\langle 4J_2(J_0 - J_0^+ - J_0^-) + \tfrac{1}{2}(J_2^+ + J_2^-)(J_0^+ + J_0^-)$$

$$+ J_2(J_0^{++} + J_0^{--})\rangle - \pi(c^2\widetilde{k}^2 - \omega^2)\,\langle J_2(J_0^{++} + J_0^{--})$$

$$+ (J_0^+ + J_0^-)(-2J_2 + \tfrac{1}{2}(J_2^+ + J_2^-))\rangle]\}$$

$$+ (i\omega_0^2/2\omega)(c^2\widetilde{k}^2 - \omega^2)\,\{-(c^2\widetilde{k}^2\sin^2\alpha - 2\omega^2)(J_0^+ + J_0^-)$$

$$+ (2c^2\widetilde{k}^3\sin^2\alpha\cos\alpha/\omega_H)(J_1^- - J_1^+)$$

$$- 4\pi(c^2\widetilde{k}^2\cos^2\alpha - \omega^2)J_2 - \delta[\omega^2\langle -4J_0 + 4(J_0^+ + J_0^-)$$

$$- 2(J_0^{++} + J_0^{--})\rangle$$

$$+ c^2\widetilde{k}^2\sin^2\alpha(-J_0^+ - J_0^- + J_0^{++} + J_0^{--})$$

$$+ 4\pi(c^2\widetilde{k}^2\cos^2\alpha - \omega^2)\langle -J_2 + \tfrac{1}{2}(J_2^+ + J_2^-)\rangle]\}$$

$$- (c^2\widetilde{k}^2 - \omega^2)^2 = 0. \qquad (1.8)$$

Here $\omega_0 = \sqrt{4\pi e^2N/m}$ is the characteristic frequency for the plasma oscillations in the isotropic case. In (1.8) we have retained thermal terms which are at least of order T; this corresponds to taking account of the thermal motion in the first approximation.

2. Using (1.8), we now consider the absorption of various kinds of waves, excluding frequency regions close to the electron gyromagnetic frequency and its multiples. We shall be interested in weakly attenuated waves (the regions of strong attenuation will also be indicated in most cases). In accordance with these remarks we assume that the following relations are satisfied:

$$\omega \gg k\sqrt{\varkappa T/m}\cos\alpha, \qquad \omega \gg \nu, \quad (2.1)$$

$$|\omega - \omega_H| \gg k\sqrt{\varkappa T/m}\cos\alpha, \qquad |\omega - \omega_H| \gg \nu,$$

$$|\omega - 2\omega_H| \gg k\sqrt{\varkappa T/m}\cos\alpha, \qquad |\omega - 2\omega_H| \gg \nu. \quad (2.2)$$

When (2.1) and (2.2) are taken into account, the integrals in (1.7) can be expanded

$$J_0 = \frac{1}{\nu - i\omega} - \frac{\widetilde{k}^2\varkappa T}{(\nu - i\omega)^3 m}\cos^2\alpha$$

$$+ \frac{1}{k\cos\alpha}\sqrt{\frac{m\pi}{2\varkappa T}}\exp\left(-\frac{m\omega^2}{2\varkappa Tk^2\cos^2\alpha}\right),$$

$$J_1 = -\frac{\varkappa T\widetilde{k}\cos\alpha}{m(\nu - i\omega)^2} + \frac{\omega}{k^2\cos^2\alpha}\exp\left(-\frac{m\omega^2}{2\varkappa Tk^2\cos^2\alpha}\right),$$

$$J_2 = \frac{1}{2\pi(\nu - i\omega)} - \frac{3\varkappa T\widetilde{k}^2}{2\pi m(\nu - i\omega)^3}\cos^2\alpha$$

$$+ \frac{\omega^2}{\sqrt{\pi}k^3\cos^3\alpha}\left(\frac{m}{2\varkappa T}\right)^{3/2}\exp\left(-\frac{m\omega^2}{2\varkappa Tk^2\cos^2\alpha}\right). \qquad (2.3)$$

The corresponding formulas for the J^+ integrals can be obtained by replacing ω by $\omega - \omega_H$, for the J^- by replacing ω by $\omega + \omega_H$, for J^{++} by replacing ω by $\omega - 2\omega_H$, etc. In the terms which contain exponentials we replace $\nu - i\omega$ by $-i\omega$ and $\widetilde{k}$ by k (for weakly attenuated waves $q \ll k$). Substituting into (1.8) a relation of the type given in (2.3), we can obtain the dispersion equation. However, this equation is too unwieldy to be given here in general form.

In view of the fact that $q \ll k$, we can in general neglect absorption at the outset [we assume that $\nu = 0$ and omit the exponential terms in (2.3)]. Thus we arrive at the equation

$$\beta^2 vRn^6 - (1 - u - v + uv\cos^2\alpha)n^4 + [2(1 - v)^2$$

$$+ uv(1 + \cos^2\alpha) - 2u]n^2$$

$$+ (1 - v)[u - (1 - v)^2] = 0. \qquad (2.4)$$

Equation (2.4), which is cubic in n^2 ($n = ck/\omega$ is the index of refraction), describes the propagation of the extraordinary ($n^2 = n_1^2$), ordinary ($n^2 = n_2^2$), and plasma waves ($n^2 = n_3^2$). In writing this equation we have used the customary notation: $v = \omega_0^2/\omega^2$, $u = \omega_H^2/\omega^2$ and $\beta^2 = \kappa T/mc^2$. The parameter β represents the ratio of the mean thermal velocity of the electrons to the velocity of light c. In the nonrelativistic case being considered here the relation $\beta^2 \ll 1$ always holds. For example, in the solar corona $\beta^2 \sim 10^{-4}$ and in the ionosphere $\beta^2 < 10^{-6}$. Because β^2 is so small we need retain in (2.4) only those terms independent of β^2 and those of order β^2. We retain only the term that contains the highest power of the quantity ck, i.e., c^6k^6. The approximation used here is adequate for studying the important features of the characteristic waves. For the quantity R in (2.4) we have

$$R = \frac{3\sin^4\alpha}{1 - 4u} + \sin^2\alpha\cos^2\alpha\left\langle 1 + \frac{5 - u}{(1 - u)^2}\right\rangle$$

$$+ 3(1 - u)\cos^4\alpha. \qquad (2.5)$$

We shall not dwell here on a number of questions related to the interpretation of Eq. (2.4) and associated problems; the appropriate discussion can be found in the review in reference 7 and in various papers of the author.[1,8,9] In the work cited curves have been given to show the features of wave propagation in a hot magnetoacoustic plasma. We shall limit ourselves to several pertinent remarks.

If we exclude from consideration the transition region between the extraordinary (ordinary) and plasma waves,[7,9] we have for waves 1 and 2 the well-known relation:[6]

$$(1-u-v+uv\cos^2\alpha)\,n^4-[2(1-v)^2+uv(1+\cos^2\alpha)-2u]\,n^2+(1-v)\,[(1-v)^2-u]=0. \tag{2.6}$$

It is possible to speak of a pure plasma wave in regions of u and v for which the following condition is satisfied:

$$1-u-v+uv\cos^2\alpha\approx 0. \tag{2.7}$$

For n_3^2 we obtain an expression which follows from (2.5) (only terms with n^4 and n^6 are taken into account):

$$n_3^2\approx(1-u-v+uv\cos^2\alpha)/\beta^2 vR. \tag{2.8}$$

Equation (2.8) does not hold at very small values of the numerator, in which case it is necessary to take account of n^2 terms, and at large values of the numerator, in which case $\beta^2 n^2\sim 1$. In the latter case strong absorption may occur. An analysis of (2.4) shows that there are values of the parameters u and v and the angle α for which certain roots may be negative ($n^2<0$); in the region defined by the condition in (2.7), certain roots can even be complex. Inasmuch as dissipation processes have been neglected in making the transition to (2.4) the suppression of the field indicates that propagation is impossible. The situation here is similar to that which obtains above points of reflection for low-frequency radio waves incident on the ionosphere from below. In such cases there are frequency regions for which propagation is impossible. If the thermal motion in the plasma is taken into account the width of the forbidden zone can be smaller than the frequency ω itself. The existence of these narrow gaps in the frequency spectrum in gyromagnetic resonance regions for quasi-transverse propagation ($\alpha\approx\pi/2$) was first noted by Gross.[10]

We now consider the absorption. In this case, in the general dispersion equation, obtained by substituting (2.3) in (1.8), we retain the terms that depend on the collision frequency ν and exponential terms [cf. (2.3)]. Because the conditions in (2.1) and (2.2) are satisfied, the resulting relation for the absorption factor can be written as a sum of two terms: one depends on collisions and the other takes account of the absorption effect due to remote interactions. From (2.1), (2.2), and (2.4) we have (we recall that $\tilde{k}=k+iq$)

$$\frac{q}{k}\{-6\beta^2 vRn^6+4(1-u-v+uv\cos^2\alpha)n^2-2[2(1-v)^2+(1+\cos^2\alpha)uv-2u]\,n^2\}$$
$$=s\Big\{-2\beta^2 vn^6\Big[3\cos^4\alpha-\frac{\sin^2\alpha\cos^2\alpha\,(u-9)}{(1-u)^3}+3\cos^4\alpha+\frac{12u\sin^4\alpha}{1-4u}\Big]+n^4(u-3+2v)+n^2(2v^2-8v-2u+6)$$
$$-3v^2+6v+u-3\Big\}+v\Big\{(u-1)\cos^2\alpha\, n^4+(1-u-v)(1+\cos^2\alpha)\,n^2$$
$$+u-(1-v)^2\}\sqrt{\frac{\pi}{2}}\,\frac{1}{(\beta n\cos\alpha)^3}\exp\Big(-\frac{1}{2\beta^2 n^2\cos^2\alpha}\Big)+v(u-1)\Big\{\frac{\sin^2\alpha\, n^4}{2u}+\Big[v\Big(\frac{1+\cos^2\alpha}{2}+\frac{\sin^2\alpha}{1+\sqrt{u}}\Big)$$
$$-\Big\langle\frac{\sin^2\alpha}{2}+1+\frac{\sin^2\alpha}{\sqrt{u}}(1-\sqrt{u})+\frac{\sin^2\alpha}{2\cos^2\alpha}(1-\sqrt{u})^2(1+\cos^2\alpha)\Big\rangle\Big]n^2$$
$$+\frac{v^2}{1+\sqrt{u}}-v\Big(\frac{2+\sqrt{u}}{1+\sqrt{u}}\Big)+1+\frac{\sin^2\alpha}{2u\cos^2\alpha}(1-\sqrt{u})^2\Big\}\sqrt{\frac{\pi}{2}}\,\frac{1}{\beta n\cos\alpha}\exp\Big(-\frac{(1-\sqrt{u})^2}{2\beta^2 n^2\cos^2\alpha}\Big)+v(u-1)\Big\{\frac{\sin^2\alpha n^4}{2u}$$
$$+\Big[v\Big(\frac{1+\cos^2\alpha}{2}+\frac{\sin^2\alpha}{1-\sqrt{u}}\Big)-\Big\langle\frac{\sin^2\alpha}{2}+1-\frac{\sin^2\alpha}{\sqrt{u}}(1+\sqrt{u})+\frac{\sin^2\alpha}{2\cos^2\alpha}(1+\sqrt{u})^2(1+\cos^2\alpha)\Big\rangle\Big]n^2+\frac{v^2}{1-\sqrt{u}}$$
$$-v\Big(\frac{2-\sqrt{u}}{1-\sqrt{u}}\Big)+1+\frac{\sin^2\alpha}{2u\cos^2\alpha}(1+\sqrt{u})^2\Big\}\sqrt{\frac{\pi}{2}}\,\frac{1}{\beta n\cos\alpha}\exp\Big(-\frac{(1+\sqrt{u})^2}{2\beta^2 n^2\cos^2\alpha}\Big), \tag{2.9}$$

where $s=\nu/\omega$.

We now consider some particular cases. Although the specific absorption [which is characterized by the exponential terms in (2.9)] is small (in accordance with our original assumptions), it is of interest when we are concerned with small values of q, i.e., when the numbers in the exponential are not very large in absolute value. For example, in the factor $\exp(-\frac{1}{2}\beta^2 n^2\cos^2\alpha)$ the quantity $(\beta n\cos\alpha)$ cannot be too small. Since $\beta n\cos\alpha\lesssim\sqrt{\kappa T/m}/v_{ph}$ ($v_{ph}=c/n$ is the phase velocity), when $\beta^2\ll 1$ attenuation due to this term can have a noticeable effect if the wave is a slow wave, i.e., when $v_{ph}\ll c$ or

$$n^2 \gg 1. \tag{2.10}$$

The factor $\exp[-(1-\sqrt{u})^2/2\beta^2 n^2 \cos^2\alpha]$ in Eq. (2.9) may become large at large values of n^2 and near the gyromagnetic frequency ω_H when $u \to 1$ (a similar picture obtains close to $2\omega_H$ and so on). Thus the effects of specific absorption can be discussed in two cases which sometimes overlap: slow waves or frequencies near the gyromagnetic resonance frequencies. We here consider the case in which the condition in (2.10) is satisfied. However, we have left terms with the indicated exponential factor in (2.9) and below, since they may make a considerable contribution when the frequency of the wave is substantially (say, several percent) different from the gyromagnetic frequency ω_H. In addition, we consider the particular case in which the condition in (2.10) is satisfied precisely in the region of the first gyromagnetic resonance.

Even if we go to $n^2 \gg 1$ [(2.10)], it does not mean that we must always neglect terms with small powers of n^2 in (2.9).

Such a procedure would deprive us of the possibility of calculating the absorption of the ordinary wave at low frequencies when (as for plasma waves) the case $n^2 \gg 1$ is possible. A simple analysis indicates that in (2.9) the quantity proportional to $\beta^2 n^6$ in the first term, which reflects the contribution of collisions, can be omitted. Then, making several omissions which are permissible when (2.10) is satisfied, we find

$$\begin{aligned}
&(q/k)\,[-6\beta^2 vRn^6 + 4(1-u-v+uv\cos^2\alpha)\,n^4] \\
&\quad = s\,[(u+2v-3)\,n^4 + 2v^2n^2] + v\,[(u-1)\cos^2\alpha \\
&\quad + (1-u-v)(1+\cos^2\alpha)\,n^2 - v^2]\sqrt{\frac{\pi}{2}}\,\frac{1}{(\beta n\cos\alpha)^3} \\
&\quad \times\exp\left(-\frac{1}{2\beta^2n^2\cos^2\alpha}\right) + \sqrt{\frac{\pi}{8}}\,\frac{v\,(u-1)\sin^2\alpha\, n^4}{u\beta n\cos\alpha} \\
&\quad \times\left\{\exp\left(-\frac{(1-\sqrt{u})^2}{2\beta^2n^2\cos^2\alpha}\right) + \exp\left(-\frac{(1+\sqrt{u})^2}{2\beta^2n^2\cos^2\alpha}\right)\right\}.
\end{aligned} \tag{2.11}$$

For plasma waves we must take account of the condition in (2.7); in other words, as follows from (2.8) and the last formula in (2.12), the absorption need not necessarily be weak. Furthermore, were we to have $v \gg 1$, the requirement for the propagation of plasma waves (2.7) would lead precisely to $u\cos^2\alpha = 1$. When $u < 1$, the last equality is not satisfied at all. When $u \gg 1$ the angle α must have a definite value, close to $\alpha = \pi/2$. Hence the case $u\cos^2\alpha = 1$ (for $v \gg 1$) is a special one and will not be considered here. Assuming that v is not large, we can neglect in (2.11) all n^2 terms and terms that do not contain n^2. Finally, taking account of (2.4) and (2.7), we have

$$\begin{aligned}
q_3 = {}& \frac{k(1-u)}{1-u-v+uv\cos^2\alpha}\left\{\frac{s}{2}\left(1+\frac{2uv\sin^2\alpha}{(1-u)^2}\right)\right. \\
&+ \sqrt{\frac{\pi}{8}}\,v\left[\frac{1}{\beta^3n^3\cos\alpha}\exp\left(-\frac{1}{2\beta^2n^2\cos^2\alpha}\right)\right. \\
&+ \frac{\sin^2\alpha}{2\beta n\cos\alpha\, u}\left[\exp\left(-\frac{(1-\sqrt{u})^2}{2\beta^2n^2\cos^2\alpha}\right)\right. \\
&\left.\left.\left.+ \exp\left(-\frac{(1+\sqrt{u})^2}{2\beta^2n^2\cos^2\alpha}\right)\right]\right]\right\}.
\end{aligned} \tag{2.12}$$

Strictly speaking this relation holds only for weak attenuation ($q \ll k$); however, it can also be used to obtain qualitative results when the absorption is strong. It is apparent from Eq. (2.12) that when $\beta n\cos\alpha \sim 1$ the absorption is not weak ($q \sim k$). For propagation α close to $\pi/2$, the quantity $\beta n\cos\alpha$ may be small even for very slow waves; however, in these cases it does not follow that we can neglect (1.5), since violation of this condition means strong absorption when $u \gtrsim 1$. It should be noted that in (2.12) the term containing the factor $\exp[-(1+\sqrt{u})^2/2\beta^2n^2\cos^2\alpha]$ is not important and is given here to show the contribution due to such terms. From Eq. (2.12) it can be shown that the absorption of plasma waves is especially strong when $u \approx 1$. It should be noted however, from Eq. (2.8), that when $u \approx 1$, for values of α which are not close to 0 or $\pi/2$, we have $n_3^2 = -(1-u)^2/4\beta^2\cos^2\alpha$; obviously, in this region the propagation of Wave 3 generally is impossible, because $n_3^2 < 0$ for both $u > 1$ and $u < 1$.

We now derive the corresponding results, using the first formulation of the problem of propagation of electromagnetic waves in a plasma (cf. Sec. 1); the field falls off asymptotically as $e^{-\gamma t}$, where γ is the damping factor. Calculations, as well as general considerations, yield the following formula for the case of weak absorption

$$\gamma = q\,d\omega/dk. \tag{2.13}$$

In the isotropic case this relation can be written $\gamma = gU_{gp}$, where U_{gp} is the group velocity.* In the anisotropic case $d\omega/dk$ is equal to the projection of the group velocity in the direction of the wave vector **k**. Using (2.7) and (2.8) (neglecting certain terms), we find for Wave 3

---

*An elementary derivation of (2.13) can be found in reference 11. Although there is no question that (2.13) holds outside the gyromagnetic-resonance regions, it may be violated inside these regions.

$$d\omega/dk = c\,(1 - u - v + uv\cos^2\alpha)/n\,(2 - u - v)$$

and, from (2.7) and (2.13) then obtain a formula for the damping factor of the plasma wave

$$\gamma_3 = \left(1 + \frac{uv\sin^2\alpha}{(1-u)^2}\right)^{-1}\left\{\frac{\nu}{2}\left(1 + \frac{2uv\sin^2\alpha}{(1-u)^2}\right)\right.$$
$$+ \sqrt{\frac{\pi}{8}}\,\omega v\left(\frac{1}{\beta^3 n^3\cos\alpha}\exp\left(-\frac{1}{2\beta^2 n^2\cos^2\alpha}\right)\right.$$
$$+ \frac{\sin^2\alpha}{2\beta n\cos\alpha\, u}\left[\exp\left(-\frac{(1-\sqrt{u})^2}{2\beta^2 n^2\cos^2\alpha}\right)\right.$$
$$\left.\left.\left.+ \exp\left(-\frac{(1+\sqrt{u})^2}{2\beta^2 n^2\cos^2\alpha}\right)\right]\right)\right\}. \qquad (2.14)$$

The part of this expression which reflects the contribution of specific attenuation effects coincides with the results obtained by Sitenko and Stepanov.[2]

However, the collision term differs from that derived in reference 4. In particular, from Eq. (36) of reference 4 it follows that $\gamma \rightarrow 0$ when $u \rightarrow 1$ and $\alpha \neq 0$, whereas in our case $\gamma \rightarrow \nu$ under the same conditions. In an earlier paper by the author[1] a formula analogous to (2.14) was given without proof, but the coefficient similar to that in front of the curly brackets of (2.14) was given incorrectly.

In analogy with the spatial absorption, the attenuation is not necessarily weak ($\gamma \sim \omega$) when $\beta n\cos\alpha \sim 1$. The other remarks made in connection with (2.12) also apply to (2.14).

We now consider the attenuation of ordinary waves at relatively low frequency; in particular we assume that

$$\omega_0 \gg \omega, \qquad \omega_H\cos\alpha \gg \omega, \qquad \omega_0 \gg \omega_H.$$

These inequalities can be written in the form

$$v \gg 1, \; u\cos^2\alpha \gg 1, \; v \gg u. \qquad (2.15)$$

The third of these conditions is not necessarily a strong one. Investigations of the ordinary waves under the conditions given in (2.15) are of interest basically in connection with the problem of propagation of whistlers.[12] The propagation is found to be quasi-longitudinal[6] and, from Eq. (2.6), leads to the equation*

$$u\cos^2\alpha\, n^4 - 2vn^2 - v^2 = 0. \qquad (2.16)$$

The second term is smaller than the others in absolute magnitude, so that as a first approximation we have

$$n_2^2 = v/\sqrt{u}\cos\alpha = \omega_0^2/\omega\omega_H\cos\alpha, \qquad (2.17)$$

which is used as a basis for the generally accepted analysis of the propagation of whistlers.[12] From Eqs. (2.15) and (2.17) it follows that $n_2^2 \gg 1$. Under these same conditions we have $n_1^2 = -v/\sqrt{u}\cos\alpha$, and propagation is impossible for the extraordinary wave.*

In calculating the absorption coefficient we can, by virtue of the condition $\omega_H \gg \omega$, omit terms that contain the parameter u in the exponent. We are left with the basic terms in Eq. (2.11); after some simple transformations, which take account of Eqs. (2.15) – (2.17), we have

$$q_2 = \frac{k}{2\sqrt{u}\cos\alpha}\left\{s + \sqrt{\frac{\pi}{8}}\,\frac{\sin^2\alpha}{(\beta n\cos\alpha)^3}\exp\left(-\frac{1}{2\beta^2 n^2\cos^2\alpha}\right)\right\}. \qquad (2.18)$$

In this case, because $\omega_H\cos\alpha \gg \omega$ the absorption is weak even when $\beta n\cos\alpha \sim 1$ and $s \sim 1$. The specific absorption described by (2.18) may apparently be realized for propagation of whistlers in the upper layers of the atmosphere in periods of intense solar corpuscular disturbance.[13] If we neglect collisions, (2.18) coincides with the results obtained by Shafranov[14] by a completely different method [cf. the appendix to reference 14, Eq. (21)]. In the latter paper the absorption was calculated by considering the intensity of the Cerenkov radiation of electrons in a plasma and applying the Kirchoff formula. Thus, whereas the ordinary absorption due to collisions of electrons with ions is due to bremsstrahlung of moving electrons in the ion field,[6] the specific absorption is due to Cerenkov radiation,[14] and also to "magnetic bremsstrahlung" losses.

We now obtain a formula for the damping of the ordinary wave. Using (2.13) and a result which follows from (2.17), $d\omega/dk = 2v_{ph}$, we find the attenuation γ to be

$$\gamma_2 = \frac{\nu}{\sqrt{u}\cos\alpha} + \omega\sqrt{\frac{\pi}{8u}}\,\frac{\sin^2\alpha}{\beta^3 n^3\cos^4\alpha}\exp\left(-\frac{1}{2\beta^2 n^2\cos^2\alpha}\right). \qquad (2.19)$$

In conclusion we consider one more example, which arises in the propagation of slow waves. It should actually be related to gyromagnetic resonance although here, as in the preceding examples, $n^2 \gg 1$. At the outset we consider purely longitudinal propagation, with $\alpha = 0$. The attenuation of the plasma waves can then be found from (2.12) and (2.14), with the latter formula becoming the Landau expression.[5] However, when $\alpha = 0$, the extraordinary wave can also be slow when ω is close to

---

*The effect of the thermal corrections on propagation is not very important here; in any case, it need not be taken into account in calculating absorption.

*It should be noted that when $\alpha = 0$ the wave described by (2.7) should be called the extraordinary wave. The case $\alpha = 0$ is exceptional and for any small values $\alpha \neq 0$ this wave becomes the ordinary wave.

ω_H. Starting from our general relations, we find the corresponding formulas for absorption (attenuation) in this case. From (2.6) with $\alpha = 0$, neglecting the effect of thermal corrections on propagation, we have for Wave 1

$$n_1^2 = 1 - v/(1 - \sqrt{u}) \approx v/(\sqrt{u} - 1). \qquad (2.20)$$

The approximate equality refers to the case $u \approx 1$. We assume further that v is not very large, taking $v \sim 1$. Then, we are justified in assuming (neglecting difference terms of the type $u - 1$) that $u = 1$. The attenuation of Wave 1 for $\alpha = 0$ is determined by collisions and the term with the factor $\exp[-(1 - \sqrt{u})^2/2\beta^2 n^2]$. From Eq. (2.9) with $\alpha = 0$, we have after certain simplifications based on (2.20)

$$q_1 = k\left\{\frac{s}{u-1} + (\sqrt{u} - 1)\sqrt{\frac{\pi}{8}}\frac{1}{\beta n}\exp\left(-\frac{(1-\sqrt{u})^2}{2\beta^2 n^2}\right)\right\}. \qquad (2.21)$$

When $s = 0$ this formula becomes the corresponding formula given by Shafranov[14] (cf. also reference 15). Using Eq. (2.13) it is easy to calculate the value of the damping factor γ. In the present case $d\omega/dk = 2cn(\sqrt{u} - 1)^2/v$ and

$$\gamma = \nu + (\sqrt{u} - 1)^2\sqrt{\frac{\pi}{2}}\frac{\omega}{\beta n}\exp\left(-\frac{(1-\sqrt{u})^2}{2\beta^2 n^2}\right). \qquad (2.22)$$

As Shafranov has emphasized,[14] damping of the kind being considered here may be especially important at large values of v. In this case the conditions which determine the degree to which the frequency ω approaches ω_H may not be especially stringent, so that it may be necessary to introduce corrections in the formulas which have been derived. It is obvious that absorption of this kind also obtains for small values of the angle α; these are determined by the condition $|1 - v| \gg v \sin^2\alpha/|1 - \sqrt{u}|$ with the supplementary requirement $v/(\sqrt{u} - 1) \gg 1$. However, when $\alpha \neq 0$ it is necessary to take account of attenuation of the ordinary wave even for very small values of α. The situation is to a considerable degree analogous to that which obtains for the low-frequency ordinary waves considered earlier, although in the latter the specific absorption is due to the nonresonance factor $\exp(-\frac{1}{2}\beta^2 n^2 \cos^2\alpha)$, whereas in the present case it is due to the resonance factor $\exp[-(1 - \sqrt{u})^2/2\beta^2 n^2 \cos^2\alpha]$.

The author is indebted to Prof. V. L. Ginzburg for his continued interest in this work.

---

[1] B. N. Gershman, JETP **24**, 659 (1953).

[2] A. G. Sitenko and K. N. Stepanov, JETP **31**, 642 (1956), Soviet Phys. JETP **4**, 512 (1957).

[3] K. N. Stepanov, JETP **35**, 283 (1958), Soviet Phys. JETP **8**, 195 (1959).

[4] K. N. Stepanov, JETP **35**, 283 (1958), Soviet Phys. (U.S.S.R.) **28**, 1789 (1958), Soviet Phys.–Tech. Phys. **3**, 1649 (1959).

[5] L. D. Landau, JETP **16**, 574 (1946).

[6] Al'pert, Ginzburg, and Feĭnberg, Распространение радиоволн (Propagation of Radiowaves), Gostekhizdat, 1953.

[7] Gershman, Ginzburg, and Denisov, Usp. Fiz. Nauk **61**, 561 (1957).

[8] B. N. Gershman, Сб. памяти А. А. Андронова (Collection in memory of A. A. Andronov), p. 599, U.S.S.R. Acad. Sci. Press, 1955; JETP **31**, 707 (1956), Soviet Phys. JETP **4**, 582 (1957).

[9] B. N. Gershman and M. S. Kovner, Изв. высш. уч. заведений. Радиофизика (Bull. of the Insts. of Higher Learning, Radiophysics) **2**, No. 1, 28 (1959).

[10] E. P. Gross, Phys. Rev. **82**, 232 (1951).

[11] V. V. Zheleznyakov, Изв. высш. уч. заведений. Радиофизика (Bull. of the Insts. of Higher Learning, Radiophysics) **2**, No. 1, 14 (1959).

[12] L. R. O. Storey, Phil. Trans. **246**, 113 (1953).

[13] B. N. Gershman, Изв. высш. уч. заведений. Радиофизика (Bull. of the Insts. of Higher Learning, Radiophysics) **1**, Nos. 5 – 6, 49 (1958).

[14] V. D. Shafranov, JETP **34**, 1475 (1958), Soviet Phys. JETP **7**, 1019 (1958).

[15] V. P. Silin, Труды ФИАН (Trans. Phys. Inst. Acad. Sci.) **6**, 201 (1955).

Translated by H. Lashinsky
136

SOVIET PHYSICS JETP VOLUME 37 (10), NUMBER 3 MARCH, 1960

CAPTURE MECHANISM IN BETATRONS

I. M. SAMOĬLOV

Submitted to JETP editor March 5, 1959

J. Exptl. Theoret. Phys. (U.S.S.R.) **37**, 705-712 (September, 1959)

The motion of electrons in a betatron is considered, with account of the Coulomb repulsion of the particles in the beam injected into the chamber during one revolution of an electron. It is shown that electron capture is due to the change in the mode of the radial oscillations, caused by the repulsion of the particles in the beam, and to the loss of electrons as a result of collisions with the injector or chamber walls.

AFTER the first attempts to explain electron capture in the betatron on the basis of a single electron analysis,[1,2] a number of authors proposed various capture mechanisms in which collective particle interactions were taken into account. Many workers[3-12] indicate that the most important effect is the Coulomb interaction. Usually in analyzing the injection process one considers the average effect of the space charge in the chamber. This procedure leads to capture mechanisms which, however, are characterized by low efficiencies. In this kind of analysis the effects due to the Coulomb repulsion of electrons in the beam in the first few revolutions, when the motion of the particles is relatively well ordered, is neglected.

We consider an arbitrary time of injection, at which there is some electron space charge present in the chamber. We isolate a group of injected particles which form a complete loop. This group will be affected by the space charge in the chamber, Q, and by the interactions between the particles themselves. If the interaction in the loop is taken into account by including the charge of the loop in Q, taking averages over the volume of the chamber as is usually done, the results do not give a true picture of the motions. Each of the particles in the loop is subjected to a force which depends on the position of the particle with respect to the space charge whereas in actuality this force is determined by the position relative to the central part of the loop, i.e., the well known transverse repulsion of electrons is a ribbon-shaped loop. (Obviously the beam has this shape, at least for some fraction of a revolution after the electrons leave the injector). Since the motion of the particles in the loop can remain ordered for several revolutions, it is of interest to investigate the effect of this ordered motion on the motion of electrons in the injection process. The Coulomb repulsion causes expansion of the beam, but because of the magnetic focusing field the expansion cannot go on indefinitely. As a result there is an increase in the amplitude of the oscillations and a shift of the focal points (if the latter continue to exist) in the azimuthal direction. The transverse repulsion of particles in a loop has been considered in a recently published paper by Matveev.[12] This work treats a particular case which is not usually realized in betatrons, i.e., the case in which the electrons leave the injector in a parallel beam. In the present paper we consider the more general case in which the electron beam is characterized by an angular divergence.

1. EFFECT OF ELECTRON REPULSION IN THE BEAM

It is convenient to treat the effect of repulsion by considering the motion of a group of particles isolated in such a way as to form a single loop. The presence of the space charge in the chamber (except for the charge of the loop itself) results in a value, n_e, which differs from the original magnetic field decay index n $(H \sim r^{-n})$. If we neglect the change in n_e during one or two revolutions the charge in the chamber does not affect the interaction of particles in the loop in any way other than a change in the effective value of n.

Consider the problem of Coulomb repulsion in that part of the beam which forms a single loop and is injected into a chamber which is free from space charge. An estimate based on the usual equations of motion indicates that the Coulomb repulsion force (F) in the loop (here we consider the radial component) does not change substantially over the greater part of the electron path. The only noticeable exceptions are the focal points, where F is several times larger than in the other parts of the trajectory. For this reason we first estimate the effect of repulsion in the focal regions.

The available evidence indicates the existence of only a single focus as the beam leaves the injector; the further behavior of the particles is determined by interaction effects in the loop. In analyzing the repulsion of particles in the vicinity of the first focus, which occupies an angle γ of the azimuthal coordinate φ, we make the following assumptions. 1) The force F is different from zero for $\varphi < \gamma$ and in the other regions the particles execute free betatron oscillations. 2) The electron distribution over flight angle α (total angular divergence 2α) is uniform; for an infinite beam height this means $F = f\alpha$ where $f = \text{const}$ and α is taken from the vertical symmetry plane of the beam. 3) The axial electrons $(\alpha = 0)$ leave the injector along a tangent to the radius of the circle r_0 on which the injector is located. 4) The magnetic field is constant from the time at which the electrons leave the injector. 5) The motion is one-dimensional, i.e., we consider only the radial motion of particles in the loop.

In the region of the first focus the equations of motion in a magnetic field described by $H \sim r^{-n}$ can be conveniently written (in the first approximation) in the form*

$$\eta'' + k^2\eta = -\delta_H + q\alpha, \tag{1.1}$$

where $\eta = (r - r_0)/r_0 = \rho/r_0$; the derivative is taken along the azimuth; $k^2 = 1 - n$; $\delta_H = \delta H/H_0 \ll 1$ is a parameter which characterizes the instantaneous orbit, where H_0 is the field at the radius r_0 and $eH_0r_0/mvc = 1$ (the usual notation is used here), $v \ll c$ and $\delta H = H(r_0) - H_0$. The Coulomb repulsion is given by the $q\alpha$ term

$$q = fr_0/mv^2 = \varkappa 4\pi r_0 e j_\alpha / mv^3 h, \tag{1.2}$$

where j_α is the current in a unit angle of the beam; κ is a coefficient which takes account of the finite height of the beam h. The solution of Eq. (1.1) can be written in the form

$$\eta_1 = q\alpha/k^2 + A_1 \sin k(\varphi + \psi_1) - (\delta_H/k^2)(1 - \cos k\varphi), \tag{1.3}$$

where

$$A_1 = (\alpha/k)\sqrt{1 + (q/k)^2}, \quad \tan k\psi_1 = -q/k.$$

Equation (1.3) can be divided into two parts; one of these, $\eta_\delta = -(\delta_H/k^2)(1 - \cos k\varphi)$, describes the motion of the beam as a whole while the other, which depends on $\alpha\ (\eta_\alpha)$, determines the motion of the particles in the beam with respect to the axial trajectory η_δ, so that

$$\eta = \eta_\delta + \eta_\alpha. \tag{1.3a}$$

Since ψ_1 is independent of α and $A_1 \sim \alpha$, in the next section of the trajectory η_2 has the form given by Eq. (1.3a) (for $q = 0$) where, as in the first part, ψ_2 is independent of α and $A_2 \sim \alpha$. It is easy to show that $\eta_{\alpha 2}$ is symmetric with respect to the azimuth φ_m at which $\eta_{\alpha 2}$ is a maximum and $\eta'_{\alpha 2} = 0$. Hence for the azimuth $\beta = 2\varphi_m - \gamma$ we have $\eta_{\alpha 2}(\beta) = \eta_{\alpha 1}(\gamma)$ and $\eta'_{\alpha 2}(\beta) = -\eta'_{\alpha 1}(\gamma)$. Since the force F is "turned off" at $\varphi = \gamma$, i.e., over the width of the beam $\eta_{\alpha 1}(\gamma)$, it must be "turned on" again in the next part, $\varphi > \beta$. The equation of motion will be similar to Eq. (1.3), where it can be shown that $A_3 = A_1$ and the phase ψ_3, as before, is independent of α. From the symmetry of the trajectory with respect to φ_m it follows (this can easily be shown by direct calculation) that when $\varphi = 2\varphi_m$, $\eta_{\alpha 3} = 0$ for any α and $\eta_{\alpha 3} = -\eta'_{\alpha 1}(0) = -\alpha$, i.e., the electron beam is focused again and the original angular divergence is maintained. It is apparent that in the next portion of the path the behavior of the beam with respect to the axial trajectory η_δ will repeat that given above since the only difference from the original initial conditions is the change in the sign of F at the focus, i.e., where the electron trajectories intersect. Thus η_α is a periodic function with period $\Phi = 4\varphi_m$ which exceeds the period of the free betatron oscillations $(2\pi/k)$ by an amount θ, where

$$\tan(k\theta/4) = (1 - \cos k\gamma)/(k/q + \sin k\gamma). \tag{1.4}$$

An expression for η_α which is valid for any φ and convenient for calculation can be obtained if we represent η_α in a form of a series using the expressions $\eta_{\alpha(1-3)}$, each of which applies for the appropriate sections:

$$\eta_\alpha = \sum_{i=0}^{\infty} [8q\alpha(1 - \cos\lambda_i\gamma)/\lambda_i\Phi(k^2 - \lambda_i^2)] \sin\lambda_i\varphi, \tag{1.5}$$

where $\lambda_i\Phi = (2i + 1)2\pi$.

Limiting ourselves to the first term in the expansion $\lambda = 2\pi/\Phi$ and small values of γ, using $\rho_\alpha = r_0\eta_\alpha$, we have from Eqs. (1.4) and (1.5)

$$\rho_\alpha \simeq (1 + q\gamma)(\alpha r_0/k)\sin\lambda\varphi. \tag{1.6}$$

We shall not discuss these results but estimate the effect of the Coulomb repulsion over the entire electron trajectory. It is apparent that this case is the particular case of the problem considered above for which $\gamma \to (\frac{1}{4})\Phi$. In the expression for $F = f\alpha$ we choose some average value of f along the trajectory. When $\gamma \to (\frac{1}{4})\Phi$, Eqs. (1.4) and (1.5) yield

$$\tan(k\theta/4) = q/k, \tag{1.7}$$

---

*The radius at the injector is taken as the reference.

$$\rho_\alpha = B\alpha \sin \lambda\varphi, \tag{1.8}$$

where

$$B = 4qr_0/\pi(k^2 - \lambda^2) \approx (qr_0/k^2)(1 + 4/k\theta). \tag{1.9}$$

In making a numerical estimate we note that at injection $q = q_f = 1.5$ in the focal regions and the minimum value of q along the trajectory is approximately $0.25\,q_f$. In this case, with $\gamma \approx 0.5$ and $n = 0.5$, it follows from Eqs. (1.4) and (1.6) that there is an increase in the amplitude by 50 – 75% while the increase in the period is about 3 – 5%; for the entire trajectory, from Eqs. (1.7) and (1.9) (with $q = 0.25\,q_f$), the increase in amplitude is 35 – 60% and in period 20 – 30%. Thus, aside from the significant increase in q_f over the minimum mean value of q along the trajectory, taking account of the Coulomb repulsion in the focal regions only is not sufficient since, as will be shown below, the change in the period of oscillation is very important in the capture mechanism.

We note that taking formal averages of the charge of the turn over the volume of the chamber also yields a change in the amplitude and frequencies of the electron oscillations. We shall not consider this effect quantitatively, but indicate the important qualitative difference of the picture described above from the "average" analysis. In the latter case each of the particles in the turn (consequently in the beam as a whole) executes oscillations at the same frequency, corresponding to some effective value of n_e. Actually, as has been shown above, the resulting trajectory has everywhere the form given by Eq. (1.3a) or

$$\rho = B\alpha \sin \lambda\varphi - a(1 - \cos k\varphi), \tag{1.10}$$

where $a = \delta_H r_0/k^2$, i.e., each of the particles in the turn participates simultaneously in two oscillatory motions (with different frequencies) and, as is apparent from Eq. (1.10), the motion of the beam as a whole at the frequency of the usual betatron oscillations is maintained.

The relation between the parameter a and the time of injection τ can be easily obtained for $H = \xi H_m \sin \omega t$ (ξ is a coefficient which takes account of the behavior of the magnetic field close to zero)

$$a \approx (\xi e H_m \omega r_0^2 / mvck^2)\,\tau, \tag{1.11}$$

where $\tau = t - t_0$ and t_0 is the time at which $H = H_0$.

In conclusion we may note that as a consequence of the nonuniform distribution of electrons over flight angle, the difference in the coefficient κ for particles with different α, and the vertical oscillations (which have not been considered in the problem), the electron beam will obviously not be focused ideally. However it will be apparent that the above analysis is qualitatively correct and that the idealized picture of the motion can be used in the calculations.

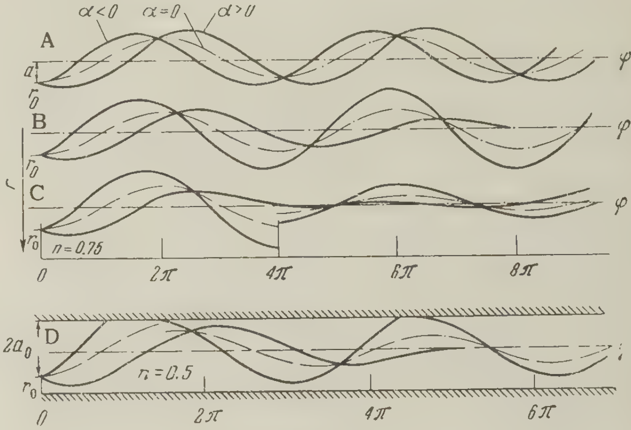

FIG. 1

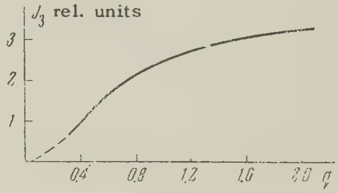

FIG. 2

2. ELECTRON CAPTURE MECHANISM

The Coulomb repulsion of electrons in a turn changes the usual particle trajectories (Fig. 1A) in such a way that for half of the electrons in the beam the motion (1.10) assumes the form of rapidly damped oscillations, Fig. 1B. However, if the conditions are not changed, as follows from the periodicity of Eq. (1.10) the amplitude of the oscillations returns to the initial value. An irreversible change in amplitude, which leads to particle capture, results from loss of part of the electrons in the turn as a result of collisions with the injector or with the chamber walls.

If there is a collision with the injector at some value $\varphi = \varphi_1$, in the remaining part of the turn the new axial electrons (which are emitted from the injector at some angle $\alpha = \alpha_c$) are no longer subject to the effect of the repulsive forces and execute free betatron oscillations with a new amplitude A_c which can be determined (for $\alpha = \alpha_c$ and $\varphi = \varphi_1$) from the expression

$$A = \{a^2 + (B\alpha)^2 [\sin^2 \lambda\varphi + (\lambda/k)^2 \cos^2 \lambda\varphi] - 2B\alpha a [(\lambda/k) \sin k\varphi \cos \lambda\varphi - \cos k\varphi \sin \lambda\varphi]\}^{1/2}. \tag{2.1}$$

At the same time the remaining electrons in the beam now move with respect to the new axial particles with the old increase in period (Fig. 1C) since the quantity q is not changed. As has been noted above, the motion of the axial particles describes the motion of the beam as a whole; hence, after loss of part of the electrons of the turn, as before, the remaining particles participate in two oscillatory motions with different frequencies and amplitudes A_c $(a \rightarrow A_c)$ and $B\alpha_i$ where α_i is now taken from α_c. Since the electrons move about the instantaneous orbit, remaining at a distance $a - \Delta$ from the edge of the injector anode (Δ is the thickness of the injector element), the injector will not be struck by those particles for which

$$A_c + B\alpha_i \leqslant a - \Delta. \tag{2.2}$$

It is apparent from Eq. (2.2) that the capture angle increases with increasing a; hence electrons will be captured most effectively at the injection time for which $a \approx a_0$, half the distance between the inner wall of the chamber and the center of the cathode. In estimating the capture angle it is necessary to take account of the collision of the beam with the chamber walls because when $a \approx a_0$ a significant fraction of the electrons are lost in the first turn, Fig. 1D.

The general picture of the collision of the beam with the wall is rather complicated because the loss of electrons is "stretched" over the azimuth. In estimating the capture angle in this case, we assume for simplicity that the electrons which strike the wall are lost "abruptly" (as in collisions with the injector) for some value of the azimuthal angle φ_0. In this case, in contrast with collisions in the turn, particles are lost both for $\alpha < 0$ and $\alpha > 0$. In determining α_c and A_c we assume that the electrons do not strike the wall if the amplitude determined from Eq. (2.1) for $\varphi = \varphi_0$ is smaller than $2a_0 - a$. Assuming that $\alpha_c = (\alpha_1 + \alpha_2)/2$ where $\alpha_{1,2}$ is the root of the expression $A \leq 2a_0 - a$, we obtain from Eq. (2.1)

$$A_c = ca, \tag{2.3}$$

where

$$c = [\sin k\varphi_0 \sin \lambda\varphi_0 + (\lambda / k) \cos k\varphi_0 \cos \lambda\varphi_0] / [\sin^2 \lambda\varphi_0 + (\lambda / k)^2 \cos^2 \lambda\varphi_0]^{1/2}. \tag{2.3a}$$

Determining the capture angle as in Eq. (2.2), we have for the two regions

$$a \leqslant a_0 + \Delta / 2, \qquad \alpha_{\text{cap}} = (a - \Delta - A_c) / B; \tag{2.4a}$$

$$a \geqslant a_0 + \Delta / 2, \qquad \alpha_{\text{cap}} = (2a_0 - a - A_c) / B. \tag{2.4b}$$

We note that after the first passage of the beam the part which remains may experience new collisions with the walls of the chamber or with the injector; as a result, the capture angle can be larger than indicated by Eq. (2.4). However it is extremely difficult to analyze the multiple losses of electrons; for this reason we take the capture angle to be the minimum value as determined by the first collision only.

Equation (2.4) allows us to estimate the critical values of the injector currents (J_{cr}) at which the collective capture mechanism starts to become effective. As the azimuth φ_0 we take the azimuth defined by $k\varphi_0 = \pi$, where the axial electrons of the beam pass closest to the inner wall of the chamber. In estimating J_{cr} we must take account of the fact that when $a < a_0$, for values of α which are not too large and values of q which are not too small, the beam passes through the azimuth $k\varphi_0 = \pi$ essentially without loss of particles and the determining azimuths become $k\varphi_0 = 2\pi$ to 3π or larger. It is apparent from Eq. (2.4) that the criterion for the operation of collective capture is the condition $(1 - c) \geq \Delta/a$ whence, expressing eq. (2.3a) in a series in powers of $\beta = k\theta/2\pi \ll 1$ and limiting ourselves to the first terms of the expansion $c \approx 1 - (\beta k\varphi_0)^2/2$, we obtain

$$q_{cr} \leqslant \pi \sqrt{\Delta / 2a} / \varphi_0. \tag{2.5}$$

With $\Delta = 0.2$ cm, $a = 1$ cm, $k^2 = 0.5$, and $k\varphi_0 = 2\pi$ to 3π we have $q_{cr} = 0.1 - 0.07$, which for $h \approx 1$ cm and $\kappa \simeq 0.4$ gives $j_{\alpha\,cr} = 2.5$ ma/deg for an injection energy $U = 10$ kv. Thus at the 30 Mev synchrotron of the Institute of Physics of the Academy of Sciences[11] $(k^2 = 0.25)$ the experimental value $J_{cr} \approx 3$ ma. If we assume $2\alpha \approx 6°$, calculation shows that $J_{cr} = 5$ to 8 ma for $U = 10$ kv and 2 to 3.5 ma for $U = 5$ kv.

Equation (2.4) can be used to determine the dependence of the capture current J_{cap} on the injection current J. Since $J_{cap} \sim \alpha_3 j_\alpha$, taking account of Eq. (2.4) (where $\Delta \ll a$) and Eqs. (1.2) and (1.9), we have

$$J_{\text{cap}} \sim ak^2(1 - c) / (1 + 4/k\theta). \tag{2.6}$$

It is apparent from Eq. (2.6) that the further the instantaneous orbit is from the injector, the larger the capture current. The quantities c and $k\theta$ are determined in the final analysis by the dimensionless parameter q/k, i.e., taking account of Eq. (1.2), Eq. (2.6) gives the qualitative dependence of J_{cap} on J shown in Fig. 2, (computed for $k\varphi_0 = \pi$). For $k^2 = 0.5$, $a = a_0 = 2$ cm, $\Delta = 0.2$ cm, $r_0 = 20$ cm, $k\varphi_0 = \pi$ and $q = 0.5$ the total capture angle is approximately 1.5°. Thus the capture mechanism due to Coulomb repulsion of the particles and the loss of part of the electrons from the turn serves to explain the observed high efficiency of injection and the threshold nature of capture.

Above we have considered the behavior of particles in a beam which is injected into the chamber during the course of one turn τ_0. In considering injection times greater than τ_0 it is necessary to take account of the interaction between turns. As we have already noted, the motion of electrons in an isolated turn with account taken of the space charge of the other turns, can be considered in terms of an effective n_e. When this effect is taken into account the dependence of J_{cap} on J will differ from that given in Fig. 2 since the function $(1-c)/(1+4/k\theta)$ will reach its limiting value for values of q which are smaller than those in Fig. 2. For large values of q, Eq. (2.6) becomes the usual curve, i.e., if we take account of the growth of space charge with q due to the previous turns the nature of the curve (2.6) is in agreement with that observed in betatron curves which shows the dependence of gamma yield on injection current.

CONCLUSION

In this paper we have considered the behavior of particles in a beam injected into a chamber to form one turn, treating the averaged motion of the particles in the space charge field of the other turns; qualitatively this analysis would seem to indicate that capture is not changed in multi-turn injection. Starting from this result one can draw several conclusions which are of practical interest. 1) The capture angle is limited by collisions of the beam with the walls of the chamber which result in a loss of a considerable fraction of the electrons, as is observed experimentally.[9] 2) It is feasible to inject a sharply focussed beam since smaller emission currents are required and this is an important factor, especially at high injection energies. 3) In view of the relatively small effect of the thickness of the injector edge Δ (especially in large machines) capture should take place effectively when electrons are injected from outside the chamber through the use of deflection plates. This method of injection appears promising from the point of view of increasing the gamma yield since it is relatively easy to use an injector at several hundred kilovolts. 4) It is possible to achieve injection in a magnetic field which is constant in time; this technique has been used successfully for the preliminary adjustment of betatrons.[9] It is also possible to achieve injection in a uniform magnetic field. 5) Electron capture can also be realized when the injector is located inside the equilibrium orbit, close to the inner wall of the chamber. It is also possible to locate the injector above (or below) the plane of the equilibrium orbit in such a way that the cathode (long-dimension) is along a radius and close to the top (bottom) of the chamber. The use of an injector of this kind may be useful for the extraction of electron beams from a betatron.

In conclusion we may note that even if a rigorous analysis of the injection process (many turns) shows that the presence of space charge due to the other turns in any way reduces the efficiency of particle capture, the single-turn injection scheme given above is still of interest. In this scheme the electrons are injected into a chamber which is space-charge free; because of the high injection efficiency (one turn) it is possible to achieve capture currents which are sufficient for producing high gamma yields. We may note that for injection from outside the chamber (through the use of deflection plates) a one-turn injection system would not represent any special technical difficulties.

The author is indebted to A. A. Sokolov for fruitful discussions.

---

[1] D. W. Kerst and R. Serber, Phys. Rev. **60**, 53 (1941).

[2] J. A. Rajchman and W. H. Cherry, J. Franklin Inst. **243**, 261 (1947).

[3] D. W. Kerst, Phys. Rev. **74**, 503 (1948).

[4] R. Wideroe, J. Appl. Phys. **22**, 362 (1951).

[5] S. E. Barden, Proc. Phys. Soc. **64B**, 85 (1951).

[6] Kerst, Adams, Koch, and Robinson, Rev. Sci. Instr. **21**, 462 (1950).

[7] V. D. Rusanov, Dissertation, Physics Inst., Acad. Sci., 1956.

[8] Logunov, Ovchinnikov, and Rusanov, J. Tech. Phys. (U.S.S.R.) **27**, 1135 (1957), Soviet Phys.–Tech Phys. **2**, 1032 (1958).

[9] Yu. S. Korobochko, J. Tech. Phys. (U.S.S.R.) **27**, 1603 (1957), Soviet Phys.–Tech Phys. **2**, 1486 (1958).

[10] Yu. N. Lobanov and V. A. Petukhov, Ускорители элементарных частиц (Elementary Particle Accelerators) Atomizdat, Moscow, 1957, p. 73.

[11] L. M. Korvizhnykh and A. N. Lebedev, JETP **34**, 984 (1958), Soviet Phys. JETP **7**, 679 (1958).

[12] A. N. Matveev, JETP **35**, 372 (1958), Soviet Phys. JETP **8**, 259 (1959).

Translated by H. Lashinsky
137

SOVIET PHYSICS JETP VOLUME 37 (10), NUMBER 3 MARCH, 1960

KINETIC THEORY OF IMPACT IONIZATION IN SEMICONDUCTORS

L. V. KELDYSH

P. N. Lebedev Physics Institute, Academy of Sciences, U.S.S.R.

Submitted to JETP editor March 23, 1959

J. Exptl. Theoret. Phys. (U.S.S.R.) **37**, 713-727 (September, 1959)

The effect of impact ionization processes on the distribution function for electrons and holes in a strong electric field is studied. It is shown that the energy dependence of the impact ionization probability near the threshold is essentially different for crystals with small and high dielectric constants; the solution of the kinetic equation is considered in both these cases. Expressions are obtained for the equilibrium number of carriers in a strong field, the impact-ionization coefficient, the critical field, etc. The dependence of the breakdown field on temperature, on specimen thickness, and on the electron-lattice interaction law is found. The connection of the expressions obtained with the known breakdown criteria of Fröhlich and Hippel is established. It is shown that increasing the electric field causes a decrease in the recombination speed, as a result of which the equilibrium number of carriers starts growing as the field increases long before the appearance of impact ionization.

THE electric breakdown of semiconductors apparently takes place as a result of the unlimited growth of carrier concentration with increasing field strength.[1] In a stationary state the number of carriers, n, is determined by the relationship

$$n\{\overline{w_i(E,T)} - \overline{w_r(n,E,T)}\} + n_0(E,T) = 0, \tag{1}$$

where $\overline{w_i(E, T)}$ and $\overline{w_r(n, E, T)}$ are the impact ionization and recombination probabilities averaged over the distribution function, $n_0(E, T)$ is the number of carriers of a given type created in unit volume of the semiconductor in unit time by thermal ionization and direct field extraction of valence electrons into the conduction band, E is the field strength and T the temperature.

With increasing field, as will be shown below, $\overline{w_r}$ decreases but $\overline{w_i}$ grows rapidly and, consequently, n increases. In the field E_c for which $\overline{w_i} = \overline{w_r}$ the carrier concentration tends to infinity, which is the breakdown criterion for the case given. Thus, quantitative consideration of the behavior of a semiconductor in the pre-breakdown region, as well as a study of the mechanism of breakdown itself, requires the solution of the kinetic equation taking into account the processes of impact ionization and recombination. This is the aim of the present work.

Following the usual method,[2] it is not difficult to obtain the following system of equations for determining the symmetric $f_0(\epsilon)$ and antisymmetric $f_1(\epsilon)$ parts of the distribution function, $f(\mathbf{P})$

$$f(\mathbf{P}) = f_0(x) + \frac{e\mathbf{EP}}{m} f_1(x) + \ldots$$

$$= f_0(x) - \frac{e\mathbf{EP}}{\varepsilon_i m}\,\frac{\tau(x)}{1 + w_i(x)\,\tau(x)}\,\frac{df_0(x)}{dx}, \tag{2}$$

$$\left[\eta(x) + \left(\frac{E}{E_i}\right)^2 \frac{\lambda^2(x)\,\delta}{x\delta(x)}\,\frac{1}{1 + w_i(x)\,\tau(x)}\right]\frac{df_0(x)}{dx}$$

$$+ f_0(x) - \frac{\tau(x)}{x^{3/2}\,\delta(x)}\,\frac{S(x)}{N_i} = 0, \tag{3}$$

$$\frac{1}{N_i x^{1/2}}\,\frac{dS(x)}{dx} - [w_i(x) + w_r(x)]\,f_0(x) + n_0(x, E, T)$$

$$+ N_i \int_1^\infty w_i(x, x')\,f_0(x')\,x'^{1/2}dx' = 0, \tag{4}$$

where $x = \epsilon/\epsilon_i$; $\epsilon = P^2/2m$ is the energy; **P** is the momentum; ϵ_i is the threshold ionization energy; τ^{-1} is the frequency of collision with phonons; $w_i(x)$ and $w_r(x)$ are the total probabilities of impact ionization and recombination; $w_i(x, x')$ is the probability of the creation by ionization of a carrier with energy x by a carrier with initial energy x', $\lambda(x) = l(x)/l(1)$; $l(x) = P\tau(x)/m$ is the mean free path; $S(x)$ is the carrier current through the surface $\epsilon(\mathbf{P}) = x\epsilon_i$, caused by the field and phonon interactions; $\frac{3}{2}N_i$ is the total number of states with energy $\epsilon < \epsilon_i$;

$$\delta(x) = 4m \int_0^{2P} B(q)\,\hbar\omega_q q\,dq \Big/ \int_0^{2P} B(q)\,(1 + 2N_q)\,q^3 dq$$

$$\sim \frac{\hbar\omega_p}{\varepsilon(N_p + 1/2)}, \tag{5}$$

$$\eta(x) = \int_0^{2P} B(q)(\hbar\omega_q)^2(2N_q+1)\,q\,dq \Big/ 2\varepsilon_i \int_0^{2P} B(q)\,\hbar\omega_q q\,dq,$$

$$\tau^{-1}(x) = \frac{Vm}{4\pi\hbar^4P^3}\int_0^{2P} B(q)(2N_q+1)\,q^3dq, \quad E_i = \frac{\sqrt{3\delta}\varepsilon_i}{el(\varepsilon_i)}. \tag{6}$$

Here, q, ω_q and N_q are the momentum, frequency, and number of phonons; B_q is the square of the matrix element of the interaction of an electron with a phonon; V is the normalization volume; E_i is the field in which the mean energy of the carriers becomes of the order ϵ_i; $\delta = \delta(1)$. The small value of δ, the average fraction of the energy lost by an electron in one collision with the lattice, is a condition for the applicability of the approximation considered. For the parameter values of interest to us, $\delta \sim 10^{-2}$. The small quantity $\eta(x)$ we will neglect henceforth. For those valence crystals in which the electrons interact mainly with acoustic phonons $B_{ac}(q) \sim q$ and $\hbar\omega_q^{ac} = cq$, where c is the velocity of sound. When the interaction is with optical phonons $B_{op}(q) = \text{const.}$ and $\hbar\omega_q^{op} = \hbar\omega_0 = \text{const.}$

From (5) and (6) it follows that

$$\delta_{ac}(x) = 4mc^2/kT, \qquad \lambda_{ac}(x) = 1,$$

$$E_i^{ac} = \sqrt{12mc^2/kT}\,\varepsilon_i/el,$$

$$\delta_{op}(x) = \hbar\omega_0/\varepsilon(N_P+{}^1\!/_2), \qquad \lambda_{op}(x) = 1,$$

$$E_i^{op} = \sqrt{3\hbar\omega_0\varepsilon_i/(N_P+{}^1\!/_2)(el)^2}\,. \tag{7}$$

Before proceeding to the solution of Eqs. (2) — (4), we make some remarks on the choice of the probabilities $w_r(x)$, $w_i(x)$ and $w_i(x, x')$. The effect of recombination on the form of the distribution function is insignificant in view of the inequality $w_r\tau \ll 1$, which is well fulfilled. Therefore, the corresponding term in (4) can be considered as a small contribution and the fact that it is in general nonlinear has no effect. In the majority of cases, however, an important part is played by the so-called "radiationless" recombination associated with carrier capture into local states. Its probability for a sufficiently large number of carriers can be considered as independent of concentration. Such a process can only take place for very slow carriers ($\epsilon \lesssim \hbar\omega_m$, where ω_m is the maximum lattice vibration frequency), which in fact are not included in the conditions considered, since for them $\delta(x)$ is not small. Therefore, it is most natural to include radiationless recombination, not in (4), but in the boundary condition for S(x) at x = 0. The last two terms in (4) can be taken into account in a similar way. In fact, the probability of creation of a carrier with energy ϵ by thermal ionization and by the field decreases exponentially with increase of ϵ. Likewise, the number of carriers with energies essentially exceeding the ionization threshold is exponentially small. Therefore, both $n_0(E, T)$ and $w_i(x, x')$ cause the creation of only very slow carriers $x \ll 1$, and we include them only in the boundary condition

$$\frac{S(0)}{N_i} - w_r^0 f_0(0) + \frac{n_0(E,T)}{N_i}$$

$$+ \sum_{e,h} N_i \int_0^\infty x^{1/2}dx \int_1^\infty w_i^{(1,2)}(x,x')\,f_0(x')\,x'^{1/2}\,dx' = 0,$$

$$w_r^0 = \int_0^\infty w_r(x)\,x^{1/2}\,dx, \tag{8}$$

where the summation takes into account the presence of two carrier types and the indices 1 and 2 refer to the creation probability of carriers of the same or opposite charge.

The quantity $w_i(x)$, as shown in Appendix 1, can increase near the threshold either linearly or quadratically, depending upon whether the value of the dielectric constant of the crystal is small or large, i.e.,

$$w_i(x) = p(x-1)^j k_j(x)/\tau(x), \qquad j = 1, 2,$$

$$k_j(x) = 1 + \sum_{n=1}^{\infty} k_{jn}(x-1)^n. \tag{9}$$

The dimensionless quantity p thus defined is rather large ($p \sim 10^2$).

Equations (3) and (4) take an essentially different form in the regions x < 1 and x > 1. It is natural, therefore, to solve them in each of these regions separately and then match the solutions obtained at x = 1. Below the ionization potential $w_i(x) = 0$, $w_r(x)$ is a small correction, and all the remaining terms in the right half of (4) do not depend on the value of $f_0(x)$ in this region. Equations (3) and (4) are consequently integrated in the general form. However, on the basis of the remarks made above, we will use a simplified form of the solution in which the value $\eta(x)$ is neglected, and $w_r(x)$, $w_i(x, x')$, and $n_0(x, E, T)$ are taken into account only in the boundary condition (8).

$$S(x) = \text{const} \equiv -\frac{N_i\delta}{\tau(1)}\sigma(E)\,f_0(1),$$

$$f_0(x) = f_0(1)\exp\left\{\left(\frac{E_i}{E}\right)^2\int_x^1 \frac{x'\delta(x')}{\lambda^2(x')\delta}\,dx'\right\}$$

$$\times\left\{1 + \left(\frac{E_i}{E}\right)^2\sigma(E)\int_x^1 \exp\left[-\left(\frac{E_i}{E}\right)^2\int_{x'}^1 \frac{t\delta(t)}{\lambda^2(t)\delta}\,dt\right]\frac{dx'}{x'\lambda(x')}\right\}. \tag{10}$$

The constants of integration $f_0(1)$ and $\sigma(E)$ must be determined from the boundary conditions. The value of $\sigma(E) \equiv -S(1)\tau(1)/N_i\delta f_0(1)$, giving the mean probability of impact ionization, is simply determined, as will be shown below, by solving the equation in the region $x > 1$. Knowing this value is sufficient to determine all the characteristics of the semiconductor in the strong electric field. In fact, we show below that in the region $x > 1$ the distribution function falls practically to zero for $x - 1 \gtrsim (\delta/p)^{1/4}\sqrt{E/E_i} = \alpha$. Consequently, the contribution of this region to all the observed quantities (number of carriers, conductivity, mean energy) is of the order $\alpha \ll 1$. In other words, all these quantities can be evaluated using the function (10) by averaging over the region $x < 1$. The single quantity completely determined by the distribution of carriers over the ionization potential is the mean probability of impact ionization. But it is equal at the same time to $-S(1) = N_i\delta\sigma(E)f_0(1)/\tau(1)$, which is easy to see by integrating (4) from 1 to ∞, and omitting the last three terms, which are insignificantly small in this region. Thus, all the information which we must obtain from the solution of the kinetic equation in the region $x > 1$ is included in the function $\sigma(E)$, proportional to the ratio $S(x)/f_0(x)$ at $x = 1$.

The total number of carriers n and the mean impact ionization and recombination probabilities are determined from the following relationships

$$n = N_i\int_0^\infty f_0(x)\,x^{1/2}dx = f_0(1)\,N_i \exp\left[\left(\frac{uE_i}{E}\right)^2\right]\left\{\varphi_{1/2}^{(1)}\left(\frac{E}{E_i}\right)\right.$$
$$\left. + \left(\frac{E_i}{E}\right)^2\sigma(E)\exp\left[-\left(\frac{uE_i}{E}\right)^2\right]\varphi_{1/2}^{(2)}\left(\frac{E}{E_i}\right)\right\}, \qquad (11)$$

$$\overline{w_i(E)} = \frac{S(1)}{n} = \frac{\delta}{\tau(1)}\sigma(E)$$
$$\times \frac{\exp[-(uE_i/E)^2]}{\varphi_{1/2}^{(1)}(E/E_i) + (E_i/E)^2\sigma(E)\exp[-(uE_i/E)^2]\,\varphi_{1/2}^{(2)}(E/E_i)}, \qquad (12)$$

$$\overline{w_r(E)} = \frac{N_i}{n}\,w_r^0 f_0(0)$$
$$= w_r^0\,\frac{1 + (E_i/E)^2\sigma(E)\exp[-(uE_i/E)^2]\,\zeta(E/E_i)}{\varphi_{1/2}^{(1)}(E/E_i) + (E_i/E)^2\sigma(E)\exp[-(uE_i/E)^2]\,\varphi_{1/2}^{(2)}(E/E_i)}, \qquad (13)$$

$$u^2 = \int_0^1 \frac{x\delta(x)}{\lambda^2(x)\,\delta}\,dx,$$

$$\zeta(z) = \int_0^1 \exp\left[\frac{1}{z^2}\int_0^x \frac{x'\delta(x')}{\lambda^2(x')\,\delta}\,dx'\right]\frac{dx}{x\lambda(x)}, \qquad (14)$$

$$\varphi_k^{(1)}(z) = \int_0^1 \exp\left[-z^{-2}\int_0^x \frac{x'\delta(x')}{\lambda^2(x')\,\delta}\,dx'\right]x^k dx,$$

$$\varphi_k^{(2)}(z) = \int_0^1 \frac{dx}{x\lambda(x)}\int_0^x \exp\left[-z^{-2}\int_x^{x'} \frac{x''\delta(x'')}{\lambda^2(x'')\,\delta}\,dx''\right]x'^k dx'. \qquad (15)$$

The integral $\zeta(z)$ in general diverges at the lower limit. This is associated with the fact that we have considered in (8) the number of recombinations as proportional to $f_0(0)$. In fact, as follows from the reasons given, this number is determined by the mean value of $f_0(E)$ in the region of very small energies $(\epsilon \lesssim \hbar\omega_m)$. Consideration of this fact should lead to the exclusion of the integral for $x \sim \hbar\omega_m/\epsilon_i$. The exact value of this limit for calculating $\zeta(z)$ has no significance, since the divergence of the integral is logarithmic.

Using the expressions (11) – (13) and the evident relationships

$$-S(1) = N_i\int_1^\infty w_i(x)\,f_0(x)\,x^{1/2}dx,$$

$$N_i\int_0^\infty w_i^{(1)}(x, x')\,x^{1/2}\,dx$$
$$= 2N_i\int_0^\infty w_i^{(2)}(x, x')\,x^{1/2}\,dx = 2w_i(x'), \qquad (16)$$

the boundary condition (8) can be rewritten in a form completely analogous to relation (1) (index e refers to electrons and h to holes),

$$[\overline{w_{re}(E)} - \overline{w_{ie}(E)}]\,n_e(E) - \overline{w_{ih}(E)}\,n_h(E) - n_{0e}(E.T) = 0,$$
$$[\overline{w_{rh}(E)} - \overline{w_{ih}(E)}]\,n_h(E) - \overline{w_{ie}(E)}\,n_e(E) - n_{0h}(E,T) = 0. \qquad (17)$$

If w_r^0 can be taken as independent of n, then (see reference 4)

$$n_e(E) = \frac{n_{0e}(E,T)}{\overline{w_{re}(E)}}\;\frac{1 + (n_{0h}(E,T)/n_{0e}(E,T) - 1)\,r_h(E)}{1 - r_e(E) - r_h(E)},$$

where

$$r(E) = \frac{\overline{w_i(E)}}{\overline{w_r(E)}}. \qquad (18)$$

We study the behavior of this expression on increasing the field. In the region $E \ll E_i$, we have $r(E) \ll 1$ and (18) takes the usual form $n(E) = n_0/\overline{w_r(E)}$. Thus, the growth of n is determined mainly by the function $\varphi_{1/2}^{(1)}(E/E_i)$ [we notice that $\sigma(E)$ becomes of the order of unity only when E is comparable with E_i]. In particular, for the cases mentioned above, involving acoustical and optical phonons in valence crystals, n is proportional to $E^{3/2}$ and E^3 respectively. This behavior is occasioned by the fact that when the field becomes sufficiently large ($E \gtrsim 10^3$ v/cm), the mean electron energy starts to increase, the relative number of slower electrons decreases, and there is an associated decrease in the recombination velocity. When the field approximates to $E_i \sim 10^5$ v/cm, $\overline{w_i(E)}$ begins to increase rapidly and at a field E_c, determined by the condition

$$r_e(E_c) + r_h(E_c) = 1, \qquad (19)$$

breakdown occurs. As a rule, the values of E_i are different for electrons and holes, therefore one of the quantities $r(E)$ is much greater than the other and the condition of breakdown takes the form $r(E_c) = 1$. The carrier type for which the value E_i is smaller is taken here. A direct comparison of (12) and (13) shows that $r(E_i) \sim \delta/w_r^0\tau \gg 1$ and, consequently, $E_c < E_i$. But the field dependence of all the quantities entering into these formulae is small compared with the exponential, and in the zero-order approximation we have

$$E_c = uE_i \ln^{-1/2}\left\{\frac{\sigma(E_c)\,\delta}{w_r^0\,\tau(1)}\left[1 + \left(\frac{E_i}{E_c}\right)^2 \sigma(E_c)\exp\left[-\left(\frac{uE_i}{E_c}\right)^2\right]\right.\right.$$

$$\left.\left.\times\,\zeta\left(\frac{E_c}{E_i}\right)\right]^{-1}\right\} \approx uE_i \ln^{-1/2}\frac{\delta}{w_r^0\tau}. \qquad (20)$$

The value of w_r^0 is of the order $(\hbar\omega_m/\epsilon_i)^{3/2}/\tau_r$ where τ_r is the recombination lifetime of carriers when the field is absent. Taking this lifetime as of the order of a microsecond, and $\tau \sim 10^{-12}$ sec, we obtain the following estimate of the critical field $E_c \approx E_i u/5$ (see reference 5).

If the region in which the field acts is sufficiently small ($\lesssim 1$ cm), then the lifetime of carriers is determined not by recombination but by their departure from this region. The carrier concentration depends in this case on the distance t from the boundary of the specimen and the number of carriers n_0 flowing through this boundary in unit time[1] ($n_{0h} = 0$):

$$n_e(E, t) = \frac{n_{oe}}{v_{ed}}\exp[\varkappa_e(E)\,t]$$

$$\times\frac{\varkappa_e(E)\exp[-\varkappa_e(E)L - \varkappa_h(E)t] - \varkappa_h(E)\exp[-\varkappa_h(E)L - \varkappa_e(E)\,t]}{\varkappa_e(E)\exp[-\varkappa_e(E)L] - \varkappa_h(E)\exp[-\varkappa_h(E)L]}. \qquad (21)$$

Here v_d is the drift velocity of the carriers in the field E, L is the dimension of the region, and $\kappa(E)$ is the so-called impact-ionization coefficient.

$$\varkappa(E) = \frac{\overline{w_i(E)}}{v_d} = \frac{\sqrt{3\delta}}{l(1)}\frac{E_i}{E}\sigma(E)$$

$$\times\frac{\exp[-(uE_i/E)^2]}{\varphi^{(1)}(E/E_i) + (E_i/E)^2\sigma(E)\exp[-(uE_i/E)^2]\,\varphi^{(2)}(E/E_i)}, \qquad (22)$$

$$\varphi^{(1)}(z) = \int_0^1 \exp\left[-z^{-2}\int_0^x \frac{x'\delta(x')}{\lambda^2(x')\delta}\,dx'\right]\frac{d}{dx}[x\lambda(x)]\,dx,$$

$$\varphi^{(2)}(z) = \int_0^1 \frac{dx}{x\lambda(x)}$$

$$\times\int_0^x \exp\left[-z^{-2}\int_x^{x'}\frac{x''\delta(x'')}{\lambda^2(x'')\,\delta}\,dx''\right]\frac{d}{dx'}[x'\lambda(x')]\,dx'. \qquad (23)$$

For the particular cases corresponding to (7)

$$\varphi_{ac}^{(1)}(z) = \frac{\sqrt{\pi}}{2z'}\Phi(z'), \quad \varphi_{ac}^{(2)}(z) = \frac{\sqrt{\pi}}{4z'}\int_0^{z'^2} e^t\Phi(\sqrt{t})\frac{dt}{t},$$

$$z' = \frac{1}{\sqrt{2z}}, \qquad \varphi_{op}^{(1)}(z) = z^2(1 - \exp[-z^{-2}]),$$

$$\varphi_{op}^{(2)}(z) = z^2\{\mathrm{Ei}(z^{-2}) + 2\ln z - C\}, \qquad (24)$$

where $\Phi(z)$ is the error integral, $\mathrm{Ei}(z)$ is the exponential integral function, and C is Euler's constant ($C \approx 0.577$).

The breakdown field for the limited region is determined according to (21) by the condition

$$[\varkappa_e(E_c) - \varkappa_h(E_c)]\,L = \ln[\varkappa_h(E_c)/\varkappa_e(E_c)] \qquad (25)$$

and is thus a function of the ratio $\sqrt{3\delta}\,L/l(1)$. As long as this ratio is small we have

$$E_c(L) = uE_i\ln^{-1/2}\left\{\frac{\sqrt{3\delta}\,L}{l(1)}\frac{E_i}{E_c}\frac{\sigma(E_c)}{\ln[\varkappa_h(E_c)/\varkappa_e(E_c)]}\right.$$

$$\left.\times\left[\varphi^{(1)}\left(\frac{E_c}{E_i}\right) + \left(\frac{E_i}{E_c}\right)^2\sigma(E_c)\exp\left[-\left(\frac{uE_i}{E_c}\right)^2\right]\varphi^{(2)}\left(\frac{E_c}{E_i}\right)\right]^{-1}\right\}$$

$$\approx uE_i\ln^{-1/2}\frac{\sqrt{3\delta}\,L}{l(1)}. \qquad (26)$$

The temperature dependence of E_c is determined mainly by the quantity $E_i \sim \sqrt{\delta}/l(1)$. For acoustical phonons $E_c \sim \sqrt{T}$, for optical $E_c \sim \coth^{1/2}(\hbar\omega_0/kT)$.

In conclusion, we make a series of remarks on the connection of the parameter we have introduced, u, with the known breakdown criteria of Fröhlich and Hippel. Since $\lambda(1) = 1$ the integrand of u^2 in (14) can be either of the order of unity if $\lambda(x)$ does not increase with increasing energy, or increases sufficiently slowly, or much greater than unity, if the mean free path increases rapidly with growth of x. In the first case, which apparently, obtains always in valence crystals, breakdown occurs in fields of the order E_i, i.e., when the mean carrier energy becomes of the order ϵ_i. In form this condition agrees with Fröhlich's criterion,[6] although the primary idea of this criterion was somewhat different. In the second case, which has been well studied and of which ionic crystals are an example, the integrand of u^2 in (14) attains a maximum for small energies and, therefore,

$E_c \sim uE_i \gg E_i$. In ionic crystals, for energies $\epsilon \gtrsim \hbar\omega_0$, the mean free path $\lambda(x)$ is proportional to x, and consequently $u \sim [\epsilon_i/\hbar\omega_0]^{1/2}$. The breakdown field is determined by the relationship

$$E_c \sim uE_i \ln^{-1/2} \frac{\delta}{w_r^0 \tau(1)} \sim \frac{\hbar\omega_0}{el\,(\hbar\omega_0)} \ln^{-1/2} \frac{\delta}{w_r^0 \tau}. \tag{27}$$

In other words, breakdown occurs in fields for which $eE_c l \sim \hbar\omega_0$ for carriers with energy $\epsilon \sim \hbar\omega_0$, which agrees qualitatively with Hippel's criterion.[9]

Starting from (5) and (6), it is not difficult to verify that Fröhlich's criterion is applicable to crystals in which $B(q)$ for $q \to 0$ increases less rapidly than $[q(1+2N_q)]^{-1}$, and Hippel's criterion applies in the opposite case.

We proceed now to the solution of our basic problem — finding the distribution function in the region $x > 1$ where the process of impact ionization is important. It will be convenient here to introduce new units of energy and current

$$y = \frac{x-1}{\alpha_j}, \qquad s(y) = \frac{\tau(1)}{\delta} \gamma_j S(x)/N_i, \tag{28}$$

$$\alpha_j = (\delta E^2/pE_i^2)^{1/(2+j)}, \qquad \gamma_j = (E_i/E)^2 \alpha_j, \qquad \beta_j = p\alpha_j^j. \tag{29}$$

The system (3) and (4), expressed in these variables, takes the following form:

$$\frac{ds(y)}{dy} - \frac{xk_j(x)}{\lambda(x)} y^j f_0(y) = 0, \tag{30a}$$

$$\frac{x\lambda(x)}{1+\beta_j k_j(x) y^j} \frac{df_0(y)}{dy} + \gamma_j \frac{x^2 \delta(x)}{\lambda(x)\,\delta} f_0(y) - s(y) = 0. \tag{30b}$$

An essential fact, on which all further discussion is based, is the smallness of α, evident directly from (29). In the most interesting region of the field $\alpha \lesssim 0.1$. The functions $f_0(x)$ and $S(x)$ are essentially different from zero only in the narrow region $x - 1 \lesssim \alpha$, outside which they fall off exponentially. In this region the coefficients of (30), in the arguments of which the substitution of y for x has not been made, are very slowly changing functions of y and with great accuracy can be taken as the first terms of corresponding series of degree $x - 1 = \alpha y$. In the zero order approximation in α, which we mainly use, all these are unity. Further, in this approximation, (30) can be solved exactly only in particular — although perhaps the most interesting — cases. We therefore now describe a general method allowing us to determine with adequate accuracy the quantity $\sigma(E)$ of direct interest to us.

Equations (30) for any values of the parameters have two linearly independent solutions; one exponentially decreasing at infinity, the other increasing. Apparently, only the first of these is physically permissible. It is determined to within an arbitrary multiplier, but the ratio of $s(y)$ to $f_0(y)$ at any point, including at $y = 0$, is strictly defined. Therefore, the requirement of a solution decreasing at infinity is equivalent to the problem of determining the value of $\sigma(E)$. We eliminate from (30) the function $f_0(y)$. Then for the current $s(y)$ we obtain a second-order equation

$$\frac{d}{dy}\left\{\frac{\lambda(x)}{xk_j(x)\,y^j} e^{\gamma_j F(y)} \frac{ds(y)}{dy}\right\} - \frac{1+\beta_j k_j(x)\,y^j}{x\lambda(x)} e^{\gamma_j F(y)} s(y) = 0,$$

$$F(y) = \int_0^y \frac{x'\delta(x')}{\lambda^2(x')\,\delta} [1 + \beta_j k_j(x')\,y'^j]\,dy'. \tag{31}$$

The quantity $\sigma(E)$ which is sought is derived from its solution in the following manner:

$$\sigma(E) = -\frac{1}{\gamma_j} \lim_{y\to 0} \left\{\frac{xk_j(x)\,y^j}{\lambda(x)} \frac{s(y)}{ds(y)/dy}\right\} \tag{32}$$

and is a function of the parameters β_j and γ_j. Instead, to find this function, we invert the problem, take fixed values of σ, and seek the inverse function $\beta_j = \beta_j(\sigma, \gamma_j)$. In these circumstances (31) appears as a typical eigenvalue problem; the given boundary conditions at $y = 0$ [Eq. (32)] and at infinity [$s(y) \to 0$] require the finding of the value of the parameter β_j, for which the equation has a nontrivial solution. Solving then the expression obtained for σ, we find the relationship of importance to us $\sigma = \sigma(\beta_j, \gamma_j) = \sigma(E)$. The eigenvalue of interest to us must, apparently, be the smallest, since, from its physical meaning, the function $f_0(y)$ cannot tend to zero anywhere except at infinity. But, from (30a) and the conditions $xk_j(x)/\lambda(x) > 0$ and $s(\infty) = 0$ it follows that $s(y)$ also has no zeros in the interval $(0, \infty)$. These properties, by virtue of the oscillation theorem, are possessed only by the eigenfunction corresponding to the lowest eigenvalue.

One of the most accurate and at the same time simplest ways of finding the lowest eigenvalue is the variational method. Equation (31) with the boundary condition (32) is equivalent to the following variational problem:[10]

$$-\beta_j = \min \frac{\int_0^\infty \left\{\frac{\lambda(x)}{xk_j(x)\,y^j}\left[\frac{ds(y)}{dy}\right]^2 + \frac{s^2(y)}{x\lambda(x)}\right\} e^{\gamma_j F(y)}\,dy - \frac{s^2(0)}{\sigma\gamma_j}}{\int_0^\infty \frac{k_j(x)}{x\lambda(x)} e^{\gamma_j F(y)}\,y^j s^2(y)\,dy} \tag{33}$$

with the additional condition that only functions satisfying (32) are permissible. The eigenvalue is obtained by this method rather accurately even when the variational functions are only rough approximations to the true solution. In the problem considered, however, one can also hope to obtain a reasonable approximation for the function (although this is not a necessity), since its quantitative behavior is very simple. Directly from (31) it is apparent that $s(y)$ is a smooth function monotonically decreasing with increase of y.

Evaluation of the integrals entering into (33) and the subsequent solution requires as a rule rather cumbersome expressions. Therefore we will utilize this method only in cases when an accurate solution cannot be found.

We proceed now to the actual solution of (30) in different cases.

I. $j = 1$. As already remarked above, this case corresponds to semiconductors with not very large dielectric constants ($\mu \sim 1$). In the null approximation with respect to α, the system (30) takes the following form

$$\frac{ds(y)}{dy} - yf_0(y) = 0,$$

$$\frac{1}{1+\beta_1 y}\frac{df_0(y)}{dy} + \gamma_1 f_0(y) - s(y) = 0. \tag{34}$$

The integration of these equations is carried out in Appendix II and leads to the following results:

$$f_0(y) = \frac{\text{const}}{\sqrt{z}}\left\{W_+(z^2) + \rho W_-(z^2)\right\}\exp\left\{-\frac{1}{4}\beta_1\gamma_1\left(y+\frac{1}{2\beta_1}\right)^2\right\}, \tag{35}$$

$$s(y) = -\frac{1}{\sqrt{\beta_1}}\left\{\frac{W_+(z^2)-\rho W_-(z^2)}{W_+(z^2)+\rho W_-(z^2)} - \frac{\sqrt{\beta_1}\gamma_1}{2}\right\}f_0(y), \tag{36}$$

where

$$z = \beta_1^{1/4}\left\{y + \frac{1}{2\beta_1}\left(1+\frac{\beta_1\gamma_1^2}{4}\right)\right\}, \qquad \rho = \frac{1}{4}\beta_1^{-3/4}\left(1-\frac{\beta_1\gamma_1^2}{4}\right),$$

$W_{\pm}(x) = W_{\rho^2\pm\frac{1}{4},\frac{1}{4}}(x)$ is the so-called Whittaker function. From (35) and (36) it follows that

$$\sigma(E) = \frac{1}{\sqrt{\beta_1}}\left\{\frac{W_+(z_0^2)-\rho W_-(z_0^2)}{W_+(z_0^2)+\rho W_-(z_0^2)} - \frac{\sqrt{\beta_1}\gamma_1}{2}\right\},$$

$$\text{where } z_0 = 2\rho\,\frac{4+\beta_1\gamma_1^2}{4-\beta_1\gamma_1^2}. \tag{37}$$

The various limiting cases of these formulae are also treated in Appendix II. Here we only remark that the quantity $\beta_1\gamma_1^2 = \delta(E_i/E)^2$ for the fields of interest to us is small, which allows formulae (35) – (37) to be greatly simplified.

II. $j = 2$. The case of large values of the dielectric permittivity. In Appendix I it is shown that μ can be considered as large if the condition

$$\mu \gg e^2/\hbar\sqrt{2\alpha\varepsilon_i/m}, \tag{38}$$

is satisfied, where e is the electronic charge. By inspection this criterion can be interpreted as follows; the quantity μ is considered large in crystals in which the binding energy of Coulombic levels $me^4/\mu^2\hbar^2$ is smaller than the width of the region $\alpha\epsilon_i$ where impact ionization takes place. In the semiconductors of most interest – germanium and silicon – the binding energy of the Coulomb levels is about 10^{-2} ev, and the quantity $\alpha\epsilon_i \sim 0.1$ ev. It is natural, therefore, to suppose that they belong to the case $j = 2$. The intermediate case when

$$w_i(x) = \frac{p}{\tau(1)}\,(x-1) + c_1(x-1)^2] \text{ and } \alpha c_1 \sim 1,$$

also leads to the case $j = 2$ by the transformation $y' = y + 1/2\alpha c_1$ and, therefore, will not detain us.

Putting $j = 2$ in the original system (30) gives

$$\frac{ds(y)}{dy} - y^2 f_0(y) = 0, \qquad \frac{1}{1+\beta_2 y^2}\frac{df_0(y)}{dy} + \gamma_2 f_0(y) - s(y) = 0. \tag{39}$$

It is not possible to find the general solution of these equations for arbitrary values of the parameters. We proceed, therefore, in the following manner: we divide the integral of possible values of the field into two partially overlapping regions, in one of which $\beta_2 \ll 1$, and in the other $\gamma_2 \ll 1$. In the first region, which is apparently the one of greater interest, we find an analytical solution of (39), and in the second utilize the general method described above for determining the function $\sigma(E)$.

We will start with a proof that these regions do, in fact, overlap, and thus the combination of the solutions we obtain contains the solution of the problem for any values of the parameters E and p. To do this, we remark that the product $\beta_2^{3/2}\gamma_2 \sim \sqrt{p\delta^2} \ll 1$, and therefore for all values of E one of the quantities β_2 and γ_2 must be small. The regions overlap when $\beta_2 \sim \gamma_2 \sim (p\delta^2)^{1/5} < 1$, although the margin in the latter inequality is not very large. The considerations given have an obvious physical significance. The energy relaxation time due to collisions with phonons is much greater than the momentum relaxation time. In ionization collisions these times are of the same order. Therefore, if the ionization processes play an important role in establishing momentum equilibrium ($\beta_2 \gtrsim 1$), then the energy relaxation is determined only by them ($\gamma_2 \ll 1$). On the other hand, if phonons make a significant contribution to establishing energy equilibrium ($\gamma_2 \gtrsim 1$), then the momentum loss in ionization for time τ is insignificantly small ($\beta_2 \ll 1$). The region $\beta_2 \ll 1$ is of the greatest interest, since it corresponds to a field $E < E_i$, and in general this condition, as was shown above, is satisfied even by breakdown fields. We commence the discussion with this case.

a) $\beta_2 \ll 1$. Region of comparatively weak fields.

In the zeroth approximation with respect to α_2 and β_2 (the method used, taking into account the corresponding corrections, is given in Appendix III) a second-order equation for $f_0(y)$ can be obtained from (39):

$$d^2 f_0(y)/dy^2 + \gamma_2 df_0(y)/dy - y^2 f_0(y) = 0. \tag{40}$$

By a series of elementary substitutions this can be reduced to the Whittaker equation and its solution takes the following form:

$$f_0(y) = \mathrm{const}\, y^{-1/2} \exp\{-{}^1/_2\gamma_2 y\}\, W_{-(\gamma_2/4)^2, 1/4}(y^2). \tag{41}$$

Using the known behavior of the Whittaker function, it is not difficult to discover the behavior of $f_0(y)$ at zero and at infinity:

$$y \gg 1:\ f_0(y) = \mathrm{const}\, y^{-(\gamma_2/4)^2 - 1/2} \exp\{-{}^1/_2(y^2 + \gamma_2 y)\}, \tag{42}$$

$$y \ll 1:\quad f_0(y) \approx \mathrm{const}\left\{\frac{\Gamma(^1/_2)}{\Gamma(^3/_4+\gamma_2^2/16)}\left(1 - \frac{1}{2}\gamma_2 y\right) + \frac{\Gamma(-^1/_2)}{\Gamma(^1/_4+\gamma_2^2/16)}\, y + O(y^2)\right\}. \tag{43}$$

With the help of the last formulae and the second of Eqs. (39) the quantity $\sigma(E)$ of interest to us can be determined:

$$\sigma(E) = -\frac{1}{\gamma_2}\left\{\frac{d}{dy}\ln f_0(y) + \gamma_2\right\}_{y=0} = \frac{2}{\gamma_2}\frac{\Gamma(^3/_4+\gamma_2^2/16)}{\Gamma(^1/_4+\gamma_2^2/16)} - \frac{1}{2}. \tag{44}$$

In the limiting cases of small $(\gamma_2 \gg 1)$ and large $(\gamma_2 \ll 1)$ fields we have

$$\sigma(E) = \begin{cases} 2/\gamma_2^4 = (2p/\delta)(E/E_i)^6, & \gamma_2 \gg 1 \\ \dfrac{2}{\gamma_2}\dfrac{\Gamma(^3/_4)}{\Gamma(^1/_4)} = 2\dfrac{\Gamma(^3/_4)}{\Gamma(^1/_4)}\left(\dfrac{p}{\delta}\right)^{1/4}\left(\dfrac{E}{E_i}\right)^{3/2}, & \gamma_2 \ll 1. \end{cases} \tag{45}$$

The distribution function (41) in the latter case $(\gamma_2 \ll 1)$ is close to that obtained by Heller.[11]

b) $\gamma_2 \ll 1$. Region of very strong fields. In the zero approximation with respect to α_2 and γ_2 we must solve the following variational problem:

$$-\beta_2 = \min \frac{\int_0^\infty \{[y^{-1}ds/dy]^2 + s^2(y)\}dy - s^2(0)/\gamma_2\sigma}{\int_0^\infty y^2 s^2(y)\, dy}$$

$$\lim_{y\to 0}\left\{\frac{1}{y^2 s(y)}\frac{ds(y)}{dy}\right\} = -\frac{1}{\gamma_2\sigma}. \tag{46}$$

The detailed method of solution is given in Appendix III. Here we confine ourselves to a summary of the results. The connection between the quantity $g = (\gamma_2\sigma)^{-2/3}$ and β_2 is given in parametric form by the two relationships

$$\beta_2 = g\{g^2\psi_1(\nu) - \psi_2(\nu)\}, \qquad g^2 = \frac{d\psi_2(\nu)}{d\nu}\Big/\frac{d\psi_1(\nu)}{d\nu}, \tag{47}$$

where

$$\psi_1(\nu) = \frac{\nu\sin\pi\nu}{\pi}\frac{\Gamma^3(\nu)\Gamma(4\nu)}{\Gamma^2(2\nu)\Gamma(3\nu)},$$

$$\psi_2(\nu) = \left[\frac{\nu\sin\pi\nu}{3\pi}\Gamma^2(\nu)\right]^{2/3}\frac{\Gamma(4\nu)}{\Gamma(8\nu/3)}\frac{\Gamma(\nu/3)\Gamma^2(4\nu/3)\Gamma(7\nu/3)}{\Gamma(\nu)\Gamma^2(2\nu)\Gamma(3\nu)}. \tag{48}$$

The corresponding function $s(y)$ takes the form

$$s(y) = z^\nu K_\nu(z), \qquad z = \left[\frac{2^{2\nu}\nu\sin\pi\nu}{3\pi\sigma}\Gamma^2(\nu)\right]^{1/2\nu} y^{3/2\nu}, \tag{49}$$

where $K_\nu(z)$ is the Macdonald function. ν varies from $\frac{3}{4}$ to $\frac{1}{2}$. In the limiting case when $\beta_2 \to 0$, ν tends to $\frac{3}{4}$ and the solution (49) agrees with that which is obtained from (41) in the limit as $\gamma_2 \to 0$. Thus, the solutions we have obtained in fact join up in the region where the conditions $\beta_2 \ll 1$ and $\gamma_2 \ll 1$ are simultaneously satisfied. In the other limiting case when $\nu \to \frac{1}{2}$, g tends to infinity. Thus, $\beta_2 \sim g^3 \sim (\gamma_2\sigma)^{-2}$. In fact, for very large fields

$$\sigma(E) = \sqrt{\psi_1(^1/_2)/\delta}\, E/E_i. \tag{50}$$

APPENDIX I

The probability of the creation of electrons with momenta $\mathbf{p}_1$ and $\mathbf{p}_2$ and a hole with momentum $\mathbf{p}_3$, due to an ionizing collision of an electron with an original momentum $\mathbf{p}_0$, can always be written in the form

$$(2\pi/\hbar)\,|M(\mathbf{p}_0;\ \mathbf{p}_1,\ \mathbf{p}_2)|^2\,\delta[\varepsilon_e(\mathbf{p}_0) - \varepsilon_e(\mathbf{p}_1) - \varepsilon_e(\mathbf{p}_2) - \varepsilon_h(\mathbf{p}_3)] \times \delta[(\mathbf{p}_0 - \mathbf{p}_1 - \mathbf{p}_2 - \mathbf{p}_3)/\hbar].$$

Hence, the following expression is obtained for the total ionization probability:

$$w_i(\varepsilon_0) = \frac{2\pi}{\hbar}V^3 \times \int |M(\mathbf{p}_0;\ \mathbf{p}_1,\ \mathbf{p}_2)|^2\,\delta[\varepsilon_0 - \varepsilon_e(\mathbf{p}_1) - \varepsilon_e(\mathbf{p}_2) - \varepsilon_h(\mathbf{p}_3)] \times \delta\left(\frac{\mathbf{p}_0 - \mathbf{p}_1 - \mathbf{p}_2 - \mathbf{p}_3}{\hbar}\right)\frac{d^3p_1 d^3p_2 d^3p_3}{(2\pi\hbar)^9}. \tag{A.1}$$

All the conservation laws can be satisfied only for sufficiently large values of $\mathbf{p}_0$. The ionization threshold is determined by the condition

$$\varepsilon_i \equiv \varepsilon_e(\mathbf{p}_i) = \varepsilon_{min}(\mathbf{p}_i) \equiv \min\{\varepsilon_e(\mathbf{p}_1) + \varepsilon_e(\mathbf{p}_2) + \varepsilon_h(\mathbf{p}_i - \mathbf{p}_1 - \mathbf{p}_2)\}.$$

The condition of a minimum in the right-hand side of the equality means that at the threshold $\nabla\epsilon_e(\mathbf{p}_1) = \nabla\epsilon_e(\mathbf{p}_2) = \nabla\epsilon_h(\mathbf{p}_3) = \mathbf{v}$, i.e., the speeds of all the final particles are equal. Close to the threshold the argument of the energy δ-function can be developed in a power series of the departure of the momenta from their values $\mathbf{p}_m(\mathbf{p}_0)$ determined from the minimum condition written down above. The coefficients of the corresponding quadratic form, after transforming to principal axes, we will label $m_k^{*-1}(\mathbf{p}_0)$. After introducing new variables of integration according to the formulae

$$p_k - p_{km}(\mathbf{p}_0) = \sqrt{2m_k^*(\mathbf{p}_0)\,[\varepsilon_e(\mathbf{p}_0) - \varepsilon_{min}(\mathbf{p}_0)]}\,\pi_k$$

etc., (A.1) acquires the following form:

$$w_i(\mathbf{p}_0) = \frac{2\pi}{\hbar}\frac{m_1^*(\mathbf{p}_0)\, m_2^*(\mathbf{p}_0) m_3^*(\mathbf{p}_0)}{(2\pi)^3(2\pi\hbar)^6}[\varepsilon_e(\mathbf{p}_0) - \varepsilon_{min}(\mathbf{p}_0)]^2$$

$$\times V^3 \int |M(\mathbf{p}_0;\ \mathbf{p}_1,\ \mathbf{p}_2)|^2 \delta\left(1 - \sum_{k=1}^{6} \pi_k^2\right) d^6\pi =$$

$$= \frac{1}{\hbar}\frac{m_1^*(\mathbf{p}_0)\, m_2^*(\mathbf{p}_0)\, m_3^*(\mathbf{p}_0)}{(2\pi)^2(2\pi\hbar)^6} V^3 \overline{|M(\mathbf{p}_0)|^2}[\varepsilon_e(\mathbf{p}_0) - \varepsilon_{min}(\mathbf{p}_0)]^2. \tag{A.2}$$

In the Born approximation $M(\mathbf{p}_0, \mathbf{p}_1, \mathbf{p}_2)$ is simply the matrix element of the corresponding interaction energy. Since the momenta which are exchanged by the particles participating in the reaction are of the order $\sqrt{m\epsilon_i}$, the collision parameters making the principal contribution to ionization at the threshold are of the order $\hbar/\sqrt{m\epsilon_i}$. In this region the interaction potential must be of Coulomb order e^2/r, since the polarization of the medium only occurs at large distances. Therefore

$$M \sim \frac{e^2}{\hbar}\sqrt{m\varepsilon_i}\frac{\hbar^3}{V(m\varepsilon_i)^{3/2}} = \frac{1}{V}\frac{e^2\hbar^2}{m\varepsilon_i},$$

so that

$$w_i(\mathbf{p}_0) \sim \frac{e^4 m}{\hbar^3} V\varepsilon_i^{-2}[(\nabla\varepsilon_e(\mathbf{p}_i) - \mathbf{v})(\mathbf{p}_0 - \mathbf{p}_i)]^2 \approx \frac{e^4 m}{\hbar^3} V\left(\frac{\varepsilon_0 - \varepsilon_i}{\varepsilon_i}\right)^2. \tag{A.3}$$

This expression is almost the same as the result obtained by Tevordt[12] from an exact analysis of a somewhat simplified model. In deriving (A.3) we have neglected the difference between the slowly varying quantities $m_k^*(\mathbf{p}_0)$ and their values at the ionization threshold, and have replaced all the m_k^* by some mean value m. Also we took the speed of the final particles v as small compared with the speed of the primary $\nabla\epsilon_e(\mathbf{p}_0)$.

When the Born approximation is inapplicable, the ionization cross-section for slow electrons differs from the Born multiplier $|\psi(0, 0)|^2$, where $\psi(\mathbf{r}_1, \mathbf{r}_2)$ is the wave function of the final state describing the motion of the two electrons relative to the hole.[13] When a long-range Coulomb interaction is present, this multiplier tends to infinity as $(\epsilon - \epsilon_i)^{-1}$.[14]* The evaluation of the matrix element given above is then correct only in the region $\epsilon - \epsilon_i \gtrsim e^4 m/\mu^2\hbar^2$ (criterion for applicability of the Born approximation). The dielectric permitivity μ enters into this criterion because the growth of $|\psi(0, 0)|^2$ is determined by the long-range part of the Coulomb interaction. In the region of small energies

$$w_i(\mathbf{p}_0) \sim \frac{e^4 m}{\hbar^3} V\left(\frac{\varepsilon_0 - \varepsilon_i}{\varepsilon_i}\right)^2 \frac{e^4 m}{\mu^2\hbar^2(\varepsilon_0 - \varepsilon_i)} = \frac{\varepsilon_i}{\hbar}\left(\frac{e^4 m}{\mu\hbar^2\varepsilon_i}\right)^2 V\frac{\varepsilon_0 - \varepsilon_i}{\varepsilon_i}. \tag{A.4}$$

The energies of interest to us are of the order $\epsilon_i + \alpha\epsilon_i$. Consequently, if μ is large enough so that $\mu^2\alpha\epsilon_i\hbar^2/e^4 m \gg 1$ the Born approximation is applicable for them and Formula (A.3) can be used. In cases where $\mu \sim 1$, the situation is completely analogous to that which exists in gases and the ionization cross section close to the threshold increases linearly.

APPENDIX II

We transform the system (34) by introducing new variables according to the formulae

$$z = \beta_1^{1/4}\left[y + \frac{1}{2\beta_1}\left(1 + \frac{\beta_1\gamma_1^2}{4}\right)\right], \quad \rho = \frac{1}{4}\beta_1^{-3/4}\left(1 - \frac{\beta_1\gamma_1^2}{4}\right),$$

$$\chi_1(z) = \left\{\left(1 - \frac{\sqrt{\beta_1}\gamma_1}{2}\right) f_0(y) + \sqrt{\beta_1} s(y)\right\}$$

$$\times \exp\left[\frac{1}{4}\beta_1\gamma_1\left(y + \frac{1}{\beta_1}\right)^2\right];$$

$$\chi_2(z) = \left\{\left(1 + \frac{\sqrt{\beta_1}\gamma_1}{2}\right) f_0(y) - \sqrt{\beta_1} s(y)\right\}$$

$$\times \exp\left[\frac{1}{4}\beta_1\gamma_1\left(y + \frac{1}{\beta_1}\right)^2\right]. \tag{A.5}$$

The functions $\chi_{1,2}(z)$ then satisfy the following equations:

$$d^2\chi_{1,2}(z)/dz^2 + (4\rho^2 \mp 1 - z^2)\chi_{1,2}(z) = 0, \tag{A.6}$$

which easily lead to the Whittaker equation. The corresponding solutions are given by (35) — (37). Here we retain in the analysis some limiting cases. It was remarked above that in the region of fields of interest to us the quantity $\beta_1\gamma_1^2 = \delta(E_i/E)^2$ is small compared with unity. Therefore we will retain only terms of the order $\sqrt{\beta_1}\,\gamma_1$, and will neglect terms of the order $\beta_1\gamma_1^2$.

a) $\rho \ll 1$. Region of large fields. In this case the quantity $z_0 = 2\rho(4 + \beta_1\gamma_1^2)/(4 - \beta_1\gamma_1^2)$ is also small. In the zero approximation in ρ^2 the solution has the following form:

$$f_0(y) \approx z^{-1/2}\exp\left\{-\frac{1}{4}\beta_1\gamma_1\left(y + \frac{1}{\beta_1}\right)^2\right\} W_{1/4,\,1/4}(z^2)$$

$$\approx \exp\left\{-\frac{\sqrt{\beta_1}}{2}\left(y + \frac{1}{2\beta_1}\right)^2 - \frac{1}{4}\beta_1\gamma_1\left(y + \frac{1}{\beta_1}\right)^2\right\}, \tag{A.7}$$

---

[*] The results of Geltman[14] cannot be considered as strictly proven, since one of the terms entering into the interaction of the final particles was considered as a small perturbation. More convincing from our point of view is the fact that the experimentally measured ionization cross section in gases close to the threshold depends linearly on energy.

$$s(y) = -\{1 - \sqrt{\beta_1}\gamma_1/2\} f_0(y)/\sqrt{\beta_1}, \ \sigma(E) = 1/\sqrt{\beta_1}\gamma_1 - {}^1/_2. \tag{A.8}$$

b) $\rho \gg 1$. Region of relatively small fields. For this case it is most convenient to start directly from (A.6). We transform afresh to the independent variable $y = (4\rho)^{1/3}(z - 2\rho)$ and neglect the small quantity $\rho^{-4/3}y^2$. The functions $\chi_{1,2}(y)$ then satisfy the equation

$$d^2\chi_{1,2}(y)/dy^2 - (y \pm \sqrt{\beta_1})\chi_{1,2}(y) = 0. \tag{A.9}$$

Consequently,

$$\chi_{1,2}(y) = (y \pm \sqrt{\beta_1})^{1/2} K_{1/3}[{}^2/_3(y \pm \sqrt{\beta_1})^{3/2}], \tag{A.10}$$

$$f_0(y) \approx \sqrt{y} K_{1/3}({}^2/_3\, y^{3/2}) \exp[-{}^1/_4\, \beta_1\gamma_1 (y + 1/\beta_1)^2] + O(\beta_1),$$
$$s(y) = -[\sqrt{y} K_{2/3}({}^2/_3\, y^{3/2}) / K_{1/3}({}^2/_3\, y^{3/2}) - \gamma_1/2] f_0(y); \tag{A.11}$$

$$\sigma(E) = -3^{1/3}\Gamma({}^2/_3)/\gamma_1\Gamma({}^1/_3) - {}^1/_2. \tag{A.12}$$

If γ_1 is not small, then

$$\sigma(E) = -{}^1/_2[K_{2/3}(\gamma_1^3/12)/K_{1/3}(\gamma_1^3/12) - 1]. \tag{A.13}$$

This solution is easily obtained also from (34) under the condition $\beta_1 \ll 1$.

APPENDIX III

1. The evaluation of the corrections to the solution of (30) for $j = 2$ which are proportional to β_2, α_2, and α_2^2, can be performed in the following way. We introduce the new independent variable

$$z = \left\{2\int_0^y y \sqrt{\frac{k_2(x)\,|1 + \beta_2 k_2(x) y^2|}{\lambda^2(x)}}\, dy\right\}^{1/2}$$

and then by substitution

$$f_0(y) = \left(\frac{dz}{dy}\right)^{-1} \exp\left\{-\frac{1}{2}\int_0^z \left[\gamma_2 \frac{x^2\delta(x)}{\lambda(x)\delta} + \frac{d}{dy}\left(\frac{x\lambda(x)}{1 + \beta_2 k_2(x) y^2}\right)\right] \frac{\lambda(x)}{x k_2(x)} \frac{dz}{dy}\, dz\right\} \varphi(z) \tag{A.14}$$

arrive at the equation in the normal form

$$d^2\varphi(z)/dz^2 - \{{}^1/_4\,\gamma_2^2\Psi(z) + z^2\}\varphi(z) = 0. \tag{A.15}$$

We develop $\Psi(z)$ in a power series of z: $\Psi(z) = \Psi(0) + \Psi_1(z) + \Psi_2(z^2) + \ldots$. In essence this series is an expansion of $\Psi(z)$ in powers of α_2 and β_2: $\Psi \sim \alpha_1$, Ψ_2 contains terms proportional to α_2^2 and β_2, etc. By the transformation

$$z' = \left(1 + \frac{1}{4}\gamma_2^2\Psi_2\right)^{1/4}\left(z + \frac{1}{2}\gamma_2^2 \frac{\Psi_1}{4 + \gamma_2^2\Psi_2}\right)$$

Equation (A.15) leads to the previous form. We limit ourselves here to this preliminary treatment and shall not proceed to explicit expressions for $\Psi(z)$, Ψ_0, Ψ_1 and Ψ_2 in view of their cumbersomeness.

2. As the variational function for the problem formulated in Eq. (46), we will choose the function $s(y) = z^\nu K_\nu(z)$, where $z = (\xi y)^{3/2\nu}$. This function has the correct behavior at zero, $s(y) - s(0) \sim y^3$, and decreases monotonically with increase of y, i.e., it satisfies the basic qualitative requirements for $s(y)$. Also in the limiting cases of small $(\nu \to \frac{3}{4})$ and large $(\nu \to \frac{1}{2})$ values of β_2, it gives an accurate solution of (39) for $\gamma_2 = 0$. Of the two parameters ξ and ν, only one is disposable by virtue of the additional condition (46). We will take ν as the independent variable. The parameter ξ is expressed in terms of ν and σ in the following way:

$$\xi^3 = (2^{2\nu}/3\pi\sigma)\,\nu\Gamma^2(\nu)\sin\pi\nu. \tag{A.16}$$

The evaluation of all the integrals entering into (46) is most conveniently carried out using the known integral forms of the Macdonald functions

$$K_\nu(z) = \frac{1}{2} z^\nu \int_0^\infty t^{-\nu-1} \exp\left\{-\frac{t}{2} - \frac{z^2}{2t}\right\} dt,$$

$$\int_0^\infty z^\mu K_\nu(z) K_{\nu'}(z)\, dz$$
$$= \frac{2^{\mu-2}}{\Gamma(\mu+1)} \Gamma\left(\frac{\mu+\nu+\nu'+1}{2}\right) \Gamma\left(\frac{\mu-\nu+\nu'+1}{2}\right)$$
$$\times \Gamma\left(\frac{\mu+\nu-\nu'+1}{2}\right) \Gamma\left(\frac{\mu-\nu-\nu'+1}{2}\right). \tag{A.17}$$

As a result, (46) is reduced to

$$-\beta_2 = g \min\{-g^2\psi_1(\nu) + \psi_2(\nu)\}, \tag{A.18}$$

where the functions $\psi_1(\nu)$ and $\psi_2(\nu)$ are determined by (48). The condition for the minimum of this expression leads to the connection (47) between β_2 and g.

---

[1] S. L. Miller, Phys. Rev. **99**, 1234 (1955). A. P. Shotov, J. Tech. Phys. (U.S.S.R.) **28**, 437 (1958), Soviet Phys.–Tech. Phys. **3**, 413 (1958).

[2] B. I. Davydov, JETP **7**, 1069 (1937). W. Franz, Z. Physik **113**, 607 (1939); Encycl. Phys. **17**, 155 (1956). R. Stratton, Proc. Roy. Soc. **A242**, 355 (1957).

[3] W. Shockley and W. T. Read, Phys. Rev. **87**, 835 (1952).

[4] N. L. Pisarenko, Izv. Akad. Nauk SSSR, Ser. Fiz. **5**, 631 (1938).

[5] F. Seitz, Phys. Rev. **76**, 1376 (1949).

[6] H. Fröhlich, Proc. Roy. Soc. **A160**, 230 (1937).

[7] B. I. Davydov and I. M. Shmushkevich, JETP **10**, 1043 (1940).

[8] V. A. Chuenkov, Usp. Fiz. Nauk **54**, 185 (1954).

[9] A. von Hippel, J. Appl. Phys. **8**, 815 (1937).

[10] R. Courant and D. Hilbert, Methods of Mathematical Physics, Interscience, 1943. Chapter IV.

[11] W. R. Heller, Phys. Rev. **84**, 1130 (1951).

[12] L. Tewordt, Z. Physik **138**, 499 (1954).

[13] L. D. Landau and E. M. Lifshitz, Квантовая механика (Quantum Mechanics), Pergamon, 1958 Sec. 118.

[14] S. Geltman, Phys. Rev. **102**, 171 (1956).

Translated by K. F. Hulme
138

SOVIET PHYSICS JETP VOLUME 37 (10), NUMBER 3 MARCH, 1960

DISPERSION RELATIONS FOR THE VIRTUAL COMPTON EFFECT

I. S. ZLATEV and P. S. ISAEV

Joint Institute for Nuclear Research

Submitted to JETP editor March 23, 1959

J. Exptl. Theoret. Phys. (U.S.S.R.) **37**, 728-734 (September, 1959)

Dispersion relations for physical amplitudes have been derived by the Bogolyubov method in the center-of-mass system for electron bremsstrahlung and for pair production by a photon in the field of a nucleon, accurate to lowest order in e.

1. INTRODUCTION

AT the present time dispersion relations (d.r.) provide one of the most effective methods for taking into account effects of strong interactions. In application to electromagnetic processes such as the nucleon Compton effect, bremsstrahlung, or pair production by photons in the field of a nucleon, etc., this method, under well defined assumptions, allows information to be obtained about the nucleon structure. It should be noted that nucleon structure has been the subject of considerable attention in recent years* since it has not only intrinsic interest but is also closely related to the study of limits of applicability of quantum electrodynamics at small distances.

A theoretically rigorous study of the influence of nucleon structure on the processes of bremsstrahlung and pair production is made possible by applying d.r. to the indicated processes. From this point of view a study of d.r. for the virtual Compton effect, which describes both of the above mentioned processes, is of certain interest.

In this work d.r. are obtained for the virtual Compton effect accurate to lowest order in e by the Bogolyubov[1] method.

The proof of d.r. for the bremsstrahlung and pair production processes was given by Vladimirov and Logunov;[3] in this paper attention is concentrated on obtaining d.r. in a form useful for practical applications.

It is shown that the cross sections agree, in the one-nucleon approximation, with those calculated by lowest order perturbation theory; however, the d.r. method allows one to introduce rigorously form factors (of the type considered by Hofstadter) into those nucleon vertices in the Feynmann graphs which contain a virtual photon line. This constitutes one of the serious advantages of the d.r. method over perturbation theory.

The resultant d.r. may be further utilized at least to estimate the contribution of the one-pion state to the processes under consideration in the same way as was done for the pion photoproduction process.[4,5]

The bremsstrahlung and pair production processes have been previously calculated by the authors[6] in lowest-order perturbation theory, taking into account only Bethe-Heitler type diagrams into which Hofstadter form factors were introduced. It is clear that for incident particle energies up to ~ 150 Mev, when the contribution from the meson cloud of the nucleon and higher order electromagnetic corrections are unimportant, these results could be used to check the validity of quantum electrodynamics at small distances, i.e., to verify the local nature of the interaction between the electromagnetic field and the current of a charged particle. Analogous results were also obtained by Bjorken et al.[7] However as the energy increases to 500 or 600 Mev the contribution from the meson cloud of the nucleon should become more and more noticeable and the one-pion approximation may introduce significant changes in the cross sections for the processes under discussion. Therefore taking into account the one-pion state will noticeably move the energy limit for the check of validity of quantum electrodynamics at small distances, namely up to an electron and photon energy of the order of 500 — 600 Mev.

In this way it becomes possible, for example, to verify quantum electrodynamics down to distances $\geq 3 \times 10^{-14}$ cm in the bremsstrahlung process where the incident electron has an energy ~ 550 Mev and the emitted photon has an energy ~ 260 Mev.

---

*A detailed bibliography on the nucleon structure problem may be found in the review article by Blokhintsev, Barashenkov, and Barbashov.[2]

2. DISPERSION RELATIONS FOR THE AMPLITUDE OF THE VIRTUAL COMPTON EFFECT

The S-matrix element describing the bremsstrahlung of an electron in the field of a nucleon has the form

$$\langle f \mid S \mid i\rangle = \langle p, s;\ q, \sigma;\ k, \nu \mid S \mid q_0, \sigma_0;\ p_0, s_0\rangle =$$
$$= (2\pi)^{3/2} \langle p, s \mid b^-(\mathbf{q}, \sigma)\, a^-(\mathbf{k}, \nu)\, Sb^{+*}(\mathbf{q}_0, \sigma_0) \mid p_0, s_0\rangle, \quad (2.1)$$

where p, s (p_0, s_0) are the four-momentum and spin of the final (initial) nucleon, q, σ (q_0, σ_0) are the four-momentum and spin of the final (initial) electron, k, ν are the four-momentum and polarization of the photon, $b^-(\mathbf{q}, \sigma)$ and $b^{+*}(\mathbf{q}_0, \sigma_0)$ are creation and annihilation operators for an electron in the states ($\mathbf{q}$, σ) and ($\mathbf{q}_0$, σ_0), and $a^-(\mathbf{k}, \nu)$ is the creation operator for a photon of momentum **k** and polarization ν; $|p_0, s_0\rangle = (2\pi)^{3/2} C^{+*}(\mathbf{p}_0, s_0)\, \Phi_0$ is the initial nucleon state vector.

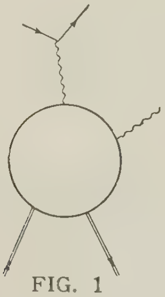

FIG. 1

Now following the method outlined in the paper by Logunov and Isaev[8] and assuming that the virtual Compton effect amplitude behaves asymptotically as ~ $1/k_0$ (where k_0 is the photon energy)* we obtain d.r. for the diagram shown in Fig. 1, in the Breit coordinate system and to lowest order in e, as follows

$$D(k_0) = \frac{\mathrm{P}}{\pi}\int_{E_1}^{\infty} \frac{A(k_0')\,dk_0'}{k_0' - k_0} - \frac{\mathrm{P}}{\pi}\int_{E_1}^{\infty} \frac{A(-k_0')\,dk_0'}{k_0' + k_0}$$
$$+ \frac{A^{(1)}(-\lambda\mathbf{a} + \Delta\mathbf{p})}{E_p - k_0} + \frac{A^{(2)}(\lambda\mathbf{a} + \Delta\mathbf{p})}{E_p + k_0}, \quad (2.2)$$

where

$$k_0 = (k_0 + \varkappa_0)/2, \quad \varkappa = q_0 - q,$$
$$D(k_0) = \frac{1}{2}[ST^{ret}(k_0, \mathbf{a}) + ST^{adv}(k_0, \mathbf{a})],$$
$$A(k_0) = \frac{1}{2i}[ST^{ret}(k_0, \mathbf{a}) - ST^{adv}(k_0, \mathbf{a})],$$

with S the **λ**-symmetrization operator.

$$A^{(1)}(-\lambda\mathbf{a} + \Delta\mathbf{p}) = (2\pi)^3 \frac{M^2 + \Delta\mathbf{p}^2}{M^2 + \mathbf{p}^2} e^n \varepsilon^l S \sum_\rho \langle \mathbf{p}, \sigma \mid j^l(0) \mid -\lambda\mathbf{a}$$
$$+ \Delta\mathbf{p}, \rho\rangle \langle -\lambda\mathbf{a} + \Delta\mathbf{p}, \rho \mid j^n(0) \mid \mathbf{p}_0, \sigma_0\rangle,$$
$$A^{(2)}(\lambda\mathbf{a} + \Delta\mathbf{p}) = (2\pi)^3 \frac{M^2 + \Delta\mathbf{p}^2}{M^2 + \mathbf{p}^2} e^n \varepsilon^l S \sum_\rho \langle \mathbf{p}, \sigma \mid j^n(0) \mid \lambda\mathbf{a}$$
$$+ \Delta\mathbf{p}, \rho\rangle \langle \lambda\mathbf{a} + \Delta\mathbf{p}, \rho \mid j^l(0) \mid \mathbf{p}_0, \sigma_0\rangle;$$
$$\lambda\mathbf{a} = \mathbf{k} + (1 - \Delta)\,\mathbf{p} = \varkappa - (1 + \Delta)\,\mathbf{p},$$
$$\Delta = m_\gamma^2 / 4\mathbf{p}^2;\ \varkappa^2 = -m_\gamma^2, \qquad \varepsilon^l = \bar{u}(\mathbf{q}, \sigma)\,\gamma^l u(\mathbf{q}_0, \sigma_0). \quad (2.3)$$

Here $\mathbf{a} = \boldsymbol{\lambda}/\lambda$ is a unit vector orthogonal to **p**; $j^l(0)$, $j^n(0)$ are the electromagnetic current operators; e^n is the polarization vector of the free photon; u (**q**, σ) is the spinor describing an electron in the state with momentum q and spin direction σ. The spinors are normalized according to $\bar{u}u = 1$.

The d.r. for pair production by a photon in the field of a nucleon are obtained from (2.2) by the simple substitutions $k \to \kappa$, $\kappa = q + q_0$, and $m_\gamma^2 = \kappa_0^2 - \kappa^2$. The one-nucleon terms (2.3) are evaluated at the points

$$k_0 = \pm E_p = \pm(1 - \Delta)\,\mathbf{p}^2/\sqrt{M^2 + p^2}. \quad (2.4)$$

The continuous spectrum in k_0 begins at the points

$$k_0 = \mp E_1 = [\mp 2M\mu$$
$$+ \mu^2 - 2(1 - \Delta)\,\mathbf{p}^2]/2\sqrt{M^2 + \mathbf{p}^2}, \quad (2.5)$$

with μ the pion mass.

In order to avoid having the one-nucleon poles ± E_p fall in the region of the continuous spectrum $|k_0| \geq E_1$, i.e., in order that $E_p < E_1$, it is necessary to require that p^2 satisfy

$$p^2 < (2M\mu + \mu^2 + m_\gamma^2)/4.$$

It is important to note that in the d.r. under study no unphysical region appears for momenta satisfying the inequality

$$|\mathbf{p}| < [(2M\mu + \mu^2)^2 + (M + \mu)^2 m_\gamma^2 + m_\gamma^2 M^2 + (2M\mu + \mu^2)$$
$$\times \sqrt{(2M\mu + \mu^2 + m_\gamma^2)^2 + 4M^2 m_\gamma^2}]^{1/2}/2\sqrt{2}\,(M + \mu). \quad (2.6)$$

For the real Compton effect $m_\gamma = 0$ and we get

$$|\mathbf{p}| < (2M\mu + \mu^2)/2(M + \mu),$$

in agreement with the results of Bogolyubov and Shirkov.[10] The one-nucleon terms (2.3) are calculated in the same manner as that outlined by Logunov and Isaev.[8] In the Breit coordinate system they take the form

---

*An analogous choice for the asymptotic behavior of the amplitude for the real Compton effect was made by Gell-Mann and Mathews.[9]

$$A_{ln}^{(1)} = -e^2 \frac{M(M^2+\Delta \mathbf{p}^2)}{2(2\pi)^3(M^2+\mathbf{p}^2)E''\sqrt{EE_0}} \bar{w}(\mathbf{p},\sigma)\Big(F_1(\varkappa^2)\gamma^l + F_2(\varkappa^2)\frac{\mu_0[\hat{\varkappa},\gamma^l]}{4M}\Big)(\hat{p}''+M) \times\Big(F_1(k^2)\gamma^n - F_2(k^2)\frac{\mu_0[\hat{k},\gamma^n]}{4M}\Big) w(\mathbf{p}_0,\sigma_0),$$

$$A_{nl}^{(2)} = -e^2 \frac{M(M^2+\Delta \mathbf{p}^2)}{2(2\pi)^3(M^2+\mathbf{p}^2)E''\sqrt{EE_0}} \bar{w}(\mathbf{p},\sigma)\Big(F_1(k^2)\gamma^n - F_2(k^2)\frac{\mu_0[\hat{k},\gamma^n]}{4M}\Big)(\hat{p}''+M) \times\Big(F_1(\varkappa^2)\gamma^l + F_2(\varkappa^2)\frac{\mu_0[\hat{\varkappa},\gamma^l]}{4M}\Big) w(\mathbf{p}_0,\sigma_0). \qquad (2.7)$$

Here F_1 and F_2 are nucleon form factors: $F_1(0) = F_2(0) = 1$ for the proton, $F_1(0) = 0$, $F_2(0) = 1$ for the neutron; μ_0 is the anomalous magnetic moment in units of nuclear magnetons.

It is important to note that in the one-nucleon approximation, i.e., when

$$\langle f|S|i\rangle = -ie\frac{me^n\varepsilon^l}{\sqrt{2k_0\varepsilon\varepsilon_0}}\frac{(2\pi)^4}{\varkappa^2}\delta(k+p-p_0-\varkappa) \times\Big(\frac{A_{ln}^{(1)}(-\lambda a)}{E_p-k_0}+\frac{A_{nl}^{(2)}(\lambda a)}{E_p+k_0}\Big) \qquad (2.8)$$

(ϵ, ϵ_0 are the electron energies in final and initial states) the expression (2.8) coincides with the sum of the matrix elements corresponding to the diagrams of Figs. 2a and 2b, in which the vertices involving the virtual photon contain $F_1(\kappa^2)$ and $F_2(\kappa^2)$ instead of the form-factor functions $\Phi_1(\kappa^2, p''^2)$ and $\Phi_2(\kappa^2, p''^2)$, and the vertices involving the real photon contain $F_1(0)$ and $F_2(0)$ instead of $\Phi_1(0, p''^2)$ and $\Phi_2(0, p''^2)$.

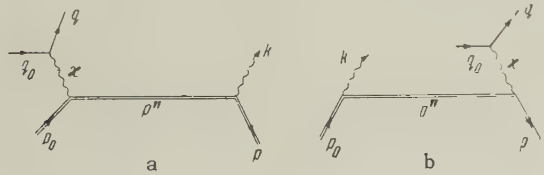

a b

FIG. 2.

In this way use of d.r. permits one to introduce in a rigorous manner into the bremsstrahlung and pair production processes (in lowest order in e approximation) the form factors depending on one variable which, for negative values of the argument, were studied by Hofstadter.[11]

3. STRUCTURE OF THE BREMSSTRAHLUNG AMPLITUDE

Making use of the results of Kawaguchi and Mugibayashi[12] we write T^c in the form

$$T^c = \sum_{i=1}^{12}\Omega_i T^i, \qquad (3.1)$$

where Ω_i are scalar functions of the invariants constructed of p_0, p, k, and κ, and T^i are relativistic and gauge invariant structures satisfying the condition

$$T^i = \pm(T^i)^+ \qquad (p \rightleftarrows p_0,\ \sigma \rightleftarrows \sigma_0,\ k \to -k,\ \varkappa \to -\varkappa). \qquad (3.2)$$

The resultant twelve structures are rather unwieldy (they are given explicitly in reference 13).

In going over to the real Compton effect four of these structures vanish and only eight remain. This is in agreement with the results of Ritus.[14]

We expand T^c in the frame $\mathbf{p} + \mathbf{p}_0 = 0$ in terms of twelve independent three-dimensional structures r_k, which we choose as follows

$$\begin{array}{lll} r_1 = \mathbf{e}\cdot\boldsymbol{\varepsilon}, & r_5 = i\ \boldsymbol{\varepsilon}\cdot\boldsymbol{\lambda}\ \boldsymbol{\sigma}\cdot\mathbf{p}\times\mathbf{e}, & r_9 = i\ \mathbf{e}\cdot\boldsymbol{\varepsilon}\ \boldsymbol{\sigma}\cdot\mathbf{p}\times\boldsymbol{\lambda}, \\ r_2 = \mathbf{e}\cdot\mathbf{p}\ \boldsymbol{\varepsilon}\cdot\boldsymbol{\lambda}, & r_6 = i\ \boldsymbol{\varepsilon}\cdot\mathbf{p}\ \mathbf{e}\cdot\mathbf{p}\ \boldsymbol{\sigma}\cdot\mathbf{p}\times\boldsymbol{\lambda}, & r_{10} = i\ \boldsymbol{\varepsilon}\cdot\mathbf{p}\ \boldsymbol{\sigma}\cdot\boldsymbol{\lambda}\times\mathbf{e}, \\ r_3 = \mathbf{e}\cdot\mathbf{p}\ \boldsymbol{\varepsilon}\cdot\mathbf{p}, & r_7 = \frac{i}{\lambda^2}\ \mathbf{e}\cdot\mathbf{p}\ \boldsymbol{\varepsilon}\cdot\boldsymbol{\lambda}\ \boldsymbol{\sigma}\cdot\mathbf{p}\times\boldsymbol{\lambda}, & r_{11} = \frac{i}{\lambda^2}\ \boldsymbol{\varepsilon}\cdot\boldsymbol{\lambda}\ \boldsymbol{\sigma}\cdot\boldsymbol{\lambda}\times\mathbf{e}, \\ r_4 = i\ \boldsymbol{\varepsilon}\cdot\mathbf{p}\ \boldsymbol{\sigma}\cdot\mathbf{p}\times\mathbf{e}, & r_8 = i\ \mathbf{e}\cdot\mathbf{p}\ \boldsymbol{\sigma}\cdot\mathbf{p}\times\boldsymbol{\varepsilon}, & r_{12} = i\ \mathbf{e}\cdot\mathbf{p}\ \boldsymbol{\sigma}\cdot\boldsymbol{\lambda}\times\boldsymbol{\varepsilon}. \end{array} \qquad (3.3)$$

The amplitude T^C may now be written as

$$T^c = \sum_{k=1}^{12} L_k(k_0, \mathbf{p}^2)\, r_k, \qquad (3.4)$$

where $L_k(k_0, \mathbf{p}^2)$ are scalar functions of the variable k_0 and the recoil $\mathbf{p}^2$. The $\boldsymbol{\lambda}$-symmetrization operation S is now performed trivially due to the explicit dependence of the structures r_k on $\boldsymbol{\lambda}$.

4. DISPERSION RELATIONS FOR THE LORENTZ INVARIANT COEFFICIENTS

As a consequence of independence of the structures r_k it is obvious that d.r. (2.2) may be written for each coefficient L_k separately (and each of these coefficients shall behave in the complex k_0-plane no worse than the amplitude T^C, and decrease asymptotically no slower than $1/k_0$). Furthermore the symmetrization operation S will cause the structures antisymmetric in $\boldsymbol{\lambda}$ to decrease no slower than k_0^{-2}.

In order to go over from d.r. for L_k to relations for the coefficients Ω_i it is first necessary to relate Ω_i and L_k and then to investigate the behavior of $\Omega_i(k_0)$ in the complex plane.

Expanding T^i in terms of the r_k and utilizing

$$T^c = \sum_{i=1}^{12}\Omega_i T^i = \sum_{k=1}^{12} L_k r_k,$$

we find

$$\sum_{i=1}^{12}\Omega_i a_{ik} = L_k \qquad (k = 1, 2, \ldots, 12). \qquad (4.1)$$

The system (4.1) separates and can be solved for Ω_i.

An analysis of the coefficients $\Omega_i(k_0)$ shows that all Ω_i are analytic functions of k_0 in the same domain in which the function T^c is analytic. For the coefficient Ω_6 we write once-subtracted d.r. since its asymptotic behavior may be like that of a constant.

Introducing the invariant variables

$$r = k(p + p_0), \qquad t = (\varkappa - k)^2 \tag{4.2}$$

and utilizing the relations

$$\operatorname{Im} \Omega_j(k_0) = -\operatorname{Im} \Omega_j^*(-k_0) \quad (j = 1, 5, 6),$$

$$\operatorname{Im} \Omega_j(k_0) = \operatorname{Im} \Omega_j^*(-k_0) \qquad (j = 2, 3, 4, 7, \ldots, 12), \tag{4.3}$$

which follow from (3.2), we obtain d.r. for the functions $\Omega_i(r, t)$ in the frame $\mathbf{p} + \mathbf{p}_0 = 0$ in the following form

$$\operatorname{Re} \Omega_i(r, t) = \frac{P}{\pi} \int_{r_0}^{\infty} \left(\frac{1}{r' - r} + \frac{1}{r' + r}\right) \operatorname{Im} \Omega_i(r', t)\, dr' + \Omega_i^0 \qquad (i = 1,5),$$

$$\operatorname{Re} \Omega_i(r, t) = \frac{P}{\pi} \int_{r_0}^{\infty} \left(\frac{1}{r' - r} - \frac{1}{r' + r}\right) \operatorname{Im} \Omega_i(r', t)\, dr' + \Omega_i^0 \qquad (i = 2, 3, 4, 7\text{—}11),$$

$$\operatorname{Re} \Omega_6(r, t) = \frac{2r^2}{\pi} P \int_{r_0}^{\infty} \frac{\operatorname{Im} \Omega_6(r', t)\, dr'}{r'(r'^2 - r^2)} + \operatorname{Re} \Omega_6(0),$$

$$\operatorname{Re} \Omega_6(0) = -\frac{t + m_\gamma^2}{2m_\gamma^2} \operatorname{Re} \Omega_5(0) + \frac{1}{m_\gamma^2} \operatorname{Re} \Omega_1(0),$$

$$\operatorname{Re} \Omega_{12}(r, t) = \frac{P}{\pi} \int_{r_0}^{\infty} \left(\frac{1}{r' - r} - \frac{1}{r' + r}\right) \operatorname{Im} \Omega_{12}(r', t)\, dr' \tag{4.4}$$

[the lower limit on the integrals is $r_0 = 2M\mu + \mu^2 + \frac{1}{2}(t + m_\gamma^2)$]. The one-nucleon terms in the d.r. for Ω_6 and Ω_{12} vanish. The remaining one-nucleon terms may be obtained from (2.7) and are given explicitly in reference 13.

5. DISPERSION RELATIONS FOR PHYSICAL AMPLITUDES IN THE BARYCENTRIC FRAME

In order to obtain d.r. for the physical amplitudes in the barycentric frame we expand T^c in terms of independent three-dimensional structures ρ_k in that frame:

$$T^c = \sum_{k=1}^{12} M_k \rho_k. \tag{5.1}$$

Here M_k are physical amplitudes which depend on the total center of mass energy W and on $\cos\theta$, where θ is the angle between the directions of the virtual and real photons. We have

$$\begin{aligned}
&\rho_1 = \mathbf{e}\cdot\boldsymbol{\varepsilon}, && \rho_5 = i\, \boldsymbol{\varepsilon}\cdot\mathbf{k}\, \boldsymbol{\sigma}\cdot\boldsymbol{\kappa}\times\mathbf{e}, && \rho_9 = i\, \mathbf{e}\cdot\boldsymbol{\varepsilon}\, \boldsymbol{\sigma}\cdot\mathbf{k}\times\boldsymbol{\kappa},\\
&\rho_2 = \mathbf{e}\cdot\boldsymbol{\kappa}\ \boldsymbol{\varepsilon}\cdot\mathbf{k}, && \rho_6 = i\, \boldsymbol{\varepsilon}\cdot\boldsymbol{\kappa}\ \mathbf{e}\cdot\boldsymbol{\kappa}\ \boldsymbol{\sigma}\cdot\mathbf{k}\times\boldsymbol{\kappa}, && \rho_{10} = i\, \boldsymbol{\varepsilon}\cdot\boldsymbol{\kappa}\ \boldsymbol{\sigma}\cdot\mathbf{k}\times\mathbf{e},\\
&\rho_3 = \mathbf{e}\cdot\boldsymbol{\kappa}\ \boldsymbol{\varepsilon}\cdot\boldsymbol{\kappa}, && \rho_7 = i\, \mathbf{e}\cdot\boldsymbol{\kappa}\ \boldsymbol{\varepsilon}\cdot\mathbf{k}\ \boldsymbol{\sigma}\cdot\mathbf{k}\times\boldsymbol{\kappa}, && \rho_{11} = i\, \boldsymbol{\varepsilon}\cdot\mathbf{k}\ \boldsymbol{\sigma}\cdot\mathbf{k}\times\mathbf{e},\\
&\rho_4 = i\, \boldsymbol{\varepsilon}\cdot\boldsymbol{\kappa}\ \boldsymbol{\sigma}\cdot\boldsymbol{\kappa}\times\mathbf{e}, && \rho_8 = i\, \mathbf{e}\cdot\boldsymbol{\kappa}\ \boldsymbol{\sigma}\cdot\boldsymbol{\kappa}\times\boldsymbol{\varepsilon}, && \rho_{12} = i\, \mathbf{e}\cdot\boldsymbol{\kappa}\ \boldsymbol{\sigma}\cdot\mathbf{k}\times\boldsymbol{\varepsilon}.
\end{aligned} \tag{5.2}$$

The relation between $\Omega_i(W, \cos\theta)$ and $M_k(W, \cos\theta)$ may be obtained by expanding the relativistically invariant structures T^i in terms of ρ_k:

$$T^i = \sum_{k=1}^{12} b_{ik} \rho_k \qquad (i = 1, 2, \ldots, 12). \tag{5.3}$$

By solving the system (5.3) we find the matrix $\| c_{ik} \| = \| b_{ik} \|^{-1}$. By an appropriate choice of the structures, namely the choice (5.2), it is possible to separate the system (5.3) and reduce it to two second order and two fourth order systems. The coefficients c_{ik} are rather complicated and will not be given here. The final form of the d.r. for the physical amplitudes M_j in the barycentric frame is as follows:

$$\begin{aligned}
\operatorname{Re} M_j(W, t, m_\gamma^2) = \frac{2}{\pi} P \int_{M+\mu}^{\infty} \sum_i \xi_i \Big(\frac{1}{W'^2 - W^2}
&+ \eta_i \frac{1}{W'^2 + W^2 - 2M^2 + m_\gamma^2 + t}\Big) \times W'dW' b_{ji}(W', t, m_\gamma^2)\\
&\times \sum_k c_{ik}(W', t, m_\gamma^2) \operatorname{Im} M_k(W', t, m_\gamma^2) + \sum_i b_{ji}(W, t, m_\gamma^2) \Omega_i^0\\
&+ b_{j,6}(W, t, m_\gamma^2) \sum_k M_k\left(\sqrt{M^2 - \frac{t + m_\gamma^2}{2}}, t, m_\gamma^2\right) \Big[\frac{1}{m_\gamma^2} c_{1k}\\
&\times \left(\sqrt{M^2 - \frac{t + m_\gamma^2}{2}}, t, m_\gamma^2\right)\\
&- \frac{t + m_\gamma^2}{2m_\gamma^2} c_{5k}\left(\sqrt{M^2 - \frac{t + m_\gamma^2}{2}},\ t,\ m_\gamma^2\right)\Big],
\end{aligned}$$

where

$$\xi_6 = r / r', \ \xi_i = 1 \ \text{ for } i \neq 6; \ \ r' = W'^2 - M^2 + \tfrac{1}{2}(t + m_\gamma^2);$$
$$\eta_i = 1 \ \text{ for } i = 1,5; \qquad \eta_i = -1 \ \text{ for } i = 2, 3, 4, 6 - 12. \tag{5.4}$$

In conclusion we express deep gratitude to A. A. Logunov for valuable discussions and constant interest in this work, and also to D. V. Shirkov and A. N. Tavkhelidze for useful advice.

---

[1] Bogolyubov, Medvedev, and Polivanov, Вопросы теории дисперсионных соотношений (Problems in the Theory of Dispersion Relations), Fizmatizdat, M., 1958.

[2] Blokhintsev, Barashenkov, and Barbashov, Usp. Fiz. Nauk **68**, 417 (1959), Soviet Phys.—Uspekhi **2**, 505 (1960).

[3] V. S. Vladimirov and A. A. Logunov, Preprint, Joint Inst. Nuc. Res. R-260 (1958).

[4] Logunov, Tavkhelidze, and Solovyev, Nucl. Phys. **4**, 427 (1957).

[5] L. D. Solovyev, Nucl. Phys. **5**, 256 (1958).

[6] I. S. Zlatev and P. S. Isaev, JETP **35**, 309 (1958), Soviet Phys. JETP **8**, 213 (1959). Report at the All-Union Conference on Quantum Field Theory and Elementary Particles Theory (October 2 — 6, 1958, Uzhgorod).

[7] Bjorken, Drell, and Frautschi, Phys. Rev. **112**, 1409 (1958).

[8] A. A. Logunov and P. S. Isaev, Nuovo cimento **10**, 917 (1958).

[9] G. F. Chew, Ann. Conf. on High Energy Physics, CERN, 1958.

[10] N. N. Bogolyubov and D. V. Shirkov, Dokl. Akad. Nauk SSSR **113**, 529 (1957), Soviet Phys.—Doklady

[11] R. Hofstadter, Usp. Fiz. Nauk **13**, 693 (1957). (Russ. transl.) [sic!].

[12] M. Kawaguchi and N. Mugibayashi, Progr. Theoret. Phys. **8**, 212 (1952).

[13] I. S. Zlatev and P. S. Isaev, Preprint Joint Inst. Nucl. Res. R-321, 1959.

[14] V. I. Ritus, JETP **35**, 1485 (1958), Soviet Phys. JETP **8**, 923 (1959).

Translated by A. M. Bincer
139

SOVIET PHYSICS JETP VOLUME 37(10), NUMBER 3 MARCH, 1960

RELATIVISTIC TRANSPORT EQUATIONS FOR A PLASMA. I.

Yu. L. KLIMONTOVICH

Moscow State University

Submitted to JETP editor March 27, 1959

J. Exptl. Theoret. Phys. (U.S.S.R.) **37**, 735-744 (September, 1959)

A connection is established between the definitions of the probability of a state and the distribution functions given in the papers of various authors, based on the example of a transport equation for a charged particle in an external electromagnetic field.

A random function which determines the number of particles in a volume element in phase space is introduced. The electromagnetic field strengths or the numbers of oscillators are also considered as random functions. The set of equations for these functions serves as the basis for deriving a chain of equations connecting the moments of the random functions or the corresponding distribution functions of different orders. Through an approximation to this chain of equations we obtain a set of relativistic self-consistent equations. We give relativistic expressions for the dispersion equations for the transverse and longitudinal plasma waves. A variational principle for a relativistic plasma is considered.

THE possibility of a consistent derivation of the relativistic transport equations for a plasma is of interest in connection with the increasing importance of the theory of the high-temperature plasma.

The most general method to obtain approximate transport equations in the non-relativistic approximation is Bogolyubov's method[1] which is based upon an approximate solution of a chain of equations for distribution functions.

One must also construct a chain of relativistic equations for distribution functions to derive the transport equations in the relativistic case. Different forms of approximating higher distribution functions in terms of lower ones in such a chain makes it possible to obtain the appropriate transport equations: the equation with a self-consistent field, the Fokker-Planck equation for a relativistic plasma, the transport equation taking radiation into account, and so on. The present paper is also devoted to this problem.

The number of papers in which the relativistic transport equations for a plasma have been considered is very small.[2-4]

In the papers by the author[2] an equation was obtained for the distribution function of a system of charged particles in an electromagnetic field. A relativistic dispersion relation for the transverse and longitudinal waves was found in the self-consistent approximation for the distribution function of eight variables. We found relativistic equations for the quantum distribution functions for scalar charged particles and for electrons. A relativistic quantum equation with a self-consistent field was considered for scalar charged particles. The normalization condition for the distribution function, given in reference 2, may be replaced by a simpler one in those cases when the rest mass of the system of particles under consideration remains constant.

Belyaev and Budker[3] considered, for particles with a Coulomb interaction, a relativistic transport equation which was a generalization of the well-known Landau transport equation. On the basis of that equation they considered the energy and momentum transfer problem from one gas to another.

In Clemmow's and Willson's papers[4] a relativistic transport equation was obtained for the basic distribution function of seven variables $\mathbf{F}(t, \mathbf{q}, \mathbf{p})$, without taking collisions into account. A relativistic dispersion equation for longitudinal plasma oscillations was found and studied.

Since equations for different distribution functions are used in the papers mentioned, we first establish a connection between the equations and distribution functions used in the various papers by using as a simple example the transport equation for the distribution function of the variables of one charged particle.

1. RELATIVISTIC DISTRIBUTION FUNCTIONS

When a charged particle moves in an electromagnetic field the square of the four-momentum

$$G = \sum_i \left(P_i - \frac{e}{c} A_i\right)^2 = -m_0^2 c^2.$$

is an integral of motion. Here P_i and A_i are the four-momentum and four-potential. Using this expression for G we obtain the relativistic equation of motion for a charged particle:[2]

$$\frac{dq_i}{ds} = \frac{1}{2m_0}\frac{\partial G}{\partial P_i} = \frac{1}{m_0}\left(P_i - \frac{e}{c}A_i\right) = u_i,$$

$$\frac{dP_i}{ds} = -\frac{1}{2m_0}\frac{\partial G}{\partial q_i} = -\frac{1}{2m_0}\frac{\partial}{\partial q_i}\left(P_i - \frac{e}{c}A_i\right)^2,$$

$$ds = dt\sqrt{1-\beta^2}. \tag{1}$$

We introduce a distribution function of eight variables $f(q_i, P_i)$, defined in such a way that the four vector

$$J_i = \int u_i f(q_i, P_i)\, d^4P$$

is the same as the particle-current four vector.[3] We can then, in the case of a constant rest mass, write down for the distribution function the equation of continuity in (q_i, P_i) space:[2]

$$\frac{\partial}{\partial q_i}\left(\frac{dq_i}{ds}f\right) + \frac{\partial}{\partial P_i}\left(\frac{dP_i}{ds}f\right) = 0. \tag{2}$$

If we integrate (2) over the spatial coordinates and over all momentum components we get

$$\frac{\partial}{\partial q_4}\int \frac{dq_4}{ds} f d^3q d^4p = \frac{\partial}{\partial t}\int \frac{(E - e\varphi)}{m_0c^2} f d^3q d^4P = 0,$$

and we can therefore consider the expression

$$f\frac{u_4}{ic}\, d^3q d^4P = f\frac{(E - e\varphi)}{m_0c^2}\, d^3q d^4P \tag{3}$$

as the probability that the particle finds itself at time t in the spatial volume element d^3q around the point q and has values of its four-momentum in the region d^4P around the point P_i; it is normalized to unity.

We can write (3) in a more symmetric form if we introduce the four-vector of the hypersurface element dS_i. We can then write instead of (3) the more general expression $f\,|(u_i/c)\,dS_i|\,d^4P$ which determines the probability that the world line of the particle intersects the hypersurface element dS_i and that the four-momentum has a value in the region d^4P around P_i. Such a definition was given in a paper by Stratonovich.* Choosing different orientations of the hypersurface element we can obtain instead of (3) other particular definitions.

The equations given above are the same as the ones given by Belyaev and Budker[3] with the only difference that in reference 3 the function $\mathcal{H} = -\sqrt{G}$ was used instead of the function G.

It is possible to define the probability for a state by expression (3) because Eqs. (2) are written for the case where the distribution function does not depend explicitly on a parameter characterizing the trajectory of the motion of the particle in four-dimension space (world line). One can choose the proper time as such a parameter. This problem will be considered in the following in more detail in connection with the quantum generalization of the results stated.

It is in many cases convenient to use instead of a distribution function for the variables q_i and P_i a distribution function for the variables q_i and $p_i = P_i - (e/c)A_i$. The equations of motion take in that case the usual form

$$dq_i/ds = u_i = p_i/m_0, \qquad dp_i/ds = (e/c)F_{ik}u_k.$$

We shall write down the corresponding equation of continuity in these variables. Its three-dimensional form is

$$\frac{\mathcal{E}}{m_0c^2}\frac{\partial f}{\partial t} + \mathbf{u}\frac{\partial f}{\partial \mathbf{q}} + e\frac{\partial}{\partial \mathbf{p}}\left\{\gamma\mathbf{E} + \frac{1}{c}[\mathbf{u}\times\mathbf{H}]\right\}f + e(\mathbf{uE})\frac{\partial f}{\partial \mathcal{E}} = 0. \tag{4}$$

Here

$$\mathcal{E} = E - e\varphi, \qquad \gamma = \sqrt{1 - u^2/c^2}, \qquad u = p/m_0.$$

In these variables we get instead of (3) the expression $f(\mathcal{E}/m_0c^2)\,d^3qd^4p$.

Because the mass of the particle is constant, the relation $\Sigma p_i^2 = -m_0^2c^2$ exists between the components of the four-momentum p_i. This makes it possible to simplify (2) and (4) by integrating, for example, over p_4 and reducing them to the equation for the distribution function of seven variables $F(t, \mathbf{q}, \mathbf{p})$. To do this we first clarify the meaning of this distribution function.

Any element of the pseudo-sphere $\Sigma p_i^2 = -m_0^2c^2$ is perpendicular to the vector p_i. If we denote the vector of the hypersurface element in q_i-space by dS_i and in p_i-space by $dS_i^{(p)}$, we have $dS_i^{(p)} \parallel p_i$. The probability that the world line passes through a hypersurface element dS_i while the values of p_i lie within the hypersurface region $dS_i^{(p)}$ will therefore be proportional to the scalar product $dS_i dS_i^{(p)}$. If the vector of the hypersurface element dS_i is in the direction of the time axis, we get for the probability for a state the expression $F(\mathbf{q}, \mathbf{p}, t)\,d^3qd^3p$, where $F(\mathbf{q}, \mathbf{p}, t)$ is an invariant function of seven variables. Such a definition of probability was used by Clemmow and Willson[4] and in earlier papers (see Synge's book[5]). We shall find a connection between the functions $f(q_i, p_i)$ and $F(\mathbf{q}, \mathbf{p}, t)$ and obtain an equation for $F(\mathbf{q}, \mathbf{p}, t)$, starting from Eq. (4).

---

*I express my thanks to R. L. Stratonovich for acquainting me with his unpublished work.

Taking it into account that only states lying on the surface $\Sigma p_i^2 = -m_0^2c^2$ are possible, we introduce a function $F(q_i, p_i)$ such that

$$f(q_i, p_i)(\mathscr{E}/m_0c^2)d^3qd^4p$$

$$= F(q_i, p_i)\delta(\mathscr{E} - c\sqrt{m_0^2c^2 + p^2})\, d^3qd^3pd\mathscr{E}.$$

From the expressions given it follows that

$$F(\mathbf{q}, \mathbf{p}, t) = \int F(q_i, p_i)\,\delta(\mathscr{E} - c\sqrt{m_0^2c^2 + p^2})\, d\mathscr{E}. \tag{5}$$

As a result we obtain the following equation

$$\frac{\partial F}{\partial t} + \mathbf{v}\frac{\partial F}{\partial \mathbf{q}} + e\left\{\mathbf{E} + \frac{1}{c}[\mathbf{v}\times\mathbf{H}]\right\}\frac{\partial F}{\partial \mathbf{p}} = 0. \tag{6}$$

This equation is the same as the one given in the papers by Clemmow and Willson.[4] If we go over from the variables $\mathbf{q}$, $\mathbf{p}$, t to the variables $\mathbf{q}$, $\mathbf{v}$, t, we get for the probability of finding the particle in a volume element of phase space the expression[5]*

$$F(t, \mathbf{q}, \mathbf{v})\, m_0^3\gamma^5 d^3qd^3v.$$

Using the distribution function $F(t, \mathbf{q}, \mathbf{p})$ we obtain expressions for the density and the current from the formulae

$$\rho = e\int F(\mathbf{q}, \mathbf{p}, t)\, d^3p, \qquad \mathbf{j} = e\int \mathbf{v}F(\mathbf{q}, \mathbf{p}, t)\, d^3p. \tag{7}$$

We must note that in the general case the equation for one distribution function is insufficient to describe relativistic processes. Indeed, when introducing the function $F(q_i, p_i)$, one must take into account the possibility of states with negative energy values, i.e., put

$$f(q_i, p_i) = F(q_i, p_i)\frac{m_0c^2}{\mathscr{E}}\left\{\delta(\mathscr{E} - c\sqrt{m_0^2c^2 + p^2})\right.$$

$$\left. + \delta(\mathscr{E} + c\sqrt{m_0^2c^2 + p^2})\right\}.$$

We get in that case instead of one Eq. (6) a set of equations for two functions F^+ and F^-:

$$\pm\frac{\partial F^\pm}{\partial t} + \mathbf{v}\frac{\partial F^\pm}{\partial \mathbf{q}} + e\left\{\mathbf{E} + \frac{1}{c}[\mathbf{v}\times\mathbf{H}]\right\}\frac{\partial F^\pm}{\partial \mathbf{p}} = 0. \tag{8}$$

The positive sign corresponds to a positive energy value and the minus sign to a negative one. The equations for F^+ and F^- differ only by the sign in front of the first term. We shall consider (8) in more detail in the following in connection with the derivation of transport equations that take pair production into account.

2. A CHAIN OF EQUATIONS FOR THE RELATIVISTIC DISTRIBUTION FUNCTIONS

There are two possible ways of obtaining chains of equations for the relativistic distribution functions. One is a direct generalization of Bogolyubov's well-known method to the relativistic case. To do this we must consider distribution functions both of the particle variables and of the coordinates and the momenta of the field oscillators. Some non-relativistic problems with such distribution functions were considered in references 6 – 8.

We shall obtain the chain of equations by a slightly different method, based upon the use of a set of equations for the random function $N_{\mathbf{qp}}(t)$ and the electrical and magnetic field strengths, which are also considered as random functions. The function $N_{\mathbf{qp}}(t)$ is defined in such a way that the expression

$$N_{\mathbf{qp}}d^3qd^3p = \sum_{1\leqslant l\leqslant N} \delta(\mathbf{q} - \mathbf{q}^{(l)})\,\delta(\mathbf{p} - \mathbf{p}^{(l)}) \tag{9}$$

determines the number of particles at time t in a volume element of phase space d^3qd^3p around the point $\mathbf{q}, \mathbf{p}$. Equations for the random functions $N_{\mathbf{qp}}$ for systems of particles with a central force interaction were considered, for instance, in references 9 – 11. A set of equations for the function $N_{\mathbf{qp}}$ and the vector and scalar potential served in a paper by the author[12] as the starting point for considering the space-time correlation functions for a system of charged particles with an electromagnetic interaction. We shall use the results of that paper to a large extent in this section.

If we can forget about states with a negative energy, the equation for the function $N_{\mathbf{qp}}(t)$ is formally the same as (6):

$$\frac{\partial N_{\mathbf{qp}}}{\partial t} + \mathbf{v}\frac{\partial N_{\mathbf{qp}}}{\partial \mathbf{q}} + e\left\{\mathbf{E} + \frac{1}{c}[\mathbf{v}\times\mathbf{H}]\right\}\frac{\partial N_{\mathbf{qp}}}{\partial \mathbf{p}} = 0. \tag{9$'$}$$

In order that the set of equations be complete, we must still add the equations for the electromagnetic field

$$\operatorname{curl}\mathbf{H} = \frac{1}{c}\frac{\partial \mathbf{E}}{\partial t} + 4\pi e\int \mathbf{v}N_{\mathbf{qp}}d^3p, \qquad \operatorname{div}\mathbf{H} = 0,$$

$$\operatorname{curl}\mathbf{E} = -\frac{1}{c}\frac{\partial \mathbf{H}}{\partial t}, \qquad \operatorname{div}\mathbf{E} = 4\pi e\left\{\int N_{\mathbf{qp}}d^3p - n_0\right\}. \tag{10}$$

The set (9) and (10) is also a closed set of relativistic equations for the random functions $N_{\mathbf{qp}}$, $\mathbf{E}$, and $\mathbf{H}$, which describe different states of the plasma electrons and the electric and magnetic field strengths. In the following we assume that the role of the positively charged ions is reduced to the role of a background which compensates the charge of the electrons. One can consider the more general case in a similar manner.

---

*A relativistic transport equation with a self-consistent field for the function $F(\mathbf{q}, \mathbf{v}, t)$ was also considered in A. A. Vlasov's book Теория многих частиц (Many-Particle Theory), Gostekhizdat, 1950.

If we take states with a negative energy into account we must introduce two random functions $N^{\pm}_{\mathbf{qp}}(t)$, the equations for which are formally the same as (8). In a corresponding fashion the expressions for the density and the current on the right-hand sides of (10) are also changed.

As an initial set of equations we can use the equation for the random function of eight variables q_i, p_i, defining it in such a way that the expression

$$N_{q_i,\,p_i}\gamma d^3q d^4p = \sum_{1\leqslant l\leqslant N}\frac{1}{\gamma^{(l)}}\,\delta(\mathbf{q}-\mathbf{q}^{(l)})\,\delta(p_i-p_i^{(l)})\,\gamma d^3q d^4p \tag{11}$$

determines the number of particles whose world lines intersect an element of hypersurface oriented along the time axis while their momenta lie in the region d^4p around the point p_i.

We can write expression (11) in the explicit relativistically-invariant form proposed by Stratonovich:

$$N_{q_ip_i} = \sum_{1\leqslant l\leqslant N}\delta(q_i-q_i^{(l)}(s^{(l)}))\,\delta(p_i-p_i^{(l)}(s^{(l)}))\,ds^{(l)}.$$

Taking into account that $ds = dt/\gamma$ and performing an integration in this expression, we get Eq. (11).

The equation of motion for the functions $N_{q_iP_i}$ has the following form in the variables q_i, P_i

$$(\partial G/\partial P_i)\,\partial N_{q_iP_i}/\partial q_i - (\partial G/\partial q_i)\,\partial N_{q_iP_i}/\partial P_i = 0,$$

and in the variables q_i, p_i

$$u_i\frac{\partial}{\partial q_i}N_{q_ip_i} + \frac{e}{c}F_{ik}u_k\frac{\partial}{\partial p_i}N_{q_ip_i} = 0. \tag{12}$$

Together with the equations

$$\partial F_{ik}/\partial q_k = 4\pi e\int u_i N_{q_ip_i}d^4p,$$

$$\partial F_{ik}/\partial q_l + \partial F_{kl}/\partial q_i + \partial F_{li}/\partial q_k = 0 \tag{13}$$

(12) forms a closed set of equations for the random function $N_{q_ip_i}$ and the tensor F_{ik} whose components are also considered to be random functions.

Using the set (9) and (10) [or (12) and (13)] we can obtain a chain of equations for the moments of the random functions or for the corresponding distribution functions. This problem has been considered before[12] for a non-relativistic plasma. There we obtained expressions for the space-time correlation functions of the charge and current density, and for the values of the vector and scalar potentials. Using (9) and (10) we can obtain similar results for a relativistic plasma.

We shall consider a more general approach, which enables us to take directly into account the thermal motion of the electromagnetic field. We determine the state of the system by giving the coordinates and momenta of the particles $\mathbf{q}_1,\ldots,\mathbf{q}_N$, $\mathbf{p}_1,\ldots,\mathbf{p}_N$ and the coordinates and momenta of the oscillators of the transverse electromagnetic field $Q^{(j)}_{\mathbf{k}}$ and $P^{(j)}_{\mathbf{k}}$ $(j = 1, 2)$.

The equations of motion for these quantities can be written in the following form in the Coulomb gauge[13]

$$\dot{\mathbf{q}}^{(l)} = \mathbf{v}^{(l)},\quad \dot{\mathbf{p}}^{(l)} = -\frac{\partial}{\partial \mathbf{q}^{(l)}}\sum_{1\leqslant l\leqslant N}\Phi(|\mathbf{q}^{(l)}-\mathbf{q}^{(l')}|) - \frac{e}{c}\frac{\partial \mathbf{A}}{\partial t} + \frac{e}{c}[\mathbf{v}\times \operatorname{curl}\mathbf{A}]; \tag{14}$$

$$\dot{Q}^{(j)}_{\mathbf{k}} = P^{(j)}_{\mathbf{k}},$$

$$\dot{P}^{(j)}_{\mathbf{k}} = -\omega_{\mathbf{k}}^2 Q^{(j)}_{\mathbf{k}} + e\sqrt{4\pi/V}\sum_{1\leqslant l\leqslant N}(\mathbf{v}\mathbf{a}_{\mathbf{k}})^{\sin}_{\cos}\mathbf{k}\mathbf{q}^{(l)}. \tag{15}$$

In those equations $\mathbf{a}_{\mathbf{k}}$ is a unit vector in the direction of the component of a vector-potential with wave vector $\mathbf{k}$. Then

$$\mathbf{A} = \sqrt{4\pi c^2/V}\sum_{\mathbf{k}}\mathbf{a}_{\mathbf{k}}(Q^{(1)}_k\sin\mathbf{kq} + Q^{(2)}_{\mathbf{k}}\cos\mathbf{kq}),\quad \Phi(q) = e^2/q.$$

The connection between the velocity and the momentum of a particle is of the form $\mathbf{v} = \gamma\mathbf{p}/m_0$.

Together with the random functions $N_{\mathbf{qp}}(t)$ we introduce another random function defined in such a way that the expression

$$N_{Q^{(j)}_{\mathbf{k}}P^{(j)}_{\mathbf{k}}}dQ^{(j)}_{\mathbf{k}}dP^{(j)}_{\mathbf{k}}\ \text{(or more briefly, } N_{Q_{\mathbf{k}}P_{\mathbf{k}}}dQ^{(j)}_{\mathbf{k}}dP^{(j)}_{\mathbf{k}})$$

is the number of oscillators of the transverse electromagnetic field with wave vector $\mathbf{k}$ whose coordinates and momenta lie at the time t in the region $dQ^{(j)}_{\mathbf{k}}dP^{(j)}_{\mathbf{k}}$ around the point $Q^{(j)}_{\mathbf{k}}P^{(j)}_{\mathbf{k}}$.

We can write down the equations for the random functions introduced in this way, using the equations of motion (14) and (15)

$$\frac{\partial N_{\mathbf{qp}}}{\partial t} + \mathbf{v}\frac{\partial N_{\mathbf{qp}}}{\partial \mathbf{q}} - \frac{\partial}{\partial \mathbf{q}}\int\Phi(|\mathbf{q}-\mathbf{q}'|)N_{\mathbf{q'p'}}d\mathbf{q}'d\mathbf{p}'\frac{\partial N_{\mathbf{qp}}}{\partial \mathbf{p}} + \frac{e}{c}\int\left(-\frac{\partial \mathbf{A}}{\partial t} + [\mathbf{v}\times\operatorname{curl}\mathbf{A}]\right)N_{Q_{\mathbf{k}}P_{\mathbf{k}}}dQ^{(j)}_{\mathbf{k}}dP^{(j)}_{\mathbf{k}}\frac{\partial N_{\mathbf{qp}}}{\partial \mathbf{p}} = 0; \tag{16}$$

$$\frac{\partial}{\partial t}N_{Q_{\mathbf{k}}P_{\mathbf{k}}} + \sum_j\left(P^{(j)}_{\mathbf{k}}\frac{\partial}{\partial Q^{(j)}_{\mathbf{k}}}N_{Q_{\mathbf{k}}P_{\mathbf{k}}} - \omega^2_{\mathbf{k}}Q^{(j)}_{\mathbf{k}}\frac{\partial}{\partial P^{(j)}_{\mathbf{k}}}N_{Q_{\mathbf{k}}P_{\mathbf{k}}}\right) + e\sqrt{\frac{4\pi}{V}}\int(\mathbf{v}'\mathbf{a}_{\mathbf{k}})^{\sin}_{\cos}\mathbf{kq}'N_{\mathbf{q'p'}}d\mathbf{q}'d\mathbf{p}'\frac{\partial}{\partial P^{(j)}_{\mathbf{k}}}N_{Q_{\mathbf{k}}P_{\mathbf{k}}} = 0. \tag{17}$$

We must take into account in the first equation that

$$A = \sqrt{4\pi c^2/V}\sum_{k,j}Q^{(j)\,\sin}_{\mathbf{k}\ \,\cos}\,\mathbf{kq}.$$

One can use the set of relativistic equations (16) and (17) to obtain a chain of equations both for single-time and for many-time distribution functions.

We shall take into consideration the connection between the distribution functions and the moments of the random functions

$$\overline{N_{\mathbf{qp}}(t)\,N_{\mathbf{q}'\mathbf{p}'}(t)} = V^{-2}N(N-1)\,f_2(\mathbf{q},\mathbf{p},\mathbf{q}',\mathbf{p}',t)$$

$$+(N/V)\,\delta(\mathbf{q}-\mathbf{q}')\,\delta(\mathbf{p}-\mathbf{p}')\,f_1(\mathbf{q},\mathbf{p},t),$$

$$\overline{N_{\mathbf{qp}}(t)\,N_{\mathbf{q}'\mathbf{p}'}(t)\,N_{\mathbf{q}''\mathbf{p}''}(t)}$$

$$= V^{-3}N(N-1)(N-2)\,f_3(\mathbf{q},\mathbf{p},\mathbf{q}',\mathbf{p}',\mathbf{q}'',\mathbf{p}'',t)$$

$$+V^{-2}N(N-1)\{\delta(\mathbf{q}-\mathbf{q}')\,\delta(\mathbf{p}-\mathbf{p}')\,f_2(\mathbf{q},\mathbf{p},\mathbf{q}'',\mathbf{p}'',t)$$

$$+\delta(\mathbf{q}-\mathbf{q}'')\,\delta(\mathbf{p}-\mathbf{p}'')\,f_2(\mathbf{q},\mathbf{p},\mathbf{q}',\mathbf{p}',t)$$

$$+\delta(\mathbf{q}'-\mathbf{q}'')\,\delta(\mathbf{p}'-\mathbf{p}'')\,f_2(\mathbf{q},\mathbf{p},\mathbf{q}',\mathbf{p}',t)\}$$

$$+(N/V)\,\delta(\mathbf{q}-\mathbf{q}')\,\delta(\mathbf{p}-\mathbf{p}')$$

$$\times\delta(\mathbf{q}-\mathbf{q}'')\,\delta(\mathbf{p}-\mathbf{p}'')\,f_1(\mathbf{q},\mathbf{p},t),$$

$$\overline{N_{\mathbf{qp}}(t)\,N_{\mathbf{q}'\mathbf{p}'}(t)\,N_{Q_{\mathbf{k}}P_{\mathbf{k}}}(t)}$$

$$= V^{-2}N(N-1)\,\Phi_3(\mathbf{q},\mathbf{p},\mathbf{q}',\mathbf{p}',Q_{\mathbf{k}},P_{\mathbf{k}},t)$$

$$+(N/V)\,\delta(\mathbf{q}-\mathbf{q}')\,\delta(\mathbf{p}-\mathbf{p}')\,\Phi_2(\mathbf{q},\mathbf{p},Q_{\mathbf{k}},P_{\mathbf{k}},t).$$

In these equations f_1, f_2, and f_3 are the first, second, and third distribution functions of the electrons, normalized in such a way that $V^{-s}\int f_s d\mathbf{q}d\mathbf{p} = 1$, and Φ_2 and Φ_3 are the second and third compound distribution functions for the electrons and the oscillators of the electromagnetic field. Using the expressions that follow from (16) and (17) we get, after averaging, the following equations for the first distribution functions for the electrons and for the oscillators $f_1(\mathbf{q},\mathbf{p},t)$, $F_1(Q_{\mathbf{k}}^{(j)}, P_{\mathbf{k}}^{(j)}, t)$

$$\frac{\partial f_1}{\partial t}+\mathbf{v}\frac{\partial f_1}{\partial \mathbf{q}}-n\frac{\partial}{\partial \mathbf{q}}\int\Phi(|\mathbf{q}-\mathbf{q}'|)\frac{\partial}{\partial \mathbf{p}}f_2 dq'dp'$$

$$+\frac{e}{c}\int\left(-\frac{\partial \mathbf{A}}{\partial t}+[\mathbf{v}\times\operatorname{curl}\mathbf{A}]\right)$$

$$\times\frac{\partial}{\partial \mathbf{p}}\Phi_2(\mathbf{q},\mathbf{p},Q_{\mathbf{k}}^{(j)},P_{\mathbf{k}}^{(j)},t)\,dQ_{\mathbf{k}}^{(j)}dP_{\mathbf{k}}^{(j)}=0, \tag{18}$$

$$\frac{\partial F_1}{\partial t}+\sum_j\left(P_{\mathbf{k}}^{(j)}\frac{\partial}{\partial Q_{\mathbf{k}}^{(j)}}-\omega_{\mathbf{k}}^2 Q_{\mathbf{k}}^{(j)}\frac{\partial}{\partial P_{\mathbf{k}}^{(j)}}\right)$$

$$\times F_1+en\sqrt{\frac{4\pi}{V}}\int(\mathbf{v}'\mathbf{a}_{\mathbf{k}})\genfrac{}{}{0pt}{}{\sin}{\cos}\mathbf{k}\mathbf{q}'\frac{\partial}{\partial P_{\mathbf{k}}^{(j)}}\Phi_2 dq'dp'=0. \tag{19}$$

The single-time second distribution functions f_2 and Φ_2 for which we can obtain equations by similar means, enter into these equations, only the single-time third distribution functions enter in the equations for the second distribution functions, and so on.

The initial set (16) and (17) can be written in relativistically invariant form if we use instead of the equation for $N_{\mathbf{qp}}(t)$ the equation for the function $N_{q_i p_i}$ and the corresponding relativistically invariant equation for the function that determines the number of field oscillators.

The chain of equations deduced here can be obtained from the equation for the distribution function for the coordinates and momenta of all particles and field oscillators at one and the same time

$$f(\mathbf{q}_1,\ldots,\mathbf{q}_N,\mathbf{p}_1,\ldots,\mathbf{p}_N,\ldots,Q_{\mathbf{k}}^{(j)},\ldots,P_{\mathbf{k}}^{(j)},\ldots,t).$$

The equation for this distribution function is of the following form

$$\frac{\partial f}{\partial t}+\sum_{1\leqslant l\leqslant N}\mathbf{v}^{(l)}\frac{\partial f}{\partial \mathbf{q}^{(l)}}+\sum_{1\leqslant l\leqslant N}\left\{-\frac{\partial f}{\partial \mathbf{q}^{(l)}}\sum_{l'}\Phi(|\mathbf{q}^{(l)}-\mathbf{q}^{(l')}|)\right.$$

$$\left.+\frac{e}{c}\left(-\frac{\partial \mathbf{A}}{\partial t}+[\mathbf{v}^{(l)}\times\operatorname{curl}\mathbf{A}]\right)\right\}\frac{\partial f}{\partial \mathbf{p}^{(l)}}$$

$$+\sum_{k,j}\left(P_{\mathbf{k}}^{(j)}\frac{\partial f}{\partial Q_{\mathbf{k}}^{(j)}}-\omega_{\mathbf{k}}^2 Q_{\mathbf{k}}^{(j)}\frac{\partial f}{\partial P_{\mathbf{k}}^{(j)}}\right)$$

$$+e\sqrt{\frac{4\pi}{V}}\sum_{k,j,l}(\mathbf{v}^{(l)}\mathbf{a}_{\mathbf{k}})\genfrac{}{}{0pt}{}{\sin}{\cos}\mathbf{k}\mathbf{q}^{(l)}\frac{\partial f}{\partial P_{\mathbf{k}}^{(j)}}=0. \tag{20}$$

3. A VARIATIONAL PRINCIPLE FOR A RELATIVISTIC PLASMA

It is well known that the action function for a system of charged particles and the electromagnetic field can be written, for instance, in the form[14]

$$S=\sum_{1\leqslant l\leqslant N}\left\{-m_0c\int\sqrt{-u_i^{(l)2}}\,ds^{(l)}+\frac{e}{c}\int A_i u_i^{(l)}ds^{(l)}\right\}$$

$$+\frac{i}{16\pi c}\int F_{ik}^2 d^4q.$$

Using the function $N_{q_i p_i}$ and taking into account that $ds = dt/\gamma$ and $dq_4 = icdt$ we can write this expression in the form

$$S=\frac{1}{ic}\int\left\{-m_0c\sqrt{-u_i^2}+\frac{e}{c}A_i u_i\right\}N_{q_i p_i}d^4q\,d^4p$$

$$+\frac{i}{16\pi c}\int F_{ik}^2 d^4q. \tag{21}$$

Using the latter expression we determine the equations of motion in the following way

$$P_i=\frac{\partial}{\partial u_i}\frac{\delta S}{\delta N_{q_i p_i}}=p_i+\frac{e}{c}A_i,$$

$$\dot{P}_i=\frac{\partial}{\partial q_i}\frac{\delta S}{\delta N_{q_i p_i}}=\frac{e}{c}\frac{\partial}{\partial q_i}(A_i u_i).$$

Taking into account that

$$dA_i/ds=u_k\partial A_i/\partial q_k,$$

$$\partial(A_k u_k)/\partial q_i=u_k\partial A_i/\partial q_k+F_{ik}u_k,$$

we get the equations of motion in the usual form

$$m_0 du_i / ds = (e/c) F_{ik} u_k.$$

The equations for the field are obtained as usual by varying the vector potential and are the same as (13), while the equation for the function $N_{q_i p_i}$ itself, which follows from the equations of motion is the same as (12).

We shall average expression (21) for the action function over the whole system; such an average will be denoted by a superior bar. This average value of the action function is determined not only by the average values $\overline{N}_{q_i p_i}$, $\overline{A}_i$, $\overline{F}_{ik}$, but also by the values of the correlation functions of the field and particle variables and of the field fluctuations. We shall introduce the deviations from the average values $\delta N_{q_i p_i}$ and δF_{ik}. We have then

$$\overline{A_i N_{q_i p_i}} = \overline{A}_i \overline{N}_{q_i p_i} + \overline{\delta A_i \delta N_{q_i p_i}}, \qquad \overline{F^2_{ik}} = \overline{F}^2_{ik} + \overline{\delta F^2_{ik}}.$$

If we neglect the correlation functions $\overline{\delta A_i \delta N_{q_i p_i}}$ and the field fluctuations, the expression for $\overline{S}$ takes the form

$$\overline{S} = \frac{1}{ic} \int \left(- m_0 c \sqrt{- u^2_i} + \frac{e}{c} \overline{A}_i u_i \right) \overline{N}_{q_i p_i} d^4 q d^4 p$$
$$+ \frac{i}{16\pi c} \int \overline{F}^2_{ik} \, d^4 q.$$

This relation can be used to derive the relativistic equations for the particle distribution function $\overline{N}_{q_i p_i}$ and the components of the tensor $\overline{F}_{ik}$ with a self-consistent field (without taking correlation into account).

If we introduce instead of the function $N_{q_i p_i}$ the random function $N_{\mathbf{qp}}(t)$, the average value of which is the normal distribution function of seven variables $\mathbf{q}$, $\mathbf{p}$, and t, we are led to the following expression for S after integrating over the energy

$$S = \int \left\{ - m_0 c^2 + \frac{e}{c} A_i u_i \right\} N_{qp} d^3 q d^3 p ds + \frac{i}{16\pi c} \int F^2_{ik} d^4 q.$$

In the non-relativistic approximation this expression takes the form

$$S = \int \left\{ \frac{mv^2}{2} + \frac{e}{c} \mathbf{A}\mathbf{v} - e\varphi \right\} N_{\mathbf{qp}} d^3 q d^3 p dt$$
$$+ \frac{1}{8\pi} \int (\mathbf{E}^2 - \mathbf{H}^2) \, d^3 q dt, \qquad \mathbf{v} = \frac{\mathbf{p}}{m}.$$

If we average the last expression, neglecting correlation and field fluctuations, we get an approximate expression for the average value of the action function

$$\overline{S} = \int \left\{ \frac{mv^2}{2} + \frac{e}{c} \overline{\mathbf{A}}\mathbf{v} - e\overline{\varphi} \right\} \overline{N}_{qp} d^3 q d^3 p dt$$
$$+ \frac{1}{8\pi} \int (\mathbf{E}^2 - \mathbf{H}^2) \, d^3 q dt.$$

This equation is the same as the expression for the action function used in Low's work.[15]

4. RELATIVISTIC EQUATIONS WITH A SELF-CONSISTENT FIELD

In the present section we consider the relativistic transport equation in the self-consistent field approximation.

We first consider the set (9) and (10). We introduce functions that characterize the deviations of the random functions from their average values $\delta N_{\mathbf{qp}}$, $\delta \mathbf{E}$, and $\delta \mathbf{H}$, and express the second moments of the random functions in terms of the central moments; for instance,

$$\overline{EN_{\mathbf{qp}}} = \overline{E}\, \overline{N}_{\mathbf{qp}} + \overline{\delta E \delta N_{\mathbf{qp}}}.$$

If we break off the chain of equations right at the beginning by neglecting the second central moments we obtain a set of relativistic self-consistent equations

$$\frac{\partial \overline{N}_{\mathbf{qp}}}{\partial t} + \mathbf{v} \frac{\partial \overline{N}_{\mathbf{qp}}}{\partial \mathbf{q}} + e \left(\overline{\mathbf{E}} + \frac{1}{c} [\mathbf{v} \times \overline{\mathbf{H}}] \right) \frac{\partial \overline{N}_{\mathbf{qp}}}{\partial \mathbf{p}} = 0, \qquad p = m_0 v \gamma;$$

$$\mathbf{curl}\ \overline{\mathbf{H}} = \frac{1}{c} \frac{\partial \overline{\mathbf{E}}}{dt} + 4\pi e \int \mathbf{v} \overline{N}_{\mathbf{qp}} d^3 p, \qquad \operatorname{div} \overline{\mathbf{H}} = 0;$$

$$\mathbf{curl}\ \overline{\mathbf{E}} = - \frac{1}{c} \frac{\partial \overline{\mathbf{H}}}{\partial t}, \qquad \operatorname{div} \overline{\mathbf{E}} = 4\pi e \left\{ \int \overline{N}_{\mathbf{qp}} d^3 p - n_0 \right\}. \tag{22}$$

This set of equations differs only by the relativistic dependence of the momentum on the velocity from the classical set of self-consistent field equations for a plasma, first considered by Vlasov.[16]

We give here expressions for the dispersion relations for transverse and longitudinal plasma waves obtained under the assumption that the distribution function $\overline{N}_{\mathbf{qp}}(t) = n f_1(\mathbf{q}, \mathbf{p}, t)$ differs little from the stationary uniform distribution for which we must take in this case the relativistic Maxwell distribution

$$\overline{N}_{\mathbf{p}} = A \exp\{ - c \sqrt{m^2_0 c^2 + p^2} / \varkappa T \}.$$

The relativistic dispersion relations have the following form

$$1 = \frac{4\pi e^2 \omega}{\varkappa T (\omega^2 - c^2 k^2)} \int \frac{(\gamma u_y)^2 \overline{N}_{\mathbf{p}}}{\omega - \gamma u_x k} d^3 p$$

for transverse oscillations and

$$1 = \frac{4\pi e^2}{\varkappa T \omega} \int \frac{(\gamma u_x)^2 \overline{N}_{\mathbf{p}}}{\omega - \gamma u_x k} d^3 p$$

for longitudinal oscillations. The last expression is the same as the dispersion relation given by Clemmow and Willson.[4]

The set of self-consistent equations for the distribution function $\overline{N}_{q_i p_i}$ has the following form

$$u_i \partial \overline{N}_{q_i p_i} / \partial q_i + \frac{e}{c} F_{ik} u_k \frac{\partial}{\partial p_i} \overline{N}_{q_i p_i} = 0,$$

$$\partial \overline{F}_{ik} / \partial q_k = 4\pi e \int u_i \overline{N}_{q_i p_i} d^4 p,$$

$$\partial F_{ik} / \partial q_l + \partial F_{kl} / \partial q_i + \partial F_{li} / \partial q_k = 0.$$

The relativistically invariant dispersion relations had been obtained earlier.[2]

By averaging (16) and (17) or by using the first equations of the chain for the distribution functions [Eqs. (18) and (19)] we can obtain a more general set of self-consistent equations for the distribution functions of the electrons and the field oscillators, taking the thermal motion of the electromagnetic field into account. This set of equations has the following form:

$$\frac{\partial f_1}{\partial t} + \mathbf{v} \frac{\partial f_1}{\partial \mathbf{q}} - n \frac{\partial}{\partial \mathbf{q}} \int \Phi\left(|\mathbf{q} - \mathbf{q}'|\right) f_1 d\mathbf{q}' d\mathbf{p}' \frac{\partial f_1}{\partial \mathbf{p}}$$

$$+ \frac{e}{c} \int \left(- \frac{\partial \mathbf{A}}{\partial t} + [\mathbf{v} \times \operatorname{curl} \mathbf{A}] \right)$$

$$\times F_1 \left(Q_{\mathbf{k}}^{(j)} P_{\mathbf{k}}^{(j)} t\right) dQ_{\mathbf{k}}^{(j)} dP_{\mathbf{k}}^{(j)} \frac{\partial f_1}{\partial \mathbf{p}} = 0,$$

$$\frac{\partial F_1}{\partial t} + \sum_j \left(P_{\mathbf{k}}^{(j)} \frac{\partial F_1}{\partial Q_{\mathbf{k}}^{(j)}} - \omega_{\mathbf{k}}^2 Q_{\mathbf{k}}^{(j)} \frac{\partial F_1}{\partial P_{\mathbf{k}}^{(j)}} \right)$$

$$+ en \sqrt{\frac{4\pi}{V}} \int (\mathbf{v}' \mathbf{a}_{\mathbf{k}}) \begin{matrix} \sin \\ \cos \end{matrix} \mathbf{k}\mathbf{q}' f_1 d\mathbf{q}' d\mathbf{p}' \frac{\partial F_1}{\partial P_{\mathbf{k}}^{(j)}} = 0.$$

In forthcoming parts of the present paper we shall consider more accurate transport equations and equations for the correlation functions.

I use this opportunity to express my deep gratitude to Academician N. N. Bogolyubov for a discussion of the problems touched upon in the present paper.

---

[1] N. N. Bogolyubov, Проблемы динамической теории в статистической физике, (Problems of Dynamic Theory in Statistical Physics), Gostekhizdat, 1946.

[2] Yu. L. Klimontovich, Dokl. Akad. Nauk SSSR **87**, 927 (1952); Тр. Московского авиационного технологич. ин-та (Proc. Moscow Aviation Technological Inst.) No. 26 (1955).

[3] S. T. Belyaev and G. I. Budker, Dokl. Akad. Nauk SSSR **107**, 807 (1956), Soviet Phys.–Doklady **1**, 218 (1956).

[4] P. C. Clemmow and A. J. Willson, Proc. Roy. Soc. (London) **A237**, 117 (1956); Proc. Cambridge Phil. Soc. **53**, 222 (1957).

[5] J. L. Synge, The Relativistic Gas (North Holland Publ. Co., Amsterdam, 1957).

[6] W. E. Brittin, Phys. Rev. **106**, 843 (1957).

[7] R. N. Gurzhi, JETP **33**, 451 (1957), Soviet Phys. JETP **6**, 352 (1958).

[8] Yu. L. Klimontovich, JETP **35**, 1276 (1958), Soviet Phys. JETP **8**, 891 (1959); Yu. L. Klimontovich and S. V. Temko, JETP **35**, 1141 (1958), Soviet Phys. JETP **8**, 799 (1959).

[9] Yu. L. Klimontovich, Dokl. Akad. Nauk SSSR **96**, 43 (1954); JETP **33**, 982 (1957), Soviet Phys. JETP **6**, 753 (1958).

[10] R. L. Stratonovich, Thesis, Moscow State University (1956).

[11] B. B. Kadomtsev, JETP **32**, 943 (1957), Soviet Phys. JETP **5**, 771 (1957); JETP **33**, 151 (1957), Soviet Phys. **6**, 117 (1958).

[12] Yu. L. Klimontovich, JETP **34**, 173 (1958), Soviet Phys. JETP **7**, 119 (1958).

[13] W. Heitler, Quantum Theory of Radiation (Oxford University Press, 1954).

[14] L. D. Landau and E. M. Lifshitz, Теория поля (Field Theory), Gostekhizdat, 1948 [The Classical Theory of Fields, Addison-Wesley, 1951].

[15] F. E. Low, Proc. Roy. Soc. (London) **A248**, 282 (1958).

[16] A. A. Vlasov, Уч. зап. МГУ, (Sci. Notes, Moscow State Univ.) No. 76, part 1, 1944; JETP **8**, 291 (1938).

Translated by D. ter Haar
140

SOVIET PHYSICS JETP VOLUME 37 (10), NUMBER 3 MARCH, 1960

ROTATION OF THE PLANE OF POLARIZATION OF ELASTIC WAVES IN MAGNETICALLY POLARIZED MAGNETOELASTIC MEDIA

K. B. VLASOV and B. Kh. ISHMUKHAMETOV

Institute for the Physics of Metals, Academy of Sciences, U.S.S.R.

Submitted to JETP editor March 28, 1959

J. Exptl. Theoret. Phys. (U.S.S.R.) 37, 745-749 (September, 1959)

Some peculiarities of the propagation of magnetoelastic waves in magnetically polarized media are studied; the medium considered is one with uniaxial symmetry. It is shown that a magnetoelastic wave propagated along the axis of symmetry consists of three waves: a longitudinal wave and two circularly polarized waves, whose speeds of propagation are different and are determined by the magnetic state of the medium — the magnitude of the magnetization or of the polarization field. The last circumstance should lead to rotation of the plane of polarization of linearly polarized elastic waves. The treatment is based on phenomenological "equations of state" that describe the dynamic properties of magnetoelastic media. Some remarks are made regarding the physical meaning of the constants that determine the rotation of the plane of polarization in certain specific types of magnetoelastic media; and an estimate is made of the frequencies at which an appreciable effect is to be expected.

1. The elastic, magnetic, and magnetoelastic properties of a magnetoelastic medium in the dynamic range can be described by equations of the form[1]

$$\sigma^*_{ij} - \left(d'_{ijkl} \frac{\partial u_k}{\partial x_l} + h'_{ij,n} J_n \right) = d''_{ijkl} \frac{\partial \dot{u}_k}{\partial x_l} + h''_{ij,n} \dot{J}_n ,$$

$$H_m + a_{mnpq} \frac{\partial^2 J_p}{\partial x_n \partial x_q} - \left(h'_{m,kl} \frac{\partial u_k}{\partial x_l} + \gamma'_{mn} J_n \right)$$

$$= h''_{m,kl} \frac{\partial \dot{u}_k}{\partial x_l} + \gamma''_{mn} \dot{J}_n , \qquad (1)$$

where H_m, J_n, and u_k are the components of the vector magnetic field intensity, the vector magnetization, and the vector displacement at points of the elastic medium, and where the σ^*_{ij}'s are the components of a certain tensor related to the elastic stresses; d'_{ijkl}, $h'_{ij,n} = h'_{n,ij}$, γ'_{mn}, and a_{mnpq} are components of the tensors formed, respectively, by the elastic moduli, the magnetostrictive constants, the inverse magnetic susceptibilities, and the exchange-interaction constants.

By way of illustration we consider a homogeneous magnetoelastic medium with uniaxial symmetry. Let the medium furthermore be magnetically polarized: that is, let it be subject to a constant, homogeneous polarizing magnetic field H_0, or let it possess a constant, homogeneous polarization magnetization J_0. We shall also suppose that the polarization magnetization or the polarizing field is directed along the axis of symmetry, the x_3 axis. We assume in addition that $J \ll J_0$ and $H \ll H_0$.

In this case it can be shown[1] that the tensor constants that appear in (1) have the form

$$\begin{pmatrix} \gamma'_{11} & \gamma''_{12} & 0 \\ -\gamma''_{12} & \gamma'_{11} & 0 \\ 0 & 0 & \gamma'_{33} \end{pmatrix}, \qquad (2)$$

$$\begin{pmatrix}
d'_{1111} & d'_{1122} & d'_{1133} & 0 & 0 & 0 & 0 & d''_{1112} & d''_{1121} \\
d'_{1122} & d'_{1111} & d'_{1133} & 0 & 0 & 0 & 0 & -d''_{1121} & -d''_{1112} \\
d'_{1133} & d'_{1133} & d'_{3333} & 0 & 0 & 0 & 0 & d''_{3312} & -d''_{3312} \\
0 & 0 & 0 & d'_{2323} & d'_{2332} & d''_{2331} & d''_{2313} & 0 & 0 \\
0 & 0 & 0 & d'_{2332} & d'_{3232} & d''_{3231} & d''_{2331} & 0 & 0 \\
0 & 0 & 0 & -d''_{2331} & -d''_{3231} & d'_{3232} & d'_{2332} & 0 & 0 \\
0 & 0 & 0 & -d''_{2313} & -d''_{2331} & d'_{2332} & d'_{2323} & 0 & 0 \\
-d''_{1112} & d''_{1121} & -d''_{3312} & 0 & 0 & 0 & 0 & d'_{1212} & d'_{1221} \\
-d''_{1121} & d''_{1112} & d''_{3312} & 0 & 0 & 0 & 0 & d'_{1221} & d'_{1212}
\end{pmatrix}. \qquad (3)$$

$$d'_{1221} = d'_{1111} - d'_{1122} - d'_{1212};$$

$$\begin{pmatrix} 0 & 0 & 0 & h''_{1,23} & h''_{1,32} & h'_{1,31} & h'_{1,13} & 0 & 0 \\ 0 & 0 & 0 & h'_{1,13} & h'_{1,31} - h'_{1,32} - h''_{1,23} & & & 0 & 0 \\ h'_{3,11} & h'_{3,11} & h'_{3,33} & 0 & 0 & 0 & 0 & h''_{3,12} - h''_{3,12} & \end{pmatrix},$$

$$h'_{11,3} = h'_{22,3} = h'_{3,11}, \quad h'_{33,3} = h'_{3,33}, \quad h'_{31,1} = h'_{32,2} = h'_{1,31},$$
$$h'_{13,1} = h'_{23,2} = h'_{1,13}, \quad h''_{23,1} = -h'_{13,2} = -h'_{1,23},$$
$$h''_{32,1} = -h''_{31,2} = -h''_{1,32}, \quad h''_{12,3} = -h''_{21,3} = -h'_{3,12}. \quad (4)$$

We remark that such a simultaneous entry, in a single table, of the single-primed and double-primed components of the tensor constants became possible by virtue of the fact that in this work we did not take account of those tensor components (double-primed) that describe energy absorption. The nature of the dependence of the components of the tensor constants on the polarizing field or magnetization was discussed earlier.[1]

As is easily seen, the "stress" tensor σ^*_{ij} is unsymmetrical and differs from the stress tensor that appears in the equation of motion of elasticity theory,

$$\rho \ddot{u}_i = \partial \sigma_{ij} / \partial x_j, \quad (5)$$

the latter, by definition (as the momentum flow tensor, taken with reversed sign), must be symmetric. An expression for the tensor σ_{ij} can be obtained by symmetrizing the tensor σ^*_{ij}, i.e., by separating it into symmetric and antisymmetric terms

$$\sigma_{ij} = {}^1/_2 (\sigma^*_{ij} + \sigma^*_{ji}), \quad T_{ij} = {}^1/_2 (\sigma^*_{ij} - \sigma^*_{ji}). \quad (6)$$

The second term determines the force couple that acts on unit volume. This couple is always equilibrated by some other couple that acts on unit volume; its nature can vary. In anisotropic media it can be, for example, a couple produced by the noncoincidence of the orientations of the vector magnetic field intensity and of the magnetization (for a more detailed discussion of this question, see references 2 and 3).

It appears that the following additional conditions[4] must still be imposed on the constants d'_{ijkl}:

$$d'_{ijkl} + d'_{jilk} = d'_{ijlk} + d'_{jikl}. \quad (7)$$

2. We now consider the specific problem of the propagation of plane magnetoelastic waves along the direction of the symmetry axis. Hereafter we shall neglect displacement currents and conduction currents. Therefore in the joint solution of the equations of elasticity (5) and the equations of electrodynamics, we shall need only the following two of Maxwell's equations:

$$\operatorname{curl} \mathbf{H} = 0, \quad \operatorname{div} \mathbf{B} = 0.$$

Furthermore we shall suppose that all variable quantities vary as $\exp[i(\omega t - kx_3)]$; and we shall also assume that the exchange interaction, for a medium with uniaxial symmetry, is described by just two independent tensor components a_{mnpq} (a_1 and a_2). As a result we get the following two independent systems of homogeneous equations:

$$\omega^2 \rho u_3 = \rho (c_l^0)^2 k^2 u_3 + i h_{33} k J_3,$$
$$-4\pi J_3 = -i h_{33} k u_3 + (\gamma'_{33} + a_2 k^2) J_3; \quad (8)$$

$$\omega^2 \rho u_1 = \rho (c_t^0)^2 k^2 u_1 - i\omega B k^2 u_2 + i h_{15} k J_1 - \omega h''_{14} k J_2,$$
$$\omega^2 \rho u_2 = i\omega B k^2 u_1 + \rho (c_t^0)^2 k^2 u_2 + \omega h''_{14} k J_1 + i h_{15} k J_2,$$
$$0 = -i (h_{15} - h^*_{15}) k u_1 + \omega (h''_{14} + h^{*''}_{14}) k u_2$$
$$+ (\gamma'_{11} + a_1 k^2) J_1 + i\omega \gamma''_{12} J_2,$$
$$0 = -\omega (h''_{14} + h^{*''}_{14}) k u_1 - i (h_{15} - h^*_{15}) k u_2$$
$$- i\omega \gamma''_{12} J_1 + (\gamma'_{11} + a_1 k^2) J_2, \quad (9)$$

Here the following symbols have been introduced:

$$c_t^0 = [(d'_{2323} + d'_{2332}) / 2\rho]^{1/2}, \quad c_l^0 = [d'_{3333} / \rho]^{1/2},$$
$$B = c''_{45} - c^{*''}_{45} = {}^1/_2 (d''_{2313} + d''_{2331}),$$
$$h_{33} = h'_{3,33}, \quad h_{15} = {}^1/_2 (h'_{1,13} + h'_{1,31}), \quad h^*_{15} = h_{15} - h'_{1,13},$$
$$h''_{14} = \tfrac{1}{2} (h''_{1,23} + h''_{1,32}), \quad h^{*''}_{14} = h''_{1,23} - h''_{14}. \quad (10)$$

The system of homogeneous equations (8) determines the propagation of a longitudinal magnetoelastic wave. For the speed of propagation of this wave, $c_l = \omega/k$, we get the expression

$$c_l = c_l^0 [1 - h_{33}^2 / \rho (c_l^0)^2 (\gamma'_{33} + a_2 k^2 + 4\pi)]^{1/2}. \quad (11)$$

On setting the determinant of the system of homogeneous equations (9) equal to zero, we get a characteristic equation of the sixth degree in ω; it separates into the two equations

$$\rho\omega^2 - \rho (c_t^0)^2 k^2 \mp \omega B k^2 + k^2 (\gamma'_{11} + a_1 k^2 \mp \omega \gamma''_{12})^{-1} (h_{15} \mp \omega h''_{14})$$
$$\times [(h_{15} - h^*_{15}) \mp \omega (h''_{14} + h^{*''}_{14})] = 0, \quad (12)$$

We shall henceforth neglect the term $a_1 k^2$; this is permissible when $a_1 k^2 \ll |\gamma'_{11} \mp \omega \gamma''_{12}|$. Then it is easy to find two positive roots k_+ and k_- of Eq. (12). To these there will correspond two transverse magnetoelastic waves that are circularly polarized: that is, $u_1/u_2 = \mp i$ and $J_1/J_2 = \mp i$. Since the speeds of propagation of these waves are different, this should lead to rotation of the plane of polarization of a linearly polarized elastic wave.

The angle through which the plane of polarization rotates upon propagation of a linearly polarized elastic wave through unit distance is $\varphi = (k_+ - k_-)/2$, or

$$\varphi = \frac{\omega^2}{2\rho\,(c_t^0)^3}\left\{B + \varkappa'_{11}\frac{[h_{15}\,(h''_{14} + h^{*''}_{14}) + h''_{14}\,(h_{15} - h^*_{15})]}{1 - (\omega\,/\,\omega_0)^2} - \varkappa'_{11}\frac{\omega_0^{-1}\;[h_{15}\,(h_{15} - h^*_{15}) + \omega^2 h''_{14}\,(h''_{14} + h^{*''}_{14})]}{1 - (\omega\,/\,\omega_0)^2}\right\}, \qquad (13)$$

where $\kappa'_{11} = 1/\gamma'_{11}$ is the susceptibility measured in a direction perpendicular to the symmetry axis, and $\omega_0 = \gamma'_{11}/\gamma''_{12}$ is the magnetic resonance frequency. Here it has been assumed that the expression in curly brackets, multiplied by $\omega/\rho\,(c_t^0)^2$, is small in comparison with unity.

3. We shall now discuss the results obtained. As is evident from relation (11), the speed of propagation of a longitudinal magnetoelastic wave along the symmetry axis in a magnetically polarized medium is dependent not only on the elastic constants but also on the magnetic state of the medium. In connection with this we recall that in ferromagnetics both h_{33} and γ'_{33} depend appreciably on the magnetization. Formally this phenomenon can be described by introducing an elastic-modulus tensor d^H_{ijkl} measured at constant field. For quasistationary processes, a definite relation[5] holds between the tensor component $d^J_{ijkl} = d'_{ijkl}$ measured at constant magnetization and the tensor component d^H_{ijkl} measured at constant field; in our case this takes the form

$$d^H_{3333}\,/\,d^J_{3333} = 1 - h^2_{33}\,/\,d^J_{3333}\,\gamma'_{33}.$$

In the dynamic range, as is evident from (11), two additional terms a_2k^2 and 4π must be added to γ'_{33}. This may be one of the reasons for the differences between the values of elastic moduli obtained experimentally in measurements made in the quasistationary and in the dynamic ranges. We recall that in the case of ferromagnets, the dependence of the elastic moduli on magnetic state bears the name "ΔE -effect."

As is evident from (13), the rotation of the plane of polarization is determined by several constants. Their physical meaning for specific types of medium can be established on the basis of a microscopic theory of the kinetic processes that occur in a specific magnetoelastic medium. We consider several types of medium.

The role of the constant B was considered earlier,[6] and it has been shown[7] that in metals the constant c''_{45} that appears in B may be dependent on the effect of the polarizing magnetic field on the electron distribution function, as perturbed by the elastic wave. A specific calculation[7] of the constant c''_{45}, carried out within the framework of the free-electron model, gives, in particular, for low frequencies $(kl \ll 1)$ or for strong polarizing fields $(\omega_c\tau \gg kl)$, the relation

$$c''_{45} = -c''_{54} = -c''_{44}\,\omega_c\tau, \qquad (14)$$

where $\omega_c = eH_0/cm$; e, m, τ, and l are, respectively, the charge, mass, collision time, and free path length of an electron; $c''_{44} = \frac{1}{5}nmlv_0 \times (1 + \omega_c^2\tau^2)^{-1}$ is the imaginary part of the complex elastic-modulus tensor and determines the losses caused by transfer of the energy of the elastic wave to the conduction electrons;[8] v_0 is the speed of electrons at the Fermi surface. Calculation shows that appreciable rotation of the plane of polarization (through angles φ of the order of a few degrees or more in a field $H_0 \sim 10^3$ oe) may be expected in pure metals at low temperatures at frequencies of the order of tens of megacycles/sec.[7]

Concerning the constants that appear in the subsequent terms in the curly brackets in (13), it is possible to draw some conclusions from relations (1) and (6). The constant h^*_{15} determines the torque that acts on an anisotropic body because of noncoincidence of the directions of the vector magnetization and of the vector magnetic field intensity, or the field that must be applied in order to keep the magnetization unchanged upon rotation of the volume element. The value of this constant is determined by the magnetocrystalline anisotropy constant. In magnetically uniaxial ferromagnetics, the constant h^*_{15} and the magnetostrictive constant h_{15} (which depends on the magnetostriction constants) are in order of magnitude approximately the same and equal to 10^4 oe. The constant $h^{*''}_{14}$ describes gyromagnetic effects, and the constant h''_{14} is apparently related to possible anisotropy of the gyromagnetic effects. The value of the constant $h^{*''}_{14}$ is determined by the gyromagnetic ratio and is of order of magnitude 10^{-7} oe sec. In uniaxial ferromagnetics, the ferromagnetic resonance frequency is $\omega_0 \sim 10^9$ sec^{-1}.

Thus in ferromagnetics, the second and third terms in curly brackets in (13) can provide an appreciable amount of rotation of the plane of polarization at elastic-wave frequencies of order 10^9 sec^{-1}.

We emphasize that the different constants appearing in (13) have different types of temperature dependence.

We remark also that in the works of Akhiezer et al.[9] and of Kittel,[10] only one possible cause of rotation of the plane of polarization was taken into account — namely, the magnetostrictive constant h_{15}. The expression derived by Kittel for the rotation of the plane of polarization (which is correct for frequencies $\omega > \omega_0$) can be obtained from formula (13) by setting B, $h_{14}^{*\prime\prime}$, $h_{14}^{\prime\prime}$, and h_{15}^{*} equal to zero.

---

[1] K. B. Vlasov, Физика металлов и металловедение (Physics of Metals and Metal Research) **5**, 385 (1957); Izv. Akad. Nauk SSSR, Ser. Fiz., **22**, 1159 (1958), Columbia Tech. Transl. p. 1149.

[2] L. D. Landau and E. M. Lifshitz, Электродинамика сплошных сред (Electrodynamics of Continuous Media), GITTL, M., 1957.

[3] W. F. Brown, Jr., Revs. Modern Phys. **25**, 131 (1953); Amer. J. Phys. **19**, 290 and 333 (1951).

[4] N. Joel and W. A. Wooster, Nature **182**, 1078 (1958).

[5] K. B. Vlasov, Тр. Ин-та физики металлов Уральского филиала АН СССР (Proceedings of the Institute for the Physics of Metals, Ural' Branch, Academy of Sciences, USSR), Sverdlovsk, 1958, Sect. 20, p. 71.

[6] K. B. Vlasov and B. Kh. Ishmukhametov, JETP **36**, 1301 (1959), Soviet Phys. JETP **9**, 921 (1959).

[7] K. B. Vlasov, Физика металлов и металловедение (Physics of Metals and Metal Research) **7**, 447 (1959).

[8] M. S. Steinberg, Phys. Rev. **110**, 772 (1958).

[9] Akhiezer, Bar'yakhtar, and Peletminskiĭ, JETP **35**, 228 (1958), Soviet Phys. JETP **8**, 157 (1959).

[10] C. Kittel, Phys. Rev. **110**, 836 (1958).

Translated by W. F. Brown, Jr.
141

SOVIET PHYSICS JETP VOLUME 37 (10), NUMBER 3 MARCH, 1960

RESONANCE SCATTERING OF GAMMA-QUANTA BY Mg^{24}

I. Sh. VASHAKIDZE, T. I. KOPALEĬSHVILI and G. A. CHILASHVILI

Institute of Physics, Academy of Sciences, Georgian S.S.R.

Submitted to JETP editor March 31, 1959

J. Exptl. Theoret. Phys. (U.S.S.R.) **37**, 750-755 (September, 1959)

Resonance scattering of γ quanta from Mg^{24} nuclei, with excitation of the first two levels at 1.37 and 4.23 Mev has been investigated. Analysis of the correlation formula enables one to draw conclusions concerning the character of the excitation of the nucleus.

1. Until recently the problem of resonance scattering of γ quanta by nuclei was not amenable to experimental investigation because of the fact that usually $\Delta = h\nu_1 - h\nu_2 > \Gamma$, where ν_1 and ν_2 are the frequencies of the absorbed and emitted quanta, and Γ is the natural width of the excited level. As a result, the emission line $h\nu_2$ and the absorption line $h\nu_1$ hardly overlap, thus making it difficult to establish the occurrence of the resonance scattering. However this difficulty has now been essentially overcome, and there are many papers devoted to resonance scattering by various nuclei.[1-4]

The reason for the interest in this phenomenon is that by studying it one can not only determine some of the quantum numbers of excited nuclear states, but one can also decide whether the excitation occurs via a collective or a single-particle mechanism, since in many cases, as we shall show later, the expressions for the correlation function depend essentially on the assumed nuclear model.

2. The present paper gives a theoretical treatment of resonance scattering of γ quanta by Mg^{24}, with excitation of the 2^+ levels at 1.37 and 4.23 Mev (cf. Fig. 1).

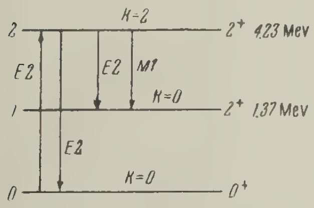

FIG. 1

Metzger[2] and Burgov and Terekhov[3] used the method of resonance scattering to determine experimentally the width of the 2^+ level at 1.37 Mev. Metzger gives a lower limit of $\Gamma_\gamma > 1.6 \times 10^{-4}$ ev, while reference 3 gives a definite value of $\Gamma_\gamma = 3.8 \times 10^{-4}$ ev. Assuming that the Mg^{24} nucleus is highly deformed,[5,6] the 2^+ level at 1.37 Mev can be treated either as a collective (rotational) level with angular momentum $I = 2$ and projection on the nuclear symmetry axis $K = 0$, or as a single-particle level resulting from the perturbed motion of a single particle in the field of the deformed nucleus. For a collective level, the reduced probability of transition from the excited state to the ground state is[7]

$$B = \tfrac{3}{5}\,(Ze\beta R_0^2 / 4\pi)^2, \tag{1}$$

where R_0 is the equilibrium radius of the sphere, and β is the equilibrium value of the nuclear deformation parameter. Formula (1) is usually used for determining the parameter β from the observed value of B. Setting the radius $R_0 = 1.45\,A^{1/3} \times 10^{-13}$ cm, one finds for Mg^{24} the value $\beta = 0.45$.

For the case of single-particle excitation, the expression for the transition probability to the ground state was given by Nilsson.[8] It is obvious that in Mg^{24} the transition from the 2^+ level at 1.37 Mev to the ground state occurs mainly by emission of E2 quanta. The corresponding level width is[8]

$$\Gamma = (4\pi / 75\hbar)\,(\omega / c)^5\, B\,(E2), \tag{2}$$

$$B\,(E2) = (5e/\sqrt{4\pi})^2 \Big| \sum_{l_1} \sum_{l_2} \sum_{\sigma} A_{l_1,\,\Omega-\sigma} A'_{l_2\Omega'-\sigma}\, \delta_{\Omega,\Omega'}$$

$$\times \frac{B_{l_1 l_2}}{\sqrt{(2l_1+1)(2l_2+1)}}$$

$$\times\, (2l_1 00 \,|\, 2l_1 l_2 0)\,(2l_1 0\,\Omega-\sigma \,|\, 2l_1 l_2 \Omega-\sigma)\Big|^2. \tag{3}$$

Here l_1 and l_2 are the orbital angular momenta of the nucleon in the ground and excited states, having the values 0 and 2 (N=2 shell); Ω is the projection of the angular momentum of the nucleon on the nuclear symmetry axis; σ is the spin: $A_{l_1,\Omega-\sigma}$ and $A'_{l_2,\Omega'-\sigma}$ are the diagonalization coefficients corresponding to the single-particle functions in the ground and first excited states;[8]

$$B_{l_1 l_2} = \int R_{2l_1} R_{2l_2} r^4 dr, \tag{4}$$

where R_{2l_1} and R_{2l_2} are oscillator wave functions for the nucleon, which depend only on the parameter

r'_0 which determines the level spacing corresponding to the spherical oscillator potential

$$\hbar\omega = \hbar^2 / 2M_p r'^2_0. \qquad (5)$$

The expression for B(E2) depends on the parameters $\delta = \beta/0.95$ and r'_0.

The nucleons in the N = 2 shell can be in states with $\Omega = \pm 1/2$, $\pm 3/2$, and $\pm 5/2$; there are three different states for $\Omega = \pm 1/2$, two for $\Omega = \pm 3/2$, and one for $\Omega = \pm 5/2$. The spacing of the levels depends on the value of $\hbar\omega$ and the deformation parameter δ. If we require that the level spacing agree with experiment, we can determine the parameter δ from the Nilsson model. In the Mg^{24} nucleus the $\pm 1/2$ and $\pm 3/2$ levels are filled if $\delta > 0$, while the $\pm 5/2$ and $\pm 1/2$ levels are filled if $\delta < 0$. The selection rules permit only $1/2 \rightarrow 1/2$ and $3/2 \rightarrow 3/2$ transitions in Mg^{24}. For the values of the parameter δ we get $\delta = \pm 0.2$ from the $1/2 \rightarrow 1/2$ transition, and $\delta = 0$ from the $3/2 \rightarrow 3/2$ transition, setting $r'_0 = 1.9 \times 10^{-13}$ cm in (5).

δ	$10^4 \Gamma_{theor}$, ev	$10^4 \Gamma_{exp}$, ev
0.2	63	3.8[4]
−0.2	0.8	
0.3	11.8	>1.6[3]

The values of the width of the excited level at 1.37 Mev are given in the table. We see that the value $\delta = -0.2$ must be discarded, since the resulting level width contradicts the experimental value. The theoretical value of the width for $\delta = 0.2$ is considerably greater than the experimental value. But if we take a somewhat greater value for δ, say 0.3, the theoretical value of the width Γ is much closer to experiment. Of course, the excitation energy is then different from the experimental value, but not very much, since with $\delta = 0.3$ we get 1.72 Mev for the excitation energy. Unfortunately, in Nilsson's paper the diagonalization coefficients are tabulated only up to $\delta = 0.3$. It is to be expected that for a somewhat greater value of δ the agreement with experiment will be more satisfactory with respect to both the width of the level and the value of the energy of excitation. As for the width of the excited level found from the collective model, nothing definite can be said since no satisfactory way has yet been found for determining the deformation parameter β independently of formula (1).

The angular distribution of the scattered γ quanta is

$$I(\theta) = I(0)\{1 - 3\cos^2\theta + 2\cos^4\theta\}. \qquad (6)$$

As was to be expected, the angular distribution does not depend on the model, since we are dealing with a pure E2 transition.

3. We can get a different result concerning the dependence of the angular distribution on the nuclear model if we consider the resonance scattering of γ quanta by Mg^{24} with excitation of the second 2^+ level at 4.23 Mev. Actually γ transitions can occur from this level to the ground state as well as to the first excited 2^+ level. For the transition to the ground state, the angular distribution of the γ quanta will not depend on the model since this transition is pure E2. For the transition to the first 2^+ level, both E2 and M1 transitions are possible. If the probabilities of these transitions are of the same order of magnitude, then because of the interference term the correlation function will now depend essentially on the assumed nuclear model, and a comparison with experiment will enable us to determine the validity of the models. One must keep in mind that the probabilities of E2 transitions to the ground state and first excited state should be of the same order of magnitude. Of course the nucleus in the first excited state later makes a transition to the ground state, but this can give nothing new concerning the dependence of the angular distribution on the assumed nuclear model, since this transition is a pure E2. For this reason we shall in what follows regard the first excited state as the final state. To obtain the correlation between the quanta absorbed and emitted in the transition $2 \rightarrow 1$, we shall start from the two models: collective and single-particle. However before doing this we must check whether the conditions

$$W[E2(2 \rightarrow 1)] \sim W[E2(2 \rightarrow 0)],$$
$$W[M1(2 \rightarrow 1)] \sim W[E2(2 \rightarrow 1)],$$

are satisfied, where the numbers 0, 1, and 2 denote the ground state, the first and the second excited states, respectively.

Since both excited levels have the same angular momentum 2^+, we can use the assumption of Davydov and Filippov[9,10] that the nucleus can be represented as an asymmetric top, which has rotational levels of different energies but with the same total angular momentum. The authors cited have found the relation between these levels as a function of asymmetry parameter γ. Since the Mg^{24} nucleus is highly deformed, we apply the model of Davydov and Filippov to it, and calculate the probabilities of the radiative transitions for the same value of the asymmetry parameter which gives the observed value for the ratio of the energies of the levels ($\gamma = 22°$). We find

$$W\,[E2\,(2\rightarrow 1)]\,/\,W\,[E2\,(2\rightarrow 0)]\sim 1,$$
$$W\,[M1\,(2\rightarrow 1)]\,/\,W\,[E2\,(2\rightarrow 1)]\sim 10^{-2}. \qquad (7)$$

We see that the probability of the magnetic transition in this case is very small compared to the probability of the E2 transition. The correlation function will therefore not depend on the nuclear model, and will be given by formula (6). If however we treat the 2^+ levels at 4.23 and 1.37 Mev as single particle levels according to the Nilsson model, then as is easily shown we get for the ratio of the radiative transition probabilities

$$W\,[E2\,(2\rightarrow 1)]\,/\,W\,[E2\,(2\rightarrow 0)]$$
$$\sim W\,[M1\,(2\rightarrow 1)]\,/\,W\,[E2\,(2\rightarrow 1)]\sim 1. \qquad (8)$$

From this it follows that the transition $2\rightarrow 1$ is not a pure E2 transition, and that the correlation function on this model will differ from formula (6). To find the function we use the general correlation formula

$$I\,(\mathbf{n}_\gamma)\sim\sum_{pp'}\sum_{M_0}\sum_{M_2}$$
$$\times\left|\sum_{M_1}(M_0I_0K_0\,|\,\hat{H}_0\,|\,I_1M_1K_1)\,(I_1M_1K_1\,|\,\hat{H}_1\,|\,I_2M_2K_2)\right|^2, \qquad (9)$$

where $(I_0M_0K_0\,|\,\hat{H}_0\,|\,I_1M_1K_1)$ is the matrix element for E2 absorption of the γ quantum with transition of the nucleus from the ground state to the 2^+ state at 4.23 Mev; $(I_1M_1K_1\,|\,\hat{H}_1\,|\,I_2M_2K_2)$ is the matrix element for the transition $2\rightarrow 1$, in which (E2 + M1) quanta are emitted; $(I_0M_0K_0)$, $(I_1M_1K_1)$, and $(I_2M_2K_2)$ are the values of the total angular momentum of the nucleus, its projection on a space-fixed axis and its projection on the nuclear symmetry axis, in the initial, intermediate, and final states, respectively. The operators for absorption and emission of γ quanta have the well-known form[12]

$$\hat{H}_0=-\sqrt{\pi/15}\,ep'\,(kr)^2Y_{2p'},$$
$$\hat{H}_1=-\sqrt{\pi/15}\,ep\sum_{M=-2}^{2}D^2_{Mp}\,(\mathbf{n}_\gamma)\,(kr)^2Y_{2M}-(\pi e\hbar\,/\,M_pc)\sqrt{3}$$
$$\times\sum_{M\mu}D^1_{Mp}\,(\mathbf{n}_\gamma)\,f_1\,(kr)\,(11-\mu\,\mu+M\,|\,111M)\,Y_{1,\,\mu+M}\nabla_{-\mu}, \qquad (10)$$

where $f_L(kr)$ are spherical Bessel functions, multiplied by $(2\pi)^{1/2}$, and $D^l_{mm'}(\mathbf{n})$ is the transformation matrix.

For the wave function of the nuclear system in the initial, intermediate, and final states, we have[7,8]

$$\Psi_{000}=\sqrt{1/8\pi^2}\,\chi_{\Omega_0\Omega_0^0},$$
$$\Psi_{2M_12}=\sqrt{5/16\pi^2}\,\{\chi_{\Omega_1\Omega_1^0}D^2_{M_12}+\chi_{-\Omega_1,\,-\Omega_1^0}D^2_{M_1\,-2}\},$$
$$\Psi_{2M_20}=\sqrt{5/8\pi^2}\,\chi_{\Omega_2\Omega_2^0}D^2_{M_20}, \qquad (11)$$

where Ω_i ($i = 0, 1, 2$) is the projection on the nuclear symmetry axis of the angular momentum of the nucleon excited in the N = 2 shell, in the initial, intermediate, and final states, Ω_i^0 is the sum of the projections of the angular momenta of the other nucleons in the shell.

In addition we have

$$\chi_{\Omega_i\Omega_i^0}=\chi_{\Omega_i^0}\chi_{\Omega_i}, \qquad (12)$$

where

$$\chi_{\Omega_i}=\sum_{l_i\,m_i\,\sigma_i}A^i_{l_i\Omega_i-\sigma_i}R_{2l_i}D^{l_i}_{m_i\,\Omega_i-\sigma_i}Y_{l_im_i}(\theta,\,\varphi)\,\chi\,(\sigma_i) \qquad (12')$$

is the wave function of the nucleon in the undeformed nucleus,[8] $A^i_{l_i\Omega_i-\sigma_i}$ are the diagonalization coefficients, $\chi(\sigma_i)$ are spin functions, χ_{Ω_i} is the wave function of the other nucleons in the N = 2 shell.

If we use these expressions, we find, after quite involved calculations,

$$I\,(\mathbf{n}_\gamma)\sim\sum_{pp'}\sum_{M_0M_2}\Big|\tfrac{5}{8}\,e^2\,(k_{20}R_0)^2\sqrt{5/3}\,N\,(\Omega_0\Omega_1)$$
$$\times\Big\{\sum_{M_1}B\,(20m_1M_2\Omega_1\Omega_2)\,[O\,(20m_1pM_2)\,D^1_{p'-M_2,\,p}\,(\mathbf{n}_\gamma)$$
$$+\,C\,(20m_1pm_2)\,D^2_{p'-M_2,\,p}\,(\mathbf{n}_\gamma)]$$
$$+\sum_{m_1}B\,(22m_1p'M_2\Omega_1\Omega_2)\,[O\,(22m_1pM_2)\,D^1_{p'-M_2,\,p}\,(\mathbf{n}_\gamma)$$
$$+\,C\,(22m_1pM_2)\,D^2_{p'-M_2,\,p}\,(\mathbf{n}_\gamma)]\Big\}\Big|^2, \qquad (13)$$

where

$$N\,(\Omega_0\Omega_1)=\sum_{l_0}\sum_{l_1}\frac{\sqrt{2l_1+1}}{(2l_0+1)^{3/2}}\,(l_1200\,|\,l_12l_00)\,\mathfrak{M}_2\,(l_1l_0)$$
$$\times\sum_{\sigma_1}\{A^1_{l_1\Omega_1-\sigma_1}\,A^0_{l_2\Omega_0-\sigma_1}\,(l_12\Omega_1-\sigma_12\,|\,l_22l_0\Omega_1-\sigma_1+2)$$
$$+\,A^1_{l_1,\,-\Omega_1-\sigma_1}A^0_{l_0,\,\Omega_0-\sigma_1}$$
$$\times\,(l_12-\Omega_1-\sigma_12\,|\,l_12l_0-\Omega_1-\sigma_1+2)\},$$

$$B\,(l_1l_2mp'M_2\Omega_1\Omega_2)=\sum_{L=l_1-2}^{l_1+2}\frac{1}{(2L+1)}\,(l_12m_1p'\,|\,l_12Lm_1+p')$$
$$\times\,(l_22m_1+p'-M_2,\,M_2\,|\,l_22Lm_1+p')$$
$$\times\sum_{\sigma'}[A^2_{l_2\Omega_2-\sigma_1},\;A^1_{l_1\Omega_1-\sigma_1}\,(l_12\Omega_1-\sigma_12\,|\,l_12L\Omega_1-\sigma_1+2)$$
$$\times\,(l_22\Omega_2-\sigma_10\,|\,l_22L\Omega_2-\sigma_1)+A^2_{l_2\Omega_2-\sigma_1}\,A^1_{l_1,-\Omega_1-\sigma_1}$$
$$\times\,(l_12-\Omega_1-\sigma_1,\,-2\,|\,l_12L-\Omega_1-\sigma_1-2)$$
$$\times\,(l_22\Omega_2-\sigma_10\,|\,l_22L\Omega_2-\sigma_1)],$$

$$O\,(l_1l_2m_1p'M_2)=\frac{e\hbar k_{21}}{2\sqrt{2}\,M_pc}\,\frac{1}{\sqrt{2l_2+1}}$$
$$\times\sum_{\mu=-1}^{1}(11-\mu\mu+p'-M_2\,|\,111p'-M)\{(l_11m_1-\mu\,|\,l_11l_1$$
$$+\,1m_1-\mu)\,(1l_1+1\mu+p'-M_2m_1-\mu\,|\,1l_1+1l_2m_1$$
$$+\,p'-M_2)\,T_1\,(l_1l_2)-(l_11m_1-\mu\,|\,l_11l_1-1m_1-\mu)$$

$$\times (1 l_1 - 1\mu + p' - M_2 m_1 - \mu \mid 1 l_1 - 1 l_2 m_1$$
$$+ p' - M_2) T_2 (l_1 l_2)\},$$
$$T(l_1 l_2) = \sqrt{(l_1 + 1)} (1 l_1 + 100 \mid 1 l_1 + 1 l_2 0) [(l_2 - l_1 - 2)$$
$$\times (l_1 + l_3 + 3) \mathfrak{M}_0 (l_1 l_2) + 2 M_p c k_{21} R^2 \hbar^{-1} \mathfrak{M}_2 (l_1 l_2)],$$
$$T_2 (l_1 l_2) = \sqrt{l_1} (1 l_1 - 100 \mid 1 l_1 - 1 l_2 0) [\mathfrak{M}_0 (l_1 l_2)$$
$$+ 2 M_p c k_{21} R^2 \hbar^{-1} \mathfrak{M}_2 (l_1 l_2)],$$
$$C (l_1 l_2 m_1 M_1 M_2) = - \sqrt{\frac{2 l_1 + 1}{3 (2 l_2 + 1)}} (l_1 2 m_1 M_1 - M_2 \mid l_1 2 l_2 m_1$$
$$+ M_1 - M_2) (kR)^2 \mathfrak{M}_2 (l_1 l_2).$$

In these formulas M_p is the proton mass and c is the velocity of light; k_{20} and k_{21} are the wave numbers of the γ quanta emitted in the transitions $2 \rightarrow 0$ and $2 \rightarrow 1$, respectively, while the symbols $\mathfrak{M}_L(l_1 l_2)$ denote radial integrals, i.e.

$$\mathfrak{M}_L (l_1 l_2) = \int R_{2 l_1} (r / R)^L R_{2 l_2} r^2 dr.$$

From the selection rules we have $|\Omega_1 - \Omega_0| = 2$, $|\Omega_1 - \Omega_2| = 2$. Thus in the absorption of an E2 quantum we will have the transitions $\frac{1}{2} \rightarrow \frac{5}{2}$, $\frac{1}{2} \rightarrow -\frac{3}{2}$, $\frac{3}{2} \rightarrow -\frac{1}{2}$, if $\delta > 0$. If we require that the calculated level spacing agree with the experimental value, (4.23 Mev), we will have only the $\frac{1}{2} \rightarrow -\frac{3}{2}$ transition. In this case the theoretical values are $\Delta E = 3.8$ Mev for $\delta = 0.3$, and $\Delta E = 2.9$ Mev for $\delta = 0.2$, (The lack of tables of the diagonalization coefficients for $\delta > 0.3$ prevents us from getting closer to the experimental value $\Delta E = 4.23$ Mev.) In this case, in the transition $2 \rightarrow 1$ to the final state only the single-particle transition $-\frac{3}{2} \rightarrow \frac{1}{2}$ will occur. If we substitute the computed values of k_{20} and k_{21} in formula (13), we finally get the correlation function

$$I (\theta) \sim (1 + A \cos \theta + B \cos^2 \theta + C \cos^3 \theta + D \cos^4 \theta), \quad (14)$$

where θ is the angle between the absorbed and emitted γ quanta. For $\delta = 0.3$, the values of the coefficients in (14) are

$$A = 0.11, \quad B = -1.5, \quad C = -0.3, \quad D = 0.7.$$

The correlation function given by formula (14) is not symmetric around 90° (cf. Fig. 2), whereas in the case of collective excitation the corresponding curve determined from (6) is symmetric. Thus the experimental investigation of the correlation of γ quanta in the excitation of Mg^{24} with an energy of 4.23 Mev would enable us to draw definite conclusions concerning the nature of the excitation of this nucleus. Unfortunately, so far as we know, no one has as yet done such experiments.

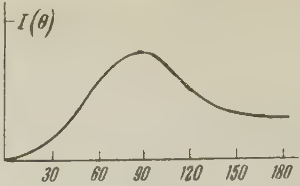

FIG. 2

In conclusion, it is our pleasant duty to express our thanks to V. I. Mamasakhlisov for his direction and continued interest in our work.

---

[1] P. Moon, Proc. Phys. Soc. (London) **64**, 76 (1951).

[2] F. Metzger, Phys. Rev. **83**, 842 (1951).

[3] N. A. Burgov and Yu. V. Terekhov, Атомная энергия (Atomic Energy) **2**, 514 (1957).

[4] D. G. Alkhazov et al., JETP **35**, 1056 (1958), Soviet Phys. JETP **8**, 737 (1959).

[5] G. Rakavy, Nucl. Phys. **4**, 375 (1957).

[6] V. I. Mamasakhlisov and T. I. Kopaleĭshvili, JETP **34**, 1169 (1958), Soviet Phys. JETP **7**, 809 (1958).

[7] A. Bohr and B. Mottelson, Kgl. Danske Videnskab. Selskab Mat. fys. Medd. **27**, No. 16 (1953).

[8] S. G. Nilsson, Kgl. Danske Videnskab. Selskab Mat. fys. Medd. **29**, No. 16 (1955).

[9] A. S. Davydov and G. F. Filippov, JETP **35**, 441 (1958), Soviet Phys. **8**, 303 (1959).

[10] A. S. Davydov and G. F. Filippov, JETP **35**, 703 (1958), Soviet Phys. JETP **8**, 488 (1959).

[11] V. I. Mamasakhlisov and T. I. Kopaleĭshvili, JETP **37**, 131 (1959), Soviet Phys. JETP **10**, 93 (1960).

[12] M. E. Rose, Multipole Fields, J. Wiley and Sons, New York, 1955, Russ. Transl. IIL 1957.

Translated by M. Hamermesh
142

SOVIET PHYSICS JETP VOLUME 37(10), NUMBER 3 MARCH, 1960

SIMPLE WAVES IN THE CHEW-GOLDBERGER-LOW APPROXIMATION

I. A. AKHIEZER, R. V. POLOVIN, and N. L. TSINTSADZE

Physico-Technical Institute, Academy of Sciences, Ukrainian S.S.R.; Institute of Physics, Academy of Sciences, Georgian S.S.R.

Submitted to JETP editor April 3, 1959

J. Exptl. Theoret. Phys. (U.S.S.R.) **37**, 756-759 (September, 1959)

Simple waves in a plasma with anisotropic pressure are treated in the Chew-Goldberger-Low approximation. It is shown that there exist three types of simple waves. The direction of the variations of the magnetohydrodynamic quantities in these waves is investigated.

CHEW, Goldberger, and Low[1] have shown that a rarefied plasma in a magnetic field, in which collisions play a negligible role, can be described by a system of magnetohydrodynamic equations with an anisotropic pressure. Small vibrations of the plasma have been studied by means of these equations.[2] It is of interest to use these same equations for the study of nonlinear motions of the plasma, and primarily for the study of simple waves. The present paper is devoted to this last problem.

1. In the Chew-Goldberger-Low approximation the system of magnetohydrodynamic equations has the following form:

$$\rho\frac{d\mathbf{v}}{dt}=\mathbf{F}+\frac{1}{4\pi}(\operatorname{curl}\mathbf{H})\times\mathbf{H}, \qquad F_i=-\frac{\partial p_{ik}}{\partial x_k},$$

$$\frac{\partial\mathbf{H}}{dt}=\operatorname{curl}\,[\mathbf{v}\times\mathbf{H}], \qquad \operatorname{div}\mathbf{H}=0, \qquad \frac{\partial\rho}{\partial t}+\operatorname{div}(\rho\mathbf{v})=0,$$

$$p_{ik}=p_\perp\delta_{ik}+(p_\parallel-p_\perp)h_ih_k, \qquad \mathbf{h}=\mathbf{H}/H,$$

$$\frac{d}{dt}\left(\frac{p_\perp}{\rho H}\right)=0, \qquad \frac{d}{dt}\left(\frac{p_\parallel H^2}{\rho^3}\right)=0. \tag{1}$$

We shall consider one-dimensional simple waves, in which all the magnetohydrodynamic quantities are functions of one such quantity, for example ρ, which in turn depends on the coordinate x and the time t:

$$x-V_{\mathrm{ph}}(\rho)\,t=f(\rho), \tag{2}$$

where $V_{\mathrm{ph}}(\rho)$ is the rate of displacement of a point at which the density ρ has a given value, and $f(\rho)$ is the function inverse to the density distribution $\rho(x)$ at the initial time $t = 0$.

In regions of compression $f'(\rho) < 0$; in regions of rarefaction $f'(\rho) > 0$; and the condition for self-similar waves is $f(\rho)\equiv 0$.

Simple waves are closely related to waves of small amplitude.[3] The differential equations connecting the changes of all the magnetohydrodynamic quantities with the change of the density ρ are easily found from the relations between the amplitudes of the waves of small intensity.

Just as in magnetohydrodynamics with a scalar pressure, there exist three types of simple waves, in which the magnetohydrodynamic quantities satisfy the following differential equations.

Alfven waves:*

$$dv_z=-(u_A/H_x)\,dH_z, \qquad dv_y=-(u_A/H_x)\,dH_y,$$

$$H_y dH_y+H_z dH_z=0,$$

$$dv_x=dH_x=d\rho=dp_\parallel=dp_\perp=0, \tag{3}$$

where u_A is the speed of the Alfven waves, defined by the formula

$$u_A=V_{Ax}\sqrt{1+4\pi H^{-2}(p_\perp-p_\parallel)}, \qquad \mathbf{V}_A=\mathbf{H}/\sqrt{4\pi\rho}. \tag{4}$$

Magnetoacoustic waves

$$\frac{dv_x}{d\rho}=\frac{u_\pm}{\rho}, \qquad \frac{dH_x}{d\rho}=0, \qquad \frac{dv_z}{d\rho}=0, \qquad \frac{dH_z}{d\rho}=0,$$

$$\frac{dH_y}{d\rho}=\frac{H^2}{\rho H_y}\left(1+\frac{s_\perp^2H_x^2}{u_\pm^2H^2-3s_\parallel^2H_x^2}\right),$$

$$\frac{dv_y}{d\rho}=-\frac{u_\pm}{\rho}\frac{H_x}{H_y}\left(1-\frac{s_\perp^2H_y^2}{u_\pm^2H^2-3s_\parallel^2H_x^2}\right)\left(1+\frac{s_\perp^2H_x^2}{u_\pm^2H^2-3s_\parallel^2H_x^2}\right)^{-1},$$

$$\frac{dp_\parallel}{d\rho}=\frac{p_\parallel}{\rho}\left[1+\frac{2s_\perp^2H_x^2}{u_\pm^2H^2+H_x^2(s_\perp^2-3s_\parallel^2)}\right],$$

$$\frac{dp_\perp}{d\rho}=\frac{p_\perp}{\rho}\left[1+\frac{u_\pm^2H^2-3H_x^2s_\parallel^2}{u_\pm^2H^2+H_x^2(s_\perp^2-3s_\parallel^2)}\right], \tag{5}$$

where

$$s_\parallel^2=p_\parallel/\rho, \quad s_\perp^2=p_\perp/\rho.$$

The speeds $u_\pm$ of the magnetoacoustic waves are given by the formula

---

*In the limiting case $p \ll H$ these waves have been discussed by Ferraro.[4]

$$u_\pm = \Big\{\tfrac{1}{2}[s_\perp^2(2-\cos^2\varphi)+2s_\parallel^2\cos^2\varphi+V_A^2]$$

$$\pm\Big[\tfrac{1}{4}(s_\perp^2(2-\cos^2\varphi)+2s_\parallel^2\cos^2\varphi+V_A^2)^2$$

$$+s_\perp^4\sin^2\varphi\cos^2\varphi-3s_\parallel^2s_\perp^2\cos^2\varphi(2-\cos^2\varphi)$$

$$+3s_\parallel^4\cos^4\varphi-3s_\parallel^2V_A^2\cos^2\varphi\Big]^{1/2}\Big\}^{1/2}. \qquad (6)$$

The plus sign corresponds to the fast, the minus to the slow, acoustic wave; φ is the angle between the direction of the magnetic field and the direction of propagation of the wave.

The quantity V_{ph} appearing in (2) is connected with the phase velocities in the following ways:

$$V_{ph}=v_x+u_A \qquad (7)$$

for the Alfven waves, and

$$V_{ph}=v_x+u_\pm$$

for the magnetoacoustic waves.

It follows from (3) that $dV_{ph}/d\rho = 0$; this means that the Alfven wave is propagated without change of shape.

2. The study of (5) in general form entails great mathematical difficulties. We shall confine ourselves to the most interesting case, in which the hydrostatic pressure is much smaller than the magnetic pressure:

$$s_\perp \ll V_A, \quad s_\parallel \ll V_A.$$

Under these conditions the formulas (5) and (6) take the following form for the fast magnetoacoustic wave:

$$dv_x/d\rho = u_+/\rho, \qquad dv_y/d\rho = -u_+H_x/\rho H_y,$$

$$dH_y/d\rho = H^2/\rho H_y,$$

$$dp_\parallel/d\rho = p_\parallel/\rho, \qquad dp_\perp/d\rho = 2p_\perp/\rho, \qquad u_+ = V_A. \qquad (9)$$

From Eq. (9) we have*

$$dV_{ph}/d\rho > 0. \qquad (10)$$

This means that in regions of rarefaction the density gradient decreases, and that it increases in regions of compression.

From the relation (2) and the equation of continuity it follows that

$$-\frac{1}{u_\pm(\rho)}[fV'_{ph}(\rho)+f'(\rho)]\frac{d\rho}{dt}=1. \qquad (11)$$

It can be seen from this that in regions of rarefaction ($f' > 0$) and in self-similar waves ($f \equiv 0$) the density decreases. In regions of compression ($f' < 0$) the density increases up to the point at which the expression in square brackets ceases to be negative. A compressional shock wave appears when this expression becomes zero.

It follows from the relations (9) that in a fast magnetoacoustic wave the quantities $p_\parallel$, $p_\perp$, H, $p_\perp/p_\parallel$ change in the same direction as the density.*

3. Let us now consider the slow magnetoacoustic wave. With the conditions $s_\perp \ll V_A$, $s_\parallel \ll V_A$ satisfied, the equations that hold on a slow magnetoacoustic wave are

$$\frac{dv_x}{d\rho}=\frac{u_-}{\rho}, \qquad \frac{dv_y}{d\rho}=\frac{H_y}{H_x}\frac{u_-}{\rho}, \qquad \frac{dp_\parallel}{d\rho}=\frac{3p_\parallel}{\rho}, \qquad \frac{dp_\perp}{d\rho}=\frac{p_\perp}{\rho},$$

$$H_y\frac{dH_y}{d\rho}=\frac{s_\perp^2V_A^2H^4}{-\rho A(\rho)}, \qquad 2u_-\frac{dV_\Phi}{d\rho}=\frac{6s_\parallel^2s_\perp^2V_A^2H_x^2}{\rho A(\rho)},$$

$$u_-=s_\parallel\sqrt{3}\cos\varphi, \qquad A(\rho)=s_\perp^4H_y^2-3s_\parallel^2H_x^2(s_\perp^2-s_\parallel^2). \qquad (12)$$

We must distinguish two cases, depending on the sign of the quantity $A(\rho)$.

1) Normal case†

$$A(\rho)>0, \qquad dV_{ph}/d\rho>0.$$

Here the density changes in just the same way as in the fast magnetoacoustic wave. In particular, shock waves are formed in regions of compression, and the self-similar waves are waves of rarefaction. According to Eq. (12) the changes of the quantities $p_\parallel$, $p_\perp$ are in the same direction as those of the density, and those of the quantities H and $p_\perp/p_\parallel$ are in the opposite direction.

2) Anomalous case‡

$$A(\rho)<0, \qquad dV_{ph}/d\rho<0.$$

Here the density gradient decreases in regions of compression, and increases in regions of rarefaction. It follows from (11) that in regions of compression the density rises, and in regions of rarefaction it falls. In self-similar waves the density rises. According to Eq. (12), in the anomalous case the quantities $p_\parallel$, $p_\perp$, and H change in the same direction as the density, and the quantity $p_\perp/p_\parallel$

---

*This fact has been noted by Sagdeev[5] in the case in which the direction of propagation of the wave is perpendicular to the magnetic field.

*The decrease of the ratio $p_\perp/p_\parallel$ with decrease of the magnetic field is due to the conservation of a particle's magnetic moment.[6]

†This case is always realized, for example, if the wave is propagated perpendicular to the magnetic field ($H_x = 0$), or if the plasma is isotropic ($p_\parallel = p_\perp$).

‡This case is realized, for example, if the wave is propagated along the magnetic field ($H_y = 0$) and the quantity $p_\perp/p_\parallel$ is greater than unity.

changes in the opposite direction.*

It follows from (11) that shock waves arise in regions of rarefaction. Thus in this case, unlike that of magnetohydrodynamics with a scalar pressure, shock waves of rarefaction can be produced.

At the instant of production of a shock wave the plasma has the density ρ_s that satisfies the equation[8]

$$f''(\rho_s)/f'(\rho_s) = V''_{\mathrm{ph}}(\rho_s)/V'_{\mathrm{ph}}(\rho_s). \qquad (13)$$

We note that in both the normal case and the anomalous case the quantity A increases: $dA/dt > 0$. Therefore the plasma can be in the anomalous state for only a finite time. The density value ρ_n at which the transition from the anomalous to the normal state occurs satisfies the equation $A(\rho_n) = 0$.

If $\rho_s > \rho_n$, a shock wave is formed in the region of rarefaction; if $\rho_n > \rho_s$, the plasma makes the transition to the normal state before a shock wave of rarefaction is formed. Which event happens first depends on the initial density distribution $f(\rho)$.

We note that the point ρ_n is not a singular point for the system of differential equations (12). At this point we merely have vanishing of the derivatives $d\rho/dH_y$, $dp_{\parallel}/dH_y$, $dp_{\perp}/dH_y$, dv_x/dH_y, and dv_y/dH_y.

The writers express their gratitude to A. I. Akhiezer and G. Ya. Lyubarskiĭ for valuable discussions.

---

*This is in agreement with Parker's[7] result of an inverse dependence between $p_{\perp}/p_{\parallel}$ and H in the static case when the particles move along the magnetic field. The decrease of $p_{\perp}/p_{\parallel}$ with the increase of H, in spite of the conservation of magnetic moment (proportional to $p_{\perp}/H$) is explained by the fact that particles with larger values of $p_{\perp}/p_{\parallel}$ are more strongly reflected from the region of strong magnetic field.[6]

[1] Chew, Goldberger, and Low, Proc. Roy. Soc. **A236**, 112 (1956).

[2] L. I. Rudakov and R. Z. Sagdeev, Физика плазмы и проблемы управляемых термоядерных реакций (Plasma Physics and Problems of Controlled Thermonuclear Reactions), U.S.S.R. Acad. Sci., 1958, Vol. 3, p. 268.

[3] Akhiezer, Lyubarskiĭ, and Polovin, Укр. физ. журн., (Ukr. Phys. J.) **3**, 433 (1958).

[4] V. C. A. Ferraro, Proc. Roy. Soc. **A233**, 310 (1956).

[5] R. Z. Sagdeev, Физика плазмы и проблемы управляемых термоядерных реакций (Plasma Physics and Problems of Controlled Thermonuclear Reactions), U.S.S.R. Acad. Sci., 1958, Vol. 4, p. 384.

[6] L. Spitzer, The Physics of Fully Ionized Gases (Russ. Transl.), IIL, 1957.

[7] E. N. Parker, Phys. Rev. **107**, 924 (1957).

[8] G. Ya. Lyubarskiĭ and R. V. Polovin, Укр. физ. журн., (Ukr. Phys. J.) **3**, No. 5 (1958).

Translated by W. H. Furry
143

SOVIET PHYSICS JETP VOLUME 37(10), NUMBER 3 MARCH, 1960

CIRCULAR POLARIZATION OF γ QUANTA EMITTED BY A NUCLEUS AFTER μ^- CAPTURE

I. S. SHAPIRO and L. D. BLOKHINTSEV

Submitted to JETP editor April 3, 1959

J. Exptl. Theoret. Phys. (U.S.S.R.) **37**, 760-764 (September, 1959)

Formulas for the circular polarization of γ quanta emitted by a nucleus after μ^- capture are deduced. The hyperfine splitting of the mesic atom levels is taken into account.

SINCE the μ^- mesons emitted in the decay of π^- mesons are longitudinally polarized, the nuclear μ^- capture leads to the formation of polarized nuclei. If, therefore, the daughter nucleus is formed in an excited state, the γ rays emitted by it will, in general, be polarized (the angular distribution will here be isotropic). In the present paper we consider the circular polarization of the γ rays for the case when the nucleus goes into a discrete state in the μ^- capture, i.e., when no neutron is emitted. The process under consideration is the following: a nucleus A_Z with spin j_1 captures in the K shell a polarized μ^- meson and goes over into an excited nuclear state A_{Z-1} with spin j_2,* which, under emission of a γ quantum with multipolarity J (the formulas obtained can easily be generalized for the case of mixed multipoles), goes over into the ground state with spin j_3.

We took the Hamiltonian of the four-fermion interaction in the form of a superposition of vector (v), axial-vector (a), and pseudoscalar (p) coupling with the coupling constants g_v, g_a, and g_p. The presence of v and a coupling follows from the theory of the universal Fermi interaction, as proposed by Feynman and Gell-Mann and by Sudarshan and Marshak.[1] The p coupling was added in view of the fact that the effects connected with the emission of virtual π mesons lead to the appearance of terms analogous to the pseudoscalar coupling in the S matrix describing the weak interaction.[2] The effective coupling constant g_p is proportional to the mass of the lepton, and while it is negligibly small in β decay, it does have a considerable magnitude in μ^- capture: according to the estimates of Goldberger and Treiman[2] $g_p \approx 8 g_a$, so that the inclusion of the pseudoscalar variant becomes inevitable, despite the fact that the constant g_p enters in the expressions for the probabilities of the processes under consideration with the factor v/c, where v is the velocity of the nucleons.

The circular polarization of the γ quanta, C_γ, is given by

$$C_\gamma = (W_+ - W_-)/(W_+ + W_-), \qquad (1)$$

where W_+ and W_- are the probabilities for the emission of γ quanta whose spin is oriented in the direction of the momentum (right polarization) and in the opposite direction of the momentum (left polarization), respectively. The calculation leads to the following expression for C_γ in the case of the longitudinal neutrino:

$$C_\gamma = P_\mu \alpha \cos\theta, \qquad \alpha = B/A, \qquad (2)$$

where P_μ is the polarization of the μ^- meson at the instant of its entrance in the K orbit of the mesic atom,* and θ is the angle between the direction of the polarization vector of the μ^- meson and the direction of emission of the γ quantum;

$$\begin{aligned} A = \mathrm{Re}\,(& |g_v|^2 \langle Y_\Lambda\rangle|^2 + |g_a|^2 |\langle i\gamma_5 Y_{\Lambda-1}\rangle|^2 \\ & + |g_p|^2 \langle i\gamma_4\gamma_5 Y_{\Lambda-1}\rangle|^2 + 2g_p^* g_a \langle i\gamma_4\gamma_5 Y_{\Lambda-1}\rangle^* \langle i\gamma_5 Y_{\Lambda-1}\rangle \\ & + \sum_l \{|g_a|^2 |\langle \mathcal{J}_{l\Lambda}\rangle|^2 + |g_v|^2 |\langle i\gamma_5 \mathcal{J}_{l\Lambda-1}\rangle|^2\} \\ & + 2 \sum_{\Lambda'=\Lambda\pm1} \Big\{\Big(-|g_v|^2 \langle Y_\Lambda\rangle^* \langle i\gamma_5 \mathcal{J}_{\Lambda\Lambda'}\rangle \\ & + |g_a|^2 \langle i\gamma_5 Y_{\Lambda'}\rangle^* \langle \mathcal{J}_{\Lambda'\Lambda}\rangle \\ & + g_p^* g_a \langle i\gamma_4\gamma_5 Y_{\Lambda'}\rangle^* \langle \mathcal{J}_{\Lambda'\Lambda}\rangle) a_1(\Lambda, \Lambda') \\ & + \sum_l g_v^* g_a \langle i\gamma_5 \mathcal{J}_{l\Lambda'}\rangle^* \langle \mathcal{J}_{l\Lambda}\rangle a_2(\Lambda, \Lambda')\Big)\Big\}, \end{aligned} \qquad (3a)$$

$$\begin{aligned} B = \mathrm{Re}\,(& |g_v|^2 |\langle Y_\Lambda\rangle|^2 b_1(\Lambda) + [|g_a|^2 |\langle i\gamma_5 Y_{\Lambda-1}\rangle|^2 \\ & + |g_p|^2 |\langle i\gamma_4\gamma_5 Y_{\Lambda-1}\rangle|^2 + 2g_p^* g_a \langle i\gamma_4\gamma_5 Y_{\Lambda-1}\rangle^* \langle i\gamma_5 \mathcal{J}_{\Lambda-1}\rangle] \end{aligned}$$

---

*For $j_2 = 0$ the γ quanta are, of course, not circularly polarized.

*For $j_1 = 0$ P_μ coincides with the polarization of the μ^- meson at the instant of its capture by the nucleus, P_μ^0, which is experimentally observed in measurements of the asymmetry of electrons from μ^- decay in matter; in the general case P_μ and P_μ^0 are connected by the relation

$$P_\mu^0 = {}^1\!/_3\, P_\mu\, [1 + 2(2j_1 + 1)^{-2}].$$

$$\begin{aligned}
&\times b_1(\Lambda-1)+2\sum_I\Big\{g_v^*g_a\langle Y_\Lambda\rangle^*\langle\mathcal{Y}_{I\Lambda}\rangle b_2(\Lambda)\\
&+[g_v^*g_a\langle i\gamma_5\mathcal{Y}_{I\Lambda-1}\rangle^*\langle i\gamma_5\mathcal{Y}_{\Lambda-1}\rangle\\
&+g_p^*g_v\langle i\gamma_4\gamma_5Y_{\Lambda-1}\rangle^*\langle i\gamma_5\mathcal{Y}_{I\Lambda-1}\rangle]\,b_2(\Lambda-1)\\
&+\sum_{II'}\{|g_a|^2\langle\mathcal{Y}_{I\Lambda}\rangle^*\langle\mathcal{Y}_{I'\Lambda}\rangle b_3(\Lambda)\\
&+|g_v|^2\langle i\gamma_5\mathcal{Y}_{I\Lambda-1}\rangle^*\langle i\gamma_5\mathcal{Y}_{I'\Lambda-1}\rangle b_3(\Lambda-1)\}\\
&+2\sum_{\Lambda'=\Lambda\pm1}\Big\{[g_v^*g_a\langle Y_\Lambda\rangle^*\langle i\gamma_5Y_{\Lambda'}\rangle\\
&+g_p^*g_v\langle i\gamma_4\gamma_5Y_{\Lambda'}\rangle^*\langle Y_\Lambda\rangle]\,b_4(\Lambda,\ \Lambda')\\
&+\sum_I[-|g_v|^2\langle Y_\Lambda\rangle^*\langle i\gamma_5\mathcal{Y}_{I\Lambda'}\rangle+|g_a|^2\langle i\gamma_5Y_{\Lambda'}\rangle^*\langle\mathcal{Y}_{I\Lambda}\rangle\\
&+g_p^*g_a\langle i\gamma_4\gamma_5Y_{\Lambda'}\rangle^*\langle\mathcal{Y}_{I\Lambda}\rangle]\,b_5(\Lambda,\Lambda')\\
&+\sum_{II'}g_v^*g_a\langle i\gamma_5\mathcal{Y}_{I\Lambda'}\rangle^*\langle\mathcal{Y}_{I'\Lambda}\rangle b_6(\Lambda,\ \Lambda')\Big\}\Big),
\end{aligned}\tag{3b}$$

where Λ is the orbital angular momentum of the neutrino, and the index I takes the values Λ, $\Lambda \pm 1$.

The quantity A is, up to a constant factor, the total probability for the process under consideration. The abovementioned nuclear matrix elements and the coefficients a_n, b_n are given in the Appendix.

Formulas (3) apply to the case when the neutrino is emitted with the definite angular momentum $\Lambda = \Lambda_{min}$, the smallest possible according to the selection rules. Here the values of Λ_{min} for relativistic transitions (whose matrix elements contain γ_5) differ by ±1 from the values of Λ_{min} for nonrelativistic transitions between the same states. Strictly speaking, the expressions for A and B should be summed over $\Lambda \geq \Lambda_{min}$, since the condition $k_\nu R \ll 1$ is not satisfied in the μ^- capture owing to the large energy released (k_ν is the wave number of the emitted neutrino, and R is the radius of the nucleus). However, various estimates and actual calculations show[3] that the probability for the emission of the neutrino with $\Lambda = \Lambda_{min}$ is considerably higher than the probability for the emission of the neutrino with larger angular momenta.

It should be noted that formulas (3) contain Gell-Mann's[4] correction to the allowed transitions on account of the "weak magnetism." In order to see this, we consider the transition $\Delta j \equiv j_2 - j_1 = \pm 1$ (no). It is mainly due to the forbidden axial-vector interaction (matrix element $\langle\mathcal{Y}_{10}\rangle \sim \langle\sigma\rangle$). The correction caused by the "weak magnetism" is determined by the matrix element $\langle i\gamma_5\mathcal{Y}_{11}\rangle$. Indeed, the total matrix element for the μ transition, M_V, corresponding to the nuclear matrix element $\langle i\gamma_5\mathcal{Y}_{11}\rangle$ in the first approximation in $(v/c)_{nucl}$ and neglecting terms containing $(k_\nu r)^3$, can be written in the form (up to constant factor)

$$\begin{aligned}
&M_v\sim g_v\sum_m\langle i\gamma_5\mathcal{Y}_{11m}^*\rangle\,(\bar{u}_\nu i\,[1-\gamma_5]\,\mathcal{Y}_{11m}(\mathbf{k}_\nu/k_\nu)\,u_\mu)\\
&\qquad\sim\frac{\mu g_v\hbar}{2Mc}\int dV\psi_{j_2}^*\{(-i\,[\mathbf{r}\times\nabla]+\sigma)\,\mathbf{curl}\ \mathbf{A}\}\,\psi_{j_1},\\
&\mathbf{A}=(\mathbf{k}_\nu\mathbf{r})\,(\bar{u}_\nu\,[1-\gamma_5]\,\sigma u_\mu),
\end{aligned}\tag{4}$$

where M is the mass of the nucleon, and u_ν and u_μ are the Dirac bispinors for the neutrino and the μ^- meson. We see that the structure of M_V is analogous to that of the energy operator for the interaction of a magnetic moment with the magnetic field. The quantity μ, the total magnetic moment for the transition in units of a nuclear magneton, takes, according to Gell-Mann,[4] account of the virtual π mesons. It is, however, easy to show that for transitions of the type $\Delta j = \pm 1$ (no) the corrections for "weak magnetism" and other relativistic corrections of the same order of smallness [of first order in $(v/c)_{nucl}$] do not affect the polarization of the γ rays, although they contribute to the total probability of the process. The problem of such corrections in the μ^- capture was treated in more detail by Ioffe.[5]

In deriving the expression for C_γ we took into account the effect of the hyperfine splitting of the levels of the mesic atom, which plays an essential role in the process under consideration. In particular, in transitions obeying the Fermi selection rules the circular polarization of the γ quanta is entirely due to the presence of the hyperfine interaction which leads to the polarization of the nucleus in the intermediate state. In this case the circular polarization may have a considerable magnitude. For example, for $j_1 = \frac{1}{2}$, $\Lambda = 0$ ("allowed" transition), and $J = 1$ (dipole γ quantum) we have for a pure Fermi transition

$$\alpha=\begin{cases}\ \ {}^1\!/_2, & j_3={}^1\!/_2\\ -{}^1\!/_4, & j_3={}^3\!/_2.\end{cases}$$

Without account of the hyperfine interaction we would have obtained $\alpha = 0$. As another example we consider an allowed transition followed by dipole radiation ($\Lambda = 0$, $J = 1$) with $j_1 = j_2 = j_3 = \frac{1}{2}$ and Gamow-Teller coupling. Neglecting the hyperfine structure we obtain $\alpha = {}^2\!/_3$, while its inclusion leads to $\alpha = {}^1\!/_6$. The maximal value of α is $\alpha_{max} = 1$, corresponding to $|(C_\gamma)_{max}| = P_\mu \approx$ 15 to 20%.[6] A polarization of such magnitude occurs, for example, in the transition $0 \to 1 \to 0$ with $\Lambda = 0$ and $J = 1$. The formulas for A and B become much simpler for $j_1 = 0$, when there is no hyperfine splitting. The expressions for the quantities a_n and b_n for $j_1 = 0$ and also for $\Lambda = 0$ ("allowed" transitions) are given in the Appendix.

The occurrence of the circular polarization of the γ rays in the process under consideration is not connected with the nonconservation of spatial parity in the interaction $(\bar{n}p)(\bar{\nu}\mu)$. The measurement of C_γ cannot, therefore, serve to determine the handedness of the neutrino emitted in the μ^- capture. On the other hand, it is precisely this circumstance which makes possible the independent determination of the sign of the longitudinal polarization of the μ^- meson via the quantity C_γ.

The measurement of C_γ is best performed for nuclei with zero spin, since the hyperfine interaction leads to an additional depolarization of the μ^- mesons. Besides this, the lifetime of the μ^- mesons in mesoatomic orbits is larger than $\hbar/E_{hyp}$, where E_{hyp} is the shift of the mesoatomic levels due to the hyperfine interaction. The μ^- meson, therefore, will interact with the spin of the nucleus until its transition to the K orbit (unless, of course, it is captured immediately in the K orbit). This implies that at the instant of the entrance of the μ^- meson in the K orbit the nucleus may be partly polarized, which was not taken into account in the derivation of (3). It is very difficult to take this effect into account consistently (see reference 7).

It should be noted that the isotopic spin selection rules ($\Delta T = 0$ for Fermi coupling, $\Delta T = 0, \pm 1$ for Gamow-Teller coupling) are important for the μ^- capture by light nuclei. Since stable nuclei in the ground state have the lowest possible isotopic spin, and the number of neutrons in them is greater or equal to the number of protons, the μ^- capture, which increases the number of neutrons, will lead to an increase in the isotopic spin. The transitions obeying the Gamow-Teller selection rules will therefore predominate in the μ^- capture by light nuclei with excitation of discrete nuclear levels.

We note that the μ^- capture leads in the majority of cases to the emission of a neutron by the nucleus. Nevertheless, the transition of the nucleus into a discrete state may have a considerable probability. For example, the μ^- capture in C^{12} leads, with a probability of 13%, to the formation of a bound state of B^{12}.[3] The theoretical calculations of the probability for the transition of the nucleus into a particular state are not sufficiently reliable owing to our scarce knowledge of the nuclear wave functions. The observation of the spectrum of the γ rays emitted by the nucleus after the μ^- capture, which must precede the measurement of their circular polarization, is therefore of interest in itself.

APPENDIX

The aforementioned nuclear matrix elements are determined by the following formulas:

$$\langle Y_\Lambda \rangle \equiv \langle j_2 m_2 | j_\Lambda(k_\nu r) R_\mu(r) Y_{\Lambda m} | j_1 m_1 \rangle / C^{j_2 m_2}_{j_1 m_1 \Lambda m};$$

$$\langle \mathcal{Y}_{l\Lambda} \rangle \equiv \langle j_2 m_2 | j_\Lambda(k_\nu r) R_\mu(r) \mathcal{Y}_{l\Lambda m} | j_1 m_1 \rangle | C^{j_2 m_2}_{j_1 m_1 l m}.$$

Here $j_\Lambda(x)$ is the spherical Bessel function;* $R_\mu(r)$ is the normalized wave function of the ground state of the mesic atom; for nuclei with not too large Z we can set $R_\mu(r) \approx \text{const} = R_\mu(0)$; $Y_{\Lambda m}$ is the associated Legendre function,

$$\mathcal{Y}_{l\Lambda m} = \sum_{m_\Lambda, \lambda} C^{lm}_{\Lambda m_\Lambda 1\lambda} Y_{\Lambda m \Lambda} \sigma_\lambda,$$

$$\sigma_{\pm 1} = \mp (\sigma_x \pm i\sigma_y)/\sqrt{2}, \quad \sigma_0 = \sigma_z,$$

σ_x, σ_y, and σ_z are the Pauli matrices, and $C^{c\gamma}_{a\alpha b\beta}$ are the Clebsch-Gordan coefficients.

The matrix elements for the relativistic transitions, containing the matrix $\gamma_5 = \gamma_1\gamma_2\gamma_3\gamma_4$, are defined in a similar manner:

$$a_1(\Lambda, \Lambda') = (-)^{(\Lambda+\Lambda'+1)/2} \sqrt{(2\Lambda+1)/3}\, C^{10}_{\Lambda 0 \Lambda' 0};$$

$$a_2(\Lambda, \Lambda') = (-)^{(\Lambda-\Lambda'+1)/2+l} \sqrt{2} \sqrt{(2\Lambda+1)(2\Lambda'+1)}$$

$$\times C^{10}_{\Lambda 0 \Lambda' 0} W(\Lambda\Lambda' 11;\ 1l).$$

$$b_1(\Lambda) = (-)^{-j_1+j_3+\Lambda+J+1} \sqrt{3/2} \sum_j C_1(j) C_2(j) \delta_{l\Lambda}.$$

$$b_2(\Lambda) = 3(-)^{j_1+j_3+\Lambda+J+1} \sum_j \sqrt{2l+1}\, W$$

$$\times (j j\, {}^1\!/_2\, {}^1\!/_2;\ 1 j_1) C_1(j) C_3(j) \delta_{l'\Lambda};$$

$$b_3(\Lambda) = \sqrt{{}^3\!/_2}\, (-)^{-j_1+j_3+l+J+1} \sum_j C_1(j) \{\delta_{ll'} C_2(j)$$

$$+ 6(-)^{\Lambda+l+2j_1} \sqrt{(2l+1)(2l'+1)}$$

$$\times W(ll'11;\ 1\Lambda) W(j j\, {}^1\!/_2\, {}^1\!/_2;\ 1 j_1) C_3(j)\},$$

$$b_4(\Lambda, \Lambda') = (-)^{(\Lambda+\Lambda'-1)/2} \sqrt{(2\Lambda'+1)/3}\, C^{10}_{\Lambda 0 \Lambda' 0} \delta_{l\Lambda} b_2(\Lambda);$$

$$b_5(\Lambda, \Lambda') = (-)^{(\Lambda+\Lambda'+1)/2} \sqrt{(2\Lambda+1)/3}\, C^{10}_{\Lambda 0 \Lambda' 0} \delta_{l'\Lambda'} b_3(\Lambda);$$

---

*In view of the great magnitude of the released energy in the μ^- capture it is impossible to replace the Bessel function $j_\Lambda(k_\nu r)$ in the nuclear matrix elements by the first term in its expansion in powers of $k_\nu r$, as is usually done in β decay.

$$b_6(\Lambda,\ \Lambda') = (-)^{(\Lambda+\Lambda'-1)/2}\sqrt{3}\sqrt{(2\Lambda+1)(2\Lambda'+1)}$$

$$\times C^{10}_{\Lambda 0 \Lambda' 0}(-)^{J+j_1+j_3}$$

$$\sum_j C_1(j)\Big\{(-)^{\Lambda+2j_1+1}\, C_2(j)\, W(\Lambda\Lambda' 11;\ 1I)\,\delta_{II'}$$

$$+(-)^{I'}\,\frac{\sqrt{(2I+1)(2I'+1)}}{2\Lambda'+1}$$

$$\times[\delta_{I'\Lambda'}+6(2\Lambda'+1)\,W(\Lambda\Lambda' 11;\ 1I')\,W(II' 11;\,1\Lambda')]$$

$$\times C_3(j)\, W(jj\,{}^1\!/_2\,{}^1\!/_2;\ 1j_1)\Big\}_j .$$

$$C_1(j) = (2j_2+1)(2j+1)^2\sqrt{(2J+1)/J(J+1)}$$

$$\times W(JJj_2j_2;\ 1j_3)$$

$$C_2(j) = W(jjj_1j_1;\ 1\,{}^1\!/_2)\,W(jj\,{}^1\!/_2\,{}^1\!/_2;\ 1j_1)\,W(j_1j_1j_2j_2;\ 1I),$$

$$C_3(j) = \sum_f (2f+1)\,W(II'\,{}^1\!/_2\,{}^1\!/_2;\ 1f)\,W(jj_1fI,\ {}^1\!/_2 j_2)$$

$$\times W(jj_1fI';\ {}^1\!/_2 j_2)\,W(j_2j_2jj;\ 1f).$$

In these formulas $W(abcd;\,ef)$ is a Racah coefficient. If $j_1 = 0$, we have (a_n^0, b_n^0 are the values of a_n, b_n for $j_1 = 0$):

$$a_1^0(\Lambda,\ \Lambda') = a_1(\Lambda,\ \Lambda');\qquad a_2^0(\Lambda,\ \Lambda') = a_2(\Lambda,\ \Lambda'),$$

$$b_1^0(\Lambda) = b_4^0(\Lambda) = 0;$$

$$b_2^0(\Lambda) = (-)^{j_2+j_3+J+1}\sqrt{2j_2+1}\sqrt{\frac{2J+1}{J(J+1)}}$$

$$\times W(JJj_2j_2;\ 1j_3)\,\delta_{\Lambda j_2}\delta_{Ij_2};$$

$$b_3^0(\Lambda) = \sqrt{6}\,(-)^{\Lambda+J+j_3+1}(2j_2+1)\sqrt{\frac{2J+1}{J(J+1)}}\,W(j_2j_2 11;\ 1\Lambda)$$

$$\times W(JJj_2j_2;\ 1j_3)\,\delta_{Ij_2}\delta_{I'j_2};$$

$$b_5^0(\Lambda,\ \Lambda') = (-)^{(\Lambda+j_2+1)/2}\sqrt{(2\Lambda+1)/3}\,C^{10}_{\Lambda 0 j_2 0}\delta_{I'j_2}b_3^0(\Lambda);$$

$$b_6^0(\Lambda;\ \Lambda') = (-)^{(\Lambda+\Lambda'-1)/2}\sqrt{\frac{2\Lambda+1}{3(2\Lambda'+1)}}$$

$$\times C^{10}_{\Lambda 0\Lambda' 0}(-)^{J+j_2+j_3}(2j_2+1)\sqrt{\frac{2J+1}{J(J+1)}}\,W(JJj_2j_2;\ 1j_3)$$

$$\times[\delta_{j_2\Lambda'}+6(2\Lambda'+1)\,W(\Lambda\Lambda' 11;\ 1j_2)\ W(j_2j_2 11;\ 1\Lambda')].$$

If simultaneously $j_1 = 0$ and $j_2 = 0$, then

$$a_1^0(0,1) = -1/\sqrt{3},\qquad a_2^0(0,1) = -\sqrt{\tfrac{2}{3}},$$

$$b_1^0(0) = b_2^0(0) = b_4^0(0) = 0;$$

$$b_3^0(0) = \sqrt{6}\,(-)^{j_3+J}\sqrt{\frac{2J+1}{J(J+1)}}\,W(JJ11;\ 1j_3)\,\delta_{I1}\delta_{I'1};$$

$$b_5^0(0,1) = b_3^0(0)/\sqrt{3},$$

$$b_6^0(0,1) = 2(-)^{J+j_3+1}\sqrt{\frac{2J+1}{J(J+1)}}\,W(JJ11;\ 1j_3)\,\delta_{I1}\delta_{I'1}.$$

---

[1] R. P. Feynman and M. Gell-Mann, Phys. Rev. **109**, 193 (1958). E. C. G. Sudarshan and R. E. Marshak, Phys. Rev. **109**, 1890 (1958).

[2] L. Wolfenstein, Nuovo cimento **8**, 882 (1958). M. L. Goldberger and S. B. Treiman, Phys. Rev. **111**, 354 (1958).

[3] Jackson, Treiman, and Wyld, Jr., Phys. Rev. **107**, 327 (1957).

[4] M. Gell-Mann, Phys. Rev. **111**, 362 (1958).

[5] B. L. Ioffe, JETP **37**, 159 (1959), Soviet Phys. JETP **10**, 113 (1960).

[6] Ignatenko, Egorov, Khalupa, and Chultém, JETP **35**, 1131 (1958), Soviet Phys. JETP **8**, 792 (1959).

[7] É. I. Dolinskiĭ, JETP **36**, 1179 (1959), Soviet Phys. JETP **9**, 838 (1959).

Translated by R. Lipperheide
144

SOVIET PHYSICS JETP VOLUME 37 (10), NUMBER 3 MARCH, 1960

THERMOELECTRIC COEFFICIENTS OF METALS IN STRONG MAGNETIC FIELDS AND THE EFFECT OF DRAG OF ELECTRONS BY PHONONS

L. É. GUREVICH and G. M. NEDLIN

Leningrad Physico-Technical Institute, Academy of Sciences, U.S.S.R.

Submitted to JETP editor April 4, 1959

J. Exptl. Theoret. Phys. (U.S.S.R.) **37**, 765-775 (September, 1959)

The behavior of the thermoelectric tensor in strong magnetic fields, when the electron Larmor frequency is greater than the collision frequency, is considered by the methods proposed by Lifshitz, Azbel', and Kaganov.[1-3] Drag of the electrons by phonons is taken into account, and it is shown that this latter effect significantly changes the asymptotic values of the tensor (for large values of the magnetic field) and also its dependence on the direction of the magnetic field relative to the crystal axes (in the case of a complex topology of the Fermi surface).

THE asymptotic behavior of the thermoelectric tensor in strong magnetic fields was studied by I. M. Lifshitz and Peschanskiĭ.[4] However, they did not take into account the phenomenon of the drag on electrons by phonons. The aim of the present work is the consideration of this latter effect. We shall consider the region of low temperatures, where $T \ll \Theta$ (Θ is the Debye temperature and T the temperature of the specimen).

1. THE KINETIC EQUATIONS FOR ELECTRONS AND PHONONS

The linearized kinetic equations for the electron and phonon distribution functions, $n(\mathbf{p})$ and $N(\mathbf{q})$, in the presence of a temperature gradient, a magnetic field directed along the z axis, and a chemical potential gradient $\nabla\mu$, have the form

$$\frac{\partial(n-n_0)}{\partial t} = -\frac{\partial(n-n_0)}{\partial\tau}\omega^* - t_{ed}^{-1}\hat{W}_{ed}(n-n_0) + x\frac{\partial n_0}{\partial x}\frac{\mathbf{v}\nabla T}{T}$$
$$+\frac{\partial n_0}{\partial x}\frac{\mathbf{v}\nabla\mu}{T} + \int\frac{d^3q}{(2\pi\hbar)^3}V_{\mathbf{p},\,\mathbf{p}+\mathbf{q}}\{[(N_{\mathbf{q}}+1)(1-n_{\mathbf{p}})n_{\mathbf{p}+\mathbf{q}} - n_{\mathbf{p}}$$
$$\times(1-n_{\mathbf{p}+\mathbf{q}})N_{\mathbf{q}}]\,\delta(\varepsilon_{\mathbf{p}+\mathbf{q}}-\varepsilon_{\mathbf{p}}-\hbar\omega_{\mathbf{q}}) + [n_{\mathbf{p}+\mathbf{q}}(1-n_{\mathbf{p}})N_{-\mathbf{q}}$$
$$-n_{\mathbf{p}}(1-n_{\mathbf{p}+\mathbf{q}})(N_{-\mathbf{q}}+1)]\,\delta(\varepsilon_{\mathbf{p}+\mathbf{q}}-\varepsilon_{\mathbf{p}}+\hbar\omega_{\mathbf{q}})\};$$

$$\frac{\partial(N-N_0)}{\partial t} = -(N-N_0)t_{fd}^{-1} + \xi\frac{\partial N_0}{\partial\xi}\frac{\mathbf{s}\nabla T}{T} + \int\frac{2d^3p}{(2\pi\hbar)^3}V_{\mathbf{p},\,\mathbf{p}+\mathbf{q}}$$
$$\times[n_{\mathbf{p}+\mathbf{q}}(1-n_{\mathbf{p}})(N_{\mathbf{q}}+1) - n_{\mathbf{p}}(1-n_{\mathbf{p}+\mathbf{q}})N_{\mathbf{q}}]$$
$$\times\delta(\varepsilon_{\mathbf{p}+\mathbf{q}}-\varepsilon_{\mathbf{p}}-\hbar\omega_{\mathbf{q}}).$$

By the substitutions

$$n(\mathbf{p}) = n_0(\varepsilon - \mathbf{p}\mathbf{v}_e(\mathbf{p}))\,\text{and}\,N(\mathbf{q}) = N_0(\hbar\omega_{\mathbf{q}} - \mathbf{q}\mathbf{v}_f(\mathbf{q}))$$

and for small $\mathbf{v}_e$ and $\mathbf{v}_f$, these equations take the form

$$\frac{\partial}{\partial t}\left(\frac{\mathbf{p}\mathbf{v}_e}{T}\right) = -\frac{\partial}{\partial\tau}\left(\frac{\mathbf{p}\mathbf{v}_e}{T}\right)\omega^* - x\frac{\mathbf{v}\nabla T}{T} - \frac{\mathbf{v}\nabla\mu}{T} - t_{ed}^{-1}\hat{W}_{ed}\left(\frac{\mathbf{p}\mathbf{v}_e}{T}\right)$$
$$+\int\frac{d^3q}{(2\pi\hbar)^3}V_{\mathbf{p},\,\mathbf{p}+\mathbf{q}}\left\{\frac{\mathbf{v}_e(\mathbf{p})-\mathbf{v}_f(\mathbf{q})}{T}\mathbf{q}\left[\frac{n(x+\xi)}{n(x)}(N(\xi)+1)\right.\right.$$
$$\left.+\frac{n(x-\xi)}{n(x)}N(\xi)\right]\delta(\varepsilon_{\mathbf{p}+\mathbf{q}}-\varepsilon_{\mathbf{p}}) + \frac{\mathbf{v}_e(\mathbf{p}+\mathbf{q})-\mathbf{v}_e(\mathbf{p})}{T}(\mathbf{p}+\mathbf{q})$$
$$\times\left[\frac{n(x+\xi)}{n(x)}(N(\xi)+1)\,\delta(\varepsilon_{\mathbf{p}+\mathbf{q}}-\varepsilon_{\mathbf{p}}-\hbar\omega_{\mathbf{q}}) + \frac{n(x-\xi)}{n(x)}N(\xi)\right.$$
$$\left.\left.\times\,\delta(\varepsilon_{\mathbf{p}+\mathbf{q}}-\varepsilon_{\mathbf{p}}+\hbar\omega_{\mathbf{q}})\right]\right\};$$

$$\frac{\partial}{\partial t}\left(\frac{\mathbf{q}\mathbf{v}_f}{T}\right) = \int\frac{2d^3p}{(2\pi\hbar)^3}\left\{\frac{\mathbf{v}_e(\mathbf{p})\,\mathbf{p}}{T}\left[\frac{n(x)(1-n(x-\xi))}{N(\xi)}\right.\right.$$
$$\left.\left.-\frac{n(x+\xi)(1-n(x))}{N(\xi)}\right] - \frac{\mathbf{v}_f(\mathbf{q})\,\mathbf{q}}{T}\frac{n(x+\xi)(1-n(x))}{N(\xi)}\right\}$$
$$\times V_{\mathbf{p},\,\mathbf{p}+\mathbf{q}}\,\delta(\varepsilon_{\mathbf{p}+\mathbf{q}}-\varepsilon_{\mathbf{p}}) - t_{fd}^{-1}\frac{\mathbf{q}\mathbf{v}_f}{T} - \xi\frac{\mathbf{s}\nabla T}{T}. \qquad (1)$$

Here τ is a quantity defining the phase of the electron in the Larmor orbit; $\omega^* = 2\pi/T_0$, where T_0 is the characteristic time for motion around the orbit, after which the momentum of the electron changes by a quantity of the order of the period of the reciprocal lattice or (in the case of a closed trajectory) returns to its initial value (see references 2 and 3), $\mathbf{p}$ is the quasi-momentum of the electron, $\mathbf{v} = \partial\epsilon/\partial\mathbf{p}$ is its velocity, $\mathbf{q}$ is the quasi-momentum of the phonon, $\mathbf{s} = \partial(\hbar\omega)/\partial\mathbf{q}$ is its group velocity, $\hat{W}_{ed} \sim 1$ and t_{ed} are the dimensionless collision operator and the characteristic relaxation time of electrons on lattice defects and on each other. The latter is of the order $\hbar E/T^2$, where E is an energy of atomic order[8] and can be shown to be important at low temperatures for sufficiently pure metals; t_{fd} is the relaxation time of phonons on lattice defects and on each other; $\xi = \hbar\omega_q/T$; $x = (\epsilon_p - \mu)/T$; T is the temperature in energy units. In the latter system, and in what follows, $n(x)$ and $N(\xi)$ denote the equilibrium distributions for electrons and phonons. When $\mathbf{v}_e$ does not appear under the integral sign, the inelasticity is taken into account in $n(x \pm \xi)$, and is neglected in the δ-function, which is valid. The vectors $\mathbf{v}_e(\mathbf{p})$ and $\mathbf{v}_f(\mathbf{p})$ have the meaning of drift velocities of electrons and phonons, respectively. Their interaction tends to equalize these velocities. In this case, the drag on the electrons by the phonons is expressed by an integral containing $(\mathbf{v}_e - \mathbf{v}_f)$.

If (for its estimate) we consider $\mathbf{v}_e - \mathbf{v}_f$ to be constant, then the remaining integral I, multiplied by T/p, determines the order of magnitude of the reciprocal of the relaxation time for scattering of electrons on phonons in terms of the momentum t_5^{-1}.

The law of conservation of energy for $\Theta \gg T \gg ms^2$ gives $\epsilon(\mathbf{p}+\mathbf{q}) - \epsilon(\mathbf{p}) = \mathbf{v}\cdot\mathbf{q} + \frac{1}{2}\sum m_{\alpha\beta}^{-1} \times q_\alpha q_\beta = 0$. Here $m_{\alpha\beta}^{-1} = \partial^2\epsilon/\partial p_\alpha \partial p_\beta$. We set $\mathbf{q} = \mathbf{q}_\perp + q_\parallel \mathbf{v}/v$, where $\mathbf{q}_\perp \cdot \mathbf{v} = 0$. Since $q \ll mv$, then, in first approximation, $q_\parallel = 0$, and in second, $q_\parallel = -\sum' m_{\alpha\beta}^{-1} q_\alpha q_\beta / 2v$, where the primes on the sums indicate that the directions of α and β are orthogonal to $\mathbf{v}$. After integration over $q_\parallel$ in I, we get an integral of the form

$$\int d^2q_\perp (\mathbf{q}_\perp + q_\parallel \mathbf{v}/v)\,\Phi(\mathbf{q}). \tag{2}$$

In $\Phi(\mathbf{q})$, we can set $\mathbf{q} = \mathbf{q}_\perp$, and since $\Phi(\mathbf{q}) = \Phi(-\mathbf{q})$, there remains only the integral over the second component. Since $V_{\mathbf{p},\mathbf{p}+\mathbf{q}} \sim q$, while $q_\parallel \sim q_\perp^2$, then $t_5^{-1} \sim T^5$, i.e., actually, the time of equalization of the drift velocities of the electrons and phonons is connected with momentum relaxations (see references 5 — 7), which is physically understandable, since the drag on the electrons by the phonons takes place as a result of the change in their momentum due to interaction with the phonons. The integral containing the difference $\mathbf{v}_e(\mathbf{p}+\mathbf{q}) - \mathbf{v}_e(\mathbf{p})$ expresses the trend to equalization of the drift velocities of electrons with different momenta by the agency of their interaction with phonons. Since $\epsilon_{p+q} - \epsilon_p = \hbar\omega_q$, while the angular separation of the vectors $\mathbf{p}+\mathbf{q}$ and $\mathbf{p}$ is insignificant, then this is actually the energy relaxation of electrons due to phonons. In a manner similar to the above, it is not difficult to show that the corresponding reciprocal of the relaxation time is $t_3^{-1} \sim T^3$.

The drift velocity of the phonon can be eliminated from (1) in the stationary case. Inasmuch as we are interested here in the case in which the electron current $j = 0$, we can neglect the integral term containing $\mathbf{v}_e$ in the phonon equation. It can be shown that consideration of this term in the calculation of the electric conductivity leads to the "renormalization" of the relaxation time, so that the effective relaxation time of the electrons is

$$\tau_e^{-1} = t_e^{-1} - \alpha t_5^{-1} t_f t_{fe}^{-1},$$

where $t_f^{-1} = t_{fd}^{-1} + t_{fe}^{-1}$, $\quad t_e^{-1} = t_{ed}^{-1} + t_{ef}^{-1}$;

t_{ef} is the relaxation time of electrons on phonons, t_{fe} is the relaxation time of phonons on electrons, determined by the integral for $\mathbf{v}_f \cdot \mathbf{q}/T$ in the phonon equation (1), and α is a numerical coefficient. If the metal is "dirty," i.e., if $t_f \ll t_{fe}$, or $t_e \ll t_{ef}$, then $\tau_e = t_e$. If the metal is "clean," then τ_e has the same temperature dependence as $t_e(t_{ef})$, and differs only numerically from it.

Physically, the latter effect represents the change in the scattering of electrons by phonons as a result of the fact that the drift velocity of the latter increases because of the presence of drift in the electrons ("mutual" drag).

Turning to our case, we get for $\mathbf{v}_e$ the equations

$$\frac{\partial}{\partial\tau}\left(\frac{\mathbf{p}\mathbf{v}_e}{T}\right)\omega^* + t_0^{-1}\hat{W}\left\{\frac{\mathbf{v}_e\mathbf{p}}{T}\right\} = -\frac{\mathbf{v}\nabla\mu}{T} - x\frac{\mathbf{v}\nabla T}{T} - \frac{\nabla T}{T}\mathbf{F}; \tag{3}$$

$$\mathbf{F} = \int \frac{d^3q}{(2\pi\hbar)^3} t_f(\mathbf{q})\,\xi s V_{\mathbf{p},\mathbf{p}+\mathbf{q}} \left[\frac{n(x+\xi)}{n(x)}(N(\xi)+1) + \frac{n(x-\xi)}{n(x)}N(\xi)\right]\delta(\varepsilon_{\mathbf{p}+\mathbf{q}} - \varepsilon_{\mathbf{p}}). \tag{4}$$

Here

$$t_0^{-1}\hat{W} = t_{ed}^{-1}\hat{W}_{ed} + t_{ef}^{-1}\hat{W}_{ef}.$$

We can get the order of the quantity F by equating the integral for it to the integral determining the relaxation time t_5:

$$F \sim \frac{p}{q} t_f s t_5^{-1} \sim s\frac{\Theta}{T} t_f t_5^{-1}. \tag{5}$$

2. SOLUTION OF THE KINETIC EQUATION IN THE CASE OF SCATTERING OF THE ELECTRONS BY LATTICE DEFECTS OR BY EACH OTHER

We must solve the equation

$$\frac{\partial}{\partial\tau}\left(\frac{\mathbf{p}\mathbf{v}_e}{T}\right)\omega^* + t_0^{-1}\hat{W}\left(\frac{\mathbf{p}\mathbf{v}_e}{T}\right) = -x\frac{\mathbf{v}\nabla T}{T} - \frac{\nabla T}{T}\mathbf{F}. \tag{6}$$

Solving it, we can find the current $j_i^{(T)} = \sum_k \beta_{ik}\nabla_k T$; here, the desired thermoelectric tensor α_{ik}, which is determined from the relation $\nabla_i\mu = -e\sum_k \alpha_{ik}\nabla_k T$ for the condition $j = 0$, is

$$\alpha_{ik} = -\sum_l \sigma_{il}\beta_{lk}.$$

The tensor σ_{ik} is known (see references 2 and 3); therefore it is necessary to find the tensor β_{ik}.

We shall seek a solution of Eq. (6) in the form

$$\mathbf{p}v_c/T = -t_0\sum_i \psi_i \nabla_i T/T.$$

For ψ_i, we obtain the equation

$$\frac{\partial\psi_i}{\partial\tau} + \gamma_0\hat{W}(\psi_i) = \gamma_0 x v_i + \gamma_0 F_i. \tag{6'}$$

Here $\gamma_0 = 1/\omega^* t_0 \ll 1$. To each of the two terms of inhomogeneity in Eq. (6′), we can juxtapose ψ_{i1}, and ψ_{i2}, respectively.

In accord with this, we also have

$$\beta_{ik} = \beta_{ik}^{(1)} + \beta_{ik}^{(2)}, \qquad \alpha_{ik} = \alpha_{ik}^{(1)} + \alpha_{ik}^{(2)}.$$

In this case, quantities with index (1) are defined directly by the effect of the temperature gradient on the electron, and those with index (2) by the drag of electrons by phonons. The asymptotic value of the tensor $\alpha^{(1)}$ was found in reference 4. If $\alpha_{ik} = \gamma_0^{p_{ik}} a_{ik}$, then the order of the $a_{ik}^{(1,2)}$ can easily be estimated.* Let

$$\beta_{ik}^{(1)} = \gamma_0^{r_{ik}} b_{ik}^{(1)}, \qquad \sigma_{ik} = \gamma_0^{s_{ik}} c_{ik};$$

Then $a^{(1)} \sim b^{(1)}/ec$. But $b^{(1)}/c$ is of the order of the ratio of the right sides of the kinetic equations determining $\beta^{(1)}$ and σ, multiplied by T/μ (in view of the presence of the factor x in the inhomogeneity of the equation for $\beta^{(1)}$) so that

$$a_{ik}^{(1)} \sim T/e\mu. \tag{7}$$

Equating the same two terms in the inhomogeneity of the equation and taking (5) into account, and also the fact that F_i is an (almost) even function of x, we find

$$a^{(2)} \sim a^{(1)}\frac{s}{v}\frac{\Theta}{T}\frac{t_f}{t_5}\frac{\mu}{T} \sim a^{(1)}\left(\frac{\Theta}{T}\right)^2\frac{t_f}{t_5}, \tag{8}$$

since $s/v = (\hbar s/a)a/\hbar v \approx \Theta/\mu$ (a is the lattice constant). If the phonons are scattered by the electrons, then $t_f \sim (\hbar/\Theta)\mu/T$, $t_5 \sim (\hbar/\Theta)(\Theta/T)^5$ (see references 5 – 7), so that,

$$a^{(2)} \sim a^{(1)}(T/\Theta)^2\mu/\Theta. \tag{8'}$$

Therefore, for not very low temperatures, i.e.,

$$\Theta > T > T_\alpha \sim \Theta(\Theta/\mu)^{1/2} \tag{9}$$

the drag effect predominates even in those elements of the tensor α_{ik} in which the asymptotic values of $\alpha_{ik}^{(1)}$ and $\alpha_{ik}^{(2)}$ are identical in γ_0. But, as will be seen below, the asymptotic value (in γ_0) of $\alpha_{ik}^{(2)}$ is always smaller than the asymptotic value of $\alpha_{ik}^{(1)}$. In what follows, only $\beta_{ik}^{(2)}$ and $\alpha_{ik}^{(2)}$ are computed. Therefore the index 2 is omitted for brevity.

For calculation of β_{ik}, it is necessary to solve

$$\frac{\partial\psi_i}{\partial\tau} + \gamma_0\hat{W}(\psi_i) = \gamma_0 F_i, \tag{6''}$$

$$\beta_{ik} = \lim_{G\to\infty}\frac{2et_0}{(2\pi\hbar)^3}\frac{1}{G}\iint d\varepsilon\, dp_z \frac{\partial n}{\partial\varepsilon}\frac{T_0 eH}{c}\int v_i\psi_k d\tau. \tag{10}$$

Integration is carried out over all momentum space; G is the number of cells included in the limits of integration. As in references 2 and 3, it is necessary to treat the following cases separately ($|\epsilon - \mu| \sim T$):

1. The trajectories $\epsilon = \text{const}$, $p_z = \text{const}$ are closed and lie within the limits of a single cell of the reciprocal lattice.
2. There is a layer of open trajectories.
3. The approximation to "critical" directions (see reference 3).

1. Closed Trajectories Lying Within the Limits of a Single Cell

As in reference 2, we seek ψ_i in the form

$$\psi_i = \sum_{n=0}^{\infty}\gamma_0^n\psi_i^{(n)}; \tag{11}$$

We then obtain the set of recurrent equations

$$\partial\psi_i^{(0)}/\partial\tau = 0, \quad \partial\psi_i^{(1)}/\partial\tau + \hat{W}(\psi_i^{(0)}) = F_i,$$
$$\partial\psi_i^{(n)}/\partial\tau + \hat{W}(\psi_i^{(n-1)}) = 0 \quad \text{при } n \geqslant 2. \tag{12}$$

The periodicity in τ serves as an additional condition on these equations, i.e.,

$$\oint\hat{W}(\psi_i^{(0)})\,d\tau = \oint F_i d\tau, \qquad \oint\hat{W}(\psi_i^{(n)})\,d\tau = 0, \; n \geqslant 2. \tag{13}$$

Integration is carried out over τ along the closed trajectory. Since all $\oint F_i d\tau \neq 0$, then all

$$\psi_i^{(0)} = C_i^{(0)}(\varepsilon, p_z) \neq 0.$$

We also take it into account that $\oint v_{x,y} d\tau \sim \oint dp_{y,x} = 0$; then the tensor in this case generally has the form

$$\beta_{ik} = \begin{vmatrix} \gamma_0 b_{xx} & \gamma_0 b_{xy} & \gamma_0 b_{xz} \\ \gamma_0 b_{yx} & \gamma_0 b_{yy} & \gamma_0 b_{yz} \\ b_{zx} & b_{zy} & b_{zz} \end{vmatrix}. \tag{14}$$

The symmetry properties of the crystal can change the asymptotic value of the tensor β. Thus, for example, if there is mirror symmetry relative to the plane zx, then, inasmuch as both v_i and F_i are transformed in the symmetry transformation as p_i, and the operator $\partial/\partial\tau \sim v_y\partial/\partial p_x$ is odd, while $\hat{W}$

---

*As in references 1–3, we denote by γ_0 the small ratio $\gamma_0 = H_0/H$, where H_0 is a characteristic value of the magnetic field (for which the Larmor period is of the order of the relaxa-time t_0).

is even relative to the transformation $p_y, p'_y \to -p_y, -p'_y$, the equation for ψ_i can be written in the form

$$\hat{L}(\psi_i) = \gamma_0 \dot{F}_i, \text{ where } L_{p_y, p'_y}(\mathbf{H})| = -L_{-p_y, -p'_y}(-\mathbf{H}),$$

i.e.,

$$\psi_{x,z}(p_y, \mathbf{H}) = \psi_{x,z}(-p_y, -\mathbf{H}),$$

$$\psi_y(p_y, \mathbf{H}) = -\psi_y(-p_y, -\mathbf{H}).$$

Therefore β_{xz}, β_{zx}, β_{xx}, β_{yy}, β_{zz} are even, and β_{xy}, β_{yx}, β_{zy}, β_{yz} are odd functions of $\mathbf{H}$, so that $\beta_{xz} \sim \gamma_0^2$; $\beta_{zx} \sim \gamma_0^2$; $\beta_{xx} \sim \gamma_0^2$; $\beta_{yy} \sim \gamma_0^2$; $\beta_{zy} \sim \gamma_0^2$.

This result is found to be in agreement with the requirements imposed in the macroscopic theory on the tensor β_{ik}. Actually, if we write

$$\beta_{ik} = c_{ik} + c_{kllm} H_{lm} + c_{iklml'm'} H_{lm} H_{l'm'},$$

where H_{lm} is an antisymmetric tensor, the dual to the pseudovector $\mathbf{H}$, and c is a tensor of the corresponding rank, and if we consider that, when $\mathbf{H} = (0, 0, H)$, only $H_{xy} = -H_{yx} \neq 0$, then it is easy to see, from the presence of mirror symmetry relative to the plane zx, that the components of the tensor β_{ik} which contain an even number of signs ik equal to y are even functions of $\mathbf{H}$, and vice versa.

Returning to the general case, we have (making use of the expression for σ^{-1} from reference 3):

$$\alpha_{ik} = \begin{vmatrix} a_{xx} & a_{xy} & a_{xz} \\ a_{yx} & a_{yy} & a_{yz} \\ a_{zx} & a_{zy} & a_{zz} \end{vmatrix}. \qquad (15)$$

The case in which the Fermi surface is closed and the number of electrons is equal to the number of holes should be specially noted. In such a case (see reference 2), the asymptotic value of the tensor σ is such that

$$\alpha_{i\kappa} = \begin{vmatrix} \gamma_0^{-1} a_{xx} & \gamma_0^{-1} a_{xy} & \gamma_0^{-1} a_{xz} \\ \gamma_0^{-1} a_{yx} & \gamma_0^{-1} a_{yy} & \gamma_0^{-1} a_{yz} \\ a_{zx} & a_{zy} & a_{zz} \end{vmatrix}. \qquad (16)$$

2. Open Trajectories

Equations (12) must be solved in this case under the additional condition of finiteness, i.e.,

$$\overline{\hat{W}(\psi_i)} = \overline{F_i}, \text{ where } \bar{f} = \lim_{\tau \to \infty} \frac{1}{2\tau} \int_{-\tau}^{+\tau} f\, d\tau$$

and integration is carried out over the entire trajectory. This means that

$$\overline{\hat{W}(\psi_i^{(0)})} = \overline{F_i}, \qquad \overline{\hat{W}(\psi_i^{(n)})} = 0 \quad \text{for } n \geqslant 1.$$

Generally, all $\overline{F}_i \neq 0$, so that all $C_i^{(0)}(\epsilon, p_z) \neq 0$. However, if all trajectories have infinite extension in one direction, chosen to be the x axis, then

$$\bar{v}_x \sim \lim_{\tau \to \infty} \frac{1}{2\tau} \int dp_y = 0,$$

since p_y changes within finite limits. Consequently, in this case,

$$\beta_{i\kappa} = \begin{vmatrix} \gamma_0 b_{xx} & \gamma_0 b_{xy} & \gamma_0 b_{xz} \\ b_{yx} & b_{yy} & b_{yz} \\ b_{zx} & b_{zy} & b_{zz} \end{vmatrix}. \qquad (17)$$

The expressions for the α_{ik} have the form

$$\alpha_{i\kappa} = \begin{vmatrix} \gamma_0^{-1} a_{xx} & \gamma_0^{-1} a_{xy} & \gamma_0^{-1} a_{xz} \\ a_{yx} & a_{yy} & a_{yz} \\ a_{zx} & a_{zy} & a_{zz} \end{vmatrix}. \qquad (18)$$

3. Approximation to "Critical" Directions

Let us consider the case here in accord with the classification given by I. M. Lifshitz and Peschanskiĭ.[3] For simplicity of calculation, we set $\hat{W} = 1$.

a) Approximation to an isolated direction, in which a layer of open trajectories appears. In this approximation, there are greatly extended trajectories whose period of motion is $\tau_0 \sim T_0/\vartheta$, where ϑ is the angle between the direction of the magnetic field and the direction in which the open trajectories occur.

The equation for ψ_i has the form

$$\partial\psi_i/\partial\tau + \gamma\psi_i = \gamma F_i, \qquad \gamma = \tau_0/t_0 \sim \gamma_0/\vartheta. \qquad (19)$$

Applying the Fourier method (see reference 2), we obtain

$$\beta_{i\kappa} = -\frac{2et_0}{(2\pi\hbar)^3} \lim_{G \to \infty} \frac{1}{G} \iint d\varepsilon\, dp_z \frac{\partial n}{\partial x} \frac{eH\tau_0}{c} \left\{ v_i^{(0)} F_\kappa^{(0)} + \gamma \sum_{n=1}^{\infty}{}' \frac{\gamma\left(v_i^{(n)} F_\kappa^{(-n)} + v_i^{(-n)} F_\kappa^{(n)}\right) + in\left(v_i^{(n)} F_\kappa^{(-n)} - v_i^{(-n)} F_\kappa^{(n)}\right)}{n^2 + \gamma^2} \right\}. \qquad (20)$$

Here, $v_i^{(n)}$, $F_k^{(n)}$ are the Fourier components of the corresponding quantities as functions of τ. Taking it into account that $v_0^{(n)} \sim \vartheta$, while the factor $1/\vartheta$ which comes from τ_0, is compensated by the factor $1/G$, and that $v_x^{(0)} = v_y^{(0)} = 0$, we obtain

$$\beta_{ik} = \begin{vmatrix} \gamma_0 b_{xx} & \gamma_0 b_{xy} & \gamma_0 b_{xz} \\ b_{yx} & b_{yy} & b_{yz} \\ b_{zx} & b_{zy} & b_{zz} \end{vmatrix}. \qquad (21)$$

Here, all the b_{ik} are functions of the ratio $\eta = \gamma_0/\vartheta$, while $\beta_{ik}(\infty) = \text{const}$, and as $\eta \to 0$:

$$b_{ik} = \begin{vmatrix} b_{xx}(0) & b_{xy}(0) & b_{xz}(0) \\ \eta b'_{yx} & \eta b'_{yy} & \eta b'_{yz} \\ b_{zx}(0) & b_{zy}(0) & b_{zz} \end{vmatrix}. \qquad (22)$$

Hence we obtain for the tensor α_{ik}:

$$\alpha_{i\kappa} = \begin{vmatrix} \gamma_0^{-1} a_{xx} & \gamma_0^{-1} a_{xy} & \gamma_0^{-1} a_{xz} \\ a_{yx} & a_{yy} & a_{yz} \\ a_{xz} & a_{zy} & a_{zz} \end{vmatrix}, \qquad (23)$$

where all a_{ik} are functions of η.

As $\eta \to \infty$, all $a_{ik} \to a_{ik}(\infty) = \text{const}$, and as $\eta \to 0$,

$$a_{ik} = \begin{vmatrix} \eta a'_{xx} & \eta a'_{xy} & \eta a'_{xz} \\ a_{yx}(0) & a_{yy}(0) & a_{yz}(0) \\ a_{xz}(0) & a_{zy}(0) & a_{zz}(0) \end{vmatrix} \tag{24}$$

in agreement with Eqs. (15) and (18).

b) Approximation to the direction in which the layer of open trajectories disappears. If we denote by ϑ the angle between the direction of the magnetic field and the critical direction, then, since the contribution to the tensor β_{ik} from the open trajectories $\sim \vartheta$, in this case $\beta_{ik} = g_{ik} + \vartheta d_{ik}$, where the tensor g_{ik} has a structure of the type (14), and the tensor d_{ik} has the type (17). By means of Eq. (29) of reference 3, we get the following expression for α_{ik}:

$$\alpha_{ik} = \begin{vmatrix} a_{xx} + \vartheta\gamma_0^{-1}c_{xx} & a_{xy} + \vartheta\gamma_0^{-1}c_{xy} & a_{xz} + \vartheta\gamma_0^{-1} c_{xz} \\ a_{yx} & a_{yy} & a_{yz} \\ a_{zx} & a_{zy} & a_{zz} \end{vmatrix}. \tag{25}$$

3. CASE OF SCATTERING OF ELECTRONS BY PHONONS

In view of the presence of two relaxation times for electrons relative to phonons, t_{ef} (see Sec. 1), it is necessary to investigate the role of the operators of relaxation for the direction $\hat{W}_5/t_5$ and the energy $\hat{W}_3/t_3$. If we introduce the function $n_1 = -\mathbf{v}_e \cdot \mathbf{p}\, \partial n_0/\partial \epsilon$, and multiply the electron equation in the system (1) by $\partial n_0/\partial x$, then the term containing $\mathbf{v}_e \cdot (\mathbf{p}+\mathbf{q}) - \mathbf{v}_e(\mathbf{p})$, has the form

$$\int M(x\Omega;\ x'\Omega')\, n_1(x'\Omega')\, dx'd\Omega'$$
$$- n_1(x\Omega) \int K(x\Omega;\ x''\Omega'')\, dx''d\Omega''.$$

Here Ω is the set of angular coordinates of the momentum $\mathbf{p}$. We write

$$\int M(x\Omega,\ x'\Omega')\, n_1(x'\Omega')\, dx'd\Omega'$$
$$= \int M(x\Omega,\ x'\Omega')\,[n_1(x'\Omega') - n_1(x'\Omega)]$$
$$\times dx'd\Omega' + \int dx' \int M(x\Omega,\ x'\Omega')\, n_1(x'\Omega)\, d\Omega'.$$

The first of the integrals can be combined with $\hat{W}_5$, which represents a relaxation in direction, such that

$$t_3^{-1}\hat{W}_3(x\Omega,\ x'\Omega') = \delta(\Omega - \Omega')\Big\{\int M(x\Omega,\ x'\Omega'')\, d\Omega''$$
$$- \delta(x - x') \times \int K(x\Omega,\ x''\Omega'')\, dx''d\Omega''\Big\}.$$

Here,

$$M(x\Omega,\ x'\Omega') = V_{p,p'}\Delta\Big\{N_0(x'-x)\frac{n_0(x)}{n_0(x')}\delta(x'-x-\xi_{\mathbf{p}'-\mathbf{p}})$$
$$+ N_0(x-x')e^{x-x'}\frac{n_0(x)}{n_0(x')}\delta(x'-x+\xi_{\mathbf{p}'-\mathbf{p}})\Big\},$$
$$K(x\Omega,\ x'\Omega') = V_{\mathbf{pp}'}\Delta\Big\{N_0(x-x')\frac{n_0(x')}{n_0(x)}\delta(x'-x+\xi_{\mathbf{p}'-\mathbf{p}})$$
$$+ N_0(x'-x)e^{x'-x}\frac{n_0(x')}{n_0(x)}\delta(x'-x-\xi_{\mathbf{p}'-\mathbf{p}})\Big\}$$

(Δ = number of states in the interval $dx d\Omega$).

It is easy to establish the fact that, with accuracy up to terms $\sim T/\mu$, we have $K(x\Omega, x'\Omega') = M(x'\Omega, x\Omega')$, so that

$$t_3^{-1}\hat{W}_3(x\Omega,\ x'\Omega') = \delta(\Omega - \Omega')\Big\{L(x,\ x') - \delta(x - x')$$
$$\times \int L(x'',\ x)\, dx''\Big\},$$
$$\iint \hat{W}_3(x\Omega,\ x'\Omega')\, t_3^{-1} f(x')\, dx'dx \equiv 0. \tag{26}$$

This property of the operator $\hat{W}_3$ expresses the fact that a change in the total number of electrons in a solid angle can be brought about only as a result of collisions with a change in momentum.

We set $n_1 = \varphi(p_z, \tau)\chi(\epsilon)\,\partial n_0/\partial\epsilon$, which is possible in view of the δ-like character of the function $\partial n_0/\partial\epsilon$. The current is

$$j = \frac{2e}{(2\pi\hbar)^3}\iint dp_z d\tau \int \mathbf{v}\varphi(p_z,\ \tau)\chi(\varepsilon)\frac{eHT_0}{c}\frac{\partial n_0}{\partial\varepsilon}\, d\varepsilon$$
$$= \frac{2e}{(2\pi\hbar)^3}\iint dp_z d\tau \frac{eHT_0}{c}\mathbf{v}(\mu)\varphi(p_z\tau),$$

since $\chi(\epsilon)$ can always be chosen in such a fashion that

$$\int \frac{\partial n_0}{\partial\varepsilon}\chi(\varepsilon)\, d\varepsilon = 1.$$

The kinetic equation for n_1 has the form

$$\frac{\partial n_1}{\partial\tau}\omega^* + t_5^{-1}\hat{W}_5(n_1) + t_3^{-1}\hat{W}_3(n_1) = -R\frac{\partial n_0}{\partial\varepsilon}. \tag{27}$$

If $R(x) = R(-x)$, then the corresponding function $n_1(x) = n_1(-x)$, since $W(x, x') = W(-x, -x')$ (see reference 6).

Integrating Eq. (27) with respect to ϵ with account of Eq. (26), we obtain an equation for $\varphi(p_z\tau)$:

$$\omega^*\partial\varphi/\partial\tau + \hat{W}'(\varphi)/t_5 = R(0), \qquad W'(p_z\tau;\ p'_z\tau')$$
$$= \iint dx'dx W_5(xp_z\tau;\ x'p'_z\tau')\chi(\varepsilon')\,\partial n_0/\partial\varepsilon'. \tag{28}$$

Consequently, the function φ is determined by the directional relaxation time t_5. If $R(x) = -R(-x)$, then, correspondingly, $n_1(-x) = -n_1(x)$ and is determined from Eq. (27), where it is possible to discard the term $\hat{W}_5/t_5$ since $1/t_5 \ll 1/t_3$.

Inasmuch as the inhomogeneity in the kinetic equation, which determines the electrical conductivity and the drag effect, is an even function of x, then the tensors σ_{ik} and $\beta_{ik}^{(2)}$ contain $\gamma_5 \sim 1/\omega t_5$, and the coefficients in the expansion in powers of γ_5 are proportional to t_5. In the calculation of the tensor $\beta_{ik}^{(1)}$, it is necessary to take it into account that the even part (in x) in the equation determining the tensor is smaller than the odd by the factor T/μ, but in the calculation of the current from the odd part, a factor of the same order of magnitude appears.

We note that in view of the sharp difference between t_3 and t_5, a case can occur in which $t_3 < t_{ed}$ and $t_5 > t_{ed}$. In such a case we must replace t_5 by t_{ed}. Moreover, in certain magnetic fields it can happen that $1/\omega t_3 = \gamma_3 \gg 1$, while $\gamma_5 = (\omega t_5)^{-1} \gg 1$. In such a case, the asymptotic value will evidently be an expansion in γ_5 and γ_3^{-1}. We shall not linger over these cases. Then,

$$\beta_{ik}^{(1)} = t_3 f_{ik}(\gamma_3) + t_5 g_{ik}(\gamma_5).$$

Since $t_5 \gg t_3$, i.e., $\gamma_5 \ll \gamma_3$, then the zero order terms (in γ) are proportional to t_5, and terms of second order $\sim \gamma_3^2 t_3$. The two first-order terms are equal, since $\gamma_3 t_3 = \gamma_5 t_5 = \gamma t$. Therefore, the tensor $\alpha_{ik}^{(2)}$ remains the same as in Sec. 2, if we set $\gamma_0 = \gamma_5$ in all formulas for $\alpha_{ik}^{(2)}$. The tensors $\beta_{ik}^{(1)}$, and correspondingly, the $\alpha_{ik}^{(1)}$, have the following form (see reference 4):

1) The case of close trajectories lying within the limits of a single cell:

$$\beta_{ik}^{(1)} = \begin{vmatrix} \gamma_3^2 t_3 c_{xx} & \gamma t c_{xy} & \gamma t c_{xz} \\ \gamma t c_{yx} & \gamma_3^2 t_3 c_{yy} & \gamma t c_{yz} \\ \gamma t c_{zx} & \gamma t c_{zy} & t_5 c_{zz} \end{vmatrix}. \tag{29}$$

Using σ_{ik} from references 2 and 3 we get

$$\alpha_{ik}^{(1)} = \begin{vmatrix} a_{xx} & \gamma_3 a_{xy} & a_{xz} \\ \gamma_3 a_{yx} & a_{yy} & a_{yz} \\ \gamma_5 a_{zx} & \gamma_5 a_{zy} & a_{zz} \end{vmatrix}. \tag{30}$$

The tensor for $\alpha_{ik}^{(2)}$ has the form (15). In the case of a closed Fermi surface, for an equal number of electrons and holes, the $\alpha_{ik}^{(1,2)}$ have the form (16) if we set $\gamma_0 = \gamma_5$.

2) Open trajectories. In correspondence with the above, we have

$$\beta_{ik}^{(1)} = \begin{vmatrix} \gamma_3^2 t_3 c_{xx} & \gamma t c_{xy} & \gamma t c_{xz} \\ \gamma t c_{yx} & t_5 c_{yy} & t_5 c_{yz} \\ \gamma t c_{zx} & t_5 c_{zy} & t_5 c_{zz} \end{vmatrix}, \tag{31}$$

$$\alpha_{ik}^{(1)} = \begin{vmatrix} \gamma_3 \gamma_5^{-1} a_{xx} & \gamma_5^{-1} a_{xy} & \gamma_5^{-1} a_{xz} \\ \gamma_3 a_{yx} & a_{yy} & a_{yz} \\ \gamma_3 a_{zx} & a_{zy} & a_{zz} \end{vmatrix}, \tag{32}$$

$\alpha_{ik}^{(2)}$ has the form (18) with $\gamma_0 = \gamma_5$.

3) Approximation to the critical directions.

a) Approximation to the direction in which the layer of open trajectories disappears. As above, in Sec. 2, $\beta_{ik}^{(1)} = g_{ik}^{(1)} + \vartheta d_{ik}^{(1)}$, while $g_{ik}^{(1)}$ has the form of (29), and $d_{ik}^{(1)}$ has the form of (31). Taking this into account, we get the following expression for $\alpha_{ik}^{(1)}$:

$$\alpha_{ik}^{(1)} = \begin{vmatrix} a_{xx} + \gamma_3 \gamma_5^{-1} \vartheta c_{xx} & \gamma_3 a_{xy} + \vartheta \gamma_5^{-1} c_{xy} & a_{xz} + \vartheta \gamma_5^{-1} c_{xz} \\ \gamma_3 a_{yx} & a_{yy} & a_{yz} \\ \gamma_5 a_{zx} + \vartheta \gamma_3 c_{zx} & \gamma_5 a_{zy} + \vartheta c_{zy} & a_{zz} \end{vmatrix}; \tag{33}$$

$\alpha_{ik}^{(2)}$ has the form of (25) with $\gamma_0 = \gamma_5$.

b) Approximation to the isolated direction in which a layer of open trajectories arises. If ϑ is the angle between the z axis and the critical direction, while $\eta_3 = \gamma_3/\vartheta$, $\eta_5 = \gamma_5/\vartheta$, then the tensor $\alpha_{ik}^{(2)}$ has a structure of the type (23), (24), if we set $\gamma_0 = \gamma_5$, $\eta = \eta_5$ in the latter equations.

In the approximation of the tensor $\alpha_{ik}^{(1)}$ we consider three regions:

1) $\eta_3 \ll 1$; $\eta_5 \ll 1$. With consideration of the relation between γ_3 and γ_5, we get the expression

$$\beta_{ik}^{(1)} = \begin{vmatrix} \gamma_3^2 t_3 c_{xx} & \gamma t c_{xy} & \gamma t c_{xz} \\ \gamma t c_{yx} & \eta_3^2 t_3 c_{yy} & \eta t c_{yz} \\ \gamma t c_{zx} & \eta t c_{zy} & t_5 c_{zz} \end{vmatrix} \tag{34}$$

for $\beta_{ik}^{(1)}$, and by means of $\sigma_{ik}(\gamma_5, \eta_5)$ from reference 3, we determine $\alpha_{ik}^{(1)}$:

$$\alpha_{ik}^{(1)} = \begin{vmatrix} a_{xx} & \gamma_5^{-1} \eta_3 \eta_5 a_{xy} & \gamma_5^{-1} \eta_5 a_{xz} \\ \gamma_3 a_{yx} & a_{yy} & a_{yz} \\ \gamma_5 a_{zx} & \eta_5 a_{zy} & a_{zz} \end{vmatrix}. \tag{35}$$

2) $\eta_3 \gg 1$; $\eta_5 \ll 1$. In this case,

$$\beta_{ik}^{(1)} = \begin{vmatrix} \gamma_3^2 t_3 c_{xx} & \gamma t c_{xy} & \gamma t c_{xz} \\ \gamma t c_{yx} & t_3 (c_{yy} + \eta_3 \eta_5 c'_{yy}) & \eta t c_{yz} \\ \gamma t c_{zx} & \gamma t c_{zy} & t_5 c_{zz} \end{vmatrix} \tag{36}$$

and correspondingly,

$$\alpha_{ik}^{(1)} = \begin{vmatrix} a_{xx} + \eta_3 \eta_5 b_{xx} & \gamma_3^{-1} (a_{xy} + \eta_3 \eta_5 b_{xy}) & \gamma_5^{-1} \eta_5 a_{xz} \\ \gamma_3 a_{yx} & a_{yy} & a_{yz} \\ \gamma_3 \eta_5 a_{zx} & \eta_5 a_{zy} & a_{zz} \end{vmatrix}. \tag{37}$$

3) $\eta_3 \gg 1$; $\eta_5 \gg 1$. Under these conditions,

$$\beta_{ik}^{(1)} = \begin{vmatrix} \gamma_3^2 t_3 c_{xx} & \gamma t c_{xy} & \gamma t c_{xz} \\ \gamma t c_{yx} & t_5 c_{yy} & t_5 c_{yz} \\ \gamma t c_{zx} & t_5 c_{zy} & t_5 c_{zz} \end{vmatrix}, \tag{38}$$

$$\alpha_{ik}^{(1)} = \begin{vmatrix} \gamma_3 \gamma_5^{-1} a_{xx} & \gamma_5^{-1} a_{xy} & \gamma_5^{-1} a_{xz} \\ \gamma_3 a_{yx} & a_{yy} & a_{yz} \\ \gamma_3 a_{zx} & a_{zy} & a_{zz} \end{vmatrix}. \tag{39}$$

As is seen, the elements of the tensor $\alpha_{ik}^{(2)}$ always have an asymptotic value (asymptotic in γ and η) no higher than the asymptotic value of the corresponding elements of the tensor $\alpha_{ik}^{(1)}$. Thus, as has already been pointed out, the coefficients in the expansion in γ and η in $\alpha^{(2)}$, (if the phonons are scattered by the electrons) are of order $(T/\Theta)^3/e$, while in $\alpha^{(1)}$, they are of order $\sim T/e\mu$ [(7), (8′)]; above the temperature T_γ [Eq. (9)] the drag effect predominates, except for the case (37), when $\alpha^{(1)}$ can exceed $\alpha^{(2)}$ [Eqs. (23) and (24)].

In the isotropic model (for this the asymptotic values of $\alpha^{(2)}$ and $\alpha^{(1)}$ coincide for scattering of electrons by other than phonons, expanding $\beta^{(1,2)} = \sum_r \beta_r^{(1,2)} \gamma_0$, we get $\beta_r^{(2)}/\beta_r^{(1)} = (T/T_\gamma^{(r)})^2$, where

$$T_\gamma^{(r)} \approx 5.4 \left| \frac{(r+2) - (1-r)\delta}{(n/n_0)^{1/3}} + \frac{1-r}{(m^*/m_0)(v/v_0)} \right|^{1/2} \times \left(\frac{(s/s_0)^3 n/n_0}{v/v_0} \right)^{1/2} \text{deg};$$

$$m^* = (d^2\varepsilon/dp^2)^{-1}, \qquad \delta = -d(\ln t_0)/d(\ln p).$$

Here n is the concentration of electrons, $m_0 = 10^{-27}$ gm;

$$s_0 = 3 \cdot 10^5 \text{ cm-sec}^{-1}, \quad v_0 = 10^8 \text{ cm-sec}^{-1}, \quad n_0 = 3 \cdot 10^{22} \text{ cm}^{-3}.$$

[1] I. M. Lifshitz and M. Ya Azbel', JETP **32**, 1188 (1957), Soviet Phys. JETP **5**, 967 (1957).

[2] Lifshitz, Azbel', and Kaganov, JETP **31**, 63 (1956), Soviet Phys. JETP **4**, 41 (1957).

[3] I. M. Lifshitz and V. G. Peschanskiĭ, JETP **35**, 1251 (1958), Soviet Phys. JETP **8**, 875 (1959).

[4] Bychkov, Gurevich, and Nedlin, JETP **37**, 534 (1959), Soviet Phys. JETP **10**, 377 (1960).

[5] L. É. Gurevich, Основы физ. кинетики (Foundations of Physical Kinetics), Gostekhizdat, 1940.

[6] L. É. Gurevich, JETP **16**, 193 (1946).

[7] H. Bethe and A. Sommerfeld, Electron Theory of Metals (Russian translation, Gostekhizdat, 1940).

[8] L. D. Landau and I. Ya. Pomeranchuk, Phys. Z. Sowjetunion **10**, 649 (1939); JETP **7**, 379 (1937).

Translated by R. T. Beyer
145

SOVIET PHYSICS JETP VOLUME 37 (10), NUMBER 3 MARCH, 1960

ANGULAR DISTRIBUTION AND POLARIZATION OF β PARTICLES IN SECOND FORBIDDEN TRANSITIONS

A. Z. DOLGINOV and E. V. KHARITONOV

Submitted to JETP editor April 9, 1959

J. Exptl. Theoret. Phys. (U.S.S.R.) **37**, 776-785 (September, 1959)

Explicit formulas for the polarization and angular distribution of β electrons in second forbidden transitions involving V and A coupling are derived. The angular correlations in unique transitions are examined in the case of arbitrary order of forbiddenness. Unique second forbidden transitions are treated in detail.

1. SECOND FORBIDDEN TRANSITIONS Δj = 2 (no)

THE results of a great number of recent papers indicate that the time reversal invariant vector and axial vector interactions play the fundamental role in β decay processes. Together with the further refinement of these results it becomes of interest to investigate the forbidden β transitions with the aim of determining the nuclear matrix elements. Many papers have been devoted to the study of forbidden β transitions. However, detailed explicit formulas for the angular distribution and polarization of β particles have been given only for transitions of first order of forbiddenness. In the present paper we consider β processes of second and higher order of forbiddenness. Since the method of calculation has already been described in a series of papers,[1] we give at once the final formulas.

a. Angular Distribution of β Electrons for Second Forbidden β Transitions in Oriented Nuclei

We shall characterize the orientation of the nuclear spins by the quantity

$$\rho_g = \sum_{\mu_0}{}' C^{j_0\mu_0}_{j_0\mu_0 g 0} w(\mu_0), \qquad \sum_{\mu_0}{}' w(\mu_0) = 1, \tag{1}$$

where j_0 is the angular momentum of the initial nucleus, μ_0 is its projection on the axis along which most of the nuclear spins are oriented (chosen as the Z axis), $w(\mu_0)$ is the probability that the nucleus has a spin projection with the value μ_0, and $C^{\cdots}_{\cdots}$ are Clebsch-Gordan coefficients.[2] The number g is even for aligned nuclei, and even or odd for polarized nuclei.

$$\sqrt{2g+1}\,\rho_g = \sqrt{2j_0+1}\,j_0^g f_g,$$

where f_g are quantities which are tabulated in the papers of Cox and Tolhoek.[3]

The angular distribution for second forbidden transitions with a change of the nuclear spin by two units ($|j_0 - j_1| = \Delta j = 2$) and without change of parity is given by the formula

$$w(\mathbf{j}_0\mathbf{p}) = 1 + \frac{p}{E} \sum_{g=1,\ldots,4}{}' r_g(j_0, j_1) B_g(E, q, p) P_g(\cos\vartheta), \tag{2}$$

where j_1 is the spin of the nucleus after the β decay, $P_g(\cos\vartheta)$ is the Legendre polynomial in the angle of the electron momentum vector $\mathbf{p}(p, \vartheta, \varphi)$, E is the total energy of the electron (including the rest mass), q is the momentum (energy) of the neutrino (we choose units for which $\hbar = m = c = 1$),

$$r_g = U(j_1 2 j_0 g;\ j_0 2)\rho_g = \sqrt{5(2j_0+1)}\,W(j_1 2 j_0 g;\ j_0 2)\rho_g,$$

where W (abcd; ef) is the Racah function (tables of Racah functions are given in reference 4), and

$$\xi B_g = A_1 + A_2 E + A_3(E + V) + A_4(p^2 + 2EV + V^2)$$

$$+ A_5 E(p^2 + 2p^2 V E^{-1} + V^2) + A_6(p^2 + EV),$$

$$\xi = a_1 + a_2(p^2 + 2p^2 V E^{-1} + V^2) + a_3(p^2 E^{-1} + V). \tag{3}$$

Assuming uniform distribution of the charge over the volume of the nucleus, we have $V = 6\alpha Z/5R$. For the case where the charge is distributed over the nuclear surface, we find $V = \alpha Z/R$ (Z is the nuclear charge, R is the nuclear radius).

The quantities a_i are equal to

$$a_1 = \gamma_1(p^2 + q^2) + (\gamma_2 q^4 + \gamma_3 p^4 + \gamma_4 p^2 q^2) + \gamma_5 q\left(p^2 + \tfrac{3}{5}q^2\right),$$

$$a_2 = \gamma_1\left(p^2 + \tfrac{25}{9}q^2\right),$$

$$a_3 = \zeta_1\left(q^2 + \tfrac{3}{5}p^2\right) + \zeta_2 q(p^2 + q^2). \tag{4}$$

The quantities A_i for different values of g have the following values:

$g = 1$:

$$A_1 = (\varphi_1 q^4 + \varphi_2 p^4 + \varphi_3 p^2 q^2) + \varphi_4 q (p^2 + q^2) + \varphi_5 p^2 + \varphi_6 q,$$

$$A_2 = q(\lambda_1 q^2 + \lambda_2 p^2) + (\lambda_3 q^2 + \lambda_4 p^2),$$

$$A_3 = \varphi_7 q \left(p^2 + \tfrac{5}{9} q^2\right) + \varphi_8 \left(p^2 + \tfrac{25}{9} q^2\right),$$

$$A_4 = \varphi_9 \left(\frac{125}{\sqrt{6}} q^2 + p^2\right),$$

$$A_5 = 0, \qquad A_6 = \lambda_5 q^2 + \lambda_6 p^2;$$

$g = 2$:

$$A_1 = p\,[q(\chi_1 q^2 + \chi_2 p^2) + (\chi_3 q^2 + \chi_4 p^2)],$$

$$A_2 = p\,[(\omega_1 q^2 + \omega_2 p^2) + \omega_3 q + \omega_4],$$

$$A_3 = A_4 = 0, \qquad A_5 = \omega_5 p, \qquad A_6 = p(\omega_6 q + \omega_7);$$

$g = 3$:

$$A_1 = -2\sqrt{7/3}\, p^2 \left[\left(-\frac{5}{42}\varphi_2 q^2 + \frac{1}{\sqrt{6}}\varphi_3 p^2\right) + \varphi_4 q + \varphi_5\right],$$

$$A_2 = -2\sqrt{7/3}\, p^2 (\lambda_2 q + \lambda_4),$$

$$A_3 = -2\sqrt{7/3}\, p^2 (\varphi_7 q + \varphi_8),$$

$$A_4 = -2\sqrt{7/3}\,\varphi_9 p^2, \qquad A_5 = 0, \quad A_6 = -2\sqrt{7/3}\,\lambda_6 p^2;$$

$g = 4$:

$$A_1 = -6p^3(\chi_2 q + \chi_4), \quad A_2 = -\tfrac{3}{4}\omega_2 p^3,$$

$$A_3 = A_4 = A_5 = A_6 = 0. \tag{5}$$

The coefficients γ_i, η, ζ_i, φ_i, λ_i, χ_i, and ω_i, which depend on the coupling constants and on the three nuclear matrix elements, are given in Appendix A.

In expression (2) we have made the approximation $(\alpha Z)^2 \ll 1$, $(\alpha Z/p)^2 \ll 1$. In the limiting case where $Z \gg 2A^{1/3}E$ (A is the mass number of the decaying nucleus), the angular distribution no longer depends on the nuclear matrix elements, as in the case of unique transitions. In this case we have

$$w(\mathbf{j}_0\mathbf{p}) = 1 - \frac{p}{E}\sum_{g=1,2,3} r_g B_g P_g(\cos\vartheta), \tag{6}$$

where

$$\xi B_1 = \sqrt{6}\left(\tfrac{5}{3}q^2 + \tfrac{9}{25}p^2\right), \qquad \xi B_2 = \tfrac{3}{5}\sqrt{14}\,pE,$$

$$\xi B_3 = -\tfrac{18}{25}\sqrt{14}\,p^2, \quad \xi = \tfrac{10}{3}q^2 + \tfrac{6}{5}p^2.$$

Formula (6) corresponds to the two-component theory of the neutrino.

b. Longitudinal Polarization of the β Particles

For β^- transitions with $\Delta j = 2$ (no), the longitudinal polarization vector for the β^- particles in the rest system of the electron can be written in the form

$$\zeta = -\frac{\mathbf{p}}{E}\left(a + \frac{b}{E} + \frac{\alpha Z}{p}c\right). \tag{7}$$

The quantity $a\xi$ is different from ξ in that the constants β_{ik} (which enter in the coefficients γ_i, η, and ζ_i) are replaced by the constants α_{ik}:

$$\alpha_{ik} = C_i C_k'^{*} + C_i' C_k^{*}, \qquad \beta_{ik} = C_i C_k^{*} + C_i' C_k'^{*},$$

$$i, k = V, A\ T. \tag{8}$$

C_i and C_i' are the coupling constants of the β interaction corresponding to the terms which, respectively, do or do not conserve parity. $b\xi = Va_2 + a_3$, where we also replace the β_{ik} in the quantities a_2 and a_3 on the right hand side of this equation by the α_{ik}.

$$c\xi = 2\,\mathrm{Im}\left[\varkappa_1 q\left(q^2 + \tfrac{1}{2}p^2\right) + \varkappa_2\left(q^2 + \tfrac{3}{10}p^2\right)\right]. \tag{7'}$$

The energy dependence of ξ, a_2, and a_3 is given by (3) and (4). The coefficients κ_i which depend on the constants C, C′ and the nuclear matrix elements, are given in Appendix A.

If the strong interactions are invariant under time reversal the combinations of matrix elements entering in κ_i are real. A possible violation of time reversal invariance in β interactions is determined by the third term on the right hand side of (7). In the two-component theory of the neutrino $\alpha_{ik} = \beta_{ik}$ and $a = 1$.

In (7) we made the approximation $(\alpha Z)^2 \ll 1$ and $(\alpha Z/p)^2 \ll 1$. If $Z \gg 2A^{1/3}E$ for a given nucleus, the formulas for the longitudinal polarization no longer depend on the nuclear matrix elements: $\boldsymbol{\zeta} = -\mathbf{p}/E$ (here we use the two-component theory of the neutrino).

We note that the general form of (7) is the same for β transitions of arbitrary order of forbiddenness, where the energy dependence of a, b, and c is determined by the order of forbiddenness.

2. UNIQUE TRANSITIONS $\Delta j = N + 1$

The formulas for the angular correlations in forbidden β transitions of the unique type, in which the change of the nuclear spin exceeds the order of forbiddenness by one (i.e., $\Delta j = |j_0 - j_1| = N + 1$), do not depend on the nuclear matrix elements. It is therefore impossible to obtain from a study of the unique transitions, any information about the structure of the nucleus, except information on the angular momenta and the parities of the nuclear levels. The latter, though, is the most definite information on these quantities that we have.

The unique transitions are determined by the Gamow-Teller interaction, where apparently only the axial vector (A) coupling gives a significant contribution.

In this part of the paper we consider the angular distribution and polarization of β particles for unique β transitions of arbitrary (N-th) order of forbiddenness in oriented and non-oriented nuclei. The detailed form of the formulas obtained is given for the case of second forbidden transitions: $\Delta j = 3$ (no).

a. Longitudinal Polarization of β Electrons

We shall characterize the polarization of the electrons by the angle χ between the electron momentum $\mathbf{p}$ and the direction of the spin ζ. The polarization is then given by the formula

$$w(\zeta\mathbf{p}) = 1 + \zeta\cos\chi.$$

In the approximation $(\alpha Z)^2 \ll 1$, $(\alpha Z/p)^2 \ll 1$ (the exact formulas are given in Appendix B) we have

$$\zeta = \frac{\mathbf{p}}{E+\Delta}\left(\frac{\alpha_{TT}-\alpha_{AA}}{\beta_{TT}+\beta_{AA}} - \frac{\alpha Z}{p}\,\frac{2\,\mathrm{Im}\,\alpha_{AT}}{\beta_{TT}+\beta_{AA}}\,d_N\right),$$
$$\Delta = 2\,(\mathrm{Re}\,\beta_{TA})/(\beta_{TT}+\beta_{AA}), \tag{9}$$

where α_{ik} and β_{ik} are given by (8). The weakly energy dependent coefficient d_N is different for different orders of forbiddenness of the β transition, N:

$$\sigma d_N = \sum_j \mathscr{D}_j^N \left(j+\tfrac{1}{2}\right)^{-1}, \qquad \sigma = \sum_j \mathscr{D}_j^N,$$
$$\mathscr{D}_j^N = \frac{4^N(2N+3)(N!)^2}{(2N+1)!}\,\frac{p^{2j-1}q^{2N-2j+1}}{(2j)!\,(2N-2j+2)!}\,. \tag{10}$$

The summation in (10) goes over all half odd integer values of j with $j < N+1$.

It is seen from (9) that the interference terms (between the interactions T and A) violate the time reversal invariance. However, this interference is apparently absent in the β interaction.

For "pure" T or A coupling we obtain:*

$$\zeta = \pm\frac{\mathbf{p}}{E}\,\frac{2\,\mathrm{Re}\,CC'^*}{|C|^2+|C'|^2}\,. \tag{9'}$$

b. Angular Distribution of the Electrons

If we characterize, as before, the orientation of the nuclear spins by the quantity ρ_g [see formula (1)], the angular distribution of the electrons emitted by oriented nuclei in unique transitions has the form

$$w(\mathbf{j}_0\mathbf{p}) = 1 + \sum_{g=1,\dots}^{2N+1} r_g(j_0, j_1)\,B_g(E, q, p)\,P_g(\cos\vartheta). \tag{11}$$

Here

$$r_g = U(j_1N+1\,j_0g;\; j_0N+1)\,\rho_g,$$
$$\sigma B_g = a_g + \frac{p\,\mathrm{Re}\,S}{EQ-X}\,b_g + \frac{\alpha Z\,\mathrm{Im}\,S}{EQ-X}\,b_g', \tag{12}$$
$$a_g = \sum_j \mathscr{D}_j^N \xi_j^g, \qquad b_g = \sum_j \mathscr{D}_j^N \eta_j^g, \qquad b_g' = \sum_j \mathscr{D}_j^N \eta_j^g \left(j+\tfrac{1}{2}\right)^{-1},$$
$$Q = \beta_{TT} + \beta_{AA}, X = -2\,\mathrm{Re}\,\beta_{TA},$$
$$\mathrm{Re}\,S = \alpha_{TT} - \alpha_{AA},\ \mathrm{Im}\,S = -2\,\mathrm{Im}\,\alpha_{AT}. \tag{13}$$

In the general case of N-th order of forbiddenness the numerical coefficients ξ_j^g and η_j^g are given in terms of the Racah functions and the Clebsch-Gordan coefficients:

$$\xi_j^g = (-)^{j-1/2}\sqrt{(2j+g+1)(2j-g)(2g+1)(2N+3)}$$
$$\times C^{g0}_{j-1/2\,0\,j-1/2\,0}\,W(N-j+1\,N+1\,jg;\; jN+1),$$
$$g \text{ — even};$$
$$\eta_j^g = (-)^{j-1/2}\sqrt{g(g+1)(2g+1)(2N+3)}\,C^{g0}_{j-1/2\,0\,j+1/2\,0}$$
$$\times W(N-j+1\;\,N+1\,jg;\; jN+1),$$
$$g \text{ — odd}. \tag{14}$$

For "pure" T or A coupling we have:

$$\sigma B_g = a_g \pm \frac{p}{E}\,\frac{2\,\mathrm{Re}\,CC'^*}{|C|^2+|C'|^2}\,b_g. \tag{12'}$$

The numerical values of the coefficients $R_j^{(2)}$, ξ_j^g, and η_j^g for second forbidden β transitions (N=2) are given in Appendix C.

c. Polarization of Electrons Emitted by Oriented Nuclei

The probability for observing an electron with momentum $\mathbf{p}$ and polarization ζ in unique β transitions is

$$w(\mathbf{j}_0, \mathbf{p}, \zeta) = 1 + |\zeta|\cos\chi + \sum_{g=1,\dots}^{2N+1} r_g B_g P_g(\cos\vartheta)$$
$$+ \sum_{g,\,s} r_g C_{gs} F_{gs}(\vartheta, \chi, \omega). \tag{15}$$

The directions of the vectors $\mathbf{j}_0$, $\mathbf{p}$, and ζ and the angles between them are given in the figure. The values of $|\zeta|$, r_g, and B_g are determined by the corresponding formulas (9) and (12). The index s in the last term of (15) takes on the values $s = g$, $g \pm 1$, so that the summation over s goes from $s = 0$ to $s = 2N + 2$. Furthermore,

---

*Here, as well as in the analogous formulas below, the upper indices refer to T, and the lower indices to A.

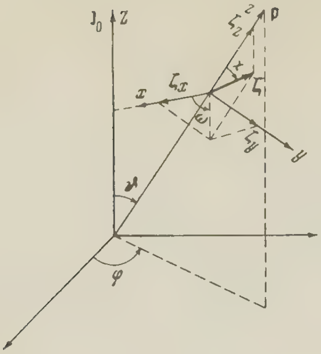

$$\sigma C_{gs} = \left[k_{gs}^{+} + \frac{EX - Q}{EQ - X}\, k_{gs}^{-}\right] + \frac{p}{EQ - X}(l_{gs}\operatorname{Re} S + t_g \operatorname{Im} S)$$

$$+ \frac{\alpha Z}{EQ - X}(- t_g' \operatorname{Re} S + l_{gs}' \operatorname{Im} S),$$

$$k_{gs}^{\pm} = \sum_j \mathcal{D}_j^N \cdot \tfrac{1}{2}(\varepsilon_{j^1/_2} \pm \varepsilon_{j-{}^1/_2}),$$

$$l_{gs} = \sum_j \mathcal{D}_j^N \zeta_j, \qquad l_{gs}' = \sum_j \mathcal{D}_j^N \zeta_j (j + \tfrac{1}{2})^{-1},$$

$$t_g = \sum_j \mathcal{D}_j^N \tau_j, \qquad t_g' = \sum_j \mathcal{D}_j^N \tau_j (j + \tfrac{1}{2})^{-1}. \tag{16}$$

The angular dependence of $F_{gs}(\vartheta, \chi, \omega)$ for different values of s and g is expressed in the following form:

$$F_{gg} = \sqrt{\frac{3(2g+1)}{g(g+1)}} \sin\chi \sin\omega P_g^1(\cos\vartheta),$$

$$F_{gg+1} = \sqrt{3(g+1)} \cos\chi P_g(\cos\vartheta)$$

$$+ \sqrt{\frac{3}{g+1}} \sin\chi \cos\omega P_g^1(\cos\vartheta),$$

$$F_{gg-1} = -\sqrt{3g} \cos\chi P_g(\cos\vartheta)$$

$$+ \sqrt{3/g} \sin\chi \cos\omega P_g^1(\cos\vartheta).$$

$P_g^1(\cos\vartheta)$ is the first associated Legendre function. The constants Q, X, and S are given by (13).

In the general case of N-th order of forbiddenness the coefficients $\varepsilon_{j\lambda}$, ζ_j, and τ_j are given in terms of the functions of Racah and Fano[5] and the Clebsch-Gordan coefficients:

$$\varepsilon_{j\lambda} = (-)^{l-1}(2j+1)(2l+1)\sqrt{2(2g+1)(2N+3)}\, C_{l0l0}^{s0}$$

$$\times W(jN+1\, jg;\ jN+1) X(lls,\ jjg,\ \tfrac{1}{2}\tfrac{1}{2}1),$$

$$g - \text{odd},$$

$$\zeta_j = (-)^{j+{}^1/_2}(2j+1)\sqrt{4j(2j+2)(2g+1)(2N+3)}$$

$$\times C^{s0}_{j-\frac{1}{2}0j+\frac{1}{2}0} W(iN+1\, jg;\ jN+1)$$

$$\times X(j+\tfrac{1}{2}\, j-\tfrac{1}{2}\, s,\ jjg,\ \tfrac{1}{2}\tfrac{1}{2}1), \qquad g - \text{even}$$

$$\tau_j = (-)^{j-{}^1/_2}(2j+1)\sqrt{(2N+3)/3}\, C^{g0}_{j-\frac{1}{2}0j+\frac{1}{2}0}$$

$$\times W(iN+1\, jg;\ jN+1), \qquad g - \text{odd}$$

$$l = j + \lambda, \quad \lambda = \pm\tfrac{1}{2}, \quad i = N - j + 1. \tag{17}$$

A significant polarization of order $\sim p/E$ of the electrons in the direction $[\mathbf{p}\times\mathbf{j}_0]$ can be observed only if time reversal invariance is violated and if there is TA interference. If time reversal invariance holds, or if there is no TA interference, the polarization in this direction is $\sim \alpha Z/E$, i.e., small as compared to unity.

In the case of "pure" T or A coupling the quantity σC_{gs} [formula (16)] is given by

$$\sigma C_{gs} = k_{gs}^{+} - \frac{1}{E} k_{gs}^{-} \pm \frac{p}{E} \frac{2\operatorname{Re} CC'^*}{|C|^2 + |C'|^2} l_{gs}$$

$$\mp \frac{\alpha Z}{E} \frac{2\operatorname{Re} CC'^*}{|C|^2 + |C'|^2} t_g'. \tag{16'}$$

The numerical values of the coefficients $\epsilon_{j\lambda}^{(gs)}$, $\zeta_j^{(gs)}$, and $\tau_j^{(g)}$ for second forbidden β transitions are given in Appendix C.

All formulas quoted above correspond to β^- decay. In the case of positron decay we must make the following substitutions in these formulas:

$$C_A \to -C_A^*, \quad C_A' \to C_A'^*, \quad C_{V,T} \to C_{V,T}^*, \quad C_{V,T}' \to -C_{V,T}'^*,$$
$$\alpha Z \to -\alpha Z.$$

APPENDIX A

Coefficients γ_i, η, and ζ_i in the expressions (4):

$$\gamma_1 = |L_V|^2 \beta_{VV}, \qquad \gamma_2 = \tfrac{1}{25}(|K_A|^2\beta_{AA} + |K_V|^2\beta_{VV});$$

$$\gamma_3 = \tfrac{1}{125}(2|K_A|^2\beta_{AA} + 3|K_V|^2\beta_{VV} - 2\sqrt{6}\operatorname{Re} K_A K_V^* \beta_{AV});$$

$$\gamma_4 = \tfrac{5}{9}\gamma_2 + \tfrac{25}{9}\gamma_3,$$

$$\gamma_5 = \tfrac{2}{3\sqrt{5}}(-\sqrt{2}\beta_{VV}\operatorname{Re} K_V L_V^* + \sqrt{3}\operatorname{Re} K_A L_V^* \beta_{AV});$$

$$\eta = \tfrac{1}{125}(3|K_A|^2\beta_{AA} + 2|K_V|^2\beta_{VV} + 2\sqrt{6}\operatorname{Re} K_A K_V^* \beta_{AV});$$

$$\zeta_1 = -\tfrac{2}{3\sqrt{5}}(\sqrt{2}\beta_{VV}\operatorname{Re} K_V L_V^* + \sqrt{3}\operatorname{Re} K_A L_V^* \beta_{AV});$$

$$\zeta_2 = \tfrac{2}{75}(-3|K_A|^2\beta_{AA} + 2|K_V|^2\beta_{VV}).$$

Nuclear matrix elements:

$$K_A = [C^{j_0\mu_0}_{2\Lambda j_1\mu_1}]^{-1}\int \psi^*_{j_1\mu_1}\sigma \mathbf{Y}^{0*}_{2\Lambda}\psi_{j_0\mu_0} r^2\,\mathbf{dr};$$

$$K_V = [C^{j_0\mu_0}_{2\Lambda j_1\mu_1}]^{-1}\int \psi^*_{j_1\mu_1}\mathbf{Y}^*_{2\Lambda}\psi_{j_0\mu_0} r^2\,\mathbf{dr};$$

$$L_V = [C^{j_0\mu_0}_{2\Lambda j_1\mu_1}]^{-1}\int \psi^*_{j_1\mu_1} i\alpha \mathbf{Y}^{-1*}_{2\Lambda}\psi_{j_0\mu_0} r\,\mathbf{dr}.$$

In these expressions σ and α are the four-rowed Dirac matrices, and $\mathbf{Y}^{\tau}_{\mathrm{L}\Lambda}$ is the spherical vector function. Its components are expressed in terms of the spherical functions:

$$[\mathbf{Y}^{\tau}_{L\Lambda}]_{\gamma} = (-)^{1-\gamma} C^{L\Lambda}_{L+\tau,\, M1,\, -\gamma} Y_{L+\tau,\, M},$$
$$M = \Lambda + \gamma, \quad \gamma = 0, \pm 1.$$

The scalar product of two vectors $(\mathbf{AB})$ is here conveniently represented in the form

$$(\mathbf{AB}) = \sum_{\gamma} (-)^{\gamma} A_{\gamma} B_{-\gamma},$$
$$A_0 = A_z, \qquad A_{\pm 1} = \pm (A_x \pm iA_y)/\sqrt{2}.$$

Coefficients φ_i, λ_i, χ_i, and ω_i in the expressions (5):

$$\varphi_1 = -\tfrac{1}{25}\left(\sqrt{\tfrac{1}{6}}|K_A|^2\alpha_{AA} + \tfrac{2}{5}\operatorname{Re} K_A K_V^*\alpha_{AV}\right);$$

$$\begin{aligned}\varphi_2 = {}&-(2\sqrt{6}/625)\left(|K_A|^2\alpha_{AA} + \tfrac{3}{2}|K_V|^2\alpha_{VV}\right.\\ &\left.-\sqrt{6}\operatorname{Re} K_A K_V^*\alpha_{AV}\right);\end{aligned}$$

$$\begin{aligned}\varphi_3 = {}&-\tfrac{1}{225}\sqrt{\tfrac{2}{3}}\,(7|K_A|^2\alpha_{AA} + |K_V|^2\alpha_{VV}\\ &-\sqrt{6}\operatorname{Re} K_A K_V^*\alpha_{AV});\end{aligned}$$

$$\varphi_4 = \tfrac{1}{5}\sqrt{\tfrac{6}{5}}\left(\sqrt{3}\operatorname{Re} K_A L_V^*\alpha_{AV} - \sqrt{2}\,\alpha_{VV}\operatorname{Re} K_V L_V^*\right);$$

$$\begin{aligned}\varphi_5 = {}&-\tfrac{1}{5}\sqrt{\tfrac{2}{3}}\left(\tfrac{1}{2}|K_A|^2\alpha_{AA} + \tfrac{1}{3}|K_V|^2\alpha_{VV}\right.\\ &\left.+\sqrt{\tfrac{2}{3}}\operatorname{Re} K_A K_V^*\alpha_{AV}\right);\end{aligned}$$

$$\varphi_6 = -\sqrt{\tfrac{3}{2}}\,|L_V|^2\alpha_{VV};$$

$$\begin{aligned}\varphi_7 = {}&\tfrac{18}{125}\sqrt{6}\left(\tfrac{1}{2}|K_A|^2\alpha_{AA} - \tfrac{1}{3}|K_V|^2\alpha_{VV}\right.\\ &\left.-\sqrt{\tfrac{2}{3}}(\alpha Z/p)\operatorname{Im} K_A K_V^*\alpha_{AV}\right);\end{aligned}$$

$$\begin{aligned}\varphi_8 = {}&-\tfrac{3}{25}\sqrt{\tfrac{6}{5}}\,[\operatorname{Re}(\sqrt{3}K_A L_V^*\alpha_{AV} - \sqrt{2}K_V L_V^*\alpha_{VV})\\ &+(\alpha Z/p)\operatorname{Im}(\sqrt{3}K_A L_V^*\alpha_{AV} + \sqrt{2}K_V L_V^*\alpha_{VV})];\end{aligned}$$

$$\varphi_9 = -\tfrac{2}{625}\left(\tfrac{1}{2}|K_A|^2\alpha_{AA} + \tfrac{1}{3}|K_V|^2\alpha_{VV} + \sqrt{\tfrac{2}{3}}\operatorname{Re} K_A K_V^*\alpha_{AV}\right);$$

$$\begin{aligned}\lambda_1 = {}&\tfrac{1}{75}\sqrt{\tfrac{2}{3}}\,[|K_V|^2\alpha_{VV} - \sqrt{6}\operatorname{Re} K_A K_V^*\alpha_{AV}\\ &-(\alpha Z/4p)\sqrt{6}(5E + E^{-1})\operatorname{Im} K_A K_V^*\alpha_{AV}];\end{aligned}$$

$$\begin{aligned}\lambda_2 = {}&(\sqrt{6}/125)\left[|K_V|^2\alpha_{VV} + 2|K_A|^2\alpha_{AA}\right.\\ &-3\sqrt{6}\operatorname{Re} K_A K_V^*\alpha_{AV}\\ &\left.+(\alpha Z/2p)\sqrt{\tfrac{1}{6}}(7E + E^{-1})\operatorname{Im} K_A K_V^*\alpha_{AV}\right];\end{aligned}$$

$$\begin{aligned}\lambda_3 = {}&-(2/\sqrt{15})\,[\alpha_{VV}\operatorname{Re} K_V L_V^*\\ &-(\alpha Z/4p)(5E - E^{-1})\alpha_{VV}\operatorname{Im} K_V L_V^*];\end{aligned}$$

$$\begin{aligned}\lambda_4 = {}&(6/25\sqrt{5})[\sqrt{2}\operatorname{Re} K_A L_V^*\alpha_{AV} - \sqrt{3}\,\alpha_{VV}\operatorname{Re} K_V L_V^*\\ &+(\alpha Z/12p)(7E - E^{-1})\operatorname{Im}(-\sqrt{2}K_A L_V^*\alpha_{AV}\\ &+\sqrt{3}K_V L_V^*\alpha_{VV})];\end{aligned}$$

$$\begin{aligned}\lambda_5 = {}&\tfrac{1}{15}\sqrt{\tfrac{2}{3}}\,[|K_V|^2\alpha_{VV} + \sqrt{6}\operatorname{Re} K_A K_V^*\alpha_{AV}\\ &-(\alpha Z/4p)\sqrt{6}(5E - E_V^{-1})\operatorname{Im} K_A K_V^*\alpha_{AV}];\end{aligned}$$

$$\begin{aligned}\lambda_6 = {}&(3\sqrt{6}/625)\,[-|K_A|^2\alpha_{AA} + 2|K_V|^2\alpha_{VV}\\ &-\sqrt{6}\operatorname{Re} K_A K_V^*\alpha_{AV}\\ &+(\alpha Z/4p)\sqrt{6}(7E - E_V^{-1})\operatorname{Im} K_A K_V^*\alpha_{AV}];\end{aligned}$$

$$E_V \equiv E + p^2 V^{-1};$$

$$\chi_1 = (\sqrt{14}/100)(\alpha Z/p)(|K_V|^2\beta_{VV} - \sqrt{6}\operatorname{Re} K_A K_V^*\beta_{AV});$$

$$\begin{aligned}\chi_2 = {}&(1/30\sqrt{14})(\alpha Z/p)(|K_A|^2\beta_{AA} + |K_V|^2\beta_{VV}\\ &-5\sqrt{\tfrac{2}{3}}\operatorname{Re} K_A K_V^*\beta_{AV});\end{aligned}$$

$$\begin{aligned}\chi_3 = {}&(\sqrt{14}/180)(\alpha Z/p)\,[5E|K_V|^2\beta_{VV} + 3(E + V)|K_V|^2\beta_{VV}\\ &+9\sqrt{10}\,\beta_{VV}\operatorname{Re} K_V L_V^*];\end{aligned}$$

$$\begin{aligned}\chi_4 = {}&-(6/125\sqrt{14})(\alpha Z/p)\left[\tfrac{7}{24}E\,(|K_A|^2\beta_{AA} - |K_V|^2\beta_{VV}\right.\\ &-7\sqrt{\tfrac{2}{3}}\operatorname{Re} K_A K_V^*\beta_{AV}) + \tfrac{5}{12}(E + V)(|K_A|^2\beta_{AA}\\ &-|K_V|^2\beta_{VV} - 5\sqrt{\tfrac{2}{3}}\operatorname{Re} K_A K_V^*\beta_{AV})\\ &+\tfrac{5}{6}\sqrt{\tfrac{5}{6}}(\sqrt{2}\operatorname{Re} K_A L_V^*\beta_{AV} - \sqrt{3}\operatorname{Re} K_V L_V^*\beta_{VV})\\ &\left.+(\alpha Z/p)^{-1}7/\sqrt{6}\operatorname{Im} K_A K_V^*\beta_{AV}\right];\end{aligned}$$

$$\begin{aligned}\omega_1 = {}&-(\sqrt{14}/15)\left(\tfrac{1}{2}|K_A|^2\beta_{AA} + \tfrac{1}{3}|K_V|^2\beta_{VV}\right.\\ &\left.-\sqrt{\tfrac{2}{3}}\operatorname{Re} K_A K_V^*\beta_{AV}\right);\end{aligned}$$

$$\begin{aligned}\omega_2 = {}&-\tfrac{24}{125}\sqrt{\tfrac{2}{7}}\left(\tfrac{1}{3}|K_A|^2\beta_{AA} + \tfrac{1}{2}|K_V|^2\beta_{VV}\right.\\ &\left.-\sqrt{\tfrac{2}{3}}\operatorname{Re} K_A K_V^*\beta_{AV}\right);\end{aligned}$$

$$\omega_3 = \tfrac{1}{3}\sqrt{\tfrac{14}{5}}\,(\sqrt{3}\,\mathrm{Re}\,K_A L_V^* \beta_{AV} - \sqrt{2}\,\beta_{VV}\,\mathrm{Re}\,K_V L_V^*);$$

$$\omega_4 = -\tfrac{2}{9}\sqrt{7}\,|L_V|^2 \beta_{VV};$$

$$\omega_5 = -(3\sqrt{14}/125)\Big(\tfrac{1}{2}|K_A|^2\beta_{AA} + \tfrac{1}{3}|K_V|^2\beta_{VV}$$

$$+\sqrt{\tfrac{2}{3}}\,\mathrm{Re}\,K_A K_V^* \beta_{AV}\Big);$$

$$\omega_6 = -(\sqrt{14}/25)\Big(-|K_A|^2\beta_{AA} + \tfrac{1}{3}|K_V|^2\beta_{VV}\Big);$$

$$\omega_7 = -\tfrac{1}{5}\sqrt{\tfrac{14}{5}}(\sqrt{3}\,\mathrm{Re}\,K_A L_V^* \beta_{AV} + \sqrt{2}\,\beta_{VV}\,\mathrm{Re}\,K_V L_V^*)\,.$$

Coefficients κ_i in the expression (7′):

$$\varkappa_1 = \tfrac{2}{25}\sqrt{\tfrac{2}{3}}\,K_A K_V^* \alpha_{AV};$$

$$\varkappa_2 = -(1/3\sqrt{5})(\sqrt{2}\,K_V L_V^* \alpha_{VV} + \sqrt{3}\,K_A L_V^* \alpha_{AV}).$$

APPENDIX B

Expressions for the angular correlations in unique transitions have been given in the approximation $(\alpha Z)^2 \ll 1$ and $(\alpha Z/p)^2 \ll 1$. To obtain the exact formulas for arbitrary Z, we must make the following changes.

1. In the expressions for σ in (10) and a_g in (12) we must replace $\mathscr{D}_j^N$ by D_j^N, where

$$D_j^N = [\varkappa(EQ - X)]^{-1}\mathscr{D}_j^N p^{1-2j}[(2j)!!]^2$$

$$\times\Big\{a^2_{j_{1/2}}(Q+X) + a^2_{j-1/2}(Q-X)\Big\}\omega_j,$$

$$\omega_j = 1 - 3(\varkappa R)^2/10(j+1). \qquad \text{(B.1)}$$

Here $\kappa^2 + 1 = (E + \alpha Z/R)^2$ in the case of a uniform surface distribution of the nuclear charge and $= (E + 6\alpha Z/5R)^2$ in the case of a uniform volume distribution. The $a_{j\lambda}$ are coefficients determined by the condition of smooth joining of the radial parts of the electron wave function inside and outside the nucleus. The values of $a_{j\lambda}$ are given in the tables of Sliv and Volchek.[6] The expression

$$[k_{gs}^+ + (EX - Q)(EQ - X)^{-1} k_{gs}^-]$$

in formula (16) must be replaced by $\sum_j D_j^N$, but in the curly brackets in the expression for D_j^N [formula (B.1)] we must have

$$\Big\{a^2_{j\frac{1}{2}}\varepsilon_{j\frac{1}{2}}(Q+X) + a^2_{j-\frac{1}{2}}\varepsilon_{j-\frac{1}{2}}(Q-X)\Big\}.$$

2. The expression

$$(EQ - X)^{-1}\sum_j \mathscr{D}_j^N \eta_j^g\left[p\,\mathrm{Re}\,S + \alpha Z\Big(j+\tfrac{1}{2}\Big)^{-1}\mathrm{Im}\,S\right]$$

in the formulas (12) must be replaced by $\sum_j \Gamma_j^N \eta_j^g$, where

$$\Gamma_j^N = 2[\varkappa(EQ - X)]^{-1}\mathscr{D}_j^N p^{1-2j}[(2j)!!]^2 a_{j\frac{1}{2}} a_{j-\frac{1}{2}}$$

$$\times\{\cos\delta_j\,\mathrm{Re}\,S - \sin\delta_j\,\mathrm{Im}\,S\}\,\omega_j,$$

$$\sin\delta_j = -\frac{\alpha Z}{p(j+{}^1/_2)}\cos\delta_j$$

$$= -\frac{\alpha Z}{p(j+{}^1/_2)}\left[1 + \left(\frac{\alpha Z}{p(j+{}^1/_2)}\right)^2\right]^{-1/2}. \qquad \text{(B.2)}$$

Exactly the same changes have to be made in the terms of (16) which contain l_{gs} and l'_{gs} (with the coefficient ζ_j).

In the quantities of (16) containing t_g and t'_g we must make the substitution (B.2) (with the coefficient τ_j), but in the curly brackets in (B.2) we must have

$$\{\cos\delta_j\,\mathrm{Im}\,S + \sin\delta_j\,\mathrm{Re}\,S\}.$$

For example, the exact expression for the longitudinal polarization of the electrons in unique transitions is then written in the form

$$\zeta = \sum_j \Gamma_j^N \Big/ \sum_j D_j^N.$$

APPENDIX C

Numerical values of the coefficients in the expressions (10) to (17) for second forbidden transitions (N = 2):

$$\mathscr{D}_j^{(2)} = R_j^{(2)} p^{2j\ 1} q^{5-2j}$$

$R_j^{(2)}$

j	
$\frac{1}{2}$	1
$\frac{3}{2}$	$\frac{10}{3}$
$\frac{5}{2}$	1

γ_{lj}^g

j	$g=1$	$g=3$	$g=5$
$\frac{1}{2}$	$\frac{2}{3}\sqrt{3}$	0	0
$\frac{3}{2}$	$\frac{1}{10}\sqrt{3}$	$-\frac{3}{5}\sqrt{6}$	0
$\frac{5}{2}$	$\frac{2}{7}\sqrt{3}$	$-\frac{2}{3}\sqrt{6}$	$\frac{10}{21}\sqrt{33}$

ξ_j^g

j	$g=2$	$g=4$
$\frac{1}{2}$	0	0
$\frac{3}{2}$	$-\frac{2}{5}\sqrt{15}$	0
$\frac{5}{2}$	$-\frac{4}{7}\sqrt{15}$	$\frac{3}{7}\sqrt{22}$

$\zeta_j^{(gs)}$

j	$g=2$		$g=4$	
	$s=1$	$s=3$	$s=3$	$s=5$
$\frac{1}{2}$	0	0	0	0
$\frac{3}{2}$	$\frac{2}{5}\sqrt{\frac{2}{5}}$	$-\frac{2}{5}\sqrt{\frac{3}{5}}$	0	0
$\frac{5}{2}$	$\frac{4}{7}\sqrt{\frac{2}{5}}$	$-\frac{4}{7}\sqrt{\frac{3}{5}}$	$-\frac{2}{21}\sqrt{\frac{22}{3}}$	$\frac{1}{21}\sqrt{\frac{110}{3}}$

$\tau_j^{(g)}$

j	$g=1$	$g=3$	$g=5$
$\frac{1}{2}$	$\frac{2}{3}\sqrt{\frac{2}{3}}$	0	0
$\frac{3}{2}$	$\frac{4}{5}\sqrt{\frac{2}{3}}$	$-\frac{2}{5}\sqrt{\frac{6}{7}}$	0
$\frac{5}{2}$	$\frac{6}{7}\sqrt{\frac{2}{3}}$	$-\frac{2}{3}\sqrt{\frac{6}{7}}$	$\frac{2}{7}\sqrt{\frac{10}{3}}$

$\varepsilon_{j\lambda}^{(gs)}$

j	λ	$g=1$		$g=3$		$g=5$	
		$s=0$	$s=2$	$s=2$	$s=4$	$s=4$	$s=6$
$\frac{1}{2}$	$-\frac{1}{2}$	$-\frac{2}{3}$	0	0	0	0	0
	$\frac{1}{2}$	$\frac{2}{9}$	$\frac{4}{9}\sqrt{2}$	0	0	0	0
$\frac{3}{2}$	$-\frac{1}{2}$	$-\frac{2}{3}$	$-\frac{2}{15}\sqrt{2}$	$\frac{1}{5}\sqrt{6}$	0	0	0
	$\frac{1}{2}$	$\frac{2}{5}$	$\frac{2}{5}\sqrt{2}$	$-\frac{1}{35}\sqrt{6}$	$-\frac{12}{35}\sqrt{2}$	0	0
$\frac{5}{2}$	$-\frac{1}{2}$	$-\frac{2}{3}$	$-\frac{4}{21}\sqrt{2}$	$\frac{2}{7}\sqrt{6}$	$\frac{2}{21}\sqrt{2}$	$-\frac{2}{21}\sqrt{55}$	0
	$\frac{1}{2}$	$\frac{10}{21}$	$\frac{8}{21}\sqrt{2}$	$-\frac{2}{21}\sqrt{6}$	$-\frac{10}{21}\sqrt{2}$	$\frac{2}{21}\sqrt{\frac{5}{11}}$	$\frac{20}{21}\sqrt{\frac{6}{11}}$

---

[1] A. Z. Dolginov, Nucl. Phys. **5**, 512 (1958). A. Z. Dolginov, JETP **33**, 1363 (1957); Soviet Phys. JETP **6**, 1047 (1958). G. E. Lee-Whiting, Can. J. Phys. **36**, 1199 (1958).

[2] K. Alder, Helv. Phys. Acta **25**, 235 (1952). E. Condon and G. Shortley, The Theory of Atomic Spectra, Cambridge (1935).

[3] J. A. M. Cox and H. A. Tolhoek, Physica **19**, 106 and 673 (1953).

[4] Biedenharn, Blatt, and Rose, Revs. Modern Phys. **24**, 249 (1952). H. Jahn, Proc. Roy. Soc. **205**, 192 (1951).

[5] Arima, Horie, and Tanabe, Progr. Theor. Phys. **11**, 143 (1954). H. Matsunobu and H. Takebe, Progr. Theor. Phys. **14**, 589 (1955).

[6] L. A. Sliv and B. A. Volchek, Таблицы кулоновских фаз и амплитуд при учете конечных размеров ядра, (Tables of Coulomb Phases and Amplitudes with Account of the Finite Dimensions of the Nucleus) (1956).

Translated by R. Lipperheide
146

SOVIET PHYSICS JETP VOLUME 37 (10), NUMBER 3 MARCH, 1960

QUANTUM THEORY OF SPATIAL DISPERSION OF ELECTRIC AND MAGNETIC SUSCEPTIBILITIES

O. V. KONSTANTINOV and V. I. PEREL'

Leningrad Physico-Technical Institute, Academy of Sciences, U.S.S.R.

Submitted to JETP editor April 9, 1959

J. Exptl. Theoret. Phys. (U.S.S.R.) **37**, 786-792 (September, 1959)

A general expression is obtained for the electric and magnetic susceptibilities when spatial dispersion is taken into account. It is shown that electromagnetic effects in a uniform medium can be described by means of a conductivity which depends on frequency and wave vector and a magnetic susceptibility which depends only on the wave vector. A universal relation is obtained between the conductivity and the magnetic susceptibility.

In recent years a number of papers have appeared which have been devoted to an investigation of the effects of spatial dispersion in the propagation of electromagnetic waves through matter.[1-9]

In the papers by Ginzburg[2] and Agranovich and Rukhadze[3] the dielectric tensor (with spatial dispersion taken into account) was obtained on the basis of phenomenological considerations. In papers by Shafranov,[4] Drummond,[5] and Klimontovich[7] this tensor was investigated for a classical gas of charged particles. We may note that in the classical analysis it is impossible in principle to take account of the diamagnetic currents. Quantum mechanical expressions for the dielectric tensor have been considered on the basis of particular models by a number of authors.[1,8-10]

In a paper by Nakajima,[11] a method developed by Kubo[12] was used to obtain a general quantum mechanical expression for the current density in the case of a uniform medium. This expression includes the diamagnetic currents. However, Nakajima did not obtain expressions for the magnetic susceptibility and did not relate this quantity to the electrical conductivity. In the present paper we have obtained expressions for the magnetic susceptibility and the conductivity in which spatial dispersion has been taken into account. Certain properties of the magnetization current have been derived and a universal relation has been established between the conductivity and the magnetic susceptibility.

1. AVERAGING OF THE CURRENT DENSITY

We consider a system with a weak electromagnetic field which is described by the vector and scalar potentials $\mathbf{A}(\mathbf{x}, t)$ and $U(\mathbf{x}, t)$. The electromagnetic field is not quantized.

In the approximation in which the field is linear the Hamiltonian of the system can be written in the form

$$\mathcal{H} = \mathcal{H}_0 + V, \qquad (1)$$

where $\mathcal{H}_0$ is the Hamiltonian of the unperturbed system and

$$V = \int \rho(\mathbf{x})\, U(\mathbf{x}, t)\, d\mathbf{x} - \frac{1}{c}\int J_\mu(\mathbf{x})\, A_\mu(\mathbf{x}, t)\, d\mathbf{x}. \qquad (2)$$

Here

$$\rho(\mathbf{x}) = \sum_n e_n \delta(\mathbf{x} - \mathbf{x}_n) \qquad (3)$$

is the charge density operator and

$$\mathbf{J}(\mathbf{x}) = \sum_n (e_n/2m_n)\,[\mathbf{p}_n \delta(\mathbf{x} - \mathbf{x}_n) + \delta(\mathbf{x} - \mathbf{x}_n)\,\mathbf{p}_n] + c\,\mathrm{curl} \sum_n \boldsymbol{\mu}_n \delta(\mathbf{x} - \mathbf{x}_n) \qquad (4)$$

is the current density operator for the unperturbed system. $\mathbf{p}_n$ is the kinetic momentum of a particle with the perturbing field neglected and μ_n is the operator for the inherent magnetic moment of the particle. The summation is taken over all particles of the system.

The system is described by the density matrix F which obeys the equation

$$i\hbar \dot{F} = [(\mathcal{H}_0 + V),\ F].$$

We assume that the perturbation appears adiabatically and that $F \rightarrow F_0$ when $t \rightarrow -\infty$, where

$$F_0 = e^{-\beta\mathcal{H}_0}(\mathrm{Sp}\, e^{-\beta\mathcal{H}_0})^{-1}, \qquad \beta = 1/kT.$$

Using a method analogous to that used by Nakajima,[11] we obtain the following expression for the mean value of the change in current density proportional to the external field

$$\langle \Delta \mathbf{j}(\mathbf{x}, t)\rangle = \mathbf{j}^{(1)}(\mathbf{x}, t) + \mathbf{j}^{(2)}(\mathbf{x}, t), \qquad (5)$$

where

$$j_\mu^{(1)}(\mathbf{x}, t) = \int_{-\infty}^{t} dt' \int d\mathbf{x}' \, \varphi_{\mu\nu}(\mathbf{x}, \mathbf{x}', t, t') E_\nu(\mathbf{x}', t'), \tag{6}$$

$$j_\mu^{(2)}(\mathbf{x}, t) = \int d\mathbf{x}' \, \varphi_{\mu\nu}(\mathbf{x}, \mathbf{x}', 0, 0) \frac{1}{c} A_\nu(\mathbf{x}', t) - A_\mu(\mathbf{x}, t) \, \mathrm{Sp}\left\{F_0 \sum_n \frac{e_n}{m_n} \delta(\mathbf{x} - \mathbf{x}_n)\right\}, \tag{7}$$

$$\varphi_{\mu\nu}(\mathbf{x}, \mathbf{x}', t, t') = \int_0^\beta \mathrm{Sp}\,\{F_0 J_\nu(\mathbf{x}', t' - i\hbar\lambda) J_\mu(\mathbf{x}, t)\}\, d\lambda. \tag{8}$$

Equations (5) — (8) becomes Nakajima's Eqs. (7) — (10) if we assume that the medium is uniform and neglect spin terms in the expressions for the current density (4).

2. PROPERTIES OF THE RESPONSE FUNCTION

a) Symmetry Properties

In the representation in which $\mathcal{H}_0$ is diagonal $\varphi_{\mu\nu}$ has the form

$$\varphi_{\mu\nu}(\mathbf{x}, \mathbf{x}', t, t') = \sum_{mk} e^{-i\omega_{mk}(t-t')} \times J_\nu(\mathbf{x}')_{mk} J_\mu(\mathbf{x})_{km} \frac{e^{-\beta E_k} - e^{-\beta E_m}}{E_m - E_k} (\mathrm{Sp}\, e^{-\beta\mathcal{H}_0})^{-1}. \tag{9}$$

The following properties of $\varphi_{\mu\nu}$ follow directly from this equation:

1) $\varphi_{\mu\nu}(\mathbf{x}, \mathbf{x}'; t, t')$

depends only on the time difference $t - t' = \tau$. In what follows we denote this dependence by $\varphi_{\mu\nu}(\mathbf{x}, \mathbf{x}', \tau)$.

2) $\varphi_{\mu\nu}(\mathbf{x}, \mathbf{x}', \tau)$ — is real,
3) $\varphi_{\mu\nu}(\mathbf{x}, \mathbf{x}', \tau) = \varphi_{\nu\mu}(\mathbf{x}', \mathbf{x}, -\tau)$,
4) $\varphi_{\mu\nu}(\mathbf{x}, \mathbf{x}', \tau, \mathrm{H}) = \varphi_{\mu\nu}(\mathbf{x}, \mathbf{x}', -\tau, -\mathrm{H})$.

Here H is a magnetic field. From 3) and 4) it follows that

5) $\varphi_{\mu\nu}(\mathbf{x}, \mathbf{x}', \tau, \mathrm{H}) = \varphi_{\nu\mu}(\mathbf{x}', \mathbf{x}, \tau, -\mathrm{H})$.

b) Properties of the Response Function for Coinciding Times

In what follows the following relation, which can be easily verified by direct calculation, will be found useful

$$[\rho(\mathbf{x}'), J_\mu(\mathbf{x})] = -i\hbar(\partial\delta(\mathbf{x} - \mathbf{x}')/\partial x'_\mu) \sum_n (e_n^2/m_n)\, \delta(\mathbf{x} - \mathbf{x}_n). \tag{10}$$

Whence we obtain

$$\partial\varphi_{\mu\nu}(\mathbf{x}, \mathbf{x}', 0)/\partial x'_\nu = (\partial\delta(\mathbf{x}' - \mathbf{x})/\partial x'_\mu, \mathrm{Sp})\left\{F_0 \sum_n (e_n^2/m_n)\, \delta(\mathbf{x} - \mathbf{x}_n)\right\}, \tag{11}$$

so that for any function $g(\mathbf{x}')$ we have

$$\int \varphi_{\mu\nu}(\mathbf{x}, \mathbf{x}', 0) \frac{\partial g(\mathbf{x}')}{\partial x'_\nu} dx' = \frac{\partial g(\mathbf{x})}{\partial x_\mu} \mathrm{Sp}\left\{F_0 \sum_n \frac{e_n^2}{m_n} \delta(\mathbf{x} - \mathbf{x}_n)\right\}. \tag{12}$$

Further

$$\int \varphi_{\mu\nu}(\mathbf{x}, \mathbf{x}', 0)\, d\mathbf{x}' = \delta_{\mu\nu} \mathrm{Sp}\left\{F_0 \sum_n (e_n^2/m_n)\, \delta(\mathbf{x} - \mathbf{x}_n)\right\}. \tag{13}$$

c) Relation Between the Response Function and the Correlation Functions

Following references 6 and 12, we introduce the current correlation function

$$\psi_{\mu\nu}(\mathbf{x}, \mathbf{x}', \tau) = \frac{1}{2} \mathrm{Sp}\,\{F_0 (J_\nu(\mathbf{x}', 0) J_\mu(\mathbf{x}, \tau) + J_\mu(\mathbf{x}, \tau) J_\nu(\mathbf{x}', 0))\}. \tag{14}$$

We denote the Fourier components of the functions $\psi_{\mu\nu}$ and $\varphi_{\mu\nu}$ by $\tilde{\psi}_{\mu\nu}$ and $\tilde{\varphi}_{\mu\nu}$, so that for example

$$\tilde{\psi}_{\mu\nu}(\mathbf{x}, \mathbf{x}', \omega) = \frac{1}{2\pi} \int e^{i\omega\tau} \psi_{\mu\nu}(\mathbf{x}, \mathbf{x}', \tau)\, d\tau.$$

Using Eq. (9) in a way similar to that given in reference 6 we obtain the relation between $\tilde{\psi}_{\mu\nu}(\mathbf{x}, \mathbf{x}', \omega)$ and $\tilde{\varphi}_{\mu\nu}(\mathbf{x}, \mathbf{x}', \omega)$:

$$\tilde{\varphi}_{\mu\nu}(\mathbf{x}, \mathbf{x}', \omega) = \tilde{\psi}_{\mu\nu}(\mathbf{x}, \mathbf{x}', \omega)/E_\beta(\omega). \tag{15}$$

Here $E_\beta(\omega)$ is the mean energy of the oscillator for a given temperature

$$E_\beta(\omega) = (\hbar\omega/2) \coth(\hbar\omega/2kT).$$

3. MAGNETIZATION CURRENT

As is apparent from Eq. (7), the current $\mathbf{j}^{(2)}(\mathbf{x}, t)$ does not contain a delay with respect to the vector potential $\mathbf{A}(\mathbf{x}, t)$. When $\omega = 0$, in the absence of an electric field the total current density of the system reduces to $\mathbf{j}^{(2)}$. Hence, when $\omega = 0$, $\mathbf{j}^{(2)}$ has the significance of a magnetization current. When $\omega \neq 0$ this simple significance no longer holds since $\mathbf{j}^{(1)}$ contains terms which are proportional to the induced electric field and, consequently, are proportional to the magnetic field. However, for convenience we will call the current $\mathbf{j}^{(2)}$ the magnetization current. We may note several of its general properties.

a) The gauge invariance; this is easily demonstrated by means of Eq. (12).

b) div $\mathbf{j}^{(2)} = 0$. This property follows directly from Eq. (11). It allows us to write $\mathbf{j}^{(2)} = c \operatorname{curl} \mathbf{M}(\mathbf{x}, t)$; $\mathbf{M}(\mathbf{x}, t)$ may be called the magnetic moment density of the system. [Actually $\mathbf{M}(\mathbf{x}, t)$ has the meaning of a magnetic moment density only when $\omega = 0$.]

c) Using Eq. (13) we can write $\mathbf{j}^{(2)}$ in the form

$$j_\mu^{(2)}(\mathbf{x}, t) = \frac{1}{c}\int d\mathbf{x}' \cdot \varphi_{\mu\nu}(\mathbf{x}, \mathbf{x}', 0)\,[\mathbf{A}_\nu(\mathbf{x}', t) - A_\nu(\mathbf{x}, t)]. \quad (16)$$

From Eq. (13) it follows that $\int \mathbf{j}^{(2)}(\mathbf{x}, t)\,d\mathbf{x} = 0$.

d) From Eq. (12) we have

$$\partial j_\mu^{(2)}(\mathbf{x}, t)/\partial t$$

$$= -\int d\mathbf{x}' \cdot \varphi_{\mu\nu}(\mathbf{x}, \mathbf{x}', 0)\,[E_\nu(\mathbf{x}', t) - E_\nu(\mathbf{x}, t)]. \quad (17)$$

e) As is apparent from Eq. (15), in the classical limit

$$\varphi_{\mu\nu}(\mathbf{x}, \mathbf{x}', \tau) = \beta \langle J_\nu(\mathbf{x}', 0)\, J_\mu(\mathbf{x}, \tau)\rangle.$$

Here the angular brackets denote averages over the classical canonical distribution. In this case a direct calculation yields $\mathbf{j}^{(2)} = c \operatorname{curl} \mathbf{M}_{\mathrm{cl}}$, where

$$\mathbf{M}_{\mathrm{cl}} = \langle \sum_n \mu_n\, \delta(\mathbf{x} - \mathbf{x}_n)\, \frac{1}{kT} \sum_m (\mu_m, \mathbf{H}(\mathbf{x}_m))\rangle.$$

$\mathbf{M}_{\mathrm{cl}}$ is the classical paramagnetic moment density of the system.

Thus we obtain a well-known result: the diamagnetic moment computed from classical mechanics is zero.

4. CASE OF AN EXTERNAL FIELD THAT VARIES HARMONICALLY IN TIME

Let $E_\mu(\mathbf{x}, t) = E_\mu(\mathbf{x})\, e^{-i\omega t}$. Then, using Eq. (11) we have

$$j_\mu^{(1)}(\mathbf{x}, t) = e^{-i\omega t} \int K_{\mu\nu}(\mathbf{x}, \mathbf{x}', \omega)\, E_\nu(\mathbf{x}')\, d\mathbf{x}',$$

$$K_{\mu\nu}(\mathbf{x}, \mathbf{x}', \omega) = \int_0^\infty e^{i\omega t}\, \varphi_{\mu\nu}(\mathbf{x}, \mathbf{x}', \tau)\, d\tau. \quad (18)$$

Using Eqs. (11), (17), and (18) (with $\omega \neq 0$) we can express the total current density in terms of the electric field:

$$\langle \Delta j_\mu(\mathbf{x}, t)\rangle = e^{-i\omega t} \Big\{ E_\nu(\mathbf{x}) \int K_{\mu\nu}(\mathbf{x}, \mathbf{x}', \omega)\, d\mathbf{x}'$$

$$+ \int K'_{\mu\nu}(\mathbf{x}, \mathbf{x}' \ \omega)\, [E_\nu(\mathbf{x}') - E_\nu(\mathbf{x})]\, d\mathbf{x}' \Big\}. \quad (19)$$

Here

$$K'_{\mu\nu}(\mathbf{x}, \mathbf{x}', \omega) = -\frac{1}{i\omega} \int_0^\infty e^{i\omega\tau}\, \frac{\partial \varphi_{\mu\nu}(\mathbf{x}, \mathbf{x}', \tau)}{\partial \tau}\, d\tau.$$

The quantity $K'_{\mu\nu}(\mathbf{x}, \mathbf{x}', \omega)$ is given by the relation

$$K'_{\mu\nu}(\mathbf{x}, \mathbf{x}', \omega) = K_{\mu\nu}(\mathbf{x}, \mathbf{x}', \omega) - (i/\omega)\, \varphi_{\mu\nu}(\mathbf{x}, \mathbf{x}', 0). \quad (20)$$

The divergence in $K'_{\mu\nu}(\mathbf{x}, \mathbf{x}', \omega)$ when $\omega = 0$ is due to the fact that it is impossible to express the total current density in terms of the electric field alone when $\omega = 0$. In this case it is necessary to use Eqs. (16) and (18).

5. CASE OF A UNIFORM MEDIUM

In the case of a uniform medium $\varphi_{\mu\nu}(\mathbf{x}, \mathbf{x}', \tau)$ depends only on the difference $\mathbf{x} - \mathbf{x}' = \mathbf{r}$ and, for a medium which has a center of inversion, is an even function of $\mathbf{r}$. In what follows, for the case of a uniform medium we will designate the response function by $\varphi_{\mu\nu}(\mathbf{r}, \tau)$:

$$\varphi_{\mu\nu}(\mathbf{r}, \tau) = \int_0^\beta \operatorname{Sp}\{F_0 J_\nu(0, -i\hbar\lambda)\, J_\mu(\mathbf{r}, \tau)\}\, d\lambda. \quad (21)$$

We list the symmetry properties of this function which follow from the results of Sec. 2:

1) $\varphi_{\mu\nu}(\mathbf{r}, \tau) = \varphi_{\nu\mu}(-\mathbf{r}, -\tau)$,

2) $\varphi_{\mu\nu}(\mathbf{r}, \tau, \mathbf{H}) = \varphi_{\mu\nu}(\mathbf{r}, -\tau, -\mathbf{H})$,

3) $\varphi_{\mu\nu}(\mathbf{r}, \tau, \mathbf{H}) = \varphi_{\nu\mu}(-\mathbf{r}, \tau, -\mathbf{H})$. (22)

Let

$$E_\mu(\mathbf{x}, t) = E_\mu(\mathbf{k}, \omega)\, e^{i(\mathbf{kx} - \omega t)} \quad \text{etc.}$$

Then Eq. (6) yields:

$$j_\mu^{(1)}(\mathbf{x}, t) = \sigma_{\mu\nu}(\mathbf{k}, \omega)\, E_\nu(\mathbf{x}, t). \quad (23)$$

Here

$$\sigma_{\mu\nu}(\mathbf{k}, \omega) = \int_0^\infty e^{i\omega\tau} \int e^{-i\mathbf{kr}}\, \varphi_{\mu\nu}(\mathbf{r}, \tau)\, d\mathbf{r}\, d\tau. \quad (24)$$

Equation (16) can be written in the form

$$j_\mu^{(2)} = (1/c) \int \varphi_{\mu\nu}(\mathbf{r}, 0)\, [A_\nu(\mathbf{x} - \mathbf{r}) - A_\nu(\mathbf{x})]\, d\mathbf{r},$$

whence, by means of Eq. (12) and the relation $\mathbf{H} = \operatorname{curl} \mathbf{A}$, we have

$$\operatorname{curl}_\mu \mathbf{j}^{(2)}(\mathbf{x}, t)$$

$$= (1/c) \int \varkappa_{\mu\nu}(\mathbf{r})\, [H_\nu(\mathbf{x} - \mathbf{r}, t) - H_\nu(\mathbf{x}, t)]\, d\mathbf{r}, \quad (25)$$

where

$$\varkappa_{\mu\nu}(\mathbf{r}) = \delta_{\mu\nu} \sum_\alpha \varphi_{\alpha\alpha}(\mathbf{r}, 0) - \varphi_{\mu\nu}(\mathbf{r}, 0).$$

From Eq. (16) and property b) of the current $\mathbf{j}^{(2)}$ (cf. Sec. 3) we have

$$\mathbf{j}^{(2)} = c \operatorname{curl} \mathbf{M}, \qquad M_\mu(x, t) = \chi_{\mu\nu}(\mathbf{k})\, H_\nu(\mathbf{x}, t),$$

where

$$\chi_{\mu\nu}(\mathbf{k}) = (kc)^{-2}\int \varkappa_{\mu\nu}(\mathbf{r})\,(e^{-i\mathbf{kr}} - 1)\,d\mathbf{r}. \qquad (26)$$

It is clear from these relations that to describe electromagnetic effects in uniform media it is sufficient to introduce a conductivity $\sigma_{\mu\nu}(\mathbf{k}, \omega)$ which depends on ω and a magnetic susceptibility $\chi_{\mu\nu}(\mathbf{k})$ which is independent of ω.

When $\omega \neq 0$, in general it is not possible to introduce a magnetic susceptibility. From Eq. (19) we obtain the following expression for the total current density:

$$\langle \Delta j_\mu(\mathbf{x}, t)\rangle = [\sigma_{\mu\nu}(0, \omega) + \sigma'_{\mu\nu}(\mathbf{k}, \omega)]\,E_\nu(\mathbf{x}, t).$$

Here

$$\sigma_{\mu\nu}(0, \omega) = \int_0^\infty e^{i\omega\tau}\,d\tau \int \varphi_{\mu\nu}(\mathbf{r}, \tau)\,d\mathbf{r},$$

$$\sigma'_{\mu\nu}(\mathbf{k}, \omega) = -\frac{1}{i\omega}\int_0^\infty e^{i\omega\tau}\,d\tau \int \frac{\partial\varphi_{\mu\nu}(\mathbf{r}, \tau)}{\partial\tau}(e^{-i\mathbf{kr}} - 1)\,d\mathbf{r}. \qquad (27)$$

The Kramers-Kronig relation and the fluctuation-dissipation theorem can be obtained from the following formula

$$\sigma_{\mu\nu}(\mathbf{k}, \omega) = \frac{\pi}{E_\beta(\omega)}\widetilde{\psi}_{\mu\nu}(\mathbf{k}, \omega) + i\int_{-\infty}^{\infty} \frac{1}{E_\beta(\omega')}\frac{\widetilde{\psi}_{\mu\nu}(\mathbf{k}, \omega')}{\omega - \omega'}\,d\omega'. \qquad (28)$$

This follows directly from Eqs. (15) and (24) where

$$\widetilde{\psi}_{\mu\nu}(\mathbf{k}, \omega) \equiv \int e^{-i\mathbf{kr}}\,\widetilde{\psi}_{\mu\nu}(\mathbf{r}, \omega)\,d\mathbf{r}.$$

We may note the symmetry properties of $\sigma_{\mu\nu}$ and $\chi_{\mu\nu}$ which follow from Eq. (19) [the same properties are possessed by $\sigma'_{\mu\nu}(\mathbf{k}, \omega)$]:

$$\overset{*}{\sigma}_{\mu\nu}(\mathbf{k}, \omega) = \sigma_{\mu\nu}(-\mathbf{k}, -\omega), \quad \sigma_{\mu\nu}(\mathbf{k}, \omega, \mathbf{H}) = \sigma_{\nu\mu}(-\mathbf{k}, \omega, -\mathbf{H}). \qquad (29)$$

The last relation is the Onsager relation. If there is a center of inversion

$$\varphi_{\mu\nu}(\mathbf{r}, \tau) = \varphi_{\mu\nu}(-\mathbf{r}, \tau), \quad \sigma_{\mu\nu}(\mathbf{k}, \omega) = \sigma_{\mu\nu}(-\mathbf{k}, \omega). \qquad (30)$$

Similar properties are possessed by $\chi_{\mu\nu}(\mathbf{k})$.

The properties in (29) are a particular case of the general symmetry properties of the kinetic coefficients.[6]

The tensor $\chi_{\mu\nu}$ is related to the tensor $\sigma_{\mu\nu}$ by the following relation:

$$\chi_{\mu\nu}(\mathbf{k}) = \frac{1}{2\pi k^2c^2}\int_{-\infty}^{\infty} d\omega\,\Big\{\delta_{\mu\nu}\sum_\alpha [\sigma^s_{\alpha\alpha}(\mathbf{k}, \omega) - \sigma^s_{\alpha\alpha}(0, \omega)] - [\sigma^s_{\mu\nu}(\mathbf{k}, \omega) - \sigma^s_{\mu\nu}(0, \omega)]\Big\}. \qquad (31)$$

Here

$$\sigma^s_{\mu\nu}(\mathbf{k}, \omega) = \sigma_{\mu\nu}(\mathbf{k}, \omega, \mathbf{H}) + \sigma_{\mu\nu}(\mathbf{k}, -\omega, -\mathbf{H}),$$

$\mathbf{H}$ is the magnetic field in the unperturbed Hamiltonian.

Thus the magnetic susceptibility is closely related to the spatial dispersion of the conductivity.

In the expression $j_\mu = ic\epsilon_{\mu\nu l}k_\nu\chi_{ln}H_n$ the components χ_{ln} do not appear when l or n are equal to z if $\mathbf{k}$ is directed along the z-axis. Hence the longitudinal part of $\chi_{ln}(\mathbf{k})$ has no physical significance.

For a given direction of the vector $\mathbf{k}$, when $k \to 0$, we can determine from Eq. (26) only four (transverse) components of the magnetic susceptibility tensor $\chi_{ln}(0)$ for a uniform magnetic field. In order to obtain all ten components of this tensor it is necessary to use Eq. (26) with $k \to 0$ for three mutually perpendicular directions of $\mathbf{k}$. In this case the diagonal components of the tensor χ_{ln} appear twice; for example the component χ_{xx} is obtained when $\mathbf{k}$ is along the y axis or along the z axis. In the first case

$$\chi_{xx} = -\frac{1}{2c^2}\int \varkappa_{xx}\,y^2 d\mathbf{r} = -\frac{1}{2c^2}\int \varphi_{zz}y^2\,d\mathbf{r},$$

and in the second case

$$\chi_{xx} = -\frac{1}{2c^2}\int \varkappa_{xx}z^2 d\mathbf{r} = -\frac{1}{2c^2}\int \varphi_{yy}z^2 d\mathbf{r}.$$

These integrals are equal because of the relation

$$\sum_\mu \int \varphi_{x\mu}(\mathbf{r}, 0)\,\nabla_\mu(xy^2)\,d\mathbf{r} = \sum_\mu \int \varphi_{y\mu}(\mathbf{r}, 0)\,\nabla_\mu(y^2x)\,d\mathbf{r} = 0,$$

which follows from Eq. (12).

A comparison of the results obtained for $k \to 0$ for three mutually perpendicular directions of $\mathbf{k}$ leads to the following expression for the complete tensor $\chi_{\mu\nu}(0)$:

$$\chi_{\mu\nu}(0) = -\frac{1}{2c^2}\int \Big[\frac{1}{2}\delta_{\mu\nu}\sum_\alpha \varphi_{\alpha\alpha}(\mathbf{r}, 0) - \varphi_{\mu\nu}(\mathbf{r}, 0)\Big] r^2 d\mathbf{r}. \qquad (32)$$

In the case of a fixed uniform (i.e., varying only slightly in a distance of the order of a correlation radius) field the magnetic susceptibility $\chi_{ln}(0)$ is related to the specific magnetic moment by the relation $\chi_{ln}(0) = \partial M_l(\mathbf{H})/\partial H_n$, where $\mathbf{H}$ is the magnetic field in the unperturbed Hamiltonian.

In this work we have used the conventional scheme of a self-consistent field in which the remote interactions are included in the macroscopic electromagnetic field which satisfy Maxwell's equations; only the near interactions appear in the unperturbed Hamiltonian. In this scheme the electromagnetic fields $\mathbf{E}$ and $\mathbf{H}$ are the resultants of the fields of the external sources and the fields produced by the charges and currents of the system. However, it is possible to include all interactions between the particles of a system in the unperturbed Hamiltonian; in this case, by $\mathbf{E}$ and $\mathbf{H}$ we are to understand the fields of the external sources.

The authors are indebted to Prof. L. É. Gurevich for advice and valuable discussions.

---

[1] S. I. Pekar, JETP **33**, 1022 (1957), Soviet Phys. JETP **6**, 785 (1958).

[2] V. L. Ginzburg, JETP **34**, 1593 (1958), Soviet Phys. JETP **7**, 1096 (1958).

[3] V. M. Agranovich and A. A. Rukhadze, JETP **35**, 982, 1171 (1953), Soviet Phys. JETP **8**, 819 (1959).

[4] V. D. Shafranov, JETP **34**, 1475 (1958), Soviet Phys. JETP **7**, 1019 (1958).

[5] J. E. Drummond, Phys. Rev. **110**, 293 (1958).

[6] L. D. Landau and E. M. Lifshitz, Электродинамика сплошных сред, (Electrodynamics of Continuous Media) Gostekhizdat, 1957.

[7] Yu. L. Klimontovich, JETP **34**, 173 (1958), Soviet Phys. JETP **7**, 119 (1958).

[8] G. E. H. Reuter and E. H. Sondheimer, Proc. Roy. Soc. **A195**, 336 (1948).

[9] F. G. Bass and M. I. Kaganov, JETP **34**, 1154 (1958), Soviet Phys. JETP **7**, 799 (1958).

[10] J. Lindhard, Det. Kong. Dan. Vid. Mat.-fys. Medd. **28**, 8 (1954).

[11] S. Nakajima, Proc. Phys. Soc. **69A**, 441 (1956).

[12] R. Kubo, J. Phys. Soc. (Japan) **12**, 570 (1957).

Translated by H. Lashinsky
147

SOVIET PHYSICS JETP VOLUME 37(10), NUMBER 3 MARCH, 1960

PAIR PRODUCTION IN COLLISIONS BETWEEN CHARGED PARTICLES

F. F. TERNOVSKIĬ

Moscow State University

Submitted to JETP editor April 11, 1959

J. Exptl. Theoret. Phys. (U.S.S.R.) **37**, 793-798 (September, 1959)

Pair production due to collisions between fast charged particles and atoms is considered. Expressions for the cross sections are obtained which are valid for positron and electron energies comparable with that of the parent particle.

1. INTRODUCTION

THE effect of pair production in collisions between charged particles has been discussed in references 1 to 5. The expressions obtained in these articles for cross sections agree in the region of pair particle energies ϵ_+ and ϵ_- which satisfy the inequality $\epsilon_+ + \epsilon_- \ll E/m$ (region I). The cross sections in the region $\epsilon_+ + \epsilon_- \gg E/m$ (region II) were discussed in the articles by Bhabha[2] and Murota and others.[5] The latter article, written not long ago, shows the error of Bhabha's results in region II. However, it seems that even Murota's work is not exact.

Two types of processes contribute to the cross section for the effect under consideration: (a) processes of the first order, where the pair particles are considered free; (b) processes of the second order, where the parent particle is considered free. Processes of the second order make the main contribution to the integral cross section. However, if we look over the cross sections in region II the contribution of processes of the first order can be decisive.

Finally we note, in reviewing radiative processes in the high-energy region, that the influence of multiple scattering is substantial. Landau and Pomeranchuk[6,7] were the first to draw attention to this fact. The cross sections for bremsstrahlung and pair production by γ quanta were obtained by Migdal[8] taking this effect into consideration. The following article discusses the influence of multiple scattering on pair production by charged particles.

2. CONTRIBUTION OF SECOND-ORDER PROCESSES

We shall examine pair production by singly charged particles with the mass $m \gg 1$ and the energy $E \gg m$.* We also will assume the energy of the electron to be $\epsilon_- \gg 1$ and the energy of the positron to be $\epsilon_+ \gg 1$. The contribution to the differential cross section of second order processes in the lowest approximation theory of excitation gives the expression

$$d\sigma = \frac{e^4}{(k^2-\omega^2)^2}\overline{|P_\mu G_\mu|^2}\frac{\delta(E-E'-\omega)\,d^3p'd^3p_+d^3p_-}{(2\pi)^8 J}, \qquad (1)$$

where $\mathbf{p}$ is the initial momentum and $\mathbf{p}'$ is the final momentum of the parent particle;

$$\mathbf{k}=\mathbf{p}-\mathbf{p}'; \quad E=\sqrt{p^2+m^2}, \quad E'=\sqrt{p'^2+m^2},$$

$$\omega=\varepsilon_+ + \varepsilon_-, \quad \varepsilon_\pm=\sqrt{p_\pm^2+1},$$

$$\mathbf{q}=\mathbf{k}-\mathbf{p}_+-\mathbf{p}_-; \quad J = p/E\approx 1;$$

P_μ is the transition current of the parent particle equal to $(p+p')_\mu/2\sqrt{EE'}$ for the scalar particles and $(\bar{u}_{\mathbf{p}'}\gamma_\mu u_{\mathbf{p}})$ for particles with spin $\frac{1}{2}$;

$$G_\mu = \left(u_{\mathbf{p}_-}\left[\gamma_4\frac{i(\hat{k}-\hat{p}_+)-1}{(\mathbf{k}-\mathbf{p}_+)^2+1}\gamma_\mu + \gamma_\mu\frac{i(\hat{p}_- - \hat{k})-1}{(\mathbf{p}_- - \mathbf{k})^2+1}\gamma_4\right]v_{\mathbf{p}_+}\right)V_{\mathbf{q}} \qquad (2)$$

is the matrix element for pair production by a virtual quantum; the dash indicates an averaging over the initial state spins and the summation over the final state spins.

It is convenient to do the calculation in the coordinate system whose z axis is directed along the vector $\mathbf{n}=\mathbf{k}/k$ (k-system).

Because of gauge invariance in the k-system, the following equations hold:

$$P_3 k + i\omega P_4 = 0, \qquad G_3 k + i\omega G_4 = 0,$$

therefore

$$P_\mu G_\mu = P_i G_i + (1-\omega^2/k^2)P_4 G_4,$$

with the summation for i going from 1 to 2. After integrating over the angles, quantities of the type $\overline{(P_\mu P_\nu^*)}$ with $\mu \neq \nu$ vanish, and $\overline{|P_1|^2}$ and $\overline{|P_2|^2}$ give equal contributions. Therefore we can substitute

---

*A system of units is used in which $\hbar = m_e = c = 1$.

$$\overline{|P_\mu G_\mu|^2} \rightarrow {}^1/_2 \overline{|P_\perp|^2}\,\overline{|G_\perp|^2} + (1-\omega^2/k^2)^2\,\overline{|P_4|^2}\,\overline{|G_4|^2}, \quad (3)$$

where

$$|P_\perp|^2 = |P_1|^2 + |P_2|^2, \qquad |G_\perp|^2 = |G_1|^2 + |G_2|^2.$$

The first term in the right side of (3) describes the contribution of transverse photons and the second term describes the contribution of longitudinal and scalar photons.

The calculations of the quantities included in (3) are somewhat more complex than in the theory of pair production by real quanta. We obtain

$$\overline{|G_\perp|^2} = 4\Big[\Big(\frac{1}{M^2+p_+^2\theta_+^2} - \frac{1}{M^2+p_-^2\theta_-^2}\Big)^2$$

$$+\frac{p_+^2+p_-^2}{k^2}\Big(\frac{p_+\theta_+}{M^2+p_+^2\theta_+^2} - \frac{p\_\theta\_}{M^2+p_-^2\theta_-^2}\Big)^2\Big]|\mathbf{V_q}|^2, \quad (4)$$

which includes notations understandable from the following equations:

$$\mathbf{p}_\pm = \mathbf{n}p_\pm\Big(1-\frac{1}{2}\theta_\pm^2\Big) + p_\pm\boldsymbol{\theta}_\pm, \qquad \mathbf{p} = \mathbf{n}p\Big(1-\frac{1}{2}\theta^2\Big)+p\boldsymbol{\theta},$$

$$\mathbf{p}' = \mathbf{n}\Big(p-k-\frac{1}{2}p\theta^2\Big) + p\boldsymbol{\theta},$$

$$M^2 = 1 + p_+p_-(m^2+p^2\theta^2)/p(p-k). \quad (5)$$

The matrix element for pair production by real quanta is obtained from (4) with $M^2 = 1$.

The calculation of $\overline{|G_4|^2}$ is not difficult. With the required accuracy we obtain

$$\overline{|G_4|^2} = 8p_+^2p_-^2k^{-2}[1/(M^2+p_+^2\theta_+^2)$$

$$-1/(M^2+p_-^2\theta_-^2)]^2|V_\mathbf{q}|^2. \quad (6)$$

For scalar particles

$$|P_\perp|^2 = p^2\theta^2/p(p-k),$$

$$|P_4|^2 = (p-k/2)^2/p(p-k); \quad (7)$$

for particles with spin $\frac{1}{2}$

$$\overline{|P_\perp|^2} = \frac{m^2k^2+[p^2+(p-k)^2]p^2\theta^2}{2p^2(p-k)^2}, \qquad \overline{|P_4|^2} = 1. \quad (8)$$

In addition we find

$$k^2-\omega^2 = k^2(m^2+p^2\theta^2)/p(p-k). \quad (9)$$

Using (5), the vector $\mathbf{p}'$ can be represented in the form

$$\mathbf{p}' = (p-k)(\mathbf{p}/p-\boldsymbol{\theta}) + p\boldsymbol{\theta} = (\mathbf{p}/p)(p-k) + k\boldsymbol{\theta},$$

whence

$$\delta(E-E'-\omega)\,d^3p'd^3p_+d^3p_-$$

$$- k^2d\boldsymbol{\theta}p_+^2d\boldsymbol{\theta}_+dp_+p_-^2d\boldsymbol{\theta}_-dp_-. \quad (10)$$

Finally, for the neutral atom

$$V_\mathbf{q} = Ze^2/(q^2+q_0^2), \quad (11)$$

where $q_0 = Z^{1/3}/137$ is the inverse Thomas-Fermi radius, and for $\mathbf{q}^2$ we obtain from (5)

$$\mathbf{q}^2 = (p_+\boldsymbol{\theta}_+ + p_-\boldsymbol{\theta}_-)^2$$

$$+\tfrac{1}{4}(p_+\theta_+^2+p_-\theta_-^2+kM^2/p_+p_-)^2. \quad (12)$$

Now, using (1) to (12) we can obtain the expression for the differential cross section.

Integration over angles must be done next. For this we note that the angles $\theta_\pm < \max\{1/k, m/p\}$ give the main contribution, so that the quantities $p_\pm\theta_\pm^2$ included in q^2 can be ignored. After this we introduce new variables

$$\mathbf{y} = (2M)^{-1}(p_+\boldsymbol{\theta}_+ + p_-\boldsymbol{\theta}_-),$$

$$\mathbf{x} = (2M)^{-1}(p_+\boldsymbol{\theta}_+ - p_-\boldsymbol{\theta}_-), \quad (13)$$

in which integration over $d\mathbf{x}$ is easily done. As a result we obtain

$$\int\overline{|G_\perp|^2}p_+^2d\boldsymbol{\theta}_+p_-^2d\boldsymbol{\theta}_-$$

$$=2^6\pi^2Z^2e^4\int_0^\infty\frac{[\psi(y)+M^2(p_+^2+p_+^2)k^{-2}\varphi(y)]\,ydy}{[4M^2y^2+(k/2p_+p_-)^2M^4+q_0^2]^2}, \quad (14)$$

$$\int\overline{|G_4|^2}\,p_+^2d\boldsymbol{\theta}_+p_-^2d\boldsymbol{\theta}_-$$

$$=2^7\pi^2Z^2e^4\,\frac{p_+^2p_-^2}{k^2}\int_0^\infty\frac{\psi(y)\,y\,dy}{[4M^2y^2+(k/2p_+p_-)^2M^4+q_0^2]^2}, \quad (15)$$

where

$$\psi(y) = 1-\frac{1}{y\sqrt{1+y^2}}\sinh^{-1}y,$$

$$\varphi(y) = \frac{2y^2+1}{y\sqrt{1+y^2}}\sinh^{-1}y-1. \quad (16)$$

In integrals (14) and (15) the values of y are very small so that they may be calculated approximately with logarithmic accuracy. The lower limit of integration as can be seen from (12) is determined by the largest of the quantities $kM/4p_+p_-$ and $q_0/2M$. In determining the upper limit it is necessary to consider the final size of the nucleus which limits the maximum magnitude of the transmitted momentum to the values $\sim 1/R$ where $R = 0.5\,r_0Z^{1/3}$ is the radius of the nucleus so that $y_{\max} \sim 1/RM$. On the other hand, the functions $\psi(y)$ and $\varphi(y)$ significantly increase for values $y \lesssim 1$, therefore the upper limit in any case is not above $y_{\max} \sim 1$. Thus we obtain

$$\int \overline{|G_\perp|^2} p_+^2 d\theta_+ p_-^2 d\theta_- = \frac{8\pi^2 Z^2 e^4}{3M^4}\left[1 + 2M^2 \frac{p_+^2 + p_-^2}{k^2}\right] L,$$

$$\int \overline{|G_4|^2}\, p_+^2 d\theta_+ p_-^2 d\theta_- = \frac{16\pi^2 Z^2 e^4}{3M^4} \frac{p_+^2 p_-^2}{k^2} L, \qquad (17)$$

where $L = \ln(y_{\max}/y_{\min})$, with

$$y_{min} = \begin{cases} kM/p_+p_- & \text{for } kM/p_+p_- > q_0/M \\ q_0/M & \text{for } kM/p_+p_- < q_0/M \end{cases},$$

$$y_{max} = \begin{cases} 1 & \text{for } 2MR < 1 \\ 1/2MR & \text{for } 2MR > 1 \end{cases} \qquad (18)$$

It is possible to ignore the dependence of the quantity M on θ inside the logarithm sign without introducing any error, so that in (18) we can assume

$$M = \sqrt{1 + m^2 p_+ p_- / p(p-k)} = \sqrt{1+x}.$$

We also must integrate over $d\theta$. As a result for particles with spin $\frac{1}{2}$

$$d\sigma_{1/2} = \frac{2\alpha^2 Z^2 r_0^2}{3\pi k^2} L \left\{ \frac{p^2 + (p-k)^2}{p^2}\left[A(x) + 2\frac{p_+^2 + p_-^2}{k^2} B(x)\right]\right.$$

$$+ \frac{k^2}{p^2}\left[C(x) + 2\frac{p_+^2 + p_-^2}{k^2} D(x)\right]$$

$$\left. + \frac{8p_+p_-}{k^2} \frac{p-k}{p(1+x)}\right\} dp_+ dp_-, \qquad (19)$$

and for particles with spin 0

$$d\sigma_0 = \frac{4\alpha^2 Z^2 r_0^2}{3\pi k^2} L \left\{ \frac{p-k}{p}\left[A(x) + 2\frac{p_+^2 + p_-^2}{k^2} B(x)\right]\right.$$

$$\left. + \frac{4p_+p_-}{k^2} \frac{(p-k/2)^2}{p^2(1+x)}\right\} dp_+ dp_-. \qquad (20)$$

Here

$$x = m^2 p_+ p_- / p(p-k),$$

$$A(x) = (1+2x)\ln\left(1 + \frac{1}{x}\right) - 2,$$

$$B(x) = (1+x)\ln\left(1+\frac{1}{x}\right) - 1,$$

$$C(x) = \frac{1+2x}{1+x} - 2x\ln\left(1+\frac{1}{x}\right),$$

$$D(x) = 1 - x\ln\left(1+\frac{1}{x}\right). \qquad (21)$$

The first terms in (19) and (20) describe the contribution of transverse photons emitted without spin flip. The last terms are the contribution of longitudinal and scalar photons. The second term in (19) describes the contribution of transverse photons emitted with spin flip of the parent particle.

Now we turn to limiting cases.

I. $k \ll p/m$. Then $x \ll 1$ and according to (19) and (20) we find

$$d\sigma_{1/2} \approx d\sigma_0 \approx \frac{8\alpha^2 Z^2 r_0^2}{3\pi} L \frac{dp_+ dp_-}{k^2}\left[1 + 2\frac{p_+^2 + p_-^2}{k^2}\right] \ln\frac{\varkappa p}{km}, \quad (22)$$

where we have replaced $\sqrt{p_+p_-}$ by k inside the logarithm symbol and introduced the magnitude $\varkappa \approx 1$. The result is in complete accord with the results of other authors and can be obtained using the Weiszäcker-Williams method.

IIa. $k \gg p/m$, $x \gg 1$. In this case we obtain from (21) for the functions A, B, C and D

$$2A(x) \approx C(x) \approx 1/3x^2, \qquad B(x) \approx D(x) \approx 1/2x. \quad (23)$$

Then

$$d\sigma_{1/2} = \frac{4\alpha^2 Z^2 r_0^2}{3\pi k^2} \frac{p(p-k)}{m^2 p_+ p_-} L \left[\frac{p_+^2 + p_-^2}{k^2}\left(1 - \frac{k}{p} + \frac{k^2}{p^2}\right)\right.$$

$$\left. + \frac{4p_+p_-}{k^2}\left(1 - \frac{k}{p}\right)\right] dp_+ dp_-, \qquad (24)$$

$$d\sigma_0 = \frac{4\alpha^2 Z^2 r_0^2}{3\pi k^2} \frac{p(p-k)}{m^2 p_+ p_-} L \left[\frac{p_+^2 + p_-^2}{k^2}\left(1 - \frac{k}{p}\right)\right.$$

$$\left. + \frac{4p_+p_-}{k^2}\left(1 - \frac{k}{2p}\right)^2\right] dp_+ dp_-. \qquad (25)$$

IIb. $k \gg p/m$, $x \ll 1$. In this case we obtain

$$d\sigma_{1/2} = \frac{2\alpha^2 Z^2 r_0^2}{3\pi k^2} L \frac{p^2 + (p-k)^2}{p^2}\left(1 + 2\frac{p_+^2 + p_-^2}{k^2}\right)$$

$$\times \ln\frac{p(p-k)}{m^2 p_+ p_-} dp_+ dp_-; \qquad (26)$$

$$d\sigma_0 = \frac{4\alpha^2 Z^2 r_0^2}{3\pi k^2} L \frac{p-k}{p}\left(1 + 2\frac{p_+^2 + p_-^2}{k^2}\right)$$

$$\times \ln\frac{p(p-k)}{m^2 p_+ p_-} dp_+ dp_-. \qquad (27)$$

The latter results, like the general formulas (19) to (21), are different from those obtained by Murota et al.[5] Even though these authors computed by a somewhat different method they obtained an expression for the differential cross section practically the same as ours. However, in doing the integration over angles they made an inadmissible approximation* that led to substantial mistakes when $k > p/m$.

3. CONTRIBUTION OF FIRST-ORDER PROCESSES

The contribution of first order processes can be found using the same method mentioned in Sec. 2. The calculation of the contribution of interference processes is considerably more difficult and therefore we were forced to limit ourselves to a review of the limiting cases where the contribution of processes of either the first or second order can be ignored.

---

*It was assumed that the substantial values of y are smaller than M/k, which obviously is not true. See (18).

The influence of the external field on the state of the parent particle can be taken into account using a diffraction approximation (see reference 9). Then the contribution of first order processes will be given by a formula analogous to (1), where we must assume

$$\mathbf{P} = \frac{\pi}{\sqrt{EE'}}\left(\frac{2\mathbf{p} - \mathbf{k}}{p' - |\mathbf{p} - \mathbf{k}|} + \frac{2\mathbf{p}' + \mathbf{k}}{p - |\mathbf{p}' + \mathbf{k}|}\right) G,$$

$$P_0 = \frac{\pi}{\sqrt{EE'}}\left(\frac{E + E'}{p' - |\mathbf{p} - \mathbf{k}|} + \frac{E + E'}{p - |\mathbf{p}' + \mathbf{k}|}\right) G,$$

$$G_\mu = (\bar{u}_{p_-} \gamma_\mu v_{p_+}).$$

The quantity G is connected to the scattering matrix

$$\Omega(\rho) = \begin{cases} 0 & \rho < R \\ e^{2i\eta(\rho)} & \rho > R \end{cases}, \quad \eta(\rho) = Z\alpha \ln k\rho$$

by the relation

$$G = \frac{1}{2\pi} \int (1 - \Omega(\rho))\, e^{i(\mathbf{p}-\mathbf{k})\boldsymbol{\rho}}\, d\boldsymbol{\rho},$$

where the integration over $d\boldsymbol{\rho}$ is done along the plane perpendicular to the vector $\mathbf{p}'$ and going through the center of the nucleus.

In calculating the quantities $p' - |\mathbf{p} - \mathbf{k}|$ and $p - |\mathbf{p}' + \mathbf{k}|$ it is necessary to use the law of conservation of energy $E' + \omega = E$. In this case it turns out that the magnitudes of $E - E' - k$ and $\omega - k$ can be of the same order of magnitude, and therefore to ignore the second of them in comparison with the first, as done by Rabinovich,[10] is invalid.

All the calculations are done in the same way as in Sec. 2, therefore we only mention the end result. The contribution of first-order processes to the differential cross section, for particles with spin 0, is equal to

$$dw = \frac{8\alpha^2}{\pi} \frac{p - k}{p} \frac{dp_+ dp_-}{k^2} \int_0^\infty dy \int_0^\infty q\, dq\, |G(2\widetilde{M}q)|^2$$
$$\times \left[\frac{\widetilde{M}^2}{(1+y)^2}\left(1 + \frac{p_+^2 + p_-^2}{k^2} y\right)\varphi(q) + \frac{2(p - k/2)^2}{k^2}\psi(q)\right], \tag{28}$$

where $\widetilde{M}^2 = (1 + x + y)m^2/x$ and the functions φ and ψ are given by (16).

In integrating over dq in (28) we can approximately assume

$$|G(\xi)|^2 \approx R^2 J_1^2(R\xi)/\xi^2 + 4Z^2\alpha^2/(\xi^2 + q_0^2)^2.$$

Then the cross section is broken down into the sum of two terms: diffraction dw_d and Coulomb dw_c. In the region $x \ll 1$ both dw_d and dw_c are insignificantly small. But with $x \gg 1$ we find from (28)

$$dw_{c,0} = \frac{8\alpha^2 r_0^2 Z^2}{3\pi m^2} \frac{dp_+ dp_-}{k^2} \frac{p - k}{p} \frac{p_+^2 + p_-^2}{k^2}$$
$$\times \ln \frac{m^2 p_+ p_-}{p(p-k)} \ln \frac{1}{mRy_{min}}. \tag{29}$$

For particles with spin $\frac{1}{2}$, analogous calculations give

$$dw_{c,1/2} = \frac{4\alpha^2 r_0^2 Z^2}{3\pi m^2} \frac{dp_+ dp_-}{k^2} \frac{p^2 + (p-k)^2}{p^2} \frac{p_+^2 + p_-^2}{k^2}$$
$$\ln \frac{m^2 p_+ p_-}{p(p-k)} \ln \frac{1}{mRy_{min}}. \tag{30}$$

In both formulas $y_{min} = \max\{q_0/m,\ km/p(p-k)\}$.

Nuclear interaction makes a more essential contribution for π mesons:

$$dw_{d,0} = \frac{2\alpha^2 R^2}{\pi} \frac{p - k}{p} \frac{dp_+ dp_-}{k^2} \ln \frac{m^2 p_+ p_-}{p(p-k)}$$
$$\times \left[\frac{p_+^2 + p_-^2}{k^2} \int_0^\infty \frac{\varphi(q)}{q} J_1^2(2mRq)\, dq\right.$$
$$\left. + \frac{2p_+ p_-}{k^2} \frac{(p - k/2)^2}{p(p-k)} \int_0^\infty \frac{\psi(q)}{q} J_1^2(2mRq)\, dq\right]. \tag{31}$$

Comparing these results with (24) and (25) we see that the contribution of first-order processes can be ignored for $x \ll m^2$ if the parent particle does not partake in the nuclear interaction. In the opposite case in the whole region of $x \gg 1$ the contributions of first order processes are more substantial.

4. DISCUSSION OF RESULTS

We see thus that the most likely pair production takes place with $x = m^2 p_+ p_- / p(p-k) \ll 1$. Corresponding expressions for cross sections are given in (22), (26), and (27).

Formula (31) gives the cross section for $x \gg 1$ if the parent particle is nuclear active. If the parent particle is not nuclear active, for $1 \ll x \ll m^2$ the cross section is given by (24), (25), and for $m^2 \ll x$, by (29) and (30).

The theory we have outlined is applicable to electrons in the region $k \ll p$. The region $k \ll p/m$ gives the main contribution to the integral cross section. In agreement with reference 5, independent of the particle spin we find from (22), in the absence of screening,

$$\sigma = (28\alpha^2 r_0^2 Z^2 / 27\pi) \ln^3 (\varkappa p/m),$$

and with complete screening

$$\sigma = \frac{28\alpha^2 r_0^2 Z^2}{27\pi} \ln 190 Z^{-1/3} \left[3 \ln \frac{\varkappa p}{m} \ln \frac{pZ^{1/3}}{190m} + (\ln 190 Z^{-1/3})^2\right].$$

In both formulas $\kappa \sim 1$. Corrections to these formulas contain lower orders of the lograrithm of the energy.

---

[1] L. D. Landau and E. M. Lifshitz, Sow. Phys. 6, 244 (1934).

[2] H. Bhabha, Proc. Roy. Soc. (London), **A152**, 559 (1935), H. Bhabha, Proc. Cambridge Phil. Soc. **31**, 394 (1935).

[3] G. Racah, Nuovo cimento, **14**, 93 (1935).

[4] Nishina, Tomonaga, and Kobayasi, Papers Inst. Phys. Chem. Res. Tokyo, **137** (1937).

[5] Murota, Ueda, and Tanaka, Progr. Theor. Phys. **16**, 482 (1956).

[6] L. D. Landau and I. Ya. Pomeranchuk, Dokl. Akad. Nauk SSSR, **92**, 535 (1953).

[7] L. D. Landau, I. Ya. Pomeranchuk, Dokl. Akad. Nauk SSSR **92**, 735 (1953).

[8] A. B. Migdal, JETP **32**, 633 (1957), Soviet Phys. JETP **5**, 527 (1957).

[9] A. I. Akhiezer and I. Ya. Pomeranchuk, Usp. Fiz. Nauk. **65**, 593 (1958).

[10] E. M. Rabinovich, JETP **32**, 1563 (1957), Soviet Phys. JETP **5**, 1272 (1957).

Translated by Genevra Gerhart
148

SOVIET PHYSICS JETP VOLUME 37 (10), NUMBER 3 MARCH, 1960

NONLINEAR LANGMUIR ELECTRON OSCILLATIONS IN A PLASMA

M. V. KONYUKOV

Tula Pedagogical Institute

Submitted to JETP editor April 15, 1959

J. Exptl. Theoret. Phys. (U.S.S.R.) **37**, 799-801 (September, 1959)

An exact solution has been obtained for the nonlinear oscillations of the electron density in a plasma at zero electron temperature. The initial conditions necessary for these oscillations are determined.

1. Langmuir and Tonks,[1] in studying the motion of electrons in a plasma, established the fact that small perturbations lead to harmonic oscillations at a frequency $\omega_0 = (4\pi e^2 n_0/m)^{1/2}$ which are localized in the region of the initial perturbation. However perturbations are not always small. Hence it is of interest to study these oscillations when the magnitude of the perturbation is arbitrary. This problem is considered below.*

2. If we assume that the positive ions of the plasma remain fixed and that the electron temperature is zero,[1,2] in the hydrodynamic approximation the behavior of the plasma is described by the following system of equations:

$$\frac{\partial n}{\partial t} + \frac{\partial}{\partial x}(nv) = 0, \qquad \frac{\partial v}{\partial t} + v\frac{\partial v}{\partial x} = \frac{e}{m}\frac{\partial \varphi}{\partial x},$$
$$\partial^2\varphi/\partial x^2 = 4\pi e\,(n - n_0), \quad \text{curl}\ \mathbf{H} = 0, \tag{1}$$

where e, m, v and n are the charge, mass, hydrodynamic velocity, and electron density; φ is the potential of the self-consistent field; n_0 is the positive ion density (in the equilibrium state the plasma may be assumed to be neutral).†

3. The direct solution of the equations in (1) involves considerable mathematical difficulty; however this difficulty can be easily surmounted if the Lagrangian form of the equations of motion is used. By some elementary transformations we obtain the following system from (1):‡

$$n\frac{d^2 n}{dt^2} - 2\left(\frac{dn}{dt}\right)^2 + \frac{4\pi e^2}{m}n^2(n - n_0) = 0, \tag{2a}$$

$$\frac{d^2 v}{dt^2} + \frac{4\pi e^2 n_0}{m}v = 0. \tag{2b}$$

Introducing the following variables in Eq. (2a):

$$y = \ln(1 + \nu), \qquad \nu = (n - n_0)/n_0, \tag{3}$$

we obtain

$$d^2y/dt^2 - (dy/dt)^2 + \omega_0^2(e^y - 1) = 0. \tag{4}$$

The exact solution of Eq. (4) is

$$\nu = b\sin(\omega_0 t + \varphi)/[1 - b\sin(\omega_0 t + \varphi)], \tag{5}$$

where b and φ are constants of integration.* Returning to the variable n we have

$$n = n_0/[1 - b\sin(\omega_0 t + \varphi)]. \tag{6}$$

The law of motion of the point is found from Eq. (2). Taking the origin of coordinates in the plane of symmetry of the perturbation, integrating the equation dx/dt = v we obtain

$$x - x_0 = a(x_0)[1 - \sin(\omega_0 t + \varphi_1)], \tag{7}$$

where $a(x_0)$ is a function which determines the distribution of oscillation amplitudes of the points while φ_1 is the initial phase. If the velocities of the points are zero at t = 0, Eqs. (6) and (7) become

$$n = n_0/[1 - b\cos\omega_0 t],$$
$$x - x_0 = a(x_0)[1 - \cos\omega_0 t]. \tag{8}$$

To determine $b(x_0)$ and $a(x_0)$ from the initial distribution $n(x_0)$ we use the relation $n(x_0, t) = dn(x_0)/dx_0$, where $dn(x_0)$ is the number of electrons in the volume element dx_0 at the starting time. As a result we obtain

$$b = \frac{n(x_0) - n_0}{n(x_0)}, \qquad a = \frac{1}{n_0}\int_0^{x_0} n(x_0)\,dx_0 - x_0. \tag{9}$$

---

*Published studies on nonlinear plasma oscillations refer chiefly to the case of beams or plasmas with initial velocities.[2,3] In a note published by Polovin[4] concerning a fixed plasma it was shown that the frequency of the electron oscillations is independent of the initial perturbations.

†Because of the motion of the electrons the last equation of (1) is valid when the conduction currents are compensated by the displacement currents. This condition is one of the basic properties of longitudinal Langmuir oscillations.

‡In making the transformation use is made of the relation $4\pi env + \partial E/\partial t = 0$; d/dt denotes the total derivative.

*The constant b depends on the initial density perturbation while φ depends on the initial velocity distribution.

4. Equations (8) and (9) give the final solution for nonlinear Langmuir oscillations in Lagrangian form (for an arbitrary initial density distribution but vanishing initial velocities) and gives $n(x, t)$ in parametric form.

By using the Eulerian form we can eliminate x_0 from Eqs. (8) and (9), but this procedure generally means the solution of a transcendental equation. In the case of a linear density distribution at the initial time this elimination process can be carried out relatively easily.

The nonlinear Langmuir oscillations (8) take place at a frequency $\omega_0 = (4\pi e^2 n_0/m)^{1/2}$, which is independent of the initial perturbation.[4] The oscillation amplitudes for individual points (for zero initial velocities) depend only on the initial density distribution. If this distribution is such that $n(x_0)/n_0 \leq \frac{1}{2}$ oscillations are impossible because the corresponding electron density becomes infinite or negative. This situation is a result of the approximation being used. In neglecting the temperature of the electrons we have the eliminated gas-kinetic pressure, which reduces the force tending to compress particles which are initially separated. In the case $n(x_0)/n_0 \leq \frac{1}{2}$ the absence of forces which oppose compression leads to relative particle velocities such that the coordinates of points which are initially separated coincide at later times (generally speaking, for later times $x_1 > x_2$ even if $x_{01} < x_{02}$). The velocities of contiguous points are different. This ambiguity in the velocity field indicates a violation of the conditions required for applying the hydrodynamic approximation.

Taking account of the pressure in the analysis of the nonlinear electron oscillations would lead to an effect similar to that of a discontinuity in a medium with a temperature different from zero.

In conclusion I wish to express my gratitude to Prof. Ya. P. Terletskiĭ for advice in the course of this work.

---

[1] L. Tonks and I. Langmuir, Phys. Rev., **33**, 195 (1929).

[2] A. I. Akhiezer and R. V. Polovin, Dokl. Akad. SSSR, **80**, 193 (1951).

[3] H. K. Sen, Phys. Rev., **97**, 849 (1955).

[4] R. V. Polovin, JETP **31**, 354 (1956), Soviet Phys. JETP **4**, 290 (1957).

Translated by H. Lashinsky
149

ON THE INFLUENCE OF COHERENT MAGNETIC DIPOLE RADIATION ON MAGNETIC RESONANCE

G. V. SKROTSKIĬ and A. A. KOKIN

Ural' Polytechnical Institute

Submitted to JETP editor April 17, 1959

J. Exptl. Theoret. Phys. (U.S.S.R.) **37**, 802-804 (September, 1959)

Corrections to the relaxation time, necessitated by the effect of the radiation field, are computed. The effect of the resonator on the nature of the observed phenomenon is taken into account.

1. When a spin system radiates electromagnetic quanta of wavelength exceeding the dimensions of the system coherent phenomena occur which lead to a considerable increase in the radiation line width.[1,2] The role of this phenomenon first noted by Mandel'shtam[3] and investigated by Dicke[1] was discussed in detail in connection with magnetic resonance in the paper by Bloembergen and Pound[4] where an estimate was made of the effect of coherent phenomena on the damping of radiation in the sample placed in the receiver coil of the circuit or in a resonator. Faĭn[5] noted that if the interaction of spins through their common radiation field is taken into account this leads in the radio frequency region to a shift of the resonance frequency.

In this paper we give a consistent calculation of corrections to the relaxation times and to the additional shift of the resonance frequency due to the influence of the coherent radiation field. In the course of this calculation it turns out, as expected, that within the limits of the approximation considered, quantum theory leads to the same results as classical theory. In conclusion the question is discussed of the changes in the characteristics of the signal due to the finite figure of merit of the resonator. The conditions are established under which radiation corrections will be significant.

2. Ginzburg[6] has shown that the classical equation of motion for the magnetic moment μ of a homogeneously magnetized sample of dimensions small compared to the wavelength of the radiation has the form

$$\dot{\boldsymbol{\mu}} = \gamma\,[\boldsymbol{\mu}\times\mathbf{H}] - \frac{4\gamma\omega_m}{3\pi v^3}\,[\boldsymbol{\mu}\times\ddot{\boldsymbol{\mu}}] + \frac{2\gamma}{3v^3}\,[\boldsymbol{\mu}\times\dddot{\boldsymbol{\mu}}], \qquad (1)$$

where $v = c/\sqrt{\epsilon\mu}$ is the phase velocity of light in the material of the sample, while $\omega_m \approx cV^{-1/3}$.

On introducing the magnetization $M = \mu/V$ and including terms due to other relaxation mechanisms, in terms of the circularly polarized variables M_α ($\alpha = 0, \pm 1$):

$$M_{\pm 1} = \mp (M_x \pm iM_y)/\sqrt{2}, \qquad M_0 = M_z,$$

we obtain

$$\dot{M}_\alpha + \frac{M_\alpha}{T_\alpha} = \gamma\,[\mathbf{M}\times\mathbf{H}]_\alpha + \frac{\chi_0 h_\alpha(t)}{T_\alpha} - \frac{4\gamma\omega_m V}{3\pi v^3}\,[\mathbf{M}\times\dddot{\mathbf{M}}]_\alpha + \frac{2\gamma V}{3v^3}\,[\mathbf{M}\times\dddot{\mathbf{M}}]_\alpha. \qquad (2)$$

We shall assume that the sample in addition to being situated in a constant field $H_0 = H_z$, is also placed into a weak variable magnetic field $h(t) \ll H_0$ ($\mathbf{h} \perp \mathbf{H}_0$). By linearizing (2) near the equilibrium position for the case $1/T_\alpha \ll \omega_0 = \gamma H_0$, we obtain

$$\dot{M}_\alpha + (1/T_\alpha^* + i\alpha\omega_0^*)\,M_\alpha = i\alpha\omega_0\chi_0 h_\alpha(t), \qquad (3)$$

where

$$1/T_\alpha^* = 1/T_\alpha + 1/T_\alpha^r, \qquad 1/T_\alpha^r = {}^2/_3\,(2-\alpha^2)\,\chi_0\omega_0^4 v^{-3} V, \qquad (4)$$

$$\omega_0^* - \omega_0 = {}^4/_3\chi_0\,(\omega_0^3\omega_m/\pi v^3)\,V. \qquad (5)$$

As can be seen from (4), the longitudinal relaxation time $T_{||}^r = T_0^r$ is by a factor of two smaller than the transverse relaxation time $T_\perp^r = T_{\pm 1}^r$. The expression for the shift of the resonance frequency $\omega_0^* - \omega_0$ in the form (5) was obtained by Faĭn.[5] Corrections due to the interaction of the particles through their common radiation field increase rapidly with the field H_0 and are proportional to the volume of the sample. Under favorable conditions in the range of strong magnetic fields T_α^r may become comparable to T_α.

3. The quantum theory of the phenomenon under consideration for the case of weak radio frequency fields may be developed on the basis of the method of Kubo and Tomita.[7]

If we restrict ourselves to taking into account only the interactions of the magnetic moments through the radiation field then the part of the Hamiltonian independent of the time may be written in the form

$$\hat{\mathscr{H}} = \hat{\mathscr{H}}_1 + \hat{\mathscr{H}}_2 + \hat{\mathscr{H}}' = \hat{\mathscr{H}}_0 + \hat{\mathscr{H}}',$$

$$\hat{\mathscr{H}}_1 = -\hbar\omega_0 \sum_j^N \hat{I}_{j0}, \qquad \hat{\mathscr{H}}_2 = \sum_{k\lambda} (\hat{a}^+_{k\lambda}\hat{a}_{k\lambda} + {}^1/_2)\,\hbar v k, \tag{6}$$

where $\hat{\mathscr{H}}_1$ describes the interaction of the magnetic moments with an external constant magnetic field, $\hat{\mathscr{H}}_2$ is the Hamiltonian of the radiation field, $\lambda = \pm 1$ corresponds to the two possible values of the polarization, while v is the phase velocity of light in the medium into which the magnetic moments are immersed. We shall treat the Hamiltonian of the interaction of the magnetic moments with the radiation field as a perturbation. In the case when the dimensions of the system are considerably smaller than a wavelength it has the form

$$\hat{\mathscr{H}}' = -i\gamma\hbar \sum_{k,\lambda} \sqrt{2\pi\hbar v k/V} \sum_{j\alpha}^N (-1)^\alpha \hat{I}_{j\alpha}\varepsilon_{k-\lambda-\alpha} (\hat{a}_{k\lambda} - \hat{a}^+_{k\lambda}). \tag{7}$$

The relaxation times and the shift of the resonance frequency may be determined in a manner similar to the way this is done in our earlier paper.[8] By utilizing equations (40), (46), and (47) of that article for the case $\hbar\omega_0 \gg kT$ we shall obtain expressions for T^*_α and ω^*_0 which coincide with those obtained above by a classical method.

4. The foregoing calculations have been carried out for the case when the sample is situated in free space. In making observations of magnetic resonance the sample is placed either into a coil or into a resonator of finite figure of merit. The resonator may affect in an essential manner the nature of the phenomenon being observed.

The figure of merit of an ideal resonator of volume V_p, in which the losses are due only to the presence of a magnetic sample of volume V situated in a constant field H_0 and which absorbs energy from the radio-frequency field $h(t)$, is given by*

$$Q'(\omega) = V_p/4\pi\chi''(\omega)V. \tag{8}$$

If a small sample is placed within such a region inside the resonator where the variable magnetic field of resonance frequency ω_0 may be regarded as homogeneous and linearly polarized, then $2\chi''(\omega_0) = \chi_0\omega_0T^*_\perp$ and

$$Q'(\omega_0) = (V_p/V)/2\pi\chi_0\omega_0T^*_\perp. \tag{9}$$

Further, we denote by $Q_0(\omega_0)$ the figure of merit of a real resonator with the sample in the absence of the constant magnetic field H_0.

Then $Q(\omega_0)$ of a real resonator with the sample situated in a magnetic field H_0 in conditions of resonance is related to $Q'(\omega_0)$ and $Q_0(\omega_0)$ by the relation

$$Q'(\omega_0) = \frac{Q_0(\omega_0)}{Q_0(\omega_0)/Q(\omega_0) - 1}. \tag{10}$$

The ratio Q_0/Q and Q_0 can be measured directly in an experiment and, thus, the dependence of $1/T^*_\perp$ on the frequency ω_0 may be found.

---

*The figure of merit of a system is defined as $Q(\omega) = \omega \times$(total energy of the system/energy absorbed per second).

[1] R. H. Dicke, Phys. Rev. **93**, 99 (1954).

[2] M. M. Al'perin, Укр. физ. журн., (Ukr. Phys. J.) 2, 322 (1957), V. M. Faĭn, Usp. Fiz. Nauk **64**, 273 (1958).

[3] L. I. Mandel'shtam, Сочинения, (Collected Works) vol. 1, U.S.S.R. Acad. Sci., 1948, p. 125.

[4] N. Bloembergen and R. V. Pound, Phys. Rev. 95, 8 (1954).

[5] V. M. Faĭn, JETP **36**, 798 (1959), Soviet Phys. JETP **9**, 562 (1959).

[6] V. L. Ginzburg, JETP **13**, 33 (1943).

[7] P. Kubo and K. Tomita, J. Phys. Soc. Japan **9**, 888 (1954).

[8] G. V. Skrotskiĭ and A. A. Kokin, JETP **36**, 169 (1959), Soviet Phys. JETP **9**, 116 (1959).

Translated by G. Volkoff.
150

SOVIET PHYSICS JETP VOLUME 37(10), NUMBER 3 MARCH, 1960

THE METHOD OF DISPERSION RELATIONS AND PERTURBATION THEORY

N. N. BOGOLYUBOV, A. A. LOGUNOV, and D. V. SHIRKOV

Joint Institute for Nuclear Research

Submitted to JETP editor April 17, 1959

J. Exptl. Theoret. Phys. (U.S.S.R.) **37**, 805-815 (September, 1959)

Both the idea and the results of the present investigation are related to Redmond's recent paper[1] on the exclusion of nonphysical poles from the Green's function. In contrast to that work based on the relation between the spectral representations of the Green's function and of the polarization operator we base ourselves on the principle of summing the information obtained from perturbation theory in the integrand of the Källen-Lehmann spectral integral. On summing in this way the contributions from the "principal logarithmic diagrams" we obtain expressions for the photon propagation function in quantum electrodynamics and for the meson propagation function in the symmetric theory which have all the essential properties of Redmond's result: the correct analytic behavior in the complex plane of the momentum variable p^2 and a singularity with respect to the variable of the square of the charge e^2 at the point $e^2 = 0$. However, in contrast to Redmond's result, which yields correctly only the lowest order of perturbation theory, the expressions obtained by us correspond to terms of arbitrarily high order in the perturbation theory expansions in the region of large p^2.

By taking into account the lowest order logarithmic terms, it is shown that the region of applicability of the new formulas coincides with the region of applicability of the old formulas containing the logarithmic singularities, since it is restricted by the condition of smallness of the invariant charge. The technique of reducing the expressions so obtained to the renormalization-invariant form is illustrated by the example of the photon Green's function. In conclusion some remarks are made with respect to the possible situation in nonrenormalizable theories.

1. INTRODUCTION

IN Redmond's recent paper[1] an interesting result was obtained, that by requiring analyticity it is possible to obtain expressions for the Green's function which correspond to perturbation theory and at the same time do not contain the well-known logarithmic singularities.

Redmond's method consists of the following. By postulating, on the basis of considerations of correspondence with perturbation theory, a spectral representation for the polarization operator, Redmond writes the meson Green's function in the form

$$\Delta(p^2) = (\mu^2 - p^2 - i\varepsilon)^{-1}\left[1 + (\mu^2 - p^2)\int\limits_{(3\mu)^2}^{\infty} \frac{\rho(m^2)dm^2}{m^2 - p^2 - i\varepsilon}\right]^{-1}. \tag{1.1}$$

By comparing this representation with the well known Källen-Lehmann representation

$$\Delta(p^2) = \frac{1}{\mu^2 - p^2} + \int\limits_{(3\mu)^2}^{\infty} dm^2 \frac{I(m^2)}{m^2 - p^2 - i\varepsilon} \tag{1.2}$$

and by utilizing the obvious relation

$$\pi I(m^2) = \operatorname{Im}\Delta(m^2 + i\varepsilon), \tag{1.3}$$

Redmond expresses the spectral function I in terms of ρ and obtains

$$\Delta(p^2) = \frac{1}{\mu^2 - p^2} + \int\limits_{(3\mu)^2}^{\infty} \frac{\rho(m^2)\,dm^2}{D(m^2)(m^2 - p^2 - i\varepsilon)}, \tag{1.4}$$

where

$$D(m^2) = R^2(m^2) + \pi^2(m^2 - \mu^2)^2\rho^2(m^2),$$

$$R(m^2) = 1 - (m^2 - \mu^2)\,\mathrm{P}\int\limits_{(3\mu)^2}^{\infty} \frac{\rho(l^2)\,dl^2}{m^2 - l^2}.$$

Formula (1.3) corresponds to the expression for the boson Green's function obtained by Lehmann, Symanzik, and Zimmerman[2] if a subsidiary condition is imposed on the function ρ

$$\int\limits_{(3\mu)^2}^{\infty} \rho(m^2)dm^2 \leqslant 1. \tag{1.5}$$

Then by utilizing for ρ the expression $\rho_0(m^2)$

which corresponds to the lowest order of perturbation theory he obtains for the meson Green's function the following expression

$$\Delta(p^2) = (\mu^2 - p^2)^{-1}\left[1 - (\mu^2 - p^2)\int\limits_{4M^2}^{\infty}\frac{dm^2\rho_0(m^2)}{m^2 - p^2}\right]^{-1} - \frac{Z^{-1}}{p_0^2 - p^2}, \tag{1.6}$$

where p_0^2 is the value of the variable p^2 for which the first term in (1.6) has a pole, while Z^{-1} is the residue at the pole.

Expression (1.6) has the following interesting properties: 1) it does not have a nonphysical pole, since in the neighborhood of the pole the second term exactly compensates the singularity of the first term; 2) considered as a function of g^2, it has an essential singularity at $g^2 = 0$; 3) in the neighborhood of the point $g^2 = 0$ it admits an asymptotic expansion in powers of g^2 whose first term (of order g^2) coincides with the result of perturbation theory.

It should be noted that formula (1.6) does not lead to any correspondence with higher orders of perturbation theory, in particular, it gives incorrect principal logarithmic terms. This is not surprising since, as is well known,[3,4] as a result of summing the principal logarithmic terms for the meson Green's function the following expression is obtained

$$\Delta(p^2) = \frac{1}{(\mu^2 - p^2)\,[1 - (5g^2/4\pi)\ln(-p^2/\mu^2)]^{4/5}}, \tag{1.7}$$

which contains not a "false pole," but a nonphysical singularity of fractional power. It may be easily seen that Redmond's method based on the polarization operator is very inconvenient for the investigation of singularities of type (1.7). This is connected with the fact that a singularity of type (1.7) does not correspond to any simple approximation for the polarization operator.

In the following we present a somewhat different approach to the problem of the removal of nonphysical singularities from the approximate expressions for the Green's function in quantum field theory which, it seems to us, has a greater degree of generality. We base ourselves on the principle of the summation of the perturbation theory series in the integrand of the Källen-Lehmann spectral integral. In this way, by summing the principal logarithmic diagrams, we shall obtain expressions for the photon and the meson Green's functions which, on the one hand, will possess the required analytic properties, and, on the other, will correspond to the perturbation theory expansions in the ultra violet region. This principle of summation is very close to Symanzik's ideas[5] by means of which he studied the analytic properties of the Green's function.

2. ELIMINATION OF THE "LOGARITHMIC" POLE FROM THE PHOTON GREEN'S FUNCTION

The most natural method of studying the analytic properties of the Green's function is the method of dispersion relations. At the present time this method is the only approach to problems of quantum field theory which is apparently free of internal difficulties. Therefore, it appears to be quite natural that further progress in quantum field theory must be associated with this method.

The method of dispersion relations based on the most general principles of covariance, causality, unitarity, and spectrality* enables us to obtain expressions for quantities of the type of Green's functions and of transition-matrix elements in the form of spectral expansions. In this way the problem is reduced to the investigation of the properties of the corresponding spectral functions. These spectral functions, on being expanded in terms of a complete system of states, can be expressed in terms of Green's functions for more complicated processes. In this way a possibility appears in principle of obtaining a system of equations for the determination of the Green's functions. It should be noted that in contrast, for example, to the system of Schwinger's equations, no ultraviolet divergences arise in this case. However, a consistent development of such a program encounters a number of obstacles, since, for example, no spectral representations have yet been obtained for the higher Green's functions.

At this point a palliative possibility appears of obtaining the lacking information about the spectral functions with the aid of perturbation theory data. Symanzik[5] has adopted this particular approach. By considering the n-th perturbation-theory term for a certain vertex part he showed that this term can be represented in a definite spectral form. Then, by making use of the hypothesis of the possibility of summing the series for the spectral function, Symanzik concluded that the vertex part under investigation could be represented as a whole in the given spectral form.

Symanzik utilized this approach to obtain general theoretical conclusions leading to the proof of the dispersion relations. In our opinion it would be of considerable interest to investigate on the basis of the "principle of summation in the integrand of the spectral representation" the different possibilities for making approximations. As the simplest example we shall investigate by this method the Källen-Lehmann spectral formula for the boson Green's function, and instead of summing the whole perturbation theory series we shall restrict ourselves to summing only that class of diagrams the study of which in the opinion of a number of authors[6] leads to the proof of the existence of nonphysical singularities.

---

*In speaking of the principle of spectrality we have in mind the condition of the existence of a complete set of physical states of positive energy.

In the case of the photon Green's function in quantum electrodynamics, such diagrams can be represented in the form of a photon line with an arbitrary number of simplest insertions — second order electron-positron loops. It is customary to call such diagrams "principal logarithmic diagrams." The contribution of the n-th term of diagrams of this class is of the form

$$-(e^2F(k^2,m^2))^n/k^2, \tag{2.1}$$

where $F(k^2, m^2)$ corresponds to the second order loop. An explicit expression for F is given, for example, in Sec. 32.1 of reference 4.

In the region $|k^2| \gg m^2$ the function F has the form

$$F(k^2,m^2)=\frac{1}{3\pi}\ln\frac{4m^2-k^2}{4m^2}. \tag{2.2}$$

We have introduced the term $4m^2$ into the argument of the logarithm in order to represent correctly the imaginary part of the function F

$$\operatorname{Im}F(k^2,m^2)=-\tfrac{1}{3}\theta(k^2-4m^2),\qquad \theta(x)=\begin{cases}1 & x>0\\ 0 & x<0\end{cases},$$

at the same time retaining its normalization $F(0, m^2) = 0$.

We note that a direct summation of the terms of (2.2), which was for the first time carried out in reference 7, leads to the expression

$$-\frac{1}{k^2}\left[1-\frac{e^2}{3\pi}\ln\frac{4m^2-k^2}{4m^2}\right]^{-1}, \tag{2.3}$$

on the basis of which it was concluded[6] that a logarithmic pole exists, and that, consequently, there is an internal contradiction in the theory.

We shall now apply to the diagrams under investigation the principle of summing in the integrand of the spectral representation. It may be easily seen that the n-th term of (2.1) can be represented in the Källen-Lehmann spectral form. By restricting ourselves to the approximation (2.2) we obtain

$$D_n=-\frac{1}{k^2}\left(\frac{e^2}{3\pi}\ln\frac{4m^2-k^2}{4m^2}\right)^n=\int\limits_{4m^2}^{\infty}\frac{I_n(z)}{z-k^2}dz,$$

where the function $I_n(z)$ is defined by the imaginary part of the function D_n by means of (1.3). On carrying out the summation under the integral sign of the spectral representation for the function I

$$I(z)=\sum_{n=1}^{\infty}I_n(z),$$

we see that $I(z)$ as a whole is represented by the imaginary part of (2.3). On substituting (2.3) into (1.3) we obtain

$$I(z)=\begin{cases}\dfrac{e^2}{3\pi z}\left[\left(1-\dfrac{e^2}{3\pi}\ln\dfrac{z-4m^2}{4m^2}\right)^2+\dfrac{e^4}{9}\right]^{-1}, & z\geqslant 4m^2\\ 0 & z<4m^2\end{cases} \tag{2.4}$$

We thus obtain for the photon Green's function the following expression

$$D(k^2)=-\frac{1}{k^2}+\frac{e^2}{3\pi}\int\limits_{4m^2}^{\infty}\frac{dz}{z(z-k^2-i\varepsilon)\left[\left(1-\dfrac{e^2}{3\pi}\ln\dfrac{z-4m^2}{4m^2}\right)^2+\dfrac{e^4}{9}\right]}. \tag{2.5}$$

We note that a formula of this type was recently investigated by Redmond and Uretsky.[10]

It is easily seen* that (2.5) represents the function

$$D(k^2)=-\frac{1}{k^2}\left(1-\frac{e^2}{3\pi}\ln\frac{4m^2-k^2}{4m^2}\right)^{-1}-\frac{3\pi/e^2}{[1-4\exp(-3\pi/e^2)][k^2-4m^2+4m^2\exp(3\pi/e^2)]},$$

which, on taking into account the fact that e^2 is small, can be written for the case of $|k^2|$ much greater than m^2 in the form

$$D(k^2)=-\frac{1}{k^2[1-(e^2/3\pi)\ln(-k^2/4m^2)]}-\frac{3\pi/e^2}{k^2+4m^2\exp(3\pi/e^2)}. \tag{2.6}$$

The function (2.6) has the following remarkable properties: 1) it does not have a logarithmic pole; 2) in the neighborhood of the point $e^2 = 0$ it has, regarded as a function of e^2, a singularity of "superconducting" type $\exp(-3\pi/e^2)$; 3) in the neighborhood of the point $e^2 = 0$ it has an asymptotic expansion that coincides with the ordinary perturbation-theory expansion and can be represented in the form (2.3). It is also clear that the second term in the right-hand side of (2.6) cannot be obtained as a matter of principle from perturbation theory[8] because of its exponential order of smallness, as a result of which it does not correspond to any Feynman diagrams.

We also note that the final expression (2.6) is consistent with the initial approximation (2.3). In the region in which we have utilized (2.3) for the calculation of the spectral function, it differs from the final expression (2.6) by negligibly small terms of order $\exp(-3\pi/e^2)$.

We see thus that the procedure of summing the principal logarithmic diagrams is not a unique operation. A direct summation of the logarithmic terms leads to (2.3). Summation in the integrand of the Källen-Lehmann spectral integral leads to (2.6). Assuming that quantum electrodynamics has physically sensible solutions which are in agreement with the basic principles of quantum field theory, and that consequently the photon Green's function satisfies the Källen-Lehmann theorem, we must choose from these two possibilities the formula (2.6). This equation, which does not contain any paradoxes such as the "zero-charge difficulty,"[6] is thus the result of summing the main logarithmic terms carried out in agreement with the basic physical foundations of the theory.

---

*Cf., for example, reference 10.

Naturally, (2.6) is not the only expression with correct analytic behavior in the complex plane of the variable k^2, whose asymptotic expansion into a series in powers of e^2 coincides with the usual perturbation theory. Examples of expressions of this type, other than (2.6), can be obtained by adding terms containing $\exp(-e^{-2})$ to the spectral function (2.4).

We have obtained (2.4) from (2.3), which corresponds to the main logarithmic terms of perturbation theory. We also could have started not with (2.3), but with (cf. Sec. 43.1 of reference 4)

$$-1/k^2[1-e^2F(k^2,\ m^2)],$$

which describes the sum of the main logarithmic diagrams for arbitrary values of k^2 and which reduces to (2.3) in the limit $|k^2| \gg m^2$. The corresponding spectral function has a more awkward form in comparison with (2.4) but at the same time retains all its essential properties.

We also note that (2.5) and (2.6) are very close to Redmond's formulas (1.4) and (1.6). This is due to the fact that the usual expression for the photon propagation function (2.3) has a nonphysical singularity in the form of a pole, which can be well represented by an approximate expression for the polarization operator.

An interesting feature of the spectral function (2.4) is its resonance nature. As already pointed out, this formula was obtained on the basis of summing the main logarithmic terms. It is therefore of interest to find out whether the resonance character will be retained in the spectral functions obtained on the basis of summing logarithmic terms of a higher order of smallness, and to discover in what range expressions of type (2.4) can be regarded as sensible approximations.

For this purpose we take for the initial expression for the photon propagation function a formula (Sec. 43.2 of reference 4) obtained by summing terms of the form $(e^2 \ln z)^n$ and $e^2(e^2 \ln z)^m$

$$D(z) = -\frac{1}{z}\Big[1-t+\frac{ie^2}{3}\theta(z-4m^2) + \frac{3e^2}{4\pi}\ln\Big(1-t+\frac{ie^2}{3}\theta(z-4m^2)\Big)\Big]^{-1},$$

where

$$t = \frac{e^2}{3\pi}\ln\frac{z-4m^2}{4m^2}.$$

From this expression we shall obtain in place of (2.4) (for $z \geq 4m^2$):

$$I(z) = \frac{e^2}{3\pi z} \times \frac{1+\dfrac{9}{4\pi}\tan^{-1}\dfrac{e^2/3\pi}{1-t}}{\Big\{1-t+\dfrac{3e^2}{2\pi}\ln\Big[(1-t)^2+\dfrac{e^4}{9}\Big]\Big\}^2+\dfrac{e^4}{9}\Big[1+\dfrac{9}{4\pi}\tan^{-1}\dfrac{e^2/3\pi}{1-t}\Big]^2}. \tag{2.7}$$

It can be seen from (2.7) that the resonance character of the spectral function is retained when higher logarithmic terms are taken into account. However, the effect of these higher terms on the behavior of the spectral function in the resonance region and above, is not small. By comparing (2.7) with (2.4) we see, for example, that in the resonance region (2.7) differs from (2.4) by the factor 8/17, while for very large values of z it differs by the factor 13/4. These factors do not depend on the degree of smallness of the parameter e^2.

It should be emphasized that the improvement of perturbation theory obtained by summing logarithmic terms of different orders of smallness is not a consistent operation. As is well known (cf. Sec. 42.4 of reference 4), the corresponding formulas can be trusted only in the region in which the quantity

$$e^2d(k^2) = -e^2k^2D(k^2)$$

is small compared to unity.

It follows from this that the expressions obtained above for the spectral functions represent sensible approximations only in the region below "resonance." In the resonance region and above these formulas cannot be trusted, since we are making use here of the initial approximation outside the region of its applicability, actually going outside the framework of weak coupling. Therefore, we can only make assumptions about the resonance character of spectral functions.

The inapplicability of the expressions obtained above for the spectral functions in the region of very large z is not surprising, since the problem of determining the true asymptotic behavior even for the single-particle Green's function requires the simultaneous investigation of the asymptotic behavior of other higher Green's functions and vertex parts.

3. REMOVAL OF NONPHYSICAL SINGULARITIES FROM THE MESON GREEN'S FUNCTION

A similar correction of the logarithmic summation formulas may be carried out also for other Green's functions. Let us consider, for example, the meson propagation function in the symmetric pseudoscalar theory of meson-nucleon interaction. An expression for this Green's function, obtained[3,4] by improving the ordinary perturbation theory, has the form (1.7). The corresponding spectral function arising as a result of the summation in the integrand of the spectral representation will be of the form

$$I(z)=\frac{1}{\mu^2-z}\,\frac{\sin\left(\frac{4}{5}\tan^{-1}\frac{5g^2/4}{1-t}\right)}{\pi\,[(1-t)^2+25g^4/16]^{2/5}}, \tag{3.1}$$

where

$$t=(5g^2/4\pi)\ln(z/\mu^2).$$

We now inquire as to what constitutes the difference between the meson Green's function calculated by means of (3.1) and the initial approximation (1.7). The expression (1.7) has a branch point at $p^2=-\mu^2\exp(4\pi/5g^2)$. Therefore in the present case the elimination of the nonphysical singularity is reduced to the subtraction from (1.7) of the integral along the cut which may be made from the point $-\mu^2\exp(4\pi/5g^2)$ along the negative real axis to $-\infty$. It can be easily seen that this integral will have an order of smallness of $\exp(-4\pi/5g^2)$, as a result of which it will not correspond to any perturbation-theory terms.

4. REDUCTION OF THE PHOTON GREEN'S FUNCTION TO THE RENORMALIZATION-INVARIANT FORM

It is not difficult to see that the expressions obtained above for the Green's functions are not renormalization-invariant. In this section using the photon Green's function as an example we shall show the manner in which they may be brought to invariant form.

We start with (2.6), rewritten in the form

$$\frac{e^2 d}{3\pi}=-\frac{e^2k^2D}{3\pi}=\frac{1}{3\pi/e^2-\ln(k^2/m^2)}+\frac{1}{1-\exp[3\pi/e^2-\ln(|k^2|/m^2)]}. \tag{4.1}$$

The function e^2d, called the invariant charge, must be an invariant of the transformation of the renormalization group (cf. Sec. 42 in reference 4). However, (4.1) clearly does not satisfy this requirement.

The usual technique of bringing expressions to the renormalization-invariant form utilizes the apparatus of the Lie differential equations and also makes use of considerations of correspondence with the ordinary perturbation theory. Since expressions of the type (4.1) cannot be expanded in powers of e^2, it will be technically more convenient to start not from the Lie differential equations, but from the functional equations of the renormalization group.

With this object in view we shall seek the analogue of the usual function d normalized to unity for $|k^2|=\lambda^2$ in the form

$$\frac{e_\lambda^2}{3\pi}\,d\left(\frac{k^2}{\lambda^2},e_\lambda^2\right)=\frac{1}{\Phi(e_\lambda^2/3\pi)-\ln(k^2/\lambda^2)}+\frac{1}{1-\exp[\Phi(e_\lambda^2/3\pi)-\ln(k^2/\lambda^2)]}, \tag{4.2}$$

being guided by the fact that (as shown originally by Gell-Mann and Low[9] on the basis of group theoretic considerations) the invariant function can depend on e_λ^2 and λ^2 only through the argument

$$\varphi(e_\lambda^2)+\ln\lambda^2.$$

The requirement that the function e^2d be invariant has the form

$$e_\lambda^2\,d(k^2/\lambda^2,e_\lambda^2)=e_0^2\,d(k^2/m_0^2,e_0^2)=e_{\lambda_1}^2\,d(k^2/\lambda_1^2,e_{\lambda_1}^2), \tag{4.3}$$

where m_0 is a quantity of the order of magnitude of the electron mass, while e_0 is the corresponding value of the charge. This requirement determines the relationship between the laws of transformation of charge and of the normalizing momentum by means of the function Φ

$$\Phi\left(\frac{e_\lambda^2}{3\pi}\right)-\ln\frac{k^2}{\lambda^2}=\Phi\left(\frac{e_0^2}{3\pi}\right)-\ln\frac{k^2}{m_0^2}=\Phi\left(\frac{e_{\lambda_1}^2}{3\pi}\right)-\ln\frac{k^2}{\lambda_1^2},$$

from where, in particular, it follows that

$$\Phi(e_\lambda^2/3\pi)-\Phi(e_0^2/3\pi)=-\ln(\lambda^2/m_0^2). \tag{4.4}$$

A qualitative restriction on the function Φ follows from (4.4). When $\lambda^2\to\infty$ the function $\Phi(e_\lambda^2/3\pi)$ must tend monotonically to $-\infty$. The explicit form of this function may now be determined from the condition of normalization of d. By setting $k^2=\lambda^2$ in (4.2) we obtain

$$\frac{e_\lambda^2}{3\pi}=\frac{1}{\Phi(e_\lambda^2/3\pi)}+\frac{1}{1-\exp[\Phi(e_\lambda^2/3\pi)]},$$

i.e.

$$x=1/\Phi(x)-1/[e^{\Phi(x)}-1].$$

From this equation it can be seen that Φ is indeed a monotonically decreasing function of its argument. For small x, $\Phi(x) \sim 1/x$ and (4.2) goes over into (4.1). At $x = \frac{1}{2}$ the function Φ goes through zero and reverses sign. As $x \to 1$ the function Φ tends to $-\infty$.

From the condition of normalization of the function d and from (4.3) and (4.4) it follows that

$$\Phi\left(\frac{e_0^2}{3\pi}\, d\left(\frac{\lambda^2}{m_0^2},\, e_0^2\right)\right) = \Phi\left(\frac{e_0^2}{3\pi}\right) - \ln\frac{\lambda^2}{m_0^2},$$

from which we obtain

$$\lim_{\lambda\to\infty} \frac{e_0^2}{3\pi}\, d\left(\frac{\lambda^2}{m_0^2},\, e_0^2\right) = 1. \qquad (4.5)$$

If now, following the generally accepted rules (cf., for example, reference 9), we determine from (4.5) the renormalization constant Z_3 for the photon Green's function, we obtain for it the finite value

$$Z_3 = e_0^2/3\pi. \qquad (4.6)$$

Naturally no final interpretation should be given to (4.6).

We have carried through the above arguments in order to show how expressions can be brought to the renormalization-invariant form without utiliz the Lie equations.

5. ON ONE POSSIBILITY IN NONRENORMALIZABLE THEORIES

A model expression for the Green's function in a nonrenormalizable theory was given by Redmond and Uretsky.[10] We now attempt to obtain an expression of this type by making use of the method developed earlier of summing in the integrand of a spectral representation. We shall carry through the argument using as an example the nonlinear fermion theory with a fourth order interaction Lagrangian $g\bar{\psi}O\psi\bar{\psi}O\psi$, and we shall consider the 4-fermion vertex Green's function $\Gamma(p', q', p, q)$.

By basing ourselves on renormalization-invariant considerations, we can assume that the symmetric asymptotic expression in the ultraviolet region has for its principal approximation the form*

$$\Gamma(p, p, p, p) = \Gamma(p) = 1/[1 + gF(p)], \qquad (5.1)$$

where $F(p)$ is the contribution from the simplest fermion-antifermion loop. Perturbation theory calculations for $\Gamma(p)$ lead to the expansion

$$\Gamma(p) = 1 + \sum_n g^n \Gamma_n(p), \qquad (5.2)$$

where, for example, for $|p^2| \gg m^2$ an expression of the type

$$\Gamma_1 = -p^2 \ln(p^2/m^2) + p^2 I_1 + I_0. \qquad (5.3)$$

holds for Γ_1.

Here I_0 and I_1 are divergent constants. In the general case the term Γ_n contains a polynomial in p^2 of degree n with divergent coefficients. By means of the usual subtraction methods it is possible to eliminate from Γ only the divergent term which does not depend on p^2 (of the type I_0) since the introduction of counter terms proportional to powers of p^2 leads in the final analysis to nonlocal effects (cf., for example, Sec. 28.3 in reference 4).

Therefore the formal subtraction of divergent terms of the type I_0 and $p^2 I_1$, leading to (5.1) when $F(p) = p^2 \ln(p^2/m^2)$, is not quite consistent.

Here we can make a hypothesis that Γ regarded as a function of g has an essential singularity* at $g = 0$ in the neighborhood of which there exists no asymptotic expansion for it in powers of g. An attempt to expand formally in powers of the coupling constant leads to divergent expressions in each order [the terms $I_0 + p^2 I_1$ in (5.3)].

On the basis of this hypothesis, and taking into account the fact that the finite terms in (5.2) have the form $[gp^2 \ln(p^2/m^2)]^n$, we can attempt to sum the series (5.2) with the aid of the following spectral representation

$$\Gamma(p) = 1 + p^2 \int_{m_0^2}^{\infty} \frac{\rho(z)\, dz}{z(z - p^2)}. \qquad (5.4)$$

At the present time we do not have for the 4-vertex function an analogue of the Källen-Lehmann spectral formula. Therefore we actually have to postulate the representation (5.4). However, it appears to be a fairly natural one, since, for example, it corresponds to the separate terms given by perturbation theory.

Naturally, the representation of the individual terms of the sum (5.2) in the spectral form (5.4) is purely formal, in view of the divergences contained in them. However, in accordance with the assumption which we have made, the complete expression of the form (5.4) for Γ obtained by means of summing the series

$$\rho(z) = \sum_n g^n \rho_n(z) \qquad (5.5)$$

for the spectral function ρ may turn out to be finite. The individual terms ρ_n in the sum (5.5) are determined by the imaginary components of the logarithm. Therefore, in order to evaluate the sum (5.5) we must make use of expression (5.1) with

---

*The equations of the renormalization group for this case are given in reference 11.

*In this connection see references 12 and 13.

$$F(p^2) = p^2 \{\ln(|p^2|/m^2) - i\pi\theta(p^2 - m_0^2)\}.$$

In this way we arrive at a spectral formula of the type

$$\Gamma(p) = 1 + gp^2 \int_{m_0^2}^{\infty} \frac{dz}{(z - p^2)[(1 + gz\ln(z/m^2))^2 + \pi^2 g^2 z^2]}, \quad (5.6)$$

which is quite close to the model expression of reference 10. This formula has the following important property. The integral in the right hand side of (5.6) is convergent; however, when we attempt to expand it into a power series in the coupling constant, we obtain divergent expressions in each order. Thus, (5.6) is in complete agreement with our assumptions.

With the aid of Cauchy's theorem for the function $\Gamma(p)/p^2$, we can rewrite (5.6) in the form

$$\Gamma(p) = \frac{1}{1 + gp^2\ln(p^2/m^2)} - \frac{p^2}{gp_0^2(p^2 - p_0^2)[1 + \ln(-p_0^2/m^2)]}, \quad (5.7)$$

where p_0^2 is a root of

$$1 + gp_0^2\ln(-p_0^2/m^2) = 0.$$

In the limit of small $g > 0$, the root p_0^2 tends to $-1/g$, and the second term in (5.7) takes on the form

$$gp^2/(1 + gp^2)(1 - \ln gm^2). \quad (5.8)$$

The function $f(x) = [1 - \ln x]^{-1}$ has the following properties:

$$f(0) = 0,\ f'(0) = f''(0) = \ldots = f^{(n)}(0) = \ldots = \infty. \quad (5.9)$$

Therefore since the term (5.8) is small for small gm^2, it does not give an asymptotic expansion in powers of g. An attempt at a formal expansion leads in accordance with (5.9) to a series with diverging coefficients.

The following circumstance is curious. The second term in (5.7) turns out to be (for small g) quite small everywhere for p^2 not too close to p_0^2. In this region the function Γ is practically equal to the first term in (5.7). This fact may serve as the justification for the formal subtraction of a polynomial in powers of p^2 with divergent coefficients from the expansion (5.2) with a subsequent summation of the finite terms with the aid of (5.1).

We emphasize again that the argument given above does not pretend to be rigorous to any degree, and represents an attempt of describing one of the presently possible variants of the situation in nonrenormalizable theories.

6. CONCLUSION

Let us now take stock of the situation. As has been just demonstrated, even a very preliminary attempt at a synthesis of the method of dispersion relations and of perturbation theory allows us to obtain expressions for the Green's functions which do not contain nonphysical singularities. It should, of course, be emphasized that the range of applicability of the new formulas does not differ from the range of applicability of the old formulas, being limited by considerations of going outside the framework of weak coupling, and that in this region the new formulas practically do not differ from the old ones.

Therefore, the procedure of eliminating nonphysical singularities does not in itself provide an actual method of going outside the framework of the generally adopted approximations. However, a deeper synthesis of the approximation methods and of the dispersion relations initiated by the papers of Redmond and Symanzik may be of great significance in principle.

We shall clarify this remark by using the Lee model as an example. As is well known, the exact solution of the Lee model contains the difficulty of a logarithmic pole. On the other hand, the nonrelativistic Lee model has the property of causality with respect to time and, consequently, on the basis of the principle of spectrality the one-dimensional analogue of the Källen-Lehmann theorem, with respect to the variable E, holds for this model. Since the exact expression for the Green's function does not satisfy the Källen-Lehmann theorem, this means that the initial Hamiltonian contradicts the condition of spectrality, i.e., that (as is well known) the system of eigenfunctions of this Hamiltonian includes states with negative energy. Since such states are physically meaningless, this means that the initial Hamiltonian was not well chosen.

By applying the correction described above to the Lee model Green's function, we shall obtain for it an expression without the logarithmic pole, which will be equivalent to the subtraction from the Hamiltonian of terms corresponding to negative energy states, i.e., to its reduction to a physically sensible form.

In electrodynamics two hypotheses can be made with respect to the cause of the appearance of the logarithmic pole: 1) the initial Lagrangian is a nonphysical one, i.e., its complete system of eigenfunctions does not satisfy the requirement of spectrality; 2) the reason for the appearance of the logarithmic pole is contained in the inappropriate choice of the approximation method used.

From the point of view of the first possibility, which is equivalent to the situation in the Lee model, the correction described above for the photon Green's function corresponds to correcting the Lagrangian. In the second variant this procedure reduces to the automatic elimination of parasitic singularities which do not correspond to the physical content of the theory. Naturally, at present, it is not possible to choose between these two possibilities.

It can now be seen that the method of summation in the integrand of spectral representations appears as a certain new "super-subtraction" procedure which removes nonphysical singularities irrespectively of the reason for their appearance. It should be emphasized that this "second subtraction" procedure is a perfectly natural one, since it represents a mathematical formation of the requirement of the correspondence of the results to which it leads with the initial physical principles of the theory.

The authors express their gratitude to Prof. D. I. Blokhintsev, B. V. Medvedev, and M. K. Polivanov for discussion of the results.

---

[1] P. J. Redmond, Phys. Rev. **112**, 1404 (1958).

[2] Lehmann, Symanzik and Zimmerman, Nuovo cimento **2**, 425 (1955).

[3] Galanin, Ioffe, and Pomeranchuk, JETP **29**, 51 (1955), Soviet Phys. JETP **2**, 37 (1956).

[4] N. N. Bogolyubov and D. V. Shirkov. Введение в теорию квантованных полей (Introduction to the Theory of Quantized Fields) Moscow, Gostekhizdat, 1957 [English translation, New York, Interscience, 1959].

[5] K. Symanzik, Progr. Theoret. Phys. **20**, 690 (1958).

[6] L. D. Landau and I. Ya. Pomeranchuk, Dokl. Akad. Nauk SSSR **102**, 489 (1955); cf. also the article by L. D. Landau in the collection "Niels Bohr and the Development of Physics," London, 1955.

[7] Landau, Abrikosov, and Khalatnikov, Dokl. Akad. Nauk SSSR **95**, 773, 1177; **96**, 261 (1954).

[8] K. Ford, Phys. Rev. **105**, 320 (1957).

[9] M. Gell-Mann and F. Low, Phys. Rev. **95**, 1300 (1954).

[10] P. J. Redmond and J. L. Uretsky, Phys. Rev. Letters **1**, 147 (1958).

[11] M. É. Maĭer and D. V. Shirkov, Dokl. Akad. Nauk SSSR **122**, 45 (1958), Soviet Phys.—Doklady **3**, 931 (1959).

[12] R. Arnowitt and S. Deser, Phys. Rev. **100**, 349 (1955).

[13] L. N. Cooper, Phys. Rev. **100**, 362 (1955).

Translated by G. M. Volkoff
151

SOVIET PHYSICS JETP VOLUME 37(10), NUMBER 3 MARCH, 1960

ON THE DETERMINATION OF THE POTENTIAL IN QUANTUM FIELD THEORY

M. A. BRAUN

Leningrad State University

Submitted to JETP editor April 17, 1959

J. Exptl. Theoret. Phys. (U.S.S.R.) **37**, 816-822 (September, 1959)

The problem of the determination of the potential in quantum field theory is studied in relation to the limitations that are imposed on the transition amplitude by the conditions of orthonormality and completeness for the systems of states of the noninteracting and interacting particles. A nonlinear integral equation for the transition amplitude is used for the construction of the potential. It is shown that the potential so constructed correctly describes the scattering of particles in the range of energies in which production of new particles does not occur, and also the bound states. Problems associated with the nonuniqueness of the potential are discussed.

In the theoretical literature of recent years much space has been given to papers devoted to the study of the interaction of particles in quantum field theory by means of some sort of effective potential (cf., e.g., the survey article by Klein,[1] which gives an extensive bibliography, and also references 2 — 6). Nevertheless, the problem of the potential in quantum field theory cannot be regarded as solved. The methods proposed for its construction are not satisfactory. Some of them are in essence approximate (for example, the particles are assumed to be bound, and as the potential one takes their energy when they are a given distance apart). In other papers the authors get a potential that depends on the energy, so that they do not arrive at the Schrödinger equation for the eigenvalues, but at an equation of the form $[h_0 + V(E)]\psi_E = E\psi_E$. The methods for eliminating the dependence of the potential on the energy that have been proposed in a number of papers (cf. reference 1) are extremely artificial and complicated, and are not very effective, in the opinion of the authors themselves.

We shall be guided by an idea due to Novozhilov, that a potential independent of the energy can be determined by means of a nonlinear equation for the transition amplitude.[3] The present paper develops and refines this idea.

For our purposes the basic quantities are $\langle\varphi_\alpha|\psi_\beta^{(+)}\rangle$ in the quantum mechanics of two particles and $\langle\Phi_\alpha|\Psi_\beta^{(+)}\rangle$ in quantum field theory, where φ_α and Φ_α are states of the two particles without interaction, and $\psi_\alpha^{(+)}$ and $\Psi_\alpha^{(+)}$ are states of the interacting particles with the outgoing-wave condition. The nonlinear equations for the transition amplitude relate $\langle\varphi_\alpha|\psi_\beta^{(+)}\rangle$ to the potential in a simple way. Thus the problem is to relate $\langle\varphi_\alpha|\psi_\beta^{(+)}\rangle$ to $\langle\Phi_\alpha|\Psi_\beta^{(+)}\rangle$ (in the construction of the potential the latter quantities are regarded as known). As is shown in Sec. 1 of the present paper, direct identification of $\langle\varphi_\alpha|\psi_\beta^{(+)}\rangle$ with $\langle\Phi_\alpha|\Psi_\beta^{(+)}\rangle$ is impossible. In virtue of the orthonormality and completeness of the systems φ_α and $\psi_\alpha^{(+)}$, the $\langle\varphi_\alpha|\psi_\beta^{(+)}\rangle$ satisfy definite relations. On the other hand, the $\langle\Phi_\alpha|\Psi_\beta^{(+)}\rangle$ do not satisfy these relations, because the system of states $\Psi_\beta^{(+)}$ (α is a two-particle state) is not complete, i.e., because of the possibility of the production of new particles.

In Sec. 2 the $\langle\Phi_\alpha|\Psi_\beta^{(+)}\rangle$ are replaced by other quantities $\langle\tilde{\Phi}_\alpha|\Psi_\beta^{(+)}\rangle$, where the $\tilde{\Phi}_\alpha$ are chosen in such a way that, firstly, they agree asymptotically with the Φ_α, and secondly, the relations mentioned above are satisfied. On the basis of the $\langle\tilde{\Phi}_\alpha|\Psi_\beta^{(+)}\rangle$ it is possible to construct a potential which, as will be rigorously proved, correctly describes the scattering of the particles at energies below the threshold for the production of new particles, and makes it possible to find the levels of the bound states.

At the end of Sec. 2 we give expressions for the potential that are suitable for concrete calculations. They are an improvement on the corresponding formulas given by Novozhilov,[3] who did not examine the question of the possibility of identifying the $\langle\varphi_\alpha|\psi_\beta^{(+)}\rangle$ and the $\langle\Phi_\alpha|\Psi_\beta^{(+)}\rangle$. It must be emphasized, however, that this improvement does not extend to the results of the calculation of the nucleon-nucleon potential made by Novozhilov and Terent'ev,[4] since it is outside the scope of the approximation used in that paper (the correction terms fall off as $e^{-3\mu r}$ and faster with increase of the distance r between the nucleons; μ is the mass of the π meson).

Section 3 contains a brief discussion of some peculiarities of the potential constructed here. It turns out that the very statement of the problem of describing a quantum-field system by potentials does not permit an unambiguous definition of the potential. All the possible potentials are connected by transformations of a special type, and differ only at small distances between the particles. Considerations of simplicity and convenience enable us to single out uniquely the potential that is most suitable for applications. Here also it is shown that, generally speaking, the potential so obtained has a nonlocal character.

In our work we use some formulas of the general theory of scattering, which can be found, for example, in a paper by Ekstein.[7]

1. STATEMENT OF THE PROBLEM

Let us consider the Schrödinger equation for a system of two particles that interact with the potential V:

$$i\partial\psi/\partial t = (h_0 + V)\psi = h\psi. \tag{1}$$

Let us introduce the eigenvectors φ_α of the unperturbed Hamiltonian, where α denotes the spins and momenta of the two particles. Let $h_0\varphi_\alpha = E_\alpha\varphi_\alpha$ and $\langle\varphi_\alpha|\varphi_\beta\rangle = \delta_{\alpha\beta}$. We denote the corresponding orthonormal eigenvectors of the total Hamiltonian, with outgoing waves, by $\psi_\alpha^{(+)}$. We define $t_{\alpha\beta}$ by the equation

$$\langle\varphi_\alpha|\psi_\beta^{(+)}\rangle = \delta_{\alpha\beta} - t_{\alpha\beta}/(E_\alpha - E_\beta - i0). \tag{2}$$

Let there exist also bound states ψ_m, so that $h\psi_m = E_m\psi_m$, where $E_m < E_\alpha$ when the total momenta of these states are the same. We set

$$\langle\varphi_\alpha|\psi_m\rangle = t_{\alpha m}/(E_m - E_\alpha). \tag{3}$$

A matrix element of the S matrix is defined by the formula

$$S_{\alpha\beta} = \delta_{\alpha\beta} - 2\pi i\delta(E_\alpha - E_\beta)\,t_{\alpha\beta}. \tag{4}$$

For $t_{\alpha\beta}$ we can write the linear equation

$$t_{\alpha\beta} = V_{\alpha\beta} - \sum_\gamma \frac{V_{\alpha\gamma}t_{\gamma\beta}}{E_\gamma - E_\beta - i0} \tag{5}$$

and the nonlinear equation

$$t_{\alpha\beta} = V_{\alpha\beta} - \sum_\gamma \frac{t_{\alpha\gamma}t_{\gamma\beta}^{+}}{E_\gamma - E_\beta - i0} - \sum_m \frac{t_{\alpha m}t_{m\beta}^{+}}{E_m - E_\beta}. \tag{6}$$

A peculiarity of the nonlinear equation (6) is its simple dependence on the potential. In reference 3 it is therefore suggested that one insert in (6) instead of $t_{\alpha\beta}$ the corresponding expressions from quantum field theory, whereupon the potential in momentum space is determined from (6). Of course, to determine the potential in terms of $t_{\alpha\beta}$ one could start from (5), as Klein did.[1] This, however, would have given nothing new, since (6) in fact is the solution of (5) that gives the potential explicitly. We thus get

$$V_{\alpha\beta} = t_{\alpha\beta} + \sum_\gamma \frac{t_{\alpha\gamma}t_{\gamma\beta}^{+}}{E_\gamma - E_\beta - i0} + \sum_m \frac{t_{\alpha m}t_{m\beta}^{+}}{E_m - E_\beta}. \tag{7}$$

The question arises: can one insert arbitrary quantities for the $t_{\alpha\beta}$ in (7)? It turns out that they cannot be arbitrary. The point is that the $t_{\alpha\beta}$ must satisfy certain integral relations that arise from the orthonormality and completeness of the systems $\psi_\alpha^{(+)}$, ψ_m and φ_α. These relations were first obtained by Wigner and Eisenbud.[8] As an example we give one of these relations here:

$$\frac{t_{\alpha\beta}^{+} - t_{\alpha\beta}}{E_\alpha - E_\beta - i0} + \sum_\gamma \frac{t_{\alpha\gamma}t_{\gamma\beta}^{+}}{(E_\alpha - E_\gamma - i0)(E_\beta - E_\gamma + i0)}$$
$$+ \sum_m \frac{t_{\alpha m}t_{m\beta}^{+}}{(E_m - E_\alpha)(E_m - E_\beta)} = 0 \tag{8}$$

[hereafter when we refer to (8), we shall take it to mean all the relations of this type].

It can be shown by direct verification that the relations (8) for the $t_{\alpha\beta}$ are not only necessary, but also sufficient conditions for the quantity V determined from (7) to be capable of being interpreted as a potential. One of these relations guarantees the Hermitian character of V, and the others assure that (5) with the potential V will have as its solution the same $t_{\alpha\beta}$ as appear in (7).

Thus we conclude that the quantum-field quantities inserted in (7) instead of the $t_{\alpha\beta}$ must satisfy the conditions (8).

Let us now turn to the quantum-field system. The usual definition of the transition amplitude in field theory is*

$$T_{\Gamma\Delta} = \langle\Phi_\Gamma|H - E_\Gamma|\Psi_\Delta^{(+)}\rangle. \tag{9}$$

Here Φ are the so-called asymptotically stationary states.[9] The quantities that correspond to them in ordinary quantum mechanics are the states of noninteracting particles. H is the field-theory Hamiltonian, and $\Psi_\Delta^{(+)}$ are its eigenstates with outgoing waves, corresponding to the asymptotically stationary states Φ_Δ and energies E_Δ. The S matrix is expressed in terms of the $T_{\Gamma\Delta}$ by a formula analogous to (4). We further define the quantities $T_{\Gamma M} = \langle \Phi_\Gamma | H - E_\Gamma | \Psi_M \rangle$, where the Ψ_M are bound states in the field theory. The indices Γ and M characterize all the states of the quantum-field system, including both the states corresponding to the two particles with which we are concerned ($\Gamma = \gamma$ and $M = m$) and also states corresponding to other sets of particles ($\Gamma \neq \gamma$ and $M \neq m$).

---

*We denote quantities relating to the quantum field theory by capital letters.

For the quantities $T_{\alpha\beta}$ and $T_{\alpha m}$ we can write relations of the type of (8), but with one extremely important difference. In (8) the summations are over the spins and momenta of the two particles and their bound states. In the relations for the $T_{\alpha\beta}$, on the other hand, the summations must be taken over all the states in the field theory, i.e., as compared with (8) we have additional terms corresponding to the summations over all $\Gamma \neq \gamma$ and $M \neq m$.

From this there follows our most important conclusion: $T_{\alpha\beta}$ and $T_{\alpha m}$ do not satisfy the required conditions (8) and cannot be inserted instead of $t_{\alpha\beta}$ in (5) – (7).

We shall show, however, that there exist quantities $\widetilde{T}_{\alpha\beta}$ and $\widetilde{T}_{\alpha m}$ that on one hand satisfy (8) and on the other hand are equal to $T_{\alpha\beta}$ for $E_\alpha = E_\beta$, if processes of creation and annihilation of particles do not occur. Substitution of $\widetilde{T}_{\alpha\beta}$ and $\widetilde{T}_{\alpha m}$ in (7) gives the desired potential. The construction of the $\widetilde{T}_{\alpha\beta}$ and $\widetilde{T}_{\alpha m}$ will be carried out in the next section.

2. CONSTRUCTION OF THE POTENTIAL

Let us separate out from all the states $\Psi_\Gamma^{(+)}$ the states with $\Gamma = \gamma$. Let P be the operator for projection onto these states, so that

$$\langle \Psi' | P\Psi'' \rangle = \sum_\gamma \langle \Psi' | \Psi_\gamma^{(+)} \rangle \langle \Psi_\gamma^{(+)} | \Psi'' \rangle + \sum_m \langle \Psi' | \Psi_m \rangle \langle \Psi_m | \Psi'' \rangle. \tag{10}$$

If the two particles under consideration form certain bound states, then in the sum over m we may include not all of these states m but an arbitrary selection from them.

Let us orthogonalize and normalize the Φ_α with respect to the metric (10). If

$$\langle \Phi_\alpha | P\Phi_\beta \rangle = \delta_{\alpha\beta} + N_{\alpha\beta}, \tag{11}$$

then the state vectors

$$\widetilde{\Phi}_\alpha = \sum_\gamma [1 + N]_{\gamma\alpha}^{-1/2} \Phi_\gamma \tag{12}$$

will obviously have the required properties:

$$\langle \widetilde{\Phi}_\alpha | P\widetilde{\Phi}_\beta \rangle = \delta_{\alpha\beta}. \tag{13}$$

By N in (12) we mean the Hermitian integral operator whose kernel is defined by (11). We shall assume that $[1 + N]\Phi_\alpha \neq 0$.

We assume that the orthonormal system $P\widetilde{\Phi}_\alpha$ so obtained is complete in space determined by the projection operator P. In fact, if this were not so there would exist a linear combination of the $\Psi_\gamma^{(+)}$ and Ψ_m that would be orthogonal to all the $P\widetilde{\Phi}_\alpha$, and consequently to all the Φ_α (in view of the fact that $1 + N$ cannot vanish). But the expression $\langle \Psi_\gamma^{(+)} | \Phi_\alpha \rangle$ is analogous in meaning to the phenomenological function of the state γ in the momentum representation, and for such quantities it is natural to assume linear independence.

Let us set

$$\langle \widetilde{\Phi}_\alpha | \Psi_\beta^{(+)} \rangle = \delta_{\alpha\beta} - \frac{\widetilde{T}_{\alpha\beta}}{E_\alpha - E_\beta - i0},$$

$$\langle \widetilde{\Phi}_\alpha | \Psi_m \rangle = \frac{\widetilde{T}_{\alpha m}}{E_m - E_\alpha}. \tag{14}$$

In virtue of the orthonormality and completeness of the systems of states $\Psi_\gamma^{(+)}$, Ψ_m, and $P\widetilde{\Phi}_\gamma$, the quantities $\widetilde{T}_{\alpha\beta}$ and $\widetilde{T}_{\alpha m}$ defined by (14) satisfy the conditions (8). Substitution of these quantities in (7) gives us a Hermitian potential V for which solution of the Schrödinger equation (1) at once gives the quantities $\widetilde{T}_{\alpha\beta}$ and $\widetilde{T}_{\alpha m}$.

Let us now verify that the $\widetilde{T}_{\alpha\beta}$ correctly describe the scattering, i.e., that on the energy surface $E_\alpha = E_\beta$ they are identical with $T_{\alpha\beta}$. According to (9) and (14), it is sufficient for this to show that

$$\lim_{E_\alpha \to E_\gamma} (E_\alpha - E_\gamma) \langle \widetilde{\Phi}_\alpha | \Psi_\gamma^{(+)} \rangle = \lim_{E_\alpha \to E_\gamma} (E_\alpha - E_\gamma) \langle \Phi_\alpha | \Psi_\gamma^{(+)} \rangle. \tag{15}$$

It follows from (11) that

$$N_{\alpha\beta} = \langle \Phi_\alpha | \Phi_\beta \rangle - \delta_{\alpha\beta} - \sum_{\Gamma \neq \gamma} \langle \Phi_\alpha | \Psi_\Gamma^{(+)} \rangle \langle \Psi_\Gamma^{(+)} | \Phi_\beta \rangle. \tag{16}$$

If processes of creation and annihilation are impossible, then in the sum over $\Gamma \neq \gamma$ none of the terms has a denominator that gives a singularity, and $N_{\alpha\beta}$ is not singular for $E_\alpha = E_\beta$. Under these conditions (15) indeed holds, since the singular terms of $\langle \widetilde{\Phi}_\alpha | \Psi_\beta^{(+)} \rangle$ and $\langle \Phi_\alpha | \Psi_\beta^{(+)} \rangle$ are the same.

The potential determined in terms of $\widetilde{T}_{\alpha\beta}$ and $\widetilde{T}_{\alpha m}$ by (7) is

$$V_{\alpha\beta} = \widetilde{T}_{\alpha\beta} + \sum_\gamma \frac{\widetilde{T}_{\alpha\gamma} \widetilde{T}_{\gamma\beta}^{+}}{E_\gamma - E_\beta - i0} + \sum_m \frac{\widetilde{T}_{\alpha m} \widetilde{T}_{m\beta}^{+}}{E_m - E_\beta}. \tag{17}$$

We transform (17) to an expression more convenient for study:

$$\widetilde{T}_{\alpha\beta}=\langle\widetilde{\Phi}_\alpha|H-E_\alpha|\Psi_\beta^{(+)}\rangle=\langle\widetilde{\Phi}_\alpha|H-E_\alpha|\,P\widetilde{\Phi}_\beta\rangle$$

$$+\sum_\gamma\langle\widetilde{\Phi}_\alpha|H-E_\alpha|\Psi_\gamma^{(+)}\rangle\langle\Psi_\gamma^{(+)}|\Psi_\beta^{(+)}-P\widetilde{\Phi}_\beta\rangle$$

$$+\sum_m\langle\widetilde{\Phi}_\alpha|H-E_\alpha|\Psi_m\rangle\langle\Psi_m|\Psi_\beta^{(+)}-P\widetilde{\Phi}_\beta\rangle$$

$$=\langle\widetilde{\Phi}_\alpha|H-E_\alpha|P\widetilde{\Phi}_\beta\rangle-\sum_\gamma\frac{\widetilde{T}_{\alpha\gamma}\widetilde{T}^+_{\gamma\beta}}{E_\gamma-E_\beta-i0}-\sum_m\frac{\widetilde{T}_{\alpha m}\widetilde{T}^+_{m\beta}}{E_m-E_\beta}.$$

Comparing this with (17), we find

$$V_{\alpha\beta}=\langle\widetilde{\Phi}_\alpha|H-E_\alpha|P\widetilde{\Phi}_\beta\rangle. \tag{18}$$

The Hermitian character of the potential that has been constructed can be seen directly from (18). By using (18) one can check by an elementary calculation that the Schrödinger equation with the potential V leads to the scattering amplitudes $\widetilde{T}_{\alpha\beta}$. In fact,

$$\sum_\gamma V_{\alpha\gamma}\langle\widetilde{\Phi}_\gamma|\Psi_\beta^{(+)}\rangle=\sum_\gamma\langle\widetilde{\Phi}_\alpha|H-E_\alpha|P\widetilde{\Phi}_\gamma\rangle\langle\widetilde{\Phi}_\gamma|\Psi_\beta^{(+)}\rangle$$

$$=\langle\widetilde{\Phi}_\alpha|H-E_\alpha|\Psi_\beta^{(+)}\rangle=(E_\beta-E_\alpha)\langle\widetilde{\Phi}_\alpha|\Psi_\beta^{(+)}\rangle.$$

Consequently, $\langle\widetilde{\Phi}_\alpha|\Psi_\beta^{(+)}\rangle$ is an eigenfunction of the Schrödinger equation in question, and to it there indeed corresponds the scattering amplitude $\widetilde{T}_{\alpha\beta}$.

In just as simple a way one also proves the important fact that the Schrödinger equation with the potential V will not contain any extra features: to each of its eigenfunctions there will correspond an eigenstate in the field theory for the same energy. Suppose, for example, $f_\beta(\alpha)$ is an eigenfunction of the Schrödinger equation for the energy E_β. Then

$$(H-E_\beta)\sum_\gamma f_\beta(\gamma)P\widetilde{\Phi}_\gamma=\sum_{\gamma\alpha}f_\beta(\gamma)P\widetilde{\Phi}_\alpha\langle\widetilde{\Phi}_\alpha|H-E_\beta|P\widetilde{\Phi}_\gamma\rangle$$

$$=\sum_\alpha P\widetilde{\Phi}_\alpha\sum_\gamma[(E_\alpha-E_\beta)\delta_{\alpha\gamma}+V_{\alpha\gamma}]f_\beta(\gamma)=0.$$

Thus to $f_\beta(\gamma)$ there corresponds the state $\sum_\gamma f_\beta(\gamma)P\widetilde{\Phi}_\gamma$ in the field theory.

We can summarize the properties of the potential (18) in the form of the following theorem.

The Schrödinger equation

$$E_\alpha f_\gamma(\alpha)+\sum_\beta V_{\alpha\beta}f_\gamma(\beta)=E_\gamma f_\gamma(\alpha) \tag{19}$$

with the potential $V_{\alpha\beta}$ defined by (18) has the following properties:

1) To each eigenstate $\Psi^{(+)}_{\Gamma=\gamma}$ or $\Psi_{M=m}$ of the Hamiltonian H of the quantum field theory there corresponds an eigenfunction of (19) for the same eigenvalue $E_{\gamma,m}$, determined by the rules:

$$f_\gamma^{(+)}(\alpha)=\delta_{\gamma\alpha}-\frac{1}{E_\alpha-E_\gamma-i0}\langle\widetilde{\Phi}_\alpha|H-E_\alpha|\Psi_\gamma^{(+)}\rangle,$$

$$f_m(\alpha)=\frac{1}{E_m-E_\alpha}\langle\widetilde{\Phi}_\alpha|H-E_\alpha|\Psi_m\rangle \tag{20}$$

[the bound states m here are only those that were used in the scalar product (10)].

2) Conversely, to every eigenfunction $f_\gamma^{(+)}(\alpha)$ (with outgoing wave) or $f_m(\alpha)$ (for a bound state) there corresponds in the quantum field theory an eigenstate $\Psi_\gamma^{(+)}$ or Ψ_m, respectively, for the same eigenvalue, which is constructed according to the rules:

$$\Psi_\gamma^{(+)}=\sum_\alpha f_\gamma^{(+)}(\alpha)P\widetilde{\Phi}_\alpha,\qquad \Psi_m=\sum_\alpha f_m(\alpha)P\widetilde{\Phi}_\alpha. \tag{21}$$

3) In the range of energies of the colliding particles in which creation and annihilation processes are impossible, the scattering cross sections obtained from (19) and from quantum field theory are the same.

In conclusion we present an expression for the potential that is convenient for concrete calculations, and that follows directly from (18):

$$V_{\alpha\beta}=\{[1+N]^{-1/2}\widetilde{V}(E_\alpha,E_\beta)[1+N]^{-1/2}\}_{\alpha\beta},$$

$$[\widetilde{V}(E_\alpha,E_\beta)]_{\gamma_1\gamma_2}=\left\langle\Phi_{\gamma_1}\left|H-\frac{E_\alpha+E_\beta}{2}\right|\Phi_{\gamma_2}\right\rangle$$

$$+\sum_{\Gamma\neq\gamma}\frac{T_{\gamma_1\Gamma}T^+_{\Gamma\gamma_2}(E_\Gamma-{}^1/_2(E_\alpha+E_\beta))}{(E_{\gamma_1}-E_\Gamma-i0)(E_\Gamma-E_{\gamma_2}-i0)}. \tag{22}$$

The formula (22) explicitly shows the Hermitian character of the potential, its lack of singularities, and also the fact that V actually does not depend on the states $\Psi_\gamma^{(+)}$ and Ψ_m.

3. DISCUSSION

The potential V that we have constructed is of course not the only potential that correctly describes the scattering of the particles and their bound states [in the sense of Eq. (21)]. In the derivation of V we have encountered a certain arbitrariness. In making the system P orthonormal, we could have used instead of (12) the vectors

$$\widetilde{\Phi}_\alpha=\sum_\beta U_{\beta\alpha}\widetilde{\Phi}_\beta, \tag{23}$$

where U is an arbitrary unitary Lorentz-invariant operator, which can be written in the form $U = 1 + U_1$, and $U_{1\alpha\beta}$ is a nondiagonal matrix that goes to zero if we set $N = 0$ and has no singularity at $E_\alpha = E_\beta$ when $N_{\alpha\beta}$ does not have such a singularity. All the further arguments would have remained valid. Therefore one could also use as the potential the expression

$$V'_{\alpha\beta} = \sum_{\gamma_1 \gamma_2} U^{+}_{\alpha\gamma_1} \langle \widetilde{\Phi}_{\gamma_1} | H - E_\alpha | P \widetilde{\Phi}_{\gamma_2} \rangle U_{\gamma_2\beta} \qquad (24)$$

(we note that this is not a unitary transformation of V).

The cause of this sort of ambiguity is concealed in the very statement of the problem. We have been looking for a potential that gives the same scattering and the same bound-state levels as in the field theory. In ordinary quantum mechanics, however, one can have Schrödinger equations with different potentials corresponding to the same scattering and bound-state spectrum. The wave functions for these potentials will differ at small distances between the particles, and therefore the mean values of physical quantities in a bound state will be different for different potentials, and in general will not agree with those found in quantum field theory. We indeed do not demand such agreement, however, since such a requirement is scarcely realizable in practice and seems extremely artificial from the theoretical point of view. Thus we get a whole set of potentials (24) that give equally good descriptions of the behavior of the particles within the framework of the problem as stated.

The potential (18) is distinguished from the others by its simplicity and convenience for calculations and by the absence of any arbitrary quantities not determined by the theory itself. For this reason, in our opinion, it is reasonable to adopt this particular equation (18) as the definition of the potential in quantum field theory.

It must be remarked that the arbitrariness discussed here bears no relation to the well known ambiguity in the expression for the fourth-order nucleon-nucleon potential. The reasons the latter ambiguity arises have been analyzed, for example, by Fukuda, Sawada, and Taketani.[5]

A few words about the spatial properties of the potential. Equation (18) gives the potential in the momentum representation. A Fourier transformation leads to the potential in coordinate space, which is an integral operator with the kernel $V(\mathbf{r}_1 - \mathbf{r}_2, \mathbf{r}'_1 - \mathbf{r}'_2)$, where $\mathbf{r}_1$ and $\mathbf{r}_2$ are the radii vectors of the two particles; that is, we arrive at a nonlocal interaction in the configuration space. As is well known, one cannot get a strictly local potential, if one requires that it describe the scattering correctly. In fact, the transition amplitude obtained from a local potential is analytic in the upper half of the energy plane and on the real axis; the same is true of the amplitude in quantum field theory. If we require that these amplitudes be exactly equal on some segment of the real axis of the energy plane (for which there is no production of new particles), then because they are analytic they will agree also on the entire real axis. This cannot be true, however, since at high energies new particles can be produced. Consequently, the idea of a strictly local potential must be rejected. We shall not concern ourselves here with the question of the approximately local character of the potential in individual cases.

In conclusion the writer takes occasion to express his deep gratitude to Yu. V. Novozhilov for his constant interest and for helpful comments.

---

[1] A. Klein, Prog. Theor. Phys. **20**, 257 (1958).

[2] A. Klein and B. H. McCormick, Prog. Theor. Phys. **20**, 876 (1958).

[3] Yu. V. Novozhilov, JETP **35**, 742 (1958), Soviet Phys. JETP **8**, 515 (1959).

[4] Yu. V. Novozhilov and I. A. Terent'ev, JETP **36**, 129 (1959), Soviet Phys. JETP **9**, 89 (1959).

[5] Fukuda, Sawada, and Taketani, Prog. Theor. Phys. **12**, 156 (1954).

[6] Inoue, Machida, Taketani, and Toyoda, Prog. Theor. Phys. **15**, 122 (1956).

[7] H. Ekstein, Phys. Rev. **101**, 880 (1956).

[8] E. Wigner and L. Eisenbud, Phys. Rev. **72**, 29 (1947).

[9] L. Van Hove, Physica **21**, 901 (1955); **22**, 343 (1956).

Translated by W. H. Furry
152

SOVIET PHYSICS JETP VOLUME 37(10), NUMBER 3 MARCH, 1960

NONRESONANCE ABSORPTION OF OSCILLATING MAGNETIC FIELD ENERGY BY A FERROMAGNETIC DIELECTRIC

M. I. KAGANOV and V. M. TSUKERNIK

Physico-Technical Institute, Academy of Sciences, Ukrainian S.S.R.

Submitted to JETP editor April 18, 1959

J. Exptl. Theoret. Phys. (U.S.S.R.) 37, 823-832 (September, 1959)

Spin-wave theory is used to calculate the imaginary part of the longitudinal magnetic susceptibility of a ferromagnetic dielectric.

A ferromagnet can absorb the energy of a weak alternating magnetic field $H' \sim e^{-i\omega t}$ that is polarized either perpendicular or parallel to its equilibrium magnetic moment. In the first case the magnetic field "rotates" the magnetic moment without changing its magnitude, while in the second case a process of magnetization changes the absolute value of the magnetic moment. In both cases dissipative processes occur that are associated with interactions of spin waves with each other and with phonons.[1-3] We assume saturation magnetization of the ferromagnetic dielectric at a given temperature so that our sample consists of a single domain, and that it is pure enough so that we may disregard effects due to impurities.

In the present paper we confine ourselves to the case in which the magnetic field of frequency ω is polarized parallel to the equilibrium magnetic moment of the ferromagnetic dielectric. The imaginary part of the longitudinal magnetic susceptibility $\mu_{||} = \mu'_{||} + i\mu''_{||}$ must therefore be determined in order to calculate the absorption. The complicated character of relaxation processes in ferromagnetic dielectrics[4] leads to a complicated frequency dependence of $\mu''_{||}(\omega)$.

Our calculation will be based on the simplest model of a ferrodielectric as a body with a single magnetic moment whose oscillations are propagated as spin waves. This is valid at sufficiently low temperatures; we then have no vibrations of one magnetic sublattice with respect to the other, which correspond to high frequency limits ($\sim \Theta_c/\hbar$). The real bodies to which the present form of the theory of spin waves can be applied are evidently ferrites, the semiconductor properties of which are unimportant at low temperatures (the number of free electrons vanishes exponentially as the temperature is reduced).

1. LOW FREQUENCIES

When the magnetic field frequency is considerably smaller than the reciprocal of the spin-spin relaxation time τ_{ss}, i.e.,

$$\omega\tau_{ss} \ll 1, \tag{1}$$

this field can be regarded classically as the cause of spin-wave nonequilibrium. This condition (1) enables us to assume that the spin-wave system has quasi-equilibrium energy levels, i.e.,

$$E = \sum_{\mathbf{k}} \varepsilon_{\mathbf{k}} n_{\mathbf{k}}, \qquad \varepsilon_{\mathbf{k}} = \Theta_c (ak)^2 + \mu H(t). \tag{2}$$

Here ϵ_k is the energy of a spin wave.* We shall make use of (2), which is valid for relatively large values of the wave vector number $\mathbf{k}$, so that the results of this section are correct only when $T \gg 2\pi\mu M_0 \sim 1°K$. The mean occupation numbers n_k are determined by means of a kinetic equation, written schematically as

$$\partial n_{\mathbf{k}}/\partial t = (\partial n_{\mathbf{k}}/\partial t)_{ss} + (\partial n_{\mathbf{k}}/\partial t)_{sl}. \tag{3}$$

The first term on the right is the part of the collision integral which describes the interaction between spin waves, while the second term pertains to the interaction between spin waves and phonons. The specific form of the collision operator has been given in references 2 and 3. It is very important in what follows that at temperatures T considerably above $T_0 = \mu M_0(\Theta_c/\mu M_0)^{3/7} \sim 10°$ the principal part in the interaction of spin waves is played by the exchange interaction and for $T \ll T_0$ by the relativistic interaction. This difference results in an essential distinction between the frequency dependence of the imaginary part of the magnetic susceptibility at low $(T \ll T_0)$ and high $(T \gg T_0)$ temperatures.

---

*The notation of references 2 and 3 is used.

For the low-temperature region $(T \ll T_0)$ we have, from reference 2*

$$\frac{1}{\tau_{ss}} \approx \frac{\mu M_0}{\hbar} \frac{\mu M_0}{\Theta_c} \left(\frac{T}{\Theta_c}\right)^{1/2} \approx 10^6 \left(\frac{T}{T_0}\right)^{1/2} (\mathrm{sec}^{-1}) (\mu M_0 \ll T \ll T_0),$$

and (3) will be solved in the form

$$n_{\mathbf{k}} = n_0(\varepsilon_{\mathbf{k}}/T) + n'_{\mathbf{k}}, \quad |n'_{\mathbf{k}}| \ll n_0, \tag{4}$$

where n_0 is the equilibrium Bose function. It must also be remembered that ϵ_k and T depend on the time. This form of the solution denotes that in the spin-wave system a quasi-equilibrium state can be established with its own temperature, different from the lattice temperature. Dissipation is here associated with two basically different mechanisms, the transfer of energy to phonons and the departure of the distribution from equilibrium. We therefore write $\mu'' = \mu''_1 + \mu''_2$. The first mechanism is naturally characterized by the time τ_{sl} required for temperature equalization[3] and the second mechanism by the spin-spin relaxation time τ_{ss}. Since $\tau_{ss} \ll \tau_{sl}$, at frequencies $\omega\tau_{sl} \ll 1$ the principal part in dissipative processes will be played by energy transfer to phonons and at frequencies $1/\tau_{sl} \ll \omega \ll 1/\tau_{ss}$ by the departure of the distribution from equilibrium.

To calculate the time dependence of the temperature T we must use the heat-balance equation

$$\dot{T} + (T - T_l)/\tau_{sl} = q\mu\dot{H}, \quad \tau_{sl} = C_s/\alpha, \quad q \sim 0.4, \tag{5}$$

which is easily obtained from (3) and (4). Here α is the coefficient of heat transfer between spin waves and the lattice which was calculated in reference 3. An analogous equation can be derived for the phonon temperature T_l, although the problem of the interaction between phonons and the external medium now arises. On the other hand, if we assume excellent thermal contact, so that all heat entering the lattice can be removed by the external medium (unlimited heat elimination) the lattice temperature T_l can be regarded as constant. We shall hereinafter limit ourselves to this case.†

From (5) we have

$$T = T_l + T', \qquad T' = \frac{qC_s\mu\dot{H}}{\alpha - i\omega C_s} = -\frac{i\omega qC_s\mu H'}{\alpha - i\omega C_s}. \tag{6}$$

As already stated, the dissipation is described by the imaginary part of the magnetic susceptibility, which is obtained from the imaginary part of the coefficient relating the spin temperature to the magnetic field; we have

$$M = M_0 - \mu \sum_{\mathbf{k}} n_0(\varepsilon_{\mathbf{k}}/T).$$

From this equation and (6) we obtain

$$\mu''_1 = \varkappa \frac{\mu^2}{a^3\Theta_c} \left(\frac{T}{\Theta_c}\right)^{1/2} \frac{\omega\tau_{sl}}{1 + \omega^2\tau_{sl}^2},$$

$$\varkappa = \frac{3}{40\pi^{3/2}} \frac{\zeta^2(3/2)}{\zeta(5/2)} \approx 10^{-2}. \tag{7}$$

It is shown in reference 3 that for $T \ll T_0$ the coefficient of heat transfer from spin waves to the lattice depends exponentially on the temperature (heat is transferred through the "Cerenkov" production of phonons by spin waves); also

$$C_s = (15\zeta(5/2)/32\pi^{3/2})(T/\Theta_c)^{3/2}.$$

Therefore

$$\frac{1}{\tau_{sl}} \approx \frac{64\beta_1^2}{5\pi^{3/2}\zeta(5/2)} \frac{\Theta_c}{\hbar} \frac{T^{7/2}}{ms_l^2\Theta_c^{5/2}} \exp\{-\Theta_l^2/4\Theta_c T\}, \qquad m = \rho a^3; \tag{8}$$

$$\mu''_1 \approx 5 \cdot 10^{-3} \frac{\mu^2}{a^3} \frac{ms_l^2 h\omega}{T^3} \exp\left(\frac{\Theta_l^2}{4\Theta_c T}\right), \qquad \omega\tau_{sl} \ll 1. \tag{8'}$$

We shall now calculate μ''_2, the part of μ'' that is associated with the departure of the distribution from equilibrium. This dissipation mechanism is important at relatively high frequencies $(\omega\tau_{sl} \gg 1)$, when we can still make use of (2) [in virtue of (1)] and of the kinetic equation (3). In the latter the second term of the right member may be neglected; when $\omega \gg 1/\tau_{sl}$ energy "cannot" be transferred to phonons. Since $(\partial n_k^0/\partial t)_{ss} \equiv 0$ we have

$$\partial n_{\mathbf{k}}^0/\partial t + \partial n'_{\mathbf{k}}/\partial t = (\partial n'_{\mathbf{k}}/\partial t)_{ss}. \tag{9}$$

The neglect of the term $(\partial n_k/\partial t)_{sl}$ in the kinetic equation corresponds to the neglect of heat elimination in the thermal balance equation (5). Therefore when $\omega\tau_{sl} \gg 1$ we have $\dot{T} = q\mu\dot{H}$, and (9) can be written as follows:

$$\left(1 - q\frac{\varepsilon}{T}\right) \frac{\partial n_0}{\partial(\varepsilon/T)} \frac{\mu\dot{H}}{T} = \frac{1}{\tau_{ss}} \hat{L}\{n'\}. \tag{10}$$

Here

$$1/\tau_{ss} = (\mu M_0/h)(\mu^2/a^3\Theta_c)(T/\Theta_c)^{1/2}, \tag{11}$$

while $\hat{L}$ is a dimensionless collision operator which is easily derived from (34) of reference 2 by changing from summation to integration over the wave vectors k and introducing the dimensionless wave vector $\mathbf{x} = \sqrt{\Theta_c/T}\, ak$.

In (10) we have omitted the term containing the time derivative of the nonequilibrium correction to the distribution function; this is valid for $\omega\tau_{ss} \ll 1$.

---

*We have assumed $\Theta_c \sim 10^{-13}$ erg, $T_0 \sim 10$°K; the unimportant logarithmic dependence on temperature has been disregarded.

†The adiabatic temperature-equalization time t_{sl} was calculated in reference 3.

From (10) we have

$$n' = \tau_{ss}(\mu\dot{H}/T)\,\varphi(x), \tag{12}$$

where $\varphi(x)$ is a dimensionless function which cannot be determined without solving the integral equation (10).

When the temperature dependence of n' is known the temperature dependence of μ_2'' can be determined. This requires calculating the variation of the entropy S per unit time resulting from the departure of the spin-wave distribution from equilibrium. A familiar formula[5] gives the amount of absorbed magnetic field energy:

$$Q = (\omega\mu''/4\pi)\,\overline{H'^2}. \tag{13}$$

This equation in conjunction with $T\dot{S} = Q$ gives μ'' (μ_2'' in the present case). We shall therefore determine $T\dot{S}$, using the following expression for the entropy of a nonequilibrium Bose gas:[6]

$$S = \sum_{\mathbf{k}} \{(n_{\mathbf{k}} + 1)\ln(n_{\mathbf{k}} + 1) - n_{\mathbf{k}}\ln n_{\mathbf{k}}\}.$$

By differentiating this expression with respect to time and taking into account the energy conservation law

$$\sum_{\mathbf{k}} \varepsilon_{\mathbf{k}} n_{\mathbf{k}}^{0} = 0$$

[a corollary of the linearized kinetic equation (9)], we obtain

$$Q \equiv T\dot{S} = -T\sum_{\mathbf{k}} (\dot{n}'_{\mathbf{k}})_{ss}\, n'_{\mathbf{k}}/n_{\mathbf{k}}^{0}(n_{\mathbf{k}}^{0} + 1). \tag{14}$$

From (14), (12), and (13) we then have

$$\mu_2'' = \varkappa_2\,(\mu^2/a^3\Theta_c)\,(T/\Theta_c)^{1/2}\,\omega\tau_{ss}, \tag{15}$$

where κ_2 is a numerical constant that can be determined only by solving the kinetic equation exactly.

Equation (15) is valid for $1/\tau_{sl} \ll \omega \ll 1/\tau_{ss}$. A comparison with (7) shows that μ_1'' and μ_2'' coincide when $\omega \approx (\tau_{sl}\,\tau_{ss})^{-1/2}$. At lower frequencies $\mu_1'' > \mu_2''$ and at higher frequencies $\mu_1'' < \mu_2''$. As the frequency approaches $1/\tau_{ss}$ the value of μ_2'' must be reduced since the spin system "cannot" depart from equilibrium. This can be taken into account by retaining the term $\partial n'/\partial t$ in (10). We then obtain

$$\mu_2'' = \varkappa_2 \frac{\mu^2}{a^3\Theta_c}\left(\frac{T}{\Theta_c}\right)^{1/2} \frac{\omega\tau_{ss}}{1 + \omega^2\tau_{ss}^2}. \tag{16}$$

A comparison of (15) and (11) shows that for frequencies in the interval $(\tau_{sl}\,\tau_{ss})^{-1/2} \ll \omega \ll 1/\tau_{ss}$ the imaginary part μ'' of the magnetic susceptibility is independent of temperature and is linearly dependent on frequency:

$$\mu'' \approx \hbar\omega/\mu M_0. \tag{17}$$

We shall now consider the case of relatively high temperatures $T \gg T_0$. As previously we shall assume that the temperature is considerably below both the Curie temperature Θ_C and the Debye temperature Θ_0. In this temperature region exchange forces play the principal part in the interaction between spin waves. It is therefore convenient to write the kinetic equation as follows:

$$\frac{\partial n_{\mathbf{k}}}{\partial t} = \left(\frac{\partial n_{\mathbf{k}}}{\partial t}\right)_{ss}^{\text{exch}} + \left(\frac{\partial n_{\mathbf{k}}}{\partial t}\right)_{ss}^{\text{rel}} + \left(\frac{\partial n_{\mathbf{k}}}{\partial t}\right)_{sl}. \tag{18}$$

We cannot drop the small relativistic term, which is responsible for energy dissipation in one of the frequency regions. The large exchange interaction between spin waves does not change their number; this is reflected mathematically in the fact that the Bose distribution with an arbitrary value of the chemical potential γ causes vanishing of the first term in the right member of (18). We recall that the equilibrium chemical potential of the spin-wave gas is zero.

The solution of (18) must be found in the form

$$n = n_0\left(\frac{\varepsilon - \gamma}{T}\right) + n', \qquad |n'| \ll n_0, \tag{19}$$

taking into account the time dependence of the energy ϵ, chemical potential γ and spin-wave temperature T. We shall use (2) for the energy of a spin wave, regarding it as valid also for $k = 0$. This is permissible if we assume that the ferromagnet has a large anisotropy constant or is in a relatively strong magnetic field. The spin-wave energy for $k = 0$ without an external alternating field will hereinafter be denoted by ϵ_0 ($\epsilon_0 = \mu H_{\text{eff}}$, $H_{\text{eff}} = H_0 + \beta M_0$).

From (18) and (19) we easily obtain the following relations between the variable part of the spin temperature T, the chemical potential γ and the alternating magnetic field:

$$(A_{T\gamma} - i\omega q C_s)T' + (T A_{\gamma\gamma} - i\omega B)\gamma = B\mu\dot{H},$$

$$(A_{TT} - i\omega C_s)T' + (A_{T\gamma} - i\omega C_s)\gamma = qC_s\mu\dot{H}. \tag{20}$$

Here

$$B = T^2/8\pi\Theta_c^{3/2}\varepsilon_0^{1/2}, \tag{21}$$

and the A coefficients were calculated in reference 7, where magnetic-moment relaxation in a ferromagnetic dielectric was studied. In the given temperature interval ($T \gg T_0$, Θ_0^2/Θ_C)*

$$A_{T\gamma} = (\hbar/6\pi^2\rho a^5)\,(\gamma_1\mu M_0/\Theta_c)^2\,(T/\Theta_c)^2,$$

$$A_{TT} = (2\pi^2\hbar/45\rho a^5)\,[2\beta_1^2 + (2\beta_1 + \beta_2)^2]\,(T/\Theta_c)^4,$$

$$A_{\gamma\gamma} = (\chi/\hbar)\,(\mu M_0/\Theta_c)^2\,(T^2/\varepsilon_0\Theta_c), \qquad \chi \approx 0.1.$$

---

*The notation is that of references 2 and 3.

T' and γ can be calculated by means of (20). The formula

$$M = M_0 - \mu \sum_{\mathbf{k}} n_{\mathbf{k}} \left(\frac{\varepsilon - \gamma}{T}\right)$$

for the magnetic moment is then used to give the imaginary part of the magnetic susceptibility. Retaining only the principal terms, we obtain

$$\mu'' = \frac{5\pi}{4\chi} \frac{\hbar\omega}{a^3 M_0^2} \frac{1 + \omega^2 \tau_2^2}{(1 + \omega^2\tau_1^2)^2 + \omega^2\tau_3^2} \qquad (T \gg T_0), \tag{23}$$

where

$$1/\tau_1 = (T A_{\gamma\gamma} A_{TT}/BC_s)^{1/2}$$
$$\approx (\mu M_0/\hbar)(\Theta_0^2/ms^2\Theta_c)^{1/2}(T/\Theta_c)^{3/2}(T/\varepsilon_0)^{1/4},$$
$$1/\tau_2 = A_{TT}/C_s \sim (\Theta_0/\hbar)(\Theta_0/ms^2)(T/\Theta_c)^{5/2},$$
$$1/\tau_3 = T A_{\gamma\gamma}/B \sim (T/\hbar)(\mu M_0/\Theta_c)^2(\Theta_c/\varepsilon_0)^{1/2}. \tag{24}$$

The frequency dependence of the imaginary part of the susceptibility is shown in (23), where all relaxation times satisfy the following sequence of inequalities:

$$\tau_{ss} \ll \tau_1 \ll \tau_2 \ll \tau_3,$$

and the reciprocal spin-spin relaxation time $1/\tau_{ss}$ is now given by[3]

$$1/\tau_{ss} \sim (\Theta_c/\hbar)(T/\Theta_c)^4. \tag{24'}$$

At low frequencies

$$\mu'' \sim \hbar\omega/\mu M_0 \qquad (\omega\tau_3 \ll 1;\ T \gg T_0).$$

We assume that $M_0 \sim \mu/a^3$.

It can be shown that an additional loss mechanism exists at frequencies $1/\tau_1 \ll \omega \ll 1/\tau_{ss}$, due to the departure of the spin-wave distribution from equilibrium. (This is analogous to the second mechanism at low temperatures.) However, it is easily seen that this mechanism always (at all frequencies) results in values of μ'' which are considerably smaller than those calculated from (23). This results from the fact that the exchange forces, which play the principal part in this temperature region, cannot produce dissipation without the cooperation of relativistic interactions, since the former do not change the magnetic moment.

This section will be concluded by specifying the imaginary part of the longitudinal magnetic susceptibility in different frequency and temperature ranges. From (7), (16), and (23) we have

$$\mu'' \sim \begin{cases} \dfrac{M_0\mu}{\Theta_c}\left(\dfrac{T}{\Theta_c}\right)^{1/2} \dfrac{\omega\tau_{sl}}{1 + \omega^2\tau_{sl}^2}, & \omega\sqrt{\tau_{sl}\tau_{ss}} \ll 1, \qquad T \ll T_0; \\[2ex] \dfrac{\mu M_0}{\Theta_c}\left(\dfrac{T}{\Theta_c}\right)^{1/2} \dfrac{\omega\tau_{ss}}{1 + \omega^2\tau_{ss}^2}, & \omega\sqrt{\tau_{sl}\tau_{ss}} \gg 1, \qquad T \ll T_0; \\[2ex] \dfrac{\hbar\omega}{\mu M_0} \dfrac{1 + \omega^2\tau_2^2}{(1 + \omega^2\tau_1^2)^2 + \omega^2\tau_3^2}, & \omega\tau_{ss} \ll 1, \qquad T \gg T_0. \end{cases}$$

The relaxation times are given by (8), (11), (24), and (24'). We recall that $T_0 \sim \mu M_0(\Theta_c/\mu M_0)^{3/7}$.

2. HIGH FREQUENCIES

Since at frequencies $\omega \gg 1/\tau_{ss}$ spin waves cannot depart from equilibrium, the attenuation of the magnetic field can be regarded as the absorption of photons by an equilibrium spin-wave gas.[8,9]

The interaction Hamiltonian of the field and spin waves is obviously

$$\hat{\mathcal{H}}_{int} = \mu \int \hat{H}_z \hat{a}^*(\mathbf{r})\hat{a}(\mathbf{r})\,dv.$$

The expansion of the operators $\hat{a}(\mathbf{r})$ and $a^*(\mathbf{r})$ in terms of the spin waves is given by (12) – (20) of reference 2, and the magnetic field operator is[10]

$$\hat{H}_z = i\sqrt{2\pi\hbar\omega/V}\,\{\hat{q}_\omega e^{i\omega x/c} - \hat{q}_\omega^* e^{-i\omega x/c}\}.$$

The operators $\hat{q}_\omega$ and $\hat{q}_\omega^*$ have the nonvanishing matrix elements

$$\overset{*}{q}_{n_\omega, n_\omega - 1} = \sqrt{n_\omega}\, e^{i\omega t}, \qquad q_{n_\omega, n_\omega + 1} = \sqrt{n_\omega + 1}\, e^{-i\omega t}; \tag{25}$$

n_ω is the number of protons with frequency ω. The magnetic field wave vector $\mathbf{q}$ ($|\mathbf{q}| = \omega/c$) is parallel to the x axis.

The interaction Hamiltonian in terms of spin-wave creation and annihilation operators is

$$\mathcal{H}_{int} = i\mu\sqrt{2\pi\hbar\omega V} \sum_{\mathbf{k},\mathbf{k}'} \{\overset{*}{v}_{\mathbf{k}} u_{\mathbf{k}'} \overset{*}{a}_{\mathbf{k}} \overset{*}{a}_{\mathbf{k}'} q_\omega$$
$$+ (\overset{*}{u}_{\mathbf{k}} u_{\mathbf{k}'} + \overset{*}{v}_{\mathbf{k}} v_{\mathbf{k}'})\, \overset{*}{a}_{\mathbf{k}} a_{\mathbf{k}'} q_\omega\} + \text{compl. conj.} \tag{26}$$

This equation reveals two possible processes for photon absorption—through splitting into two spin waves (the first term in the brace) or through absorption by a spin wave (the second term). The first process corresponds to the momentum conservation law

$$\mathbf{k} + \mathbf{k}' = \mathbf{q}, \tag{27}$$

while the second process corresponds to $\mathbf{k} = \mathbf{k}' + \mathbf{q}$. However, a photon cannot be absorbed by a spin wave since for this process energy and momentum conservation would require the velocity of the spin wave to be greater than that of light. To be sure, if the dielectric constant of the ferrodielectric is greater than unity this process is possible in principle (analogously to Cerenkov emission), but it is easily seen that its mean probability will then be exponentially small. Photon absorption by spin waves will therefore not be considered hereinafter.

The splitting of a photon into two spin waves can, of course, occur only if the energy of the photon is greater than twice the minimum spin-wave energy, i.e.,

$$\hbar\omega > 2\mu H_{eff}, \qquad H_{eff} = H_0 + \beta M_0$$

when it is assumed that the magnetic field H_0 is in the direction of easiest magnetization.

For $\hbar\omega < 2\mu H_{\text{eff}}$ (when the external field frequency can satisfy the condition $\omega \gg 1/\tau_{ss}$) the absorption of the magnetic field energy is mainly associated with inelastic scattering of photons by spin waves. This process occurs in the second perturbation approximation and its probability is very small. When $\omega\tau_{ss} \gg 1$ energy is, of course, also absorbed through the mechanisms considered in the first section.

However, for $\hbar\omega \geq 2\mu H_{\text{eff}}$ increased absorption of magnetic field energy should be observed because of the new mechanism. We shall hereinafter consider frequencies greater than $2\mu H_{\text{eff}}/\hbar$.

Thus

$$\mathcal{H}_{int} = i\mu\sqrt{2\pi\hbar\omega V}\sum_{\mathbf{k},\mathbf{k}'} \overset{*}{v}_{\mathbf{k}}\overset{*}{u}_{\mathbf{k}'}\overset{*}{a}_{\mathbf{k}}\overset{*}{a}_{\mathbf{k}'}q_{\omega} + \text{compl. conj.} \quad (28)$$

Non-zero matrix elements of the Hamiltonian (28) correspond to transitions $n_{\mathbf{k}}$, $n_{\mathbf{k}'}$, $n_{\omega} \rightarrow n_{\mathbf{k}}+1$, $n_{\mathbf{k}'}+1$, $n_{\omega}-1$ and the inverse transitions, and give the transition probability

$$4\pi^2 V\omega\mu^2\,|v_{\mathbf{k}}u_{\mathbf{k}'} + v_{\mathbf{k}'}u_{\mathbf{k}}|^2\,(n_{\mathbf{k}}+1)(n_{\mathbf{k}'}+1)\,n_{\omega}\delta(\varepsilon_{\mathbf{k}} + \varepsilon_{\mathbf{k}'} - \hbar\omega);$$

the δ function insures conservation of energy.

The photon absorption coefficient is defined as the difference between the probabilities of all photon absorption and emission processes:

$$\Gamma = \sum_{\mathbf{k},\mathbf{k}'} 4\pi^2 V\omega\mu^2\{(n_{\mathbf{k}}+1)(n_{\mathbf{k}'}+1) - n_{\mathbf{k}}n_{\mathbf{k}'}\}$$
$$\times\,|v_{\mathbf{k}}u_{\mathbf{k}'} + u_{\mathbf{k}}v_{\mathbf{k}'}|^2\delta(\varepsilon_{\mathbf{k}} + \varepsilon_{\mathbf{k}'} - \hbar\omega).$$

Here $n_{\mathbf{k}}$, $n_{\mathbf{k}'}$ are understood to be equilibrium Bose functions. The summation over **k** and **k′** in the last equation is subject to the momentum conservation expressed by (27).

Since the wave vector number of a spin wave is considerably greater than that of a photon,[*] we have

$$\Gamma = 4\pi^2 V\omega\mu^2 \sum_{\mathbf{k}} (n_{\mathbf{k}} + n_{-\mathbf{k}} + 1)$$
$$\times\,|v_{\mathbf{k}}u_{-\mathbf{k}} + u_{\mathbf{k}}v_{-\mathbf{k}}|^2\,\delta(\varepsilon_{\mathbf{k}} + \varepsilon_{-\mathbf{k}} - \hbar\omega).$$

Since $\epsilon_{\mathbf{k}}$, $u_{\mathbf{k}}$ and $v_{\mathbf{k}}$ are even functions of the wave vector the last equation leads to

$$\Gamma = (2\pi)^{-3}\,32\pi^2V^2\omega\mu^2\int|v_{\mathbf{k}}u_{\mathbf{k}}|^2\left(n_{\mathbf{k}} + \frac{1}{2}\right)\delta(2\varepsilon_{\mathbf{k}} - \hbar\omega)\,d\tau_{\mathbf{k}}.$$

By using (12) – (20) of reference 2 we therefore obtain

$$\Gamma = \frac{\mu^2(2\pi\mu M_0)^{3/2}}{2\Theta_c^{3/2}a^3\hbar}\coth\frac{\hbar\omega}{2T}\,J(\nu,\eta),$$
$$\nu = \hbar\omega/4\pi\mu M_0, \qquad \eta = H_{eff}/2\pi M_0. \quad (29)$$

Here

$$J(\nu,\eta) = \int_0^1 \frac{x^2[\sqrt{x^2+\nu^2} - (x+\eta)]^{1/2}}{\sqrt{(1-x)(x^2+\nu^2)}}\,dx, \quad (30)$$

when $\nu > \sqrt{\eta^2 + 2\eta}$ and

$$J(\nu,\eta) = \int_0^{(\nu^2-\eta^2)/2\eta} \frac{x^2[\sqrt{x^2+\nu^2} - (x+\eta)]^{1/2}}{\sqrt{(1-x)(x^2+\nu^2)}}\,dx, \quad (31)$$

when $\nu < \sqrt{\eta^2 + 2\eta}$.

We note that the condition $\hbar\omega/2 > \mu H_{\text{eff}}$ gives $\nu > \eta$. When $\nu < \eta$ ($\hbar\omega < 2\mu H_{\text{eff}}$) we have $\Gamma = 0$ in this approximation. We shall calculate the integrals (30) and (31) in different limiting cases.

1. $\eta \gg 1$ (strong magnetic field or large anisotropy energy):[*]

$$J(\nu,\eta) \approx \begin{cases} 16/15\sqrt{\nu}, & \nu \gg \eta; \\ \dfrac{1}{3\eta}\left\{1 - \dfrac{5}{4\eta} + \dfrac{3}{2}(\eta + 1 - \nu)\ln(\nu - \eta - 1)\right\}, & \nu \gtrsim \eta + 1; \\ \dfrac{1}{3\eta}\left\{1 - \dfrac{5}{4\eta} + \dfrac{3}{2}(\eta + 1 - \nu)\ln(\eta + 1 - \nu)\right\}, & \nu \lesssim \eta + 1; \\ 16(\nu - \eta)^3/105\eta, & \nu \gtrsim \eta. \end{cases}$$

2. $\eta \ll 1$ (weak magnetic field and small anisotropy energy):[†]

$$J(\nu,\eta) \approx \begin{cases} 16/15\sqrt{\nu}; & \nu \gg 1; \\ \dfrac{2}{3}\sqrt{\eta}\left\{1 + \dfrac{3}{2}\dfrac{\nu - \sqrt{2\eta}}{\sqrt{2\eta}}\ln\dfrac{\sqrt{2\eta}}{\nu - \sqrt{2\eta}}\right\}, & 0 < \dfrac{\nu - \sqrt{2\eta}}{\sqrt{2\eta}} \ll 1; \\ \dfrac{2}{3}\sqrt{\eta}\left\{1 - \dfrac{3}{2}\dfrac{\sqrt{2\eta} - \nu}{\sqrt{2\eta}}\ln\dfrac{\sqrt{2\eta}}{\sqrt{2\eta} - \nu}\right\}, & 0 < \dfrac{\sqrt{2\eta} - \nu}{\sqrt{2\eta}} \ll 1; \\ (\pi/8\sqrt{2})\sqrt{\eta}(\nu - \eta)^2, & \nu \gtrsim \eta. \end{cases}$$

Substituting our results into (29), we can determine the frequency dependence of the photon absorption coefficient in all limiting cases. At high frequencies we have

$$\Gamma = \frac{16}{15}\frac{\mu^2}{a^3\hbar}\left(\frac{2\pi\mu M_0}{\Theta_c}\right)^{3/2}\left(\frac{2\pi\mu M_0}{\hbar\omega}\right)^{1/2}\coth\frac{\hbar\omega}{2T}$$
$$(\hbar\omega \gg 2\pi\mu M_0, \mu H). \quad (32)$$

---

[*] $k \sim (\hbar\omega/\Theta_c)^{1/2}/a$ is comparable with the wave vector q only at a frequency that satisfies the condition $\omega \sim c^2\hbar/a^2\Theta_c \sim 10^{22}$ sec⁻¹. We of course always have $\omega \ll \hbar c^2/\Theta_c a^2$.

[*] We note that in this case $\sqrt{\eta^2 + 2\eta} \approx \eta + 1$ and ν is also considerably greater than unity since $\nu > \eta$.

[†] In this case $\sqrt{\eta^2 + 2\eta} \approx \sqrt{2\eta}$, and ν can be either greater or smaller than unity.

We note that for $\hbar\omega/2 = \sqrt{(\mu H)^2 + 4\pi\mu^2 M_0 H}$ the derivative of the absorption coefficient with respect to frequency becomes infinite.

The attenuation coefficient of the magnetic field is obviously equal to half the photon absorption coefficient ($\delta = \Gamma/2$). The imaginary part μ'' of the magnetic susceptibility is thus easily obtained by means of the dispersion equation for an electromagnetic wave with $\omega = qc/\sqrt{\epsilon\mu_{||}}$.

Since the magnetic field is parallel to the magnetic moment there is no need for taking the gyrotropy of the magnetic susceptibility tensor into account. Assuming $\omega = \omega_0 - i\delta$, $\mu_{||} = \mu'_{||} + i\mu''_{||}$, $\epsilon \sim \mu' \sim 1$, we obtain $\mu'' = 2\delta/\omega$, i.e., $\mu'' = \Gamma/\omega$. Thus (7), (15) — (17), (29), and (32) solve our problem of determining the imaginary part of the longitudinal magnetic susceptibility for a ferromagnetic dielectric over a broad range of temperatures and frequencies.

In the limit $\omega \rightarrow \infty$ the magnetic susceptibility approaches unity, while its imaginary part approaches zero. The frequency dependence of μ'' at very high frequencies is*

$$\mu'' \approx \frac{8\sqrt{2}}{15}\frac{\mu^2}{a^3}\frac{(2\pi\mu M_0)^2}{\Theta_c^{3/2}(\hbar\omega)^{3/2}} \qquad \left(\hbar\omega \gg \frac{\hbar}{\tau_{ss}},\ T,\ \mu H_{eff}\right).$$

Thus the decrease of μ'' at higher frequencies is inversely proportional to $\omega^{3/2}$ and is independent of temperature.

We are not aware of any sufficiently thorough experiments (with a fully magnetized sample† at low temperatures) with which our results might be compared. Our entire discussion shows that such experimental investigations could greatly extend our knowledge of the character of interactions between different quasi-particles (spin waves and phonons) in a ferromagnetic dielectric.

In conclusion the authors take this opportunity to thank V. G. Bar'yakhtar for useful discussions.

---

[1] A. I. Akhiezer, J. Phys. (U.S.S.R.) **10**, 217 (1946).

[2] M. I. Kaganov and V. M. Tsukernik, JETP **34**, 1610 (1958), Soviet Phys. JETP **7**, 1107 (1958).

[3] M. I. Kaganov and V. M. Tsukernik, JETP **36**, 224 (1959), Soviet Phys. JETP **9**, 151 (1959).

[4] Akhiezer, Bar'yakhtar, and Peletminskiĭ, JETP **36**, 216 (1959), Soviet Phys. JETP **9**, 146 (1959).

[5] L. D. Landau and E. M. Lifshitz, Электродинамика сплошных сред (Electrodynamics of Continuous Media), Gostekhizdat, Moscow, 1957.

[6] L. D. Landau and E. M. Lifshitz, Статистическая физика (Statistical Physics), Gostekhizdat, M.-L., 1951.

[7] V. G. Bar'yakhtar, Dissertation, Khar'kov State University, 1959.

[8] L. D. Landau and Yu. B. Rumer, Sow. Phys. **11**, 18 (1937).

[9] Akhiezer, Kaganov, and Lyubarskiĭ, JETP **32**, 837 (1957), Soviet Phys. JETP **5**, 685 (1957).

[10] W. Heitler, The Quantum Theory of Radiation, Oxford U. Press, 1936, (Russ. Transl. Gostekhizdat, M.-L., 1940).

Translated by I. Emin
153

*Our treatment is, of course, subject to the high frequency limit $\omega \ll \Theta_c/\hbar$, since we have not taken into account the excitation of vibrations of sublattices with respect to each other (see the Introduction).

†In a polydomain sample most absorption of the magnetic field will obviously be accounted for by the motion of domain boundaries.

SOVIET PHYSICS JETP VOLUME 37 (10), NUMBER 3 MARCH, 1960

THE CRITICAL SUPERCOOLING FIELD IN SUPERCONDUCTIVITY THEORY

L. P. GOR' KOV

Institute for Physical Problems, Academy of Sciences, U.S.S.R.

Submitted to JETP editor April 23, 1959

J. Exptl. Theoret. Phys. (U.S.S.R.) **37**, 833-842 (September, 1959)

The magnitude of the critical supercooling field H_{c1} in superconductivity theory[1] is determined. It is found that the field H_{c1} is larger than or smaller than the critical field H_c, depending on whether the superconductor in a weak field is of the London or of the Pippard type. The superconductor in the first case must in a strong field display a behavior similar to that of alloys. The magnitude of the ratio H_{c1}/H_c depends weakly on the temperature in the whole temperature range.

It is well known that superconducting metals in a magnetic field undergo at some value of the field a phase transition from the normal to the superconducting phase. For a bulk specimen this transition is a first-order transition; the value of the critical magnetic field H_c can thus be obtained from thermodynamic considerations and was evaluated by Bardeen, Cooper, and Schrieffer (BCS) in their theory of superconductivity.[1] Along with the thermodynamic field there exist, apparently, for a given temperature, still two other critical field values corresponding to the so-called "superheating" field and the "supercooling" field H_{c1}. These fields determine a region of possible hysteresis: for fields above H_c, but below the superheating field the superconducting phase is metastable and, on the other hand, for field values below H_c, but above H_{c1} the normal phase is metastable. (We understand by metastability, as always, an instability with respect to a finite perturbation.) To determine the magnitude of these fields thermodynamic considerations are insufficient and one must turn to the microscopic theory of superconductivity. Using an earlier developed method[2] the existence in the BCS theory of a "supercooling" field is proved in the present paper and its magnitude is found.

In the method mentioned above, the superconductor is described by two Green functions $G(x, x')$ and $F^+(x, x')$, and equations for these in a magnetic field can in the usual manner be obtained from the field-free equations. We shall first consider the absolute zero. These equations are then of the form

$$\left\{i\frac{\partial}{\partial t}+\frac{1}{2m}\left(\frac{\partial}{\partial \mathbf{r}}-ie\mathbf{A}(\mathbf{r})\right)^2+\mu\right\}G(x,x')+i\Delta(\mathbf{r})F^+(x,x')=\delta(x-x'),$$

$$\left\{i\frac{\partial}{\partial t}-\frac{1}{2m}\left(\frac{\partial}{\partial \mathbf{r}}+ie\mathbf{A}(\mathbf{r})\right)^2-\mu\right\}F^+(x,x')-i\Delta^*(\mathbf{r})G(x,x')=0, \tag{1}$$

where

$$\Delta^*(\mathbf{r})=|g|F^+(x,x), \tag{2}$$

In a constant magnetic field $G(x, x')$ and $F^+(x, x')$ are functions of the difference in the time variables, $t-t'$; expanding all quantities in Fourier integrals in this difference we get for the Fourier components $G_\omega(\mathbf{r}, \mathbf{r}')$ and $F^+_\omega(\mathbf{r}, \mathbf{r}')$ the following set of equations

$$\left\{\omega+\frac{1}{2m}\left(\frac{\partial}{\partial \mathbf{r}}-ie\mathbf{A}(\mathbf{r})\right)^2+\mu\right\}G_\omega(\mathbf{r},\mathbf{r}')+i\Delta(\mathbf{r})F^+_\omega(\mathbf{r},\mathbf{r}')=\delta(\mathbf{r}-\mathbf{r}'),$$

$$\left\{-\omega+\frac{1}{2m}\left(\frac{\partial}{\partial \mathbf{r}}+ie\mathbf{A}(\mathbf{r})\right)^2+\mu\right\}F^+_\omega(\mathbf{r},\mathbf{r}')+i\Delta^*(\mathbf{r})G_\omega(\mathbf{r},\mathbf{r}')=0; \tag{1'}$$

$$\Delta^*(\mathbf{r})=|g|(2\pi)^{-1}\int_{-\infty}^{+\infty}d\omega F^+_\omega(\mathbf{r},\mathbf{r}). \tag{2'}$$

The value H_{c1} of the supercooling field is the boundary itself of the metastability of the normal phase; at smaller fields the normal phase is absolutely unstable with respect to the appearance of a superconducting phase. We are, of course, not talking of the appearance of small layers of the superconducting phase but about the possibility that there appears that specific correlation between electrons which is caused by the interaction between them and which leads to the superconductivity phenomenon, and which finds an expression in the existence of a non-vanishing function $F^{+}(x, x')$. The metastability of the normal phase for fields $H > H_{c1}$ means instability with respect to the occurrence of finite values of $F^{+}(x, x')$ and $\Delta(\mathbf{r})$. In the point H_{c1} there occurs for the first time a solution with infinitesimal $\Delta(\mathbf{r})$ and $F^{+}(x, x')$. This makes it possible to simplify the set (1′) essentially, retaining in the equations only the first nonvanishing terms for small $\Delta(\mathbf{r})$. Furthermore, the magnetic field is uniform in the normal phase; it is convenient to take the vector potential $\mathbf{A}(\mathbf{r})$ in the form $A_x = -Hy$, $A_y = A_z = 0$. The second of Eqs. (1′) takes the following form

$$\left\{-\omega + \frac{1}{2m}\left[\left(\frac{\partial}{\partial x} - \frac{ieHy}{c}\right)^2 + \frac{\partial^2}{\partial y^2} + \frac{\partial^2}{\partial z^2}\right] + \mu\right\} F_{\omega}^{+}(\mathbf{r}, \mathbf{r}') - i\Delta^{*}(\mathbf{r})\tilde{G}_{\omega}(\mathbf{r}, \mathbf{r}') = 0. \tag{3}$$

In this equation $\tilde{G}_{\omega}(\mathbf{r}, \mathbf{r}')$ is the Green function of the electrons in the normal metal:

$$\left\{\omega + \frac{1}{2m}\left[\left(\frac{\partial}{\partial x} + \frac{ieHy}{c.}\right)^2 + \frac{\partial^2}{\partial y^2} + \frac{\partial^2}{\partial z^2}\right] + \mu\right\} \tilde{G}_{\omega}(\mathbf{r}, \mathbf{r}') = \delta(\mathbf{r} - \mathbf{r}'). \tag{4}$$

If we rewrite (4) in such a way that the differentiation is with respect to the variables $\mathbf{r}'$:

$$\left\{\omega + \frac{1}{2m}\left[\left(\frac{\partial}{\partial x'} - \frac{ieHy'}{c}\right)^2 + \frac{\partial^2}{\partial y'^2} + \frac{\partial^2}{\partial z'^2}\right] + \mu\right\} \tilde{G}_{\omega}(\mathbf{r}, \mathbf{r}') = \delta(\mathbf{r} - \mathbf{r}'), \tag{4′}$$

we can use (4′) and (3) to write the function $F_{\omega}^{+}(\mathbf{r}, \mathbf{r}')$ in the following form

$$F_{\omega}^{+}(\mathbf{r}, \mathbf{r}') = -i\int \tilde{G}_{\omega}(\mathbf{s}, \mathbf{r}')\,\tilde{G}_{-\omega}(\mathbf{s}, \mathbf{r})\,\Delta^{*}(\mathbf{s})\,d^3s. \tag{5}$$

Substitution of (5) into (2) leads to an integral equation for $\Delta^{*}(\mathbf{s})$:

$$\Delta^{*}(\mathbf{r}) = -i|g|\frac{1}{2\pi}\int_{-\infty}^{+\infty} d\omega \int \tilde{G}_{\omega}(\mathbf{s}, \mathbf{r})\,\tilde{G}_{-\omega}(\mathbf{s}, \mathbf{r})\,\Delta^{*}(\mathbf{s})\,d^3s. \tag{6}$$

The value of the magnetic field for which there occurs for the first time (coming from large fields) a nonvanishing solution of this equation is then just the value of the supercooling field H_{c1} which interests us.

For what follows, it is necessary to determine the form of the function $\tilde{G}_{\omega}(\mathbf{r}, \mathbf{r}')$. We perform the transformation

$$\tilde{G}_{\omega}(\mathbf{r}, \mathbf{r}') = \exp\left\{-\frac{ieH}{2c}(y + y')(x - x')\right\}\tilde{G}'_{\omega}(\mathbf{r} - \mathbf{r}'). \tag{7}$$

After substituting this expression into (4) the coefficients in the equation for $\tilde{G}_{\omega}(\mathbf{r} - \mathbf{r}')$ are functions of the difference, namely,

$$\left\{\omega + \frac{1}{2m}\left(\frac{\partial}{\partial \mathbf{r}} - \frac{ie}{2c}\mathbf{H}\times[\mathbf{r} - \mathbf{r}']\right)^2 + \mu\right\}\tilde{G}'_{\omega}(\mathbf{r} - \mathbf{r}') = \delta(\mathbf{r} - \mathbf{r}'). \tag{8}$$

Thanks to this $\tilde{G}'_{\omega}(\mathbf{r} - \mathbf{r}')$ clearly also depends only on the difference $\mathbf{R} = \mathbf{r} - \mathbf{r}'$. If there is no field the Green function $G_{0\omega}(R)$ is, as can easily be checked, of the form

$$G_{0\omega}(\mathbf{R}) = \begin{cases} -(m/2\pi R)\exp[ip_0R + i\omega R/v], & \omega > 0 \\ -(m/2\pi R)\exp[-ip_0R + i\omega R/v], & \omega < 0 \end{cases} \quad (|\omega| \ll \mu). \tag{9}$$

Such a choice of the solutions of (8) without a field was made in accordance with the requirement that the imaginary part of the Green function changes sign when the frequency changes sign.[3] We shall show that the function $\tilde{G}'_{\omega}(\mathbf{R})$ in (7) is the same as its value (9) without a field. Looking ahead we note that in the following we require distances R of the order of ξ_0 where ξ_0 is the parameter in the BCS theory which is connected with the value Δ_0 of the gap in the spectrum at $T = 0$ and which is equal to $\xi_0 \sim \hbar v/\Delta_0$. It turns out that one can neglect at those distances the term quadratic in the field in (8), or in other words, that the curving of the electrons in the fields of interest to us is very small. Under those conditions it is convenient, because of the large value of p_0, to look for solutions of (8) in the form $\exp\{i\varphi(R)\}G_{0\omega}(R)$, where $G_{0\omega}(R)$ is the Green function (9) when there is no field present. Substituting this expression into (8) leads to the following equation for $\varphi(R)$, which contains only quadratic terms in the field:

$$\mp p_0\partial\varphi/\partial R - (e^2/4c^2)([\mathbf{H}\times\mathbf{R}])^2 = 0,$$

[the ± sign in this equation depends on the sign of the frequency in accordance with (9)]. As will become clear below, the fields of interest to us are such that $eH\xi_0^2/c \sim 1$. Therefore, $\varphi(R)$ which is determined by this equation will give a correction in the phase factor in (7) of the order of $1/p_0\xi_0$, i.e., an insignificant quantity of the order 10^{-4}.

Substituting (7) and (9) into (6) and integrating over the frequency we get the following equation

$$\Delta^{*}(\mathbf{r}) = \frac{mp_0}{2\pi^2}\frac{|g|}{2\pi}\int\frac{\exp\{(ieH/c)(y + y')(x - x')\}}{|\mathbf{r} - \mathbf{r}'|^3}\Delta^{*}(\mathbf{r}')\,d^3r'. \tag{10}$$

The kernel of this equation leads to a logarithmic divergence when we integrate the right hand side for $\mathbf{r} = \mathbf{r}'$, which is connected with the fact that the relation (2) determines the gap $\Delta(\mathbf{r})$ as the value of the function F^+ for equal arguments. This definition is somewhat inaccurate. The fact is that in the BCS model the interaction Hamiltonian which leads to superconductivity was chosen in the form

$$H_{int} = \frac{g}{2} \sum_{p_1 + p_2 = p_3 + p_4} a^+_{\mathbf{p}_1\sigma_1} a^+_{\mathbf{p}_2\sigma_2} a_{\mathbf{p}_3\sigma_2} a_{\mathbf{p}_4\sigma_1} \tag{11}$$

with a constant coupling constant for all electrons with energies in a narrow layer $\hbar\tilde{\omega}$ in the neighborhood of the Fermi surface. This cutting off is realized in (11) by the functions θ_{p}:

$$\theta_p = \begin{cases} 1, & |\varepsilon_p - \varepsilon_F| < \tilde{\omega} \\ 0, & |\varepsilon_p - \varepsilon_F| > \tilde{\omega} . \end{cases}$$

The quantity $\tilde{\omega}$ enters logarithmically in the determination of the gap Δ_0, in the Fermi spectrum:

$$1 = |g| (mp_0 / 2\pi^2) \ln (2\tilde{\omega} / \Delta_0).$$

To the cut-off in momentum representation there corresponds, in coordinate space, some spreading out over distances of the order $\hbar v/\tilde{\omega}$. Using (11) for the interaction Hamiltonian and repeating the derivation of the equations in reference 2, we find easily that the quantity $\Delta^*(\mathbf{r})$ is connected with the function $F^+(x, x')$ in the following manner:

$$\Delta^*(\mathbf{r}) = \iint \theta(\mathbf{r} - \mathbf{s})\, \theta(\mathbf{r} - \mathbf{m})\, F^+(t, \mathbf{s}; t, \mathbf{m})\, d^3s\, d^3m, \tag{2''}$$

where $\theta(\mathrm{R})$ is a smearing out function corresponding to the cut-off function θ_{p} in the momentum representation:

$$\theta(\mathbf{R}) = (2\pi)^{-3} \int e^{i\mathbf{pR}} \theta_p d^3p = \frac{p_0}{\pi^2} \frac{\sin p_0 R}{R} \frac{\sin(\tilde{\omega} R / v)}{R} . \tag{12}$$

On this basis we must, strictly speaking, write Eq. (6) in the form

$$\Delta^*(\mathbf{r}) = i|g| \int_{-\infty}^{+\infty} \frac{d\omega}{2\pi} \int \overline{G_\omega(\mathbf{s}, \mathbf{r})}\, \overline{G_{-\omega}(\mathbf{s}, \mathbf{r})}\, \Delta^*(\mathbf{s})\, d^3s, \tag{6'}$$

denoting by $\tilde{G}_\omega(\mathbf{r}, \mathbf{r}')$ the integral over the Green function (7):

$$\overline{G_\omega(\mathbf{r}, \mathbf{r}')} = \int \theta(\mathbf{r} - \mathbf{s})\, G_\omega(\mathbf{s}, \mathbf{r}')\, d^3s.$$

The field dependent phase factor in (7) can be taken out from under the integral sign in the last expression since $\theta(\mathbf{r} - \mathbf{s})$ has the character of a δ-function. It amounts thus practically to replacing $G_{0\omega}(\mathrm{R})$ in the previous calculations [see Eq. (9)] by

$$\overline{G_{0\omega}(R)} = (2\pi)^{-3} \int e^{i\mathbf{pR}} G_{0\omega}(\mathbf{p})\, \theta_p d^3p.$$

Following this, all expressions stay finite. We have succeeded in eliminating the cut-off quantity using the relation (2″), which determines the gap in the energy spectrum at $T = 0$ when there is no field. One verifies easily, by evaluating the corresponding function $F_0^+(t, \mathbf{r}; t, \mathbf{r}')$ through the Fourier components found in reference 2, that

$$F_0^+(t, \mathbf{r}; t, \mathbf{r}') = \frac{m\Delta_0}{2\pi^2} \frac{\sin p_0 R}{R} K_0\left(\frac{R\Delta_0}{v}\right), \tag{13}$$

where K_0 is a Bessel function of imaginary argument which tends logarithmically to infinity for small R.

Substituting (13) into (2″) and noting that the function $\theta(\mathbf{r})$ possesses the following δ-function property

$$\int \theta(\mathbf{r} - \mathbf{s})\, \theta(\mathbf{s})\, d^3s = \theta(\mathbf{r})$$

(this equation can be most easily checked by the Fourier components) we get, using the form (12) for the function $\theta(\mathbf{R})$ and averaging the fast oscillating factors:

$$1 = |g| \frac{mp_0}{4\pi^4} \int K_0\left(\frac{R\Delta_0}{v}\right) \frac{\sin(\tilde{\omega} R / v)}{R^3} d^3R$$

$$= \frac{m^2 |g|}{4\pi^4} \int \left(\int_0^{\tilde{\omega}} \frac{\cos(R\xi / v)}{R^2} d\xi \right) K_0\left(\frac{R\Delta_0}{v}\right) d^3R.$$

Integrating over $d|\mathbf{R}|$ in the last expression by parts we find

$$\frac{1}{|g|} = -\frac{m^2\Delta_0}{4\pi^4} \int_0^{\tilde{\omega}} \frac{d\xi}{\xi} \int \frac{\sin(R\xi / v)}{R^2} K_1(R\Delta_0 / v)\, d^3R.$$

This expression for $1/|g|$ is convenient because the integral over d^3R posssesses the same singularity as Eq. (10) when $\tilde{\omega} \to \infty$.

After substituting this expression into (6) we get an equation in which the logarithmically diverging terms are cancelled after which $\tilde{\omega}$ can tend to infinity. Omitting the intermediate calculations we shall give the final form of (10), taking into account that the function $\Delta^*(\mathbf{r})$ depends on the coordinate y only:

$$\Delta^*(y) \ln\left(\frac{e\gamma\Delta_0}{v} \varepsilon\right)$$

$$= -\frac{1}{2} \int_{-\infty}^{\infty} \frac{\exp\{-|(eH / c)(y^2 - y'^2)|\}}{|y - y'|} \Delta^*(y')\, d_\varepsilon y' .$$

[We shall show below that the general form of the function $\Delta^*(\mathbf{r})$ corresponding to a given value of H_{c1} can be found by a simple method in terms of the solution of this equation.] Here γ is Euler's constant, ϵ an infinitesimal constant introduced to cause the integration on the right hand side to be performed only over a distance $|y - y'| \geq \epsilon$. Thanks to the logarithmic character of the singularity on the right hand side, ϵ disappears from the final results. It is convenient to introduce dimensionless variables $\xi = y\sqrt{eH/c}$ in which the equation becomes

$$\Delta^*(\xi)\ln\left(\frac{e\gamma\Delta_0\delta}{v\sqrt{eH/c}}\right) = -\frac{1}{2}\int_{-\infty}^{\infty}\frac{\Delta(\xi')\exp\{-|\xi^2-\xi'^2|\}}{|\xi-\xi'|}\,d\xi'. \tag{14}$$

The largest value of the magnetic field, for which a solution that decreases at infinity exists for (14), is just the value of the critical field H_{c1}, the "supercooling" field. Equation (14) can only be solved numerically. We shall show that (14) has a maximum eigenvalue for the magnetic field and we shall estimate its magnitude. To do this we add to and subtract from $\Delta(\xi')$ under the integral on the right hand side of (14) the value $\Delta(\xi)$. After this (14) is transformed to the following form, which no longer contains the infinitesimal constant δ:

$$\Delta^*(\xi)\ln\left(\frac{\Delta_0 e}{v}\sqrt{\frac{\gamma c}{eH}}\right) = \Phi(\xi)\Delta^*(\xi) - \frac{1}{2}\int_{-\infty}^{\infty}\frac{\exp\{-|\xi^2-\xi'^2|\}}{|\xi-\xi'|}[\Delta^*(\xi')-\Delta^*(\xi)]\,d\xi'. \tag{15}$$

The function $\Phi(\xi)$ is here equal to

$$\Phi(\xi) = e^{-\xi^2}\int_0^{|\xi|} e^{\xi'^2}\xi'\ln\frac{|\xi|+\xi'}{|\xi|-\xi'}\,d\xi'.$$

Multiplying (15) by $\Delta(\xi)$ and integrating over ξ we get

$$|\Delta|^2\ln\left(\frac{e\Delta_0}{v}\sqrt{\frac{\gamma c}{eH}}\right) = \int_{-\infty}^{\infty}\Phi(\xi)|\Delta(\xi)|^2\,d\xi + \frac{1}{4}\int\int_{-\infty}^{\infty}\frac{\exp\{-|\xi^2-\xi'^2|\}}{|\xi-\xi'|}|\Delta(\xi)-\Delta(\xi')|^2\,d\xi'd\xi. \tag{15'}$$

Since $\Phi(\xi) > 0$ it follows from the fact that the right-hand side is positive that

$$eH/c \leqslant \Delta_0^2 e^2\gamma/v. \tag{16}$$

We can obtain the value of H_{c1} approximately (and conceivably with great accuracy) by a variational method if we choose $\Delta(\xi)$ in the form of $\exp(-\alpha\xi^2)$. With such a form for $\Delta(\xi)$ all integrals in the variational principle for (14) can be evaluated and the maximum value of H arises when $\alpha = 1$ and is equal to

$$H_{c1} \approx (e^2\gamma/2)(c\Delta_0^2/ev).$$

One can show that a lower limit is then obtained for the value of H_{c1}. The theory gives for the thermodynamic critical field H_c at $T = 0$

$$H_c = \Delta_0\sqrt{2mp_0/\pi}.$$

The ratio of the two fields is

$$H_{c1}/H_c = 1.77\,(3\pi T_c mc/e)(2\pi m/7\zeta(3)p_0^5)^{1/2} \tag{17}$$

[$\xi(x)$ is Riemann's zeta-function; $\vartheta(3) = 1.202$]. It is convenient to write this quantity as follows. We have shown earlier[4] that in a sufficiently narrow region of temperatures near T_c the equations of the phenomenological Ginzburg-Landau theory[5] with a double charge follow from the theory of superconductivity. The phenomenological constant κ of this theory was defined microscopically and turned out to be equal to

$$\varkappa = (3\pi T_c mc/e)(2\pi m/7\zeta(3)p_0^5)^{1/2}. \tag{18}$$

If the ratio (17) is expressed in terms of this constant it can be written as follows

$$H_{c1}/H_c = 1.77\,\varkappa. \tag{19}$$

Near T_c the result of the Ginzburg-Landau theory[5] must hold, i.e.,

$$H_{c1}/H_c = \sqrt{2}\,\varkappa. \tag{20}$$

We see that the change in the ratio H_{c1}/H_c is small in the whole of the temperature range and does not exceed 25%.

It is interesting that according to (18) — (20) the magnitude of the field H_{c1} does by no means have to be less than H_c, not even for pure superconductors. Moreover, it is well known that in the new theory we can distinguish among the pure superconductors two classes depending on their properties in a weak magnetic field. For superconductors of the first class the penetration depth δ is at all temperatures appreciably larger than the parameter ξ_0 of the BCS theory. Such superconductors satisfy the electrodynamics of the Londons and may be called London superconductors (see the survey by Abrikosov and Khalatnikov[6]). The criterion for this case $\delta \gg \xi_0$ can be written as the condition $\kappa \gg 1$ (more accurately $\kappa \gg 0.4$). The opposite case may be called the Pippard case. Here, the penetration depth is in the whole of the temperature range, except in the immediate vicinity of T_c, much less than ξ_0, and the London equation is replaced by a more complicated nonlocal relation. The corresponding criterion will be $\kappa \ll 1$. The majority of the known pure superconductors belongs to the last or to an intermediate type. It is clear from (18) and (20) that if a superconductor belongs to the Pippard class the condition $H_{c1} \ll H_c$ is sure to be satisfied. In the London case, however, H_{c1} must be larger than H_c. In other words, a metal the behavior of which in a weak field shows the London character must display in a strong field the characteristic properties of alloys: a negative surface energy, a smeared out transition, and so on. Abrikosov[7] studied alloys in the phenomenological Ginzburg-Landau theory from this point of view and showed that superconductors with $\kappa > 1/\sqrt{2}$ possess such properties.

Apart from T_c, the combination of quantities that make up the constant κ according to (18) contains also the effective electron mass m at the Fermi surface and the Fermi momentum p_0; expressing κ in terms of the density of the number of "free electrons" $n = p_0^3/3\pi^2$ we get

$$\varkappa = 0.485\, kT_c c m^{3/2} / e\hbar^2 n^{5/6}.$$

To determine m and n from experimental data we choose as one of the quantities the value of the critical magnetic field H_{c0} at $T = 0$, which is expressed as follows in terms of m and n:

$$H_{c0} = 2{,}48\, \hbar^{-1} m^{1/2} n^{1/6} kT_c.$$

We can take as the second quantity, for instance, data on the anomalous skin-effect in the normal state. The magnitude of the active part of the resistance R yields n directly:[8]

$$n = (\pi^{5/2} 3^{5/4} \omega^3 \hbar^{3/2} / c^6 e^3)\, R^{-9/2}.$$

When we evaluate the processed data on the specific heat in the normal state and the magnitude of R for the anomalous skin effect in reference 1 (see reference 9) we find $\kappa = 0.011$ for aluminum and $\kappa = 0.135$ for tin. At the same time we must note that this method is rather unreliable, since the result is very sensitive to a change in the magnitude of R (R^6 enters into κ). It is therefore advisable to use other data. The evaluation must proceed differently for Pippard and for London superconductors.

It is convenient to use for London superconductors the fact that the equations of the Ginzburg-Landau theory hold for them over a wide range near the critical temperature. We can thus use the well-known relation[5] with the doubled charge[4]

$$\varkappa = (\sqrt{2}\, 2e / \hbar c)(H_{cT} \delta_T^2)_{T=T_c}, \tag{21}$$

where H_{cT} is the critical field at the given temperature and δ_T the penetration depth. We can also use this relation for metals intermediate between London and Pippard types, since in that case the region of applicability of (21) is sufficiently wide. The majority of the most studied superconductors belongs apparently to the intermediate type. Tin[10] ($\kappa = 0.158$), lead[11] ($\kappa = 0.234$) and indium[11] ($\kappa = 0.22$) are, for instance, such superconductors.

The Ginzburg-Landau equations are, finally, applicable also for Pippard metals in the immediate vicinity of T_c, but this neighborhood is very small ($\Delta T/T_c \sim \kappa^2$). For aluminum the London temperature region begins at $\Delta T/T_c \sim 10^{-4}$. Equation (21) can therefore not be used to determine κ in the range of temperatures which is easily accessible. The value of κ can in that case be determined from data on the magnitude of the magnetic field H_{c0} and the penetration depth δ_0 at $T = 0$. The theoretical expression for δ_0 in the Pippard case is according to the BCS theory of the following form:

$$\delta_0 = (\sqrt{3}/2)(\pi^2 p_0^2 kT_c / \gamma \hbar^4 c^3)^{-1/3}.$$

Expressing the constant κ in terms of δ_0 and H_{c0} we get

$$\varkappa = 213\, (eH_{c0} / c\hbar)^3 \delta_0^6. \tag{22}$$

For aluminum we find in this way $\kappa \approx 0.012$.

The available experimental data of Faber's on the magnitude of the supercooling field refer to a temperature range near T_c.[12] For tin, the value of H_{c1}/H_c as given by (20), with $\kappa = 0.16 - 0.226$, agrees very well with the experimental[12] value 0.232. For indium with $\kappa = 0.22$ the theoretical value $H_{c1}/H_c = 0.32$ is nearly twice as large as the experimental[12] one, 0.16. It is difficult to understand the causes of such a discrepancy.

At first sight Eq. (20) for aluminum pertains only to that temperature range where the Ginzburg-Landau equations are applicable. This range is very narrow, but we shall see in the following that the region of applicability of (20) is for a Pippard metal appreciably wider than the London temperature region* near T_c. It is, in particular, helpful to note that at $T = 0$ the character of the solution of (14) does not depend on whether the metal is a Pippard or a London metal in a weak field. With the value of κ found above for aluminum near T_c we have $H_{c1}/H_c \approx 0.017$ while the experimental[12] value is 0.036, i.e., larger than the theoretical one by a factor two. Such a discrepancy should not cause any surprise for a Pippard metal if we take into account how rough the model is and the high powers of the experimental quantities which enter into (22). At the same time Eq. (20) can itself serve to determine κ for Pippard metals. The smallness of the ratio H_{c1}/H_c (or, what is the same, the large magnitude of the surface energy) is a criterion for a metal being of the Pippard type.

In conclusion we wish to discuss some additional points. First we touch upon the general form of the solution of (6). Up to now we assumed that the magnitude of the gap $\Delta(\mathbf{r})$ depended only on y. Such an assumption is permissible, since an appropriate choice for the vector potential A had been made in the equations of the basic set (1′). It is also rather obvious from uniformity considerations that the value of the field equal to H_{c1} will correspond to a constant solution $\Delta(x, y)$ in the direction of the field. At the same time the problem is degenerate in the x, y plane, i.e., many solutions $\Delta(x, y)$ correspond to one value of H_{c1}. One can easily verify with the aid of (3) and (4) that if $\Delta(y)$ is a solution of (6) the function

---

*This fact was already noted by Ginzburg.[13]

$$\Delta(x, y) = \exp(ieHax/c)\,\Delta(y-a)$$

is also a solution, and the general form of the function which corresponds to a given value of H_{c1} will thus be

$$\Delta(x, y) = \sum_j \exp(ieHxa_j/c)\,A_j\Delta(y-a_j)$$

with arbitrary a_j and A_j.

We shall finally dwell on the problem of the temperature dependence of the field H_{c1}. If the temperature is different from absolute zero, one must use instead of (1′) the appropriate thermodynamic technique.[14] We applied this technique earlier[4] to a superconductor; we shall here only indicate to what differences from the foregoing results it leads. The mathematical change in the formalism used above consists of the following: it is sufficient to replace ω by $i\omega_n$ [where $\omega_n = \pi T(2n+1)$, n is an integer] in all equations, beginning with (4), and to replace the integration over $d\omega$ by summation over n, as follows:

$$-\frac{i}{2\pi}\int_{-\infty}^{\infty} d\omega\,(\ldots)_\omega \to T\sum_{-\infty}^{+\infty}(\ldots)_{i\omega_n}.$$

The field dependence of the Green functions remains as before, and the further calculations lead instead of to Eq. (14) to

$$\Delta_T(\xi)\ln\left(\frac{e\gamma\Delta_0}{v}\sqrt{\frac{c}{eH}}\,\delta\right) = -\frac{1}{2}\int_{-\infty}^{\infty} K_T(\xi, \xi')\,\Delta_T(\xi')\,d\xi', \quad (23)$$

where

$$K_T(\xi, \xi') = \frac{2\pi T}{v}\sqrt{\frac{c}{eH}}\int_1^{\infty}\frac{J_0\{(\xi^2-\xi'^2)\sqrt{u^2-1}\}}{u\sinh(2\pi T v^{-1}\sqrt{c/eH}\,u\,|\xi-\xi'|)}\,du. \quad (24)$$

Because of the complexity of this kernel one can in the general case only obtain the dependence of H_{c1} on T by a numerical integration. We shall consider limiting expressions.

The kernel (24) can for low temperatures be written in the following form:

$$K_T(\xi, \xi') = K_0(\xi, \xi') - \frac{2\pi^2T^2c^2}{3eH_{c1}v^2}\,\frac{\exp\{-|\xi^2-\xi'^2|\}}{|\xi+\xi'|}, \quad (25)$$

where $K_0(\xi, \xi')$ is the kernel of (14). This expansion loses its validity in the neighborhood of $\xi = -\xi'$, where the temperature dependent correction term in (25) has a singularity. In that point one cannot expand the hyperbolic sine in (24) in powers of T since it just guarantees the convergence of (24) for large u. One sees easily that the width of the region $\Delta\xi = |\xi+\xi'|$ where (25) is inapplicable is of the order $\Delta\xi \sim (2\pi T/v)\sqrt{c/eH_{c1}}$. We rewrite (23) in the following form:

$$\lambda(\xi)\ln\left(\frac{e\gamma\Delta_0}{v}\sqrt{\frac{c}{eH_{c1}}}\,\delta\right) + \frac{1}{2}\int_{-\infty}^{+\infty} K_0(\xi, \xi')\,\lambda(\xi')\,d\xi'$$

$$= \Delta_0(\xi)\,\frac{\delta H_T}{H_{c1}} - \frac{1}{2}\int_{-\infty}^{+\infty}\delta K_T(\xi, \xi')\,\Delta_0(\xi')\,d\xi',$$

where

$$\lambda(\xi) = \Delta_T(\xi) - \Delta_0(\xi).$$

One must determine $\delta H_T/H_{c1}$ from the condition that the right hand side be orthogonal to the solution of the homogeneous Eq. (14). If we use an approximate solution for $\Delta_0(\xi) \sim \exp(-\xi^2)$ we can find the main term in the additional term in H_{c1}/H_{cT} at low temperatures, using (25), which is of the form $(T^2/T_c^2)\ln(T/T_c)$. Integrating with logarithmic accuracy, we get

$$H_{c1}/H_{cT} = 1.77\varkappa\,[1 + 0.65\,(T/T_c)^2\ln(\mathrm{const}\cdot T/T_c)] \quad (26)$$

with an unknown constant [if $T \ll T_c$ we have:[6] $H_{cT} = H_{c0}(1-\gamma^2T^2/3T_c^2)$].

Near the transition temperature the field H_{c1} is small, and the equation becomes considerably simpler. It is clear from (23) and (24) that in that case in the integration the essential $|\xi-\xi'|$ are of the order of $\xi_0\sqrt{eH/c}$ because of the exponential character of the kernel (24), while it is natural to assume that $\Delta(\xi)$ changes little over those distances. Using this, it turns out that near T_c the integral equation (23) is changed into a differential equation which to a first approximation is the same as the corresponding equation for the same problem in the Ginzburg-Landau theory with a doubled charge,[4,5] the known solution of which leads to (20).

Taking the next terms into account, we can find after some calculations the temperature dependence of the ratio H_{c1}/H_c near T_c:

$$H_{c1}/H_c = \sqrt{2}\,\varkappa\,(1+0.41\,t); \quad t = 1 - T/T_c. \quad (27)$$

We should like to note here that the condition for the applicability of (20) and (27) follows from the derivation: $\Delta T \ll T_c$, whereas the applicability of the general equations of the Ginzburg-Landau theory obtained in reference 4 near T_c was confined to a much narrower temperature range near T_c. In discussing the penetration depth problem, for instance, for these equations to be applicable it is necessary that not only $\Delta T/T_c$ be small, but also that the superconductor be in the London region at the temperatures considered, i.e., that the penetration depth be large compared to ξ_0. For this it is necessary that the condition $\sqrt{\Delta T/T_c} \ll \kappa$ is satisfied which for superconductors with a small κ (Pippard superconductors) may be an appreciably stronger restriction. In the problem of the supercooling field, therefore, the question whether a superconductor belongs to the Pippard or to the London class is not a decisive factor over the whole temperature range.

We saw already that the change in the ratio H_{c1}/H_c is small in the whole of the temperature range. We can thus believe that an interpolation formula, combining (26) and (27) can represent adequately the variation of H_{c1}/H_c over the whole temperature range. Since the logarithm in (26) is a slowly-varying function, we can take simply for such a formula the polynomial

$$H_{c1}/H_c = \varkappa[1.77 - 0.43(T/T_c)^2 + 0.07(T/T_c)^4].$$

Returning, in conclusion, to the problem of the possibility whether there exist pure superconductors with alloy properties, i.e., with $\kappa > 0.56$, we note that among the best studied superconductors, lead and indium, have the largest κ, about 0.23. To increase κ it is necessary to have a larger value of H_c and a larger penetration depth. From this point of view, La, V, U, and Nb are worthy of attention. Unfortunately there are, apparently, no data about the penetration depth for these superconductors. There are in reference 11 some indications about the anomalous properties of these metals which are similar to the properties of alloys, although it is not clear whether these anomalies are caused by the presence of impurities. There is at any rate considerable interest in clarifying the problem of the existence of pure superconductors with $\kappa > 0.56$, since they should possess all anomalous properties of alloys.

In conclusion the author expresses his gratitude to Academician L. D. Landau for his interest in this work and for valuable advice and to Professor V. L. Ginzburg for remarks made.

---

[1] Bardeen, Cooper, and Schrieffer, Phys. Rev. **108**, 1175 (1957).

[2] L. P. Gor'kov, JETP **34**, 735 (1958), Soviet Phys. JETP **7**, 505 (1958).

[3] L. D. Landau, JETP **34**, 262 (1958), Soviet Phys. JETP **7**, 182 (1958).

[4] L. P. Gor'kov, JETP **36**, 1918 (1959), Soviet Phys. JETP **9**, 1364 (1959).

[5] V. L. Ginzburg and L. D. Landau, JETP **20**, 1064 (1950); V. L. Ginzburg, JETP **31**, 541 (1956), Soviet Phys. JETP **4**, 594 (1957).

[6] A. A. Abrikosov and I. M. Khalatnikov, Usp. Fiz. Nauk **65**, 551 (1958), Adv. Phys. **8**, 45 (1959).

[7] A. A. Abrikosov, JETP **32**, 1442 (1957), Soviet Phys. JETP **5**, 1174 (1957).

[8] G. E. H. Reuter and E. H. Sondheimer, Proc. Roy. Soc. (London) **A195**, 336 (1948).

[9] T. E. Faber and A. B. Pippard, Proc. Roy. Soc. (London) **A231**, 336 (1955).

[10] V. L. Ginzburg, JETP **36**, 1930 (1959), Soviet Phys. JETP **9**, 1372 (1959).

[11] D. Shoenberg, Superconductivity, (Cambridge Univ. Press, 1952).

[12] T. E. Faber, Proc. Roy. Soc. (London) **A241**, 531 (1957).

[13] V. L. Ginzburg, Physica, **24**, S42 (1958).

[14] Abrikosov, Gor'kov, and Dzyaloshinskiĭ, JETP **36**, 900 (1959), Soviet Phys. JETP **9**, 636 (1959); E. S. Fradkin, JETP **36**, 1286 (1959), Soviet Phys. JETP **9**, 912 (1959).

Translated by D. ter Haar
154

SOVIET PHYSICS JETP VOLUME 37 (10), NUMBER 3 MARCH, 1960

GROWTH OF ELECTROMAGNETIC WAVES IN INTERPENETRATING INFINITE MOVING MEDIA

G. G. GETMANTSEV

Radiophysics Institute, Gorkiĭ State University

Submitted to JETP editor April 27, 1959

J. Exptl. Theoret. Phys. (U.S.S.R.) 37, 843-846 (September, 1959)

An investigation is made of the propagation of monochromatic plane waves in interpenetrating moving media. Equations are obtained for the refractive index; these equations are used to investigate the stability of the propagating waves. The time growth (damping) factor for the wave is found for the case of motion of a plasma through a dispersionless dielectric.

As is well known, under certain conditions growing electromagnetic waves can be produced in the motion of electron streams in a plasma or any other medium. The growing plane waves (with longitudinal electric fields) produced in the motion of an electron stream in a plasma have been considered by Akhiezer and Faĭnberg[1] and by Ginzburg and Zheleznyakov.[2] Below we give a phenomenological method which can be used to analyze the building (damping) of electromagnetic waves in moving media.

We consider two infinite, uniform, isotropic, lossless and nonmagnetic media, I and II. Medium II is at rest in the laboratory Cartesian coordinate system K and has a dielectric constant ϵ_2. Medium I, in which the coordinate system K′ is fixed, moves uniformly along the x axis of system K with a velocity v and has a dielectric constant ϵ_1 in the K′ system.

If ϵ_1 and ϵ_2 are approximately equal to unity, or if we consider the motion of a plasma in a plasma, the effective electric field is equal to the average macroscopic field and the polarization vectors of medium I and medium II add.* The material equations that relate the electromagnetic field vectors **D**, **B**, **E**, and **H**, in the K coordinate system can be written as follows:†

$$\mathbf{D} = \frac{1}{(1-\varepsilon_1\beta^2)}\left\{\varepsilon_1(1-\beta^2)\mathbf{E} + (\varepsilon_1-1)\left(\left[\frac{\mathbf{v}}{c}\times\mathbf{H}\right] - \varepsilon_1\frac{\mathbf{v}}{c}\left(\frac{\mathbf{v}}{c}\mathbf{E}\right)\right)\right\} + (\varepsilon_2-1)\mathbf{E},$$
$$\mathbf{B} = \frac{1}{(1-\varepsilon_1\beta^2)}\left\{(1-\beta^2)\mathbf{H} - (\varepsilon_1-1)\left(\left[\frac{\mathbf{v}}{c}\times\mathbf{E}\right] + \frac{\mathbf{v}}{c}\left(\frac{\mathbf{v}}{c}\mathbf{H}\right)\right)\right\}, \qquad \beta = \frac{v}{c}. \tag{1}$$

These differ from the well known electrodynamic equations for moving media in that the first equation contains the additional term $(\epsilon_2 - 1)\mathbf{E}$ which characterizes the contribution to the electric induction **D** due to the polarization of the fixed medium, II.‡

Using the material equations (1) and Maxwell's equations we solve the problem of propagation of plane electromagnetic waves in medium I and medium II. Because of the symmetry of the wave propagation pattern with respect to the x and x′ axes, which coincide with the velocity vector **v**, we will assume that the plane electromagnetic wave is propagated in the direction of the unit vector γ which lies in the xy plane and forms an angle θ with the x and x′ axes and **v**. As is well known, the Maxwell curl equations lead to the following relation[5] when the expression for the plane wave is used

---

*If the effective field for the combination of medium I and medium II is known, in principle all of the following results can be generalized for media with high dielectric constants.

†In the monographs by Veksler[3] and Pauli[4] in the equation for $\mathbf{B}(\mathbf{E}, \mathbf{H})$ the minus sign in front of the term $\mathbf{v}(\mathbf{vH})/c^2$ is incorrect.

‡If medium I and medium II move with different velocities with respect to the laboratory coordinate system, K, these equations become considerably more complicated. They may be obtained by computing the total tensor of the moments in the K coordinate system and comparing it with the electromagnetic field tensors. In a similar manner it is possible to find the equations for the motion of an anisotropic medium through another anisotropic medium (a practical example of a system of this kind is the motion of a plasma in a plasma in the presence of an external fixed magnetic field).

$$\mathbf{D} = -n[\gamma\times\mathbf{H}], \quad \mathbf{B} = n[\gamma\times\mathbf{E}], \tag{2}$$

where n is the "refractive index" of the medium in which wave propagation takes place. Substituting (2) in (1) and eliminating the components of the electromagnetic fields **E** and **H**, we obtain after some simple manipulation the following equations for the refractive index:

$$f_1(n^*) = n^{*2}$$
$$\times\left\{\frac{(1-\varepsilon_1\beta^2)(\varepsilon_1+\varepsilon_2-1)\cos^2\theta + [\varepsilon_1(1-\varepsilon_2\beta^2)+(\varepsilon_2-1)]\sin^2\theta}{(\varepsilon_1+\varepsilon_2-1)}\right\}$$
$$+ 2n^*(\varepsilon_1-1)\beta\cos\theta$$
$$-\frac{(1-\beta^2)[\varepsilon_1(1-\varepsilon_2\beta^2)+(\varepsilon_2-1)]-(\varepsilon_1-1)^2\beta^2}{1-\varepsilon_1\beta^2} = 0,$$

$$f_2(n^{**}) = n^{**2}[(1-\beta^2)\sin^2\theta + (1-\varepsilon_1\beta^2)\cos^2\theta]$$
$$+ 2n^{**}(\varepsilon_1-1)\beta\cos\theta$$
$$-\frac{(1-\beta^2)[\varepsilon_1(1-\varepsilon_2\beta^2)+(\varepsilon_2-1)]-(\varepsilon_1-1)^2\beta^2}{1-\varepsilon_1\beta^2} = 0, \tag{3}$$

These differ in the coefficient of the n^2 term. As is well known, the difference in the equations in (3) when $\theta \neq 0$ denotes the existence of two characteristic waves with different polarization and velocities. The equation $f_1(n^*) = 0$ refers to the wave with the field components E_x, E_y and H_z while the equation $f_2(n^{**}) = 0$ refers to the wave with the components H_x, H_y and E_z. When $\theta = 0$ both equations coincide and, since it can be shown that

$$n^* H_z \sin\theta = -(\varepsilon_1+\varepsilon_2-1)E_x, \qquad n^{**}E_z\sin\theta = H_x,$$

the field components E_x and H_x (parallel to the velocity of medium I) vanish.*

For a given frequency and known dielectric constants [$\epsilon_1(\omega)$ and $\epsilon_2(\omega)$] the two equations of (3) determine the velocity of propagation of the electromagnetic waves in both media (one moving). The solutions of these equations determine the "growth factor" of the electromagnetic wave in the moving medium. In this connection we determine the growth of an electromagnetic wave in a plasma moving in vacuum, since it is of some interest.

For a plasma that moves with nonrelativistic velocity ($v \ll c$) in the absence of a magnetic field in the laboratory system (K) we have $n^2 = 1 - \omega_0^2/\omega^2$, where ω is the frequency in this reference system. Thus, the flow velocity v does not appear in the expressions for the "refractive index" and the "drag" of the wave does not appear in explicit form. On the other hand

$$n^2 = 1 - \omega_0^2(1-n\beta)^2/\omega^2(1-n\beta)^2 \approx 1 - \omega_0^2(1-2n\beta)/\omega'^2,$$
$$n\beta \ll 1, \tag{4}$$

where $\omega' = \omega(1-n\beta)$ is the frequency of the wave in the K′ reference system, which moves with the plasma (for simplicity it is assumed that the wave is propagated in the direction of motion of the plasma). Equation (4), which is quadratic in n, coincides with Eq. (3) in the case of longitudinal propagation ($\theta = 0$) when $\beta \ll 1$ and $\epsilon_2 = 1$ if the quantity $\epsilon_1 = 1 - \omega_0^2/\omega'^2$ is the dielectric constant of the plasma in the reference system that moves with the plasma. Solving Eq. (4) for n we have

$$n \approx -(\varepsilon_1-1)\beta \pm \sqrt{\varepsilon_1}. \tag{5}$$

This equation indicates that the wave is dragged. Thus a plasma is an example of a medium in which dispersion leads to the appearance (disappearance) of a drag effect, depending on the choice of the reference system* used for computing ϵ.

Equation (3) can also be used to compute growth (decay) of the electromagnetic waves [when the dispersion relations for $\epsilon_1(\omega)$ and $\epsilon_2(\omega)$ are known] by replacing n by kc/ω and solving these equations for ω for real wave numbers, k. In this case ϵ_1 must obviously be expressed in the K′ coordinate system (fixed in the moving medium) by transforming the frequency from the laboratory reference system to the K′ coordinate system.

As an example we solve the problem given above for the case in which an infinite uniform plasma moves in a nondispersive medium characterized by a dielectric constant ϵ_2. In the K′ coordinate system (fixed in the moving plasma) the dielectric constant is

$$\varepsilon_1 = 1 - \frac{\omega_0^2(1-\beta^2)}{\omega^2(1-n\beta\cos\theta)^2} = 1 - \frac{\omega_0^2(1-\beta^2)}{(\omega-kv\cos\theta)^2}, \tag{6}$$

where ω and k are the frequency and wave number of the electromagnetic wave in the K coordi-

---

*In the derivation of the first equation of (3) one actually obtains a somewhat more complicated expression: $f_1(n^*)(\varepsilon_1+\varepsilon_2-1)E_x/\sin\theta = 0$. The requirement $E_x \neq 0$ means that either $f_1(n^*) = 0$ or $\varepsilon_1+\varepsilon_2-1 = 0$. In the case in which medium I and medium II are plasmas the last condition corresponds to a plasma wave with a longitudinal electric field. Replacing ε_1 and ε_2 by the appropriate expressions which apply in the plasma for nonrelativistic velocities ($\beta \ll 1$) it is easy to obtain the dispersion equation $\omega_0^2/\omega^2 + \Omega^2/(\omega - kv)^2 = 0$ which coincides (if the thermal-motion corrections are neglected) with the equation obtained in references 1 and 2 on the basis of a kinetic analysis. In the equation given above ω_0^2 is the square of the plasma frequency of the fixed plasma, Ω^2 is the square of the plasma frequency of the moving plasma, and k is the wave vector.

*This situation has been clarified in a discussion with B. N. Gershman and V. V. Zheleznyakov.

nate system. If we substitute the expressions which have been derived for ϵ_1 in Eq. (3) for $n = n^*$ and $n = n^{**}$ and take $\omega = \tilde{\omega} + \xi$ and $\tilde{\omega} - kv \cos\theta = 0$, very complicated algebraic equations are obtained for ξ. If it is assumed that the plasma is rarefied $(\omega_0^2 \to 0)$ and we impose the additional condition $\omega_0^2/\xi^2 \to 0$ when $\omega_0 \to 0$ so that $\epsilon_1 \to 1$ when $\omega_0 \to 0$ and assume that $\xi \ll \tilde{\omega}$, the equations can be simplified considerably:

$$\xi^3 2\tilde{\omega}\varepsilon_2 - \xi^2\tilde{\omega}^2 \frac{1 - \varepsilon_2\beta^2\cos^2\theta}{\beta^2\cos^2\theta} - \tilde{\omega}^2\omega_0^2 \tan^2\theta \frac{\varepsilon_2 - 1}{\varepsilon_2} = 0,$$

$$\xi^3 2\tilde{\omega}\varepsilon_2 - \xi^2\tilde{\omega}^2 \frac{1 - \varepsilon_2\beta^2\cos^2\theta}{\beta^2\cos^2\theta} = 0, \tag{7}$$

where $\tilde{\omega} = kv \cos\theta$ and k is real. We note that in the derivation of Eq. (7), because $\omega_0^2 \ll \xi^2 \ll \tilde{\omega}^2$ we have neglected terms which contain ξ^4 and higher powers of ξ and terms proportional to ω_0^4. The first equation in (7) corresponds to a wave whose polarization coincides with the polarization of the Cerenkov wave $(E_x \neq 0)$ while the second is for a wave with $H_x \neq 0$. When $1 - \epsilon_2\beta^2 \cos^2\theta = 0$, which is the Cerenkov condition for a single charged particle, the solution of the first equation in (7) is

$$\xi = [\omega_0^2\tilde{\omega} \tan^2\theta\,(\varepsilon_2 - 1)/2\varepsilon_2^2]^{1/3}, \tag{8}$$

while the solution of the second equation is $\xi = 0$.

In extracting the roots in Eq. (8) it is found that two values are complex; one of these corresponds to a wave whose amplitude increases in time. It is apparent from the solution to Eq. (8) that the original assumption (for which $\omega_0^2/\xi^2 \to 0$ when $\omega_0^2 \to 0$) is actually satisfied. When $\epsilon_2 \to 1$ we find $\xi \to 0$, which is to be expected. We note also that when $\theta \to \pi/2$ the quantity ξ remains finite because when $1 - \epsilon_2\beta^2\cos^2\theta = 0$ and $\cos\theta \to 0$, $\epsilon_2 \to \infty$. If $\theta \to 0$, $\xi \to 0$ and consequently a wave which propagates in the direction of motion of the plasma exhibits no growth. In this case, as has been noted above, the electric field component E_x also tends to zero. Since this component is parallel to the direction of motion of medium I, the work done by the plasma on the wave, by virtue of which the amplitude of the field increases, also tends to zero. The same interpretation applies for the absence of the growing solution in the second equation of (7), which refers to the wave for which $H_x \neq 0$ but $E_x = 0$.

Equation (8), which determines the growth of the transverse waves at an angle found from the "Cerenkov" condition (in the sense of the dependence of ξ on ω_0 and $\tilde{\omega}$) is analogous to the growth factor for longitudinal plasma waves.[1,2] The only difference is that in plasma waves the plasma frequency of the fixed plasma is used rather than $\tilde{\omega}$.

Incidentally, if we assume formally that ϵ_2 in Eq. (8) is large, the expression obtained coincides exactly with the expression for the gain in a traveling wave tube (derived in the nonrelativistic approximation) transformed for the case of propagation of the wave at the "Cerenkov angle" with respect to the motion of the electron beam.*

The author is indebted to A. V. Gaponov and V. V. Zheleznyakov for valuable advice in the execution of this work and for many useful discussions.

---

[1] A. I. Akhiezer and Ya. B. Faĭnberg, JETP **21**, 1262 (1951).

[2] V. L. Ginzburg and V. V. Zheleznyakov, Астр. Ж. (Astron. J.), **35**, 694 (1958), Soviet Astronomy **2**, 653 (1959).

[3] R. Becker, Elektronentheorie , ONTI, 1936, p. 335. [Edwards Bros., Ann Arbor, 1944].

[4] W. Pauli, Theory of Relativity, Gostekhizdat, M.-L., 1947, (Russ. Transl.).

[5] I. E. Tamm, Основы теории электричества (Fundamentals of the Theory of Electricity) Gostekhizdat, M.-L., 1946, Sec. 114.

Translated by H. Lashinsky
155

---

*This has been pointed out by A. V. Gaponov.

SOVIET PHYSICS JETP VOLUME 37(10), NUMBER 3 MARCH, 1960

Letters to the Editor

ON THE MASSEY PARAMETER IN THE THEORY OF ATOMIC COLLISIONS

G. F. DRUKAREV

Leningrad Physico-Technical Institute,
Academy of Sciences, U.S.S.R.

Submitted to JETP editor May 7, 1959

J. Exptl. Theoret. Phys. (U.S.S.R.) **37**, 847-848 (September, 1959)

It has been shown by Hasted and Stedeford[1] and Fogel' and coworkers[2,3] that the extensive experimental material on the capture of electrons in collisions of atoms and ions can be well accounted for within the framework of the so-called adiabatic hypothesis of Massey.[4] Thus the magnitude of the cross section is determined by the parameter $|\Delta E|a/hv$, where $|\Delta E|$ is the change in the internal energy in the collision, v is the relative velocity of the atoms before the collision, and a is a quantity with the dimension of a length whose magnitude is of the order of atomic dimensions. For $a|\Delta E|/hv \gg 1$, when the process is adiabatic, the cross section is small. As the velocity increases the cross section becomes larger and reaches its maximal value for $|\Delta E|a/hv \sim 1$. For still higher velocities the cross section drops again.

With a defined as

$$a = hv_m / |\Delta E|, \qquad (1)$$

where v_m is the velocity for which the cross section is maximal, it appears that the numerical value of a is mainly determined by the type of process and is almost independent of the nature of the colliding particles. Thus, according to the data of Hasted, $a \sim 8$ A for the capture of an electron by singly charged ions, and $a \sim 1.5$ A, from the data of Fogel', for the capture of two electrons.

It is of interest to clarify what physical characteristic of the process corresponds to the parameter a as defined by formula (1). For this purpose we consider the known formulas for the momentum $q(\theta)$ imparted in the scattering into the angle θ with a change ΔE in the internal energy (in the center of mass system). Let $\mathbf{p}_0$ and $\mathbf{p}$ be the momentum of the particle before and after the collision. Using the relation $(p_0^2 - p^2)/2m = \Delta E$ and observing that $|\mathbf{p}_0 - \mathbf{p}| \ll p_0$ (which is usually true in the case of atomic collisions), we obtain

$$q(\theta) = |\mathbf{p}_0 - \mathbf{p}| = [(\Delta E / v)^2 + 4p_0^2 \sin^2(\theta/2)]^{1/2}.$$

In the small angle forward scattering $(0 \leq \theta \ll |\mathbf{p}_0 - \mathbf{p}|/p_0)$ the momentum $q(0) = |\Delta E|/v$ is imparted. In particular, if $v = v_m$, we have $q_m = |\Delta E|/v_m$. Since the velocity v_m corresponds to the maximal cross section, q_m represents the most probable momentum imparted in the forward scattering.

We therefore have

$$a = h / q_m,$$

i.e., a is inversely proportional to the most probable momentum imparted in the forward scattering. The abovementioned characteristic peculiarities of the quantity a, therefore, express the fact that each process is characterized by a definite most probable momentum transfer q_m which is almost independent of the nature of the colliding particles. The circumstance that a is smaller for the double capture than for the single capture has, from this point of view, an obvious explanation: the momentum transfer in the double capture is, of course, larger than in the single capture.

The actual numerical values of a indicate that the magnitude of q_m is of the order of the atomic unit of momentum $\hbar/a_0$ (a_0 is the Bohr radius). Hence the adiabatic condition corresponds to $q \gg \hbar/a_0$.

I am grateful to Ya. M. Fogel' for a discussion.

---

[1] J. B. Hasted and J. Stedeford, Proc. Roy. Soc. **A227**, 466 (1955).

[2] Fogel', Mitin, Kozlov, and Romashko, JETP **35**, 565 (1958); Soviet Phys. JETP **8**, 390 (1959).

[3] Fogel', Ankudinov, and Pilipenko, JETP **35**, 868 (1958); Soviet Phys. **8**, 601 (1959).

[4] H. S. Massey, Rep. Progr. Phys. **12**, 248 (1948).

Translated by R. Lipperheide
156

ELECTRON-ELECTRON SCATTERING AND QUANTUM ELECTRODYNAMICS AT SMALL DISTANCES

G. V. AVAKOV

Submitted to JETP editor May 26, 1959

J. Exptl. Theoret. Phys. (U.S.S.R.) **37**, 848-849 (September, 1959)

THE most direct experiments that could give us information about the electron would be experiments on the scattering of electrons by electrons. Assuming that the interaction is of vector type and gauge invariant up to sufficiently high energies, we can determine the electric and magnetic form-factors of the electron by a comparison of the theoretical formula with the experimental data. We note that when we take the electric form-factor into account we must also regard the magnetic form-factor of the electron as nonvanishing. Then the vertex operator Γ_μ corresponding to a vertex in the Feynman diagram for the scattering will in the most general case have the well known form[1-3]

$$\Gamma_\mu = a(q^2)\gamma_\mu + \gamma_\mu\gamma_\nu \frac{q_\nu}{\sqrt{-q^2}} b(q^2), \tag{1}$$

where the invariant functions $a(q^2)$ and $b(q^2)$ of the square of the four-momentum transfer $(q^2 = q_0^2 - \mathbf{q}^2)$ are respectively the electric and magnetic form-factors.

Omitting the cumbersome calculations, we present the formula for the scattering cross section in the center-of-mass system of the colliding electrons:

$$\begin{aligned}\frac{d\sigma}{\sigma_0 d\Omega} = {} & f^2(q^2)\frac{2+2x+x^2}{8x^2} + f(q^2) f(p^2)\frac{(1+x)^2}{4x} \\ & + f^2(p^2)\frac{1+2x+2x^2}{8} + \varepsilon^4\frac{\varphi^2(q^2)}{q^4}\frac{(2+x)^2}{(1+x)^2} \\ & + \varepsilon^4\frac{\varphi(q^2)\varphi(p^2)}{q^2p^2}\frac{2+2x^2+5x}{(1+x)^2} + \varepsilon^4\frac{\varphi^2(p^2)}{p^4}\frac{(2x+1)^2}{(1+x)^2} \\ & + 2\varepsilon^2 f(q^2)\frac{\varphi(q^2)}{-q^2}\frac{1}{x} + 2\varepsilon^2 f(p^2)\frac{\varphi(p^2)}{-p^2}x \\ & + \varepsilon^2 f(q^2)\frac{\varphi(p^2)}{-p^2}\frac{2+6x+3x^2}{2x(1+x)^2} \\ & + \varepsilon^2 f(p^2)\frac{\varphi(q^2)}{-q^2}\frac{x(2x^2+6x+3)}{2(1+x)^2},\end{aligned} \tag{2}$$

where $\sigma_0 = e^4/16\varepsilon^2$; $e^2 = 1/137$; $f = a^2$, $\varphi = b^2$; $x = \tan^2(\vartheta/2)$,

$q^2 = -4\varepsilon^2 x/(1+x) = -4\varepsilon^2\sin^2(\vartheta/2)$,
$p^2 = -4\varepsilon^2/(1+x) = -4\varepsilon^2\cos^2(\vartheta/2)$,
ϵ is the energy of the electron, and ϑ is the scattering angle.

In (2) we can make the replacements $x = q^2/p^2$, $\epsilon^2 = -(q^2+p^2)/4$. Then on the right side we have a function of q^2 and p^2 only. Equation (2) actually contains four unknown functions (since a single form-factor for different values of the argument amounts to different unknowns). By varying x and ϵ we can get six quadratic equations with the six unknowns $f(p_i)$ and $\varphi(p_i)$. In fact, by changing x and ϵ in a special way through six pairs of values, we get the table of values of q^2 and p^2:

$$\begin{array}{lll} p_1^2, p_1^2 & p_1^2, p_2^2 & p_1^2, p_3^2 \\ & p_2^2, p_2^2 & p_2^2, p_3^2 \\ & & p_3^2, p_3^2. \end{array}$$

Here the values on the left are those of q^2, and those on the right, of p^2. The first element in the table, p_1^2, p_1^2 (which means a choice of x and ϵ such that $q^2 = p^2 = p_1^2$), gives an equation with two unknowns. The second element, p_1^2, p_2^2, is obtained by changing p^2 with constant q^2. This adds one more equation and increases the number of unknowns by two. The element p_1^2, p_3^2 does the same. It is easy to see that the remaining elements of the table give new equations but do not form new unknowns.

After finding the functions φ and f, we can compare their ratio with the value of μ obtained from the scattering of electrons by α particles.[4]

In conclusion the writer wishes to express his gratitude to K. A. Ter-Martirosyan for suggesting this topic.

---

[1] Akhiezer, Rozentsveĭg, and Shmushkevich, JETP **33**, 765 (1957), Soviet Phys. JETP **6**, 588 (1958).

[2] G. Salzman, Phys. Rev. **99**, 973 (1955).

[3] Yennie, Lévy, and Ravenhall, Revs. Modern Phys. **29**, 144 (1957).

[4] G. V. Avakov and K. A. Ter-Martirosyan, Nuclear Phys. (in press).

Translated by W. H. Furry

ELECTRIC QUADRUPOLE γ TRANSITIONS IN EVEN-EVEN NUCLEI

N. N. DELYAGIN

Institute of Nuclear Physics, Moscow State University

Submitted to JETP editor April 1, 1959

J. Exptl. Theoret. Phys. (U.S.S.R.) 37, 849-851 (September, 1959)

LET us consider the first excited states of even-even nuclei, which have quantum numbers 2^+ and are deexcited by electric quadrupole radiation. The extensive experimental data available at present concerning lifetimes of these states enable us to compute for these E2 transitions the reduced probabilities B(E2), which are equal (to within a statistical factor which is the same for all the nuclei considered) to the square of the transition matrix element. One then discovers a connection between the value of B(E2) and the energy E of the excited state.

Earlier, McGowan[1] treated the nuclei in the mass number range $90 < A < 130$ from this point of view. He showed that for these nuclei the relation between B(E2) and E can be represented satisfactorily in the form $B(E2) \sim E^{-1}$, independently of the atomic number Z. We have considered the nuclei in the broad range of mass numbers from A = 46 (Ti) to A = 198 (Pt). In computing the values of B(E2) we used experimental data collected in summaries[2,3] as well as original papers published during 1958-1959 and not included in the survey reports.

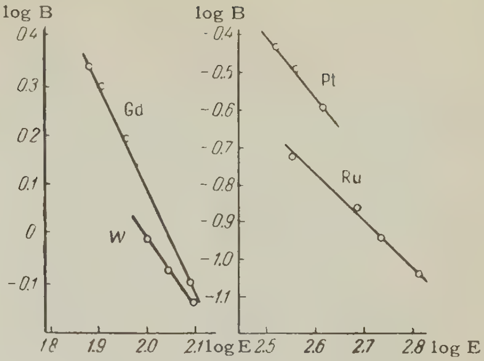

The comparison of B(E2) and E was made separately for the isotopes of different elements. For the isotopes of all the elements considered, B(E2) decreases when E increases. For nuclei with a large deformation parameter, whose first excited state is a rotational state, this relation between B(E2) and E is natural: an increase in deformation in such nuclei is associated with an increase of the quadrupole moment and the moment of inertia, which causes an increase of B(E2) and a decrease of the excitation energy. It appears that such a dependence of B(E2) on E holds not only for nuclei with large deformation parameters but for even-even nuclei in general. The relation between B(E2) and E becomes even more apparent if we look at the dependence of log B(E2) on log E. This dependence is shown in the figure for the isotopes of Ru[2-4], Gd[2,3], W[2,3,5] and Pt[2,3]. [B(E2) is in units of $e^2 \times (\text{barns})^2$ and E is in kev.] It is apparent that the relation between log B(E2) and log E is linear and can be represented by the formula

$$\log B\,(E2) = a \log E + b, \qquad (1)$$

where a and b are constant for the isotopes of a given element. For isotopes whose first excited state is a rotational state, formula (1) could have been predicted, by taking account of the quadratic dependence of B(E2) on the deformation parameter for such levels, and by assuming a power law dependence of the nuclear moment of inertia on the deformation parameter. However formula (1) proves to be valid for nuclei in various regions of mass number, independently of whether or not these nuclei have a rotational spectrum of their low lying excited states; a linear dependence similar to that shown on the figure for the isotopes of Ru, Gd, W and Pt also holds for the isotopes of Se, Pd, Cd, Te, Sm and Dy. For these ten elements, the values of the constant a in (1) were computed from the experimental data using least squares. For seven of the elements (Ru, Pd, Cd, Te, Sm, W, Pt) the values of a were very close to one another, lying in the range -1.2 ± 0.2, which shows that the power law dependence of B(E2) on E is approximately the same for these elements. Of these seven elements, the isotopes of W and two of the four Sm isotopes have rotational spectra for their lowest excited states, whereas the other nuclei do not have such spectra, and are treated as spherically symmetric in the uniform model of the nucleus.[2] A typical example is samarium, whose isotopes with A = 152 and 154 are deformed nuclei whose lowest states are rotational in character, while the isotopes with A = 148 and 150 do not have rotational spectra, and their excitation is treated in the uniform model as resulting from quadrupole vibration. However the experimental data favor the same dependence of B(E2) on E for all four isotopes of Sm, and the computed value of the constant a differs from that for Ru, W, Pt, and the other elements by no more than 15%.

For a large class of nuclei (in the mass number interval $150 < A < 190$ and $A > 222$) the lowest excited states of even-even nuclei are uniquely interpreted to be rotational states. Nuclei lying outside this mass number range are treated on the uniform model as spherically symmetric and their excitation attributed to quadrupole vibration. The lack of a quantitative theory of such vibrations makes a direct test of this assumption difficult. An alternative point of view was proposed in the paper of Davydov and Filippov,[6] where it was shown that the lowest excited states of even-even nuclei can be interpreted to be rotational states even if they are outside the mass number range $150 < A < 190$, $A > 222$, if one assumes that the nucleus is not axially symmetric. Then when we go from highly deformed nuclei to nuclei which are close to a filled shell the nature of the excitation does not change; only the parameters describing the deformation and the axial asymmetry change, resulting in a change in the energy of the levels and the separation of levels with the same spin. Possibly the regularities noted here in the dependence of B(E2) on energy could be explained on the basis of such a model.

---

[1] F. K. McGowan, Comptes Rendus du Congres International de physique nucleaire, Paris, 1959, p. 225.

[2] Alder, Bohr, Huus, Mottelson, and Winther, Revs. Modern Phys. **28**, 432 (1956).

[3] Strominger, Hollander, and Seaborg, Revs. Modern Phys. **30**, 585 (1958).

[4] P. H. Stelson and F. K. McGowan, Phys. Rev. **110**, 489 (1958).

[5] F. K. McGowan and P. H. Stelson, Phys. Rev. **109**, 901 (1958).

[6] A. S. Davydov and G. F. Filippov, JETP **35**, 440 (1958), Soviet Phys. JETP **8**, 303 (1959).

Translated by M. Hamermesh
158

EXCITATION OF ROTATIONAL STATES OF NONAXIAL NUCLEI IN ALPHA-PARTICLE SCATTERING

E. A. ROMANOVSKIĬ

Institute of Nuclear Physics, Moscow State University

Submitted to JETP editor April 6, 1959

J. Exptl. Theoret. Phys. (U.S.S.R.) **37**, 851-853 (September, 1959)

IN the present paper an estimate is made of the probability of excitation of the second 2^+ level in even-even nonaxial nuclei resulting from scattering of α particles with energy $E \gtrsim E_B$ (where E_B is the height of the Coulomb barrier), for the purpose of determining the role of the competing mechanisms of excitation — direct nuclear interaction and Coulomb excitation.

Since the quasi-classical approximation is valid for the scattering of α particles with $E \gtrsim E_B$ by heavy nuclei ($kR \gg 1$), in solving our problem we can use a method which was developed in the classical theory of Coulomb excitation. In this treatment the excitation of the nucleus occurs as the result of time-dependent nuclear and electric interactions.

It is not hard to show (cf. reference 1) that the conditions under which one can treat the potential energy of interaction as a perturbation are expressible in the following form: $(kR_0)^2 M(I_i \rightarrow I_f) \ll 1$ (for the nuclear interaction) and $\eta^2 M(I_i \rightarrow I_f) \ll 1$ (for the Coulomb interaction). Here

$$M(I_i \rightarrow I_f) = \frac{1}{2I_i+1} \sum_{m_i m_f} |\langle I_i m_i | a_\mu | I_f m_f \rangle|^2$$

is the matrix element for transition of the nucleus from the ground state to the excited state, a_μ are coordinates characterizing the deformation of the nuclear surface in a coordinate system fixed in the nucleus, and $\eta = Z_1 Z_2 e^2/\hbar v$. In the case of excitation of the second 2^+ level in a nonaxial nucleus (denoted in the sequel by 2^+) we have, according to Davydov and Filippov:[2]

$$M(0 \rightarrow 2^+) = \frac{\beta^2}{10}\left[1 - \frac{3 - 2\sin^2 3\gamma}{\sqrt{9 - 8\sin^2 3\gamma}}\right], \qquad \beta^2 = \sum_\mu |a_\mu|^2,$$

where γ is the parameter describing the deviation of the nucleus from axial symmetry. The quantity $M(0 \rightarrow 2^+)$ goes to zero for $\gamma \rightarrow 0$ and $\gamma \rightarrow 30°$, while it attains its maximum value $\sim 7 \times 10^{-3} \beta^2$ for $\gamma \approx 20°$. From these estimates it follows that perturbation theory is applicable to the excitation of the 2^+ level.

If we take account of the change of the orbit of the bombarding particles and the change of the electric multipole fields when the particles enter the nucleus by using the method proposed by the author,[3] then in calculating the probability of excitation of the 2^+ level we can use the perturbation formula:

$$P = \sum_{m_f} \left| \frac{1}{i\hbar} \int_{-\infty}^{\infty} \langle \psi_f \,|H(t)|\, \psi_i \rangle e^{i\omega t} dt \right|^2,$$

where $\omega = (E_f - E_i)/\hbar$, and $H(t)$ is the interaction energy. The quadrupole component of the interaction energy, which causes the transition, has the form

$$H(t) = -r \frac{\partial V(r)}{\partial r} \sum_{\mu\nu} D^{(2)}_{\mu\nu}(\Theta_i)\, a_\mu Y_{2\mu}(\Theta, \Phi) + \frac{4\pi}{5} Z_1 e \sum_{\mu} \hat{Q}_{2\mu} Y_{2\mu}(\Theta, \Phi)\, r^{-3}.$$

Here

$$V(r) = -V_0 \left[1 + \exp \frac{r - R_0}{d} \right]^{-1}$$

is the potential of the interaction of the α particle with the nucleus, $d \sim 0.5 \times 10^{-13}$ cm;[4] $D^{(2)}_{\mu\nu}(\Theta_i)$ are generalized spherical functions, depending on the Euler angles, which determine the transformation from a coordinate system fixed in the nucleus to a space-fixed system; r, Θ, and Φ are the polar coordinates of the incident particle; $\hat{Q}_{2\mu}$ is the nuclear quadrupole moment operator. Choosing for the wave functions ψ_i and ψ_f the wave functions of rotational states of a nonaxial nucleus,[2] and carrying out calculations analogous to those of the classical theory of Coulomb excitation, we find

$$P = \frac{16\pi^2\eta^2 B(E2; 0 \rightarrow 2^+)}{125 a^4 Z_2^2 c^2} \times \sum_{\mu} \left| I_{2\mu}(\vartheta, \xi) - \frac{5kR_0V_0a^4}{6\eta ER^2R_0 d} I_{2\mu}(\vartheta, \xi, a, R_0, d) \right|^2 \left| Y_{2\mu}\left(\frac{\pi}{2}, 0\right) \right|^2,$$

$$I_{2\mu}(\vartheta, \xi, a, R_0, d) = \int_{-\infty}^{\infty} e^{i\xi(\varepsilon \sinh w + w)} \frac{(\cosh w + \varepsilon + i\sqrt{\varepsilon^2 - 1}\, \sinh w)^{\mu}}{(\varepsilon \cosh w + 1)^{\mu - 2}} \times g(\vartheta, a, R_0, d, w)\, dw,$$

$$g(\vartheta, a, R_0, d, w) = \frac{\exp\left[\frac{a(\varepsilon \cosh w + 1) - R_0}{d}\right]}{\left[1 + \exp\left(\frac{a(\varepsilon \cosh w + 1) - R_0}{d}\right)\right]^2};$$

$$a = \frac{Z_1 Z_2 e^2}{\mu v^2}, \quad \xi = \frac{\Delta E}{2E}\eta, \quad \varepsilon = 1/\sin(\vartheta/2),$$

where ϑ is the scattering angle, μ is the reduced mass, R_0 is the radius of interaction of the α particle and the nucleus, R is the nuclear radius, $I_{2\mu}(\vartheta, \xi)$ are tabulated functions of the classical theory of Coulomb excitation,[5] and $B(E2; 0 \rightarrow 2^+)$ is the reduced probability for excitation of the 2^+ level.

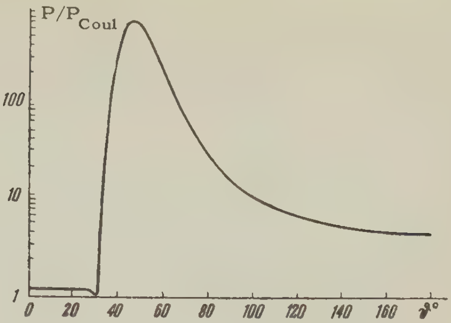

As an example we show in the figure the angular dependence of the ratio of the probability of excitation of the 2^+ level in Cd^{114}_{48} [$\Delta E = 1.2$ Mev, $B(E2; 0 \rightarrow 2^+) = 1.25 \times 10^{-50}\,\mathrm{cm}^4$][6] to the probability of excitation by the Coulomb field of incident α particles with energy $E = 30$ Mev. As we see from the figure, in the region of angles ϑ corresponding to impact parameters $\sim R_0$, the probability of excitation of the nucleus is approximately two orders of magnitude greater than the probability of Coulomb excitation. The rapid increase in the ratio P/P_{Coul} with increasing scattering angle is associated with the fact that the maximum value of P occurs at small scattering angles ϑ. In this angle region, the strong dependence of the impact parameter on angle results in an even stronger dependence of the function $g(\vartheta, a, R_0, d, w)$ on ϑ, and this function essentially determines the change in the probability of excitation as a function of angle of scattering.

The maximum cross section for inelastic scattering is approximately an order of magnitude less than the cross section for elastic scattering of α particles by this nucleus. The large value of the cross section for excitation of the 2^+ level, which is caused by the interaction of the α particles with the nuclear surface, makes it possible to study the properties of second excited 2^+ states in even-even non-axial nuclei by recording inelastically scattered α particles.

In conclusion, I express my thanks to V. G. Neudachin for discussion of this work.

---

[1] L. D. Landau and E. M. Lifshitz, Quantum Mechanics, Pergamon Press, 1958, Section 45.

[2] A. S. Davydov and G. F. Filippov, JETP **35**, 440, 703 (1958), Soviet Phys. JETP **8**, 303, 488 (1959).

[3] E. A. Romanovskiĭ, JETP **37**, 83 (1959), Soviet Phys. JETP **10**, 59 (1960).

[4] R. Woods and D. Saxon, Phys. Rev. **95**, 577 (1954).

[5] Alder, Bohr, Huus, Mottelson, and Winther, Revs. Modern Phys. **28**, 432 (1956).

[6] H. Motz, Phys. Rev. **104**, 1353 (1956).

Translated by M. Hamermesh

159

MECHANISM FOR THE PRODUCTION OF RELATIVISTIC ELECTRONS IN THE ATMOSPHERES OF NONSTATIONARY STARS

I. M. GORDON

Submitted to JETP editor May 10, 1959

J. Exptl. Theoret. Phys. (U.S.S.R.) **37**, 853-855 (September, 1959)

TYPE I supernovae exhibit at maximum tremendous luminous intensities; in some cases these intensities are two orders of magnitudes greater than the intensity of the galaxy in which the supernova is located. The radiation from supernovae is nonthermal and is due to the synchrotron radiation of relativistic electrons.[1,2]

The author has offered observations to support the view that relativistic electrons responsible for the radiation of the Crab nebula arise in the stellar atmospheres.[3] Since the energy of these electrons is $10^{11} - 10^{12}$ ev, they cannot be produced in nuclear processes or as a result of induction acceleration processes. The latter mechanism is highly ineffective for electrons because of the high "magnetic bremsstrahlung" losses. Thus there is some basis for the suggestion that these electrons are produced in secondary processes and that the primary process is the acceleration of protons.[3]

We show below that this hypothesis may explain the characteristic features of the luminosity curves of type I supernovae and certain other nonstationary stars.

Baade has shown that the luminosity curve of a type I supernova consists of two parts: a maximum followed by a rapid reduction in intensity, and then a slower exponential drop with a half-life of 55 days. The second phase starts 50 — 100 days after the maximum. An attempt to explain this characteristic of the luminosity curve was made by Borst[4] who invoked radioactive decay, and by Burbridge et al.[5] who invoked fission of Cf^{254}. The shortcomings of the first explanation were indicated by Burbridge et al.[5] while those of the second have been indicated by the present author.[3] We may note that in reference 5 it was also indicated that the source of radiation of supernovae may be relativistic electrons as had been proposed earlier by us.[1,2]

The suggestion that the radiation of supernovae is due to relativistic electrons produced in secondary processes[3] can be used to explain the exponential decay of the luminous intensity if it is assumed that 50 — 100 days after the maximum there is no significant production of new relativistic protons and that the density in the shell remains constant in the region in which the secondary processes and electron radiation occur.

In the motion of a beam of particles in a gas with constant velocity and mean free path (λ), the number of noncolliding particles varies exponentially as $\exp(-x/\lambda)$, where λ is the particle mean free path, or as $\exp(-t/T)$ where T is the mean free time. The number of electrons which are formed is proportional to the number of protons that move in the shell and also varies exponentially. A calculation shows that the radiation time for relativistic electrons is approximately 100 sec, whereas the collision time corresponding to a reduction in intensity by a factor of two in 55 days is approximately 70 days, a number which is significantly larger. Thus the intensity is proportional to the number of relativistic electrons and also varies exponentially.

Taking the proton range in hydrogen[6] as 70 g/cm^2, it is possible to determine (using the time in which the intensity is reduced by a factor of two) the density in the shell $p \approx 3 \times 10^{-16}$ g/cm^3 and the mass, starting with an expansion velocity of 10^8 cm/sec and an expansion time of 10^7 sec, corresponding to the beginning of the exponential phase. The mass which is obtained (10^{30} g) is in agreement with the astronomical data. The first part of the luminosity curve would seem to correspond to the period in which the formation of relativistic protons continues while the density changes.

This general behavior is exhibited by the luminosity curve of H Lac 1950.[7] However, superimposed on the first phase there are observed brief rapid reductions of intensity ("dips"); the second phase exhibits rapid, isolated intensity bursts. It is possible that the dips in the first phase are due to the fact that the luminosity curve reproduces the source density curve and its behavior is related to the weakening of the sources. The bursts in the second part of the curve apparently indicate the formation of new protons in the regions which are more dense than those from which most of the particles are emitted. This result follows from the greater curvature in the decay curve as compared with the main curve. It is important that the first part of the curve exhibits dips and sometimes bursts whereas the second part exhibits bursts only. Similar bursts and dips are observed in stars such as SS Cyg and R Cor Bor, indicating that the atmospheres of these stars may contain relativistic electrons of secondary origin. An exponential luminosity decay is also seen in stars such as UV Cet. From the point of view of the suggestion presented here it may be of interest to note that the composition of the primary component of cosmic rays exhibits the same anomaly[8] as the chemical composition of certain types of non-stationary stars.

The author is deeply indebted to Academician V. A. Ambartsumyan for a fruitful discussion of this problem and for valuable advice.

---

[1] I. M. Gordon, Dokl. Akad. Nauk SSSR **94**, 413 (1954).

[2] I. M. Gordon, Труды 4-го космогонического совещания (Proc. of the 4th Conf. on Cosmogony) U.S.S.R. Acad. Sci. Press, M., 1955, p. 121.

[3] I. M. Gordon, Труды астрономической обсерватории Харьковского гос. ун-та, (Proc. of the Kharkov State Univ. Astronomical Observatory) **12**, 15 (1957).

[4] L. Borst, Phys. Rev. **78**, 807 (1950).

[5] Burbridge, Hoyle, Burbridge, Christy, and Fowler, Phys. Rev. **103**, 1145 (1956).

[6] V. L. Ginzburg, Usp. Fiz. Nauk **62**, 37 (1957).

[7] G. Larssen-Leander, Stockholm Observatory Ann. **18**, 3, (1954).

[8] Koshiba, Schulz, and Schein, Nuovo cimento **9**, 1 (1958).

Translated by H. Lashinsky
160

THE LANDAU CORRECTION COEFFICIENT IN THE DETERMINATION OF THE VISCOSITY OF A LIQUID

G. A. GAMTSEMLIDZE

Tbilisi State University

Submitted to JETP editor May 12, 1959

J. Exptl. Theoret. Phys. (U.S.S.R.) **37**, 855-857 (September, 1959)

THE solution of the Navier-Stokes equation for a circular disc undergoing torsional vibrations in its own plane in an unbounded liquid yields the following expression for the coefficient of viscosity of a liquid

$$\eta = 4I^2(\gamma - \gamma_0)^2\theta / \pi^3 R^8 \rho N^2, \qquad (1)$$

where I is the moment of inertia of the disc, R is its radius, θ is the period of vibration of the disc in the liquid, ρ is the density of the liquid, N is the number of discs entering into the system, and γ and γ_0 are the damping coefficients of the disc in the liquid under study and in a vacuum.

Equation (1) was obtained under the approximations $\gamma/\omega \ll 1$, $R/\lambda \gg 1$, $\theta_0/\theta \approx 1$, where θ_0 is the period of rotation of the disc in a vacuum. The difference $\gamma - \gamma_0$ is the proper absorption coefficient, whose presence is brought about by the action of the liquid on the upper and lower surface of the disc only. In view of the fact that in the derivation of (1) edge effects were not taken into account (in particular, the effects of the liquid on the lateral surface of the disc), they should be excluded in some way or other.

In the determination of the viscosity by means of (1), L. D. Landau introduced a correction coefficient and the equation for η was written in the form

$$\eta = 4I^2(\gamma - \gamma_0)^2\theta / \pi^3 R^8 \rho N^2 (1 + 2d/R + 2\lambda/R)^2. \qquad (2)$$

Here d is the thickness of the disc used in the systems, and λ is the penetration depth of the viscous wave.

In this paper, an experimental method is described for the measurement of the viscosity of a liquid by means of rotating discs which excludes the action of viscous forces on the lateral surface of the disc without the introduction of any correction coefficients. A test of the method was carried out on measurements in helium II.

The essence of the experiment is as follows. A compound disc of thickness D was divided parallel to the plane of the characteristic oscillations into two, three, etc., parts which formed a rather complicated but nonetheless single oscillatory system. Depending on into how many parts the disc was divided, several oscillatory systems with the same moment of inertia and the same lateral surfaces were obtained; however, in each individual case there was a different number of discs (N = 1, 2, 3, 6), in the system. The discs in this case were separated from each other by distances $l \gg \lambda$, where λ is the penetration depth.

If we determine the damping coefficients γ_N and γ_0 for these systems, both in helium II and in vacuo, and compute the expression $(\gamma_N - \gamma_0)/N$ for each system, then this expression, in view of the additivity of the damping, should give the total value of the damping (brought about both by the front surfaces and the lateral surfaces) of the individual disc entering into the various systems. Since the thickness of the individual discs $d_N = D/N$ is different in different systems, the ratios obtained from their values must differ from one another.

If we plot $(\gamma_N - \gamma_0)/N$ vs. d_N for a given temperature, and extrapolate this curve to $d_N = 0$, we obtain the damping brought about by the action of the liquid alone on the upper and lower surfaces of a single disc, i.e., the difference $(\gamma - \gamma_0)_{d=0}$. Knowing $\gamma - \gamma_0$, and making use of Eq. (1), it is possible to construct the curve for the temperature dependence of the viscosity.

Values are given in Fig. 1 for the viscosity coefficient η_n of the normal component of helium II for different temperatures, obtained from (1) upon substitution in it of our measured values of $(\gamma - \gamma_0)_{d=0}$ and the values of ρ_n taken from the work of Andronikashvili.[2] The values of η_n, taken from the work of Andronikashvili,[1] which were obtained by him according to (2), are plotted in the same figure (the solid curve in the drawing was drawn through the mean values).

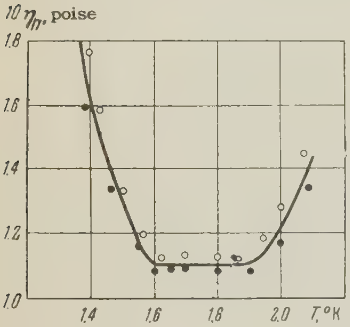

FIG. 1. Temperature dependence of the viscosity of the normal component of helium II. o – data of Andronikashvili, • – data obtained according to Eq. (1).

It is seen from Fig. 1 that within the limits of error of the experiment (5 – 7%), the values of the coefficient of viscosity obtained by the usual method are in excellent agreement with one another, which also indicates the validity of the application of the Landau correction coefficient for thin discs. At the same time this circumstance again confirms the reliability of the temperature curve $\eta_n(T)$ given by Andronikashvili.

We now investigate up to what upper limit of the ratio $(d+\lambda)/R$ does the correction coefficient remain applicable. For this purpose we find the dependence $\eta_n(T)$ from the measured values of γ_N for all four systems, by means of (2), making use of the method of successive approximations (see Fig. 2). In the calculations it was taken into consideration that the number of discs in the first system $N = 1$ and the thickness $d_1 = 0.276$ cm; in the second case, $N = 2$ and $d_2 = 0.138$ cm; in the third $N = 3$ and $d_3 = 0.092$ cm; in the fourth $N = 6$ and $d_6 = 0.046$ cm.

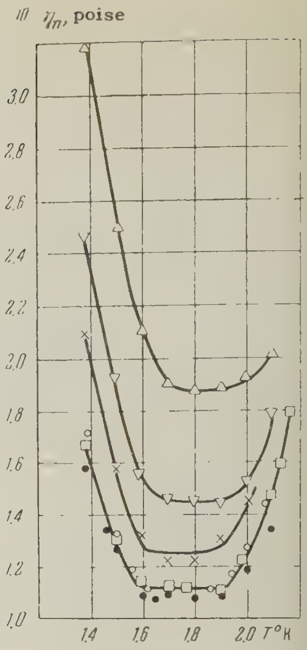

FIG. 2. The temperature dependence of the viscosity of the normal component of helium II, computed by Eq. (2) for different values of $(d+\lambda)/R$; Δ – 0.19 to 0.25, ∇ – 0.10 to 0.16, × – 0.07 to 0.13, □ – 0.05 to 0.1, o – data of Andronikashvili, • – data obtained from Eq. (1).

As is seen from Fig. 2, the temperature dependence of the coefficient of viscosity is strongly dependent on the value of $(d+\lambda)/R$. In this case the correction coefficient gives an excellent result only for the fourth system; therefore the concept of the thin disc must be limited to the values $(d+\lambda)/R < 0.05$ to 0.1. It is necessary to note that the experimental method of measurement of η_n just described does not include that part of the damping brought about by the presence of "angles" of the disc, which are formed by the front and lateral surfaces, i.e., the corner effect. But, since at all temperatures the values of the viscosity coefficient determined by the method of elimination of the effect of lateral surface are in excellent agreement with data obtained by Eq. (2) for thin discs, one must regard the correction for the corner effect to be negligibly small.

The author expresses his thanks to Professor É. L. Andronikashvili and Yu. G. Mamaladze for participation in discussion of the results and for valuable advice.

---

[1] É. L. Andronikashvili, JETP **18**, 429 (1948).

[2] É. L. Andronikashvili, JETP **18**, 424 (1948).

Translated by R. T. Beyer
161

$0^+ - 0^+$ *TRANSITION IN THE DECAY* $Pr^{140} \rightarrow Ce^{140}$

B. S. DZHELEPOV, I. F. UCHEVATKIN, and S. A. SHESTOPALOVA

All-Union Institute for Metrology

Submitted to JETP editor May 16, 1959

J. Exptl. Theoret. Phys. (U.S.S.R.) **37**, 857-859 (September, 1959)

IN 1958 it was established[1] that the Ce^{140} nucleus has a 0^+ excited level with excitation energy 1902 kev. This level resulted from the decay of La^{140}. The ground and excited states of Ce^{140} can also result from electron capture and β^+ decay of Pr^{140} (see Fig. 1).

We attempted to find out whether the 1902 kev level of Ce^{140} is excited in the decay of Pr^{140}. We expected this level to be excited by allowed β^+ decay and electron capture since the ground state of Pr^{140} is of the 1^+ type.[2]

To this end we placed an equilibrium preparation of $Nd^{140} + Pr^{140}$ in a beta spectrometer with triple focusing (radius of curvature 14.5 cm). The pressure in the apparatus was 5×10^{-5} mm Hg. The thickness of the celluloid films on the windows of the first counter was ~ 0.2 mg/cm². The counters were filled with a mixture of argon plus 15% alcohol to a total pressure of 100 mm Hg.

In Fig. 2a we show the conversion line K = 1902 kev (the energy determination is that of reference 1), and Fig. 2b is the Kurie plot of the end of the β^+ spectrum of Pr^{140}. It is known[4,5] that the β^+ spectrum of Pr^{140} has an allowed shape. Since our apparatus, using coincidences, could distort the spectrum at low energies we measured only the high energy part of the spectrum and from it reconstructed the entire spectrum. The e^-/β^+ ratio turned out to be 0.2%.

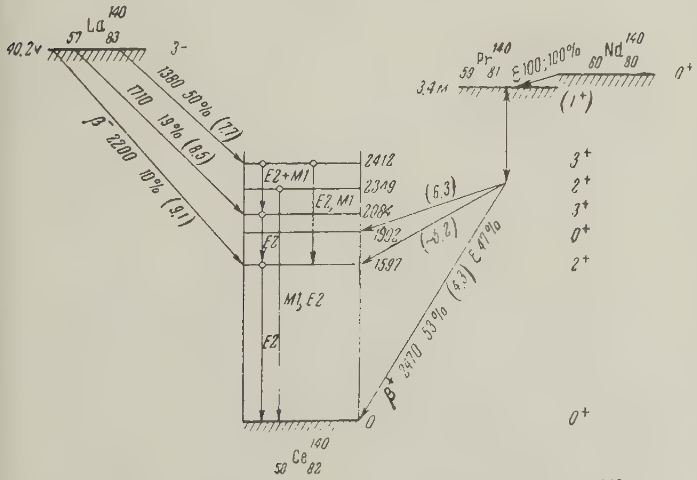

FIG. 1. Decay scheme to lower excited states of Ce^{140}; the log (ft) value is given in brackets for lines due to β transitions.

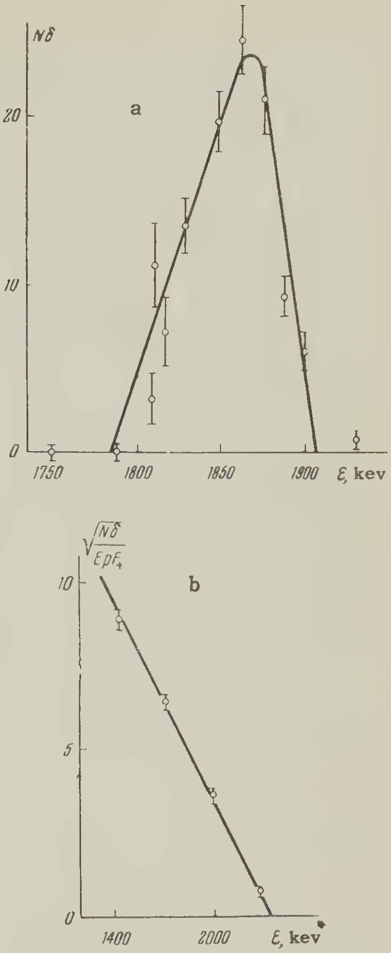

FIG. 2

To determine e^- (1902) per decay it is necessary to take into account the fact that K and L capture for an allowed transition to the ground level should amount to $\sim 47\%$.[6] It then follows that the number of conversion electrons amounts to 0.1% per decay. Consequently the level Ce^{140} (0^+) 1902 kev is excited much more frequently in the decay of Pr^{140} than in the decay of La^{140} (0.013% according to the data of references 1 and 7).

The 1902-kev level of Ce^{140} probably results from both e^- capture and β^+ decay of Pr^{140}. Taking into account values of f_K, f_L and f_+ for allowed transitions we find that $ft = 2 \times 10^6$.

Consequently, two β^+ decays from the ground level of Pr^{140} to two 0^+ levels of Ce^{140} differ in reduced time by a factor of approximately 100 (Fig. 1). This is evidence of a different intrinsic structure of these levels.

---

[1] Dzhelepov, Prikhodtseva, and Khol'nov, Dokl.

Akad. Nauk SSSR **121**, 995 (1958), Soviet Phys.—Doklady **3**, 803 (1958).

[2] B. S. Dzhelepov and L. K. Peker, Схемы распада радиоактивных ядер (Decay Schemes of Radioactive Nuclei), Izv. Akad. Nauk SSSR, 1958.

[3] Dzhelepov, Anton'eva, and Shestopalova, Dokl. Akad. Nauk SSSR **64**, 309 (1949).

[4] Browne, Rasmussen, Surls, and Martin, Phys. Rev. **85**, 146 (1952).

[5] Gromov, Dzhelepov, Dmitriev, and Preobrazhenskiĭ, Izv. Akad. Nauk SSSR, Ser. Fiz. **22**, 153 (1958), Columbia Tech. Transl. p. 151.

[6] B. S. Dzhelepov and L. N. Zyryanova, Влияние электрического поля атома на бета-распад, (Effect of Atomic Electric Field on Beta Decay), U.S.S.R. Acad. Sci., 1956. Band, Zyryanova, and Tsin Chen-Zhui, Izv. Akad. Nauk SSSR, Ser. Fiz. **20**, 1387 (1956), Columbia Tech. Transl. p. 1269. Band, Zyryanova, and Suslov, Izv. Akad. Nauk SSSR, Ser. Fiz. **22**, 952 (1958), Columbia Tech. Transl. p. 943.

[7] Bashilov, Dzhelepov, Novosil'tseva, and Chervinskaya, Izv. Akad. Nauk SSSR, Ser. Fiz. **22**, 179 (1958), Columbia Tech. Transl. p. 176.

Translated by A. M. Bincer
162

SPONTANEOUS FISSION OF Am^{241}

V. L. MIKHEEV, N. K. SKOBELEV, V. A. DRUIN, and G. N. FLEROV

Submitted to JETP editor May 26, 1959

J. Exptl. Theoret. Phys. (U.S.S.R.) **37**, 859-861 (September, 1959)

AMONG the nuclei which undergo spontaneous fission those with an odd number of protons or neutrons are usually distinguished by the low probability of such fission, their half-lives being a few orders of magnitude longer than those of neighboring even-even isotopes.

Most of our information about the spontaneous fission of odd nuclei was obtained at different times by groups at Los Alamos and Berkeley. Segre and his group[1] determined the spontaneous fission half-lives of $U^{233,235}$, $Np^{237,239}$, Pu^{239}, and Am^{241}. In most instances they gave only the upper limit of the fission probability, because of the small samples available and the difficulty of working with these isotopes, whose low fission probability is accompanied by large specific α activity. Ghiorso and his group[2] studied the spontaneous fission of Bk^{249}, Cf^{249}, $E^{253,254}$ and Fm^{255}. Their careful experiments enabled them to determine the half-lives to within 25%; only in the case of Fm^{255} was merely the lower limit of $T_{1/2}$ established.

The recent development of a technique[3,4] employing detectors with high resolving power and millimicrosecond pulses permits experimentation under more favorable conditions. The work can now be done with large samples and an appreciable effect can be observed in a considerably shorter time.

The fragment detector used in the present work was a gaseous scintillation counter, with a xenon-filled chamber constructed of the high-vacuum materials copper and teflon. A photomultiplier was mounted in contact with a glass-covered window of the chamber; a layer of quaterphenyl ($\sim 50\ \mu g/cm^2$) on the inner surface of the glass served to transform ultraviolet radiation into visible light. Reflection from the magnesium oxide coating of the chamber wall enhanced light collection. The seal between the glass and the chamber was a teflon gasket. The chamber was evacuated to 5×10^{-6} mm Hg and was filled with xenon to 2 atmos. During vacuum conditioning, the chamber was heated by water vapor. A thin layer of americium was deposited electrolytically on a platinum backing; the amount of material ($\sim 60\ \mu g$ on an area of $1.8\ cm^2$) was determined by measuring the α activity of the layer.

A FEU-33 photomultiplier with $\sim 3 \times 10^{-9}$ sec resolution was used. Fission fragments were detected against the large alpha-particle background by means of a high-speed discriminator of the Moody type.[5] A DGTs-7 crystal diode was the nonlinear element of the circuit, which was triggered by a LP-34 secondary-emission tube sensitive to small signals.

A preliminary test was conducted with a Pu^{240} target, using the same geometry as with Am^{241} in the subsequent experiments. 1.20×10^{11} years was obtained for the spontaneous fission half-life of this plutonium isotope, in good agreement with other data.[6] A 30% reduction of pulse amplitude was observed after a month of work.

For the work with Am^{241} the apparatus was calibrated by placing in the chamber a target ($\sim 200\ \mu g$) of U^{235}, which possesses a large slow-neutron fission cross section. The entire counter was surrounded by paraffin, and a (Po + Be) neutron source was used to study the counting response (see the figure). The response was found to be essentially the same for Pu^{240} and for Am^{241}, when fragments were counted against a strong α-particle background. These experiments estab-

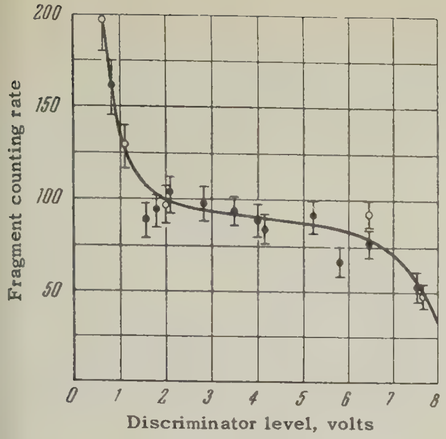

Counting response for two runs: ○ – at the beginning of the experiment with Am^{241}; ● – at the end of the experiment.

lished the optimum conditions for counting fission fragments from Am^{241}. Measurements with Am^{241} ($\sim 60\,\mu g$) were conducted for 160 hours with a 4-volt discriminator threshold. Twenty-six pulses were recorded; control experiments showed that at least 18 of these belonged to the background. The corresponding lower limit of the spontaneous fission half-life of Am^{241} is 2×10^{14} years.

The counter was surrounded by a layer of cadmium and paraffin in order to obviate neutron-induced fission. Imitation of the observed effect by the spontaneous fission of Cm^{242} impurity is excluded since an estimate showed that not more than $10^{-10}\%$ of Cm^{242} could have been present.

In Segre's experiment[1] on the spontaneous fission of Am^{241} the target consisted of only $\sim 10^{-7}$ g and in 2700 hours three pulses from fission fragments were registered; this led to the lower limit $T_{1/2} \geq 1.4 \times 10^{13}$ years. The enhanced sensitivity of our technique resulted in a value of $T_{1/2}$ which is greater by a factor of ~ 15; this result is $\sim 10^5$ times greater than would be expected for an even-even nucleus with the given value of Z^2/A.

Approximately the same factor of lifetime increase was observed for the spontaneous fission of Pu^{239}, Bk^{249}, Cf^{249}, and Es^{253,254}. The spontaneous fission probabilities of the other odd nuclei must evidently be determined more precisely.

The authors wish to thank V. F. Gerasimov for a number of valuable suggestions concerning the construction of the counter.

---

[1] E. Segre, Phys. Rev. **86**, 21 (1952).

[2] A. Ghiorso, Proceedings of the International Conference on the Peaceful Uses of Atomic Energy, Geneva, 1955, Report 718.

[3] C. Eggler and C. M. Huddleston, Nucleonics **14**, 34 (April, 1956).

[4] J. A. Northrup and R. A. Nobles, Nucleonics **14**, 36 (April, 1956).

[5] I. A. D. Lewis and F. H. Wells, Millimicrosecond Pulse Techniques, Pergamon Press, London, 1954 (Russ. Transl. IIL, 1956, p. 275).

[6] Chamberlain, Farwell, and Segre, Phys. Rev. **94**, 156 (1954).

Translated by I. Emin
163

ANGULAR ANISOTROPY OF GAMMA QUANTA THAT ACCOMPANY FISSION

V. M. STRUTINSKIĬ

Submitted to JETP editor May 26, 1959

J. Exptl. Theoret. Phys. (U.S.S.R.) **37**, 861-863 (September, 1959)

A certain anisotropy relative to the direction of fragment divergence was recently observed for the gamma quanta that accompany nuclear fission.[1] The gamma intensity is greatest in the direction of fragment divergence, and the magnitude of the anisotropy $[W_\gamma(180°) - W_\gamma(90°)]/W_\gamma(180°)$ amounts to 9 and 5% for the fission of Pu^{239} and U^{235} respectively by thermal neutrons. Leachman's review[1] mentions also one of the possible causes of the angular anisotropy, namely that the initial deformations of the fragments, and consequently also the initial electric moments of the fragments, are correlated in a definite manner with the fission direction. This explanation, however, is subject to the objection that the time required for the nucleus to radiate gammas with energies on the order of 1 Mev is too long for any reasonable value of the electric moments. The quanta are therefore emitted by the fragments apparently already after thermal equilibrium has been established and after the neutron evaporation. This is also confirmed by the fact that both the shape of the gamma spectrum and the number of gammas (~ 4 or 5 per fragment) are close to what is observed for gammas that accompany the capture of thermal neutrons.[2]

Another possible cause of angular anisotropy of the quanta may be the presence of a large fragment angular momentum correlated with the fission direction. The momentum dependence of the density of nuclear levels leads in this case to anisotropy of the quanta even if complete thermal equilibrium is established in the nucleus.[3,4] A fragment momentum of large magnitude, oriented relative to the scattering direction, can occur, for example, if the scission of the nucleus is not strictly symmetric about the fission axis. The scission is a rapid, nonadiabatic process[5] and both the place of its occurrence and its direction can be assumed to fluctuate over a wide range. The fluctuation in the place of scission can explain the unique dependence of the number of secondary neutrons on the fragment mass,[6] if it is assumed that at the instant of scission there is concentrated in the neck a considerable mass, on the order of the fragment mass difference for the most probable asymmetric fission (private communication from O. Bohr). The presence of a transverse component of the Coulomb repulsion between the stubs, when the fission is asymmetric about the axis causes the fragments to rotate after scission in opposite directions about an axis perpendicular to the fission direction. The rotational momentum of the fragments will have an order of magnitude

$$\hbar j \approx f_{\perp}\tau R \sim (Z_1 Z' e^2/R^2)(a/R)\,\tau R,$$

where Z_1 and R are the charge and radius of the fragment, Z' the charge of the stub, a a quantity on the order of the neck thickness, and τ is a characteristic time, equal to the smaller of either the time required for the fragments to diverge by a distance equal to the nuclear radius or the time required for the nucleus to resume its spherical shape. Taking $a \approx 2 \times 10^{-13}$ cm, $Z_1 = 50$, and $Z' = 5$ we find $j \approx 20$ for $\tau = 10^{-21}$ sec.

The angular distribution of the gamma quanta is calculated most readily in the following manner. The probability of emitting a quantum with momentum L is proportional to

$$\exp\{-\hbar^2(\mathbf{j}-\mathbf{L})^2/2JT\} \sim \exp\{-\hbar^2 jM/JT\},$$

where J is the moment of inertia, T the temperature, j the initial momentum of the fragment, and M the projection of the photon momentum on the direction of $\mathbf{j}$ ($\mathbf{j}$ is the classical vector).[3,4] The probability of emitting a photon making an angle θ with $\mathbf{j}$ will consequently contain the following angle-dependent factor

$$W_j^{(L)}(\theta) = \sum_{M=-L}^{L} \exp\{-\hbar^2 jM/JT\}\,|\mathbf{Y}_{LM}^{(\lambda)}(\theta)|^2,$$

where $\mathbf{Y}_{LM}^{(\lambda)}$ is a vector spherical function.[7] Expanding the exponential, we get

$$W_j^{(L)}(\theta) \approx 1 + \tfrac{1}{2}(\hbar^2 j/JT)^2 \sum_{M=-L}^{L} M^2\,|\mathbf{Y}_{LM}^{(\lambda)}(\theta)|^2. \qquad (1)$$

The sum over M is easiest to calculate by using the specific expressions for the functions $\left|\mathbf{Y}_{LM}^{(\lambda)}\right|^2$ (cf. reference 7). After summation over M, only one term with $\cos^2\theta$ remains in (1). To obtain the distribution about the fragment direction, it is necessary to average this term also over the orientation of $\mathbf{j}$. Noting that the mean value is

$$\cos^2\theta = \tfrac{1}{2}\sin^2\vartheta,$$

where ϑ is the angle to the direction of fragment divergence, we find

$$W_{\gamma}^{(L)}(\vartheta) = 1 + k_L(\hbar^2 j/JT)^2 \sin^2\vartheta,$$

where the values of k_L are $+1/8$, $-3/8$, and $-81/64$ for $L = 1$ (dipole radiation), 2 (quadrupole radiation), and 3 (octupole radiation) respectively. The negative sign of anisotropy for $L = 1$ is due to the fact that the dipole quanta are emitted predominantly along the spin $(L = |M| = 1)$ When $j = 10$, $T = 1$ Mev, $J = (2/5)\,AmR^2$, and $A = 100$, the anisotropy of the fission gammas is found to be $\sim -1\%$ for dipole radiation and from $+2$ to $+3\%$ for quadrupole radiation. At the orientation of fragment angular momentum indicated above, the observed sign of the anisotropy leads to the conclusion that $L > 1$ for the anisotropic part of the radiation. The observed anisotropy is possibly connected with gamma transitions between the lower levels of the fragments, where the quadrupole radiation is relatively more probable, particularly considering that the presence of a large nuclear momentum leads, from the point of view of level density, to a certain preference for radiation with larger momentum, especially at low temperature. The increase in anisotropy with decreasing temperature also leads to an increased contribution from the transitions between the lower levels to the observed anisotropy of radiation. The smaller anisotropy of the gammas in the case of fission of U^{235} is possibly due to the poorer orientation of the fragment angular momentum at the large spin of the fissioning nucleus, the value of which is 3 or 4 for U^{235} fission and 0 or 1 in the case of Pu^{239}.

The foregoing results for the anisotropy of gamma quanta are correct also for other cases, when nuclei with large oriented momenta are obtained, for example, in the the capture of heavy ions.

I thank B. T. Geĭlikman, S. T. Belyaev, and G. A. Pik-Pichak for valuable comments.

---

[1] R. B. Leachman, Proc. 2nd Internat. Conf. on Peaceful Uses of Atomic Energy, 15, Geneva, 1958, P/665.

[2] L. Grochev, A. Demidov, et al. ibid., P/2029.

[3] V. M. Strutinskiĭ, Сб. Ядерные реакции при малых и средних энергиях, (Anthology, Nuclear Re-

actions at Low and Medium Energies), M., 1959, p. 522.

[4] T. Erikson and V. Strutinski, Nucl. Phys. **8**, 284 (1958); **9**, 689 (1958/59).

[5] B. T. Geĭlikman, Paper delivered at the first Geneva Conference on Peaceful Uses of Atomic Energy, August 1955.

[6] R. B. Leachman, Proc. 2nd Internat. Conf. on Peaceful Uses of Atomic Energy, **15**, Geneva, 1958 P/2467.

[7] A. I. Akhiezer and V. B. Berestetskiĭ, Квантовая электродинамика (Quantum Electrodynamics), M., 1953. AEC Tr. 2876, 1957.

Translated by J. G. Adashko
164

CROSS SECTIONS FOR ELASTIC SCATTERING OF 195-Mev POSITIVE PIONS BY CARBON AND LITHIUM NUCLEI

V. G. IVANOV, V. T. OSIPENKOV, N. I. PETROV, and V. A. RUSAKOV

Joint Institute for Nuclear Research

Submitted to JETP editor May 28, 1959

J. Exptl. Theoret. Phys. (U.S.S.R.) **37**, 863-866 (September, 1959)

THE elastic-scattering cross sections were measured at the Joint Institute for Nuclear Research with the aid of the synchrocyclotron and the same cloud chamber in magnetic field as used in the experiments with negative particles.[1] The source of positive pions was a polythene block 25 g/cm^2 thick, placed in the external 670-Mev proton beam. Particles of specified momentum were guided to the chamber by a deflecting magnet and a four-meter collimator placed in the concrete shield of the accelerator. Carbon and lithium targets (natural mixtures of the isotopes of these elements), 1.72 and 0.8 g/cm^2 thick, respectively, were placed in the working volume of the chamber. The intensity of the magnetic field in which the chamber was placed was 13,500 oe.

The experimental procedure and the processing of the photographs were the same as in the experiment with the negative pions.[1] In particular, the criterion for distinguishing elastic from inelastic scattering was the minimum measured energy loss, equal to 35 Mev. Taking into account corrections for detection efficiency in the angle interval from 10 to 180°, we registered 410 and 243 events of elastic scattering of mesons by carbon and lithium respectively.

The measured total cross sections (in millibarns) are listed in the table; to determine the absolute values of the total cross sections for elastic scattering, the total inelastic-scattering cross sections were normalized to the geometric nuclear cross sections for $R = 1.4A^{1/3} \times 10^{-13}$ cm.

Nucleus	Energy, Mev	Pion sign	Elastic, 10°	πR^2
C	195	+	204±26	325
Li	195	+	156±26	226
C	230	—	200±31	325

The last row of the table contains the total cross section for the elastic scattering of negative mesons by carbon.[1] Comparison of the data given for carbon nuclei shows that, within the limits of experimental error, the elastic-scattering sections are the same for positive and negative mesons with respective energies of 195 and 230 Mev. The cross sections obtained are also in satisfactory agreement with

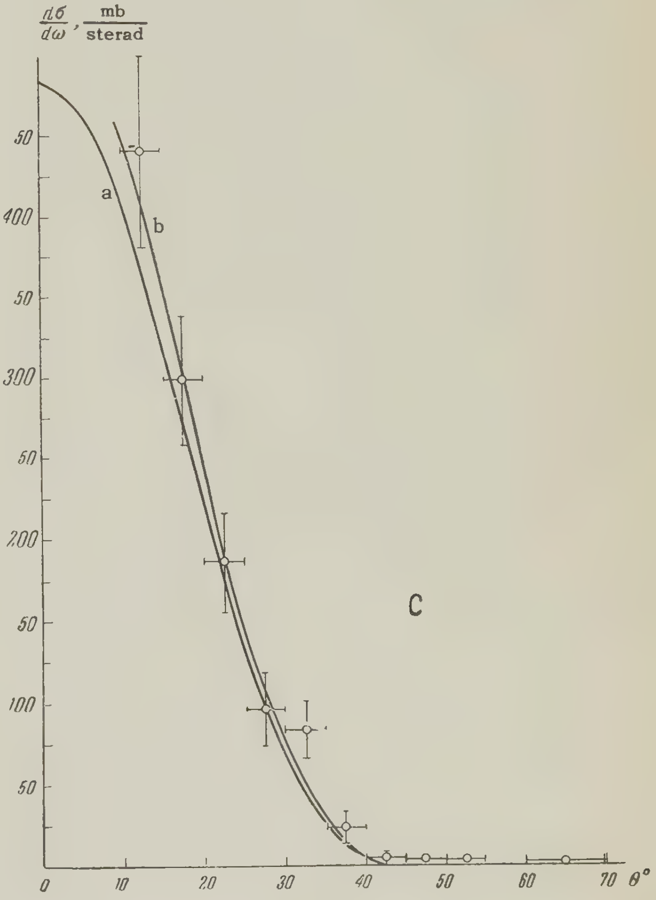

FIG. 1

the calculated values (equal to 0.6 to 0.8 of the geometric cross sections) obtained by Sternheimer[2] and by Osipenkov and Filippov[3] on the basis of the optical model, with an interaction potential in the form of a rectangular well of radius R. In these calculations, the parameters of the well (depth of well and coefficient of absorption of the pions in nuclear matter) were determined from the cross sections for the scattering of pions by free nucleons.

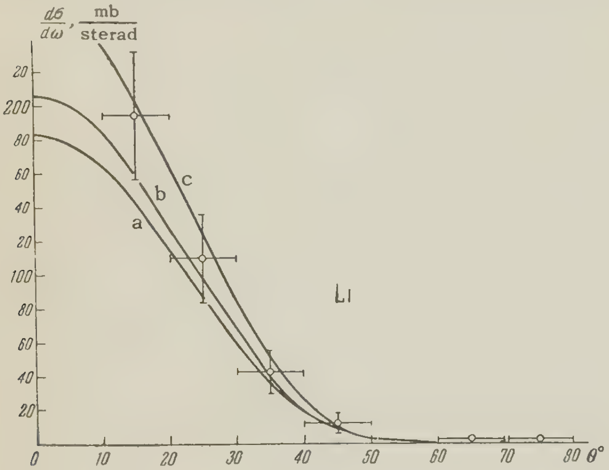

FIG. 2

The experimentally-obtained angular distribution of elastic scattering by carbon and lithium are illustrated in Figs. 1 and 2. The solid curves represent the angular distributions computed in the quasiclassical approximation from the optical-model equations* (for the range from 0° to the angle corresponding to the position of the first diffraction minimum) for the following values of the parameters: nuclear radius $R = 1.4 A^{1/3} \times 10^{-13}$ cm, coefficient of meson absorption in nuclear matter $K = 0.83 \times 10^{13}$ cm^{-1} the real part of the potential V is equal to zero for curve A and 30 Mev for curve B; $K = \infty$ and $V = 0$ for curve C. As can be seen from the diagram, the measured distributions agree with the computed ones, but within the limits of experimental error no definite conclusions can be made regarding the magnitude or sign of the real part of the potential. It is obvious that the description of the measured angular distributions with the aid of a rectangular-well potential is inadequate, since these distributions (as shown in references 5 and 6) do not exhibit the clearly-pronounced minima and maxima which characterize such a potential. For example, it was found in references 5 and 7 that to obtain correspondence between the experimental and computed data over the entire range of distribution angles it is necessary to forego, in the computations with the optical model, the homogeneous distribution of the nucleons of the nucleus and to add to the interaction potential a term proportional to the gradient of the nuclear density. No right-left asymmetry of elastic scattering of positive pions was observed in the experiment for either nucleus.

---

*The computation formula is taken from the book of Akhiezer and Pomeranchuk.[4]

---

[1] Dzhelepov, Ivanov, Kozodaev, Osipenkov, Petrov, and Rusakov, JETP **31**, 923 (1956), Soviet Phys. JETP **4**, 864 (1957).

[2] R. M. Sternheimer, Phys. Rev. **101**, 384 (1956).

[3] V. T. Osipenkov and S. S. Filippov, JETP **34**, 224 (1958), Soviet Phys. JETP **7**, 154 (1958).

[4] A. I. Akhiezer and I. Ya. Pomeranchuk, Некоторые вопросы теории ядра, (Certain Problems in Nuclear Theory), 1950, 2nd ed., p. 201.

[5] Baker, Rainwater, and Williams, Phys. Rev. **112**, 1763 (1958).

[6] Tadao A. Fujii, Phys. Rev. **113**, 695 (1959).

[7] L. S. Kisslinger, Phys. Rev. **98**, 761 (1955).

Translated by J. G. Adashko
165

ELECTROMAGNETIC MASS OF THE K MESON

CHOU KUANG-CHAO and V. I. OGIEVETSKIĬ

Joint Institute for Nuclear Research

Submitted to JETP editor May 28, 1959

J. Exptl. Theoret. Phys. (U.S.S.R.) **37**, 866-867 (September, 1959)

IN the recent experiments by Rosenfeld et al.[1] and Crawford et al.[2] it was established that the mass of the neutral K meson exceeds that of the charged K^+ meson by ~4.8 Mev. On the face of it the sign of this mass difference appears to contradict the concept that the K^+ and K^0 mesons are spinless particles belonging to the same charge doublet. Indeed, if the K^0 meson has no electromagnetic interactions and the mass difference is of electromagnetic origin then the electromagnetic self-mass of the charged K meson should make it heavier than the neutral one (see, e.g., reference 3). On this basis the above-mentioned authors are inclined to interpret their results as an argument in favor of the Pais hypothesis,[4] according to which the K^+ and K^0 meson do not form a charge doublet and may have different intrinsic parities.

It is shown below that there is not as yet sufficient basis for this conclusion since the mass difference can be explained, within the framework of the Gell-Mann–Nishijima multiplet scheme, by the electromagnetic interactions of the K^0 meson. Indeed, as noted in an interesting paper by G. Feinberg,[5] a spinless neutral particle which is different from its antiparticle, e.g., K^0, can interact with the electromagnetic field. This interaction results from a virtual dissociation of the K^0 meson into strongly interacting particles, for example a nucleon and an antihyperon. As a consequence the K^0 meson will have an electromagnetic structure.

In the general case the gauge-invariant electromagnetic interaction Lagrangian can be written as

$$L = -j_\mu(x)\,A_\mu(x) \tag{1}$$

where $j_\mu(x)$ is the operator for the total current of all interacting particles. In the β-formalism of Duffin and Kemmer the matrix element of the current taken between single K-meson states will have the form*

$$\begin{aligned}\langle p' | j_\mu(x) | p\rangle_K &= -ie\,(2\pi)^{-3}e^{-iqx}\bar{v}(p')\,\beta_\mu\,[F_{1K}(q^2)+\tau_3 F_{2K}(q^2)]\,v(p),\\ q = p'-p, &\quad \bar{v}(p') = v^+(p')\,(2\beta_4^2-1),\end{aligned} \tag{2}$$

where p' and p are the K-meson four-momenta in the final and initial states, $v(p')$ and $v(p)$ are the corresponding wave functions in the β-formalism, and $F(q^2)$ is the form factor satisfying

$$\begin{aligned}F_{K^+}(q^2) &= F_{1K}(q^2)+F_{2K}(q^2), \qquad F_{K^+}(0)=1,\\ F_{K^0}(q^2) &= F_{1K}(q^2)-F_{2K}(q^2), \qquad F_{K^0}(0)=0,\end{aligned} \tag{3}$$

since the charge of the particle is $eF(0)$.

Due to interaction (1) and by taking into account (2) we find for the self-mass of the K meson†

$$\begin{aligned}\Delta m &= \frac{ie}{(2\pi)^4}\,\frac{\bar{v}(p)}{\bar{v}v}\,\beta_\nu\int d^4q\\ &\times\frac{i(\hat{p}-\hat{q})+(\hat{p}-\hat{q})^2/2m-[(p-q)^2+m^2]/m}{[(p-q)^2+m^2]\,q^2}\,\beta_\nu\,[F_K(q^2)]^2\,v(p),\\ \hat{q} &= \beta_\mu q_\mu\end{aligned} \tag{4}$$

or

$$\Delta m = \frac{ie^2}{2\,(2\pi)^4\,m}\int d^4q\,\frac{[F_K(q^2)]^2}{q^2}\left\{\frac{(2p-q)^2}{(p-q)^2+m}-4\right\}. \tag{5}$$

The $F_K(q^2)$ as a function of q^2 can be determined only from an as yet nonexistent exact theory or a full analysis of future experiments. For our purposes it is sufficient to take, for example,

$$\begin{aligned}F_{K^+}(q^2) &= 16m^4/(q^2+4m^2)^2,\\ F_{K^0}(q^2) &= -4\lambda q^2m^2/(q^2+4m^2)^2\end{aligned} \tag{6}$$

then from (5) and (6) we obtain for the mass difference

$$\begin{aligned}m_{K^0}-m_{K^+} &= (m/8\pi^2)\,e^2\,({}^7/_3\lambda^2-1)\\ &= (m/2\pi)\,\alpha\,({}^7/_3\lambda^2-1).\end{aligned} \tag{7}$$

Comparing with the experimental value of 4.8 Mev we deduce that $\lambda \approx 2$.

We note that it will be difficult to observe experimentally other effects due to the interaction under consideration.‡

Consequently it is not necessary to give up the idea that K^+ and K^0 form a charge doublet in order to explain the observed[1,2] mass difference. Both the sign and the magnitude of the difference $m_{K^0} - m_{K^+}$ could be a consequence of electromagnetic interactions.

---

*As remarked by Feinberg in the case of the π^0 meson, which is a truly neutral particle, such a matrix element would vanish as a consequence of invariance under charge conjugation.

†Expression (5) for the self-mass may also be derived from the usual theory in which the K mesons are described by second order wave equations and the electromagnetic interaction is introduced in a gauge-invariant manner by the substitution: $\partial/\partial x_\mu \to \partial/\partial x_\mu - ieF(-\Box^2)\,A_\mu(x)$.

‡The absence of bremsstrahlung and the difficulties involved in separating the electromagnetic and nuclear scattering for K^0 were discussed by Feinberg.[5] The most characteristic experiment would involve observation of fast δ electrons from K^0 mesons. However the K^0–e scattering cross section is very small at low energies. Consequently the effect will be vanishingly small since even a 1-Bev K meson in the laboratory system will have an energy of the order of only a few Mev in the K^0–e center-of-mass system.

---

[1] Rosenfeld, Solmitz, and Tripp, Phys. Rev. Lett. **2**, 110 (1959).

[2] Crawford, Cresti, Good, Stevenson, and Ticho, Phys. Rev. Lett. **2**, 112 (1959).

[3] S. Gasiorowicz and A. Petermann, Phys. Rev. Lett. **1**, 457 (1958).

[4] A. Pais, Phys. Rev. **112**, 624 (1958).

[5] G. Feinberg, Phys. Rev. **109**, 1381 (1958).

Translated by A. M. Bincer
166

TAKING ACCOUNT OF THE GRAVITATIONAL ENERGY

D. D. IVANENKO and N. V. MITSKEVICH

Moscow State University

Submitted to JETP editor May 30, 1959

J. Exptl. Theoret. Phys. (U.S.S.R.) **37**, 868-869 (September, 1959)

EVER since the formulation of the general theory of relativity physicists have encountered serious difficulties in defining the energy and momentum of the gravitational field, needed, in particular, to take account of the transformation of these quantities into the energy and momentum of other fields. This problem has to do with the circumstance that in the formulation of the theory the equation of continuity acquires the physical meaning of a conservation law through the vanishing of the usual, not the covariant divergence. Here we call the conservation law corresponding to the vanishing of the usual divergence, the exact conservation law. The exactly conserved "pseudo-tensor" of the energy-momentum density of the gravitational field, introduced by Einstein, is, on one hand, not a generally covariant quantity; on the other hand, the energy defined in terms of it depends in an essential way on the choice of the reference systems connected with the purely spatial coordinate transformations with no change in the time coordinate. Definitions of the energy-momentum density of the gravitational field different from this have therefore been proposed, in particular by Lorentz and Levi-Civita. However, the exactly conserved tensor for all fields including the gravitational, proposed by these authors, vanishes at all points of space-time and cannot, according to Einstein's equations, have any deep physical meaning (see, for example, reference 1).

The problem of the definition of energy and momentum in the general theory of relativity has begun to be discussed again recently in the literature. Møller, in his recent papers,[2,3] has derived a new expression* for the total energy of a system of gravitational and other fields, avoiding the abovementioned difficulty concerning the critical dependence of the total energy on the spatial reference systems. At the same time, the non-tensor character of the energy-momentum density (it is an affine tensor density) turns out to be essential to the problem if only for the fact that even from a tensor quantity it is impossible to obtain a genuine vector by integration. Møller showed the uniqueness of his results from the requirement that the energy of the system be covariant with respect to purely spatial coordinate transformations and from the postulate that it can be expressed in terms of the metric tensor and its first and second derivatives.

On the other hand, our earlier formulation of Noether's theorem, when applied to the gravitational field,[4] leads to conserved quantities different from those of Einstein; as we shall show, these are closely connected with the "pseudo-tensor" derived later by Møller. For this we use a unified treatment of the gravitational and other fields to determine, for example, the conserved quantities, in particular, the canonical quasi-tensor of the energy-momentum density and the spin part of the energy-momentum. The latter is particularly important in the case of gravitation. Indeed, the gravitational field is described by a metric tensor, so that there must be particles with spin corresponding to it; it is known that in the weak field approximation the spin of these is equal to two. With the help of the expressions obtained by Møller[2] and Mitskevich[4] one easily establishes the relation

$$\mathfrak{T}^{\alpha}_{\beta} = -\,\mathfrak{U}^{\alpha}_{\beta}(\mathrm{grav}), \tag{1}$$

where $\mathfrak{T}^{\alpha}_{\beta}$ is the "pseudo-tensor" of energy-momentum of the total system of fields, introduced by Møller, and $\mathfrak{U}^{\alpha}_{\beta}(\mathrm{grav})$ is the expression for the spin part of the energy of the gravitational field, as found by us. It is also easily seen from the general derivation of the spin part of the energy-momentum[4] that this quantity has the necessary transformation properties (invariance of the integrated energy under purely spatial transformations which leave the time coordinate unchanged) also for other fields. It should be noted that the symmetric tensor found by us coincides with the expressions of Lorentz and Levi-Civita and is, owing to Einstein's equations, identically zero for the total system of fields. We therefore have the following relation

$$\mathfrak{T}^{\alpha}_{\beta}(\mathrm{sym})(\mathrm{tot}) = \mathfrak{t}^{\alpha}_{\beta}(\mathrm{tot}) + \mathfrak{U}^{\alpha}_{\beta}(\mathrm{tot}) = 0. \tag{2}$$

The canonical quasi-tensor of energy-momentum for the total system of fields, $\mathfrak{t}^{\alpha}_{\beta}$ (derived in reference 4), therefore also leads to the solution of the aforementioned problem of the determination of the total energy in the presence, and with account, of gravitation, for we can write, according to (2),

$$\mathfrak{t}^{\alpha}_{\beta}(\mathrm{f}) + \mathfrak{t}^{\alpha}_{\beta}(\mathrm{grav}) = -\,(\mathfrak{U}^{\alpha}_{\beta}(\mathrm{f}) + \mathfrak{U}^{\alpha}_{\beta}(\mathrm{grav})), \tag{3}$$

where $\mathfrak{t}^{\alpha}_{\beta}(\mathrm{f})$ and $\mathfrak{t}^{\alpha}_{\beta}(\mathrm{grav})$ refer, respectively, to the ordinary fields in the presence of gravitation and to the purely gravitational field. In particular, if ordinary matter is absent, we obtain a noteworthy relation which establishes the equality (except for the sign) of the spin part of the energy-momentum of the gravitational field and the canonical quasi-tensor of the energy-momentum density of gravitation, introduced by us and also obtained by Møller.

It seems more natural to us to regard as the energy-momentum density of the total system of fields, the sum of the canonical (unsymmetric) quasi-tensors of all fields, and not the sum of the symmetric tensor of the ordinary matter field and the canonical quasi-tensor of the gravitational field, as proposed by Møller. This is based, first of all, on the desirability of having a uniform definition of the physical quantities for all fields. On the other hand, from Møller's point of view a quantity describing the total system of fields is replaced by one which is characteristic only of the gravitational field. Our point of view corresponds also to the covariant principles of second quantization.[5] We note, however, that both methods coincide completely in the consideration of the free gravitational field.

Møller concludes from the vanishing of the energy carried by the two known forms of gravitational waves in the absence of ordinary matter, that the usual quantum theories of gravitation are not useful. It should be noted in this connection that even if we are not concerned with real, energy carrying radiation, the calculation of vacuum effects may force us to accept the quantization of gravitation and the idea of gravitons. On the other hand, if the existence of energy carrying gravitational waves were definitely established, our earlier conclusion that the gravitons can be transformed into ordinary matter would in some sense undoubtedly be true in the general case as well as in the linear weak field approximation.[6]

---

*These papers were presented at the Colloquium on Gravitation in Paris and at the 9th High Energy Conference in Kiev in 1959 by Møller and also by Geiniot, who independently arrived at similar results.

---

[1] W. Pauli, Theory of Relativity, Pergamon Press, New York (1958).

[2] C. Møller, Ann. of Phys. **4**, 347 (1958).

[3] C. Møller, Paper in the Max-Planck-Festschrift, Berlin (1958).

[4] N. V. Mitskevich, Ann. Physik **1**, 319 (1958).

[5] N. V. Mitskevich, Доклады Болгарской АН (Trans. Bulgarian Academy of Sciences) **11**, 376 (1958).

[6] A. Sokolov and D. Ivanenko, Квантовая теория поля (Quantum Theory of Fields), pt. 2, GITTL, M. (1952); D. D. Ivanenko, Paper in the Max-Planck-Festschrift, Berlin (1958); see also D. R. Brill and J. A. Wheeler, Revs. Modern Phys. **29**, 465 (1957).

Translated by R. Lipperheide
167

ON LINEAR THEORIES OF GRAVITATION

V. I. PUSTOVOĬT

Dnepropetrovsk State University

Submitted to JETP editor May 28, 1959

J. Exptl. Theoret. Phys. (U.S.S.R.) **37**, 870-871 (September, 1959)

DESPITE the fact that the general theory of relativity has now found wide recognition, attempts are still being made to approach the problem of gravitation by a somewhat different method. Here we have in mind mainly the various linear theories of gravitation based on the usual pseudo-euclidean space-time metric.[1,2] It is here essential that the linear theories yield, in first approximation, the same values for the so-called three critical effects as the general theory of relativity (see, e.g., references 1 to 4).

The linear theories involve serious theoretical difficulties. One of these is that the energy density of the gravitational field is not positive definite.[5,6] However, attempts are being made to bypass this difficulty (see, e.g., reference 7). Notwithstanding the clear superiority of the theory of Einstein, it is therefore of definite interest to find those differences between the general theory of relativity and the linear theories which can, in principle, be observed in experiment.

There is no point in looking for discrepancies in the effects of the gravitational red shift and the deflection of light in the gravitational field of the sun: these are solely determined by the field equations, which are the same as in the linear approximation of the general theory of relativity. There remains the possibility to search for discrepancies in those effects which depend on the equations of motion in addition to the field equations.

In the general theory of relativity, one of the first integrals of the equations of motion, corresponding to the second Kepler law, has the form[8]

$$(1 - 2\varkappa m/c^2 r)^{-1} r^2 d\varphi/dt = \text{const.} \tag{1}$$

Similar expressions can easily be obtained in the linear theories as well. In the theories of Birkhoff[1] and Belinfante[2] we have, respectively,

$$\exp(2\varkappa m/c^2 r)\, r^2 d\varphi/dt = \text{const}, \tag{2}$$

$$[1 + (\eta + 1)\varkappa m/2c^2 r + v^2/2c^2 - K(F - 4C_1)\varkappa m/c^2 r]\, r^2 d\varphi/dt = \text{const}. \tag{3}$$

Here $\kappa = 6.67 \times 10^{-8}\, \mathrm{g}^{-1}\, \mathrm{sec}^{-2}\, \mathrm{cm}^3$ is the gravitational constant, m is the mass of the central body, $r = p/(1 + e \cos \varphi)$ is the distance from the planet or the satellite to the central body, p is a parameter, e is the eccentricity of the orbit, c is the velocity of light in vacuum, and $\eta \approx 6$ is a constant to be determined by experiment (see the table of constants in reference 2). We note that the constants entering in the last term of the left hand side of (3) are such that

$$v^2/2c^2 - K(F - 4C_1)\varkappa m/c^2 r \geqslant 0. \tag{4}$$

Comparing the relations (1) and (3), we see that we can find a discrepancy between the Einstein theory and the theory of Belinfante by measuring the dependence of $d\varphi/dt$ on φ (say for a satellite with a large e). The maximal difference between (1) and (3) is

$$\Delta\left(\frac{d\varphi}{dt}\right)_{\max} = \left(\frac{d\varphi}{dt}\right)_{\varphi=0} \frac{\eta - 3}{2} \frac{\varkappa m (1 + e)^3}{c^2 p} \approx \frac{\eta - 3}{2} \frac{(\varkappa m)^{3/2} (1 + e)^3}{c^2 p^{5/2}}. \tag{5}$$

For an earth satellite with $e \approx 0.9$ and $p \approx 10^8$ cm, this difference is 5×10^{-12} rad sec^{-1}.

From (1), (2), and (3) one easily finds the expressions for the third Kepler law:

$$\frac{S_1 + \lambda(\varkappa m/c^2 r_1) L_1}{S_2 + \lambda(\varkappa m/c^2 r_2) L_2} = \frac{T_1}{T_2} \sqrt{\frac{a_1}{a_2}}, \tag{6}$$

where S is the area, and L, the perimeter of the orbit, a is the major half axis, and T is the period of revolution. The constant λ takes the value $\lambda = 1$ for the general theory of relativity and for the theory of Birkhoff, and $\lambda = (\eta + 1)/4$ for the theory of Belinfante ($\lambda = 0$ corresponds to the classical Kepler law in the theory of Newton).

We see from a comparison of formulas (1) and (2) that they lead to Kepler laws which differ only in second approximation, so that it is at present impossible to detect this difference in experiment. One may distinguish between the general theory of relativity and the theory of Birkhoff, however, by considering the rotation effect.

The rotation of the central body leads, according to the Einstein theory, to an additional displacement of the perihelion of the planet, which is equal to

$$\Delta\tilde{\omega} = -\frac{16\pi \sqrt{\varkappa m}\, \Omega l^2}{5c^2 p^{3/2} (1 - e^2)^3} \left(1 - 3 \sin^2 \frac{i}{2}\right). \tag{7}$$

per revolution.[9,10] In the theories of Birkhoff and Belinfante we obtain, respectively,

$$\Delta\tilde{\omega} = -\frac{3\pi \sqrt{\varkappa m}\, \Omega l^2}{5c^2 p^{3/2} (1 - e^2)^3} (3 \cos i - 1), \tag{8}$$

$$\Delta\omega = \frac{4\pi \sqrt{\varkappa m}\, \Omega l^2}{5c^2 p^{3/2} (1 - e_0^2)^3} [(7 - 3 \cos 2\omega_0 - 10.5 \sin^2 i \cos 2\omega_0) \cos i + 6 \cos^2 i - 1]. \tag{9}$$

In the theory of Belinfante we also obtain, besides the effect (9), an increase in the major half axis and in the eccentricity of the orbit, given by

$$\Delta a = \frac{36\pi e_0 \sqrt{\varkappa m}\, \Omega l^2 \sin^2 i \cos i}{5c^2 (1 - e_0^2)^{5/2} \sqrt{a_0}} (2 \sin 2\omega_0 + 1), \tag{10}$$

$$\Delta e = \frac{4\pi \sqrt{\varkappa m}\, \Omega l^2}{5c^2 a_0^{3/2}} (6 + 4{,}5 e_0 \sin 2\omega_0). \tag{11}$$

per revolution. Here i is the inclination of the orbit, ω_0 is the longitude of the perihelion, Ω is the angular velocity of the rotation, and l is the radius of the central body (the index 0 characterizes the initial values of the corresponding constants). Although the quantity (10) is also very small (for Mercury, $e \approx 0.2$; $a \approx 5.8 \times 10^{12}$ cm, $i = 7°$, $\Delta a = 1$ cm), it does have fundamental importance in that it indicates that the planetary orbits are not stationary in the theory of Belinfante.

In conclusion I express my deep gratitude to Prof. V. L. Ginzburg for his guidance, his valuable comments, and a discussion of this work.

---

[1] G. D. Birkhoff, Proc. Nat. Acad. Sci., USA **29**, 231 (1943) and **30**, 324 (1944).

[2] F. J. Belinfante and J. C. Swihart, Ann. of Phys. **1**, 168 and 196 (1957) and **2**, 88 (1957).

[3] M. Moshinsky, Phys. Rev. **80**, 514 (1950).

[4] V. L. Ginzburg, Usp. Fiz. Nauk **59**, 5 (1956) and **63**, 119 (1957).

[5] H. Weyl, Amer. J. Math. **66**, 591 (1944).

[6] F. J. Belinfante, Phys. Rev. **98**, 1175 (1955) and **95**, 630 (1954).

[7] A. A. Borgardt, JETP **34**, 1632 (1958), Soviet Phys. JETP **7**, 1121 (1958).

[8] P. G. Bergmann, Introduction to the Theory of Relativity, Prentice Hall, N. J., (1942).

[9] J. Lense and H. Thirring, Phys. Z. **19**, 156 (1918).

[10] N. St. Kalitzin, Nuovo cimento **9**, 365 (1958).

Translated by R. Lipperheide
168

ON THE POLARIZATION OF THE ELECTRONS IN BREMSSTRAHLUNG PROCESSES

A. A. KRESNIN

Submitted to JETP editor June 5, 1959

J. Exptl. Theoret. Phys. (U.S.S.R.) **37**, 872-873 (September, 1959)

THE polarization effects in the bremsstrahlung of electrons have been investigated in detail in a number of papers.[1-3] However, the question of the change of polarization of the electron beam due to the bremsstrahlung process has received almost no attention.

To investigate this question, we use the method developed by Lipps and Tolhoek[4] and Rozentsveĭg and the author.[5] We shall describe the state of polarization of the incoming electrons with momentum $\mathbf{p}_1$ by the density matrix

$$\rho(\zeta_1, \mathbf{p}_1) = \eta^{(+)}(\mathbf{p}_1)\tfrac{1}{2}(1 + \zeta\Sigma\gamma_4)\,\eta^{(+)}(\mathbf{p}_1),$$

where

$$\eta^{(+)}(\mathbf{p}) = (m - i\hat{p})\gamma_4/2\varepsilon, \quad \Sigma = i\gamma\gamma_4\gamma_5.$$

The vector $\boldsymbol{\zeta}$, which characterizes the polarization of the electron in the laboratory system, is connected with the polarization vector $\boldsymbol{\zeta}^0$ in the rest system of the electron by the relation

$$\boldsymbol{\zeta}^0 = \boldsymbol{\zeta} - \mathbf{p}(\boldsymbol{\zeta}\mathbf{p})/\varepsilon(\varepsilon + m),$$

where ϵ is the energy of the electron.

The vector $\boldsymbol{\zeta}_2$, which describes the state of polarization of the electrons emitting the bremsstrahlung quantum, is given by

$$\boldsymbol{\zeta}_2 = \mathrm{Sp}\,[\Sigma\eta^{(+)}(\mathbf{p}_2)\,S\eta^{(+)}(\mathbf{p}_1)\,\rho(\zeta_1, \mathbf{p}_1)\;\eta^{(+)}(\mathbf{p}_1)\,S^+\eta^{(+)}(\mathbf{p}_2)]/Q,$$

$$Q = \mathrm{Sp}\,[\eta^{(+)}(\mathbf{p}_2)\,S\eta^{(+)}(\mathbf{p}_1)\,\rho(\zeta_1, \mathbf{p}_1)\,\eta^{(+)}(\mathbf{p}_1)\,S^+],$$

where S is the scattering matrix element for the bremsstrahlung process. Here **k** and ω are the wave vector and the energy of the emitted photon; the indices 1 and 2 refer to the initial and final states of the electron, respectively. As a result of the calculations we obtain

$$\begin{aligned} Q\boldsymbol{\zeta}_2 = {} & Q\boldsymbol{\zeta}_1 - (p_2k)^{-2}\{-\varepsilon_1(p_1k)(p_2k)\boldsymbol{\zeta}_1 + m^2\varepsilon_1(\mathbf{k} - \mathbf{p}_1)(\boldsymbol{\zeta}_1, \mathbf{k} + \mathbf{p}_1 + \mathbf{p}_2) + \varepsilon_1[(p_2k) - (\overset{*}{p}_1p_2)]\,\mathbf{p}_2(\boldsymbol{\zeta}_1\mathbf{k}) \\ & + [m^2\varepsilon_2 - \omega(p_1p_2) + \omega(p_2k) + \varepsilon_2(p_1k)](\boldsymbol{\zeta}_1\mathbf{p}_1)\,\mathbf{p}_2 + \varepsilon_1[m^2 + (\overset{*}{p}_1k)](\boldsymbol{\zeta}_1\mathbf{p}_2)\,\mathbf{p}_2\} - (p_1k)^{-2}\{-\varepsilon_1(p_1k)(p_2k)\boldsymbol{\zeta}_1 \\ & + m^2\varepsilon_1(\boldsymbol{\zeta}_1, \mathbf{k} + \mathbf{p}_2)(\mathbf{k} - \mathbf{p}_1) + m^2(\varepsilon_2 - \omega)(\boldsymbol{\zeta}_1\mathbf{p}_1)(\mathbf{k} - \mathbf{p}_1) + \varepsilon_1[(\overset{*}{p}_2k) - (\overset{*}{p}_1p_2)](\boldsymbol{\zeta}_1\mathbf{k})\,\mathbf{p}_2 \\ & + [m^2\varepsilon_2 + \varepsilon_2(p_1k) + \omega(\overset{*}{p}_1p_2) - \omega(\overset{*}{p}_2k)](\boldsymbol{\zeta}_1\mathbf{p}_1)\,\mathbf{p}_2 + \varepsilon_1[m^2 + (p_1k)](\boldsymbol{\zeta}_1\mathbf{p}_2)\,\mathbf{p}_2\} - [2/(p_1k)(p_2k)] \\ & \times\{\varepsilon_1[(p_1k)(p_2k) - \omega^2(p_1p_2) - \omega^2m^2]\boldsymbol{\zeta}_1 + \varepsilon_1(p_1p_2)(\boldsymbol{\zeta}_1\mathbf{k})\,\mathbf{k} - [m^2\varepsilon_1 + \omega(p_1p_2) - \varepsilon_2(p_1k)](\boldsymbol{\zeta}_1\mathbf{p}_1)\mathbf{k} - \varepsilon_1[m^2 + (p_1k)](\boldsymbol{\zeta}_1\mathbf{p}_2)\,\mathbf{k} \\ & + \varepsilon_1[m^2 - p_2k](\boldsymbol{\zeta}_1\mathbf{k})\,\mathbf{p}_1 + [\varepsilon_1(p_2k) - \varepsilon_2(p_1k) - \varepsilon_2(p_1p_2)](\boldsymbol{\zeta}_1\mathbf{p}_1)\,\mathbf{p}_1 + \varepsilon_1[(p_2k) - (p_1k) - (p_1p_2)]\,\mathbf{p}_1(\boldsymbol{\zeta}_1\mathbf{p}_2) \\ & + \varepsilon_1[(\overset{*}{p}_1p_2) - \varepsilon_2\omega](\boldsymbol{\zeta}_1\mathbf{k})\,\mathbf{p}_2 + [\varepsilon_2(p_1p_2) - \varepsilon_1(p_2k) - \varepsilon_1\varepsilon_2\omega](\boldsymbol{\zeta}_1\mathbf{p}_1)\,\mathbf{p}_2 + \varepsilon_1[(p_1p_2) - (p_2k) - \varepsilon_2\omega](\boldsymbol{\zeta}_1\mathbf{p}_2)\,\mathbf{p}_2\}, \end{aligned} \tag{1}$$

$$\begin{aligned} Q = {} & \frac{\varepsilon_1}{(p_2k)^2}[-m^4 - m^2(\overset{*}{p}_1p_2) + m^2(p_2k) - m^2(\overset{*}{p}_1k) - (p_1k)(p_2k)] + \frac{\varepsilon_1}{(p_1k)^2}[-m^4 - m^2(\overset{*}{p}_1p_2) + m^2(\overset{*}{p}_2k) - m^2(p_1k) - (p_1k)(\overset{*}{p}_2k)] \\ & + \frac{2\varepsilon_1}{(p_1k)(p_2k)}[-m^2\omega^2 - m^2(p_1p_2) - (p_1p_2)(\overset{*}{p}_1p_2) + (p_2k)(\overset{*}{p}_1p_2) - (p_1k)(\overset{*}{p}_1p_2) - \omega^2(p_1p_2) + \varepsilon_1\omega(p_2k) + \varepsilon_2\omega(p_1k)], \end{aligned} \tag{2}$$

where

$$(p_1k) = \mathbf{p}_1\mathbf{k} - \varepsilon_1\omega, \quad (\overset{*}{p}_1k) = \mathbf{p}_1\mathbf{k} + \varepsilon_1\omega \quad \text{etc.}$$

The expression for Q coincides, up to a factor, with the bremsstrahlung cross section computed from the Bethe-Heitler formula.

In some special cases the expression (1) can be considerably simplified.

In the nonrelativistic limit $(\epsilon_1, \epsilon_2 \sim m)$ we obtain $\boldsymbol{\zeta}_2^0 = \boldsymbol{\zeta}_1^0$, i.e., the polarization of the beam does not change.

In the limiting case of extremely soft bremsstrahlung quanta $(\omega \rightarrow 0$, i.e., $\epsilon_2 \approx \epsilon_1 = \epsilon)$ we have

$$\boldsymbol{\zeta}_2 = \boldsymbol{\zeta}_1 + \frac{(\boldsymbol{\zeta}_1, \mathbf{p}_1 + \mathbf{p}_2)}{m^2 + \varepsilon^2 + \mathbf{p}_1\mathbf{p}_2}(\mathbf{p}_2 - \mathbf{p}_1). \tag{3}$$

Going over to the vector $\boldsymbol{\zeta}_2^0$, we see that this vector, while preserving its absolute magnitude, is rotated around the normal to the $\mathbf{p}_1$, $\mathbf{p}_2$ plane through the angle φ, given by

$$\tan\varphi = \frac{(\gamma - 1)[(\gamma + 1) + (\gamma - 1)\cos\vartheta]}{[2\gamma + (\gamma^2 - 1)\cos\vartheta + (\gamma - 1)^2\cos^2\vartheta]}\sin\vartheta, \tag{4}$$

where $\gamma = \epsilon/m$. For $\gamma \rightarrow 1$ we have $\varphi \rightarrow 0$, and for $\gamma \rightarrow \infty$: $\varphi \rightarrow \vartheta$.

[1] M. M. May, Phys. Rev. **84**, 265 (1951).

[2] Vysotskiĭ, Kresnin, and Rozentsveĭg, JETP **32**, 1078 (1957), Soviet Phys. JETP **5**, 883 (1957).

[3] K. W. McVoy, Phys. Rev. **111**, 1333 (1958).

[4] F. W. Lipps and H. A. Tolhoek, Physica **20**, 85 (1954).

[5] A. A. Kresnin and L. N. Rozentsveĭg, JETP **32**, 353 (1957), Soviet Phys. JETP **5**, 288 (1957).

Translated by R. Lipperheide
169

THE $\mu \to e + \gamma$ *AND* $\mu \to e + \nu + \bar{\nu} + \gamma$ *DECAYS*

Yu. S. KRESTNIKOV, A. G. MESHKOVSKIĬ,
Ya. Ya. SHALAMOV, V. A. SHEBANOV, and
I. Yu. KOBZAREV

Submitted to JETP editor June 9, 1959

J. Exptl. Theoret. Phys. (U.S.S.R.) **37**, 873-875 (September, 1959)

THE main characteristics of universal A-V interaction can be explained by the hypothesis of the existence of an intermediate boson of large mass.[1] One of the consequences of this hypothesis is the possibility of μ-meson decay according to the scheme $\mu \to e + \gamma$. For a point A-V interaction such a decay is forbidden. Feinberg[2] calculated the probability of the decay $\mu \to e + \gamma$ and showed that the ratio $\rho_1 = R(\mu \to e + \gamma)/R(\mu \to e + \nu + \bar{\nu})$ depends on the cutoff parameter Λ. If $\Lambda = M$, where M is the boson mass, then $\rho_1 \cong 10^{-4}$. For $\Lambda < M$, ρ_1 can be arbitrarily small.

In the present work, a search for the decay $\mu \to e + \gamma$ was made, using a 17-liter freon bubble chamber, sensitive to γ rays.[3] The chamber was placed in the external π^+ beam of the synchrocyclotron of the Joint Institute for Nuclear Research. π^+ mesons of energy approximately 200 Mev were slowed by a graphite filter, and stopped inside the chamber. About 20,000 stereophotographs were obtained and scanned twice.

In the scanning, a search was made for cases in which the π-μ-e decay was accompanied by an electron-positron pair directed along and following the end of a π- or μ-meson track. The direction of the pair corresponded to the direction of flight of the γ ray to within an accuracy of $\sim 5-7°$, and the length of the track of the μ meson from the π-meson decay was 0.16 cm. Therefore, the case in which the π-μ-e decay was accompanied by a directed pair could relate to one of three processes:

$$\mu \to e + \nu + \bar{\nu} + \gamma, \qquad (1)$$

$$\pi \to \mu + \nu + \gamma, \qquad (2)$$

$$\mu \to e + \gamma. \qquad (3)$$

In the decay (3) the angle between electron and γ ray is 180°. In 91,000 π-μ-e decays, not a single such case was found. From this, knowing the efficiency of the chamber for detecting γ rays, it is possible to determine an upper limit for the quantity ρ_1. The efficiency was calculated on an electronic computer for various γ-ray energies by the Monte-Carlo method, taking into account the distribution of the number of π mesons stopping inside the chamber. The efficiency turned out to be equal to 0.253 for the decay (3). From this, $\rho_1 \leq 4.3 \times 10^{-5}$. This quantity is in agreement with results of experiments in which the decay (3) was studied using counter methods.[4-6]

In scanning the photographs, cases of directed pairs with various angles $(e, \gamma) < 180°$ were found. One of these cases is shown in Fig. 1. We interpret

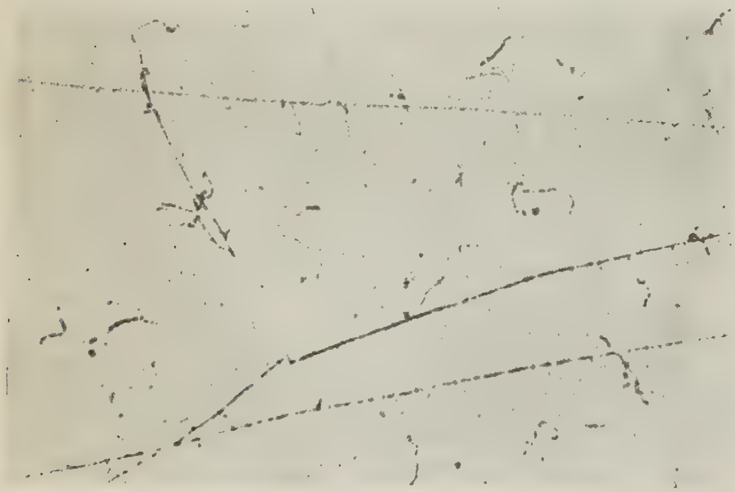

FIG. 1. Radiative decay of a μ meson by scheme (1).

No. p/p	Angle between electron and γ ray, degrees	Electron energy, Mev	γ-ray energy, Mev	Energy of the decay products, Q, Mev
1	52±3	>1	>16	$\geqslant 35$
2	61±2	>40	>15	$\geqslant 105$
3	76±2	>11	>19	$\geqslant 55$
4	98±3	>14	>18	$\geqslant 53$
5	101±2	>15	>24	$\geqslant 65$
6	120±2	>13	>13	$\geqslant 40$
7	128±3	>15	>31	$\geqslant 72$
8	143±4	>13	>13	$\geqslant 35$
9	144±2	>7	>8	$\geqslant 21$
10	151±4	>15	>20	$\geqslant 44$

such an event as the result of a radiative decay of a μ meson according to the scheme (1). This decay has not been observed before experimentally.

All of the cases in which the γ-ray energy was $\gtrsim 15-20$ Mev and the angle $(e, \gamma) \gtrsim 50-60°$ are given in the table. In addition, two doubtful cases, not given in the table, were found, so that the total number was $12^{+3.5}_{-5.5}$. In the table we indicate results of measurements of the angle (e, γ), the energy of the γ-ray and electron energy, and also the lower limit Q to the energy of the decay products, calculated from conservation laws.

For process (1), the kinetic energy of the decay products $Q_1 = 105.2$ Mev; for process (2), $Q_2 = 33.9$ Mev. As follows from the table, there is no case with $Q > Q_1$. In addition, in only one case (No. 9) is it possible that $Q < Q_2$, so that the interpretation of this event is ambiguous [(1) or (2)]. The remaining cases give $Q > Q_2$, and can therefore be related to the decay (1). The small contribution of decay (2) can be confirmed from measurements of the probability of this decay.[7] Calculations show that the background from the decay (2) constitutes about 3%.

In scanning the photographs, 109 randomly oriented pairs were found. In order to evaluate the background of random superpositions, a search was made for cases in which these pairs coincided with six markings made on the inside of the glass of the chamber. No such cases were observed. Another way of measuring the background consisted in measuring, for all observed pairs, the angle of revolution necessary to turn the pair towards the point at which the μ-meson stopped. Results of the measurements are given in Fig. 2. The distribution has a peak at 0°, coming from the effect studied. The level of events outside of the region near to 0° corresponds to random superpositions. From the graph it can be seen that the ratio of this level to that of the effect is approximately 0.2, but since there measurements were carried out for only one of the stereophotographs, the actual background is substantially lower (roughly 10 times) and, consequently, does not exceed a few per cent.

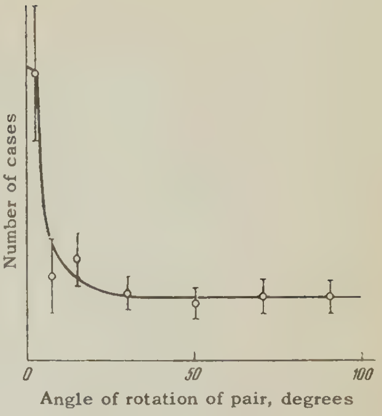

FIG. 2. Distribution of pairs with angle necessary to turn them into the point at which the μ meson stopped.

The ratio, calculated from 12 cases and taking into account the efficiency for detecting γ rays, was

$$\rho_2 = R(\mu \rightarrow e + \nu + \bar{\nu} + \gamma) / R(\mu \rightarrow e + \nu + \bar{\nu})$$

$$= \left(0.80^{+0.24}_{-0.36}\right) \cdot 10^{-3}.$$

In order to compare this result with theory, we calculated the total probability and angular distribution of the decay (1) for various values of the minimum detection energy of γ-rays for the A-V variant of interaction. We started with work of Lenard[8] in which an expression for the differential probability for the decay (1) was obtained. The calculations showed that the theoretical value of the quantity ρ_2 should lie within the limits $1.02 \times 10^{-3} < \rho_2 < 1.80 \times 10^{-3}$. These limits correspond to the indeterminacy in the minimum values of the angle (e, γ) and γ-ray energy, referred to above. We see that the experimental value of ρ_2 is near to the theoretical one.

We would like to express our gratitude to Academician A. I. Alikhanov for discussion and interest in the work, M. F. Lomanov, Yu. I. Makarov and V. I. Smetanina for help in the work, I. S. Bruk for the opportunity of carrying out the calculations on the M-2 electronic computer of the Institute of Electronic and Control Machines of the Academy of Sciences, U.S.S.R., and R. A. Ioffe for carrying out these calculations.

---

[1] R. P. Feynman and M. Gell-Mann, Phys. Rev. **109**, 193 (1958).

[2] G. Feinberg, Phys. Rev. **110**, 1482 (1958).

[3] Blinov, Lomanov, Meshkovskiĭ, Shalamov, and Shebanov, Приборы и техника эксперимента (Instruments and Measurement Engg.) 1, 35 (1958).

[4] S. Lokanathan and J. Steinberger, Phys. Rev. 98, 240 (1955).

[5] Davis, Roberts, and Zipf, Phys. Rev. Letters 2, 211 (1959).

[6] Berley, Lee, and Bardon, Phys. Rev. Letters **2**, 357 (1959).

[7] C. Castagnoli and M. Muchnik, Phys. Rev. **112**, 1779 (1958).

[8] A. Lenard, Phys. Rev. **90**, 968 (1953).

Translated by G. E. Brown
170

ON THE CONNECTION OF ISOTOPIC SPIN AND STRANGENESS WITH THE BEHAVIOR OF SPINORS UNDER INVERSION

A. M. BRODSKIĬ and D. D. IVANENKO

Moscow State University

Submitted to JETP editor June 10, 1959

J. Exptl. Theoret. Phys. (U.S.S.R.) **37**, 876-877 (September, 1959)

THE usual treatments of isotopic and strangeness properties involve an isotopic space of two, three, or four dimentions, sometimes with the possibility of transitions to a pseudo-Euclidean space. One can, however, try to describe these properties within the framework of ordinary space, by bringing in hitherto unused possibilities of different behaviors of spinors under inversions and taking into account nonconservation of the parity P. The interpretation of isotopic properties in the framework of ordinary space that we propose here is a development of earlier more special considerations.[1-8]

As has been pointed out,[8,9] under both space and time reflections spinors can behave in different ways, with transformation matrixes that differ by factors -1, i, γ_5, or products of these. In addition to $\psi' = \gamma_4\psi$ (under $x'_{1,2,3} = -x_{1,2,3}$), etc., there are also the possibilities $\psi' = \gamma_5\gamma_4\psi$ or $\psi' = i\gamma_4\psi$, etc. Thus there arise different spinor representations of the Lorentz group, some of which are equivalent by unitary transformations (but differ from each other under charge conjugation).

A more important difference between spinors, not having the property of unitary equivalence, appears when the additional factors that have been mentioned occur under space reflections only or under time reflection only. We shall characterize spinors by two pairs of indices a, b and α, β. The index a takes one of the two values 1 or 2, depending on whether or not the additional factor γ_5 is used for space reflection. Similarly, the index b = 1, 2 characterizes the geometrical time reflection T^0, which can be replaced by the Schwinger reflection $T^S = T^0 \times (\tilde{\ }) = TC$, where $(\tilde{\ })$ denotes transposition in Hilbert space and T the Wigner time reversal. The indices α, β run through the four values (0, 1, 2, 3) corresponding to the appearance of the additional factors i^α for space inversion and i^β for time inversion. The essential difference between two spinors is characterized by the differences $(a-b)$ and $(\alpha-\beta)$, or, more precisely, by their absolute values. In particular, the "mixed" spinors with $(a-b) \neq 0$ that we introduced earlier[8] provide a realization, without doubling of the number of components, of the "anomalous" representation, for which $T^0P = +PT^0$, in contrast to the usual anticommutation. For the "mixed" spinors the construction of the Dirac equation with a mass is possible only with violation of invariance with respect to P, together with preservation of the invariance with respect to the strong (combined) inversion $P^S = PC$.[8]

When there is invariance only with respect to P^S and T^S we have the question of the characteristics of spinors of distinct types. To solve it we introduce the self-adjoint ("large") spinors

$$\Psi(1) = {}^1/_2\,[(1+i\gamma_5)\,\psi + (1-i\gamma_5)\,\psi^c],$$
$$\Psi(2) = {}^1/_2\,[(1-i\gamma_5)\,\psi + (1+i\gamma_5)\,\psi^c],$$
$$\Psi^c(1,2) = C\Psi^*(1,2) = \Psi(1,2), \qquad \gamma_5^2 = -1. \qquad (1)$$

Under the strong inversions of the small ψ the quantities $\Psi(1,2)$ transform linearly, each one by itself, in complete analogy with the transformation of the ordinary ψ under geometrical inversions. Corresponding to the phase transformation $\psi' = e^{i\alpha}\psi$ we have $\Psi'(1,2) = \exp(\pm\gamma_5\alpha)\cdot\Psi(1,2)$. For self-adjoint small ψ (neutrino), $\Psi(1)$ and $\Psi(2)$ coincide. An additional difference between $\Psi(1)$ and $\Psi(2)$ is due to the possibility of different or equal relative signs under inversions. Self-adjoint ψ's are possible only for those $\Psi(1,2)$ for which these signs are the same.

For characterizing the behavior of spinors under the strong inversions P^S, T^S we need only the pairs of indices $J = a + \alpha$, $K = b + \beta$, and accordingly the one difference

$$N = J - K = (a-b) + (\alpha-\beta)\,(\mathrm{mod}\ 2). \qquad (2)$$

Here a, b, α, β relate to the original small spinors ψ from which the $\Psi(1,2)$ are constructed. $\Psi(1)$ and $\Psi(2)$ form a doublet, whose components go over into each other under geometrical inversions or charge conjugation of the original ψ. These transformations, together with the Salam-Touschek transformation, can be put in basic correspondence with three-dimensional isotopic rotations.[10] The construction of bilinear combinations (bosons) having the usual covariance properties (scalar, pseudoscalar, vector, etc.) from spinors of which the first has $N = 1$ ("mixed") and the second $N = 0$ ("normal") is impossible even when we use the strong inversions. It is also impossible to construct bosons that behave in the usual way under geometrical inversions from spinors that differ in the values of $(a-b)$ or $(\alpha-\beta)$(modulo 2). This provides a basis for identifying, for example, N with the baryon number, $(\alpha-\beta)$ with the strangeness S, and $(a-b)$ with the hypercharge Y.

We then have the usual relation $N = Y - S$. Corresponding numbers can be assigned to bosons; then bosons constructed from spinors that differ in N, S, Y form doublets, whose components transform into each other under inversions, i.e., particles of the type of the K mesons. We then get new conservation laws, in which N is conserved strictly (modulo 4), and S and Y are conserved when there is invariance only under the geometrical inversions. Therefore the fact of simultaneous violation of the conservation of P, S, Y, which has seemed accidental, can now receive a legitimate explanation. If we take as a universal invariance condition the conservation of P^S and T^S, then when there is violation of the isotopic group the ordinary parity P is also not conserved.[11]

We point out that it is convenient to carry out the construction of the interaction Lagrangian by means of the $\Psi(1,2)$, since then the invariance with respect to P^S and T^S is most explicitly manifest, and, for example, it can be seen why for two-component spinors one is confined (Feynman) to the vector and pseudovector terms, which are invariant under the Salam-Touschek transformations for the large $\Psi(1,2)$.

In conclusion we remark that it is most natural to characterize the leptons by "normal" spinors, assigning different factors ±1, i, γ_5 to the particles e, ν, μ, and the baryons by spinors that are "mixed" under strong inversions ($N \neq 0$); bosons are assigned bilinear combinations of spinors. In view of the absence of absolute conservation of the number of baryons in this formalism, they can in principle be converted into mesons and leptons; owing, however, to the existing conservation laws and the necessity of contact interaction of several particles, the probability for this conversion will be extremely small.

---

[1] C. N. Yang and J. Tiomno, Phys. Rev. **79**, 495 (1950).

[2] M. Mirianashvili, Тр. ин-та физики АН Груз ССР (Trans. Inst. Phys. Acad. Sci. Georgian SSR, No. 4 (1958).

[3] A. Salam, Proc. Seventh Rochester Conference, 1957.

[4] J. C. Taylor, Nucl. Phys. **3**, 606 (1957). J. A. McLennan, Jr., Phys. Rev. **109**, 986 (1958).

[5] F. Gürsey, Phys. Rev. Letters **1**, 98 (1958).

[6] V. I. Ogievetskiĭ and Chou Kuang-Chao, JETP **36**, 264 (1959), Soviet Phys. JETP **9**, 179 (1959); Nucl. Phys. **10**, 235 (1959).

[7] G. A. Sokolik, JETP **36**, 1098 (1959), Soviet Phys. JETP **9**, 781 (1959).

[8] A. M. Brodskiĭ and D. D. Ivanenko, JETP **33**, 910 (1957), **36**, 1279 (1959), Soviet Phys. JETP **6**, 700 (1958), **9**, 907 (1959); Dokl. Akad. Nauk SSSR **120**, 995 (1958), Soviet Phys.–Doklady **3**, 608 (1959).

[9] I. S. Shapiro, JETP **23**, 412 (1952).

[10] F. Gürsey, Nuovo cimento **7**, 411 (1958).

[11] V. G. Solov'ev, JETP **33**, 537 (1957), Soviet Phys. JETP **6**, 419 (1958).

Translated by W. H. Furry
171

BETA DECAY OF THE NEGATIVE MUON

Yu. A. BUDAGOV, S. VIKTOR, V. P. DZHELEPOV,
P. F. ERMOLOV, and V. I. MOSKALEV

Joint Institute for Nuclear Research

Submitted to JETP editor June 13, 1959

J. Exptl. Theoret. Phys. (U.S.S.R.) **37**, 878-880
(September, 1959)

ALL experiments on pion beta decay performed to date are devoted to β decay of the stopped positive mesons.[4-8] In two recent papers, the following result is obtained for the relative probability of this process:

$$(\pi^+ \rightarrow e^+ + \nu)/(\pi^+ \rightarrow \mu^+ + \nu) \approx 1\cdot 10^{-4} \pm (20-40\%).$$

This agrees with the value 1.3×10^{-4} which follows from the universal V-A theory of β decay.[7] It follows from relativistic invariance (CPT theorem)[8] that this process should have the same relative probability for negative pions as for the positive ones. However, we deemed it important to determine the relative probability of β decay of negative pions by direct experiment.

Unlike $\pi^+ \rightarrow e^+$ decay, $\pi^- \rightarrow e^-$ decay can be observed only in flight. We therefore sought for

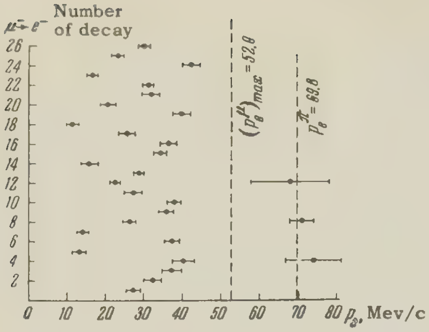

FIG. 1

β decay of negative pions among the data obtained in a diffusion chamber operating in a 9000-gauss field, used to study the interaction of 130-Mev and 160-Mev negative pions with protons as well as rare types of neutral-pion decay.[9,10] By thrice scanning approximately 100,000 stereographs, we found 29 decays in which the secondary particles were deflected by $\theta > 20°$ (the maximum angle for π-μ decay at 130 Mev is 10°). In all cases the primary and secondary particles had minimal ionizations (estimated visually). As a result of the data reduction (the method used to measure momenta and angles was analogous to the one previously described[11]), 26 cases were identified as $\mu^- \to e^-$ decays and 3 cases were classified as $\pi^- \to e^-$ decays. It should be noted that the conditions for separating the $\pi \to e$ and $\mu \to e$ decays in flight by their momenta are somewhat better than for stopped π and μ mesons, for in this case the ratio of the momentum of the $\pi \to e$ decay electron to the maximum $\mu \to e$ decay electron momentum possible at the given angle exceeds, over a wide range of angles, the ratio of these momenta for stopped π and μ mesons. Another favorable circumstance was the lower background of the $\mu \to e$ decays. Figure 1 shows the distribution of the momenta of the electrons from $\pi^- \to e^-$ decay (the three points on the right) and $\mu^- \to e^-$ decay, in the rest system of the π^- and μ^- mesons. The errors listed are the maximum errors in the measurement of the radii of curvatures of the π^- and μ^- mesons and electrons. A photograph of one of the $\pi^- \to e^- + \nu$ decay events, obtain in a diffusion chamber, is shown in Fig. 2.

The reduced data for the $\pi^- \to e^-$ decays are listed in the table.

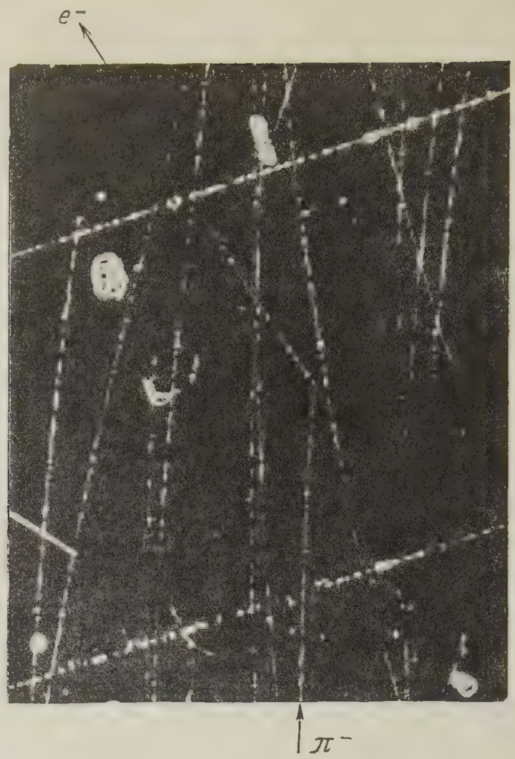

FIG. 2

As can be seen from Fig. 1 and from the table, the electron momenta in the π^--meson rest system are close to 69.8 Mev/c. If the primary particle is assumed to be the μ^- meson, then in the μ^--meson rest system the electron momenta for these three cases are 80 ± 8, 77 ± 4, and 70 ± 11 Mev/c, respectively, whereas the maximum electron momentum in $\mu \to e$ decay is 52.9 Mev/c.

Other possible processes, which may imitate $\pi^- \to e^-$ decays (inelastic scattering of π^- mesons by complex impurity nuclei in the gas in the chamber, electron bremsstrahlung, successive $\pi^- \to \mu^- \to e^-$ decay in flight with short μ^--meson track) have very low probabilities.

To determine the relative probability of the π^--meson β decay it is necessary to determine the total number of $\pi^- \to \mu^-$ decays. This number, $(5.6 \pm 0.3) \times 10^4$, was calculated from the known total path length of the π^- mesons in the chamber, which amounted to $(7.8 \pm 0.4) \times 10^7$ cm, and from the momentum, $p_\pi = 253$ Mev/c. Considering the detection efficiency of $\pi^- \to e^-$ decays to be the same as that of $\mu^- \to e^-$ decays, which has been

Number of $\pi^- \to e^-$ event	Laboratory system			Rest system of π^- meson	
	π^- meson momentum (Mev/c)	electron momentum (Mev/c)	θ deg	electron momentum (Mev/c)	θ deg
1	228±10	104±8	42.5±0.5	74±7	108±2
2	207±11	103±3	42±0.5	71±4	102±2
3	266±6	156±26	26±0.5	68±11	86±1

estimated to be 70%, and taking into account the contribution from the angle range $\theta < 20$, the relative probability of π^--meson β decay becomes

$$(\pi^- \to e^- + \bar{\nu})/(\pi^- \to \mu^- + \bar{\nu}) = (1.2 \pm 0.7)\cdot 10^{-4}.$$

Within the limits of errors, this quantity agrees with the relative probability of β decay of positive mesons and with the aforementioned value calculated on the basis of the universal V–A theory of β interaction.

The authors express their gratitude to T. S. Sazhneva, L. I. Krasnoslobdtseva, and Yu. L. Saĭkina for help in scanning the photographs.

---

[1] H. L. Friedman and J. Rainwater, Phys. Rev. **84**, 684 (1951).

[2] S. Lokanathan and J. Steinberger, Nuovo cimento **10**, 151 (1955).

[3] H. L. Anderson and C. M. G. Lattes, Nuovo cimento **6**, 1356 (1957).

[4] Fazzini, Fidecaro, Merrison, Paul, and Tollestrup, Phys. Rev. Lett. **1**, 247 (1958).

[5] Impeduglia, Plano, Prodell, Samios, Schwartz, and Steinberger, ibid. **1**, 249 (1958).

[6] Anderson, Fujii, Miller, and Tau, ibid. **2**, 53 (1959).

[7] M. Ruderman and R. Finkelstein, Phys. Rev. **76**, 1458 (1949).

[8] G. Lüders and B. Zumino, Phys. Rev. **106**, 1458 (1957).

[9] Budagov, Viktor, Dzhelepov, Ermolov, and Moskalev, Материалы совещания по камерам Вильсона, диффузионным и пузырьковым камерам, (Proceedings of the Conference on Cloud and Bubble Chambers), Joint Inst. for Nuclear Research, Dubna, 1958.

[10] Budagov, Viktor, Dzhelepov, Ermolov, and Moskalev, JETP **35**, 1575 (1958), Soviet Phys. JETP **8**, 1101 (1959).

[11] Budagov, Viktor, Dzhelepov, Ermolov, and Moskalev, JETP **36**, 1080 (1959), Soviet Phys. JETP **9**, 767 (1959).

Translated by J. G. Adashko
172

ON THE SUPERCONDUCTIVITY OF THE COMPOUND BiPt

N. N. ZHURAVLEV, A. A. STEPANOVA, and N. I. ZYUZIN

Moscow State University

Submitted to JETP editor June 13, 1959

J. Exptl. Theoret. Phys. (U.S.S.R.) **37**, 880-881 (September, 1959)

THE data of different authors on the transition temperature for the compound BiPt differ considerably one from another. According to Matthias[1] $T_c = 1.21°K$; Alekseevskiĭ found in one case $T_c = 2.4°K$ but other alloys of the composition BiPt did not become superconducting until 1.3° K.[2,3] We may, then, suppose that the different behavior of alloys with composition BiPt at helium temperatures is related to the conditions of preparation.

In their study of the phase diagram of the bismuth-platinum system, Zhuravlev and Kertes[4] found that the compound BiPt has only one crystallographic form, belonging to the hexagonal system with lattice spacings $a = 4.20$ A and $c = 5.55$ A, and has the AsNi type structure.[5,6]

We repeated the thermal analysis with differential measurement on a Pk-52 instrument and an x-ray examination from 20 to 600° C and confirmed the existence of only one crystalline form. The measurements showed that the NiAs structure was retained up to high temperatures and the coefficient of thermal expansion was derived. In the direction of the hexagonal axis $\alpha_{\|} = 4.0 \times 10^{-6} \pm 1.0 \times 10^{-6}$ deg^{-1}, and perpendicular to the axis $\alpha_{\perp} = 19.0 \times 10^{-6} \pm 2.0 \times 10^{-6}$ deg^{-1}.

We examined alloys that had various heat treatments and corresponded both to the stoichiometric composition BiPt (48.3% Pt by weight) and to higher and lower bismuth content (45 and 53% Pt by weight) than corresponds to BiPt. For alloys annealed and rapidly cooled from various temperatures which did not exceed the liquidus temperature for the given composition, the main phase (the compound BiPt) always had the AsNi type structure with $a = 4.315$ and $c = 5.490 \pm 0.005$ A.

If these same alloys were rapidly cooled from temperatures 50, 100 and 200° C above the liquidus point, then defect structures are formed.

A reduction in unit cell dimensions of the NiAs phase (BiPt) was found from x-ray powder photographs of these alloys, and the higher the temperature from which the alloys were cooled and the greater the bismuth content, the greater was the reduction in unit cell dimensions. The maximum reduction in volume of the unit cell was ~ 0.8% of the cell volume of the 48.3 wt % Pt alloy, obtained with an alloy containing 45 wt % Pt, quenched from 950° C (~ 200° above the liquidus line).

The difference in superconducting properties of various alloys prepared from bismuth and platinum and corresponding to the composition BiPt or close to it, is most likely due to the formation of a defect structure based on the BiPt structure. This is probably produced because of the high rate of cooling the liquid alloy, when on crystallizing into the NiAs structure all the vacant sites are not occupied by bismuth or platinum atoms. The defect structure is apparently formed with platinum deficiency. The decrease in unit cell dimensions leads to a reduction in the minimum bismuth-bismuth interatomic distance, which produces a change in T_c. This agrees well with the previously noted[7] increase in T_c with decreasing minimum bismuth-bismuth interatomic distance in superconducting bismuth compounds with the AsNi structure.

We are grateful to Professors G. S. Zhdanov and N. E. Alekseevskiĭ for discussion of the results.

---

[1] B. T. Matthias, Phys. Rev. **90**, 487 (1953).

[2] Alekseevskiĭ, Brandt, and Kostina, Izv. Akad. Nauk SSSR, Ser. Fiz. **16**, 233 (1952).

[3] N. E. Alekseevskiĭ and Yu. P. Gaĭdukov, JETP **25**, 383 (1953).

[4] N. N. Zhuravlev and L. Kertes, JETP **32**, 1313 (1957), Soviet Phys. JETP **5**, 1073 (1957).

[5] E. Zintl and H. Kaiser, Z. Anorg. Allgem. Chem. **211**, 113 (1933).

[6] V. P. Glagoleva and G. S. Zhdanov, JETP **25**, 284 (1953).

[7] Zhuravlev, Zhdanov, and Alekseevskiĭ, Вестник МГУ (Bulletin, Moscow State University), in press.

Translated by R. Berman
173

ON THE MAGNETO-ELECTRICAL EFFECT IN ANTIFERROMAGNETS

I. E. DZYALOSHINSKIĬ

Institute for Physical Problems, Academy of Sciences, U.S.S.R.

Submitted to JETP editor June 17, 1959

J. Exptl. Theoret. Phys. (U.S.S.R.) **37**, 881-882 (September, 1959)

LANDAU and Lifshitz[1] have shown that there may occur in some antiferromagnetic crystals a peculiar phenomenon, namely that if a crystal is placed in a constant magnetic (or electric) field, an electric (or magnetic) moment proportional to the field is produced in the crystal.

This phenomenon, which can naturally be called the magnetoelectric effect, is intimately connected with the magnetic symmetry of the substance. Indeed, the thermodynamic potential of such a solid must contain terms proportional to the product of the first powers of the electrical and magnetic field components ($\Phi \sim EH$). It is at once clear that this is impossible in a paramagnetic crystal, since its thermodynamic potential is invariant with respect to a change in the time direction ($t \rightarrow -t$, R-transformation) in which, as is well known, the magnetic field changes sign while the electrical field does not. The position is, however, essentially altered for substances which have a magnetic structure. The magnetic-symmetry group of such solids may either not contain the R-transformation at all, or may contain it only in the form of a combination with other symmetry elements, so that the appearance of terms proportional to EH in the thermodynamic potential turns out to be possible.

We should like to show here that among the well-known antiferromagnetic substances there is one, namely Cr_2O_3, where the magneto-electric effect should occur from symmetry considerations. The magnetic structure of Cr_2O_3 is well known from the neutron-diffraction studies of Brockhouse[2] and the susceptibility data (McGuire et al.[3]). It is easy to verify that the magnetic symmetry class of Cr_2O_3 consists of the following elements:

$$2C_3, \quad 3U_2, \quad IR, \quad 2S_6R, \quad 3\sigma_dR,$$

where C_3 is vertical axis of symmetry of third order, U_2 a horizontal symmetry axis of second order, I an inversion, S_6 a mirror axis of the sixth order, and σ_d a plane of symmetry.

The transformations of this class are invariants of two expressions linear in E and H: E_zH_z (the z axis is along the crystal axis) and $E_xH_x + E_yH_y$. The thermodynamic potential of Cr_2O_3 has therefore as a function of E and H the form

$$\Phi = -\frac{1}{8\pi}[\varepsilon_{\parallel} E_z^2 + \varepsilon_{\perp}(E_x^2 + E_y^2)]$$

$$-\frac{1}{8\pi}[\mu_{\parallel} H_z^2 + \mu_{\perp}(H_x^2 + H_y^2)]$$

$$-\frac{1}{4\pi}\alpha_{\parallel} E_z H_z - \frac{1}{4\pi}\alpha_{\perp}(E_x H_x + E_y H_y),$$

where $\epsilon_{\parallel}$ and $\epsilon_{\perp}$ are the longitudinal and perpendicular dielectric constants, $\mu_{\parallel}$ and $\mu_{\perp}$ the magnetic susceptibilities, and $\alpha_{\parallel}$ and $\alpha_{\perp}$ constants describing the magneto-electrical effect. Using the thermodynamic relations $4\pi\partial\Phi/\partial\mathbf{E} = -\mathbf{D}$ and $4\pi\partial\Phi/\partial\mathbf{H} = -\mathbf{B}$ we get the relations between the inductions and the field strengths:

$$D_z = \varepsilon_{\parallel} E_z + \alpha_{\parallel} H_z, \quad D_x = \varepsilon_{\perp} E_x + \alpha_{\perp} H_x,$$

$$D_y = \varepsilon_{\perp} E_y + \alpha_{\perp} H_y; \quad B_z = \mu_{\parallel} H_z + \alpha_{\parallel} E_z,$$

$$B_x = \mu_{\perp} H_x + \alpha_{\perp} E_x, \quad B_y = \mu_{\perp} H_y + \alpha_{\perp} E_y.$$

---

[1] L. D. Landau and E. M. Lifshitz, Электродинамика сплошных сред (Electrodynamics of Continuous Media), Gostekhizdat, 1958.

[2] B. N. Brockhouse, J. Chem. Phys. **21**, 961 (1953).

[3] McGuire, Scott, and Grannis, Phys. Rev. **98**, 1562 (1955).

Translated by D. ter Haar
174

NUCLEAR MOMENTS OF THE ODD ISOTOPES OF GADOLINIUM

N. I. KALITEEVSKIĬ, M. P. CHAĬKA, I. Kh. PACHEVA, and É. E. FRADKIN

Physics Institute of the Leningrad State University

Submitted to JETP editor June 19, 1959

J. Exptl. Theoret. Phys. (U.S.S.R.) **37**, 882-884 (September, 1959)

THE hyperfine structure of three lines of Gd I: 5015 A (z″G$_9$—a″F$_8$), 5103 A (z″G$_8$—a″F$_7$) and 5251 A (z″G$_8$—a″F$_8$) was investigated by means of a photoelectric spectrometer with a Fabry-Pérot interferometer.[1] The work was carried out using separated gadolinium isotopes of a high degree of enrichment (Gd^{155}—97.3%, Gd^{157}—91.4%). In agreement with paramagnetic measurements[2] it was shown unambiguously that the spin of both isotopes is $I = 3/2$. The value of the ratio of the magnetic moments $\mu_{155}/\mu_{157} = 0.79 \pm 0.02$ and the absolute values $\mu_{155} = -0.32 \pm 0.04$ and $\mu_{157} = -0.40 \pm 0.04$ agree satisfactorily within the indicated limits of error with earlier measurements.[2-4]

For the ratio of the quadrupole moments we obtain the value $Q_{155}/Q_{157} = 0.78 \pm 0.06$ which disagrees with Speck's investigation[4] in which he found that $Q_{155} \geq Q_{157}$. The absolute values of the quadrupole moments calculated from our experimental data ($Q_{155} = 1.6 \times 10^{-24}$ cm^2 and $Q_{157} = 2 \times 10^{-24}$ cm^2) are larger by almost a factor of two than those given by Speck, but it is difficult to estimate the error in the final result since the L-S coupling does not hold very well for the G-terms of gadolinium used by us, and this introduces a large indeterminacy in the estimate of the electronic matrix elements.

The values for the internal quadrupole moment $Q_0^{155} = 8 \times 10^{-24}$ cm^2 and $Q_0^{157} = 10 \times 10^{-24}$ cm^2 recalculated from the above data agree in order of magnitude with the values obtained by the method of Coulomb excitation of gadolinium nuclei.[5,6] The deformation parameters determined from our data are $\delta_{155} = 0.31$ and $\delta_{157} = 0.37$. The ratio $\delta_{155}/\delta_{157} = 0.8$ is directly obtained from the ratio of the quadrupole moments Q_{155}/Q_{157} and does not depend strongly on the possible error in the determination of the electronic wave functions. The values of the deformation parameters given above are in good agreement with the data on the variation of nuclear deformation in the series of rare earth elements obtained by the method of Coulomb excitation of even-even nuclei.[7]

By using these values of δ_{155} and δ_{157} and the values of μ_{155} and μ_{157} given above we made an estimate of g_K and g_R — the gyromagnetic ratios for the internal and the collective motions. The calculation of g_K was carried out in accordance with Nilsson's scheme, and in order to do this the expansion coefficients for the wavefunction of the unpaired nucleon tabulated by Nilsson[8] were extrapolated for the ground state of gadolinium ($N = 5$, $I = 3/2$, $h_{9/2}$) into the region of large nuclear deformations ($0.31 < \delta < 0.41$). As a result it was established that $g_{K155}/g_{K157} = 0.9 \pm 0.1$ and then $(g_R/g_K)_{157} = 1.1\,(g_R/g_K)_{155} \pm 0.2$. These relationships were obtained by utilizing only the relative values of $\delta_{155}/\delta_{157}$ and μ_{155}/μ_{157}, which are determined from the experimental data with a high degree of accuracy. The absolute values of g_K may be found with an accuracy determined by the error in the values of Q_{155} and Q_{157}. Calculations gave the values $g_{K\,155} = -0.8$ nuclear magnetons and $g_{K\,157} = -0.9$ nuclear magnetons, from which we obtain $g_{R\,155} = g_{R\,157} = 0.7$. This value differs appreciably from the approximate estimate $g_R \approx Z/A = 0.4$, and is in good agreement with the data of de Boer et al.,[6] but contradicts earlier measurements of Bjerregard and Meyer-Berkhout,[5] although the ratio $g_{K\,155}/g_{K\,157}$ determined by them experimentally is in complete agreement with the value obtained by us. This confirms to some extent the correctness of the extrapolation of Nilsson's data made by us into the region of deformations $\delta > 0.3$. Similar calculations made by Gauvin[9] for strongly deformed nuclei with an unpaired nucleon $(153 < A < 197)$ have shown that for a number of nuclei such an estimate leads to $g_R > Z/A$. The values obtained by him for g_K and g_R in the case of Gd^{155} agree with our estimate. In the case of Gd^{157} the estimates of g_K and g_R differ, since we based ours on the value $\delta_{157} = 0.37$, while Gauvin adopted $\delta_{157} = 0.31$. Gauvin discusses the possibility of a modification of the evaluation of g_K which would lead to the values of $g_R \approx Z/A$, but the new experimental data[6] on the value of g_R for Gd^{157} contradict such an estimate. Therefore an additional investigation of the odd isotopes of gadolinium by the method of Coulomb excitation is highly desirable.

The authors are grateful to V. S. Zolotarev for providing the separated isotopes and to L. K. Peker for valuable advice in the discussion of results.

---

[1] Kaliteevskiĭ, Malyshev, and Chaĭka, Оптика и спектроскопия (Optics and Spectroscopy) **6**, 820 (1959) [Am. Opt. Soc. Transl. p. 536].

[2] A. A. Manenkov and A. M. Prokhorov, JETP **33**, 1116 (1957), Soviet Phys. JETP **6**, 860 (1958).

[3] W. Low, Phys. Rev. **103**, 1309 (1956).

[4] D. R. Speck, Phys. Rev. **101**, 1725 (1956).

[5] I. H. Bjerregard and U. Meyer-Berkhout, Z. Naturfor. **11a**, 273 (1956).

[6] de Boer, Martin, and Marmier, Helv. Phys. Acta **31**, 578 (1958).

[7] Alder, Bohr, Huus, Mottleson, and Winther, Revs. Modern Phys. **28**, 432 (1956). [Russ. Trans. in the collection Деформация атомных ядер (Deformation of Atomic Nuclei), IIL, 1958].

[8] S. G. Nilsson, Kgl. Danske Videnskab. Selskab, Mat.-fys. Medd. **29**, 16, 1 (1955) [Russ. Transl. as in reference 5].

[9] J. N. L. Gauvin, Nucl. Phys. **8**, 213 (1958).

Translated by G. Volkoff
175

RESONANCE INTERACTION OF PIONS

V. S. BARASHENKOV and V. M. MAL' TSEV

Joint Institute for Nuclear Research

Submitted to JETP editor May 20, 1959

J. Exptl. Theoret. Phys. (U.S.S.R.) **37**, 884-886 (September, 1959)

In order to explain the maximum in the π^--p interaction at energy $E = 1$ Bev, Piccioni,[1] Dyson,[2] and Takeda[3] advanced the hypothesis of resonance interaction between π mesons. This hypothesis was also used to explain the high multiplicity of π mesons produced in nucleon-antinucleon annihilation[4,5] and to explain the inelastic (π^--p) scattering for $E \geq 1$ Bev.[6,8] However, the assumption of a resonance π-π interaction was not obligatory in all cases considered in these articles, since the experimental results could be explained in other ways.

It is of interest to consider what conclusions would follow from the assumption of a resonance π-π interaction in the case of inelastic interactions of particles at $E \gg 1$ Bev, where a large number of π mesons would be produced, and an assumption about the π-π interaction would have a considerable effect on the results of calculation. As an example, we consider inelastic π^--p collisions at $E = 5$ Bev. We considered this case in detail earlier[9] without taking account of a resonance π-π interaction.

We assume, as in reference 9, that statistical equilibrium is established for the K mesons in a spatial volume of radius $r_K = \hbar/m_K c$, and, for all other particles, in a spatial volume of radius $r_\pi = \hbar/m_\pi c$, where m_K and m_π are the masses of the K- and π-mesons. As we showed in reference 9, these were the best choices for explaining experimental data on multiple production of ordinary and strange particles.* We will take the same conservation laws into account and use the same method for calculating statistical weights as in our previous work.

Taking account of the resonance π-π interaction is formally equivalent to introducing a "pion isobar" of mass $\mu = 0.47$ nucleon masses,[5] spin $S = 0$ and isotopic spin $T = 0$ (variant of Dyson[2]) or $T = 1$ (variant of Takeda[3]) into the statistical theory of multiple production.†

In the table we show the ratio of the experimental results from reference 11 to the theoretical results

Variant of the theory	Number of prongs		
	2	4	6
Without the π-π interaction	0,98±0.12	0.99±0.16	2±1,14
With the π-π interaction in Dyson's variant	1,21±0.15	0.83±0.13	0.49±0.28
With the π-π interaction in Takeda's variant	1.38±0.17	0.71±0.11	0.64±0.36

for two, four, and six-prong stars, the latter calculated for three variants of the theory. (The indicated statistical experimental error is $\Delta_n = \pm\sqrt{N_n}$ where N_n is the number of n-pronged stars.)

It can be seen that the results of calculations without account of the π-π interaction agree well with experiment. Inclusion of this resonance π-π interaction, especially with Takeda's variant, worsens this agreement. The disagreement between the theoretical and experimental values for stars with a small number of prongs is a characteristic feature of the calculations which take account of the resonance π-π interaction, not only at E = 5 Bev, but also, at other energies.

The proportion of charged strange particles produced in inelastic π^--p collisions constitutes 8.6% for the theory which neglects the π-π interaction (5.5% from K^+ and 0.3% from K^- mesons) and 6.4% and 5.7% for the variants of Dyson and Takeda. Of the 110 inelastic stars in the experiment, in only four cases (i.e., in 3.5% of all cases) were strange particles produced. However, it is not possible to differentiate between the three theoretical variants on this basis, as was proposed in reference 10, because stars in which strange particles are produced, but do not decay in the chamber, may be included in the remaining 106 stars. Considering the lack of statistics of stars with strange particles, one would expect such cases to be very probable.

Thus, available experimental data can, within the limits of experimental error, be explained without employing the hypothesis of resonance π-π interaction. Further assumptions would be necessary to bring the statistical theory, with this interaction, into agreement with experiment.

We are grateful to V. I. Rus'kin for discussion of the comparison of our numerical results with his calculations.

---

*If one is interested only in the production of ordinary particles, then all reactions with strange particles can simply be discarded (i.e., set $r_K = 0$). Such a simplification has little effect on the results obtained for pions and nucleons since the proportion of strange particles produced is small.

†Inelastic π^--p scattering at 5 Bev with account of the resonance π-π interaction was considered by Rus'kin.[10] However, only part of the possible inelastic reaction channels were included here. Thus, for reactions with strange particles, the neglected channels have approximately the same statistical weight as the reactions taken into account by Rus'kin. If these channels are included, then the ratio of the cross section for the production of strange particles to the cross section for production of the observed π mesons exceeds that indicated by Rus'kin by a factor of more than two and is several times larger than the experimental value. The agreement with experiment for the distribution of stars with number of prongs is correspondingly worsened. This well-known result (see reference 9) indicates that K mesons should be taken into account differently than π mesons in the statistical theory.

[1] O. Piccioni, Proc. Rochester Conf., 1952.

[2] F. Dyson, Phys. Rev. **99**, 1037 (1955).

[3] G. Takeda, Phys. Rev. **100**, 440 (1955).

[4] T. Goto, Nuovo cimento **8**, 625 (1958).

[5] E. Eberle, Nuovo cimento **8**, 610 (1958).

[6] Cool, Piccioni, and Clark, Phys. Rev. **103**, 1082 (1956).

[7] S. L. Lindenbaum and L. C. L. Yuan, Phys. Rev. **100**, 306 (1955).

[8] Walker, Hushfar, and Shephard, Phys. Rev. **104**, 526 (1956).

[9] V. S. Barashenkov and V. M. Mal'tsev, Acta Phys. Polonica **17**, 177 (1958); V. S. Barashenkov, Nuclear Phys. **7**, 146 (1958), JETP **34**, 1016 (1958), Soviet Phys. JETP **7**, 701 (1958); É. K. Mikhul, JETP **35**, 298 (1958), Soviet Phys. JETP **8**, 205 (1959); V. S. Barashenkov and V. M. Mal'tsev, Acta Phys. Polonica **17**, 397 (1958), JETP **36**, 933 (1959), Soviet Phys. JETP **9**, 659 (1959).

[10] V. I. Rus'kin, JETP **36**, 164 (1959), Soviet Phys. JETP **9**, 113 (1959).

[11] Maenchen, Fowler, Powell, and Wright, Phys. Rev. **108**, 850 (1957).

Translated by G. E. Brown
176

ON THE DETERMINATION OF NUCLEAR DEFORMATION FROM THE ALPHA-DECAY FINE STRUCTURE

V. G. NOSOV

Submitted to JETP editor June 1, 1959

J. Exptl. Theoret. Phys. (U.S.S.R.) 37, 886-887 (September, 1959)

WE have shown earlier that by studying the α-decay fine structure it is possible to determine the form of the surface of the daughter nucleus.[1] A theory was developed for the decay of even-even nuclei, by which unique analytic expressions, valid in all space, can be obtained for the wave functions of the α particle. The resultant formula for the relative probability of excitation of the rotational level of a daughter nucleus with momentum J is found to be

$$w_J = (2J+1)\, e^{-\gamma J(J+1)} \frac{\left| \int\limits_{-1}^{1} \chi(\mu)\, e^{\beta P_2(\mu)} P_J(\mu)\, d\mu \right|^2}{\left| \int\limits_{-1}^{1} \chi(\mu)\, e^{\beta P_2(\mu)}\, d\mu \right|^2}, \quad (1)$$

where $\chi(\mu)$ is the wave function of the alpha particle on the surface of the nucleus, described by the equation $R(\mu) = R_0\{1 + \alpha_2 P_2(\mu)\}$; $\mu = \cos\vartheta$; the parameters γ and β/α_2 depend in a definite manner on the nuclear radius R_0 (we assume in the computations $R_0 = 1.4\,A^{1/3} \times 10^{-13}$ cm), the atomic number Z, the decay energy, and moment of inertia I of the daughter nucleus (it is also possible to take the right half of (1) to mean integration over some other weakly-nonspherical surface, but χ, γ, and β must then be taken to mean the corresponding quantities that pertain to that surface). Using Eq. (1) and assuming $\chi = \text{const}$, we determined the quadrupole deformations α_2 for 22 even-even daughter nuclei from the experimentally-observed probability w_2 of the excitation of the 2^+ level.

This problem was considered anew by Strutinskiĭ[2] under the same physical assumptions, but by a different method, which led to poorly-converging series. The wave function was therefore determined by him only inside a spherical surface S′ of radius $R' = 2Ze^2/E - R_0$. He then used the formula

$$w_J = (2J+1) \left| \int\limits_{-1}^{1} \chi'(\mu)\, P_J(\mu)\, d\mu \right|^2 \Bigg/ \left| \int\limits_{-1}^{1} \chi'(\mu)\, d\mu \right|^2, \quad (2)$$

where $\chi'(\mu)$ is the wave function on the surface S′. The results of references 1 (α_2^N) and 2 (α_2^S) are compared in the table. The values α_2^S deviate systematically from α_2^N, and the deviation increases with increasing $\Delta E = 3\hbar^2/I$.

Formula (2) is equivalent to stating that the penetration of the part of the barrier located outside the surface S′ is independent of the momentum of the alpha particle. To verify (2), we apply (1) to the surface S′ ($\beta = 0$). Identifying the corresponding values of w_J and γ by primes, and comparing with (2), we obtain

$$w'_J = e^{-\gamma' J(J+1)}\, w_J. \quad (3)$$

Thus in reference 2 the deformation agrees actually not with the experimentally-observed w_J, but with some quantity w'_J which has no physical meaning. Formula (3) can also be obtained by ordinary unidimensional quasi-classical methods, since the field is practically centrally-symmetrical in the region $r > R'$.

To estimate the role of the factor $\exp\{-\gamma' J \times (J+1)\}$, which describes the dependence of the penetration on the momentum of the alpha particle, we put $J = 2$ in (3); the values $e^{-6\gamma'}$ listed in the table deviate substantially from unity, indicating that the deformations obtained by Strutinskiĭ are in error.

To verify the foregoing considerations, let us insert w'_2 in the left half of (1) and calculate the corresponding deformation α'_2. Inasmuch as w'_2 is that value of the probability (not equal to the experimental one) with which the deformation in reference 2 actually agrees, α'_2 should be equal to α_2^S. As seen from the table, this is indeed so (certain discrepancies apparently do not exceed the accuracy limits of Strutinskiĭ's calculations).

The present calculation thus confirms the correctness of the deformations computed in reference 1. We note that in calculating α_2^N in accordance with (1) the error is very small. Account of all the first-order correction in the expansion in powers of the parameters $1/\kappa R_0$, α_2, and $J(J+1)/\kappa^2 R_0^2$ (κ is the wave number of the alpha particle on the surface of the nucleus) corrects the deformation by not more than 3%. Therefore

Daughter nucleus	ΔE kev	α_2^N	α_2^S	$e^{-6\gamma'}$	α'_2	Daughter nucleus	ΔE kev	α_2^N	α_2^S	$e^{-6\gamma'}$	α'_2
Em^{220}	240	0.21	0.07	0.17	0.08	U^{230}	50	0.11	0.08	0.64	0.08
Em^{222}	186	0.23	0.08	0.20	0.09	U^{232}	45	0.13	0.10	0.65	0.10
Ra^{222}	109	0.20	0.13	0.44	0.12	U^{234}	46.8	0.16	0.14	0.63	0.13
Ra^{224}	84	0.24	0.17	0.48	0.15	U^{236}	45	0.15	0.13	0.63	0.12
Ra^{226}	67.2	0.21	0.15	0.51	0.13	U^{238}	43.8	0.14	0.12	0.63	0.11
Ra^{228}	60	0.24	0.17	0.51	0.15	Pu^{238}	43.8	0.15	0.12	0.66	0.12
Th^{226}	69.6	0.22	0.17	0.55	0.15	Pu^{240}	43.2	0.15	0.12	0.65	0.12
Th^{228}	60	0.21	0.18	0.57	0.16	Cm^{242}	42	0.13	0.10	0.68	0.10
Th^{230}	52.2	0.17	0.14	0.58	0.12	Cm^{246}	37.2	0.11	0.07	0.69	0.07
Th^{232}	50	0.19	0.16	0.58	0.14	Cm^{248}	37.2	0.10	0.07	0.69	0.07
Th^{234}	50	0.17	0.14	0.57	0.13	Cf^{250}	42	0.10	0.08	0.68	0.08

the only sufficient reason for changing α_2^N would be an improvement in the experimental data, to which, in particular, the review of Perlman and Rasmussen is devoted.[3]

I thank A. S. Kompaneets for evaluating the results of this work, and also T. V. Novikova for help in the calculations.

---

[1] V. G. Nosov, Dokl. Akad. Nauk SSSR **112**, 414 (1957), Soviet Phys.–Doklady **2**, 48 (1957).

[2] V. M. Strutinskiĭ, JETP **32**, 1412 (1957), Soviet Phys. JETP **5**, 1150 (1957).

[3] I. Perlman and J. Rasmussen, Hand. d. Phys. XLII, 109 (1957).

Translated by J. G. Adashko
177

THE NON-ADDITIVITY OF LONDON-VAN DER WAALS FORCES

L. I. PODLUBNYĬ

Odessa Pedagogical Institute

Submitted to JETP editor June 6, 1959

J. Exptl. Theoret. Phys. (U.S.S.R.) **37**, 888-889 (September, 1959)

THE so-called dispersive interaction forces between neutral atoms are not additive (notwithstanding statements which are sometimes made); the additivity occurs only in the first non-vanishing perturbation theory approximation. We consider here the next terms (of third order in the coupling constant) of the perturbation series and we shall obtain an expression for the energy of the dispersive interaction of three hydrogen atoms, in its dependence on the interatomic distances R_1, R_2, R_3 as parameters and including the retardation effect.

For this purpose it is advantageous to use the Feynman-Dyson technique, as done by Dzyaloshinskiĭ[1] for the interaction of two atoms. We are interested in processes of the kind of Fig. 1a leading to a contribution

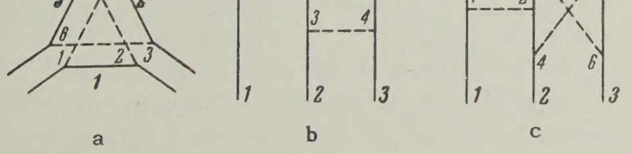

a b c

$$S^{(6)} = -\frac{4}{3}\pi^3 \int dx_1 \ldots dx_6\, D^F(1,4)\, D^F(3,6)\, D^F(2,5)$$
$$\times P[j_\delta^{(3)}(5)\, j_\nu^{(3)}(6)]\, P[j_\nu^{(2)}(3)\, j_\mu^{(2)}(4)]\, P[j_\mu^{(1)}(1)\, j_\delta^{(1)}(2)]. \quad (1)$$

To derive this expression we eliminated the variables of the intermediate electromagnetic field, used the usual, non-Heaviside system of units [$\hbar = c = 1$ up to Eq. (5)], and took into account that, for instance, for an N-particle interaction there are in all $2^{N-1}(N-1)!$ different processes of order e^{2N} corresponding to connected diagrams of the kind shown in Fig. 1a. Generally speaking we should have started our consideration with processes of the type of Fig. 1b, leading to a non-additive correction of the second order (in the coupling constant), but in the approximation chosen by us (we are only interested in the dipole interaction) all matrix elements of $S^{(4)}$ containing "propagator functions" of three interacting atoms give zero for the ground state, since two out of the three "propagator lines" are involved in only one vertex. One must drop processes depicted in Fig. 1c for similar considerations.

In the first non-vanishing order, in which the interaction energy depends simultaneously on the coordinates of all three atoms, we therefore get precisely Eq. (1). Performing in this equation the integration over all time coordinates we find:

$$U = \frac{-i}{24\pi^7} \int d^3r_1 \ldots d^3r_6 \int d^3p_1 d^3p_2 d^3p_3 \exp\{i\mathbf{p}_1(\mathbf{r}_1 - \mathbf{r}_4)$$
$$+ i\mathbf{p}_2(\mathbf{r}_3 - \mathbf{r}_6) + i\mathbf{p}_3(\mathbf{r}_5 - \mathbf{r}_2)\} \int_{-\infty}^{\infty} \frac{d\omega}{(p_1^2 - \omega^2)(p_2^2 - \omega^2)(p_3^2 - \omega^2)}$$
$$\times \sum_{k,\, m,\, n} \left[\frac{\langle 0 | j_\delta^{(3)}(r_5) | k\rangle \langle k | j_\nu^{(3)}(r_6) | 0\rangle}{\omega_{k0} - \omega}\right.$$
$$\left. + \frac{\langle 0 | j_\nu^{(3)}(r_6) | k\rangle \langle k | j_\delta^{(3)}(r_5) | 0\rangle}{\omega_{k0} + \omega}\right]$$
$$\times \left[\frac{\langle 0 | j_\nu^{(2)}(r_3) | m\rangle \langle m | j_\mu^{(2)}(r_4) | 0\rangle}{\omega_{m0} - \omega}\right.$$
$$\left. + \frac{\langle 0 | j_\mu^{(2)}(r_4) | m\rangle \langle m | j_\nu^{(2)}(r_3) | 0\rangle}{\omega_{m0} + \omega}\right]$$
$$\times \left[\frac{\langle 0 | j_\mu^{(1)}(r_1)\, n\rangle \langle n | j_\delta^{(1)}(r_2) | 0\rangle}{\omega_{n0} - \omega}\right.$$
$$\left. + \frac{\langle 0 | j_\delta^{(1)}(r_2) | n\rangle \langle n | j_\mu^{(1)}(r_1) | 0\rangle}{\omega_{n0} + \omega}\right]. \quad (2)$$

In the non-relativistic approximation we can put

$$\langle l | j_\mu(r_1) | m\rangle \langle m | j_\mu(r_2) | l\rangle = -e^2 [\psi_l^*(r_1)\psi_m(r_1)$$
$$- \delta(r_1)\delta_{lm}][\psi_m^*(r_2)\psi_l(r_2) - \delta(r_2)\delta_{ml}], \quad (3)$$

and so on. If we now introduce the polarizability

$$\alpha(\omega) = \sum_n 2\omega_{n0} | d_{on} |^2 / (\omega_{n0}^2 - \omega^2), \quad (4)$$

where d_{0n} is the dipole moment matrix element, and perform the necessary integration in (2), we get finally after elementary, but cumbersome computations

$$U(R_1, R_2, R_3) = -132\,\hbar c\alpha_1(0) \times \alpha_2(0)\,\alpha_3(0) / \pi R_1 R_2 R_3 (R_1 + R_2 + R_3)^7, \qquad (5)$$

and this formula is valid under the assumption that the distances between the atoms are much larger than the characteristic wave length λ_0 in the spectrum of the atom ($R_1, R_2, R_3 \gg \lambda_0$ so that exchange forces play no role whatever; as was already stated, we neglect the effects of higher multipoles).

---

[1] I. E. Dzyaloshinskiĭ, JETP **30**, 1152 (1956), Soviet Phys. JETP **3**, 977 (1957).

Translated by D. ter Haar
178

NUMERICAL SOLUTION OF STATIC DISPERSION RELATIONS OF THE PHOTOPRODUCTION P-WAVE

L. D. SOLOV' EV and G. N. TENTYUKOVA

Joint Institute for Nuclear Research

Submitted to JETP editor June 29, 1959

J. Exptl. Theoret. Phys. (U.S.S.R.) **37**, 889-890 (September, 1959)

WE found an exact numerical solution of the static dispersion relations obtained in references 1 and 2 for the photoproduction P-amplitudes. We used the method, proposed by Omnes[3] and based on the work of Muskhelishvili,[4] of reducing the linear singular integral equations to regular Fredholm equations. The procedure (which is not unique in the case of scattering), for the transition from the singular to the regular equations is found to be unique in this case under the following conditions: 1) the scattering phase shifts vanish at the threshold and at infinity, 2) the solution of the regular equation is bounded and has the same value at infinity as the solution of the singular equation.

The values used for the phase shifts were obtained from the Chew-Low static equations (at $f^2 = 0.08$ and a cutoff parameter $P = 7$), the solutions of which were obtained by the Salzmans[5] and repeated by Tentyukova on the "Strela" computer. The regular photoproduction equations were solved by successive approximation on the "Ural" computer of the Joint Institute for Nuclear Research.

The exact solutions for the quadrupole amplitudes and the e-parts of the magnetic dipole amplitudes behave qualitatively like the corresponding Bohr terms multiplied by $\cos\delta$.[1] The μ-parts of the magnetic dipole amplitudes (including the isotope-scalar amplitudes) behave like $\sim q^{-3}\sin\delta$. This means that the meson created upon interaction of a photon with the static magnetic moment of the nucleon always experiences secondary scattering.

It is shown further that the electric dipole amplitude is independent in the static approximation of the magnetic moments. This follows from the supplementary condition and from the dispersion relations for the longitudinal amplitudes, obtained in reference 6.

As a first attempt at comparing the complete expression for the photoproduction amplitude with experiment, with allowance for the obtained corrections, we calculated the coefficient C in the photoproduction cross section of π^0 mesons at threshold:

$$d\sigma(\gamma p \to \pi^0 p)/d\Omega = A + B\cos\theta + C\cos^2\theta.$$

In the figure, C is given in $(\hbar/\mu_0 c)^2$ units, q is the meson momentum in the c.m.s. and in units of $\mu_0 c^2$, and $q^0 = \sqrt{1-q^2}$. The solid curve corresponds to the exact solution, while the dotted one corresponds to the approximate solution obtained in reference 1; the experimental points for 160 — 240 Mev are taken from reference 7, while those for 260 Mev are from reference 8. It is seen that the exact solution leads to fair agreement with experiment near threshold. This agreement becomes somewhat worse for large energy, which can be attributed to relativistic effects. The approximate solution of reference 1 is in poor agreement with experiment, as noted by Baldin and Govorkov (private communication).

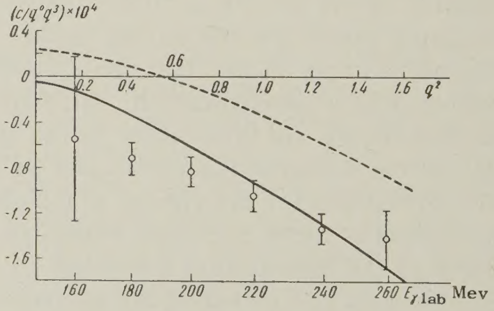

We take this occasion to express sincere gratitude to A. A. Logunov, S. V. Fomin, and N. N. Govorun for interest in the work, and also to A. M. Baldin for very valuable comments and for acquainting us with his paper prior to publication.

[1] Chew, Goldberger, Low, and Nambu, Phys. **106** 1345 (1957).

[2] Logunov, Tavkhelidze, and Solovyov, Nucl. Phys. **4**, 427 (1957). L. D. Solov'ev JETP **33**, 801 (1957), Soviet Phys. JETP **6**, 617 (1958); Nucl. Phys. **5**, 256 (1958).

[3] R. Omnes, Nuovo cimento **8**, 316 (1958).

[4] N. I. Muskhelishvili, Сингулярные интегральные уравнения (Singular Integral Equations), Gostekhizdat, 1946.

[5] G. Salzman and F. Salzman, Phys. Rev. **108**, 1619 (1957).

[6] A. A. Logunov and L. D. Solov'ev, Научные доклады высшей школы (Scientific Papers of the Higher Schools) **4**, 217 (1958); Nucl. Phys. **10**, 60 (1959). Kukin, Solov'ev, and Frenkin, Scient. Papers of the Higher Schools, No. 3, 169 (1958).

[7] Vasil'ev, Govorkov, and Gol'danskiĭ, in press.

[8] McDonald, Peterson, and Corson, Phys. Rev. **107**, 577 (1957).

Translated by J. G. Adashko
179

ON THE QUESTION OF CRITICAL VELOCITIES FOR FLOW OF He II *IN CAPILLARIES*

B. T. GEĬLIKMAN

The V. I. Lenin Moscow State Pedagogical Institute

Submitted to JETP editor June 20, 1959

J. Exptl. Theoret. Phys. (U.S.S.R.) **37**, 891-892 (September, 1959)

As is known, Onsager's[1] and Feynman's[2] ideas about vortex lines yield the right order of magnitude of critical velocities for superfluid helium rotating in a cylinder and for flow from a narrow capillary into a large beaker. In the former case the vortex lines are straight and parallel to the cylinder axis, while in the latter they are rings formed in the beaker near to the junction with the capillary.[2]

It will be shown below that similar values of the critical velocities can be calculated for the flow of helium through a long capillary. It is natural to suppose that the vortex lines will, in this case, be closed curves lying in planes perpendicular to the capillary axis. The shape of the lines will be determined by the capillary cross section, i.e., for a circular cross section the lines will be circular and for a rectangular section the lines will form closed curves nearly rectangular in shape. The angular momentum associated with such lines is evidently zero, while the linear momentum is non-zero and is directed parallel to the capillary axis, i.e., parallel to the flow velocity v. According to Landau[3] the change in energy, ΔE, of flowing helium (in a coordinate system fixed with respect to the capillary walls), associated with the formation of a vortex line, is $\Delta E = E_V - p_V v$ (E_V and p_V are the energy and momentum of a vortex line). A vortex line can be formed if $\Delta E < 0$. As superfluidity disappears when a vortex line appears, the critical velocity v_k is determined by the condition $\Delta E = 0$, i.e., $v_k = E_V / p_V$.

The momentum p_V of a narrow vortex line is given by[4] $p_V = \kappa\rho \int dF_n$, where κ is the circulation of velocity along a contour enclosing the line and ρ is the density and the integration is over a surface bounded by the vortex contour l. In calculating the line energy we shall assume that the vortex line is sufficiently far from the walls for surface effects to be neglected. Then[4]

$$E_v = \frac{\rho}{8\pi} \int \frac{(\operatorname{curl} \mathbf{v}(\mathbf{r}), \operatorname{curl} \mathbf{v}(\mathbf{r}'))}{|\mathbf{r} - \mathbf{r}'|} \, d\mathbf{r} \, d\mathbf{r}'.$$

Since p_V is proportional to the square of the linear dimensions of the line and E_V is directly proportional to it, the minimum ΔE corresponds to the maximum line length, coinciding with the transverse dimensions (for a rectangular cross section it is therefore not energetically profitable for circular vortices to be formed instead of rectangular vortices). If, in fact, the line is near the walls, Eq. (1) for E_V is inexact, but it is sufficient for calculating v_k.

According to Feynman,[2] the circulation κ is quantized: $\kappa = 2\pi n_s \hbar/m$, where $n_s = 1, 2, \ldots\ldots$. The smallest values of energy, E_V and of $|\Delta E|$ correspond to $n_s = 1$. By calculating the line energy and momentum we obtain for a circular cross section of radius r

$$v_k = (\hbar / mr)\left(\ln (r / d) + \ln 16 - {}^7/_4\right)$$

(d is the diameter of the line cross section, $d \ll r$).

For a rectangular cross section

$$v_k = \frac{\hbar}{m}\left\{\frac{1}{b}\left[\ln \frac{4a\left(\sqrt{a^2+b^2}-a\right)}{bd} - \frac{7}{4}\right] + \frac{1}{a}\left[\ln \frac{4b\left(\sqrt{a^2+b^2}-b\right)}{ad} - \frac{7}{4}\right] + 2\sqrt{\frac{1}{a^2}+\frac{1}{b^2}}\right\};$$

and for $b \ll a$

$$v_k = (\hbar / mb)\left[\ln (2b / d) + \frac{1}{4}\right].$$

a and b are the sides of the rectangle $(a, b \gg d)$. According to Lifshitz and Pitaevskiĭ[5] we should take d as 2×10^{-7} cm. For $r \approx 10^{-5}$ cm we then obtain $v_k \approx 80$ cm/sec. A similar estimate for the flow of helium from a capillary into a beaker was derived by Feynman.

We would like to thank V. M. Galitskiĭ and A. B. Migdal for interesting discussions.

---

[1] L. Onsager, Nuovo cimento **6**, Suppl. 2, 249 (1949).

[2] R. P. Feynman, Progress in Low Temperature Physics, vol I, Chap. 2, (North Holland Publishing Company, 1955).

[3] L. D. Landau, JETP **11**, 592 (1941).

[4] H. Lamb, Hydrodynamics, Russ. Transl., GTI, 1947, p. 269 and 303 [Dover, N.Y., 1945].

[5] E. M. Lifshitz and L. P. Pitaevskiĭ, JETP **33**, 535 (1957), Soviet Phys JETP **6**, 418 (1958).

Translated by R. Berman
180